UNDERSTANDING AGE AND SEX-RELATED DIFFERENCES IN THE BIOMECHANICS OF ROAD TRAFFIC ASSOCIATED INJURIES THROUGH POPULATION DIVERSITY ANALYSES

EDITED BY: Francisco J. Lopez-Valdes, Mats Yngve Svensson, Sonia Duprey and Jason Forman

PUBLISHED IN: Frontiers in Bioengineering and Biotechnology

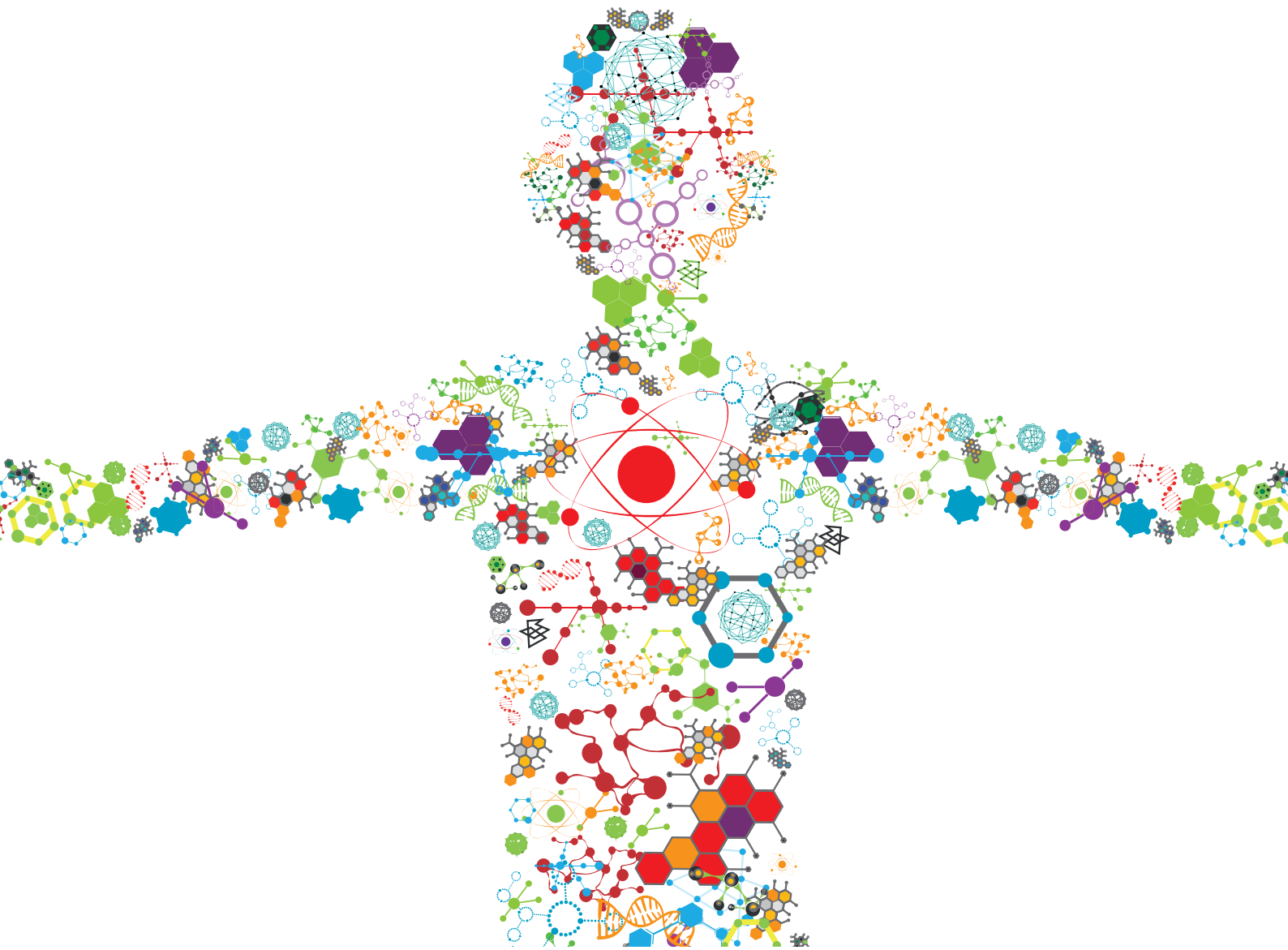

frontiers Research Topics

frontiers

ISSN 1664-8714
ISBN 978-2-88976-276-7
DOI 10.3389/978-2-88976-276-7

About Frontiers

Frontiers is more than just an open-access publisher of scholarly articles: it is a pioneering approach to the world of academia, radically improving the way scholarly research is managed. The grand vision of Frontiers is a world where all people have an equal opportunity to seek, share and generate knowledge. Frontiers provides immediate and permanent online open access to all its publications, but this alone is not enough to realize our grand goals.

Frontiers Journal Series

The Frontiers Journal Series is a multi-tier and interdisciplinary set of open-access, online journals, promising a paradigm shift from the current review, selection and dissemination processes in academic publishing. All Frontiers journals are driven by researchers for researchers; therefore, they constitute a service to the scholarly community. At the same time, the Frontiers Journal Series operates on a revolutionary invention, the tiered publishing system, initially addressing specific communities of scholars, and gradually climbing up to broader public understanding, thus serving the interests of the lay society, too.

Dedication to Quality

Each Frontiers article is a landmark of the highest quality, thanks to genuinely collaborative interactions between authors and review editors, who include some of the world's best academicians. Research must be certified by peers before entering a stream of knowledge that may eventually reach the public - and shape society; therefore, Frontiers only applies the most rigorous and unbiased reviews.
Frontiers revolutionizes research publishing by freely delivering the most outstanding research, evaluated with no bias from both the academic and social point of view. By applying the most advanced information technologies, Frontiers is catapulting scholarly publishing into a new generation.

What are Frontiers Research Topics?

Frontiers Research Topics are very popular trademarks of the Frontiers Journals Series: they are collections of at least ten articles, all centered on a particular subject. With their unique mix of varied contributions from Original Research to Review Articles, Frontiers Research Topics unify the most influential researchers, the latest key findings and historical advances in a hot research area! Find out more on how to host your own Frontiers Research Topic or contribute to one as an author by contacting the Frontiers Editorial Office: frontiersin.org/about/contact

UNDERSTANDING AGE AND SEX-RELATED DIFFERENCES IN THE BIOMECHANICS OF ROAD TRAFFIC ASSOCIATED INJURIES THROUGH POPULATION DIVERSITY ANALYSES

Topic Editors:
Francisco J. Lopez-Valdes, Comillas Pontifical University, Spain
Mats Yngve Svensson, Chalmers University of Technology, Sweden
Sonia Duprey, Université de Lyon, France
Jason Forman, University of Virginia, United States

Citation: Lopez-Valdes, F. J., Svensson, M. Y., Duprey, S., Forman, J., eds. (2022). Understanding Age and Sex-Related Differences in the Biomechanics of Road Traffic Associated Injuries Through Population Diversity Analyses. Lausanne: Frontiers Media SA. doi: 10.3389/978-2-88976-276-7

Table of Contents

frontiers | Frontiers in Bioengineering and Biotechnology

EDITORIAL
published: 13 May 2022
doi: 10.3389/fbioe.2022.869356

Editorial: Understanding Age and Sex-Related Differences in the Biomechanics of Road Traffic Associated Injuries Through Population Diversity Analyses

Francisco J. Lopez-Valdes[1]*, *Sonia Duprey*[2], *Jason Forman*[3] and *Mats Y. Svensson*[4]

[1]Institute for Research in Technology (IIT), ICAI, Universidad Pontificia Comillas, Madrid, Spain, [2]Université Claude Bernard Lyon 1, Lyon, France, [3]University of Virginia, Charlottesville, VA, United States, [4]Chalmers University of Technology, Göteborg, Sweden

Keywords: road traffic injuries (RTI), population diversity, impact biomechanics, biofidelity, human body model (HBM)

Editorial on the Research Topic

Understanding Age and Sex-Related Differences in the Biomechanics of Road Traffic Associated Injuries Through Population Diversity Analyses

Road traffic injuries account for 1.35 million deaths and approximately 50 million injuries yearly according to the World Health Organization (WHO, 2019). These injuries are unequally shared by the world's population, with several vulnerable groups being overexposed to the effects of injuries. For instance, road injuries are the leading cause of death for children and young adults (5–29 years old). Recent research has pointed out that women are at a greater risk of death and of sustaining severe injuries under the same crash configurations as men (Bose et al., 2011). Elderly car occupants have been identified as particularly vulnerable to the deployment of contemporary safety systems such as airbags and seatbelts (Kent et al., 2009).

While the seminal work done on Injury Biomechanics in the 1970's–1980's provided data to develop injury criteria that can be used with Anthropometric Test Devices (ATD), also known as crash test dummies or just dummies, there is a growing body of literature pointing out to the need of recognizing how differences between individuals may modify their specific risk to injuries (Forman et al., 2015). The source of this variability is not unique, but more and more research suggests that anthropometry, age and sex are significant factors influencing the injury tolerance of individuals.

Thus, the goal of this Research Topic is to highlight how these biomechanical differences between population groups are identified and eventually incorporated into the design of effective safety systems capable of preventing injuries for all road users.

Biomechanical research always needs to keep the connection with real world injuries. The study "Are There Any Significant Differences in Terms of Age and Sex in Pedestrian and Cyclist Accidents?" analyzes sex-specific differences in pedestrians and cyclists collisions in three European countries finding that women are at higher risk of sustaining AIS3+ lower extremity and pelvic injuries (OR = 2.11–3.03, depending on the country, but statistically significant for all analyzed countries). Two articles looked at how women and men react to longitudinal accelerations in standing position as in public transportation situations. The study "Human Response to Longitudinal Perturbations of Standing Passengers on Public Transportation During Regular Operation" found out shorter muscle response time in female volunteers compared to their

OPEN ACCESS

Edited and reviewed by:
Markus O. Heller, University of Southampton, United Kingdom

***Correspondence:**
Francisco J. Lopez-Valdes
fjlvaldes@comillas.edu

Specialty section:
This article was submitted to Biomechanics, a section of the journal Frontiers in Bioengineering and Biotechnology

Received: *04 February 2022*
Accepted: *29 April 2022*
Published: *13 May 2022*

Citation:
Lopez-Valdes FJ, Duprey S, Forman J and Svensson MY (2022) Editorial: Understanding Age and Sex-Related Differences in the Biomechanics of Road Traffic Associated Injuries Through Population Diversity Analyses. Front. Bioeng. Biotechnol. 10:869356. doi: 10.3389/fbioe.2022.869356

male counterparts, while the paper "Identifying and Characterizing Types of Balance Recovery Strategies Among Females and Males to Prevent Injuries in Free-Standing Public Transport Passengers" found no differences between the two sexes in the balance recovery outcome to longitudinal perturbations, although no statistical comparison could be made between different recovery strategies due to the sample size of the volunteer group ($n = 24$). The subject deserves further research as it was found that while seven out of 13 males used the "fighting stance" as the recovery strategy only three out 11 females adopted this strategy to maintain balance.

Two studies used computational modeling to analyze whether existing head injury criteria were suitable to predict traumatic brain injury in the elderly. "The head AIS4+ injury thresholds for the elderly vulnerable road user based on detailed accident reconstructions" reconstructed 30 real world cases to find that currently proposed injury thresholds for traumatic brain injury, both based on linear or angular magnitudes, should be substantially lowered to capture the injury likelihood of the elderly population (for instance, the found threshold of HIC_{15} for AIS4+ injuries in this study was 1,082 compared to the 1,440 threshold proposed by NHTSA). Following a similar methodology, "Evaluation of Head Injury Criteria for Injury Prediction Effectiveness: Computational Reconstruction of Real-World Vulnerable Road User Impact Accidents" identified differences between the predictions of strain-based head injury criteria (maximum principal strain was a better predictor of Diffuse Axonal Injury than cumulative strain damage). In the case of kinematics-based injury criteria, the more traditional injury criteria such as HIC and HIP provided comparably accurate results. Computer modeling was also used in "Rib cortical bone fracture risk as a function of age and rib strain: Update injury prediction using Finite Element Human Body Models" to provide an estimation of the risk of rib fractures using a probabilistic approach and experimental data from 58 individuals spanning 17–99 years old, providing a robust framework to advance the use of human body models in the prevention of road traffic injuries.

The differences with age and sex in the cervical spine was the topic of two of the studies submitted to this article collection. "The lack of sex, age and anthropometric diversity in neck biomechanical data" found out that the neck biomechanical data were biased toward males, younger volunteers and older Post Mortem Human Surrogates in a systematic review of the literature. The study "Comparison of Upper Neck Loading in Young Adult and Elderly Volunteers During Low Speed Frontal Impacts" is the first one in the literature comparing the experimentally measured cervical loading of younger ($n = 9$) and older ($n = 4$) volunteers under the same dynamic conditions to find out that there were not substantial differences between the two age groups. This finding was also supported by the study "Sex, Age, and Stature Affects Neck Biomechanical Responses in Frontal and Rear Impacts Assessed Using Finite Element Head and Neck Models" that did not identify overall kinematic differences between an aged cervical model and a younger one, which would justify that the inverse kinematics method used in the previous study could not identify important differences in the cervical loading. In parallel, the study found that aged models predicted higher ligament deformations. The female model also exhibited larger shear forces at the facet joints, agreeing with available epidemiological data. Further research on this area is needed to increase the sample size of the available experimental data and the statistical power of the comparisons between cervical loads across age groups and sexes.

Additional insight into the response of women to rear impacts was provided by three studies. "Dynamic Responses of Female Volunteers in Rear Impact Sled Tests at Two Head Restraint Systems" supplies new experimental data from female volunteers at different dynamic conditions that can be used to develop more biofidelic physical and computational female surrogates. The need for developing female models is also supported by the findings of "The effect of seat back inclination on spinal alignment in automotive seating postures" that identified differences in the lordosis and kyphosis between females and males depending on the seat back inclination in a set of 23 volunteers. The first attempt to develop a physical dummy to represent female occupants in rear impacts is included in "Design and Evaluation of the Initial 50^{th} Percentile Female Prototype Rear Impact Dummy, BioRID P50F- Indications for the need of an additional dummy size", which presented promising results about the performance of a new more women-like physical model in rear impacts.

In summary, the current Research Topic offers insights into the use of computer models to investigate the performance of existing and newly proposed injury criteria capable of capturing individual differences related to age and sex variations. It also provides new experimental data that can be used in the development of more accurate physical and computational surrogates. And, finally, the collection includes information about the development of a new physical crash test dummy intended to improve the protection of female occupants in rear impacts.

We trust that the amount of new data and developments included in this Research Topic provides valuable information to the field and, above all, contributes to reduce the number of motor vehicle related injuries that can be related to sex and age differences between road users.

AUTHOR CONTRIBUTIONS

All authors listed have made a substantial, direct, and intellectual contribution to the work and approved it for publication.

REFERENCES

Bose, D., Segui-Gomez, ScD, M., and Crandall, J. R. (2011). Vulnerability of Female Drivers Involved in Motor Vehicle Crashes: an Analysis of US Population at Risk. *Am. J. Public Health* 101, 2368–2373. doi:10.2105/ajph.2011.300275

Forman, J. L., Lopez-Valdes, F. J., Duprey, S., Bose, D., Del Pozo de Dios, E., Subit, D., et al. (2015). The Tolerance of the Human Body to Automobile Collision Impact - a Systematic Review of Injury Biomechanics Research, 1990-2009. *Accid. Analysis Prev.* 80, 7–17. doi:10.1016/j.aap.2015.03.004

Kent, R., Trowbridge, M., Lopez-Valdes, F. J., Ordoyo, R. H., and Segui-Gomez, M. (2009). How Many People Are Injured and Killed as a Result of Aging? Frailty, Fragility, and the Elderly Risk-Exposure Tradeoff Assessed via a Risk Saturation Model. Annual Proceedings/Association for the Advancement of Automotive Medicine. *Assoc. Adv. Automot. Med.* 53, 41–50.

WHO (2019). *Global Status Report on Road Safety 2018*. Geneva: World Health Organization.

Conflict of Interest: The authors declare that the research was conducted in the absence of any commercial or financial relationships that could be construed as a potential conflict of interest.

frontiers in Bioengineering and Biotechnology

ORIGINAL RESEARCH
published: 24 May 2021
doi: 10.3389/fbioe.2021.677952

Are There Any Significant Differences in Terms of Age and Sex in Pedestrian and Cyclist Accidents?

Christoph Leo[1], Maria C. Rizzi[2], Niels M. Bos[3], Ragnhild J. Davidse[3], Astrid Linder[2,4], Ernst Tomasch[1] and Corina Klug[1]*

[1] Vehicle Safety Institute, Graz University of Technology, Graz, Austria, [2] Swedish National Road and Transport Research Institute, VTI, Gothenburg, Sweden, [3] SWOV Institute for Road Safety Research, The Hague, Netherlands, [4] Mechanics and Maritime Science, Chalmers University, Gothenburg, Sweden

This study has analyzed sex-specific differences in pedestrian and cyclist accidents involving passenger cars. The most frequently injured body regions, types of injuries, which show sex-specific differences and the general accident parameters of females and males were compared. Accident data from three different European countries (Austria, Netherlands, Sweden) were analyzed. The current analysis shows that for both, females and males, pedestrian and cyclist injuries are sustained mainly to the body regions head, thorax, upper extremities and lower extremities. The results show that the odds for sustaining skeletal injuries to the lower extremities (incl. pelvis) in females are significantly higher. It was observed in all datasets, that the odds of females being involved in a rural accident or an accident at night are lower than for males. Elderly pedestrian and cyclist (≥60YO) tend to sustain more severe injuries (AIS2+ and AIS3+) than younger pedestrian and cyclists (<60YO) in some of the datasets. The findings of this study highlight the differences in males and females in both, accident scenarios and sustained injuries. Further investigations are needed to distinguish between gender- and sex-specific differences causing the different injury patterns.

Keywords: pedestrian, cyclists, epidemiology, injuries, sex-specific differences

OPEN ACCESS

Edited by:
Francisco J. Lopez-Valdes, Comillas Pontifical University, Spain

Reviewed by:
George Yannis, National Technical University of Athens, Greece
Elisabetta M. Zanetti, University of Perugia, Italy

****Correspondence:***
Christoph Leo
christoph.leo@tugraz.at

Specialty section:
This article was submitted to Biomechanics, a section of the journal Frontiers in Bioengineering and Biotechnology

Received: *08 March 2021*
Accepted: *29 April 2021*
Published: *24 May 2021*

Citation:
Leo C, Rizzi MC, Bos NM, Davidse RJ, Linder A, Tomasch E and Klug C (2021) Are There Any Significant Differences in Terms of Age and Sex in Pedestrian and Cyclist Accidents? Front. Bioeng. Biotechnol. 9:677952. doi: 10.3389/fbioe.2021.677952

INTRODUCTION

Worldwide, more than 50% of the 1.35 M road users killed annually, are vulnerable road users (VRUs) such as pedestrians, cyclists and motorcyclists (World Health Organization, 2018). Together, pedestrians and cyclists accounted for 32% of the road fatalities in the European Union in 2016 (World Health Organization, 2018). To reduce this number, a detailed analysis of the injuries is required to understand which injuries are the most common, related injury mechanisms, and finally to determine protective measures.

Awareness of sex and age specific differences in injury risks for vehicle occupants has only been identified in recent years (Kullgren and Krafft, 2010; Forman et al., 2019; Mitchell and Cameron, 2020). This may be due to the fact that vehicle safety regulations for occupants and VRUs are predominantly focused on mid-sized adult males (Simms and Wood, 2009;

Linder and Svedberg, 2019; Linder and Svensson, 2019). Studies have shown that this leads to unequal treatment in terms of vehicle safety based on sex and, as a result to significant differences in the injuries sustained by males and females (Bose et al., 2011; Starnes et al., 2011; Forman et al., 2019; Leo et al., 2019b; Linder and Svedberg, 2019; Mitchell and Cameron, 2020). Starnes et al. found for example in their study that younger males (15–55 years) were significantly more likely to suffer tibia fractures than females.

Besides sex, age has also been identified as an important factor affecting the types and severity of injuries (Davis, 2001; Niebuhr et al., 2016; Leo et al., 2019a; Saadé et al., 2020). Davis and Niebuhr et al. conclude that elderly pedestrians (≥60YO) tend to suffer more severe injuries than younger pedestrians. Also Saadé et al. conclude in their study that the pedestrian age as well as the collision speed have a statistically significant influence on injuries. Especially the age group 61+ shows statistically significant differences in that study.

Anthropometric test devices (ATDs) and Human Body Models (HBMs) used for safety evaluations have been predominantly designed to match mid-sized adult males (or in rare cases small adult females). This has led to an unequal treatment of the sexes with regard to vehicle safety regulations (Linder et al., 2020). Virtual testing (VT) will play an essential role in overcoming the unequal treatment, based on sex, in vehicle safety regulations in the near future. By means of VT it is possible to assess a much larger number of test scenarios than in physical testing. Furthermore, facilitated by state-of-the-art Human Body Models (HBMs), it is also possible to implement different anthropometries and gender specific characteristics in the loop of virtual testing. As a first step, an average female anthropometry could be considered for safety evaluations, as originally proposed by Schneider (1983). Furthermore, HBMs could be even used to generate a population of HBMs representing different statures, body mass indexes and ages by applying morphing algorithms (Zhang et al., 2017).

The development of a state-of-the-art mid-sized adult female HBM and a midsized male counterpart, is one of the main objectives of the European funded VIRTUAL project (Linder et al., 2020). Knowledge of which injuries to predict, is of utmost importance for the development of such a model.

Therefore, the current study was carried out to investigate the frequency of injury types and different body regions involved for females and males. In contrast to other studies focused on vehicle occupants (Pipkorn et al., 2020), the current study focuses on pedestrians and cyclists in collisions involving passenger cars.

In two previous studies (Leo et al., 2019a,b), some initial investigations on differences in injury patterns have been performed. In the current study, these initial findings are being further discussed. An additional dataset has been included and additional parameters were analyzed to gain a better understanding of the observed differences.

This study aimed to analyze the most frequently injured body regions, which type of injuries show sex-specific differences and compare the general accident parameters, i.e., collision speed, between females and males among pedestrians and cyclists in collisions involving passenger cars.

MATERIALS AND METHODS

Accident Data

This study is based on accident data from three different countries (Austria, Netherlands, Sweden), extracted from three different databases, for which the full abbreviated injury scale (AIS) codes of pedestrians and cyclists were available. All three databases hold data of accidents with different injury severities as well as fatalities. As the three databases differ significantly, the data of each was handled separately, and the method applied to each database as well as the results have been presented per dataset. A summary of the used data is provided in **Table 1**.

Swedish Accident Data

The Swedish Traffic Accident Data Acquisition (STRADA) database contains information related to police reported road traffic accidents occurring on public roads in Sweden. Since its inception in 1999, the data held on STRADA has continuously increased. As of 2016, all emergency care hospitals in Sweden are included, allowing the data to be considered as nationally representative (Swedish Government Offices, 1965; Mattsson and Ungerbäck, 2013). The information provided by the police includes information about the accident location and other circumstances, i.e., date and time of accident, weather and road conditions, and posted speed limit. Hospital reports normally include a number of parameters regarding accident circumstances, i.e., a brief description of the accident, accident type and location of the accident, as well as personal information about the patient, i.e., age, gender, use of protective equipment, etc., and full diagnosis classified according to the 2005 AIS (AAAM, 2005) and the International Classification of Disease (ICD-10-SE) (AAAM, 2005; National Board of Health and Welfare, 2010). A unique aspect of the STRADA database is that police and hospital reports can be matched. Matching police and hospital reports for the same accident is of particular value in accident analysis as it allows connecting important accident circumstances (provided by the police) with details of injuries sustained in the accident (provided by the hospital). Around 30% of all accidents in STRADA include both a police and hospital report (Yamazaki, 2018). For a detailed description of the STRADA database, please see Howard and Linder (2014) and Yamazaki (2018).

The present study comprises accidents in which a cyclist or pedestrian have been injured in an accident involving a passenger car in 2016–2018. Only accidents including both a police report and a hospital report were selected. This selection resulted in 1,311 pedestrians with a total of 3,182 injuries and 1,932 cyclists with a total of 3,829 injuries.

Dutch Accident Data

All road traffic accidents in the Netherlands recorded by the police are included in the national road accident registration (BRON) database. BRON contains a large number of characteristics of each accident and driver as well as any involved casualties. However, police assessment of accident severity is not always accurate. Therefore, the Dutch Institute for Road Safety Research (SWOV) supplements BRON data

TABLE 1 | Summary of accident data used for injury analyses.

	Austria		Netherland		Sweden	
	Accidents	**Injuries**	**Accidents**	**Injuries**	**Accidents**	**Injuries**
Pedestrian	308	1,083	5,272	10,436	1,311	3,182
Cyclist	144	289	15,650	29,515	1,932	3,829
Years of Recoding	2003–2019		2000–2014		2016–2018	
Filtering Criteria	– vehicle is a passenger car or van (mass up to 3.5t); – pedestrian or cyclist was struck by only one vehicle; – only one pedestrian or cyclist was involved; – AIS 2005 information is available for pedestrian or cyclist; – Only the first impact was taken into consideration.		– vehicle is a passenger car or van (mass up to 3.5t).		– vehicle is a passenger car or van (mass up to 3.5t); – accidents including both a police report and a hospital report.	
AIS version	AIS2005		AIS1990 (converted to AIS2005 using the AIS Crosswalk)		AIS2005	

with data from the National Basic Register Hospital Care (LBZ). This results in more reliable information of the actual severity of injuries sustained in traffic accidents. In LBZ, injuries are registered according to the ICDICD9 or ICD10, the latter since 2012. SWOV recodes these injuries into AIS90-codes using the software program ICDmap90 (SWOV, 2016). The data provided to this study contain the number of injuries in the Netherlands in 2000–2014 per AIS code according to AIS90 (using recode from ICD9/ICD10). The injuries coded according to AIS90 were converted to AIS2005-Update2008 using the AIS Crosswalk which can be used to convert injuries coded in one AIS version to another version. For 2000–2011, only injuries of patients reported in both police registration and hospital data were included, and only when road user type (pedestrian or cyclist) and opponent (car) were identical in both databases. In more recent years (2012–2014), hospitals have been using ICD10-coding which provides more extensive information on road user type and opponent. Therefore, for this particular period, injuries registered by hospitals only, have also been included. Since passenger cars and light goods vehicles are in the same category in ICD10, it cannot be guaranteed that all opponents were passenger cars.

The data from the Netherlands included cases from 2000 to 2014. These data were available for 5,272 pedestrians with a total of 10,436 injuries and for 15,650 cyclists with a total of 29,515 injuries.

Austrian Accident Data

The Central Database for In-Depth Accident Study (CEDATU) is an in-depth database provided by the Vehicle Safety Institute at Graz University of Technology in Austria, currently covering approximately 3,300 cases. The database includes a detailed description of accidents in Austria. Accidents with at least one injured road user are included, for which access to the court file is granted. The dataset contains accidents with fatal, serious and slight injuries. Detailed accident parameters, such as collision velocities and pre-crash trajectories are derived from accident reconstructions. Each accident case contains a set of approximately 350 core parameters. Accident parameters such as accident type, accident site, road users, etc., can be used to extrapolate findings to the national level (Tomasch and Steffan, 2006; Tomasch et al., 2008).

The following filter criteria were used to obtain the accident data set for the current study:

- vehicle is a passenger car or van (mass up to 3.5t);
- pedestrian or cyclist was struck by only one vehicle;
- only one pedestrian or cyclist was involved;
- AIS 2005 information is available for pedestrians or cyclists;
- only the first impact was taken into consideration.

These filter criteria data were available and applied for 308 pedestrians with a total of 1,083 injuries and for 144 cyclists with a total of 289 injuries. The obtained dataset includes cases from 2003 to 2019 in Austria.

Accident Data Analysis

For analyzing differences in injuries sustained by males and females, the datasets were categorized by sex. To avoid mixing up age and sex-specific differences, injuries sustained by pedestrians or cyclists younger than 60 years old (YO) and those equal or older than 60 YO, were analyzed separately. Previous studies have shown that for pedestrian-to-passenger car collisions, elderly pedestrians ($\geq$60YO) tend to suffer more severe injuries than younger pedestrians (<60YO) (Davis, 2001; Niebuhr et al., 2016; Saadé et al., 2020). This is another reason for splitting pedestrian as well as cyclist data for these two age groups. For all analyses, the odds-ratio (OR) and its 95% confidence interval (95%-Cl), as well as the p-value of the chi-square test, were calculated (McHugh, 2009; Szumilas, 2010; Andrade, 2015). As significance level for the *p*-value, 5% was chosen. The OR is thereby defined as the ratio of the frequency of its occurrence to the frequency of its non-occurrence (Andrade, 2015). For the current study the OR is

defined as given in Equation 1, where $n_{specific\ injury}$ is the number of observations for a specific injury (e.g., head injuries, femur injuries, . . .) for females or males and $n_{injuries}$ is the total number of observed injuries for females or males.

Equation 1 Calculation of OR for the current study:

$$OR = \frac{\frac{n_{specific\ injury\ female}}{n_{injuries\ female} - n_{specific\ injury\ female}}}{\frac{n_{specific\ injury\ male}}{n_{injuries\ male} - n_{specific\ injury\ male}}}$$

Minor injuries (AIS1) have not been included in the current analyses, as more severe injuries are the focus of the current study. For the analysis of the most frequent AIS2+ and AIS3+ injuries, the AIS code was grouped according to the anatomical structure, e.g., skeletal, internal organ, vessels, and if possible, according to a special organ or bone, e.g., femur, tibia, lung, heart. The different anatomical structures, coded organs and bones can be found in the AIS 2005 code book (AAAM, 2005).

The results are presented in the form of tables. In order to obtain a quick and clear overview, a forest plot was integrated into the tables. An example of this visualization is shown in **Table 2**. The vertical gray dashed line identifies an OR of 1. The red point displays the specific OR value and the whiskers show the 95% confidence interval. In Example 1, the red point lies on the dashed gray line, which means that the observed OR value is 1 and none of the analyzed groups has higher or lower odds. For Example 2, the OR as well as the full 95%-CI has been shifted to the right of the dashed gray line. For the current study, this would mean that females have significantly higher odds of sustaining such an injury. In Example 3, on the other hand, an example showing the opposite trend can be seen, where males have significantly higher odds. In Example 4, only the OR value is shifted to the left, however, the 95%-CI overlays the gray dashed line. This means that the odds for men are higher, although not significantly so.

The Austrian data also provide access to other accident parameters, such as collision speeds, accident locations and road conditions, facilitating detailed investigation and gaining an insight into the type of injuries males and females are exposed to in accidents involving passenger cars. The collision speed (speed at first contact for each participant) in the database are determined using the accident reconstruction software PC-Crash (Tomasch and Steffan, 2006). Due to the nature of accident databases, this information was unfortunately not available for the Dutch and Swedish databases. The in-depth dataset of Austrian accident data was only split by sex due to the low number of accidents for some parameters following age categorization of the datasets. The results of this analysis are displayed in the form of boxplots. The number of analyzed accidents may differ for this in-depth analysis, due to certain parameters lacking for some accidents. Only accidents for which all parameters to be evaluated have been completed have been used for this analysis.

TABLE 2 | Exemplary visualization of the statistical analyses.

ID	Visualization
1	
2	
3	
4	

RESULTS

Analysis of Injured Body Regions According AIS Classification

In **Table 3**, the share of injuries according the different AIS body regions for all three databases is shown. This table gives an overview of the most frequently injured body regions in all three databases for pedestrians and cyclists together.

Austrian Accident Data

In **Supplementary Figure 1**, the injured body regions as a function of sex and injury severity in Austria are displayed. The *p*-values and OR of all body regions are summarized in **Table 4**.

Analyzing AIS2+ injuries revealed that the three most commonly injured body regions for female pedestrians < 60YO are the lower extremities (31.9%) and head (31.9%), respectively, and the thorax (13.3%). For male pedestrians < 60YO, the three most commonly injured AIS2+ body regions are the head (39.4%) followed by the lower extremities (18.5%) and the thorax (13.5%). These statistics change when observing more severe AIS3+ injuries. Here female pedestrians < 60YO most often sustain head injuries (50%) followed by lower extremity injuries (18.5%) and injuries to the thorax (16.7%). For AIS3+ injuries, male pedestrians < 60YO most often sustain head injuries (58%) followed by thorax injuries (16%) and injuries to the spine (9.3%). Analyzing significant differences for AIS2+ and AIS3+ injuries revealed significant differences between females and males with regard to injured body regions for pedestrians < 60YO. Hence, the odds for females sustaining AIS2+ (OR = 2.05, *p*-value = 0.004) and AIS3+ (OR = 2.6, *p*-value = 0.033) lower extremity injuries are significantly higher. For other body regions, no significant differences were observed.

For female pedestrians ≥ 60YO, the three most commonly injured AIS2+ body regions are the lower extremities (29.2%) followed by the head (22.3%) and the thorax (16.3%). For male pedestrians ≥ 60YO, the three most commonly injured AIS2+ body regions are the lower extremities (30%) and head (30%), respectively, followed by the thorax (14%) and the spine (10.5%). For AIS3+ injuries we have observed the following order for females: head (41.5%) followed by thorax (24.4%) and lower extremities (20.7%). For AIS3+ injuries we have observed the following order for males: head (41.1%) followed by thorax (21.1%) and lower extremities (17.9%). Analyzing significant differences for AIS2+ and AIS 3+ did not reveal any significant differences between females and males in the Austrian data with regard to injured body regions for pedestrians ≥ 60YO.

Analyzing AIS2+ injuries, the three most commonly injured body regions for female cyclists < 60YO are the lower extremities (26.3%) followed by the upper extremities (26.3%) and the head

TABLE 3 | Share of injured body regions for AIS2+ and AIS3+ in the three different databases for pedestrians and cyclists together.

Body Region	AIS 2+						AIS 3+					
	Austria		Netherlands		Sweden		Austria		Netherlands		Sweden	
	Male	Female	Male	Female	Male	Female	Male	Female	Male	Female	Male	Female
Head	**42%**	**31%**	28%	25%	15%	11%	**63%**	**47%**	**63%**	**59%**	**31%**	**29%**
Face	3%	1%	1%	1%	6%	5%	0%	1%	0%	0%	1%	2%
Neck	1%	0%	0%	0%	1%	0%	3%	0%	3%	0%	1%	0%
Thorax	11%	14%	13%	9%	15%	10%	15%	21%	15%	8%	31%	26%
Abdomen	5%	6%	2%	2%	2%	3%	6%	7%	6%	2%	3%	5%
Spine	11%	10%	7%	7%	12%	10%	7%	4%	7%	2%	6%	6%
Upper Extremities	12%	14%	11%	10%	21%	24%	0%	3%	0%	0%	1%	2%
Lower Extremities	15%	25%	**39%**	**48%**	**30%**	**39%**	7%	19%	7%	30%	27%	30%

Bold values indicate that most frequently injured body region of each database.

(26.3%). For male cyclists < 60YO, the three most commonly injured AIS2+ body regions are the head (36%) followed by the upper extremities (26%) and the spine (14%). These statistics change when observing more severe AIS3+ injuries. Here female cyclists < 60YO most often sustain head injuries (37.5%) followed by lower extremity injuries (25%) and injuries to the thorax (25%). For AIS3+ injuries, male cyclists < 60YO most often sustain head injuries (65.2%) followed by thorax injuries (8.7%), injuries to the spine (8.7%) and neck injuries (8.7%). Analyzing significant differences for AIS2+ injuries of the lower extremities revealed significant differences between females and males with regard to injured body regions for cyclists < 60YO. Females have higher odds of suffering AIS2+ (OR = 5.33, p-value = 0.019) injuries of the lower extremities. For other body regions, no significant differences can be observed.

For female cyclists ≥ 60YO, the three most commonly injured AIS2+ body regions were the head (37.8%) followed by the lower extremities (15.6%) and thorax (15.6%), respectively, and the upper extremities (11.1%). For male cyclists ≥ 60YO, the three most commonly injured AIS2+ body regions are the head (58.5%) followed by the thorax (12.2%) and the upper extremities (9.8%). For AIS3+ injuries we observed the following order for females: head (46.2%) followed by thorax (23.1%) and lower extremities (15.4%). For AIS3+ injuries we observed the following order for males: head (81%) followed by thorax (19%). Analyzing significant differences revealed certain differences between females and males for AIS3+ with regard to injured body regions for cyclists ≥ 60YO. Males have significantly higher odds (OR = 0.21, p-value = 0.015) of sustaining AIS3+ head injuries. For other body regions or AIS2+ injuries, no significant differences were observed.

Dutch Accident Data

In **Supplementary Figure 2**, the injured body regions as a function of sex and injury severity in the Netherlands are displayed. The p-values and OR of all body regions are summarized in **Table 5**.

Analysis of the AIS2+ injuries revealed that the most commonly injured body regions for female pedestrians < 60YO are the lower extremities (57.3%) followed by the head (21.4%), the upper extremities (6.8%) and thorax (6.7%), respectively. For male pedestrians < 60YO the three most commonly injured AIS2+ body regions are the lower extremities (53%) followed by the head (23.6%) and the thorax (8.3%). These statistics change when considering more severe AIS3+ injuries. Here female pedestrians < 60YO most often suffer head injuries (61.4%) followed by lower extremity injuries (25.5%) and injuries to the thorax (9.7%). For AIS3+ injuries, male pedestrians < 60YO most often suffer head injuries (60.3%) followed by lower extremity injuries (21.8%) and injuries to the thorax (12.5%). Analyzing significant differences between females and males revealed significant differences for AIS2+ and AIS3+ injuries with regard to injured body regions for pedestrians < 60YO. Females have significantly higher odds (OR = 1.19, p-value = 0.011) of sustaining AIS2+ lower extremity injuries while the odds of males sustaining AIS3+ spinal injuries (OR = 0.25, p-value = 0.035) is significantly higher.

For female pedestrians ≥ 60YO, the three most commonly injured AIS2+ body regions are the lower extremities (56.5%) followed by the head (17.3%) and the upper extremities (10%). For male pedestrians ≥ 60YO, the three most commonly injured AIS2+ body regions are the lower extremities (47.5%) followed by the head (22%) and the thorax (13%). For AIS3+ injuries we have observed the following order for females: lower extremities (48%) followed by head (43.2%) and thorax (7.3%). For AIS3+ injuries we have observed the following order for males: head (50.4%) followed by lower extremities (36.6%) and thorax (10.1%). Analyzing significant differences revealed certain differences between females and males for AIS2+ and AIS 3+ with regard to injured body regions for pedestrians ≥ 60YO. Females have higher odds of suffering AIS2+ (OR = 1.43, p-value < 0.001) or AIS3+ (OR = 1.6, p-value = 0.006) injuries of the lower extremities while the odds are significantly higher for males sustaining AIS2+ head injuries (OR = 0.74, p-value = 0.013) and AIS2+ thorax injuries (OR = 0.7, p-value = 0.018).

Analyzing the AIS2+ injuries revealed that the three most commonly injured body regions for female cyclists < 60YO are the lower extremities (39%) followed by the head (31.6%) and the spine (9.6%) and upper extremities (9.4%), respectively. For male cyclists < 60YO the three most commonly injured AIS2+

TABLE 4 | Share of injured body regions for AIS2+ and AIS3+ injuries, OR and *p*-value in Austria for pedestrians and cyclists < 60YO and ≥ 60YO (*p-value < 5%).

	Injured Body Regions in Austria											
	AIS2+						AIS3+					
Body Region	**Male**	**Female**	**OR**	**95%-CI**	***p*-value**	**Visualization**	**Male**	**Female**	**OR**	**95%-CI**	***p*-value**	**Visualization**
	Pedestrian < 60YO						**Pedestrian < 60YO**					
	n = 297	*n* = 113					*n* = 150	*n* = 54				
Head	39.4%	31.9%	0.72	[0.45; 1.14]	0.159		58.0%	50.0%	0.73	[0.39; 1.36]	0.310	
Face	2.0%	2.7%	1.35	[0.27; 5.40]	0.695		0.0%	1.9%	–	–	–	
Neck	0.3%	0.0%	–	–	–		0.7%	0.0%	–	–	–	
Thorax	13.5%	13.3%	0.99	[0.51; 1.84]	0.959		16.0%	16.7%	1.06	[0.43; 2.40]	0.909	
Abdomen	8.4%	6.2%	0.73	[0.28; 1.66]	0.453		8.0%	7.4%	0.94	[0.25; 2.89]	0.890	
Spine	12.1%	7.1%	0.56	[0.23; 1.19]	0.141		9.3%	5.6%	0.59	[0.13; 1.94]	0.389	
Upper Extremities	5.7%	7.1%	1.27	[0.50; 2.96]	0.608		0.0%	0.0%	–	–	–	
Lower Extremities	18.5%	31.9%	2.05	[1.25; 3.36]	0.004*		8.0%	18.5%	2.6	[1.02; 6.52]	0.033*	
	Pedestrian ≥ 60YO						**Pedestrian ≥ 60YO**					
	n = 200	*n* = 202					*n* = 95	*n* = 82				
Head	30.0%	22.3%	0.67	[0.43; 1.05]	0.078		41.1%	41.5%	1.02	[0.56; 1.86]	0.956	
Face	1.5%	1.5%	0.99	[0.17; 5.82]	0.990		0.0%	0.0%	–	–	–	
Neck	0.0%	0.0%	–	–	–		0.0%	0.0%	–	–	–	
Thorax	14.0%	16.3%	1.2	[0.69; 2.08]	0.514		21.1%	24.4%	1.21	[0.59; 2.47]	0.597	
Abdomen	6.5%	4.0%	0.6	[0.23; 1.47]	0.253		11.6%	7.3%	0.61	[0.20; 1.71]	0.337	
Spine	10.5%	16.3%	1.66	[0.93; 3.03]	0.086		8.4%	6.1%	0.72	[0.20; 2.28]	0.555	
Upper Extremities	7.5%	10.4%	1.43	[0.71; 2.92]	0.309		0.0%	0.0%	–	–	–	
Lower Extremities	30.0%	29.2%	0.96	[0.63; 1.48]	0.862		17.9%	20.7%	1.2	[0.56; 2.56]	0.633	
	Cyclist < 60YO						**Cyclist < 60YO**					
	n = 50	*n* = 19					*n* = 23	*n* = 8				
Head	36.0%	26.3%	0.65	[0.18; 2.04]	0.446		65.2%	37.5%	0.34	[0.05; 1.81]	0.171	
Face	4.0%	0.0%	–	–	–		0.0%	0.0%	–	–	–	
Neck	4.0%	0.0%	–	–	–		8.7%	0.0%	–	–	–	
Thorax	4.0%	10.5%	2.77	[0.27; 28.41]	0.300		8.7%	25.0%	3.33	[0.30; 37.92]	0.236	
Abdomen	6.0%	0.0%	–	–	–		4.4%	0.0%	–	–	–	
Spine	14.0%	10.5%	0.76	[0.10; 3.65]	0.702		8.7%	0.0%	–	–	–	
Upper Extremities	26.0%	26.3%	1.03	[0.28; 3.36]	0.979		0.0%	12.5%	–	–	–	
Lower Extremities	6.0%	26.3%	5.33	[1.12; 30.63]	0.019*		4.4%	25.0%	6.41	[0.45; 224.44]	0.089	
	Cyclist ≥ 60YO						**Cyclist ≥ 60YO**					
	n = 41	*n* = 45					*n* = 21	*n* = 26				
Head	58.5%	37.8%	0.44	[0.18; 1.03]	0.054		81.0%	46.2%	0.21	[0.05; 0.77]	0.015*	
Face	4.9%	0.0%	–	–	–		0.0%	0.0%	–	–	–	
Neck	0.0%	0.0%	–	–	–		0.0%	0.0%	–	–	–	
Thorax	12.2%	15.6%	1.31	[0.37; 4.94]	0.653		19.1%	23.1%	1.26	[0.30; 5.87]	0.737	
Abdomen	0.0%	13.3%	–	–	–		0.0%	11.5%	–	–	–	
Spine	7.3%	6.7%	0.91	[0.15; 5.56]	0.906		0.0%	3.9%	–	–	–	
Upper Extremities	9.8%	11.1%	1.15	[0.27; 5.17]	0.838		0.0%	0.0%	–	–	–	
Lower Extremities	7.3%	15.6%	2.25	[0.56; 11.73]	0.234		0.0%	15.4%	–	–	–	

body regions are the head (31%) followed by the lower extremities (29.1%) and the upper extremities (15.2%). These statistics change when considering more severe AIS3+ injuries. Here female cyclists < 60YO most often suffer head injuries (70.9%) followed by lower extremity injuries (17.9%) and injuries to the thorax (6.9%). For AIS3+ injuries, male cyclists < 60YO most often suffer head injuries (65.3%) followed by lower extremity injuries (17.9%) and injuries to the thorax (11.7%). Analyzing significant differences revealed significant differences between females and males for AIS2+ as well as for AIS3+ injuries with regard to injured body regions for cyclists < 60YO. Males have significantly higher odds of sustaining AIS2+ injuries to the

TABLE 5 | Share of injured body regions for AIS2+ and AIS3+ injuries, OR and *p*-value in the Netherlands for pedestrians and cyclists < 60YO and ≥ 60YO (*p-value < 5%).

	Injured Body Regions in the Netherlands											
	AIS2+						AIS3+					
Body Region	**Male**	**Female**	**OR**	**95%-CI**	***p*-value**	**Visualization**	**Male**	**Female**	**OR**	**95%-CI**	***p*-value**	**Visualization**
	Pedestrian < 60YO						**Pedestrian < 60YO**					
	n = 2504	*n = 1291*					*n = 710*	*n = 329*				
Head	23.6%	21.4%	0.88	[0.75; 1.03]	0.122		60.3%	61.4%	1.05	[0.80; 1.37]	0.732	
Face	0.4%	0.5%	1.25	[0.45; 3.21]	0.662		0.0%	0.0%	–	–	–	
Neck	0.0%	0.1%	–	–	–		0.0%	0.3%	–	–	–	
Thorax	8.3%	6.7%	0.79	[0.61; 1.03]	0.079		12.5%	9.7%	0.75	[0.49; 1.15]	0.189	
Abdomen	3.4%	2.9%	0.84	[0.56; 1.24]	0.382		2.8%	2.7%	0.98	[0.42; 2.13]	0.941	
Spine	4.2%	4.3%	1.05	[0.75; 1.45]	0.789		2.5%	0.6%	0.25	[0.04; 0.88]	0.035*	
Upper Extremities	7.2%	6.8%	0.95	[0.72; 1.23]	0.672		0.0%	0.0%	–	–	–	
Lower Extremities	53.0%	57.3%	1.19	[1.04; 1.37]	0.011*		21.8%	25.2%	1.21	[0.89; 1.64]	0.225	
	Pedestrian ≥ 60YO						**Pedestrian ≥ 60YO**					
	n = 728	*n = 1142*					*n = 238*	*n = 354*				
Head	22.0%	21.0%	0.74	[0.59; 0.94]	0.013*		50.4%	76.1%	0.75	[0.54; 1.04]	0.085	
Face	0.3%	0.7%	2.12	[0.5; 15.76]	0.303		0.0%	0.0%	–	–	–	
Neck	0.0%	0.0%	–	–	–		0.0%	0.0%	–	–	–	
Thorax	13.0%	11.5%	0.7	[0.52; 0.94]	0.018*		10.1%	12.9%	0.71	[0.39; 1.27]	0.240	
Abdomen	2.2%	1.7%	0.63	[0.31; 1.29]	0.195		1.7%	0.5%	0.18	[0.01; 1.33]	0.068	
Spine	6.0%	5.6%	0.76	[0.50; 1.15]	0.182		1.3%	2.0%	0.88	[0.18; 4.84]	0.885	
Upper Extremities	8.9%	12.1%	1.13	[0.82; 1.56]	0.450		0.0%	0.0%	–	–	–	
Lower Extremities	47.5%	68.3%	1.43	[1.19; 1.73]	<0.001*		36.55%	84.58%	1.6	[1.15; 2.25]	0.006*	
	Cyclist < 60YO						**Cyclist < 60YO**					
	n = 5109	*n = 4077*					*n = 1685*	*n = 1247*				
Head	31.0%	31.6%	1.03	[0.94; 1.12]	0.560		65.3%	70.9%	1.29	[1.10; 1.51]	0.001*	
Face	1.1%	0.7%	0.64	[0.40; 1.00]	0.050		0.0%	0.0%	–	–	–	
Neck	0.0%	0.0%	–	–	–		0.0%	0.1%	–	–	–	
Thorax	12.5%	7.1%	0.54	[0.46; 0.62]	<0.001*		11.7%	6.9%	0.56	[0.43; 0.73]	<0.001*	
Abdomen	3.3%	2.5%	0.76	[0.59; 0.97]	0.028*		1.8%	2.0%	1.13	[0.65; 1.93]	0.658	
Spine	7.8%	9.6%	1.26	[1.09; 1.46]	0.002*		3.3%	2.2%	0.68	[0.42; 1.07]	0.100	
Upper Extremities	15.2%	9.4%	0.58	[0.51; 0.66]	<0.001*		0.0%	0.0%	–	–	–	
Lower Extremities	29.1%	39.0%	1.56	[1.43; 1.70]	<0.001*		17.9%	17.9%	1	[0.82; 1.21]	0.978	
	Cyclist ≥ 60YO						**Cyclist ≥ 60YO**					
	n = 3150	*n = 2746*					*n = 921*	*n = 1258*				
Head	33.3%	27.6%	0.77	[0.69; 0.86]	<0.001*		62.3%	59.7%	0.9	[0.75; 1.07]	0.218	
Face	0.9%	0.8%	0.89	[0.50; 1.58]	0.694		0.0%	0.0%	–	–	–	
Neck	0.0%	0.0%	–	–	–		0.1%	0.0%	–	–	–	
Thorax	17.7%	10.5%	0.54	[0.47; 0.63]	<0.001*		11.3%	7.6%	0.65	[0.48; 0.87]	0.004*	
Abdomen	1.4%	1.2%	0.87	[0.55; 1.35]	0.526		1.1%	1.2%	1.08	[0.47; 2.40]	0.86	
Spine	9.2%	7.4%	0.79	[0.66; 0.95]	0.014*		3.8%	2.2%	0.56	[0.32; 0.94]	0.029	
Upper Extremities	12.0%	12.7%	1.07	[0.91; 1.25]	0.411		0.0%	0.0%	–	–	–	
Lower Extremities	25.5%	39.8%	1.93	[1.73; 2.16]	<0.001*		21.4%	29.3%	1.52	[1.25; 1.85]	<0.001*	

thorax (OR = 0.54, p-value < 0.001), injuries to the abdomen (OR = 0.76, p-value = 0.028) and injuries to the upper extremities (OR = 0.58, p-value < 0.001). The odds for females suffering AIS2+ injuries to the spine (OR = 1.26, p-value = 0.002) and injuries to the lower extremities (OR = 1.56, p-value < 0.001), on the other hand, are significantly higher. For AIS3+ injuries, it was observed that females have significantly higher odds of suffering head injuries (OR = 1.29, p-value = 0.001) while males have significantly higher odds of suffering thorax injuries (OR = 0.56, p-value < 0.001).

For female cyclists ≥ 60YO, the three most commonly injured AIS2+ body regions are the lower extremities (39.8%) followed by the head (27.6%) and the upper extremities (12.7%). For male cyclists ≥ 60YO, the three most commonly injured AIS2+ body regions are the head (33.3%) followed by the lower extremities (25.5%) and the thorax (17.7%). For AIS3+ injuries we have observed the following order for females: head (59.7%) followed by lower extremities (29.3%) and thorax (7.6%). For AIS3+ injuries we have observed the following order for males: head (62.3%) followed by lower extremities (21.4%) and thorax (11.3%). Analyzing significant differences revealed significant differences between females and males AIS2+ as well as AIS3+ injuries with regard to injured body regions for cyclists ≥ 60YO. Males have significantly higher odds of sustaining AIS2+ injuries to the head (OR = 0.77, p-value < 0.001), injuries to the thorax (OR = 0.54, p- value < 0.001) and injuries to the spine (OR = 0.79, p-value = 0.014). The odds of females sustaining AIS2+ injuries to the lower extremities (OR = 1.93, p-value < 0.001), on the other hand, are significantly higher. For AIS3+ injuries it was observed that females have significantly higher odds of sustaining lower extremity injuries (OR = 1.52, p- value < 0.001) while males have significantly higher odds of sustaining thorax injuries (OR = 0.65, p-value = 0.004) and lower extremity injuries (OR = 1, p-value < 0.001).

Swedish Accident Data

In **Supplementary Figure 3**, the injured body regions as a function of sex and injury severity in Sweden are displayed. The p-values and OR of all body regions are summarized in **Table 6**.

By analyzing the AIS2+ injuries the most commonly injured body regions for female pedestrians < 60YO are the lower extremities (40.4%) followed by the upper extremities (14%), the head (13.1%) and the spine (13.1%). For male pedestrians < 60YO the three most commonly injured AIS2+ body regions are the lower extremities (40.7%) followed by the thorax (15.3%) and the head (14.5%). These statistics change when considering more severe AIS3+ injuries. Here female pedestrians < 60YO most often suffer thorax injuries (28.4%) followed by head injuries (27%) and injuries to the lower extremities (23%). For AIS3+ injuries male pedestrians < 60YO most often suffer thorax injuries (30.7%) followed by head injuries (29.8%) and injuries to the lower extremities (28.8%). By analyzing if there are significant differences between females and males with regard to injured body regions, it can be seen that the odds for females suffering AIS2+ spine injuries, are significantly higher (OR = 1.88, p-value = 0.014).

For female pedestrians ≥ 60YO the three most commonly injured AIS2+ body regions are the lower extremities (46.6%) followed by the upper extremities (21.7%) and the head (12.6%). For male pedestrians ≥ 60YO the three most commonly injured AIS2+ body regions are the lower extremities (42.6%) followed by the spine (14.1%) and the thorax (13.6%). For AIS3+ injuries we have observed the following order for females ≥ 60YO: lower extremities (45.5%) followed by thorax (27.3%) and the head (20%). For AIS3+ injuries we have observed the following order for males ≥ 60YO: lower extremities (36.4%) followed by thorax (29.5%) and the head (25%). Analyzing significant differences revealed certain differences between females and males for AIS2+ with regard to injured body regions for pedestrians ≥ 60YO. Males, for example, have significantly higher odds (OR = 0.3, p-value < 0.001) of sustaining AIS2+ spine injuries while the odds for females sustaining upper extremity injuries are higher (OR = 2.04, p-value = 0.008).

Analyzing the AIS2+ injuries the three most commonly injured body regions for female cyclists < 60YO are the lower extremities (35.5%) followed by the upper extremities (31%) and the spine (10.5%). For male cyclists < 60YO the most commonly injured AIS2+ body regions are the upper extremities (35.9%) followed by the lower extremities (15.9%), the spine (15.9%) and the head (13.6%). These statistics change when considering more severe AIS3+ injuries. Here female cyclists < 60YO most often suffer lower extremity injuries (38.5%) followed by head injuries (38.5%) and injuries to the thorax (11.5%). For AIS3+ injuries male cyclists < 60YO most often suffer head injuries (38.5%) followed by thorax injuries (26.2%) and injuries to the lower extremities (16.9%). Analyzing significant differences revealed significant differences between males and females for AIS2+ as well as AIS3+ injuries of the lower extremities, with regard to injured body regions for cyclists < 60YO. Females have significantly higher odds of suffering AIS2+ (OR = 2.91, p-value < 0.001) or AIS3+ (OR = 3.02, p-value = 0.028) injuries of the lower extremities. For other body regions, no significant differences were observed.

For female cyclists ≥ 60YO the three most commonly injured AIS2+ body regions are the lower extremities (32.8%) followed by the upper extremities (26.6%) and the thorax (12.5%). For male cyclists ≥ 60YO the most commonly injured AIS2+ body regions are the upper extremities (20.5%) followed by the lower extremities (20%), head (20%) and the thorax (17.9%). For AIS3+ injuries we have observed the following order for females: thorax (35.7%) followed by head (28.6%), lower extremities (14.3%) and the spine (14.3%), respectively. For AIS3+ injuries we have observed the following order for males: thorax (35.7%) followed by head (31.2%) and lower extremities (25%). Analyzing significant differences revealed certain differences between females and males for AIS2+ with regard to injured body regions for cyclists ≥ 60YO. Males for example have significantly higher odds (OR = 0.34, p-value = 0.003) of sustaining AIS2+ head injuries while the odds for females sustaining lower extremity injuries is significantly higher (OR = 1.95, p-value = 0.01). For other body regions or AIS3+ injuries, no significant differences were observed.

Detailed Injury Analyses for Significant AIS2+ and AIS3+ Injuries

Austrian Accident Data

Significant differences were only identified for pedestrian-to-passenger car collisions involving males and females in the Austrian accident data, shown in **Table 7**. Male pedestrians < 60YO have significantly higher odds of sustaining AIS2+ skull injuries (OR = 0.5, p-value = 0.008) while the odds for female < 60YO of sustaining AIS2+ lumbar spine injuries (OR = 7.89, p-value < 0.001), AIS2+ femur injuries (OR = 3.63,

TABLE 6 | Share of injured body regions for AIS2+ and AIS3+ injuries, OR and p-value in Sweden for pedestrians and cyclists < 60YO and ≥ 60YO (*p-value < 5%).

	Injured Body Regions in Sweden											
	AIS2+						AIS3+					
Body Region	**Male**	**Female**	**OR**	**95%-CI**	***p*-value**	**Visualization**	**Male**	**Female**	**OR**	**95%-CI**	***p*-value**	**Visualization**
	Pedestrian < 60YO						**Pedestrian < 60YO**					
	n = 366	*n = 314*					*n = 114*	*n = 74*				
Head	14.5%	13.1%	0.89	[0.57; 1.38]	0.592		29.8%	27.0%	0.87	[0.45; 1.67]	0.679	
Face	3.6%	2.9%	0.81	[0.32; 1.91]	0.614		0.9%	0.0%	–	–	–	
Neck	0.0%	0.6%	–	–	–		0.0%	1.4%	–	–	–	
Thorax	15.3%	10.5%	0.65	[0.41; 1.03]	0.065		30.7%	28.4%	0.90	[0.46; 1.70]	0.734	
Abdomen	5.2%	5.4%	1.05	[0.53; 2.06]	0.897		6.1%	12.2%	2.10	[0.74; 6.24]	0.148	
Spine	7.4%	13.1%	1.88	[1.13; 3.17]	0.014*		3.5%	5.4%	1.57	[0.34; 7.16]	0.529	
Upper Extremities	13.4%	14.0%	1.05	[0.68; 1.64]	0.813		0.0%	2.7%	–	–	–	
Lower Extremities	40.7%	40.5%	0.99	[0.73; 1.34]	0.944		29.0%	23.0%	0.74	[0.37; 1.44]	0.365	
	Pedestrian ≥ 60YO						**Pedestrian ≥ 60YO**					
	n = 177	*n = 277*					*n = 44*	*n = 55*				
Head	11.9%	12.6%	1.07	[0.60; 1.94]	0.808		25.0%	20.0%	0.75	[0.28; 1.98]	0.552	
Face	4.0%	3.6%	0.90	[0.34; 2.57]	0.850		2.3%	0.0%	–	–	–	
Neck	0.6%	0.0%	–	–	–		0.0%	0.0%	–	–	–	
Thorax	13.6%	9.0%	0.63	[0.35; 1.16]	0.129		29.6%	27.3%	0.89	[0.37; 2.19]	0.803	
Abdomen	1.7%	1.8%	1.05	[0.24; 5.48]	0.931		2.3%	1.8%	0.80	[0.02; 31.75]	0.873	
Spine	14.1%	4.7%	0.30	[0.15; 0.60]	<0.001*		4.6%	5.5%	1.18	[0.17; 10.57]	0.837	
Upper Extremities	11.9%	21.7%	2.04	[1.21; 3.57]	0.008*		0.0%	0.0%	–	–	–	
Lower Extremities	42.4%	46.6%	1.18	[0.81; 1.74]	0.381		36.4%	45.5%	1.45	[0.64; 3.32]	0.362	
	Cyclist < 60YO						**Cyclist < 60YO**					
	n = 359	*n = 248*					*n = 65*	*n = 26*				
Head	13.7%	8.9%	0.62	[0.36; 1.04]	0.072		38.5%	38.5%	1.0	[0.38; 2.56]	1.000	
Face	6.7%	6.1%	0.90	[0.45; 1.75]	0.753		0.0%	7.7%	–	–	–	
Neck	0.3%	0.0%	–	–	–		1.5%	0.0%	–	–	–	
Thorax	10.6%	7.3%	0.66	[0.36; 1.18]	0.164		26.2%	11.5%	0.39	[0.08; 1.31]	0.128	
Abdomen	1.1%	0.8%	0.75	[0.09; 4.10]	0.706		4.6%	0.0%	–	–	–	
Spine	15.9%	10.5%	0.62	[0.37; 1.01]	0.057		9.2%	0.0%	–	–	–	
Upper Extremities	35.9%	31.1%	0.80	[0.57; 1.13]	0.212		3.1%	3.9%	1.33	[0.04; 17.16]	0.853	
Lower Extremities	15.9%	35.5%	2.91	[1.98; 4.29]	<0.001*		16.9%	38.5%	3.02	[1.07; 8.62]	0.028*	
	Cyclist ≥ 60YO						**Cyclist ≥ 60YO**					
	n = 190	*n = 128*					*n = 48*	*n = 14*				
Head	20.0%	7.8%	0.34	[0.16; 0.70]	0.003*		31.3%	28.6%	0.9	[0.21; 3.25]	0.848	
Face	10.0%	7.8%	0.77	[0.33; 1.69]	0.506		0.0%	0.0%	–	–	–	
Neck	0.5%	0.0%	–	–	–		0.0%	0.0%	–	–	–	
Thorax	17.9%	12.5%	0.66	[0.34; 1.24]	0.195		37.5%	35.7%	0.94	[0.25; 3.23]	0.903	
Abdomen	1.1%	1.6%	1.49	[0.15; 14.47]	0.689		0.0%	7.1%	–	–	–	
Spine	10.0%	10.9%	1.11	[0.52; 2.30]	0.788		6.3%	14.3%	2.50	[0.27; 18.31]	0.331	
Upper Extremities	20.5%	26.6%	1.40	[0.82; 2.38]	0.209		0.0%	0.0%	–	–	–	
Lower Extremities	20.0%	32.8%	1.95	[1.17; 3.27]	0.010*		25.0%	14.3%	0.53	[0.07; 2.39]	0.399	

p-value = 0.042) and AIS2+ pelvic injuries (OR = 3.13, p-value < 0.001) are significantly higher.

Significant differences were only seen for female pedestrians ≥ 60YO, whereby the odds for females sustaining AIS2+ lumbar spine injuries (OR = 4.33, p-value = 0.011) and AIS2+ pelvic injuries (OR = 2.01, p-value = 0.024) were observed to be significantly higher.

It was also observed that female pedestrians < 60YO have significantly higher odds of sustaining AIS2+ femur (OR = 4.24, p-value = 0.022) and AIS2+ pelvic (OR = 2.52, p-value = 0.035)

TABLE 7 | Share of AIS2+ and AIS3+ injuries with significant differences, OR and *p*-value in Austria for pedestrians and cyclists < 60YO and ≥ 60YO.

AIS2+ Injuries Austria								
Body Region	**Anatomical Structure**	**Organ**	**Male**	**Female**	**OR**	**95%-CI**	***p*-value**	**Visualization**
			Pedestrian < 60YO					
			n = 497	*n = 315*				
Head	Skeletal	Skull	12.5%	6.7%	0.50	[0.29; 0.83]	0.008	
Spine	Lumbar Spine	–	0.6%	4.8%	7.89	[2.55; 35.77]	<0.001	
Lower Extremities	Skeletal	Femur	0.6%	2.2%	3.63	[0.97; 17.91]	0.042	
Lower Extremities	Skeletal	Pelvis	5.0%	14.3%	3.13	[1.89; 5.3]	<0.001	
								0 1 2 3 4 5
			Pedestrian ≥ 60YO					
			n = 200	*n = 202*				
Spine	Lumbar Spine	–	1.5%	6.4%	4.33	[1.35; 20.01]	0.011	
Lower Extremities	Skeletal	Pelvis	8.5%	15.8%	2.01	[1.09; 3.85]	0.024	
								0 1 2 3 4 5
AIS3+ Injuries Austria								
Body Region	**Anatomical Structure**	**Organ**	**Male**	**Female**	**OR**	**95%-CI**	***p*-value**	**Visualization**
			Pedestrian < 60YO					
			n = 245	*n = 136*				
Lower Extremities	Skeletal	Femur	1.2%	5.1%	4.24	[1.13; 21.06]	0.022	
Lower Extremities	Skeletal	Pelvis	3.7%	8.8%	2.52	[1.03; 6.41]	0.035	
								0 1 2 3 4 5

injuries. For all other groups no significant differences were observed with regard to injuries sustained by males and females.

A summary of all these findings can be seen in **Table 7**.

Dutch Accident Data

Significant differences were observed for AIS2+ injuries, in terms of frequencies between males and females, in the Dutch data, all listed in **Table 8**. It can be observed that pedestrian < 60YO females have significantly higher odds of sustaining skeletal injuries of the thorax and the lower extremities. Skeletal injuries are always related to a fracture of a specific bone. Hence, the odds of females sustaining different fractures, i.e., the pelvis (OR = 1.90, *p*-value = 0.021) are significantly higher. Male pedestrians < 60YO in the Netherlands have significantly higher odds of sustaining AIS2+ concussive injuries (OR = 0.75, *p*-value = 0.041), AIS2+ spleen injuries (OR = 0.52, *p*-value = 0.045) and AIS2+ cervical spine injuries (OR = 0.66, *p*-value = 0.042). For pedestrians ≥ 60YO, it can be observed that the odds for females and males sustaining skeletal injuries to different body parts is significantly higher. Thus, the odds of females sustaining AIS2+ hand (OR = 2.13, *p*-value = 0.04), femur (OR = 1.35, *p*-value = 0.047) and tibia (OR = 1.3, *p*-value = 0.024) injuries, are significantly higher. Males, on the other hand, have significantly higher odds of sustaining rib cage (OR = 0.68, *p*-value = 0.046) and scapula (OR = 0.43, *p*-value = 0.017) injuries.

A significant difference was observed between males and females for a large number of AIS2+ injuries sustained by cyclists in cyclist-to-passenger car accidents. Female cyclists < 60YO have significantly higher odds of sustaining different spine and lower extremity injuries. The odds for male cyclists < 60YO, on the other hand, of sustaining different AIS2+ head, thorax, abdomen and cervical spine injuries, as well as skeletal injuries of the upper extremities, are higher. A similar picture can be seen for injuries sustained by cyclists ≥ 60YO. In this group, females have significantly higher odds of sustaining different skeletal injuries to the lower extremities, however, the odds are also higher for AIS2+ hand (OR = 1.75, *p*-value = 0.004) and AIS2+ humerus (OR = 13.23, *p*-value = 0.001) injuries. Again, males have significantly higher odds of sustaining different AIS2+ head, thorax, and cervical spine injuries, as well as skeletal injuries of the scapula.

The odds for female pedestrians and cyclists sustaining AIS3+ skeletal femur injuries are significantly higher than for males in the Dutch accident data, irrespective of age. Moreover, younger female pedestrians (<60YO) have significantly higher odds of sustaining AIS3+ pelvic injuries (OR = 2.02, *p*-value = 0.013). The odds for younger male pedestrians of sustaining AIS3+ skeletal tibia injuries (OR = 0.42, *p*-value = 0.001) are significantly higher. For younger male cyclists we observed that they have significantly higher odds of sustaining different types of thorax and cortical spine injuries. Furthermore, the odds of elderly male cyclists sustaining AIS3+ cortical spine injuries (OR = 0.48, *p*-value = 0.013) are also higher.

A summary of all these findings can be seen in **Table 8**.

Swedish Accident Data

Some significant differences were observed for AIS2+ injuries in the Swedish data for females and males, shown in **Table 9**. The odds of the group of pedestrian < 60YO males of sustaining

TABLE 8 | Share of AIS2+ and AIS3+ injuries with significant differences, OR and *p*-value in the Netherlands for pedestrians and cyclists < 60YO and ≥ 60YO.

AIS2+ Injuries the Netherlands

Body Region	Anatomical Structure	Organ	Male	Female	OR	95%-CI	*p*-value	Visualization
		Pedestrian < 60YO						
			n = 3233	*n = 2435*				
Head	Concussive Injury	–	4.3%	3.2%	0.75	[0.56; 0.99]	0.041	
Thorax	Skeletal	Sternum	0.2%	0.5%	3.14	[1.15; 10.11]	0.021	
Abdomen	Internal Organs	Spleen	1.0%	0.5%	0.52	[0.25; 0.98]	0.045	
Spine	Cervical Spine	–	2.2%	1.5%	0.66	[0.44; 0.98]	0.042	
Lower Extremities	Skeletal	Foot	1.4%	2.3%	1.67	[1.12; 2.51]	0.011	
Lower Extremities	Skeletal	Femur	4.6%	7.9%	1.78	[1.43; 2.22]	<0.001	
Lower Extremities	Skeletal	Pelvis	0.6%	1.2%	1.90	[1.09; 3.39]	0.021	
		Pedestrian ≥ 60YO						
			n = 728	*n = 1143*				
Thorax	Skeletal	Rib Cage	7.4%	5.2%	0.68	[0.46; 1]	0.046	
Upper Extremities	Skeletal	Scapula	2.6%	1.1%	0.43	[0.21; 0.88]	0.017	
Upper Extremities	Skeletal	Hand	1.2%	2.6%	2.13	[1.04; 4.82]	0.040	
Lower Extremities	Skeletal	Femur	9.6%	12.6%	1.35	[1; 1.84]	0.047	
Lower Extremities	Skeletal	Tibia	19.8%	24.3%	1.30	[1.04; 1.63]	0.024	
		Cyclist < 60YO						
			n = 8261	*n = 6827*				
Head	Internal Organs	Cerebrum	18.8%	17.4%	0.91	[0.84; 0.99]	0.024	
Head	Skeletal	Skull	6.6%	5.7%	0.85	[0.74; 0.97]	0.017	
Thorax	Vessels	–	0.1%	0.0%	0.15	[0.01; 0.82]	0.025	
Thorax	Internal Organs	Lung	2.3%	1.3%	0.56	[0.43; 0.71]	<0.001	
Thorax	Internal Organs	Thoracic injury	4.3%	2.2%	0.5	[0.41; 0.6]	<0.001	
Thorax	Skeletal	Rib Cage	7.1%	4.7%	0.64	[0.56; 0.74]	<0.001	
Thorax	Skeletal	Sternum	0.5%	0.2%	0.43	[0.23; 0.77]	0.004	
Abdomen	Internal Organs	Kidney	1.1%	0.6%	0.57	[0.39; 0.82]	0.003	
Spine	Cervical Spine	–	3.3%	2.1%	0.64	[0.52; 0.78]	<0.001	
Spine	Lumbar Spine	–	2.5%	3.3%	1.33	[1.09; 1.61]	0.004	
Spine	Thoracic Spine	–	2.5%	3.3%	1.34	[1.11; 1.62]	0.003	
Upper Extremities	Skeletal	Clavicle	7.0%	5.5%	0.77	[0.67; 0.88]	<0.001	
Upper Extremities	Skeletal	Scapula	2.9%	1.1%	0.37	[0.29; 0.48]	<0.001	
Lower Extremities	Muscles, Tendons, Ligaments	–	0.3%	0.8%	2.42	[1.53; 3.95]	<0.001	
Lower Extremities	Skeletal	Foot	0.6%	1.1%	1.95	[1.36; 2.82]	<0.001	
Lower Extremities	Skeletal	Tibia	11.3%	18.6%	1.79	[1.63; 1.96]	<0.001	
Lower Extremities	Skeletal	Fibula	8.8%	11.5%	1.34	[1.21; 1.5]	<0.001	
		Cyclist ≥ 60YO						
			n = 3150	*n = 2747*				
Head	Internal Organs	Cerebrum	21.8%	17.3%	0.75	[0.66; 0.85]	<0.001	
Head	Skeletal	Skull	6.6%	5.1%	0.77	[0.61; 0.95]	0.017	
Thorax	Internal Organs	Lung	2.0%	1.2%	0.58	[0.37; 0.88]	0.011	
Thorax	Internal Organs	Thoracic injury	4.7%	2.4%	0.49	[0.36; 0.65]	<0.001	
Thorax	Skeletal	Rib Cage	10.0%	6.4%	0.62	[0.51; 0.75]	<0.001	
Spine	Cervical Spine	–	4.5%	2.4%	0.52	[0.38; 0.69]	<0.001	
Upper Extremities	Skeletal	Scapula	3.2%	1.6%	0.49	[0.34; 0.7]	<0.001	
Upper Extremities	Skeletal	Humerus	0.0%	0.5%	13.23	[2.62; 321.42]	0.001	
Upper Extremities	Skeletal	Hand	1.4%	2.4%	1.75	[1.19; 2.6]	0.004	
Lower Extremities	Skeletal	Foot	0.4%	1.2%	3.00	[1.62; 5.94]	<0.001	
Lower Extremities	Skeletal	Tibia	8.0%	17.0%	2.34	[1.99; 2.76]	<0.001	
Lower Extremities	Skeletal	Fibula	8.5%	11.2%	1.36	[1.14; 1.62]	<0.001	

(Continued)

TABLE 8 | Continued

AIS3+ Injuries the Netherlands								
Body Region	**Anatomical Structure**	**Organ**	**Male**	**Female**	**OR**	**95%-CI**	***p*-value**	**Visualization**
			Pedestrian < 60YO					
			n = 948	*n = 683*				
Lower Extremities	Skeletal	Femur	15.7%	28.3%	2.11	[1.66; 2.69]	<0.001	
Lower Extremities	Skeletal	Tibia	6.1%	2.6%	0.42	[0.24; 0.7]	0.001	
Lower Extremities	Skeletal	Pelvis	2.2%	4.4%	2.02	[1.15; 3.62]	0.013	
								0 1 2 3 4 5
			Pedestrian ≥ 60YO					
			n = 238	*n = 354*				
Lower Extremities	Skeletal	Femur	29.4%	40.7%	1.64	[1.16; 2.34]	0.005	0 1 2 3 4 5
			Cyclist < 60YO					
			n = 2943	*n = 2168*				
Thorax	Vessels	–	0.3%	0.0%	0.17	[0.01; 0.92]	0.038	
Thorax	Internal Organs	Lung	6.5%	4.1%	0.61	[0.47; 0.79]	<0.001	
Thorax	Skeletal	Rib Cage	4.7%	3.0%	0.63	[0.47; 0.85]	0.003	
Spine	Cervical Spine	–	3.0%	1.7%	0.57	[0.38; 0.84]	0.004	
Lower Extremities	Skeletal	Femur	15.8%	18.4%	1.21	[1.04; 1.4]	0.013	
								0 1 2 3 4 5
			Cyclist ≥ 60YO					
			n = 1258	*n = 921*				
Spine	Cervical Spine	–	3.3%	1.6%	0.48	[0.26; 0.86]	0.013	
Lower Extremities	Skeletal	Femur	18.1%	25.6%	1.56	[1.27; 1.91]	<0.001	
								0 1 2 3 4 5

AIS2+ lung injuries (OR = 0.47, *p*-value = 0.025) and AIS2+ thoracic injuries (OR = 0.39, *p*-value = 0.014) are significantly higher. Thoracic injuries include, among others, hemothorax, pneumothorax and hemopneumothorax. On the other hand, the odds for females < 60YO of sustaining different fractures (skeletal injuries) are higher. For the upper extremities, females have significantly higher odds of sustaining AIS2+ radius injuries (OR = 2.82, *p*-value = 0.003) while the odds for lower extremity injuries, sustaining AIS2+ pelvic injuries (OR = 2.04, *p*-value = 0.005) are significantly higher.

The group of pedestrian ≥ 60YO males have significantly higher odds of sustaining AIS2+ thoracic injuries (OR = 0.27, *p*-value = 0.042), AIS2+ injuries of the cervical spine (OR = 0.23, *p*-value = 0.006) and AIS2+ of the thoracic spine (OR = 0.28, *p*-value = 0.023). A similar trend can be seen for females for the group of ≥ 60YO as for < 60YO pedestrians. The odds for elderly females are also significantly higher for sustaining AIS2+ radius injuries (OR = 3.86, *p*-value = 0.017) and AIS2+ pelvic injuries (OR = 2.15, *p*-value = 0.043).

Significant differences were also observed in the Swedish accident data for male and female cyclists in terms of sustained injuries. Males < 60YO have significantly higher odds of sustaining AIS2+ cerebellum injuries (OR = 0.25, *p*-value = 0.013), AIS2+ lung injuries (OR = 0.23, *p*-value = 0.006) and AIS2+ skeletal injuries of the scapula (OR = 0.35, *p*-value = 0.041). The odds of females sustaining AIS2+ ulna injuries (OR = 2.78, *p*-value = 0.015), AIS2+ foot injuries (OR = 2.73, *p*-value = 0.006), AIS2+ tibia injuries (OR = 2.12, *p*-value = 0.006) and AIS2+ pelvic injuries (OR = 5.88, *p*-value < 0.001) are significantly higher. All injuries with observed significant differences for females involve skeletal injuries and thus fractures.

For elderly cyclists (≥60YO), males have significantly higher odds of sustaining AIS2+ head injuries. Furthermore, males also have significantly higher odds of sustaining AIS2+ cerebellum injuries (OR = 0.18, *p*-value = 0.047) and AIS2+ concussive injuries (OR = 0.16, *p*-value = 0.032). Again, females displayed significantly higher odds of suffering skeletal injuries. They also have significantly higher odds of sustaining AIS2+ radius injuries (OR = 3.41, *p*-value = 0.017) and AIS2+ skeletal injuries of the hands (OR = 6.89, *p*-value = 0.003).

For AIS3+ injuries, significant differences in injuries sustained by females were observed in the Swedish accident data. Hence, the odds for young female pedestrians (<60YO) and elderly female pedestrians (≥60YO) of sustaining AIS3+ pelvic injuries (OR = 3.03, *p*-value = 0.02 and OR = 6.45, *p*-value = 0.035, respectively) are significantly higher. Young female cyclists on the other hand have significantly higher odds of sustaining AIS3+ tibia injuries (OR = 8.22, *p*-value = 0.024) while elderly female cyclists are at a higher risk of suffering thoracic injuries (OR = 5.9, *p*-value = 0.037).

A summary of all these findings can be seen in **Table 9**.

Injury Severity

With regard to this section, please refer to the **Supplementary Table 13** for further evaluation of significant differences between younger (<60YO) and older (≥60YO) pedestrian and cyclists identified in all three accident datasets.

TABLE 9 | Share of AIS2+ and AIS3+ injuries with significant differences, OR and *p*-value in Sweden for pedestrians and cyclists < 60YO and ≥ 60YO.

AIS2+ Injuries Sweden								
Body Region	**Anatomical Structure**	**Organ**	**Male**	**Female**	**OR**	**95%-CI**	***p*-value**	**Visualization**
Pedestrian < 60YO								
			n = 543	*n = 591*				
Thorax	Internal Organs	Lung	4.60%	2.20%	0.47	[0.23; 0.91]	0.025	
Thorax	Internal Organs	Thoracic injury	3.90%	1.50%	0.39	[0.17; 0.84]	0.014	
Upper Extremities	Skeletal	Radius	1.80%	5.10%	2.82	[1.41; 6.16]	0.003	
Lower Extremities	Skeletal	Pelvis	4.20%	8.30%	2.04	[1.23; 3.45]	0.005	
Pedestrian ≥ 60YO								
			n = 177	*n = 277*				
Thorax	Internal Organs	Thoracic injury	4.00%	1.10%	0.27	[0.06; 1.03]	0.042	
Spine	Cervical Spine	–	6.20%	1.40%	0.23	[0.06; 0.69]	0.006	
Spine	Thoracic Spine	–	5.10%	1.40%	0.28	[0.07; 0.89]	0.023	
Upper Extremities	Skeletal	Radius	1.70%	6.50%	3.86	[1.27; 17.35]	0.017	
Lower Extremities	Skeletal	Pelvis	5.10%	10.50%	2.15	[1.03; 4.97]	0.043	
Cyclist < 60YO								
			n = 549	*n = 376*				
Head	Internal Organs	Cerebellum	3.30%	0.80%	0.25	[0.06; 0.75]	0.013	
Thorax	Internal Organs	Lung	2.00%	0.30%	0.15	[0.01; 0.77]	0.022	
Upper Extremities	Skeletal	Scapula	3.10%	1.10%	0.35	[0.10; 0.96]	0.041	
Upper Extremities	Skeletal	Ulna	1.50%	4.00%	2.78	[1.19; 7.05]	0.015	
Lower Extremities	Skeletal	Foot	2.00%	5.30%	2.73	[1.31; 6.00]	0.006	
Lower Extremities	Skeletal	Tibia	4.20%	8.50%	2.12	[1.22; 3.74]	0.006	
Lower Extremities	Skeletal	Pelvis	1.60%	9.00%	5.88	[2.89; 13.28]	<0.001	
Cyclist ≥ 60YO								
			n = 190	*n = 128*				
Head	Internal Organs	Cerebellum	4.70%	0.80%	0.18	[0.01; 0.99]	0.047	
Head	Concussive Injury	–	5.30%	0.80%	0.16	[0.01; 0.86]	0.032	
Upper Extremities	Skeletal	Radius	2.60%	8.60%	3.41	[1.19; 11.32]	0.017	
Upper Extremities	Skeletal	Hand	0.50%	3.90%	6.89	[1.04; 183.64]	0.03	

AIS3+ Injuries Sweden								
Body Region	**Anatomical Structure**	**Organ**	**Male**	**Female**	**OR**	**95%-CI**	***p*-value**	**Visualization**
Pedestrian < 60YO								
			n = 158	*n = 129*				
Lower Extremities	Skeletal	Pelvis	3.80%	10.90%	3.03	[1.16; 8.93]	0.02	
Pedestrian ≥ 60YO								
			n = 44	*n = 55*				
Lower Extremities	Skeletal	Pelvis	2.30%	14.50%	6.45	[1.09; 167.19]	0.035	
Cyclist < 60YO								
			n = 113	*n = 40*				
Lower Extremities	Skeletal	Tibia	0.90%	7.50%	8.22	[0.92; 240.77]	0.024	
Cyclist ≥ 60YO								
			n = 48	*n = 14*				
Thorax	Internal Organs	Thoracic injury	4.20%	21.40%	5.90	[0.81; 55.89]	0.037	

TABLE 10 | Injury Severity, OR and *p*-value for pedestrians and cyclists < 60YO and ≥ 60YO in Austrian, Dutch, and Swedish accident data (*p-value < 5%).

	Injury Severity in Austria						Injury Severity in the Netherlands						Injury Severity in Sweden					
Injury Severity	**Male**	**Female**	**OR**	**95%-CI**	***p*-value**	**Visualization**	**Male**	**Female**	**OR**	**95%-CI**	***p*-value**	**Visualization**	**Male**	**Female**	**OR**	**95%-CI**	***p*-value**	**Visualization**
	Pedestrian < 60YO						**Pedestrian < 60YO**						**Pedestrian < 60YO**					
	n = 410	*n = 168*					*n = 3790*	*n = 2023*					*n = 980*	*n = 1185*				
AIS1+	100.0%	100.0%	–	–	–		100.0%	100.0%	–	–	–		100.0%	100.0%	–	–	–	
AIS2+	73.9%	70.8%	0.86	[0.58; 1.28]	0.450		66.1%	63.9%	0.91	[0.81; 1.02]	0.089		37.3%	26.5%	0.6	[0.50; 0.73]	<0.001*	
AIS3+	38.0%	35.7%	0.91	[0.62; 1.31]	0.598		18.7%	16.3%	0.84	[0.73; 0.97]	0.019*		11.6%	6.2%	0.51	[0.37; 0.69]	<0.001*	
AIS4+	15.9%	13.7%	0.85	[0.50; 1.4]	0.511		1.0%	0.7%	0.69	[0.36; 1.26]	0.231		4.0%	2.7%	0.67	[0.41; 1.08]	0.096	
	Pedestrian ≥ 60YO						**Pedestrian ≥ 60YO**						**Pedestrian ≥ 60YO**					
	n = 271	*n = 275*					*n = 1018*	*n = 1566*					*n = 443*	*n = 590*				
AIS1+	100.0%	100.0%	–	–	–		100.0%	100.0%	–	–	–		100.0%	100.0%	–	–	–	
AIS2+	74.9%	76.4%	1.08	[0.73; 1.6]	0.692		71.5%	73.0%	1.08	[0.90; 1.28]	0.412		40.0%	46.9%	1.33	[1.04; 1.71]	0.025*	
AIS3+	36.2%	32.7%	0.86	[0.6; 1.22]	0.398		23.4%	22.6%	0.96	[0.79; 1.16]	0.647		9.9%	9.3%	0.93	[0.61; 1.42]	0.742	
AIS4+	14.0%	11.3%	0.78	[0.47; 1.3]	0.334		0.7%	0.3%	0.38	[0.09; 1.28]	0.099		3.4%	2.4%	0.69	[0.33; 1.47]	0.329	
	Cyclist < 60YO						**Cyclist < 60YO**						**Cyclist < 60YO**					
	n = 112	*n = 52*					*n = 8620*	*n = 7083*					*n = 1592*	*n = 1359*				
AIS1+	100.0%	100.0%	–	–	–		100.0%	100.0%	–	–	–		100%	100%	–	–	–	
AIS2+	44.6%	36.5%	0.72	[0.36; 1.41]	0.328		59.3%	57.6%	0.93	[0.88; 0.99]	0.032*		22.6%	18.2%	0.77	[0.64; 0.92]	0.004*	
AIS3+	20.5%	15.4%	0.71	[0.28; 1.68]	0.433		19.5%	17.6%	0.88	[0.81; 0.95]	0.002*		4.1%	1.9%	0.46	[0.29; 0.72]	0.001*	
AIS4+	8.9%	3.8%	0.43	[0.06; 1.76]	0.245		0.6%	0.5%	0.88	[0.57; 1.35]	0.563		1.4%	0.3%	0.21	[0.06; 0.55]	0.001*	
	Cyclist ≥ 60YO						**Cyclist ≥ 60YO**						**Cyclist ≥ 60YO**					
	n = 64	*n = 72*					*n = 4657*	*n = 4202*					*n = 517*	*n = 372*				
AIS1+	100.0%	100.0%	–	–	–		100.0%	100.0%	–	–	–		100.0%	100.0%	–	–	–	
AIS2+	67.2%	62.5%	0.82	[0.40; 1.66]	0.568		67.6%	65.4%	0.9	[0.83; 0.99]	0.024*		36.8%	34.4%	0.9	[0.68; 1.19]	0.472	
AIS3+	35.9%	36.1%	1.01	[0.50; 2.05]	0.983		27.0%	21.9%	0.76	[0.69; 0.84]	<0.001*		9.3%	3.8%	0.39	[0.20; 0.69]	0.001*	
AIS4+	12.5%	12.5%	1	[0.35; 2.87]	1.000		0.8%	0.6%	0.82	[0.49; 1.37]	0.450		1.0%	0.3%	0.31	[0.01; 2.01]	0.210	

The odds ratios and *p*-values based on the Hypothesis Tests are summarized for all three data samples in **Table 10** and **Supplementary Table 13**.

Austrian Accident Data

In the Austrian dataset, no significant differences in injury severity were identified for pedestrian-to-passenger car, as well as cyclist-to-passenger car collisions, in both age groups for females and males.

No significant differences were observed on analyzing if age group has influence on injuries sustained by pedestrians. A slightly different trend can be seen for cyclist-to-passenger car collisions. Older cyclists (≥60YO) have significantly higher odds of sustaining AIS2+ (OR = 0.4, *p*-value < 0.001) and AIS3+ (OR = 0.42, *p*-value = 0.001) injuries than younger cyclists (<60YO).

Dutch Accident Data

The odds for younger males (<60YO) in the Netherlands, involved in pedestrian-to-passenger car collisions of sustaining AIS2+ (OR = 0.84, *p*-value = 0.019) injuries, were significantly higher than for younger females. No significant differences were identified in injury severity between male and female pedestrians ≥ 60YO.

A slightly different trend can be seen for cyclist-to-passenger car collisions. Males in the cyclist < 60YO group have significantly higher odds of sustaining AIS2+ (OR = 0.93, *p*-value = 0.032) and AIS3+ (OR = 0.88, *p*-value = 0.002) injuries than females. Elderly males also have significantly higher odds of sustaining AIS2+ (OR = 0.9, *p*-value = 0.024) and AIS3+ (OR = 0.76, *p*-value < 0.001) injuries than females.

Significant differences were observed on analyzing if age group has influence on injuries sustained by pedestrians. Older pedestrians (≥60YO) have significantly higher odds of sustaining AIS2+ (OR = 0.72, *p*-value < 0.001) and AIS3+ (OR = 0.73, *p*-value < 0.001) injuries than younger pedestrians (<60YO). A similar trend can be seen for cyclist-to-passenger car collisions. Older cyclists (≥60YO) have significantly higher odds of sustaining AIS2+ (OR = 0.71, *p*-value < 0.001) and AIS3+ (OR = 0.7, *p*-value < 0.001) injuries than younger cyclists (<60YO).

Swedish Accident Data

Significant differences were observed between males and females in the group of pedestrians < 60YO. Males have significantly higher odds of sustaining AIS2+ (OR = 0.6, *p*-value < 0.001) and AIS3+ (OR = 0.51, *p*-value < 0.001) injuries.

The odds for pedestrian ≥ 60YO females of sustaining AIS2+ (OR = 1.33, *p*-value = 0.025) injuries were significantly higher.

Significant differences were again observed for male and female cyclist injuries in Sweden. The odds for males < 60YO of sustaining AIS2+ (OR = 0.77, *p*-value = 0.004), AIS3+ (OR = 0.46, *p*-value = 0.001) and AIS4+ (OR = 0.21, *p*-value = 0.001) injuries were observed to be significantly higher.

For the group of cyclists ≥ 60YO in Sweden, the odds for male cyclists ≥ 60YO of sustaining AIS3+ injuries are significantly higher (OR = 0.39, *p*-value = 0.001) when involved in a cyclist-to-passenger car collision.

Significant differences were observed on analyzing if age group has influence on injuries sustained by. Older pedestrians (≥60YO) have significantly higher odds of sustaining AIS2+ (OR = 0.58, *p*-value < 0.001) injuries than younger pedestrian (<60YO). A similar trend can be seen for cyclist-to-passenger car collisions. Older cyclists (≥60YO) have significantly higher odds of sustaining AIS2+ (OR = 0.47, *p*-value < 0.001) and AIS3+ (OR = 0.42, *p*-value < 0.001) injuries than younger cyclists (<60YO).

In-Depth Analysis of Accident Data

With regard to this section, please refer to the **Supplementary Material** for further evaluation of significant differences between females and males identified in the Austrian accident data.

For the in-depth analysis of the Austrian accident data for pedestrians involved in pedestrian-to-passenger car collisions (**Figure 1**), it can be seen that for almost all parameters, the mean collision velocities for males are higher than for females. Moreover, it can be seen that higher injury severities are also related to higher collision velocities. Analyzing if there are significant differences in accident severity for females and males, it was found that elderly male pedestrians (≥60YO) have significantly higher odds of sustaining fatal injuries (**Supplementary Table 15**). The trend of higher collision velocities for males can also be seen for the maximum abbreviated injury scale (MAIS) level. By analyzing if there are significant differences in MAIS levels for females and males, it was found that younger female pedestrians (<60YO) have significantly higher odds of sustaining MAIS4 injuries (**Supplementary Table 16**). The mean collision speed for elderly pedestrians (≥60YO) is slightly higher in the data sample than for younger pedestrians (<60YO) for both females and males. For accidents occurring in rural areas, it is noticeable that the collision speed is higher than in urban areas. Also, for accident location, significant differences were observed between males and females (**Supplementary Table 14**). The odds of elderly male pedestrians (≥60YO) being involved in an accident in rural areas were observed to be higher. As pedestrian accident location was also included in the Dutch and Swedish accident data, significant differences were observed for that region too. The odds for male pedestrians in the Netherlands and in Sweden being involved in an accident in rural areas, irrespective of age, were significantly higher. Collision speed in Austrian accident data for males in both dry and wet road conditions were higher than for females. The opposite trend was observed for slippery road surfaces, however, only a few cases had been reported. On analyzing if there are significant differences for females and males with regard to road conditions, none were found in the Austrian and Dutch accident data (**Supplementary Table 17**). Accidents at night-time (electric light or darkness) occurred at higher collision speeds than accidents in daylight. Moreover, the likelihood of males being involved in an accident in darkness was higher than for females in Austria and the Netherlands (**Supplementary Table 18**). Analyzing the influence of alcohol on pedestrian-to-passenger-car collisions, it

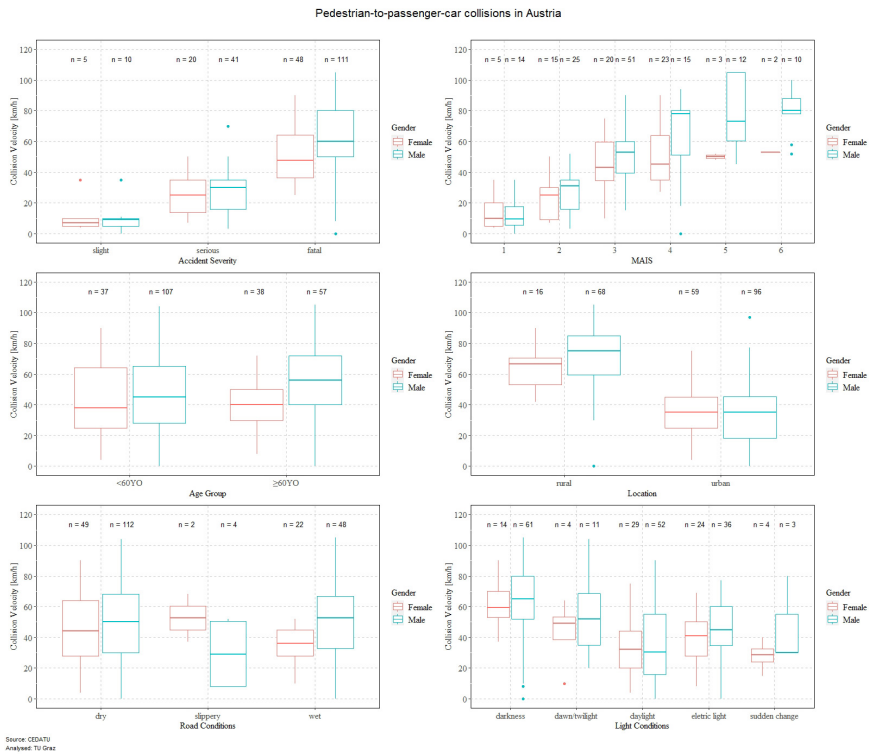

FIGURE 1 | In-depth analysis of Austrian accident data for pedestrian-to-passenger car collisions.

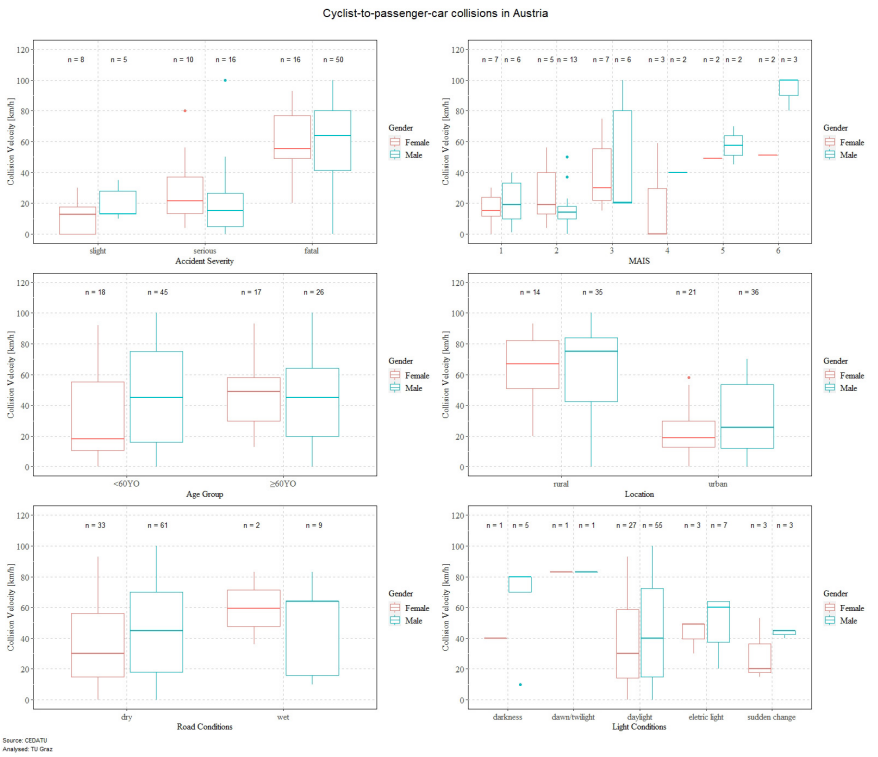

FIGURE 2 | In-depth analysis of Austrian accident data for cyclist-to-passenger car collisions.

TABLE 11 | Summary of all significant differences for different body regions and accident parameters for pedestrians and cyclists for Austria (AUT), Netherlands (NL), and Sweden (SWE).

	Pedestrian				Cyclist			
	<60YO		≥60YO		<60YO		≥60YO	
	Male	Female	Male	Female	Male	Female	Male	Female
Body Region[AUT,NL,SWE]								
Head			↑NL			↑NL	↑NL,SWE ↑AUT	
Face								
Neck								
Thorax			↑NL		↑NL ↑NL		↑NL ↑NL	
Abdomen					↑NL			
Spine	↑NL	↑SWE	↑SWE			↑NL	↑NL ↑NL	
Upper Extremities				↑SWE	↑NL			
Lower Extremities		↑AUT,NL ↑AUT		↑NL ↑NL		↑AUT,NL,SWE ↑SWE		↑NL,SWE ↑NL
Injurie Severity[AUT,NL,SWE]								
AIS1+								
AIS2+	↑SWE			↑SWE	↑NL,SWE		↑NL	
AIS3+	↑NL,SWE				↑NL,SWE		↑NL,SWE	
AIS4+					↑SWE			
Accident Location[AUT,NL,SWE]								
Urban		↑NL		↑AUT,SWE		↑NL		↑NL,SWE
Rural	↑NL,SWE		↑AUT,NL,SWE		↑NL,SWE		↑NL,SWE	
Accident Severity[AUT]								
slight								
serious				↑AUT				
fatal					↑AUT		↑AUT	
MAIS[AUT]								
MAIS1								
MAIS2								
MAIS3						↑AUT		
MAIS4		↑AUT						
MAIS5								
MAIS6								
Road Conditions[AUT,NL]								
dry								
slippery								
Wet								
Light Conditions[AUT,NL]								
darkness	↑AUT,NL		↑AUT,NL		↑NL		↑NL	
dawn/twilight		↑AUT,NL						
daylight				↑NL		↑NL		↑NL
electric light								
sudden change								
Alcohol Influence[AUT]								
yes	↑AUT		↑AUT					
no		↑AUT		↑AUT				

↑...*Significant higher OR for male or female,* ↑... *AIS2+,* ↑... *AIS3+, AUT... Austria, NL...Netherlands, SWE...Sweden.*

was found that the odds of pedestrian males being intoxicated by alcohol were higher than females (**Supplementary Table 19**).

For the in-depth analysis of cyclists involved in pedestrian-to-passenger car collisions (**Figure 2**) included in the Austrian accident data, it can also be seen that for a considerable number of parameters the mean collision velocity for males is faster than for females. It can also be seen that higher injury severities are related to higher collision velocities. On analyzing if there are significant differences in accident severity for females and males, it was found that the risk of sustaining fatal injuries is significantly higher for male cyclists, irrespective of age (**Supplementary Table 15**). The trend of higher collision velocities for males can also be seen for most of the MAIS levels. Analyzing significant differences in MAIS level for females and males, it was found that younger female cyclists (<60YO) have significantly higher odds of sustaining

MAIS3 injuries (**Supplementary Table 16**). The mean collision speed for elderly female cyclists (≥60YO) is slightly higher in the data sample than for younger female cyclists (<60YO). However, age was not found to influence speed for males. For accidents that had occurred in rural areas, it was noticeable that the collision speeds were higher than in urban areas. Accident location was not observed to make any significant difference between males and females in the Austrian data. As cyclist accident location was also included in the Dutch and Swedish accident data, significant differences could also be observed for those regions. Male cyclists in the Netherlands and Sweden have significantly higher odds of being involved in an accident in rural areas, irrespective of age (**Supplementary Table 14**). Collision speed in the Austrian accident data was found to be higher for males than females in dry road conditions. The opposite trend was observed for wet road conditions, however, only a few cases had been reported. For all road conditions no significant differences between males and females can be observed in Austrian and Dutch accident data (**Supplementary Table 17**). Most of the cyclist accidents involving passenger cars had occurred during daylight, although the collision speed was higher also for cyclist accidents at night-time (electric light or darkness). Furthermore, light conditions were not observed to have made any significant difference between males and females in Austrian accident data. In Dutch accident data it was observed that the likelihood of males being involved in an accident in darkness was higher than for females (**Supplementary Table 18**). The influence of alcohol was observed for cyclists in the Austrian accident data (**Supplementary Table 19**).

DISCUSSION

The accident databases show several significant differences due to the applied data sources and their original purpose.

Although some authors have previously tried to combine data from different databases, or extrapolate from one country to others (Kreiss et al., 2015), this was not done in the current study. Instead, trends from the different data sources have been compared and the advantages of each of the data sets were utilized. The Dutch dataset showed the highest number of cases, the Swedish dataset is the only dataset that covers all cases from one country, and is therefore most representative and unbiased. The Austrian dataset had the highest level of detail and therefore allowed the authors to perform additional analyses. It would be beneficial to have a representative, European-wide, long-term in-depth database to eliminate the limitations mentioned above.

The data in this study was collected during different time periods. However, when analyzing the Dutch data, no significant change in injuries over the years was observed, hence it has been assumed by the authors that this parameter does not influence the results. The data selection criteria, i.e., being recorded by both police and hospital or involvement of at least one vehicle, was made in order to obtain as comparable data between the countries as possible. Using this criteria is necessary, due to a significant difference in hospital and police reported data having been observed in previous studies (Juhra et al., 2012). As a consequence of using only matched police and hospital reported accidents, the data do not cover all accidents. For example, only 30% of all cases in the STRADA database are reported by both police and hospital (Yamazaki, 2018). On the other hand, as the present study includes accidents involving passenger cars, there should be a higher inclusion of the total number of crashes as the police are more likely to have reported an accident involving a motor vehicle.

For the Austrian data, a shift toward serious and fatal accidents can be seen when comparing the CEDATU database with the national statistics (**Supplementary Figure 6**). This is because the original focus of the CEDATU database was to collect data on reconstructed fatal accidents in Austria (Tomasch and Steffan, 2006; Tomasch et al., 2008). In recent years, increasingly accidents involving minor as well as severe injuries have been included in the database.

Similarly, a shift toward more severe injuries and fatal accidents can be seen in the Dutch dataset. The Dutch police register contains 90% of all fatal road accidents, although unfortunately it is less comprehensive for accidents of lesser severity (Reurings and Stipdonk, 2011).

Despite the shift toward more severe injuries and fatal accidents in the Austrian and Dutch datasets in comparison to national statistics, the datasets have been very beneficial when it comes to comparisons of injuries sustained by females and males relative to each other. For the analysis of the most relevant AIS2+ body regions, one should on the other hand mainly rely on the results based on the STRADA database.

A summary with all accident parameters and injuries showing significant differences between males and females can be seen in **Tables 11**, **12**. For more details on the exact values for OR and *p*-value have a look on the result section and the **Supplementary Material**.

Body Regions

The current analysis shows that the body regions head, thorax, upper extremities and lower extremities are more or less equally relevant for pedestrian and cyclist statistics when it comes to injury mitigation. Only a small difference was seen in the different databases, in that the order may differ between the most relevant body regions. These findings are in line with other studies which have also identified these body regions as most commonly injured by pedestrians and cyclists involved in passenger car collisions (Otte et al., 2012; Weijermars et al., 2016; Wisch et al., 2017; Saadé et al., 2020).

Predominant in the databases and groups, the head was the most frequently injured body region. The fact that the head is one of the most relevant body region when it comes to injury mitigation for pedestrian and cyclist accidents could be explained by the fact that the head is one of the most vulnerable body region. This can also be seen when having a look into the AIS Codebook (AAAM, 2005) where the majority of injuries related to the head are coded as AIS2+. Head injuries were less frequent for cyclists in the Swedish dataset. This might

TABLE 12 | Summary of all single injuries with significant differences for pedestrians and cyclists for Austria (AUT), Netherlands (NL), and Sweden (SWE).

			Pedestrian				Cyclist			
			<60YO		≥60YO		<60YO		≥60YO	
			Male	Female	Male	Female	Male	Female	Male	Female
Body Region	**Anatomical Structure**	**Organ**								
Head	Concussive Injury	–	↑NL						↑SWE	
Head	Internal Organs	Cerebrum					↑NL,SWE		↑NL,SWE	
Head	Skeletal	Skull	↑AUT				↑NL		↑NL	
Thorax	Vessels	–					↑NL ↑NL			
Thorax	Internal Organs	Lung	↑SWE				↑NL,SWE ↑NL		↑NL	
Thorax	Internal Organs	Thoracic injury	↑SWE		↑SWE		↑NL		↑NL	↑SWE
Thorax	Skeletal	Sternum		↑NL			↑NL			
Thorax	Skeletal	Rib Cage			↑NL		↑NL ↑NL		↑NL	
Abdomen	Internal Organs	Kidney					↑NL			
Abdomen	Internal Organs	Spleen	↑NL							
Spine	Cervical Spine	–	↑NL		↑SWE		↑NL ↑NL		↑NL ↑NL	
Spine	Lumbar Spine	–		↑AUT		↑AUT		↑NL		
Spine	Thoracic Spine				↑SWE			↑NL		
Upper Extremities	Skeletal	Clavicle					↑NL			
Upper Extremities	Skeletal	Scapula			↑NL		↑NL,SWE		↑NL	
Upper Extremities	Skeletal	Humerus								↑NL
Upper Extremities	Skeletal	Ulna					↑SWE			
Upper Extremities	Skeletal	Radius		↑SWE		↑SWE				↑SWE
Upper Extremities	Skeletal	Hand				↑NL				↑NL,SWE
Lower Extremities	Muscles, Tendons, Ligaments	–						↑NL		
Lower Extremities	Skeletal	Foot		↑NL				↑NL,SWE		↑NL
Lower Extremities	Skeletal	Femur		↑AUT,NL ↑AUT,NL		↑NL ↑NL		↑NL		↑NL
Lower Extremities	Skeletal	Pelvis		↑AUT,NL,SWE ↑AUT,NL,SWE		↑AUT,SWE ↑SWE		↑SWE		
Lower Extremities	Skeletal	Tibia	↑NL			↑NL		↑NL,SWE ↑SWE		↑NL
Lower Extremities	Skeletal	Fibula						↑NL		↑NL

↑. . .*Significant higher OR for male or female,* ↑. . . *AIS2+,* ↑. . . *AIS3+, AUT. . . Austria, NL. . .Netherlands, SWE. . .Sweden.*

be a result of high helmet wearing rates (Otte et al., 2015; Leo et al., 2019a).

Another fact that can be seen through all databases is that females often have significantly higher odds of sustaining injuries to the lower extremities. This was observed for pedestrians as well as for cyclists. For cyclists, this may can be explained in possible differences in the type of bicycle they ride, their riding speed and the type of accidents they are involved in Boele-Vos et al. (2017), Fyhri et al. (2019), Prati et al. (2019). Male cyclists for example more often ride on racing bikes whereas (elderly) female cyclists more often ride on pedelecs (electrically assisted bicycles) (Boele-Vos et al., 2017). Riding on a racing bike is related to higher riding speeds, a different seating position and the type of accidents may also be different. This could explain differences in injuries sustained. In addition, osteoporosis is much more common in women than in men (Alswat, 2017), which may also explain more fractures in women, such as femur/hip/pelvic fractures.

The proportion of AIS2+ injuries to the upper extremities is rather considerable, especially in Swedish accident data. However, looking at AIS3+ injuries, injuries of the upper extremities are not particularly common. Nevertheless, assessing long-term consequences of injuries, it has been shown that 85% of AIS3 upper extremity injuries, result in permanent medical impairment (Malm et al., 2008). In contrast, while thorax injuries were common for AIS 3+ injuries in all three databases, these injuries rarely result in permanent medical impairment. This illustrates that when taking long-term consequences of injuries into account, preventive measures must target upper extremity injuries as well. One last fact is that significant differences for the frequency of spinal injuries between males and females were observed in the current study. However, the trend was not consistent within the different age groups.

Detailed Injuries

For the detailed injury types, significant differences in injuries sustained by females and males were identified in all three databases. This information is very valuable with regard to the development and improvement of HBMs for virtual testing. Knowing which injuries are most common, and for which injuries significant differences can be seen between males and females, is necessary to specify what must be predicted by the HBMs.

For lower extremities (incl. pelvis), it was found that females have significantly higher odds of sustaining skeletal injuries. In all three data sets, female pedestrians showed higher odds of sustaining pelvic injuries than males. This is in line with a study by Starnes et al. (2011) and Klug et al. (2015). Starnes also concluded that males are significantly more likely to suffer tibia fractures. This, however, cannot be confirmed in the present study, due to different results being observed for tibia fractures in the different databases.

Furthermore, female cyclists showed significantly higher odds than males for tibia fractures in the Swedish and the Dutch dataset. This finding may be influenced by the fact that females and males ride on different types of bicycle frames, producing a different interaction with the lower extremities.

Injury Severity and Exposure

When comparing injury severity between males and females, males have significantly higher odds of sustaining more severe injuries compared to females in pedestrian and cyclist accidents. This is especially the case when looking at the Swedish data. From the Austrian database, which includes information on collision speeds of passenger cars, it can be seen that the collision speeds of passenger cars were higher in collisions involving males compared with females. A similar trend can also be seen when looking at cyclist-to-passenger car collisions in Austria.

The Austrian, Dutch and Swedish data shows that the odds of females being involved in a rural accident are lower than for males. It was also shown that males are more likely involved in accidents during nights. The analysis of the Austrian data has shown that these types of accidents are related to higher collision speeds. Hence, the observation of higher injury severity among males is more likely a function of the exposure to higher collision speeds of passenger cars rather than a question of the sex. In the future, it should be analyzed if any significant differences in injury severities are apparent at similar energy levels of the accidents. However, this requires additional crash data unavailable in the current datasets. Applying additional filters narrows down our numbers too much, so that no meaningful analyses can be done. Further investigations should be done to study gender-specific differences, which might lead to different accident scenarios. Some first indications have been observed in this study, showing that the types of accidents where females (more likely to be injured during daytime, inner-city) are severely injured might differ from males (higher odds to be injured during night-time at rural roads in an alcoholized state).

Regarding the age of the vulnerable road users, the Dutch and Swedish data shows that older (≥60YO) pedestrian and cyclist have significant higher odds of sustaining AIS2+ injuries. A similar trend can also be seen for AIS3+ injuries. The Austrian accident data show significant higher odds for elderly (≥60YO) cyclists sustaining AIS2+ and AIS3+ injuries as well. This is in line with previous studies which conclude that elderly pedestrians (≥60YO) tend to suffer more severe injuries than younger pedestrians (<60YO) (Davis, 2001; Niebuhr et al., 2016; Saadé et al., 2020).

Outlook

Recent studies have shown that through the implementation of autonomous emergency breaking (AEB) systems, the collision velocities in pedestrian and cyclist-to-passenger car collisions will be drastically lowered (Gruber et al., 2019; Leo et al., 2020). Reducing the collision speed will also lead to a change in impact conditions, i.e., lower head impact velocities, Leo et al. (2020). Presumably, this fact will also lead to a shift in the injuries sustained by pedestrians and cyclists in the foreseeable future.

Once comparable FE Human Body Models of an average female and male are available, the isolated sex-specific differences in injury risk caused by differences in loadings due to differences in anthropometries and influences of individual factors such as age, and injury thresholds, could and should be investigated.

Moreover, by means of virtual testing the diversity of accident scenarios and the human population can be addressed by including different pre-collision behavior.

Conclusion

The conclusion of this study is that female and male pedestrians and cyclists have significant different odds of sustaining injuries in accidents involving passenger cars. This trend can be seen for injuries to different body regions, single injuries and also for injury severity. For example, the results show that the odds of sustaining skeletal injuries to the lower extremities (incl. pelvis) in females are significantly higher. Moreover, significant differences in injuries severity for younger (<60YO) and elderly (≥60YO) pedestrians and cyclists were observed. In-depth analyses of Austrian accident data have shown that collision velocities are higher for male pedestrians and cyclists than for females in passenger car collisions. Furthermore, it was observed in all datasets, that the odds of females being involved in a rural accident or an accident at night are lower than for males.

The findings of this study highlight the need for policy makers and stakeholders to work toward developing safety features and assessment tools (e.g., integrated assessment) that take into account population diversity of sex and age and other individual related factors.

DATA AVAILABILITY STATEMENT

The data analyzed in this study is subject to the following licenses/restrictions: Raw data from accident databases from Austria, Netherlands, and Sweden are not publicly available (due to data protection regulations). Requests to access these datasets should be directed to CL, christoph.leo@tugraz.at and CK, corina.klug@tugraz.at.

AUTHOR CONTRIBUTIONS

CL carried out the data analysis and manuscript preparation. CK designed the study and supervised the data analysis. MR, NB, RD, AL, ET, and CK provided comments, feedback, and edited the manuscript. MR, NB, RD, and ET extracted the data from the Dutch, Swedish and Austrian accident databases respectively. All authors read and approved the final manuscript.

FUNDING

This study has been conducted within the VIRTUAL project that has received funding from the European Union Horizon 2020 Research and Innovation Program under Grant Agreement No. 768960.

SUPPLEMENTARY MATERIAL

The Supplementary Material for this article can be found online at: https://www.frontiersin.org/articles/10.3389/fbioe.2021.677952/full#supplementary-material

REFERENCES

AAAM (2005). *Abbreviated Injury Scale 2005*. Des Plaines IL: AAAM.

Alswat, K. A. (2017). Gender disparities in osteoporosis. *J. Clin. Med. Res.* 9, 382–387. doi: 10.14740/jocmr2970w

Andrade, C. (2015). Understanding relative risk, odds ratio, and related terms: as simple as it can get. *J. Clin. Psychiatry* 76, e857–e861. doi: 10.4088/JCP.15f10150

Boele-Vos, M. J., van Duijvenvoorde, K., Doumen, M. J. A., Duivenvoorden, C. W. A. E., Louwerse, W. J. R., and Davidse, R. J. (2017). Crashes involving cyclists aged 50 and over in the Netherlands: an in-depth study. *Accid. Anal. Prev.* 105, 4–10. doi: 10.1016/j.aap.2016.07.016

Bose, D., Segui-Gomez, M., and Crandall, J. R. (2011). Vulnerability of female drivers involved in motor vehicle crashes: an analysis of US population at risk. *Am. J. Public Health* 101, 2368–2373. doi: 10.2105/AJPH.2011.300275

Davis, G. (2001). Relating severity of pedestrian injury to impact speed in vehicle-pedestrian crashes: simple threshold model. *Transport. Res. Record* 1773, 108–113. doi: 10.3141/1773-13

Forman, J., Poplin, G. S., Shaw, C. G., McMurry, T. L., Schmidt, K., Ash, J., et al. (2019). Automobile injury trends in the contemporary fleet: belted occupants in frontal collisions. *Traffic Inj. Prev.* 20, 607–612. doi: 10.1080/15389588.2019.1630825

Fyhri, A., Johansson, O., and Bjørnskau, T. (2019). Gender differences in accident risk with e-bikes—Survey data from Norway. *Accid. Anal. Prev.* 132:105248. doi: 10.1016/j.aap.2019.07.024

Gruber, M., Kolk, H., Klug, C., Tomasch, E., Feist, F., Schneider, A., et al. (2019). "The effect of P-AEB system parameters on the effectiveness for real world pedestrian accidents," in *Proceedings of the 26th ESV Conference Proceedings*, ed. NHTSA (Washington, DC: NHTSA).

Howard, C., and Linder, A. (2014). *Review of Swedish Experiences Concerning Analysis of People Injured in Traffic Accidents*. Brussels: Belgian Road Safety Institute

Juhra, C., Wieskötter, B., Chu, K., Trost, L., Weiss, U., Messerschmidt, M., et al. (2012). Bicycle accidents - do we only see the tip of the iceberg? A prospective multi-centre study in a large German city combining medical and police data. *Injury* 43, 2026–2034. doi: 10.1016/j.injury.2011.10.016

Klug, C., Weinberger, M., Tomasch, E., Feist, F., Sinz, W., Steffan, H., et al. (2015). "Pelvic and femoral injuries in car-to-pedestrian accidents," in *Proceedings of the 2015 IRCOBI Conference Proceedings*, ed. International Research Council on the Biomechanics of Injury (Lyon: IRCOBI), 49–63.

Kreiss, J., Feng, G., Krampe, J., Meyer, M., Niebuhr, T., Pastor, C., et al. (2015). "Extrapolation of GIDAS accident data to Europe," in *Proceedings of the 24th ESV Conference Proceedings*, ed. NHTSA (Washington, DC: NHTSA).

Kullgren, A., and Krafft, M. (2010). "Gender analysis on whiplash seat effectiveness: results from real-world crashes," in *Proceedings of the 2010 IRCOBI Conference Proceedings,* Hanover, ed. International Research Council on the Biomechanics of Injury (Hanover: IRCOBI), 17–28.

Leo, C., Gruber, M., Feist, F., Sinz, W., Roth, F., and Klug, C. (2020). "The effect of autonomous emergency braking systems on head impact conditions for pedestrian and cyclists in passenger car collisions," in *Proceedings of the 2020 IRCOBI Conference Proceedings*, ed. International Research Council on the Biomechanics of Injury (Munich: IRCOBI), 330–357.

Leo, C., Klug, C., Ohlin, M., and Linder, A. (2019b). "Analysis of pedestrian injuries in pedestrian-car collisions with focus on age and gender," in *Proceedings of the*

2019 IRCOBI Conference Proceedings, ed. International Research Council on the Biomechanics of Injury (Florence: IRCOBI), 256–257.

Leo, C., Klug, C., Ohlin, M., Bos, N., Davidse, R., and Linder, A. (2019a). Analysis of Swedish and Dutch accident data on cyclist injuries in cyclist-car collisions. *Traffic Inj. Prev.* 20, S160–S162. doi: 10.1080/15389588.2019.1679551

Linder, A., and Svedberg, W. (2019). Review of average sized male and female occupant models in European regulatory safety assessment tests and European laws: gaps and bridging suggestions. *Accid. Anal. Prev.* 127, 156–162. doi: 10.1016/j.aap.2019.02.030

Linder, A., and Svensson, M. Y. (2019). Road safety: the average male as a norm in vehicle occupant crash safety assessment. *Interdiscip. Sci. Rev.* 44, 140–153. doi: 10.1080/03080188.2019.1603870

Linder, A., Davidse, R J, Iraeus, J., John, J. D., Keller, A., Klug, C., et al. (2020). "VIRTUAL - a European approach to foster the uptake of virtual testing in vehicle safety assessment," in *Proceedings of the 8th Transport Research Arena*, Helsinki: TRA.

Malm, S., Krafft, M., Kullgren, A., Ydenius, A., and Tingvall, C. (2008). Risk of permanent medical impairment (RPMI) in road traffic accidents. *Ann. Adv. Automot. Med.* 52, 93–100.

Mattsson, K., and Ungerbäck, A. (2013). *Vägtrafikolyckor: Handledning vid rapportering*. Borlänge: Transportstyrelsen.

McHugh, M. (2009). The odds ratio: calculation, usage, and interpretation. *Biochem. Med.* 120–126. doi: 10.11613/BM.2009.011

Mitchell, Z. A., and Cameron, R. B. (2020). "Female vs. Male relative fatality risk in fatal crashes," in *Proceedings of the 2020 IRCOBI Conference Proceedings*, ed. International Research Council on the Biomechanics of Injury (Munich: IRCOBI), 47–85.

National Board of Health and Welfare (2010). *International Statistical Classification of Diseases and Related Health Problems - Systematic listing: Swedish version 2011 (ICD-10-SE)*. Stockholm: National Board of Health and Welfare

Niebuhr, T., Junge, M., and Rosén, E. (2016). Pedestrian injury risk and the effect of age. *Accid. Anal. Prev.* 86, 121–128. doi: 10.1016/j.aap.2015.10.026

Otte, D., Jänsch, M., and Haasper, C. (2012). Injury protection and accident causation parameters for vulnerable road users based on German In-Depth Accident Study GIDAS. *Accid. Anal. Prev.* 44, 149–153. doi: 10.1016/j.aap.2010.12.006

Otte, D., Jänsch, M., Morandi, A., Orsi, C., Stendardo, A., Bogerd, C. P., et al. (2015). *Final Report of Working Group 1: In-Depth Accident Observations and Injury Statistics*. Brussels: COST Action TU1101 / HOPE

Pipkorn, B., Iraeus, J., Lindkvist, M., Puthan, P., and Bunketorp, O. (2020). Occupant injuries in light passenger vehicles-A NASS study to enable priorities for development of injury prediction capabilities of human body models. *Accid. Anal. Prev.* 138:105443. doi: 10.1016/j.aap.2020.105443

Prati, G., Fraboni, F., de Angelis, M., and Pietrantoni, L. (2019). Gender differences in cyclists' crashes: an analysis of routinely recorded crash data. *Int. J. Inj. Contr. Saf. Promot.* 26, 391–398. doi: 10.1080/17457300.2019.1653930

Reurings, M. C. B., and Stipdonk, H. L. (2011). Estimating the number of serious road injuries in the Netherlands. *Ann. Epidemiol.* 21, 648–653. doi: 10.1016/j.annepidem.2011.05.007

Saadé, J., Cuny, S., Labrousse, M., Song, E., Chauvel, C., and Chrétien, P. (2020). "Pedestrian injuries and vehicles-related risk factors in car-to-pedestrian frontal collisions," in *Proceedings of the 2020 IRCOBI Conference Proceedings*, ed. International Research Council on the Biomechanics of Injury (Munich: IRCOBI), 278–289.

Schneider, L. W. (1983). *Development of Anthropometrically Based Design Specifications for an Advanced Adult Anthropomorphic Dummy Family, Final Repor*t. Report Number: UMTRI-83-53-1, Vol. 1, Michigan, MI: University of Michigan Transportation Research Institute.

Simms, C., and Wood, D. (2009). *Pedestrian and Cyclist Impact: A Biomechanical Perspective*. Dordrecht: Springer Netherlands.

Starnes, M. J., Hadjizacharia, P., Chan, L. S., and Demetriades, D. (2011). Automobile versus pedestrian injuries: does gender matter? *J. Emerg. Med.* 40, 617–622. doi: 10.1016/j.jemermed.2008.03.012

Swedish Government Offices (1965). *SFS 1965:561: last update in SFS 2014:1244, 2014*. Rosenbad: Swedish Government Offices

SWOV (2016). *Data Sources*. The Hague: SWOV.

Szumilas, M. (2010). Explaining odds ratios. *J. Can. Acad. Child Adolesc. Psychiatry* 19, 227–229.

Tomasch, E., and Steffan, H. (2006). "ZEDATU – zentrale datenbank tödlicher unfälle in österreich – a central database of fatalities in Austria," in *Proceedings of the 2nd International Conference on ESAR "Expert Symposium on Accident Research"*, Hanover: ESAR.

Tomasch, E., Steffan, H., and Darok, M. (2008). "Retrospective accident investigation using information from court," in *Proceedings of the Transport Research Arena Europe 2008 (TRA)*, Ljubljana: TRA.

Weijermars, W., Bos, N., and Stipdonk, H. L. (2016). Serious road injuries in The Netherlands dissected. *Traffic Inj. Prev.* 17, 73–79. doi: 10.1080/15389588.2015.1042577

Wisch, M., Lerner, M., Vukovic, E., Hynd, D., Fiorentino, A., and Fornells, A. (2017). "Injury patterns of older car occupants, older pedestrians or cyclists in road traffic crashes with passenger cars in europe – results from SENIORS," in *Proceedings of the 2017 IRCOBI Conference Proceedings*, ed. International Research Council on the Biomechanics of Injury (Antwerp: IRCOBI), 63–78.

World Health Organization (2018). *Global Status Report on Road Safety 2018*. Geneva: World Health Organization.

Yamazaki, R. (2018). Strada Bortfallshandbok 2018 – Information om Täckning och Bortfall i Rapportering till Transportstyrelsens Vägolycksdatabas. Sweden: Swedish Transport Agency.

Zhang, K., Cao, L., Fanta, A., Reed, M. P., Neal, M. O., Wang, J.-T., et al. (2017). An automated method to morph finite element whole-body human models with a wide range of stature and body shape for both men and women. *J. Biomech.* 60, 253–260. doi: 10.1016/j.jbiomech.2017.06.015

Conflict of Interest: The authors declare that the research was conducted in the absence of any commercial or financial relationships that could be construed as a potential conflict of interest.

frontiers in Bioengineering and Biotechnology

ORIGINAL RESEARCH
published: 24 May 2021
doi: 10.3389/fbioe.2021.677768

Rib Cortical Bone Fracture Risk as a Function of Age and Rib Strain: Updated Injury Prediction Using Finite Element Human Body Models

Karl-Johan Larsson[1,2], Amanda Blennow[2], Johan Iraeus[2], Bengt Pipkorn[1,2] and Nils Lubbe[1]*

[1] Autoliv Research, Vårgårda, Sweden, [2] Division of Vehicle Safety, Department of Mechanics and Maritime Sciences, Chalmers University of Technology, Gothenburg, Sweden

To evaluate vehicle occupant injury risk, finite element human body models (HBMs) can be used in vehicle crash simulations. HBMs can predict tissue loading levels, and the risk for fracture can be estimated based on a tissue-based risk curve. A probabilistic framework utilizing an age-adjusted rib strain-based risk function was proposed in 2012. However, the risk function was based on tests from only twelve human subjects. Further, the age adjustment was based on previous literature postulating a 5.1% decrease in failure strain for femur bone material per decade of aging. The primary aim of this study was to develop a new strain-based rib fracture risk function using material test data spanning a wide range of ages. A second aim was to update the probabilistic framework with the new risk function and compare the probabilistic risk predictions from HBM simulations to both previous HBM probabilistic risk predictions and to approximate real-world rib fracture outcomes. Tensile test data of human rib cortical bone from 58 individuals spanning 17–99 years of ages was used. Survival analysis with accelerated failure time was used to model the failure strain and age-dependent decrease for the tissue-based risk function. Stochastic HBM simulations with varied impact conditions and restraint system settings were performed and probabilistic rib fracture risks were calculated. In the resulting fracture risk function, sex was not a significant covariate—but a stronger age-dependent decrease than previously assumed for human rib cortical bone was evident, corresponding to a 12% decrease in failure strain per decade of aging. The main effect of this difference is a lowered risk prediction for younger individuals than that predicted in previous risk functions. For the stochastic analysis, the previous risk curve overestimated the approximate real-world rib fracture risk for 30-year-old occupants; the new risk function reduces the overestimation. Moreover, the new function can be used as a direct replacement of the previous one within the 2012 probabilistic framework.

Keywords: rib fracture, injury risk, injury prediction, human body model, occupant safety, survival analysis, SAFER HBM

OPEN ACCESS

Edited by:
Sonia Duprey,
Université de Lyon, France

Reviewed by:
Sven Holcombe,
University of Michigan, United States
Tim McMurry,
University of Virginia, United States

****Correspondence:***
Karl-Johan Larsson
karl-johan.larsson@autoliv.com

Specialty section:
This article was submitted to Biomechanics, a section of the journal Frontiers in Bioengineering and Biotechnology

Received: *08 March 2021*
Accepted: *27 April 2021*
Published: *24 May 2021*

Citation:
Larsson K-J, Blennow A, Iraeus J, Pipkorn B and Lubbe N (2021) Rib Cortical Bone Fracture Risk as a Function of Age and Rib Strain: Updated Injury Prediction Using Finite Element Human Body Models. Front. Bioeng. Biotechnol. 9:677768. doi: 10.3389/fbioe.2021.677768

INTRODUCTION

Despite improvements in vehicle occupant safety (Kullgren et al., 2019), rib fractures remain a prevalent outcome in motor vehicle collisions (MVCs) (Forman et al., 2019; Pipkorn et al., 2020). Among patients admitted to emergency care for blunt chest trauma, MVCs are the major cause of injury; moreover, having three (or more) fractured ribs is a risk factor for mortality (Sirmali et al., 2003; Veysi et al., 2009; Battle et al., 2012). Epidemiological studies reveal that risk of thoracic injury, including rib fractures, in MVCs increases with impact speed and age—and is greater for females than for males (Bose et al., 2011; Carter et al., 2014; Weaver et al., 2015; Brumbelow, 2019; Forman et al., 2019). Increased impact speed increases the energy (and concomitant mechanical load) transferred to the occupant's thorax from vehicle safety systems, e.g., seatbelts. The increased rib fracture risk with age can be partly explained by findings from studies of human bone's mechanical properties, which show that tolerance to mechanical load until fracture decreases with age (Lindahl and Lindgren, 1967; Burstein et al., 1976; Carter and Spengler, 1978; McCalden et al., 1993; Kemper et al., 2005). Among these studies, Kemper et al. (2005) reported a difference in bone's ultimate strain due to sex, with the females showing reduced deformation before failure, but here the three female bone material donors were on average older than the three male donors, suggesting that the noted reduction may have been an effect of age rather than sex (Kemper et al., 2005). McCalden et al. (1993) reported a small increase in ultimate stress for female femoral specimens, while Lindahl and Lindgren (1967) and Burstein et al. (1976) did not find any significant differences in femoral cortical bone ultimate stress between the sexes.

In order to design safer vehicles, it is necessary to have tools and methods that can predict the influence of design changes on injury outcome. Finite element human body models (HBMs) are used in vehicle crash simulations to estimate occupant injury risk, including rib fracture risk, and to evaluate and develop countermeasures. The injury risk can be estimated using local tissue measurements, such as stress and strain in the modeled anatomical structures. Rib cortical strain has been shown to correlate to fracture in postmortem human subject (PMHS) tests (Trosseille et al., 2008). One commonly used HBM which has been validated for predicting strain in the rib cortical bone for various impact loads is the SAFER HBM (Iraeus and Pipkorn, 2019).

An injury risk function is necessary to establish a mathematical link between rib cortical strain and rib fracture risk. A variety of statistical methods have been employed in the past to create injury risk functions, as described in Petitjean and Trosseille (2011). Commonly used are logistic regression and survival analysis. While the resulting injury risk curves can differ substantially depending whether exact or censored data are used (Praxl, 2011), in most situations the two methods produce similar results (McMurry and Poplin, 2015). Petitjean and Trosseille (2011) recommend survival analysis, based on statistical simulations of theoretical samples. In addition, the International Organization for Standardization (ISO) proposed a 12-step approach to constructing injury risk curves from PMHS testing using survival analysis (International Organization for Standardization, 2014). This approach was applied to thoracic risk curves for WorldSID (Petitjean et al., 2012) and THOR (Davidsson et al., 2014).

A probabilistic framework detailing how to translate injury risk for an individual rib as calculated by injury risk functions (developed using survival analysis or otherwise) to a risk of sustaining a certain number of rib fractures in HBM simulations was presented in 2012 (Forman et al., 2012). The framework included also a specific rib cortical bone strain-based injury risk function which was based on dynamic test data from twelve human subjects (Kemper et al., 2005, 2007). The data were biased towards older subjects (only one subject was below the age of 42). Age adjustment was performed by assuming a reduction in rib cortical bone failure strain of 5.1% per decade of aging, based on test data of femur cortical bone reported by Carter and Spengler (1978). The 5.1% reduction had been originally reported by Burstein et al. (1976) from testing of material from $N = 33$ donors (21–86 years old); they also reported a 6.9% reduction in failure strain per decade of aging for tibial cortical bone samples ($N = 28$, 21–86 years old). McCalden et al. (1993) reported that the reduction of failure strain in femoral cortical bone was 9% per decade ($N = 47$, 20–102 years). Thus, Forman et al. (2012) created the risk function in the framework using relatively few, predominantly older subjects and applied a relatively small age-dependent decrease. The original risk function from Forman et al.'s (2012) study (referred to hereafter as "Forman 2012") was not based on survival analysis but presented as an empirical cumulative distribution function. The drawback with this type of function is that very small strain increments can give large risk increments, which is an undesired feature in design optimization. To overcome this limitation, the framework was updated with a smooth risk curve (Iraeus and Lindquist, 2020). The same Kemper et al. (2005); Kemper et al. (2007) strain data and 5.1% reduction used for the Forman 2012 risk curve was used, but a Weibull distribution was fitted. The resulting risk function will be referred to as "Forman smoothed".

Rib fracture risk predictions from the probabilistic framework, updated with the Forman smoothed risk curve, were validated against rib fractures observed in field data by Pipkorn et al. (2019). The rib strains used as input for the probabilistic risk calculation were obtained from the SAFER HBM. Detailed accident reconstructions and population-based stochastic vehicle impact simulations were performed. The predicted risk increased with impact speed as expected, but for younger occupants the framework overestimated the rib fracture risk at any given impact speed even more than for elderly occupants. This risk overestimation is likely a consequence of the low age-dependent decrease in the "Forman smoothed" rib strain risk function.

Recently, material coupon tensile testing was performed on human rib cortical bone samples from 61 PMHSs (32 males and 29 females) ranging in age from 17 to 99 years (Katzenberger et al., 2020). These data suffice to develop an age-dependent rib strain-based fracture risk function without relying on age scaling from other sources.

The aim of this study was to develop a strain-based rib fracture risk function using material test data spanning a wide

range of ages. The influence of age and sex on the fracture risk was investigated and modeled. A second aim was to update the probabilistic framework with the new risk function and compare probabilistic risk predictions from a set of existing HBM simulation rib strain results. The updated predictions were compared to previous predictions obtained using the Forman smoothed risk function.

MATERIALS AND METHODS

Materials

The data used in this study have previously been presented by Katzenberger et al. (2020). The authors reported mechanical properties of human rib cortical bone, measured by tensile testing of samples from PMHSs. From each PMHS, two coupons of rib cortical bone were extracted from rib levels 3 to 7. The coupons were subjected to uniaxial tensile tests to failure at medium or low strain rates (0.5 and 0.005 strain/s, respectively). The higher rate was selected to represent the strain rate measured on PMHS ribs in experiments simulating a 48 km/h frontal impact (Duma et al., 2005; Katzenberger et al., 2020). Results were obtained and reported from 58 medium-rate tests and 58 low-rate tests (55 medium and low rate test results from the same PMHS). The age and sex of the PMHSs and the reported strain at which the samples failed (failure strain, reported as engineering strains, i.e., sample elongation at failure divided by initial length) comprise the data used in this study.

Rib Fracture Risk Function

The method for developing the new rib cortical bone fracture risk function follows the 12-step procedure for developing injury risk curves, according to International Organization for Standardization (2014) and Petitjean et al. (2012): (1) collect data, (2) assign censor status, (3) check for multiple injury mechanisms, (4) separate samples by injury mechanism, (5) estimate distribution parameters, (6) identify overly influential observations, (7) check the distribution assumption, (8) choose the distribution, (9) check the validity of predictions against existing results, (10) calculate 95% confidence intervals, (11) assess the quality index, and (12) recommend one curve per body region.

In Step 1, age, sex, and failure strain of each donor PMHS in the 0.5 strain/s experiments were selected (one sample per PMHS). As the resulting fracture risk function is intended for use with HBM strains obtained in vehicle impact simulations, it was assumed that the higher strain rate will be applicable for injurious impacts. Censoring status was assigned as exact for all failure strain values (Step 2). There was no indication of more than one failure mechanism in this controlled testing (Steps 3 and 4). Thus, the collected data for creation of the injury risk curve consist of failure strain, age, and sex from 58 PMHS (31 males and 27 females). Ages ranged from 17 to 99 years (mean 56.2 years; SD 26.1). The failure strain values were then recomputed from engineering to true strain (also known as logarithmic strain) values, to correspond to the format used with explicit finite element codes.

The available data were analyzed to select relevant covariates. An ANOVA test (R software v.3.6.3; stats package v.4.0.2) (R Core Team, 2020), was used to determine whether age and sex significantly influence the failure strain (in which case they should be modeled as covariates). Survival analysis was used to calculate the probability of survival [R; flexsurv package v.1.1.1 (Jackson, 2016)], in order to model the risk of rib material fracture as a function of failure strain and covariates. The probability of fracture was then computed as 1-(probability of survival). Upon inspection, the failure strain appeared to decrease log-linearly with age, hence an accelerated failure time (AFT) model was used. Log-normal, log-logistic, and Weibull distributions were considered for the parametric AFT model formulation, and the parameters were estimated with the maximum-likelihood method (Step 5).

In Step 6, the method of DFBETAs, with a threshold of 2 divided by the square root of sample size, was used to identify any overly influential data points (Belsley et al., 1980). The distribution assumptions were checked using Q–Q plots (Step 7). Tukey-Anscombe plots of model residual versus fitted values were checked.

For Steps 8–12, 95% confidence intervals for the survival curve were determined assuming an asymptotic normal distribution. The Akaike information criteria (AIC) and Quality indices (QIs) were computed for each of the log-normal, log-logistic, and Weibull distributions. QIs were computed based on the relative size of the confidence interval (Petitjean et al., 2012) at 5, 25, and 50% risk, for the ages 25, 50, and 75 years. The resulting risk functions were visually compared to the Forman 2012 and Forman smoothed risk functions. Finally, a single risk function was chosen for strain-based rib fracture risk based on QIs and the AIC values.

Population-Based Simulations to Quantify Effect on HBM Risk Predictions

To evaluate the effect of the newly developed strain-based risk function for a population of vehicle crashes and occupants at different ages, the stochastic simulations in Pipkorn et al. (2019) were reanalyzed by re-computing (using the newly developed rib fracture risk function) the probabilistic rib fracture risk using the rib strains from each of the stochastic simulations in Pipkorn et al. (2019). No new simulations were performed in this study. The method, including the National Automotive Sampling System Crashworthiness Data System (NASS/CDS) reference risk curves, is described in detail in Iraeus and Lindquist (2016) but is briefly described here. Two datasets from the NASS/CDS database were defined, one including frontal crashes (first analyzed in Iraeus and Lindquist, 2016) and one including side impacts (first analyzed in Pipkorn et al., 2019). Both datasets included both injured and uninjured occupants. Frontal crashes were selected based on NASS/CDS variable GAD1 = "F" and near-side impact were selected based on GAD1 = "L" (for drivers) or "R" (for front seat passengers). Other inclusion criteria were; NASS/CDS case years 2000–2012; vehicle model year 2000 or later (MY 2000+); the vehicle should had a deployed airbag (steering wheel airbag for drivers or passenger airbag for front seat passengers in frontal

impacts, and side airbag in side impacts); and the occupant should be an adult belted front-seat occupant (AGE 17+). Rollovers were excluded (ROLLOVER = 0). The set of frontal impact crashes contained 5,083 cases (1,474,869 cases weighted—i.e., representing national prevalence according to NASS/CDS national inflation factors), with 185 occupants (17,810 occupants weighted) sustaining two or more fractured ribs (NFR2+). The set of side impact crashes contained 569 cases (166,209 cases weighted), with 60 occupants (3,495 occupants weighted) sustaining a NFR2+ injury. Injury risk curves were created using weighted logistic regression (R software, version 3.6.3; survey package v.4.0). Occupant age and NASS/CDS-estimated change in velocity (Delta-v, as calculated by WinSmash) were considered as covariates. In the original analysis (Iraeus and Lindquist (2016)) vehicle instrument panel intrusion was also found to be a significant covariate. However, when compared to the simulations the intrusion was set to zero (both in the NASS/CDS regression model and in the simulations). Sex was also tested as covariate but was not significant ($p = 0.92$).

Next, two stochastic simulation studies, one frontal and one lateral, were defined as described in Pipkorn et al. (2019). For both studies, the SAFER HBM version 9 (Iraeus and Pipkorn, 2019; Pipkorn et al., 2019) was positioned in a parameterized finite element model of a vehicle interior (Iraeus and Lindquist, 2016). For frontal impacts, the vehicle model included a driver airbag, a load-limited seat belt, and dashboard and floor pan intrusion modeling. For the lateral impacts, side impact countermeasures (Pipkorn et al., 2019) and side structure intrusion modeling (**Figure 1**) were added. Using Latin Hypercube sampling, the vehicle and crash pulse parameters were varied according to distributions from the NASS/CDS datasets. The study consisted of 1,000 frontal impact simulation models and 100 lateral impact simulation models. More details about the method can be found in Iraeus and Lindquist (2016).

For each simulation, the NFR2+ risk was analyzed, using the probabilistic rib fracture framework with two different rib fracture risk functions: Forman smoothed and this study's newly developed risk function. In each case, the input to the probabilistic framework was the same peak first principal strains from each of the 24 rib cortical bone meshes in the HBM, extracted from each impact simulation. For both sets of results, quasi-binominal regression was used to create population risk curves, which were then compared to the NASS/CDS population risk curves.

RESULTS

Rib Fracture Risk Function

The ANOVA showed that age had a significant effect on (true) failure strain ($p < 0.0001$). Neither sex ($p = 0.335$) nor the interaction of sex and age ($p = 0.187$) were significant as predictors for failure strain at the $\alpha = 0.05$ significance level; they were thus excluded as covariates (for the complete ANOVA analysis output, see **Appendix Table B1**).

The DFBETAS statistics highlighted six failure strain and age observations from the sample as potentially overly influential. For each of these observations, the experimental stress-strain curve was visually compared to the stress-strain curves of other observations of similar age. No differences (such as very low or high failure strain, measurement signal noise, or differences in stress magnitude) could be identified. All the highlighted observations were therefore kept in the sample.

Injury risk was computed following a parametric AFT survival model with the alternatives of log-normal, log-logistic, and Weibull distributions. The distribution's parameters are presented in **Table 1**. Parametric fracture risk expressions for each distribution are given in **Appendix A**. Tukey-Anscombe plots showed no evident trends for the residuals (**Appendix Figure B1**). Q–Q plots of survival model residuals versus each distribution did not reveal any systematic violations of distribution assumptions (**Appendix Figure B2**).

All distributions obtained good QIs, given the confidence interval sizes (**Appendix Table B2**), so the QIs could not be used to select the best model fit. The selection was therefore based on the lowest AIC value. The lowest AIC value, $AIC_{min} = -399.30$, was obtained for the log-normal distribution. Weibull and log-logistic distributions obtained AIC values of -389.50 ($AIC_{min} + 9.80$) and -397.09 ($AIC_{min} + 2.21$), respectively. Therefore, the recommended risk function for rib fracture based on strain and age is modeled with the log-normal distribution. The parametric expression of the recommended rib fracture risk function, based on the log-normal distribution, is given in Eq. 1.

$$\textit{Fracture risk}\,(\textit{strain}, \textit{AGE}) = \frac{1}{2} + \frac{1}{2}\mathrm{erf}\left[\frac{\mathrm{LN}(\mathrm{strain}) - (\beta_0 + \beta_1 \cdot \mathrm{AGE})}{\sqrt{2} \cdot \alpha}\right] \quad (1)$$

where α, β_0, and β_1 can be found in **Table 1** for log-normal distribution parameters. LN() is the natural logarithm and erf() is the Gauss error function. The resulting risk function, relating strain and age to the risk of fracture, is plotted in **Figure 2** for subjects who are 25, 50, and 75 years old.

The recommended risk function (further referred to as the "newly developed") is compared to the previously existing risk functions, Forman 2012 and Forman smoothed, in **Figure 3** for three different ages. For the oldest individuals (75 years), the new risk function predicts slightly higher fracture risks than the previous risk functions. As an example, for the new risk function, a rib strain value of 0.02 is associated with 56% fracture risk for a 75-year-old, while for the Forman 2012 and Forman smoothed risk functions, the risk is approximately 40%. For 45-year-olds, the risk predictions are similar, while for the 25-year-olds, the newly developed risk function predicts lower risk.

Population-Based Simulations to Quantify Improvement of Risk Curves

For the frontal load case, using either the Forman smoothed risk function or the newly developed risk function within the probabilistic framework, the simulation model demonstrates a higher NFR2+ risk than the NASS/CDS risk curves, regardless of occupant age; see **Figure 4**. However, the distance between

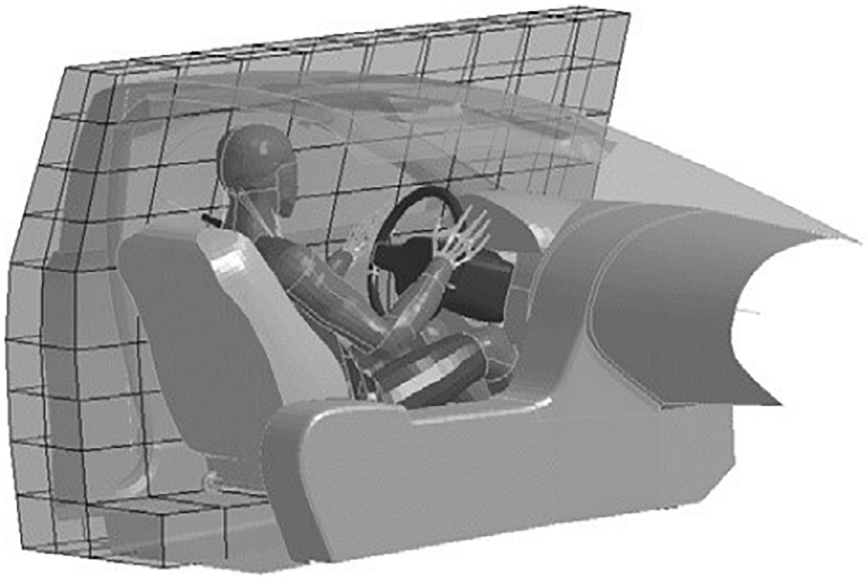

FIGURE 1 | SAFER HBM version 9 and the parametrized vehicle interior model used to estimate rib fracture risk in a population of NASS/CDS crashes. The coarse grid is used to apply the lateral velocity profile to the side structure.

the solid line (NASS/CDS estimated risk curve) and the dashed lines (simulation-based estimated risk curves) is more consistent over ages for the newly developed risk function. As an example, we examine the 50% risk: the probabilistic framework with the Forman smoothed risk function predicts 50% risk for a 30-year-old occupant at a Delta-v of 60 km/h; with the newly developed risk function, a 50% risk is predicted at a Delta-v of 69 km/h. The NASS/CDS estimate is 98 km/h, representing underestimations of 38 km/h and 29 km/h for the Forman smoothed and the new function, respectively. For a 70-year-old occupant, the corresponding underestimations of the Delta-v for the 50% NASS/CDS risk are 14 km/h (Forman smoothed) and 17 km/h (newly developed risk function). That, is, when comparing the risk for 30- and 70-year-olds, the differences between the NASS/CDS risk and the risk predicted by the simulation model are more consistent for the newly developed risk function.

The results for the lateral load case show similar trends; see **Figure 5**. Using the Forman smoothed risk function, the 50% risk for a 30-year-old occupant is predicted at a Delta-v of 43 km/h, an underestimation of 18 km/h. Using the newly developed risk function it is predicted at a Delta-v of 52 km/h, an underestimation of 9 km/h. For a 70-year-old occupant, the corresponding underestimations of the Delta-v for the 50% NASS/CDS risk are 10 km/h (Forman smoothed) and 11 km/h (newly developed risk function). As for the frontal load case, the simulation model predictions using the new function for the lateral load case are closer to the NASS/CDS risk estimates, and partly within the confidence bands.

TABLE 1 | Distribution parameters for Weibull, log-normal, and log-logistic distributions.

Distribution	α	β_0	β_1
Weibull	3.3562	−2.9236	−0.0114
Log-normal	0.3026	−2.9866	−0.0130
Log-logistic	5.6986	−2.9802	−0.0133

DISCUSSION

A new rib fracture risk function was developed using a parametric AFT survival model. AIC was used to select the log-normal distribution. It has been debated whether AIC is suitable for choosing the distribution, or if one should default to a Weibull distribution, or if the Area under the Receiver Operator

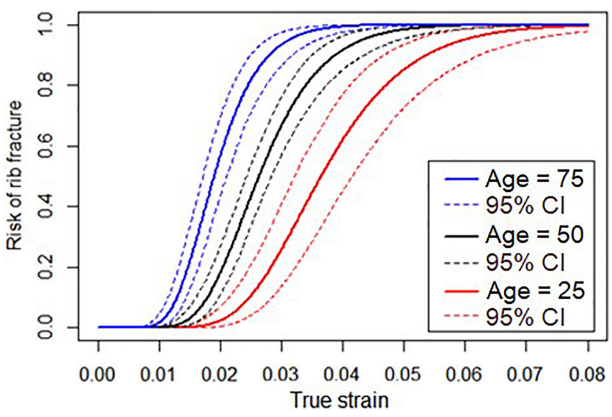

FIGURE 2 | Risk function relating true strain and risk of rib fracture for subjects who are 25, 50, and 75 years old.

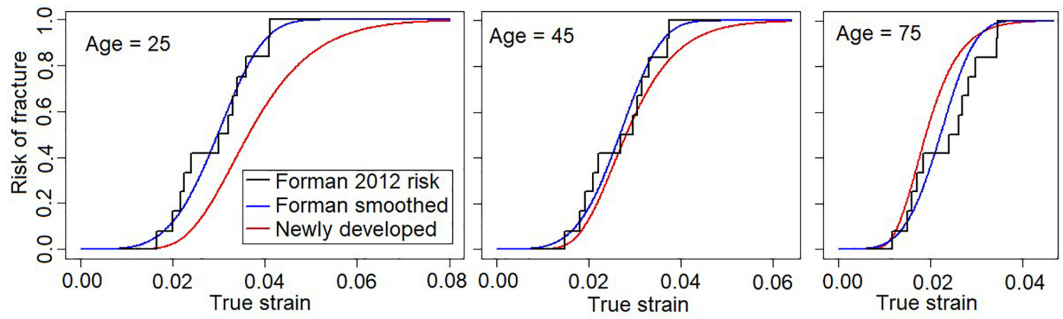

FIGURE 3 | Newly developed risk function (red) with Forman 2012 (black), and Forman smoothed (blue) functions for three different ages. **Left**, 25 years; **middle**, 45 years; **right**, 75 years.

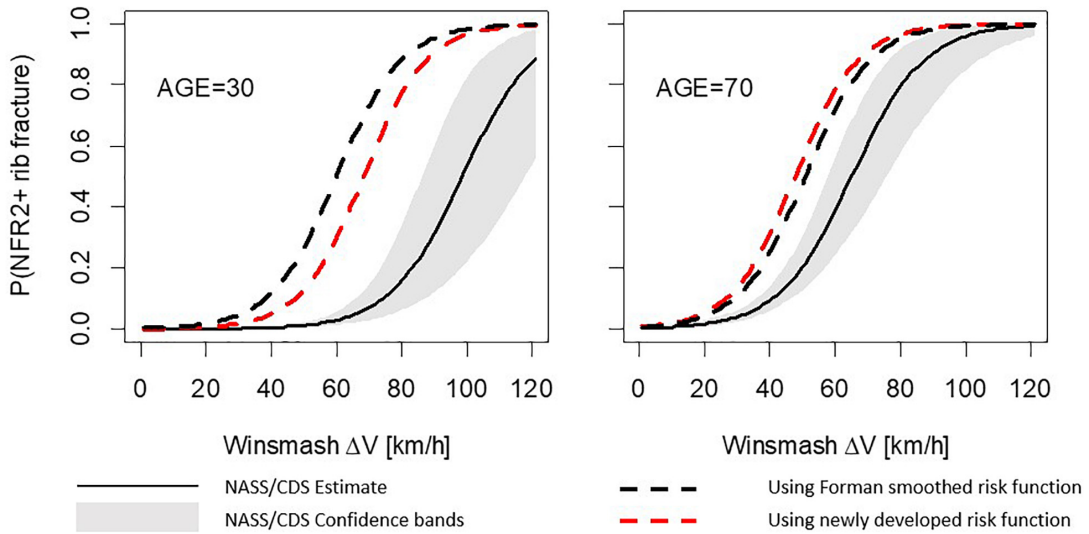

FIGURE 4 | Number of fractured ribs, NFR2+; predictions for the frontal stochastic simulations. Comparison between risk curves from probabilistic framework using the Forman smoothed and the newly developed risk functions for a 30-year-old occupant **(left)** and a 70-year-old occupant **(right)**.

Curve, indicating how good injury and non-injury data are classified, is a better metric (Yoganandan et al., 2016, 2017; McMurry and Poplin, 2017). For the developed risk curves the Weibull distribution performed worst in terms of AIC, but with an AIC delta of less than ten compared to the other distributions. As evidenced by the QIs being equally good for all distributions, there is no strong evidence against the Weibull distribution; however, there was no reason not to choose the log-normal distribution that had the lowest AIC value. Parameters for the Weibull distribution are reported in **Table 1**, should one prefer it. The dataset consisted of test-to-failure data only, hence, the Area under the Receiver Operator Curve cannot be calculated. Further details on choosing predictors of interest and identifying overly influential observations have been suggested (Yoganandan et al., 2016) and debated (McMurry and Poplin, 2017; Yoganandan et al., 2017). However, in the current data, no outliers were identified and the selection of predictors of interest was straightforward and based on previous literature, likely not requiring even more detailed analysis. Alternatives such as Bayesian survival analysis may offer improvements for small sample sizes (Cutcliffe et al., 2012), but with 58 tests the sample used is likely large enough for accurate estimations without it. Overall, the 12-step ISO approach appears to be a viable approach and well suited to the data in this study.

The age effect (the decrease in failure strain as a function of age) is greater for the newly developed risk function compared to the previous risk functions used with the probabilistic framework (Forman 2012 and Forman smoothed), see **Figure 3**. In the current study, the AFT model was used for the survival analysis, resulting in a proportional relationship between age and failure strain. The acceleration factor is $\exp(\beta_1 \cdot AGE)$. Using β_1 for the recommended log-normal distribution from **Table 1**, after 10 years of aging a subject will only require 87.8% of the strain to predict the same risk of fracture as before. In other words, according to our modeling, the failure strain in human rib cortical bone is reduced by 12.2% per decade of aging. This reduction appears greater than both the 5.1% reduction

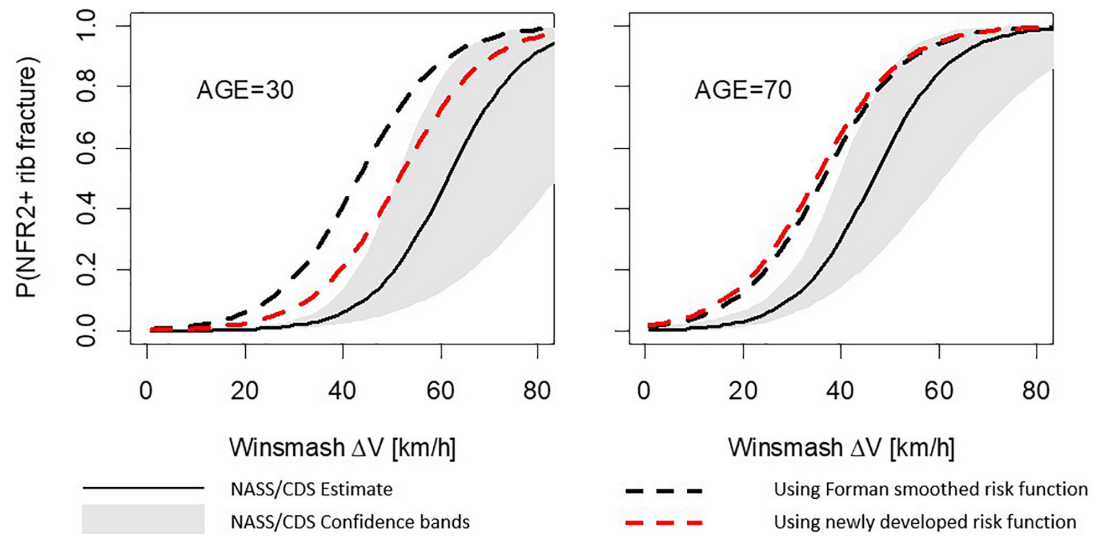

FIGURE 5 | Number of fractured ribs, NFR2+; predictions for the lateral stochastic simulations. Comparison between risk curves from probabilistic framework using Forman smoothed and the newly developed risk functions for a 30-year-old occupant **(left)** and 70-year-old occupant **(right)**.

(Carter and Spengler, 1978) used in the Forman 2012 risk function and the 9% reported by McCalden et al. (1993). To investigate if the age-dependent decrease found in the current study is reasonable, we can compare the risk predictions from the newly developed function to the failure strains in the dataset used. In **Figure 6**, the strains required for 5, 50, and 95% risk predictions from the newly developed risk function across the 17–99 year age span are plotted with the age and failure strain of each subject. A visual comparison demonstrates that the strains representing a 50% risk level appear centered between the subject failure strains across the age span. In other words, for a given strain and age, a risk prediction of 50%, corresponds well to the expectation that half of the test samples of that age failed at that level of strain. Similarly, for the 5% risk level, we can expect that most, but not all, samples will survive that level of strain. Thus, the 12.2% reduction factor appears to be a reasonable estimation of the age-dependent decrease in the subject failure strains.

Sex was not found to have a significant effect on the failure strain; this result is in agreement with the findings in Katzenberger et al. (2020), where it was shown that sex did not have any statistically significant effect on any of the rib cortical bone material parameters, yield stress and strain, elastic modulus or failure stress, at either of the strain rates (0.5 and 0.005 strain/s). Sex was not included as a covariate (as it was not significant) in the NASS/CDS regression model, and the stochastic simulations were only carried out using a model of the average male. This result is in conflict with some epidemiological studies, Bose et al. (2011); Carter et al. (2014), and Forman et al. (2019) who found an increased rib fracture risk for females compared to males. However, it should be noted that the two covariates included in the current study, Delta-v and age, are the two most important parameters as they have the largest effect size. In Forman et al. (2019) sex has the same effect on rib fracture risk as changing Delta-v by 5.8 km/h or occupant age by 11 years. Thus, including just Delta-v and age as parameters in the stochastic simulation seems to be a reasonable first approximation.

In the stochastic simulation study, it was shown that the newly developed risk function, in particular the updated age effect, gives results that are more consistent with rib fracture risk estimated directly from NASS/CDS data. In general, the stochastic simulations predicted higher risk than the NASS/CDS did. The 50% rib fracture risk for the lateral stochastic simulations was estimated for a Delta-v 9 km/h (30-year-old) to 11 km/h (70-year-old) lower than the risk for NASS/CDS data. For the frontal stochastic simulations, the corresponding values were 29 km/h (30-year-old) to 17 km/h (70-year-old). Hence, all simulation results predicted higher risk than the NASS/CDS estimates. The stochastic simulations are defined using a few parameters, with distribution based on NASS/CDS. Most likely there are many additional parameters significantly influencing injury outcome, not reported in databases like NASS/CDS (simply because they cannot be measured) and thus cannot easily be included in stochastic simulations. In addition, as safety system parameters are proprietary information, these had to be estimated based on reverse engineering from US NCAP tests. That in combination with a sampling strategy not considering potential dependency of these parameters, makes it highly likely that the generic safety system will perform less optimal compared to systems in production vehicles.

It should also be noted that the rib fracture risk estimated from the NASS/CDS data should not be considered as an absolute truth. Several studies have shown that the true fracture rate is under-reported by as much as 50–70% when fractures are diagnosed using clinical CT (Crandall et al., 2000; Lederer et al., 2004; Schulze et al., 2013), and thus the NASS/CDS risk curves might underestimate the true fracture risk. This

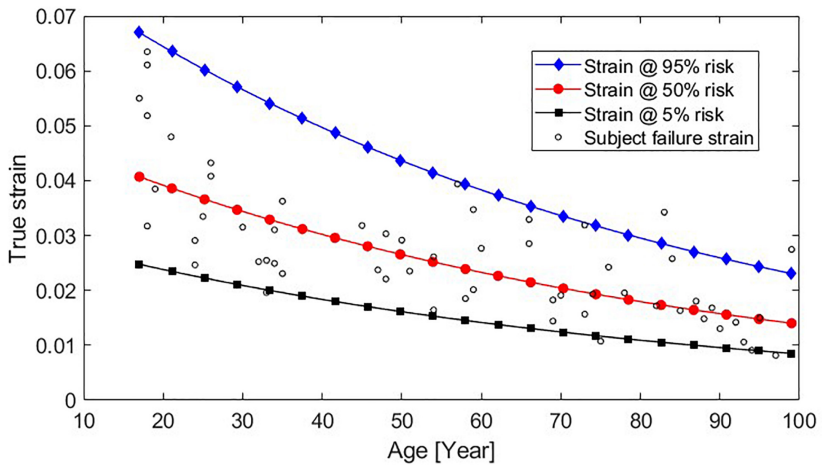

FIGURE 6 | Strains that result in 95, 50, and 5% predicted fracture risk across subjects aged 17–99 years, using the newly developed function plotted with the failure strain and age data from each subject.

means that probably neither the injury risk from the stochastic simulations nor the real-life estimated risk is correct. However, comparing the stochastic simulation results evaluated using the newly developed risk function with the Forman smoothed risk function and the NASS/CDS estimated risk, the newly developed risk curve seems to estimate the age effect better than the Forman smoothened risk function.

The main effect on HBM rib fracture risk predictions of using the newly developed risk function instead of the Forman 2012 or the Forman smoothed risk functions will be a lower rib fracture risk predicted for younger occupants for the same level of rib strain. Out of the 36,560 people fatally injured in motor vehicle accidents in the United States during 2018, 6,087 were aged between 16 and 24 years (National Center for Statistics and Analysis, 2020). Kent et al. (2005) found that 75% of fatal injuries to younger drivers (16–33 years old) protected by both a seatbelt and an airbag in a frontal impact were to the head, whereas older occupants (65+ years old) crashed at lower Delta-v's but were more likely to sustain a fatal chest injury. In order to reduce fatalities, for younger occupants a restraint system could apply a higher seatbelt restraint force in frontal impacts, in order to restrict head forward motion relative to the vehicle and thus avoid a hard head impact; for older occupants, a lower seatbelt restraint force in lower-severity accidents would be appropriate to mitigate chest injuries. That is, a plausible safety-system design solution would incorporate age-adaptive restraints. The newly developed risk function can be a useful tool in the design of such a restraint.

Limitations

The rib fracture risk curve is based on failure strains obtained in 0.5 strain/s experiments and should therefore be used for strains obtained under similar strain rates. However, Katzenberger et al. (2020) found no statistically significant differences in failure strains between the 0.5 and 0.005/s strain rates tested. Experiments performed at yet higher loading rates may reveal if there is a rate effect to rib failure strain that need to be considered in future risk modeling.

Further, the experiments were tensile, and thus the developed risk function is only applicable to tensile strain, even though the strain experienced by ribs in motor vehicle accidents is not known. By using strain gages attached to the cutaneous side of PMHS's ribs in an experiment simulating a belted frontal impact, Duma et al. (2005) demonstrated that the first principal strain was closely aligned to the axial strain (along the rib) and that a majority of ribs sustained tensile loading until fracture. Trosseille et al. (2008) measured the strain at PMHS's ribs during different impact scenarios, ranging from frontal to lateral. The pattern of axial strain along the rib ranged from tensile to compressive and the distribution of strain was dependent on both loading direction and impacting object. Hence, if there are large shear or compressive rib strains predicted by an HBM, the resulting rib fracture risks obtained from the newly developed function (with tensile rib strains from the HBM simulation) might not reveal the full extent of the fracture risk.

There are many limitations with the stochastic simulations, of which some have been discussed above. In addition to using only one anthropometry, i.e., a model of an average male, only one initial posture was used, Further, injury risk age dependency was only modeled as change in ultimate strain, where in reality there are many other age related changes on both material and structural level.

CONCLUSION

- A new strain-based, age-adjusted risk function that can be used to predict rib fracture risk together with finite element HBMs has been developed.
- The new fracture risk function indicates that human rib cortical bone failure strain is reduced by 12.2% per decade of aging.

- The new fracture risk function can be used directly within the existing probabilistic framework for estimating rib fracture risk.
- In stochastic frontal impacts the 50% risk of NFR2+ for a 30-year-old occupant was estimated at a DV of 60 km/h (Forman smoothed) and at 69 km/h with the newly developed risk function. For 70-year-olds the 50% NFR2+ Delta-v's where 51 and 48 km/h using Forman smoothed and the newly developed risk function, respectively.
- In stochastic lateral impacts the 50% risk of NFR2+ for 30-year-olds was at Delta-v's of 43 km/h (Forman smoothed) and 52 km/h (newly developed). For 70-year-olds the Delta-v's were 35 and 36 km/h for Forman smoothed and the newly developed risk function, respectively.

DATA AVAILABILITY STATEMENT

The original contributions presented in the study are included in the article/supplementary material, further inquiries can be directed to the corresponding author/s.

AUTHOR CONTRIBUTIONS

K-JL: conceptualization, methodology, project administration, supervision, validation, and writing – original draft. AB: data curation, formal analysis, visualization, and writing – original draft. JI: conceptualization, formal analysis, visualization, and writing – original draft, reviewing, and editing. BP: conceptualization, supervision, resources, and writing – reviewing and editing. NL: conceptualization, supervision, resources, methodology, funding acquisition, and writing – reviewing and editing. All authors contributed to the article and approved the submitted version.

FUNDING

The work performed in this study was partly funded by FFI-Strategic Vehicle Research and Innovation, Vinnova, the Swedish Energy Agency, the Swedish vehicle industry, by the OSCCAR project (which received funding from the European Union Horizon 2020 Research and Innovation Programme under Grant Agreement No. 768947), and Autoliv Research. This document reflects only the author's view, the funding organizations are not responsible in any way for any use that may be made of the information it contains.

ACKNOWLEDGMENTS

The work was carried out at SAFER, the Vehicle and Traffic Safety Centre at Chalmers University, Sweden. The authors thank K. Mayberry for language revisions.

REFERENCES

Battle, C. E., Hutchings, H., and Evans, P. A. (2012). Risk factors that predict mortality in patients with blunt chest wall trauma: a systematic review and meta-analysis. *Inj. Int. J. Care Inj.* 43, 8–17. doi: 10.1016/j.injury.2011.01.004

Belsley, D. A., Kuh, E., and Welsch, R. E. (1980). *Regression Diagnostics: Identifying Influential Data and Sources of Collinearity*. Hoboken, NJ: John Wiley & Sons, Inc.

Bose, D., Segui-Gomez, M., and Crandall, J. R. (2011). Vulnerability of female drivers involved in motor vehicle crashes: an analysis of US population at risk. *Am. J. Public Health.* 101, 2368–2373. doi: 10.2105/AJPH.2011.300275

Brumbelow, M. L. (2019). "Front crash injury risks for restrained drivers in good-rated vehicles by age, impact configuration, and EDR-based Delta V," in *Proceedings of the IRCOBI Conference*, (Florence).

Burstein, A. H., Reilly, D. T., and Martens, M. (1976). Aging of bone tissue: mechanical properties. *J. Bone Joint Surg. Am.* 58, 82–86. doi: 10.2106/00004623-197658010-00015

Carter, D. R., and Spengler, D. M. (1978). Mechanical properties and composition of cortical bone. *Clin. Orthop. Related Res.* 135, 192–217.

Carter, P. M., Flannagan, C. A. C., Reed, M. P., Cunningham, R. M., and Rupp, J. D. (2014). Comparing the effects of age, BMI and gender on severe injury (AIS 3+) in motor-vehicle crashes. *Accid. Anal. Prev.* 72, 146–160. doi: 10.1016/j.aap.2014.05.024

Crandall, J., Kent, R., Patrie, J., Fertile, J., and Martin, P. (2000). Rib fracture patterns and radiologic detection–a restraint-based comparison. *Annu. Proc. Assoc. Adv. Automot. Med.* 44, 235–260.

Cutcliffe, H. C., Schmidt, A. L., Lucas, J. E., and Bass, C. R. (2012). How few? Bayesian statistics in injury biomechanics. *Stapp. Car Crash J.* 56, 349–386.

Davidsson, J., Carroll, J., Hynd, D., Lecuyer, E., Song, E., Trosseille, X., et al. (2014). "Development of injury risk functions for use with the THORAX Demonstrator; an updated THOR," in *Proceedings of the IRCOBI Conference*, (Berlin).

Duma, S., Stitzel, J., Kemper, A., McNally, C., Kennedy, E., and Matsuoka, F. (2005). "Non-censored rib fracture date from dynamic belt loading tests on the human cadaver Thorax," in *Proceedings of the 19th International Technical Conference on the Enhanced Safety of Vehicles*, (Washington DC: NHTSA), 15.

Forman, J., Poplin, G. S., Shaw, C. G., McMurry, T. L., Schmidt, K., Ash, J., et al. (2019). Automobile injury trends in the contemporary fleet: belted occupants in frontal collisions. *Traffic Inj. Prev.* 20, 607–612. doi: 10.1080/15389588.2019.1630825

Forman, J. L., Kent, R. W., Mroz, K., Pipkorn, B., Bostrom, O., and Segui-Gomez, M. (2012). "Predicting rib fracture risk with whole-body finite element models: development and preliminary evaluation of a probabilistic analytical framework," in *Proceedings of the 56th AAAM Annual Conference. Annals of advances in automotive medicine*, Vol. 56, (Seattle, WA), 109–124.

International Organization for Standardization (2014). *Road Vehicles—Procedure to Construct Injury Risk Curves for the Evaluation of Occupant Protection in Crash Tests. Report No.: ISO/TS 18506*. Geneva: International Organization for Standardization.

Iraeus, J., and Lindquist, M. (2016). Development and validation of a generic finite element vehicle buck model for the analysis of driver rib fractures in real life nearside oblique frontal crashes. *Accid. Anal. Prev.* 95, 42–56. doi: 10.1016/j.aap.2016.06.020

Iraeus, J., and Lindquist, M. (2020). Analysis of minimum pulse shape information needed for accurate chest injury prediction in real life frontal crashes. *Int. J. Crashworthiness* 1–8. doi: 10.1080/13588265.2020.1769004

Iraeus, J., and Pipkorn, B. (2019). "Development and validation of a generic finite element ribcage to be used for strain-based fracture prediction," in *Proceedings of the IRCOBI Conference*, (Florence), 193–210.

Jackson, C. (2016). flexsurv: a platform for parametric survival modeling in R. *J. Stat. Softw.* 70, 1–33. doi: 10.18637/jss.v070.i08

Katzenberger, M. J., Albert, D. L., Agnew, A. M., and Kemper, A. R. (2020). Effects of sex, age, and two loading rates on the tensile material properties of human rib cortical bone. *J. Mech. Behav. Biomed. Mater.* 102:103410. doi: 10.1016/j.jmbbm.2019.103410

Kemper, A. R., McNally, C., Kennedy, E. A., Manoogian, S. J., Rath, A. L., Ng, T. P., et al. (2005). Material properties of human rib cortical bone from dynamic tension coupon testing. *Stapp Car Crash J.* 49, 199–230.

Kemper, A. R., McNally, C., Pullins, C. A., Freeman, L. J., Duma, S. M., and Rouhana, S. M. (2007). The biomechanics of human ribs: material and structural properties from dynamic tension and bending tests. *Stapp Car Crash J.* 51, 235–273.

Kent, R., Henary, B., and Matsuoka, F. (2005). On the fatal crash experience of older drivers. *Annu. Proc. Assoc. Adv. Automot. Med.* 49, 371–391.

Kullgren, A., Axelsson, A., Stigson, H., and Ydenius, A. (2019). "Developments in car crash safety and comparisons between results from EURO NCAP tests and real-world crashes," in *Proceedings of the 26th International Technical Conference on the Enhanced Safety of Vehicles (ESV)*, (Eindhoven).

Lederer, W., Mair, D., Rabl, W., and Baubin, M. (2004). Frequency of rib and sternum fractures associated with out-of-hospital cardiopulmonary resuscitation is underestimated by conventional chest X-ray. *Resuscitation* 60, 157–162. doi: 10.1016/j.resuscitation.2003.10.003

Lindahl, O., and Lindgren, A. G. H. (1967). Cortical bone in man II. variation in tensile strength with age and sex. *Acta Orthop. Scand.* 38, 141–147. doi: 10.3109/17453676708989628

McCalden, R. W., McGeough, J. A., Barker, M. B., and Court-Brown, C. M. (1993). Age-related changes in the tensile properties of cortical bone. *J. Bone Joint Surg.* 75-A, 1193–1205. doi: 10.2106/00004623-199308000-00009

McMurry, T. L., and Poplin, G. S. (2015). Statistical considerations in the development of injury risk functions. *Traffic Inj. Prev.* 16, 618–626. doi: 10.1080/15389588.2014.991820

McMurry, T. L., and Poplin, G. S. (2017). A note on "Deriving injury risk curves using survival analysis from biomechanical experiments". *J. Biomech.* 52, 187–188. doi: 10.1016/j.jbiomech.2016.09.047

National Center for Statistics and Analysis. (2020). *Traffic Safety Facts 2018 Annual Report: A Compilation of Motor Vehicle Crash Data Report No. DOT HS 812 981*. Washington, DC: National Highway Traffic Safety Administration.

Petitjean, A., and Trosseille, X. (2011). Statistical simulations to evaluate the methods of the construction of injury risk curves. *Stapp Car Crash J.* 55, 411–440.

Petitjean, A., Trosseille, X., Praxl, N., Hynd, D., and Irwin, A. (2012). Injury risk curves for the worldSID 50th male dummy. *Stapp Car Crash J.* 56, 323–347.

Pipkorn, B., Iraeus, J., Björklund, M., Bunketorp, O., and Jakobsson, L. (2019). "Multi-scale validation of a rib fracture prediction method for human body models," in *Proceedings of the IRCOBI Conference*, (Florence), 175–192.

Pipkorn, B., Iraeus, J., Lindkvist, M., Puthan, P., and Bunketorp, O. (2020). Occupant injuries in light passenger vehicles—A NASS study to enable priorities for development of injury prediction capabilities of human body models. *Accid. Anal. Prev.* 138:105443. doi: 10.1016/j.aap.2020.105443

Praxl, N. (2011). "How reliable are injury risk curves?," in *Proceedings of the 22nd Enhanced Safety Vehicles Conference*, (Washington DC), 9.

R Core Team (2020). *R: A Language and Environment for Statistical Computing*. Vienna: R Foundation for Statistical Computing.

Schulze, C., Hoppe, H., Schweitzer, W., Schwendener, N., Grabherr, S., and Jackowski, C. (2013). Rib fractures at postmortem computed tomography (PMCT) validated against the autopsy. *Forensic Sci. Int.* 233, 90–98. doi: 10.1016/j.forsciint.2013.08.025

Sirmali, M., Türüt, H., Topçu, S., Gülhan, E., Yazici, Ü, Kaya, S., et al. (2003). A comprehensive analysis of traumatic rib fractures: morbidity, mortality and management. *Eur. J. Cardiothorac. Surg.* 24, 133–138. doi: 10.1016/S1010-7940(03)00256-2

Trosseille, X., Baudrit, P., Leport, T., and Vallancien, G. (2008). Rib cage strain pattern as a function of chest loading configuration. *Stapp Car Crash J.* 52, 205–231. doi: 10.4271/2008-22-0009

Veysi, V. T., Nikolaou, V. S., Paliobeis, C., Efstathopoulos, N., and Giannoudis, P. V. (2009). Prevalence of chest trauma, associated injuries and mortality: a level I trauma centre experience. *Int. Orthop.* 33, 1425–1433. doi: 10.1007/s00264-009-0746-9

Weaver, A. A., Talton, J. W., Barnard, R. T., Schoell, S. L., Swett, K. R., and Stitzel, J. D. (2015). Estimated injury risk for specific injuries and body regions in frontal motor vehicle crashes. *Traffic Inj. Prev.* 16(Suppl. 1), S108–S116. doi: 10.1080/15389588.2015.1012664

Yoganandan, N., Banerjee, A., Hsu, F.-C., Bass, C. R., Voo, L., Pintar, F. A., et al. (2016). Deriving injury risk curves using survival analysis from biomechanical experiments. *J. Biomech.* 49, 3260–3267. doi: 10.1016/j.jbiomech.2016.08.002

Yoganandan, N., Banerjee, A., Hsu, F.-C., Bass, C. R., Voo, L., Pintar, F. A., et al. (2017). Response to letter to the editor on "Deriving injury risk curves using survival analysis from biomechanical experiments". *J. Biomech.* 52, 189–190. doi: 10.1016/j.jbiomech.2016.12.015

Conflict of Interest: The authors declare that the research was conducted in the absence of any commercial or financial relationships that could be construed as a potential conflict of interest.

APPENDIX A

Parametric expressions for fracture risk functions based on Weibull, log-normal, and log-logistic distributions are presented in Eqs A1, A2, and A3, respectively. Values for parameters α, β_0, and β_1 can be found in **Table 1**. LN() is the natural logarithm, exp() is the natural exponential function and erf() is the Gauss error function.

$$Weibull\ risk\,(strain, AGE) = 1 - exp\left(-\left(\frac{strain}{exp(\beta_0 + \beta_1 \cdot AGE)}\right)^{\alpha}\right) \tag{A1}$$

$$Log - normal\ risk\,(strain,\ AGE) = \frac{1}{2} + \frac{1}{2}\mathrm{erf}\left[\frac{\mathrm{LN}(\mathrm{strain}) - (\beta_0 + \beta_1 \cdot \mathrm{AGE})}{\sqrt{2} \cdot \alpha}\right] \tag{A2}$$

$$Log - logistic\ risk\,(strain, AGE) = 1 - \frac{1}{1 + \left(\frac{strain}{exp(\beta_0 + \beta_1 \cdot AGE)}\right)^{\alpha}} \tag{A3}$$

APPENDIX B

The output statistics from the ANOVA analysis are presented in **Table B1**.

Tukey-Anscombe plots of residuals versus fitted values are shown in **Figure B1**.

Q–Q plots of survival model residuals versus the distribution assumptions are shown in **Figure B2**.

In **Table B2** the QIs computed based on the relative sizes of the 95% confidence intervals are presented.

TABLE B1 | ANOVA analysis results.

Covariate	Coefficient	Df	Sum square	Mean square	*F*-value	*P* (>*F*)
Age	−1.54E-04	1	4.44E-03	4.44E-03	6.00E+01	2.57E-10
Sex	8.88E-03	1	7.00E-05	7.00E-05	9.45E-01	3.35E-01
Age × sex	−1.18E-04	1	1.32E-04	1.32E-04	1.79E+00	1.87E-01
Residuals		54	4.00E-03	7.40E-05		

TABLE B2 | Relative size of 95% confidence interval and the corresponding quality index (QI) for Weibull, log-normal, and log-logistic distributions.

Distribution	Age	Risk of injury (%)	Relative CI size	Quality index
		5	0.423	Good
	25	25	0.281	Good
		50	0.237	Good
		5	0.431	Good
Weibull	50	25	0.255	Good
		50	0.177	Good
		5	0.464	Good
	75	25	0.289	Good
		50	0.215	Good
		5	0.334	Good
	25	25	0.260	Good
		50	0.253	Good
		5	0.279	Good
Log-logistic	50	25	0.175	Good
		50	0.158	Good
		5	0.293	Good

(Continued)

TABLE B2 | Continued

Distribution	Age	Risk of injury (%)	Relative CI size	Quality index
	75	25	0.218	Good
		50	0.196	Good
		5	0.283	Good
	25	25	0.238	Good
		50	0.241	Good
		5	0.248	Good
Log-normal	50	25	0.181	Good
		50	0.153	Good
		5	0.262	Good
	75	25	0.205	Good
		50	0.195	Good

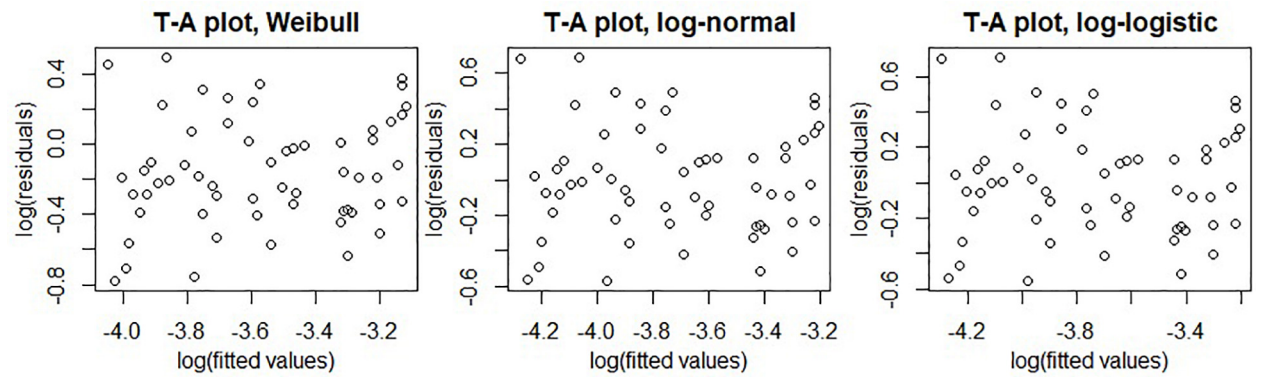

FIGURE B1 | Tukey-Anscombe plots of residuals versus fitted values for fitted Weibull **(left)**, log-logistic **(middle)**, and log-normal **(right)** survival models.

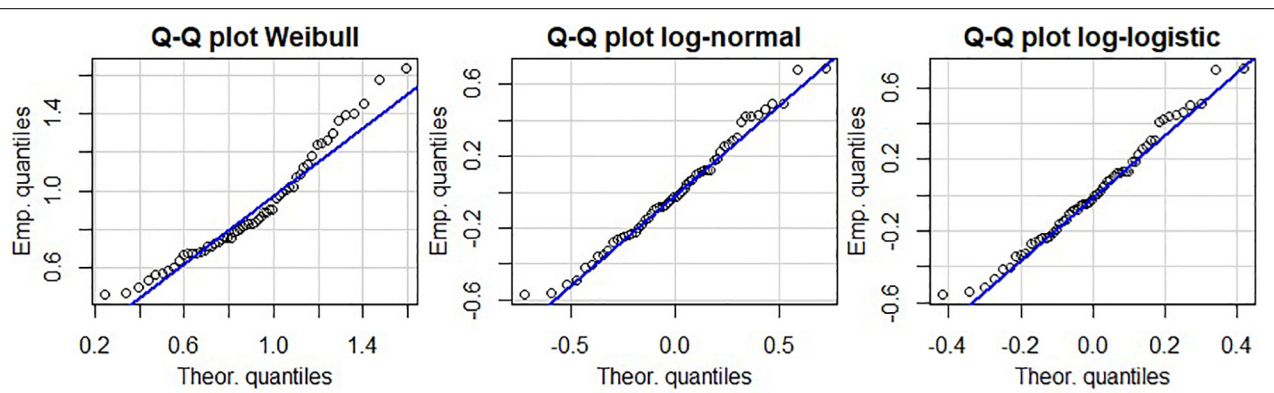

FIGURE B2 | Q–Q plots of residuals versus fitted Weibull **(left)**, log-logistic **(middle)**, and log-normal **(right)** distributions.

frontiers in Bioengineering and Biotechnology

ORIGINAL RESEARCH
published: 08 June 2021
doi: 10.3389/fbioe.2021.684003

Dynamic Responses of Female Volunteers in Rear Impact Sled Tests at Two Head Restraint Distances

Anna Carlsson[1], Stefan Horion[2], Johan Davidsson[3], Sylvia Schick[2], Astrid Linder[3,4], Wolfram Hell[2] and Mats Y. Svensson[3]*

[1] Chalmers Industrial Technology (Chalmers Industriteknik), Gothenburg, Sweden, [2] Institute for Legal Medicine, Ludwig-Maximilians-Universitaet (LMU), Munich, Germany, [3] Vehicle Safety Division, Chalmers University of Technology, Gothenburg, Sweden, [4] Swedish National Road and Transport Research Institute (VTI), Gothenburg, Sweden

OPEN ACCESS

Edited by:
Michael Kleinberger, United States Army Research Laboratory, United States

Reviewed by:
John Bolte, The Ohio State University, United States
Chantal Parenteau, Exponent Inc., United States
Shannon Kroeker, MEA Forensic Engineers & Scientists, Canada

***Correspondence:**
Anna Carlsson
anna.carlsson@chalmers.se

Specialty section:
This article was submitted to Biomechanics, a section of the journal Frontiers in Bioengineering and Biotechnology

Received: *22 March 2021*
Accepted: *14 May 2021*
Published: *08 June 2021*

Citation:
Carlsson A, Horion S, Davidsson J, Schick S, Linder A, Hell W and Svensson MY (2021) Dynamic Responses of Female Volunteers in Rear Impact Sled Tests at Two Head Restraint Distances. Front. Bioeng. Biotechnol. 9:684003. doi: 10.3389/fbioe.2021.684003

The objective of this study was to assess the biomechanical and kinematic responses of female volunteers with two different head restraint (HR) configurations when exposed to a low-speed rear loading environment. A series of rear impact sled tests comprising eight belted, near 50th percentile female volunteers, seated on a simplified laboratory seat, was performed with a mean sled acceleration of 2.1 g and a velocity change of 6.8 km/h. Each volunteer underwent two tests; the first test configuration, HR10, was performed at the initial HR distance ∼10 cm and the second test configuration, HR15, was performed at ∼15 cm. Time histories, peak values and their timing were derived from accelerometer data and video analysis, and response corridors were also generated. The results were separated into three different categories, $HR10_C$ (N = 8), $HR15_C$ (N = 6), and $HR15_{NC}$ (N = 2), based on: (1) the targeted initial HR distance [10 cm or 15 cm] and (2) whether the volunteers' head had made contact with the HR [Contact (C) or No Contact (NC)] during the test event. The results in the three categories deviated significantly. The greatest differences were found for the average peak head angular displacements, ranging from 10° to 64°. Furthermore, the average neck injury criteria (NIC) value was 22% lower in $HR10_C$ (3.9 m^2/s^2), and 49% greater in $HR15_{NC}$ (7.4 m^2/s^2) in comparison to $HR15_C$ (5.0 m^2/s^2). This study supplies new data suitable for validation of mechanical or mathematical models of a 50th percentile female. A model of a 50th percentile female remains to be developed and is urgently required to complement the average male models to enhance equality in safety assessments. Hence, it is important that future protection systems are developed and evaluated with female properties taken into consideration too. It is likely that the HR15 test configuration is close to the limit for avoiding HR contact for this specific seat setup. Using both datasets ($HR15_C$ and $HR15_{NC}$), each with its corresponding HR contact condition, will be possible in future dummy or model evaluation.

Keywords: crash testing, females, soft tissue neck injury, rear impact, sled testing, vehicle safety, volunteers, whiplash

INTRODUCTION

Today, low-to-moderate speed rear impact testing is performed with 50th percentile male dummies, mainly with the BioRID II, which limits the assessment and development of whiplash protection systems with regard to female occupant protection (Linder and Svensson, 2019). In terms of stature and mass, the 50th percentile male crash test dummy roughly corresponds to the 90th–95th percentile female (Welsh and Lenard, 2001), resulting in females not being well represented by the existing low velocity rear impact male dummy; BioRID II. Accident data shows that females have a greater risk of sustaining whiplash injuries than males, even under similar crash conditions (Kihlberg, 1969; O'Neill et al., 1972; Otremski et al., 1989; Morris and Thomas, 1996; Temming and Zobel, 1998; Chapline et al., 2000; Krafft et al., 2003; Storvik et al., 2009; Carstensen et al., 2011). According to these studies, the whiplash injury risk is up to three times higher for females compared to males.

Passenger vehicles equipped with advanced whiplash protection systems posed on average a ∼50% lower risk of long-term whiplash injuries for occupants in rear impacts, than for occupants in passenger vehicles manufactured after 1997, without whiplash protection systems installed (Kullgren et al., 2007). Nevertheless, insurance data show that whiplash injuries account for 63% of all injuries leading to permanent medical impairment sustained in passenger vehicles on the Swedish market (Gustafsson et al., 2015). In rear impacts, the risk reduction for permanent medical impairment is approximately 30% greater for males than for females according to insurance claims records (Kullgren and Krafft, 2010), which effectively means that the difference between female and male whiplash injury risk has increased, although the general whiplash injury risk has reduced. In recent years, injury statistics show that whiplash injuries still present a major problem, and that the whiplash injury risk females are exposed to is substantially higher (Kullgren et al., 2020).

Low-speed rear impact volunteer tests have shown that females have greater horizontal head accelerations, greater (or similar) horizontal T1 accelerations, lesser head and T1 rearward displacements, lesser (or similar) Neck Injury Criterion (NIC) values, and more pronounced rebound motions in comparison to males (Siegmund et al., 1997; Mordaka and Gentle, 2003; Viano, 2003; Ono et al., 2006; Linder et al., 2008; Schick et al., 2008; Carlsson et al., 2011, 2012). The results show that there are characteristic differences in the dynamic response between males and females in rear impacts.

Based on mathematical simulations, Mordaka and Gentle (2003) concluded that a "scaled down male model is not adequate to simulate female responses even though the scaling constitutes a good height and mass match" (p. 52). Additionally, Vasavada et al. (2008) found that "male and female necks are not geometrically similar and indicate that a female-specific model will be necessary to study gender differences in neck-related disorders" (p. 114). That is, a female model must be based on data from tests with females.

The greatest whiplash injury frequencies are associated with females and males of average statures (Kihlberg, 1969; Carlsson et al., 2014). Based on US injury statistics, the highest whiplash injury frequency was recorded for the statures 162.6–165.1 cm (64–65 in) for the females and 175.3–177.8 cm (69–70 in) for the males, both close to the average statures of the US population (females: 161.8 cm (63.7 in), males: 175.3 cm (69.0 in); Schneider et al., 1983). Based on Swiss and Swedish insurance records, Carlsson et al. (2014) concluded that the stature and mass of the females most frequently injured correspond well with the average stature and mass of the female populations in these countries.

Hence, there is a need for 50th percentile female models, physical and/or computational crash test dummies and human body models (HBMs), to further improve the vehicle safety for both females and males (Carlsson, 2012; Carlsson et al., 2017). Human dynamic response data is important when developing and evaluating such occupant models. Thus, the objective of this study was to generate dynamic response data and investigate differences in seat interaction for near 50th percentile females in a laboratory seat at two different head restraint (HR) configurations.

MATERIALS AND METHODS

A series of rear impact sled tests comprising female volunteers was performed at a velocity change of ∼7 km/h with two nominal HR distances. The test series was approved by the ethical committee at the Ludwig-Maximilian University in Munich, Germany, Approval Reference Number 319-07 (Address: Ethikkommission der Medizinischen Fakultät der LMU, Pettenkoferstr. 8a, 80336 Munich, Germany).

Volunteers

Female volunteers were recruited by advertisements at the Ludwig-Maximilian University in Munich, Germany. Potential subjects were preselected by telephone interviews. Exclusion criteria included any known histories of spinal symptoms; former whiplash associated disorders (WADs); former fractures and/or surgical interventions to the vertebral column; familial or hereditary spinal disorders, disc protrusion or herniations, rheumatism and rheumatoid diseases, further orthopaedic diseases, syndromes and symptoms such as, arthrosis, arthritis, multiple cartilaginous exostoses, scoliosis, spondylolisthesis; having been under treatment (massage/non-steroidal anti-inflammatory drugs/exercises/chiropractic or other therapies) for the back/neck during the 6 months preceding the tests. The volunteers were examined by a physician prior to the tests and further exclusions were made based on these objective findings or if subjective discomfort in the head/neck/shoulders/back existed on the test day. Anthropometric data were obtained on the same occasion.

Eight female volunteers participated in the test series. Their age ranged between 22 and 29 years at an average of 26 years, their stature ranged between 161 and 166 cm at an average of 163 cm, and their mass ranged between 55 and 67 kg at an average of 60 kg (**Table 1**). According to the University of Michigan Transportation Research Institute (UMTRI), the stature and mass

of the 50th percentile female is 162 cm and 62 kg, respectively, (Schneider et al., 1983). In comparison to the UMTRI data, the female volunteers were on average 1% taller and 4% lighter than the 50th percentile female.

Sled and Seat System

A stationary target sled (1,005 kg) equipped with a laboratory seat was impacted from the rear by a bullet sled (570 kg). The ram-shaped front structure of the bullet sled activated an iron band, mounted inside a band-brake on the target sled, dimensioned to create a predefined acceleration and velocity change of the target sled. The laboratory seat had the same seatback construction as in previous tests series (Davidsson et al., 1998; Carlsson et al., 2011). The seatback was designed to resemble the shape and deflection properties of a Volvo 850 car seat and consisted of four stiff panels covered with 20 mm medium quality Tempur foam. The panels were independently mounted to a rigid seatback frame by coil springs to allow easy implementation into a computational model. The seatback was adjusted to 24.1°. The seat specifications can be found in the Davidsson et al. (1999) publication. In the present study, the HR was modified and consisted of a plywood panel (dimensions: 350 × 230 × 20 mm) covered by firm padding (polyethylene 220-E) and supported by a rigid steel frame, i.e., it was not coupled to the deflecting parts of the seatback. This HR design was chosen to achieve improved reproducibility, based on experience gained in the earlier test series (Carlsson et al., 2011). The HR angle was 12.4° from the vertical plane. The targeted initial head-to-HR distance was set by adjusting the thickness of the padding on the HR for each individual (**Figure 1**). The HR surface stiffness was not affected by the change in thickness of the padding, typically from 13 to 8 cm. The seat base was rigid and the flat seat surface (dimensions: 500 × 500 × 20 mm) was angled 16.9° from the horizontal plane. A plate was mounted on the sled to resemble a passenger floor pan surface of a car (**Figure 1**). The seatback and seat base were covered with double layers of knitted lycra fabric.

TABLE 1 | The age, stature, mass, Δv and head-to-HR distance of the individual female volunteers (A–H), as well as their average values and standard deviations (SD).

Test subject				HR10 Initial HR distance 10 cm		HR15 Initial HR distance 15 cm	
	Age [years]	Stature [cm]	Mass [kg]	Δv[b] [km/h]	HR distance[d] [cm]	Δv[b] [km/h]	HR distance[d] [cm]
A[a]	27	161.0	54.5	6.95	12.0	6.89	16.3
B	26	163.8	56.8	6.61	7.8	6.75	14.4
C	27	162.8	66.8	6.73	11.5	6.86	15.3
D	23	166.0	56.8	6.72	9.1	6.87	13.5
E	25	165.3	61.2	6.94	9.2	6.69	14.1
F	29	161.4	62.2	6.89	7.3	6.85	14.2
G	22	161.9	60.4	6.73	7.6	6.88	14.9
H[a]	27	164.4	58.0	6.87	11.4	6.87	16.5
Average	**26**	**163.3**	**59.6**	**6.81**	**9.5**	**6.83**	**14.4**
SD[c]	**2**	**1.8**	**3.9**	**0.12**	**1.9**	**0.07**	**1.1**

[a] *No HR contact at HR15.*
[b] *Change of velocity.*
[c] *Standard Deviation (SD).*
[d] *At impact.*

Test Procedures and Test Configurations

The volunteers were seated on the laboratory seat, restrained by a 3-point seatbelt and instructed to obtain a natural seated posture, position their feet on the angled plate, place their hands on their lap, face forward and relax prior to the impact. Then, prior to the test, the head-to-HR distance was checked, and the volunteers were reminded to remain seated in a relaxed manner. There was no countdown, and the volunteers were aware of the impending impact since the bullet sled created sound as well as vibrations that could be sensed. Each volunteer underwent two tests; the first test configuration, labelled HR10, was performed at the targeted initial HR distance ∼10 cm, and the second test configuration labelled HR15, was performed at ∼15 cm. These two HR placements were chosen to provide additional distance, in 5 cm increments, compared to the 5 ± 2 cm in the earlier test series of Carlsson et al. (2011). The chosen head-to-HR distances are greater than what is typically found in recent passenger vehicle seats when seated in neutral, upright position (Park et al., 2018). The volunteers were asked to leave the seat for approximately 10 min between the tests. At this point the volunteers were asked if they wanted to proceed with the second test (HR15). This non-randomised order of tests was chosen to allow the volunteers to experience the smaller head-to-HR distance before continuing. A randomised order of the two tests would likely only have had a marginal effect on the head kinematics results. Siegmund et al. (2003) carried out repeated rear impact volunteer tests to study the influence of habituation on the neck response. Their results suggests that the habituation from the first to the second test had negligible influence of the onset phase of the head motion, although at a much lower rear impact severity. The same sled pulse was applied in all tests, with an average mean target sled acceleration of 2.1 g and a velocity change of 6.8 km/h. The volunteers were wearing their own clothes, a pair of shorts and a vest/T-shirt during the tests.

Instrumentation and Data Acquisition

The head of each volunteer was equipped with a harness which was fixed tightly to the head (**Figure 1**). Linear tri-axial accelerometers (MSC 322C/AM-100) were mounted on the left side of the harness and an angular accelerometer (Endevco 7302B) on the right side, approximately at the head centre of gravity. Linear accelerometers (Endevco 7264–200) in x- and z-direction were placed on a holder above the T1 vertebra. The holder was attached to the skin at four points; one above each of the proximal ends of the clavicles, and two bilateral and close to the spinal process of the T1 vertebra. The HR contact was measured by a tape switch (Barger 121 BP). Linear accelerometers (Endevco 2262A–200) recorded bullet sled and target sled accelerations in the x-direction. The start of the impact ($T = 0$) was defined by a tape switch (Barger 101 B) attached to the steel bar on the target sled. Video tracking targets were secured on the volunteers prior to the tests (**Figure 1**).

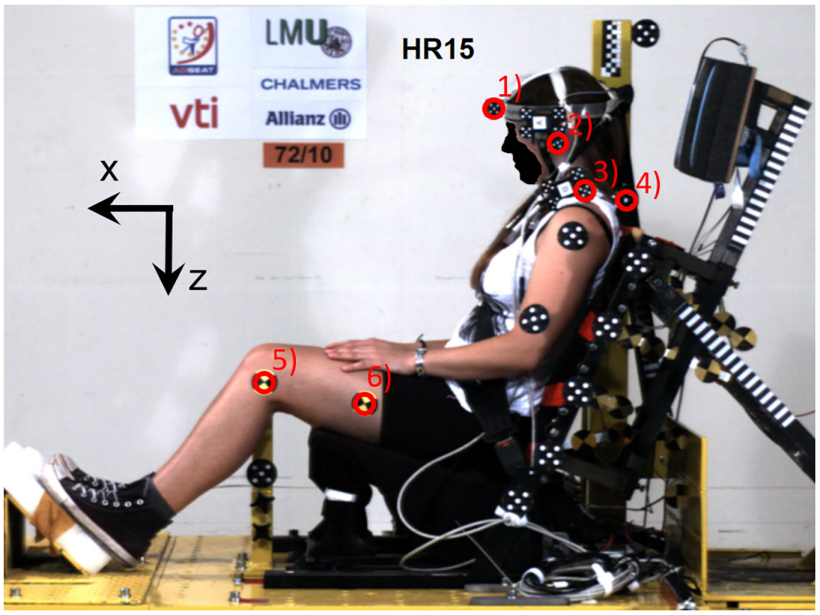

FIGURE 1 | Volunteer test setup; in this case for the head-to-HR distance 15 cm (HR15). Video tracking targets **(1)** and **(2)** for determining head displacements and targets **(3)** and **(4)** for T1 displacements. The position of the trochanter major was palpated and measured prior to the test, and its linear displacement was obtained from targets **(5)** and **(6)**. The thickness of the dark head restraint padding was adjusted to adapt the head-to-head restraint distance for each volunteer, to either 10 cm or 15 cm.

Two high-speed digital video cameras (Redlake HG100K, 1,504 × 1,128 pixels, 1,000 f/s) monitored the tests from the left side and perpendicular to the direction of the sled tracks; one providing a close-up view and one providing an overview. Both were placed approximately 6.8 m from the midplane of the volunteers. Sensor data was registered by a Kayser-Trede MiniDau acquisition unit at 10 kHz sampling rate and anti-alias filtered at 4 kHz.

Data Analysis

The sled, head and T1 accelerations were filtered at CFC60, CFC1000, and CFC60, respectively, as defined by SAE J211. Two different accelerometer coordinate systems were defined; their centres were located at respective accelerometer positions and the two systems moved as the position of the volunteer changed during impact. The coordinate systems were defined according to SAE J211 (orthogonal right-handed), with the positive x-, y-, and z-axis forward, rightward and downward, respectively, at the beginning of the impact.

Videos were digitised in Tema 3.5 software. None of the displacement data was filtered. The linear displacements of the head and T1 were obtained from video tracking targets (2) and (4), respectively (**Figure 1**). The angular displacement of the head was derived from targets (1) and (2) and the T1 from targets (3) and (4). In addition, the position of the trochanter major was palpated and measured prior to testing, and its linear displacement was obtained from targets (5) and (6). The actual head-to-HR distance at the time $T = 0$ was obtained from video analysis, and this distance deviated somewhat from the targeted distance (**Table 1**). The displacement data was set to zero at the time of impact ($T = 0$) and was expressed in a sled fixed coordinate system.

Peak values and their timing were derived from the data, and response corridors were generated. A Shapiro-Wilks test for statistical normality was performed on the data set. For each dynamic response parameter, we investigated whether the observed differences in parameter values between $HR10_C$ and $HR15_C$ were statistically significant. $HR15_{NC}$ was excluded from this analysis since this category only involved two samples. T-tests were performed with the statistical significance level of .05 with no corrections for multiple comparisons. Response corridors for the volunteers were defined as the average ± 1 standard deviation (SD). The peak values of the head and T1 x-accelerations, x- and angular displacements as well as their occurrence in time were determined for each volunteer. The HR distance was (1) adjusted (pre-test) to 10 and 15 cm, respectively, and (2) estimated from video analysis at impact ($T = 0$). The HR contact time was documented. The NIC value (Boström et al., 1996, 2000) was calculated from SAE J211/1 (2003) standard CFC60 filtered head and T1 accelerations.

RESULTS

The results were separated into three different categories, $HR10_C$, $HR15_C$, and $HR15_{NC}$, based on

(1) the targeted initial HR distance (10 or 15 cm) and (2) whether the volunteers' head had made contact with the HR during the test event [Contact (C) or No Contact (NC)]:

$HR10_C$: - 8 tests

- Initial HR distance 10 cm
- HR contact
- Represented by dark grey corridors

$HR15_C$:

- 6 tests
- Initial HR distance 15 cm
- HR contact
- Represented by light grey corridors

$HR15_{NC}$:

- 2 tests
- Initial HR distance 15 cm
- No HR contact
- Represented by solid black lines

At the time $T = 0$, the two volunteers (A and H, **Table 1**) with no HR contact ($HR15_{NC}$) were placed in a separate group since they had somewhat greater actual head-to-HR distance (16.3 and 16.5 cm) in comparison to the six volunteers with HR contact (ranging from 13.5 to 15.3 cm). The greater distance may be the reason why no contact occurred. No symptoms from the neck were reported by the volunteers after the tests.

Response corridors were defined as the average ± 1 SD from the average response for the eight female volunteers, except for two cases where no HR contact had occurred. In **Supplementary Appendix 1**, in the online supplement, each individual response curve is presented together with the corridors.

The average speed change applied was 6.8 ± 0.1 km/h (**Figure 2**).

Initial HR Distance and HR Contact

Estimated from video analysis (at $T = 0$), the HR distance was on average 9.5 cm in $HR10_C$, 14.4 cm in $HR15_C$, and 16.4 cm in $HR15_{NC}$ (**Table 2**). The HR contact started 23% ($P = 0.000$) and ended 16% ($P = 0.000$) earlier, respectively, in $HR10_C$ in comparison to $HR15_C$, however, the length of the HR contact was approximately the same (40 and 37 ms, respectively).

Linear Displacements

Linear displacements are presented in **Figure 3** and **Table 2**, as well as in **Supplementary Figures A1.1–3** in the online supplement. On average, $HR10_C$ resulted in 18% less ($P = 0.001$) and 19% earlier ($P = 0.000$) peak rearward x-displacement of the head (negative values in **Figure 3A**) compared to $HR15_C$. In T1, the peak rearward x-displacement (negative values in **Figure 3B**) was on average 7% less [not statistically significant (NS)] and 6% earlier ($P = 0.017$) compared to $HR15_C$. This

TABLE 2 | Summary of results from the tests comprising near 50th percentile female volunteers.

Variable	$HR10_C$ Initial HR distance 10 cm HR contact (*N* = 8) Peak		$HR15_C$ Initial HR distance 15 cm HR contact (*N* = 6) Peak		$HR15_{NC}$ Initial HR distance 15 cm No HR contact (*N* = 2) Peak	
	Average (SD)	Time	Average (SD)	Time	Average	Time
X-Displacement[a]	[mm]	[ms]	[mm]	[ms]	[mm]	[ms]
- Head	–113 (12)	121 (11)	–138 (9)	149 (7)	–133	156
- T1	–96 (9)	127 (5)	–104 (8)	135 (6)	–92	126
- Head relative to T1	–26 (15)	142 (47)	–50 (13)	188 (33)	–100	211
- Trochanter Major	–96 (6)	123 (5)	–94 (3)	122 (5)	–96	124
Angular displacement	[°]	[ms]	[°]	[ms]	[°]	[ms]
- Head	10 (9)	140 (44)	28 (9)	202 (13)	64	237
- T1	18 (2)	144 (6)	24 (3)	159 (8)	20	149
- Head relative to T1[b]	–12 (6)	131 (18)	–7 (2)	126 (27)	–5	100
- Head relative to T1[c]	5 (11)	263 (67)	15 (9)	235 (15)	47	242
X-Acceleration	[m/s^2]	[ms]	[m/s^2]	[ms]	[m/s^2]	[ms]
- Head	193 (35)	116 (12)	106 (40)	147 (8)	32	115
- T1	62 (10)	130 (8)	47 (6)	135 (13)	49	132
NIC	[m^2/s^2]	[ms]	[m^2/s^2]	[ms]	[m^2/s^2]	[ms]
	3.9 (1.1)	91 (19)	5.0 (2.1)	123 (23)	7.4	134
Head restraint (HR)	[mm]	[ms]	[mm]	[ms]	[mm]	[ms]
- Head-to-HR distance[d]	95 (19)	–	144 (6)	–	164	–
- Contact (start)	–	99 (12)	–	129 (8)	–	None
- Contact (end)	–	139 (11)	–	166 (7)	–	None

[a] *Relative to the sled.*
[b] *First peak.*
[c] *Second peak.*
[d] *At T = 0 ms (based on video analysis).*

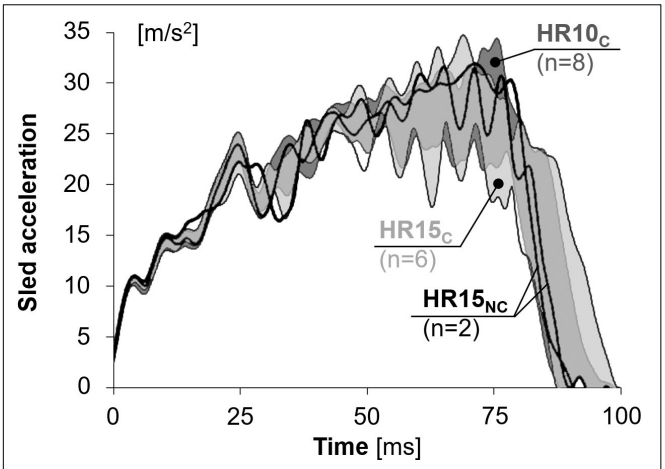

FIGURE 2 | The sled pulse for tests comprising 50th percentile female volunteers.

resulted in substantial differences between the configurations in the rearward x-displacement of the head relative to T1 (negative values in **Figure 3C**); $HR10_C$ was on average 48% less ($P = 0.009$) and 24% earlier (NS) in comparison to $HR15_C$, while $HR15_{NC}$ was 102% greater and 12% later, in comparison to $HR15_C$ (**Table 2**). In the trochanter major, the rearward x-displacement was similar for the two configurations, HR10 and HR15 (**Figure 4** and **Table 2**).

The rebound motion was most pronounced in $HR10_C$, with an earlier return to the initial position (= 0 cm) and a greater forward x-displacement after 500 ms (positive values in **Figures 3A,B**). In $HR10_C$, the head returned to the initial position on average 39% earlier ($P = 0.006$) in comparison to $HR15_C$ (217 and 356 ms, respectively). For the two volunteers in $HR15_{NC}$ the head did not return to its original position. The entire rebound motion was not captured by the cameras. After 500 ms, the average forward x-displacement of the head was 90% greater (NS) in $HR10_C$ (76 mm) compared to $HR15_C$ (40 mm) (**Figure 3A**). Correspondingly for the T1, the average forward displacement after 500 ms was 61% greater (NS) for $HR10_C$ (48 mm) than $HR15_C$ (30 mm), while the T1 lagged behind (–19 mm) for $HR15_{NC}$ (**Figure 3B**).

Angular Displacements

Angular displacements are presented in **Figure 5** and **Table 2**, as well as in **Supplementary Figures A1.4–6** in the online supplement. The rearward angular displacements showed substantial differences in the two configurations (positive angles in **Figure 5**). In comparison to $HR15_C$, the peak rearward head angular displacement was 64% less ($P = 0.003$) and 31% earlier ($P = 0.006$) in $HR10_C$ (**Figure 5A**). For the two volunteers that never made head-to-HR contact in $HR15_{NC}$, the peak rearward head angular displacement was 128% greater and 17% later than the other six volunteers in $HR15_C$. The corresponding numbers for T1 were 25% less ($P = 0.001$) and 9% earlier ($P = 0.002$) in $HR10_C$ (**Figure 5B**). Because the rearward angular displacement

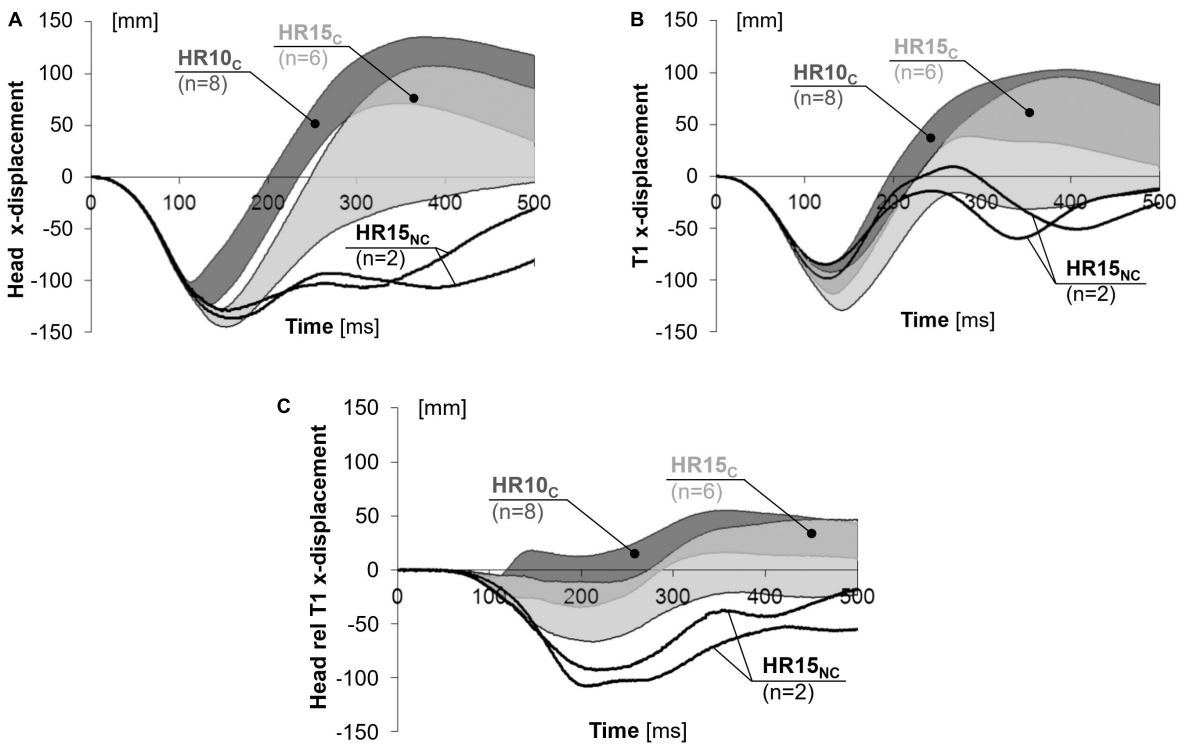

FIGURE 3 | X-displacement of the **(A)** head, **(B)** T1, and **(C)** head relative to T1 for near 50th percentile female volunteers.

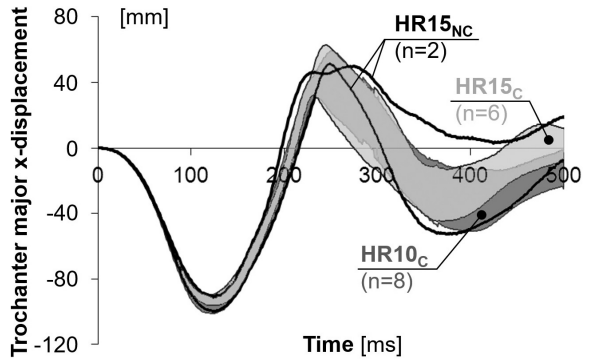

FIGURE 4 | X-displacements of the trochanter major for near 50th percentile female volunteers.

of T1 started earlier in comparison to the head, the volunteers exhibited a small forward angulation (flexion) of the head relative to T1 during the first ∼100 ms for all HR conditions (negative angles in **Figure 5C**). In $HR10_C$, this forward peak head relative to T1 angular displacement was on average 75% greater (NS) in comparison to $HR15_C$. Furthermore, the early HR contact in $HR10_C$ resulted in less rearward angulation (extension) of the head relative to T1, whereas in $HR15_C$, the extension of the head relative to T1 was more prominent. In comparison to $HR15_C$, the peak rearward head relative to T1 angular displacement was 70% less (NS) in $HR10_C$ (**Table 2**).

During the rebound, $HR10_C$ showed an earlier return of the head and T1 angles to their initial positions (= 0°), and a more pronounced forward flexion after 500 ms (negative angles in **Figures 5A,B**) compared to HR15. The head returned to the initial position on average 23% earlier in $HR10_C$ in comparison to $HR15_C$ (249 and 324 ms, respectively, based on the average curves of the corridors in **Figure 5A**). In the T1, the corresponding values were 24% earlier in $HR10_C$ compared to $HR15_C$ (236 and 312 ms, respectively, based on the average curves of the corridors in **Figure 5B**). The average curves of the corridors were used due to some of the volunteers not returning to their initial position within the time frame, 500 ms (thus calculating the significance was not meaningful). In $HR15_{NC}$, neither the head nor the T1 returned to the initial position in any of the two tests. After 500 ms, $HR10_C$ showed a 102% larger forward flexion of the head in comparison to $HR15_C$ (–13.6° and –6.7,° respectively, NS), while in $HR15_{NC}$ the head remained in extension (22°). Correspondingly, after 500 ms the T1 angular displacement was on average 179% greater in $HR10_C$ than in $HR15_C$ (–8,1° and 2,9°, respectively, NS), while in $HR15_{NC}$ the T1 remained in extension (10°).

Sensor Data

Linear head and T1 accelerations are presented in **Figure 6** and **Table 2**, as well as in **Supplementary Figures A1.5–12** in the online supplement. The peak head forward x-acceleration was on average 82% greater (P = 0.001) and 22% earlier (P = 0.000) in $HR10_C$, and 69% less and 22% earlier in $HR15_{NC}$, as compared to $HR15_C$ (positive values in **Figure 6A**). In the T1, the peak forward acceleration was on average 34% greater (P = 0.004) in $HR10_C$ compared to $HR15_C$ (positive values in **Figure 6B**).

In comparison to $HR15_C$ (5.0 m^2/s^2 at 123 ms), the NIC value was on average 22% lower (NS) and 26% earlier (P = 0.015) in $HR10_C$ (3.9 m^2/s^2 at 91 ms), and 49% greater and 9% later in $HR15_{NC}$ (7.4 m^2/s^2 at 134 ms) (**Table 2**).

DISCUSSION

To further improve vehicle safety for both females and males, 50th percentile female models, physical and/or computational crash test dummies and human-body models (HBMs), are required (Carlsson, 2012, 2017). Human dynamic response data is important when developing and evaluating these occupant models. Thus, the objective of this study was to generate response corridors and investigate differences in seat interaction for near 50th percentile females in a laboratory seat at two different HR configurations.

The eight female volunteers participating in the tests were closely matched in size (163.3 ± 1.8 cm/59.6 ± 3.9 kg, **Table 1**) to the 50th percentile female according to the UMTRI study (162 cm/62 kg, Schneider et al., 1983). It is important to note that the average anthropometry varies between different regions of the world. However, we aimed for an anthropometric definition representative for the world population. The anthropometry study of the WorldSID project (Moss et al., 2000) concluded that the size of a world-harmonised 50th percentile adult male would correspond well with the size of the 50th percentile adult male as defined by the UMTRI project (Robbins, 1983a,b; Schneider et al., 1983). We found it reasonable to make the same assumption regarding the 50th percentile adult female (Carlsson et al., 2014).

The present test setup is based on an earlier setup with an average head-to-HR distance of 5.5 cm for the female volunteers (Davidsson et al., 1999; Carlsson et al., 2011). The new setup was designed to provide a greater initial HR distance in 5 cm increments (10 and 15 cm, respectively). The increased HR distance was introduced to enable larger relative motions between the head and the upper torso. Since the initial HR distance was greater compared to previous test series, the mean sled acceleration was reduced from ∼3 to ∼2 g to ensure the volunteers' safety. The selection of the reduced mean acceleration was based on a previous study (Krafft et al., 2002), reporting that long-term whiplash injury risks approached 0% for mean vehicle accelerations below 3 g. Krafft et al. presented mean accelerations ranging from 1 to 7 g indicating that the current sled pulse is representative of the lower range of real-world rear impacts. Furthermore, in comparison to previous test series the design of the laboratory seat was simplified to facilitate computational modelling and reproducibility. The earlier Volvo 850 seat base was replaced with a rigid, flat surface. In addition, the earlier spring-mounted HR panel was replaced by a rigid, adjustable construction to obtain a more precise and reproducible position of the HR during impact (**Figure 1**). The initial HR distance was adjusted by adding padding to the HR, i.e., the geometry was similar for all volunteers in $HR10_C$ and $HR15_C$, respectively. Consequently, seatback panels were flexing like a

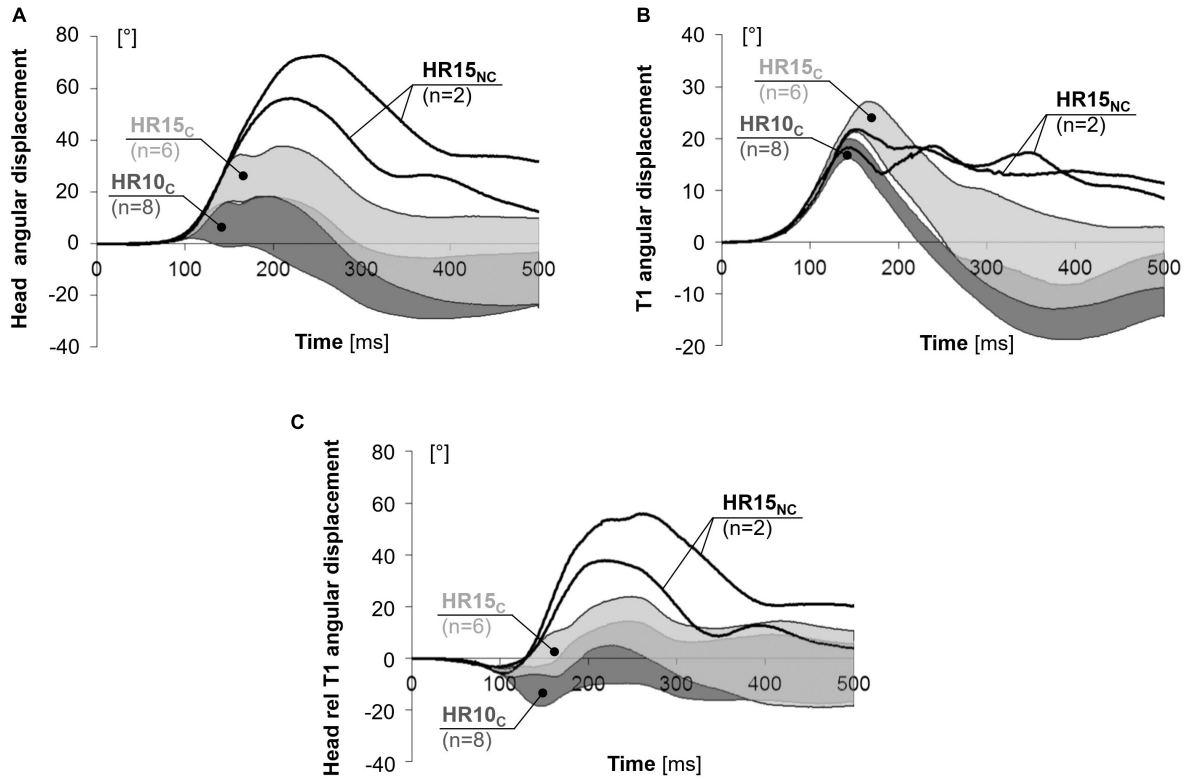

FIGURE 5 | Angular displacement of the **(A)** head, **(B)** T1, and **(C)** head relative to T1 for near 50th percentile female volunteers.

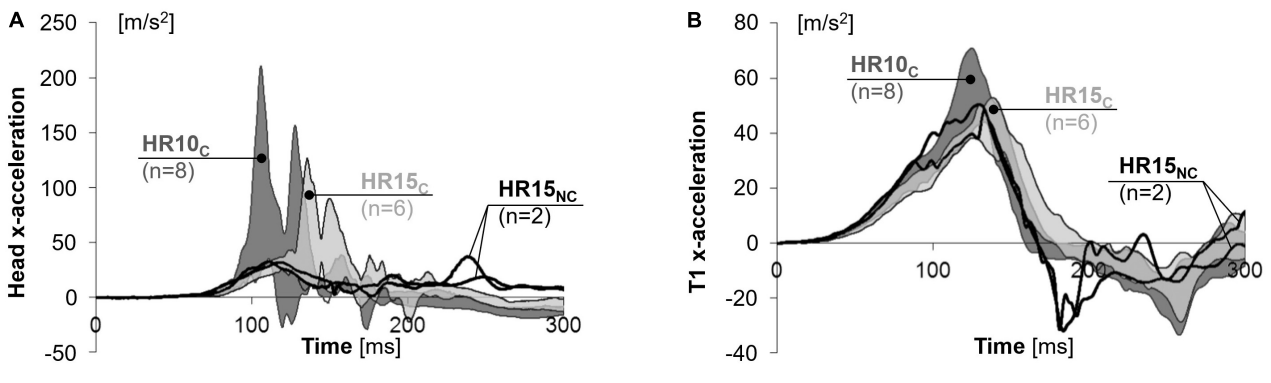

FIGURE 6 | X-accelerations of the **(A)** head and **(B)** T1 for near 50th percentile female volunteers.

standard car seat, while the HR stayed still relative to the sled during the dynamic event. This seatback and HR design deviates from a typical vehicle front seat, however, in this study, the reproducibility was given priority.

The results from the HR15 test configuration were separated into two groups. In the first group, HR15$_C$, the head did contact the HR, while in the second group, HR15$_{NC}$, HR contact did not occur. It is likely that the HR15 test configuration is close to the limit of avoiding HR contact for this specific seat setup. At the time T = 0, the HR15$_{NC}$ volunteers had a greater head-to-HR distance (16.3 and 16.5 cm) in comparison to the HR15$_C$ volunteers (ranging from 13.5 to 15.3 cm). Furthermore, HR15$_{NC}$ also had lesser x-displacements of the head (13.3 and 13.8 cm) and T1 (9.2 and 10.4 cm) (**Table 2**). The greater distance likely explains why no HR contact occurred. The results deviated significantly between the two groups after the time of HR contact in the HR15$_C$ group (on average 129 ms, **Table 2** and **Figures 3–6**). It will be possible to use both datasets in future dummy and model evaluations, each with its corresponding HR contact condition. The grey corridors of HR15$_C$ can be used in case the dummy or model contacts the HR (targeting 129 ms), while the black lines of the HR15$_{NC}$ can be used in non-contact cases.

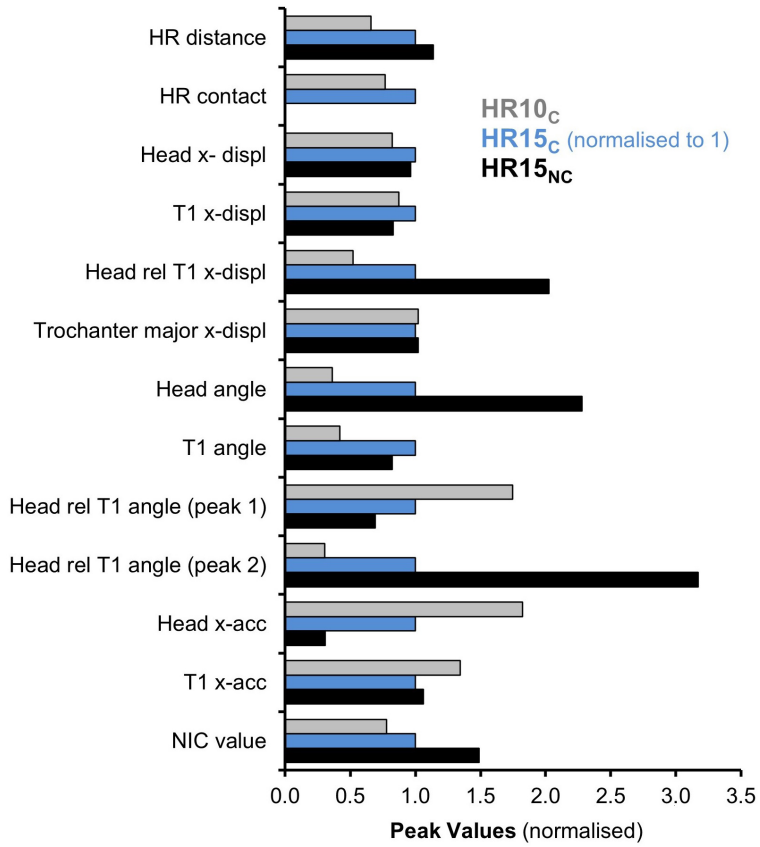

FIGURE 7 | The relative HR distance and contact time; peak x-displacements (head, T1, head relative to T1, trochanter major); angular displacements (head, T1, head relative to T1); x-accelerations (head, T1) and NIC value for $HR10_C$, $HR15_C$ (normalised to 1) and $HR15_{NC}$.

Together, the two datasets represent parts of the mid-sized female population. When evaluating a dummy or a model, it is desirable to also evaluate it against other volunteer datasets to obtain a more robust representation of the population.

The relative peak values from accelerometer signals and data from video analysis for the two configurations, HR10 and HR15, are summarised in **Figure 7**. The $HR15_C$ test was used as a reference, normalised to 1 (represented by blue bars). The greatest differences between the three categories, $HR10_C$, $HR15_C$ and $HR15_{NC}$, were found for the head and head relative to T1 angular displacements. There is also a considerable difference in the T1 angular displacement for the two test configurations, HR10 and HR15, however, not between the two categories $HR15_C$ and $HR15_{NC}$. Thus, the results indicate that the T1 angular displacement for the HR15 can be regarded as an upper limit for this test setup. Similar results can be seen for the head x-displacement, with a difference between the two test configurations, HR10 and HR15, this has not, however, been observed between the two categories $HR15_C$ and $HR15_{NC}$. This result supports the idea that the HR15 test configuration is close to the limit of whether HR contact will occur, for this setup. The data also indicate that the initial HR distance was somewhat greater for the two volunteers in the $HR15_{NC}$ category, which might explain why their heads did not reach the HR. A significant increase was observed in the head relative to T1 x-displacements for increasing HR distance, $HR10_C$, $HR15_C$ and $HR15_{NC}$. In contrast, the x-displacement of the trochanter major (pelvic region) seems unaffected by the different HR configurations. The head x-acceleration decrease for increasing HR distances, $HR10_C$, $HR15_C$, and $HR15_{NC}$, may (partly) be explained by increasing head angular displacements. Furthermore, an increase of the NIC-values for increasing HR distances, $HR10_C$, $HR15_C$, and $HR15_{NC}$, was also recorded.

This study has several limitations. Due to financial constraints, the test series was limited to eight volunteers in two HR configurations. Although additional volunteers would have been valuable, this sample size is in line with other similar studies. The volunteers were young (22–29 years); an older sample might have had a somewhat different response. However, the age of the volunteers in the present study corresponds quite well to the age group with the highest whiplash injury risk (Jakobsson et al., 2000). Moreover, the outcome might have been affected by the volunteers not being exposed to the two HR configurations in a randomised order. It was decided to make the tests non-randomised to give the volunteers the option of discontinuing their participation once they had been exposed to the shorter head-to-HR distance. Furthermore, the outcome might also have been affected by the volunteers being aware of the impending impact. An "unexpected" impact was not possible to achieve, since the noise and vibrations caused by the bullet sled could

be sensed. In addition, electromyographic (EMG) activity was not measured in this study. This type of measurement would potentially have given information about to what extent the volunteers were relaxed or tense at the time of impact ($T = 0$).

Philippens et al. (2002) compared the dynamic response of the 50th percentile male BioRID to volunteer and post-mortem human subject (PMHS) data and observed similar responses in low-speed rear impact tests. The dynamic response of the BioRID dummy was validated with regard to male volunteer tests in Davidsson et al. (1999), the same tests that the female volunteers in Carlsson et al. (2011) were compared to. However, the results from the latter study show that the female volunteers had a somewhat different dynamic response than the male volunteers. Similar findings have been reported in other studies (Siegmund et al., 1997; Mordaka and Gentle, 2003; Viano, 2003; Ono et al., 2006; Linder et al., 2008; Schick et al., 2008; Carlsson et al., 2012). There does not seem to be a simple way to "reinterpret" or "scale" data obtained with the BioRID II to address the female dynamic response (Carlsson, 2012). Thus, it is important that future whiplash protection systems are developed and evaluated with consideration of the female properties as well. With this study we have been able to supply new data that can be used for validation of a 50th percentile low speed rear impact female crash test dummy and/or computational models.

DATA AVAILABILITY STATEMENT

The raw data supporting the conclusions of this article will be made available by the authors, without undue reservation.

ETHICS STATEMENT

The studies involving human participants were reviewed and approved by the Ludwig-Maximilian University in Munich, Germany Approval Reference Number 319–07 Address: Ethikkommission der Medizinischen Fakultät der LMU, Pettenkoferstr. 8a, 80336 Munich, Germany. The patients/participants provided their written informed consent to participate in this study.

AUTHOR CONTRIBUTIONS

AC: preparation, execution, documentation, and analysis of the test series and main author. SH: preparation and execution of the test series, internal review of the manuscript. JD: preparation of the test series, advice based on earlier experience in experimental whiplash injury research including volunteer testing and crash test dummy development, and internal review of the manuscript. SS: medical responsibility, preparation of the test series, advice based on earlier experience in experimental whiplash injury research including volunteer testing, and internal review of the manuscript. AL: EU project coordinator, contributed to the planning of the test series, advice based on earlier experience in experimental whiplash injury research including volunteer testing, and internal review of the manuscript. WH: WP-leader in the ADSEAT project, contributed to the planning of the test series, and internal review of the manuscript. MS: principal investigator, WP-leader in the two involved EU-projects, initiated the work in the present study, contributed with advice based on earlier experience in experimental whiplash injury research including volunteer testing and crash test dummy development, and contributed to the writing and internal review of the manuscript. All authors contributed to the article and approved the submitted version.

FUNDING

This study was part of the ADSEAT (Adaptive Seat to Reduce Neck Injuries for Female and Male Occupants) project funded by the European Commission, Project No. 233904. The data was adapted for evaluation tasks in the project VIRTUAL (Open Access Virtual Testing Protocols for Enhanced Road User Safety) that has received funding from the European Union Horizon 2020 Research and Innovation Programme under Grant Agreement No. 768960. The writing of this paper was funded by Folksams Forskningsstiftelse, Sweden.

ACKNOWLEDGMENTS

We thank to everyone involved in the sled test series, Carsten Reinkemeyer and the staff at Allianz Test Centre, Ismaning, Germany, and Claudia Helmreich, and Claudia Oehme at Ludwig-Maximilians-Universitaet (LMU), Munich, Germany, and Elisabet Agar who performed the language review.

SUPPLEMENTARY MATERIAL

The Supplementary Material for this article can be found online at: https://www.frontiersin.org/articles/10.3389/fbioe.2021.684003/full#supplementary-material

REFERENCES

Boström, O., Fredriksson, R., Håland, Y., Jakobsson, L., Krafft, M., Lövsund, P., et al. (2000). Comparison of car seats in low speed rear-end impacts using the BioRID dummy and the new neck injury criterion (NIC). *Accid. Anal. Prev.* 32, 321–328. doi: 10.1016/s0001-4575(99)00105-0

Boström, O., Svensson, M. Y., Aldman, B., Hansson, H. A., Håland, Y., et al. (1996). "A new neck injury criterion candidate – based on injury findings in the cervical spinal ganglia after experimental neck extension trauma," in *Proceedings of the IRCOBI Conference*, (Dublin), 123–136.

Carlsson, A. (2012). *Addressing Female Whiplash Injury Protection – A Step Towards 50th Percentile Female Rear Impact Occupant Models*. [doctoral dissertation]. Gothenburg: Chalmers University of Technology.

Carlsson, A., Chang, F., Lemmen, P., Kullgren, A., Schmitt, K.-U., Linder, A., et al. (2014). Anthropometric specifications, development, and evaluation of EvaRID – A 50th percentile female rear impact finite element

dummy model. *Traffic Inj. Prev.* 15, 855–865. doi: 10.1080/15389588.2014.885647

Carlsson, A., Linder, A., Davidsson, J., Hell, W., Schick, S., and Svensson, M. (2011). Dynamic kinematic responses of female volunteers in rear impacts and comparison to previous male volunteer tests. *Traffic Inj. Prev.* 12, 347–357. doi: 10.1080/15389588.2011.585408

Carlsson, A., Pipkorn, L., Kullgren, A., and Svensson, M. (2017). Real-world adjustments of driver seat and head restraint in Saab 9-3 vehicles. *Traffic Inj. Prev.* 18, 398–405. doi: 10.1080/15389588.2016.1217522

Carlsson, A., Siegmund, G. P., Linder, A., and Svensson, M. (2012). Motion of the head and neck of female and male volunteers in rear impact car-to-car impacts. *Traffic Inj. Prev.* 13, 378–387. doi: 10.1080/15389588.2012.659362

Carstensen, T. B., Frostholm, L., Oernboel, E., Kongsted, A., Kasch, H., Jensen, T. S., et al. (2011). Are there gender differences in coping with neck pain following acute whiplash trauma? A 12-month follow-up study. *Eur. J. Pain* 16, 49–60. doi: 10.1016/j.ejpain.2011.06.002

Chapline, J. F., Ferguson, S. A., Lillis, R. P., Lund, A. K., and Williams, A. F. (2000). Neck pain and head restraint position relative to the driver's head in rear-end collisions. *Accid. Anal. Prev.* 32, 287–297. doi: 10.1016/s0001-4575(99)00126-8

Davidsson, J., Deutscher, C., Hell, W., Svensson, M. Y., Linder, A., and Lövsund, P. (1998). "Human volunteer kinematics in rear-end sled collisions," in *Proceedings of the IRCOBI Conference*, (Göteborg).

Davidsson, J., Flogård, A., Lövsund, P., and Svensson, M. Y. (1999). "BioRID P3 – design and performance compared to hybrid III and volunteers in rear impacts at $\Delta V = 7$ km/h," in *Proceedings of the 43rd Stapp Car Crash Conference*, (San Diego, CA).

Gustafsson, M., Stigson, H., Krafft, M., and Kullgren, A. (2015). Risk of Permanent Medical Impairment (RPMI) in car crashes correlated to age and gender. *Traffic Inj. Prev.* 16, 353–361. doi: 10.1080/15389588.2014.940459

Jakobsson, L., Lundell, B., Norin, H., and Isaksson-Hellman, I. (2000). WHIPS – Volvo's whiplash protection study. *Accid. Anal. Prev.* 32, 307–319. doi: 10.1016/s0001-4575(99)00107-4

Kihlberg, J. K. (1969). "Flexion–torsion neck injury in rear impacts," in *Proceedings of the 13th AAAM Conference*, (Minneapolis, MIN).

Krafft, M., Kullgren, A., Lie, A., and Tingvall, C. (2003). The risk of whiplash injury in the rear seat compared to the front seat in rear impacts. *Traffic Inj. Prev.* 4, 136–140. doi: 10.1080/15389580309862

Krafft, M., Kullgren, A., Ydenius, A., and Tingvall, C. (2002). Influence of crash pulse characteristics on whiplash associated disorders in rear impacts – crash recording in real life crashes. *Traffic Inj. Prev.* 3, 141–149. doi: 10.1080/15389580212001

Kullgren, A., and Krafft, M. (2010). "Gender analysis on whiplash seat effectiveness: results from real-world crashes," in *Proceedings of the IRCOBI Conference*, (Hanover).

Kullgren, A., Krafft, M., Lie, A., and Tingvall, C. (2007). "The effect of whiplash protection systems in real-life crashes and their correlation to consumer crash test programmes," in *Proceedings of the 20th ESV Conference*, (Lyon). doi: 10.1080/15389580212001

Kullgren, A., Stigson, H., and Axelsson, A. (2020). "Developments in car crash safety since the 1980s", in *Proceedings of the IRCOBI Conference 2020*. Available online at: www.ircobi.org/wordpress/downloads/irc20/pdf-files/14.pdf

Linder, A., and Svensson, M. Y. (2019). Road safety: the average male as a norm in vehicle occupant crash safety assessment. *Interdiscip. Sci. Rev.* 44, 140–153. doi: 10.1080/03080188.2019.1603870

Linder, A., Carlsson, A., Svensson, M. Y., and Siegmund, G. P. (2008). Dynamic responses of female and male volunteers in rear impacts. *Traffic Inj. Prev.* 9, 592–599. doi: 10.1080/15389580802384669

Mordaka, J., and Gentle, R. C. (2003). The biomechanics of gender difference and whiplash injury: designing safer car seats for women. *Acta Politechnica* 43, 47–54.

Morris, A. P., and Thomas, P. D. (1996). "Neck injuries in the UK co-operative crash injury study," in *Proceedings of the 40th Stapp Car Crash Conference*, (Albuquerque, NM).

Moss, S., Wang, Z., Salloum, M., Reed, M. P., van Ratingen, M., Cesari, D., et al. (2000). *Anthropometry for WorldSID a World-Harmonized Midsize Male side Impact Crash Dummy*. SAE Technical Paper 2000-01-2202. Warrendale, PA: Society of Automotive Engineers.

O'Neill, B., Haddon, W., Kelley, A. B., and Sorenson, W. W. (1972). Automobile head restraints—frequency of neck injury claims in relation to the presence of head restraints. *Am. J. Public Health* 62, 399–405. doi: 10.2105/ajph.62.3.399

Ono, K., Ejima, S., Suzuki, Y., Kaneoka, K., Fukushima, M., and Ujihashi, S. (2006). "Prediction of neck injury risk based on the analysis of localized cervical vertebral motion of human volunteers during low-speed rear impacts," in *Paper Presented at IRCOBI Conference*, (Madrid).

Otremski, I., Marsh, J. L., Wilde, B. R., McLardy Smith, P. D., and Newman, R. J. (1989). Soft tissue cervical injuries in motor vehicle accidents. *Injury* 20, 349–351. doi: 10.1016/0020-1383(89)90011-9

Park, J., Jones, M. L. H., Ebert, S. M., Reed, M. P., and Hallman, J. J. (2018). Driver head locations: considerations for head restraint design. *Traffic Inj. Prev.* 19, 825–831. doi: 10.1080/15389588.2018.1524889

Philippens, M., Cappon, H., Van Ratingen, M., Wismans, J., Svensson, M., Sirey, F., et al. (2002). Comparison of the rear impact biofidelity of BioRID II and RID 2. *Stapp Car Crash J.* 46, 461–476.

Robbins, D. H. (1983a). *Anthropometric Specifications for Mid-sized Male Dummy*. Final Report, UMTRI-83-53-2. Ann Arbor, MI: University of Michigan Transportation Research Institute.

Robbins, D. H. (1983b). *Anthropometric Specifications for Small Female and Large Male Dummies*. Final Report, UMTRI-83-53-3. Ann Arbor, MI: University of Michigan Transportation Research Institute.

Schick, S., Horion, S., Thorsteinsdottir, K., and Hell, W. (2008). "Differences and commons in kinetic parameters of male and female volunteers in low speed rear end impacts," in *Proceedings of the 2nd Int. Conf. TÜV SÜD, Whiplash – Neck Pain in Car Crashes*, (Erding).

Schneider, L. W., Robbins, D. H., Pflüg, M. A., and Snyder, R. G. (1983). *Development of Anthropometrically Based Design Specifications for an Advanced Adult Anthropomorphic Dummy Family*. Final Report, UMTRI-83-53-1. Ann Arbor, MI: University of Michigan Transportation Research Institute.

Siegmund, G. P., King, D. J., Lawrence, J. M., Wheeler, J. B., Brault, J. R., and Smith, T. A. (1997). "Head/neck kinematic response of human subjects in low-speed rear-end collisions," in *Proceedings of the 41st Stapp Car Crash Conference*, (Orlando, FL).

Siegmund, G. P., Sanderson, D. J., Myers, B. S., and Inglis, J. T. (2003). Rapid neck muscle adaptation alters the head kinematics of aware and unaware subjects undergoing multiple whiplash-like perturbations. *J. Biomech.* 36, 473–482. doi: 10.1016/s0021-9290(02)00458-x

Storvik, S. G., Stemper, B. D., Yoganandan, N., and Pintar, F. A. (2009). Population-based estimates of whiplash injury using NASS CDS data. *Biomed. Sci. Instrum.* 45, 244–249.

Temming, J., and Zobel, R. (1998). "Frequency and risk of cervical spine distortion injuries in passenger car accidents: significance of human factors data," in *Proceedings of the IRCOBI Conference*, (Göteborg).

Vasavada, A. N., Danaraj, J., and Siegmund, G. P. (2008). Head and neck anthropometry, vertebral geometry and neck strength in height-matched men and women. *J. Biomech.* 41, 114–121. doi: 10.1016/j.jbiomech.2007.07.007

Viano, D. C. (2003). Seat influences on female neck responses in rear crashes: a reason why women have higher whiplash rates. *Traffic Inj. Prev.* 4, 228–239. doi: 10.1080/15389580309880

Welsh, R., and Lenard, J. (2001). "Male and female car drivers – differences in collision and injury risks," in *Proceedings of the 45th AAAM Conference*, (San Antonio, TX).

Conflict of Interest: The authors declare that the research was conducted in the absence of any commercial or financial relationships that could be construed as a potential conflict of interest.

frontiers in Bioengineering and Biotechnology

ORIGINAL RESEARCH
published: 23 June 2021
doi: 10.3389/fbioe.2021.682015

The Head AIS 4+ Injury Thresholds for the Elderly Vulnerable Road User Based on Detailed Accident Reconstructions

He Wu[1,2], Yong Han[2], Di Pan[1,2], Bingyu Wang[2], Hongwu Huang[1,2], Koji Mizuno[3] and Robert Thomson[4]*

[1] School of Aeronautics and Astronautics, Xiamen University, Xiamen, China, [2] School of Mechanical and Automotive Engineering, Xiamen University of Technology, Xiamen, China, [3] Department of Mechanical Science and Engineering, Graduate School of Engineering, Nagoya University, Nagoya, Japan, [4] Chalmers University of Technology, Gothenburg, Sweden

OPEN ACCESS

Edited by:
Francisco J. Lopez-Valdes, Comillas Pontifical University, Spain

Reviewed by:
Elisabetta M. Zanetti, University of Perugia, Italy
Declan A. Patton, Children's Hospital of Philadelphia, United States
Jalaj Maheshwari, Center for Injury Research and Prevention, The Children's Hospital of Philadelphia, United States, in collaboration with reviewer DP

***Correspondence:**
Yong Han
yonghan@xmut.edu.cn

Specialty section:
This article was submitted to Biomechanics, a section of the journal Frontiers in Bioengineering and Biotechnology

Received: *17 March 2021*
Accepted: *26 May 2021*
Published: *23 June 2021*

Citation:
Wu H, Han Y, Pan D, Wang B, Huang H, Mizuno K and Thomson R (2021) The Head AIS 4+ Injury Thresholds for the Elderly Vulnerable Road User Based on Detailed Accident Reconstructions. Front. Bioeng. Biotechnol. 9:682015. doi: 10.3389/fbioe.2021.682015

Compared with the young, the elderly (age greater than or equal to 60 years old) vulnerable road users (VRUs) face a greater risk of injury or death in a traffic accident. A contributing vulnerability is the aging processes that affect their brain structure. The purpose of this study was to investigate the injury mechanisms and establish head AIS 4+ injury tolerances for the elderly VRUs based on various head injury criteria. A total of 30 elderly VRUs accidents with detailed injury records and video information were selected and the VRUs' kinematics and head injuries were reconstructed by combining a multi-body system model (PC-Crash and MADYMO) and the THUMS (Ver. 4.0.2) FE models. Four head kinematic-based injury predictors (linear acceleration, angular velocity, angular acceleration, and head injury criteria) and three brain tissue injury criteria (coup pressure, maximum principal strain, and cumulative strain damage measure) were studied. The correlation between injury predictors and injury risk was developed using logistical regression models for each criterion. The results show that the calculated thresholds for head injury for the kinematic criteria were lower than those reported in previous literature studies. For the brain tissue level criteria, the thresholds calculated in this study were generally similar to those of previous studies except for the coup pressure. The models had higher (>0.8) area under curve values for receiver operator characteristics, indicating good predictive power. This study could provide additional support for understanding brain injury thresholds in elderly people.

Keywords: the elderly, accident reconstruction, video information, head injury criteria, vulnerable road user

INTRODUCTION

The Global Status Report on Road Safety (2018) shows that 1.35 million people die each year from road traffic accidents (World Health Organization, 2018) and that more than half of the global deaths were vulnerable road users (VRUs) (specifically 23% of pedestrians, 3% of cyclists, and 28% of motorized 2–3 wheelers). In China, there were 63,772 deaths caused by traffic accidents in 2017, in which elderly people (the age $\geq$ 60 years) accounted for 30.35% (TABC, 2017).

Brain injuries have been observed as the most fatal factor to the VRUs and have been investigated thoroughly in the past five decades (Gadd, 1966; Nahum et al., 1977; Ward et al., 1980; Hertz, 1993; Arbogast et al., 1995; Hardy et al., 2001; Melvin and Lighthall, 2002; Shi et al., 2020). Due to the complexity of the head anatomical structure, many head injury tolerances (Nusholtz et al., 1984; Margulies and Thibault, 1992; Bain and Meaney, 2000; Zhang et al., 2004) and head injury criteria (HIC) (Versace, 1971; Newman, 1986; Newman and Shewchenko, 2000; Willinger and Baumgartner, 2003; Marjoux et al., 2008; Takhounts et al., 2011, 2013; Kimpara and Iwamoto, 2012) have been proposed for evaluating the human head injury risk under various crash conditions. Two types of HIC have been proposed for evaluating head injury risk; one is based on head kinematics and the other on local tissue stress and strain information. Kinematic-based criteria include the head injury criterion (HIC) (National Highway Traffic Safety Administration (NHTSA), 1972), the Brain Injury Criteria (BRIC) (Takhounts et al., 2011, 2013), the Generalized Acceleration Model for Brain Injury Threshold (GAMBIT) (Newman, 1986), and the head impact power (HIP) (Newman and Shewchenko, 2000). The development of computer technology and finite element (FE) head models facilitated brain tissue-based injury criteria such as the von Mises stress, shear stress (Donnelly and Medige, 1997; Kang et al., 1997; Darvish and Crandall, 2001), pressure, the maximal principal strain (MPS), the cumulative strain damage measure (CSDM) (Bandak and Eppinger, 1994; Takhounts et al., 2003), and the dilatation damage measure (DDM) (Nusholtz et al., 1995). For the elderly, as the brain size decreases and the subdural space increases (Genarelli and Thibault, 1982), the relative motion between the skull and the brain increases significantly under various impact conditions, which would lead to a greater risk of vein rupture and hematoma (Kleiven and Holst, 2001; Richards and Carroll, 2012). However, there are few studies on the head injury tolerances for the elderly.

Brain injury criteria and mechanism tolerances based on biomechanical experiments (Melvin and Lighthall, 2002) and indepth accident reconstructions (Yao et al., 2008; Peng et al., 2012; Bourdet et al., 2014; Giordano and Kleiven, 2014; Nie and Yang, 2014; Sahoo et al., 2016) have been intensively investigated. Shi et al. (2020) investigated the effectiveness of the various HIC in the prediction of VRUs severe head injuries caused by ground impact in 10 accidents and showed that predictors like angular acceleration, linear acceleration, HIC, coup pressure, MPS, and CSDM had good capability to predict severe head injuries. However, the correlation between those injury predictors and injury risk still needs more analyzing. With more real-world accident cases collected and reconstructed with high accuracy, the purpose of the current study was to establish the head AIS 4+ injury tolerance of elderly people based on various HIC. A total of 30 detailed real-world elderly VRU accidents with video information from the TRaffic Accident database with Video (VRU-TRAVi) (Han et al., 2018; Shi et al., 2020) was used.

MATERIALS AND METHODS

Vulnerable Road Users Accident Data

A total of 30 real-world VRU accident cases were selected and reconstructed from the VRU-TRAV database. This database was established in 2015, and more than 1,500 cases of video information have been collected at present. Among them, about 1,300 cases (only video information) were downloaded from the Internet (Youku, YouTube, Tencent, etc.). In addition, more than 220 in-depth accidents (contains video and detailed medical records) were obtained from National Automobile Accident In-Depth Investigation System (NAIS) and Academy of Forensic Science (AFS). NAIS and AFS meet the ethical procedures for incident data collection. We have intensive cooperation with NAIS workstations (Shanghai University of Engineering and Technology and Xihua University) and AFS to obtain these accident data. The selection standards for VRU accidents were:

(a) All cases were for the elderly (age $\geq$ 60 years).
(b) Each case has detailed accident sketches, vehicle damage photos, video information from the vehicle recorder or road monitoring, and detailed head injury reports.
(c) The contact area between the VRU's head and the vehicle front-end structure (such as the A-pillar, bonnet, windshield, or ground) could be obtained from the above information.
(d) From the video records, the kinematic motion of the vehicle and the VRU kinematics before/during/after collisions could be observed clearly.
(e) The injury report should record details of the type of head injury and the severity of the head injuries having been classified and coded by using the maximum degree of injury severity (MAIS) (Association for the Advancement Automotive Medicine, 2005).

Table 1 shows the basic information of the 30 accidents (detailed information listed in **Supplementary Table 1**), in which the VRU's age was mainly distributed between 60 and 80 years old, and the five most common types of head injuries (detailed head injury information listed in **Supplementary Table 2**) were subarachnoid hemorrhage (SAH), subdural hematoma (SDH), skull fracture (SF), soft tissue hematoma (STH), and scalp laceration (SL).

Accident Reconstruction

Shi et al. (2020) described the accident reconstruction flow shown in **Figure 1**. There are four steps to reconstruct the kinematic and head injury severity of the VRUs by coupling multi-body system and FE models.

Step 1: PC-Crash Modeling

The multi-body vehicle and VRUs models were reconstructed based on vehicle and VRU size information in the accident files, and the estimation of vehicle speed was obtained by the video frame-by-frame analysis method (Han et al., 2019) and direct linear transformation (DLT) method (Han X. Y. et al., 2012). The

TABLE 1 | Basic information of 30 accidents.

	VRU Types			Gender		Age		
	Pedestrian	**Cyclist**	**ETWs***	**Male**	**Female**	**61–70**	**71–80**	**>80**
No. of cases	11	4	15	20	10	14	15	1
percentage	37%	13%	50%	67%	33%	47%	50%	3%
	The type of head injury					**Injury severity**		**MAIS for head**		
	SAH	**SDH**	**SF**	**STH**	**SL**	**Death**	**No-death**	**0–1**	**2–3**	**≥4**
No. of cases	13	13	13	8	7	21	9	4	6	20
percentage	24%	24%	24%	15%	13%	70%	30%	13%	20%	67%

**ETWs, electric two-wheelers.*

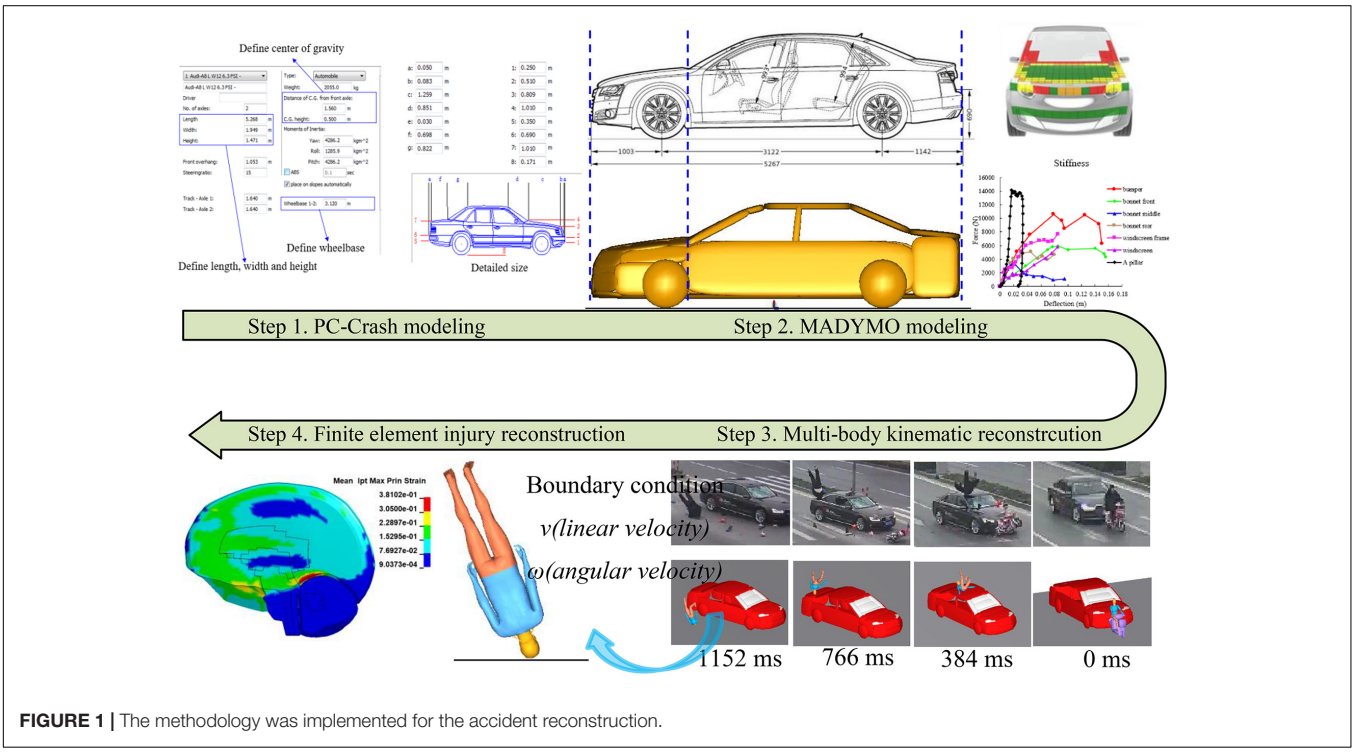

FIGURE 1 | The methodology was implemented for the accident reconstruction.

initial impact position between vehicle and VRUs were mainly determined by the video and pictures of vehicle damage parts.

Step 2: MADYMO Modeling

The vehicle multi-body model used was developed based on the detailed vehicle structural dimensions using ellipsoids, and the front-end stiffnesses were defined based on Euro-NCAP test data (Martinez et al., 2007). For the pedal bicycle and electric two-wheelers, six hinges were used to simulate the motion between each component, and the stiffness characteristics were defined based on the studies of McLundie (2007) and Maki and Kajzer (2000). The VRU's gender, stature, and weight were similarly reconstructed to the accident victims by using the scaling method on the baseline model of the 50th Chalmers Pedestrian Model (CPM) (Young, 1997; Yang et al., 2000). For the contact simulation, the elastic contact model was used to represent the contact between different multi-body models, and the friction coefficient was specified to be 0.2 between the VRU and the vehicles models, and 0.58 between the VRUs and the ground (Wood and Simms, 2000; Shi et al., 2018).

Step 3: Multi-body Kinematic Reconstruction

The final position of the vehicle and VRU was reconstructed based on the accident sketch by using PC-Crash and MADYMO code. The VRUs' kinematic in both vehicle and ground contact were reproduced by comparing with the accident video information.

Step 4: Finite Element Injury Reconstruction

The head and torso boundary conditions pre-impact were defined by the output from running the multi-body kinematic reconstruction. These boundary conditions included three-axis linear and angular velocities of the head, chest, and pelvis centers of gravity (CG) and the relative position between the pedestrian to vehicle and ground impact. Some cases have both head-to-vehicle and head-to-ground impacts, some have

only ground impacts, and the types of vehicles involved in the 30 cases are mainly sedan, SUV, and MPV. To make the FE vehicle model used for simulation match the dimensions of the accident vehicle as much as possible, a total of five FE vehicle models (Han X. Y. et al., 2012; Han Y. et al., 2012; Shi et al., 2018, 2019) were selected and used for the head-to-vehicle impacts simulations, and the ground surface was the asphalt road and defined as a rigid body (Tamura et al., 2014; Huang et al., 2020).

Head Injury Criteria

All FE simulations were performed using the LS-DYNA MPP R9.3.0 (LSTC, Livermore, CA, United States) software. Eight HIC were computed with the THUMS V4.0.2 pedestrian model. The head kinematic-based criteria were the angular velocity, the angular and linear acceleration, and HIC (Versace, 1971; National Highway Traffic Safety Administration (NHTSA), 1972). The brain tissue level-based injury criteria were the coup pressure, MPS (Thibault et al., 1990; Bain and Meaney, 2000), and CSDM (Bandak and Eppinger, 1994; Takhounts et al., 2003). The estimated injury risks were compared with the injury records with AIS codes, and their effectiveness to predict severe head injuries was examined.

Statistical Analysis

In this study, a single logistic regression method was used to establish the relationship between the head AIS 4+ injury risk and different evaluation criteria in the elderly. The injury risk curves are a sigmoid function derived based on Eq. 1 as follows:

$$P(x) = \frac{1}{1 + e^{-(\alpha_0 + \alpha_1 x)}} \tag{1}$$

Where $P(x)$ is the probability of head AIS 4+ injuries for a value of injury criterium lower than or equal to x, α_0 is the intercept, and α_1 is the regression coefficient of x. Receiver operating characteristic (ROC) curves and area under curves (AUC) were further used to assess the predictive capability of the regression models. In this study, we used a confusion matrix to obtain the ROC curves and AUC. Confusion matrix (Li, 2012) is a concept from machine learning and is a measure of the performance of a classification model, which has two dimensions, one of which represents the actual value and the other the predicted value. **Table 2** shows the expression of the confusion matrix for a typical binary classification problem. True positive (TP) means that the actual value is positive and the predicted value is also positive. False negative (FN) means that the actual value is positive and the predicted value is negative. Similarly, False positive (FP) and True negative (TN) indicated that the actual values are negative, and the predicted values are positive and negative, respectively.

To plot the ROC curves, we first need to define two measures, namely false positive rate (FPR) and true positive rate (TPR). FPR refers to the ratio of false-positive cases (the cases that predicted positive but are actually negative) out of all negative cases, it is defined by:

$$\mathrm{FPR} = \frac{\mathrm{FP}}{\mathrm{FP} + \mathrm{TN}} \tag{2}$$

True positive rate refers to the ratio of true-positive cases (the cases that predicted positive and actually are positive too) out of all positive cases, it is defined by:

$$\mathrm{TPR} = \frac{\mathrm{TP}}{\mathrm{TP} + \mathrm{FN}} \tag{3}$$

In the binary classification task, the classification result can be obtained by setting a threshold. If the predicted value is higher than the threshold, it is classified as positive, and classified as negative if lower than the threshold. By setting different thresholds, we can get different confusion matrices, and then multiple pairs of FPR and TPR values can be calculated with FPR as the X-axis and TPR as the Y-axis, thus the ROC curve can be obtained by connecting them. The ROC indicates the predictive power with AUC 1.0 indicating a perfect model.

RESULTS

Kinematic Response of Accident Reconstructions

Based on the clear and complete accident video information, the kinematic response before/during/after the collision was reconstructed for a total of 30 elderly cases. **Figure 2** shows the results of comparing the reconstruction kinematic response with the video information in case 9 (others are summarized in **Supplementary Figure 1**). The reconstructed pedestrian kinematics showed consistent results with the video records, including the relative position between the pedestrian and the vehicle, the pedestrian rotation angle (Shi et al., 2018), the pedestrian body region contact to the ground, the subsequent order of contacts (Han et al., 2018), and the final position (Wu et al., 2020). The reconstructed kinematic of the VRUs show consistency with the observed kinematics in the video records for all cases.

Results of VRU Head Injury Simulations

For the 30 real-world VRU accident reconstructions, the simulated results of the four kinematic-based HIC and four brain tissue-based criteria are shown in **Figure 3**. The histograms were reordered in terms of the magnitude of the calculated injury criterion values according to the AIS < 4 cases (in the green columns) and the cases resulting in head AIS 4+ injuries (in the red columns). For each head kinematics-based and brain tissue-based criteria, the simulated values in green columns were globally lower than those simulated for the red columns. The ranges for the kinematic-based criteria consisting of the head angular velocity and acceleration, linear acceleration, and HIC_{15} were 14.4–97.3 rad/s, 5,550–36,688 rad/s^2, 73–530.3 g, 103–4,238, respectively. The ranges for the brain tissue-based

TABLE 2 | The expression of the confusion matrix for a typical binary classification problem.

Confusion matrix		Predicted value	
		Positive	Negative
Actual value	Positive	True positive (TP)	False negative (FN)
	Negative	False positive (FP)	True negative (TN)

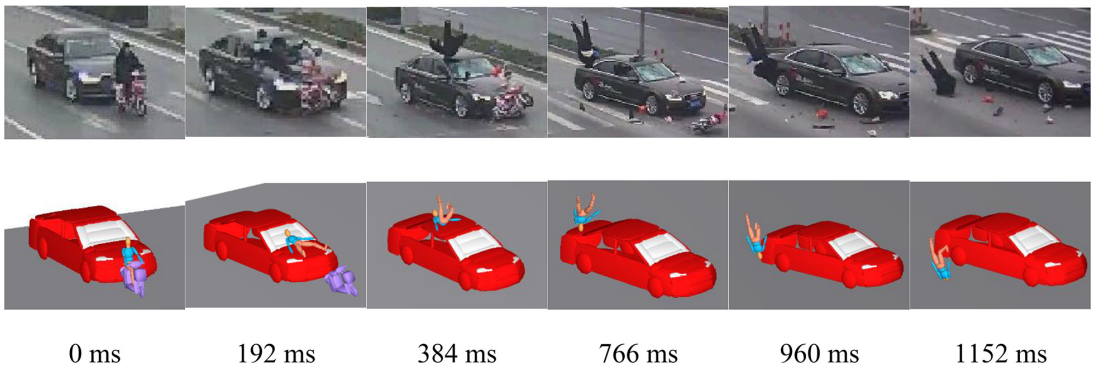

FIGURE 2 | Comparison between the elderly reconstruction kinematics and the video records in case 9.

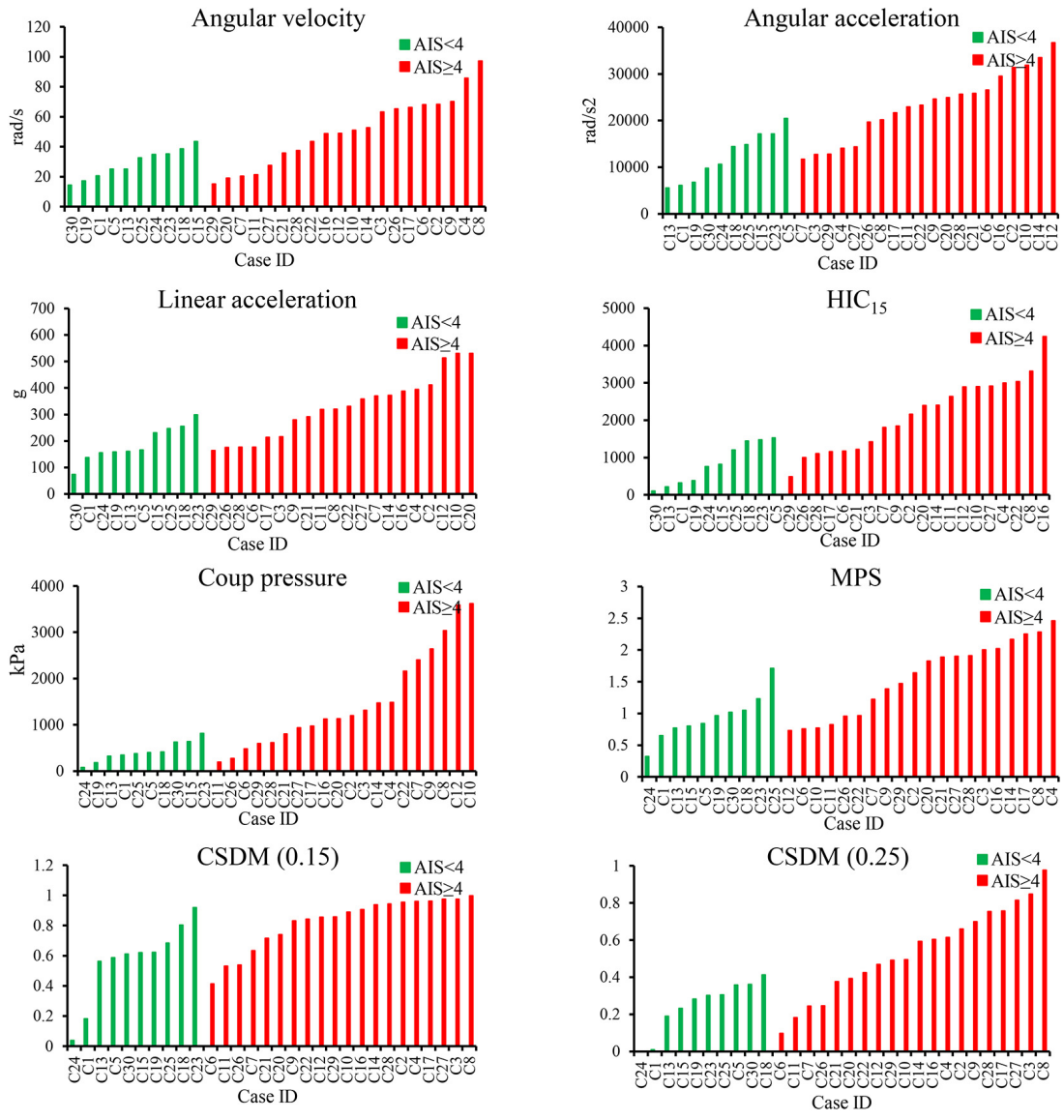

FIGURE 3 | Simulated results of all head injury criteria.

criteria consisting of the coup pressure, MPS, CSDM (0.15), and CSDM (0.25) were 78.44–3,618 kPa, 0.32–2.46, 0.04–0.996, and 0.001–0.98, respectively. The detailed parameter values for all head kinematics-based criteria and brain tissue-based criteria as determined from the simulations are listed in **Supplementary Table 2**.

Injury Risk Curves for All Head Injury Criteria

The injury risk curves for the four head kinematic based criteria and the four brain tissue based criteria were developed based on the regression of the histograms, and the resulting curves are shown in **Figure 4**, where the green circles are the experimental data, and the red pentagrams are the threshold at 50% AIS 4+ injury risk for each criterion. The subplots are the ROC curves, the blue dots are the FPR and TPR coordinates at different thresholds, and the green dots represent the FPR and TPR coordinates when the threshold is 0.5. The closer the ROC curve is to the upper left corner, and the closer the AUC = 1, the better the predictive capability of the regression equation. The AUC value for the kinematic-based criteria consisting of the head angular velocity and acceleration, linear acceleration, and HIC15 were 0.7975, 0.87, 0.8617, and 0.8575, respectively. Similarly, the AUC value for the brain tissue-based criteria consisting of the coup pressure, MPS, CSDM (0.15), and CSDM (0.25) were 0.8775, 0.7975, 0.8075, and 0.85, respectively. The logistic regression risk equations, the AUC value, and the 50% probability of head AIS 4+ injury for all HIC are summarized in **Table 3**.

DISCUSSION

The Reliability of the Accident Reconstructions

The "accident reconstructions" using the real-world accident data to reproduce the collision process and human injuries can be used to alleviate the lack of real data to some extent (Kleiven, 2007; Yao et al., 2008). The traditional accident reconstruction methods were mostly based on police investigation records, including the objective vehicle trajectory traces developed from the investigation of the collision and the subjective information such as the comments and opinions garnered from the participants involved in the accident (Yao et al., 2008; Badea-Romero and Lenard, 2013). However, due to the lack of video information, factors exist regarding the uncertainty which influences the quality and reliability of the reconstruction. These include such factors as the VRUs' kinematics, vehicle dynamics, impact area, impact angle, and landing posture, and the factors affecting the uncertainty could be alleviated by analyzing the videos for use in undertaking the accident reconstruction.

In the current study, the real-world VRU accidents with video information were selected and reconstructed by using a multi-body system (PC-Crash and MADYMO) and FE

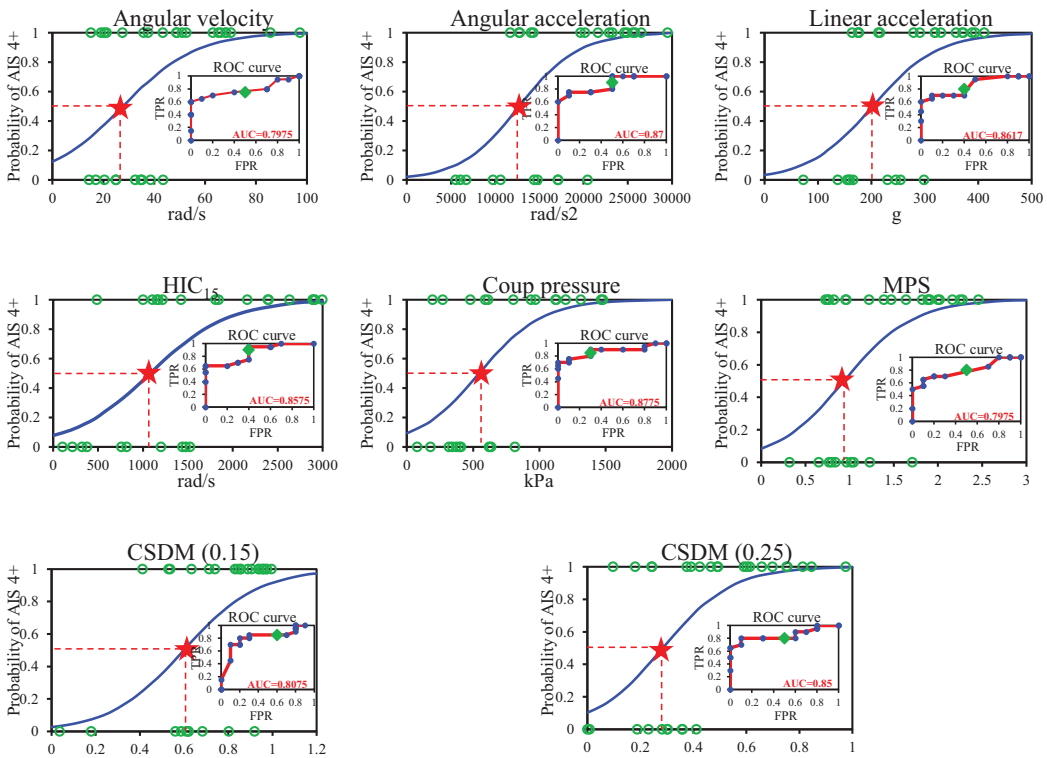

FIGURE 4 | Head AIS 4+ injury risk curves for the head kinematic based criteria.

TABLE 3 | Summary of the results of head AIS 4+ injury risk curves.

Injury criteria	Risk curve equations for AIS 4+ injuries	AUC value	50% risk of AIS 4+	Reference value	Experimental materials
Angular vel	$P(x) = 1/\left(1 + e^{(-(-1.9372+0.0697x))}\right)$	0.7975	27.8 rad/s	46.5 rad/s (Margulies and Thibault, 1992)	Animal studies, physical model and analytical model simulations
Angular acc	$P(x) = 1/\left(1 + e^{(-(-3.826+0.0003x))}\right)$	0.87	12753 rad/s^2	19000 rad/s^2 (Chinn et al., 2001)	Accident reconstruction using Bimass head model
Linear acc	$P(x) = 1/\left(1 + e^{(-(-3.3202+0.0164x))}\right)$	0.8617	202.5 g	250 g (Normalisation CED, 2011)	ATDs test
HIC_{15}	$P(x) = 1/\left(1 + e^{(-(-2.4875+0.0023x))}\right)$	0.8575	1,082	1,440 (National Highway Traffic Safety Administration (NHTSA), 1995)	Real-world accident cases
Coup pressure	$P(x) = 1/\left(1 + e^{(-(-2.3011+0.0042x))}\right)$	0.8775	548 kPa	234 kPa (Ward et al., 1980)	Animal and human cadaver tests
MPS	$P(x) = 1/\left(1 + e^{(-(-2.4121+2.5618x))}\right)$	0.7975	0.942	0.89 (Takhounts et al., 2013)	Animal tests
CSDM (0.15)	$P(x) = 1/\left(1 + e^{(-(-3.5831+5.9842x))}\right)$	0.8075	0.6	0.55 (Takhounts et al., 2003)	Animal tests
CSDM (0.25)	$P(x) = 1/\left(1 + e^{(-(-2.1784+7.6546x))}\right)$	0.85	0.285	0.25 (Takhounts et al., 2013)	Animal tests

methods. Initially, the collision speed could be calculated more accurately using the video images and the DLT method. Then, the reconstructed kinematics could be verified against video frame by frame. Finally, the head impact conditions and injury outcomes could be more objectively compared with the hospital injury reports. In some cases (e.g., in case 18), it is difficult to observe the whole process of VRUs' kinematic response after collision due to the perspective of the video; therefore, the kinematic response of the obscured part could be inferred by comparing the final position (Pascoletti et al., 2019a) and the observed kinematic response at the next moment. The 5th and 50th percentile THUMS models have different size and material properties, which could change the impact locations with the vehicle and injury severity of the head. But in this study, only the 50th percentile of THUMS was used for injury reconstruction in both male and female cases. The reasons are as follows: firstly, we used the CPM model to reconstruct the VRU's kinematic response (including the impact location of the head), and the CPM model was scaled strictly according to the VRU's height, weight, and gender in the real accident, and the reconstruction results were compared with the video information and vehicle damage photos. Then, the multi-body reconstruction results were input into the THUMS model as boundary conditions for injury reconstruction (shown in section "Accident Reconstruction"). Therefore, it can be ensured that the head-to-vehicle impact locations are consistent with the actual accident. Also, with the same loading boundary conditions (including the same linear and angular velocity, impact angle, and location), the little differences in the severity of head injury caused by the fifth and 50th THUMS models were observed, especially to simulate head impact with the ground.

Regression Models Evaluation

For the unbalanced sample of head injury level (the number of head AIS 4+ was 20 cases and no head AIS 4+ was 10 cases), the performance of the regression models was evaluated using ROC curves (shown in **Figure 5**) and AUC values (listed in **Table 3**) in this study. For all regression models, the values of AUC ranged from 0.8 to 0.88, indicating a good predictive capability. However, by comparing with previous studies (National Highway Traffic Safety Administration (NHTSA), 1995; Mertz et al., 1996), the initial probability (the probability when the horizontal coordinate is zero) of the regression model obtained in this study was slightly higher (the corresponding AIS 4+ probability was not zero (from 0.02 to 0.12) when the injury value was zero), and this phenomenon was one of the possible reasons why the AUC value could not be very close to 1. There are two reasons to explain this phenomenon: one is the insufficient sample size used to fit the regression model, and another is the unbalanced sample size and the number of on-head AIS 4+ only 10 cases. The main purpose of this study was to obtain the threshold of head AIS 4+ injury in elderly people, so the effect of the initial probability on the threshold was not significant, and the authors will subsequently increase the sample size further to obtain a more optimal regression model.

For the study of brain injuries tolerance, most human tolerance limits were constrained in the mild or moderate brain injuries (Rowson et al., 2012) because the head injury data used were mostly for football players, and there were limited data available with severe injuries, especially for the elderly. In this study, each criterion injury threshold of a 50% risk of an AIS 4+ severe brain injury for elderly people (listed in **Table 3**) was compared with those published in the literature for this field.

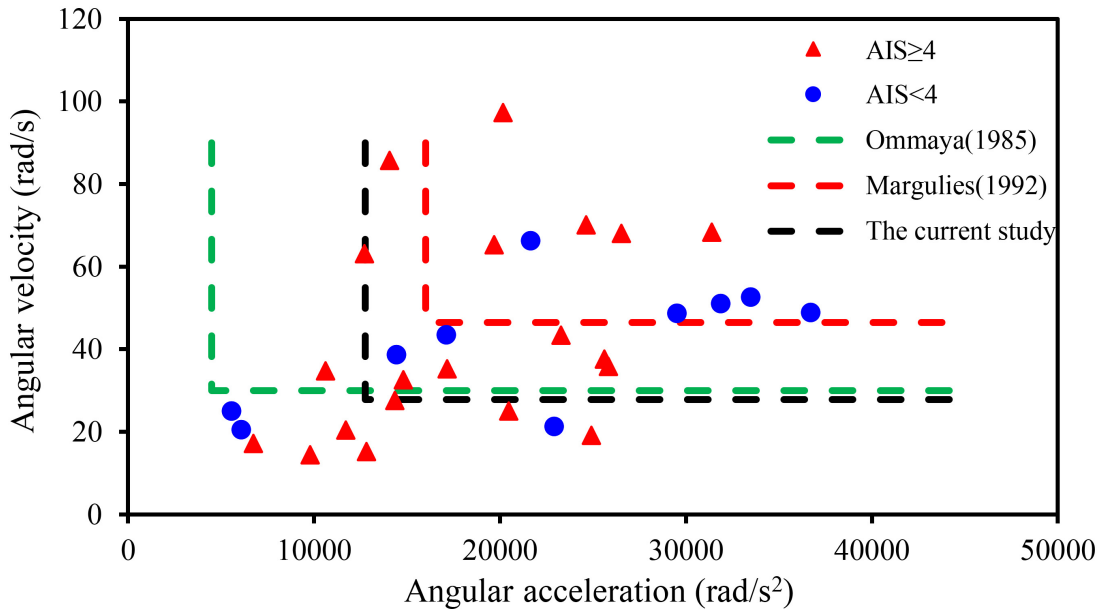

FIGURE 5 | The relationship between head angular velocity, angular acceleration, and brain strain.

Rotational Motion-Based Criteria (Angular Velocity and Angular Acceleration)

Based on animal experiments, Unterharnscheidt (1971) indicated that a rotational acceleration of 101–150 krad/s^2 leads to no injury and when the accelerations up to 197 krad/s^2, subdural hematomas combined with neurological injuries, could be observed. Ommaya (1985) used a primate model and suggested an injury threshold for sagittal plane rotation of the head of 4,500 rad/s^2 when rotational velocity is less than 30 rad/s. Pincemaille et al. (1989), based on experimental data from volunteer boxers, found that the concussion thresholds for angular acceleration and angular velocity were in the range of 13.6–16, 25–48 rad/s, respectively. Margulies and Thibault (1992) utilized a primate model and proposed a DAI-tolerance limit (AIS 4+) for humans of 46.5 rad/s with an angular acceleration of 16,000 rad/s^2. Patton et al. (2012) reported maximum rotational acceleration, respectively, a velocity of 4.5 krad/s^2, 33 rad/s as a threshold for short or no loss of consciousness, based on a set of American football players' head impact analyses. In this current study, the thresholds of angular velocity and angular acceleration (listed in **Table 3**) for the head injury level of AIS 4+ in the elderly were obtained based on logistic regression of the reconstruction results of 30 accidents, which were 27.8 rad/s and 12,753 rad/s^2, respectively (shown in **Figure 5**). These thresholds were only similar to the concussion thresholds derived by Pincemaille et al. (1989) and Patton et al. (2012) and were much lower than those derived by Unterharnscheidt (1971) and Ono et al. (1980) for subdural hematoma and brain contusion. Those suggested that the probability of brain injury was higher in the elderly under the same impact conditions.

Linear Motion-Based Criteria (Maximum Resultant Linear Acceleration and HIC)

Early HIC were maximum resultant head acceleration because of their simplicity. The head accelerations of 200 and 250 g causing an AIS 3 and AIS 4 head injury were confirmed with previous studies (Newman, 1980; Chinn et al., 2001). However, this criterion does not take into account the time duration of the impact, so HIC was developed as a new HIC based on the Wayne state tolerance curve. The National Highway Traffic Safety Administration (National Highway Traffic Safety Administration (NHTSA), 1995) developed the HIC curves for various AIS injury levels, and HIC = 1,440 means a 50% probability of head AIS 4+ injury. Mertz et al. (1996) established a risk curve for HIC_{15} and skull fracture based on cadaver's data and knowing that HIC = 1,420 means a 50% probability of skull fracture. The comparison of the linear acceleration and HIC risk curves for a head injury derived from these studies is shown in **Figures 6**, **7**. In this current study, the critical value of 50% probability of head AIS 4+ injury for linear acceleration and HIC15 were 202.5 g and 1,082, respectively, which were slightly lower than (linear acceleration and HIC15 in this study were 19 and 24.86% lower than the earlier studies, respectively) the threshold of previous studies (Chinn et al., 2001; ; National Highway Traffic Safety Administration (NHTSA), 1995; Mertz et al., 1996).

Stress-Based Criteria

Ward et al. (1980) simulated the head impacts in animal and human cadaver tests in aircraft accidents by using an original FE brain model and showed that the serious and fatal injuries would occur when the intracranial pressure exceeded 234 kPa. In the current study, the critical value of the pressure for a 50% risk brain injury was 548 kPa, which is much higher (the pressure

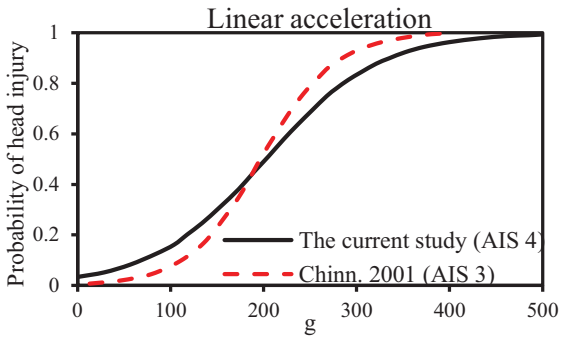

FIGURE 6 | Comparison of the linear acceleration risk curves for head injury.

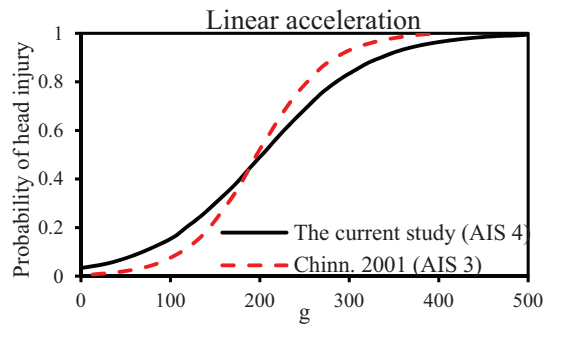

FIGURE 7 | Comparison of the head injury criteria (HIC) risk curves for head AIS 4+ injury.

threshold in this study was 134.2% higher) than Ward's and his colleagues' study. One reason for this large difference may be the difference in the material properties used, and another may the intense head-to-ground impact due to the ground being considered as a rigid body.

For the strain-based criteria, such as MPS and CSDM, Takhounts et al. (2003, 2011, 2013) proposed the 50% thresholds for MPS, CSDM0.15, and CSDM0.25 to predict concussion and DAI, which were 0.89, 0.55, and 0.25, respectively. The research was performed based on the animal experimental data simulated by the SIMon head model. It should be noted that the anatomical structure of the SIMon model was quite simplified compared to the real human head and the skull was assumed to be a rigid body. In this current study, the 50% risk of head AIS 4+ injury for MPS, $CSDM_{0.15}$, and $CSDM_{0.25}$ of 0.94, 0.6, and 0.285, respectively, in which these thresholds are very close to proposed by Takhounts et al. (2003, 2011, 2013).

According to the comparison with previous studies in the literature using different sources, it could be found that the threshold for head AIS 4+ injury in the elderly computed by the global kinematic criteria is generally lower than those of previous studies; for the brain tissue level criteria, the thresholds calculated were generally similar to those of previous studies except for the coup pressure. One reason is that all accidents involved elderly people, and another reason is that the injury threshold for all criteria in this study was obtained from the THUMS head model (Ver. 4.0.2); therefore, the model differences should be carefully considered in the future when applying the threshold.

Limitation

The first limitation was that the accident cases are too limited and the number of head AIS 4+ cases (20 cases) and no head AIS 4+ cases (10 cases) were not equivalent in this research due to the high selection standards. The second limitation was that the kinematics could not be completely replicated according to the video information due to the limitations of the CPM model. Since not all deaths were analyzed anatomically, there existed some cases (six cases in total) without weight information. Admittedly, a more accurate numerical model also requires road user weight (Pascoletti et al., 2019b) in addition to the height and age, which is another limitation in this article. The variables in the regression models were only injury criteria and head AIS level, and did not include age and sex, mainly because of the small number of cases and the unbalanced proportion of sex and age groups (listed in **Supplementary Table 1**). Moreover, for some cases, the head collided with both the vehicle and the ground, but only the collision that caused the more severe head injury was included and the cumulative effect caused by another collision was not considered (Determine the collision that caused the more serious head injury using two aspects: Firstly, the specific position of the head impact with the vehicle and the ground can be derived from the video information. Then compared to the position of head injury in the injury report to determine whether the most serious head injury was caused by the vehicle or the ground. In addition, the values for each HIC were calculated for VRU during the vehicle impact and ground impact phases based on the THUMS 4.02 model, and the head injury values resulting from the vehicle and ground impact phases were compared to determine in which impact phase that caused the more severe head injury). And the THUMS head model represents a 50th male adult, the brain tissue mass and volume were not scaled according to the different ages and genders. The head injury models also did not consider the potential difference in tissue properties (e.g., skull stiffness), which was another limitation.

CONCLUSION AND PERSPECTIVES

Thirty in-depth VRUs accident cases with video records were reconstructed with high reliability by using a multi-body system (PC-Crash and MADYMO) and the THUMS (Ver. 4.0.2) head FE model. The kinematic-based injury criteria (linear acceleration, angular velocity, and acceleration, HIC) and brain tissue-based injury criteria (coup pressure, MPS, and CSDM) were investigated for predicting the head AIS 4+ injuries in elderly VRUs. The predictive ability of the logistic regression models was evaluated using the ROC curve and AUC, where the AUC ranged from 0.8 to 0.88, indicating a good correlation between all criteria and head AIS 4+ injury in the elderly. Thereby, the relevance of their capability to predict AIS 4+ brain injuries could therefore be compared with the AIS 4+ injury thresholds determined in the previous studies identified in the literature.

In this study, the determined injury threshold could alleviate the limited data on previously available brain tolerance.

Also, the injury value acquired from in-depth real-world accident investigations could provide additional support for understanding brain injury mechanisms in elderly people. What's more, the authors recommend that the comprehensive kinematic-based and tissue-based injury criteria should be considered for future VRUs' safety studies.

DATA AVAILABILITY STATEMENT

The original contributions presented in the study are included in the article/**Supplementary Material**, further inquiries can be directed to the corresponding author.

AUTHOR CONTRIBUTIONS

YH conceptualization, methodology, writing original draft preparation, and writing reviewing and edition. HW software. HW, BW, and DP cases analysis, investigation, and joint writing the original draft preparation. YH and RT methodology, writing draft, and revising. KM conceptualization, supervision, and revising. All authors contributed to the article and approved the submitted version.

FUNDING

The authors would like to acknowledge support of the Natural Science Foundation of China (Grant Number 51775466), Fujian Provincial Science foundation for distinguished young scholars (Grant Number 2019J06022), the State Key Laboratory of Automotive Safety and Energy under Project No. KF2005, and the Natural Science Foundation of Fujian Province (Grant Number 2020J05235).

SUPPLEMENTARY MATERIAL

The Supplementary Material for this article can be found online at: https://www.frontiersin.org/articles/10.3389/fbioe.2021.682015/full#supplementary-material

REFERENCES

Arbogast, K., Meaney, F., and Thibault, L. (1995). *Biomechanical Characterization Of The Constitutive Relationship For The Brainstem. SAE Technical Paper. 952716*. Warrendale, PA: SAE.

Association for the Advancement Automotive Medicine (2005). *The Abbreviated Injury Scale–Copyright 2005*. Barrington, IL: Association for the Advancement of Automotive Medicine, 60011.

Badea-Romero, A., and Lenard, J. (2013). Source of head injury for pedestrians and pedal cyclists: striking vehicle or road? *Accid. Anal. Prev.* 50, 1140–1150. doi: 10.1016/j.aap.2012.09.024

Bain, A., and Meaney, D. (2000). Tissue-level thresholds for axonal damage in an experimental model of central nervous system white matter injury. *J. Biomech. Eng.* 122, 615–622. doi: 10.1115/1.1324667

Bandak, F. A., and Eppinger, R. H. (1994). A three-dimensional finite element analysis of the human brain under combined rotational and translational accelerations. *SAE Trans.* 103, 1708–1726.

Bourdet, N., Deck, C., Serre, T., Perrin, C., Llari, M., and Willinger, R. (2014). In-depth real-world bicycle accident reconstructions. *Int. J. Crashworthiness* 19, 222–232. doi: 10.1080/13588265.2013.805293

Chinn, B., Canaple, B., Derler, S., Doyle, D., Otte, D., Schuller, E., et al. (2001). *Cost 327 Motorcycle Safety Helmets*. Brussels: European Commission.

Darvish, K., and Crandall, J. (2001). Nonlinear viscoelastic effects in oscillatory shear deformation of brain tissue. *Med. Eng. Phys.* 23, 633–645. doi: 10.1016/s1350-4533(01)00101-1

Donnelly, B. R., and Medige, J. (1997). Shear properties of human brain tissue. *J. Biomech. Eng. Trans. ASME* 119, 423–432. doi: 10.1115/1.2798289

Gadd, C. (1966). *Use of a Weighted-Impulse Criterion For Estimating Injury Hazard. SAE Technical Paper. 660793*. Warrendale, PA: SAE.

Genarelli, T. A., and Thibault, L. E. (1982). Biomechanics of acute subdural hematoma. *J. Trauma* 22, 680–686.

Giordano, C., and Kleiven, S. (2014). Evaluation of axonal strain as a predictor for mild traumatic brain injuries using finite element modeling. *Stapp Car Crash J.* 58, 29–61.

Han, X. Y., Jin, X. L., Zhang, X. Y., and Miao, X. (2012). Vehicle movement information reconstruction based on video images and DLT theory. *Automot. Eng.* 12, 1145–1149.

Han, Y., Li, Q., Qian, Y. B., Zhou, D. Y., and Svensson, M. (2018). Comparison of the landing kinematics of pedestrians and cyclists during ground impact determined from vehicle collision video records. *Int. J. Veh. Saf.* 10, 212–234. doi: 10.1504/ijvs.2018.10018889

Han, Y., Li, Q., Wang, F., Wang, B. Y., Mizuno, K., and Zhou, Q. (2019). Analysis of pedestrian kinematics and ground impact in traffic accidents using video records. *Int. J. Crashworthiness* 24, 211–220. doi: 10.1080/13588265.2018.1429520

Han, Y., Yang, J. K., Nishimoto, K., Mizuno, K., Matsui, Y., Nakane, D., et al. (2012). Finite element analysis of kinematic behaviour and injuries to pedestrians in vehicle collisions. *Int. J. Crashworthiness* 17, 141–152. doi: 10.1080/13588265.2011.632243

Hardy, W., Foster, C., Mason, M., Yang, K., King, A., and Tashman, S. (2001). Investigation of head injury mechanisms using neutral density technology and high-speed biplanar X-ray. *Stapp Car Crash J.* 45, 337–368.

Hardy, W., Mason, M., Foster, C., Shah, C. S., Kopacz, J., Yang, K., et al. (2007). A study of the response of the human cadaver head to impact. *Stapp Car Crash J.* 51, 17–80.

Hertz, E. (1993). "A note on the head injury criterion (HIC) as a predictor of the risk of skull fracture," in *Proceedings of the Association for the Advancement of Automotive Medicine Annual Conference* (San Antonio, TX: AAAM).

Huang, Y., Zhou, Q., Koelper, C., Li, Q., and Nie, B. (2020). Are riders of electric two-wheelers safer than bicyclists in collisions with motor vehicles? *Accid Anal. Prev.* 134, 105336. doi: 10.1016/j.aap.2019.105336

Kang, H. S., Willinger, R., Diaw, B. M., and Chinn, B. (1997). *Validation of a 3D Anatomic Human Head Model And Replication Of Head Impact In Motorcycle Accident By Finite Element Modeling*. Warrendale, PA: SAE Transactions, 3849–3858.

Kimpara, H., and Iwamoto, M. (2012). Mild traumatic brain injury predictors based on angular accelerations during impacts. *Ann. Biomed. Eng.* 40, 114–126. doi: 10.1007/s10439-011-0414-2

Kleiven, S. (2007). Predictors for traumatic brain injuries evaluated through accident reconstructions. *Stapp Car Crash J.* 51, 81–114.

Kleiven, S., and Holst, H. (2001). "Consequences of brain size following impact in prediction of subdural hematoma evaluated with numerical techniques," in *Proceedings of the International IRCOBI Conference* (Isle of Mann: IRCOBI).

Li, H. (2012). *Statistical Learning Methods*. Beijing: Tsinghua University Press.

Maki, T., and Kajzer, J. (2000). The behavior of bicyclists in frontal and rear crash accidents with cars. *JSAE Rev.* 22, 357–363. doi: 10.1016/s0389-4304(01)00112-6

Margulies, S. S., and Thibault, L. (1992). A proposed tolerance criterion for diffuse axonal injury in man. *J. Biomech.* 25, 917–923. doi: 10.1016/0021-9290(92)90231-o

Marjoux, D., Baumgartner, D., Deck, C., and Willinger, R. (2008). Head injury prediction capability of the hic, hip, simon and ulp criteria. *Accid. Anal. Prev.* 40, 1135–1148. doi: 10.1016/j.aap.2007.12.006

Martinez, L., Guerra, L., Ferichola, G., Garcia, A., and Yang, J. K. (2007). "Stiffness corridors of the european fleet for pedestrian simulations," in *Proceedings of the 20th International Technical Conference on the Enhanced*

Safety of Vehicles (ESV) (Washington, DC: National Highway Traffic Safety Administration.NHTSA).

McLundie, W. (2007). *Investigation of Two-Wheeled Road Traffic Accidents Using Explicit FE Techniques*. PhD's thesis. Bedford: Cranfield university.

Melvin, J., and Lighthall, J. W. (2002). "Brain-injury biomechanics," in *Accidental Injury*, eds A. M. Nahum and J. W. Melvin (New York, NY: Springer), 277–302. doi: 10.1007/978-0-387-21787-1_13

Mertz, H., Motors, G., and Nushdh, G. (1996). *Head Injury Risk Assessment for Forehead Impacts. SAE Technical Papers. 960099*. Warrendale, PA: SAE.

Nahum, A., Smith, R., and Ward, C. (1977). *Intracranial Pressure Dynamics During Head Impact. SAE Technical Paper. 770922*. Warrendale, PA: SAE.

National Highway Traffic Safety Administration (NHTSA) (1972). *Occupant Crash Protection-Head Injury Criterion. (S6. 2 of FMVSS 571.208)*. Washington, DC: National Highway Traffic Safety Administration.

National Highway Traffic Safety Administration (NHTSA) (1995). *Final Economic Assessment, FMVSS No. 201, Upper Interior Head Protection. Office of Regulatory Analysis, Plans and Policy*. Washington DC: National Highway Traffic Safety Administration.

Newman, J. (1980). *Head Injury Criteria In Automotive Crash Testing*. Warrendale, PA: SAE Transactions, 4098–4115.

Newman, J. (1986). "A generalized acceleration model for brain injury threshold (GAMBIT)," in *Proceedings of the International IRCOBI Conference* (Isle of Mann: IRCOBI).

Newman, J., and Shewchenko, N. (2000). A proposed new biomechanical head injury assessment function-the maximum power index. *Stapp Car Crash J.* 44, 215–247.

Nie, J., and Yang, J. K. (2014). A study of bicyclist kinematics and injuries based on reconstruction of passenger car–bicycle accident in China. *Acci. Anal. Prev.* 71, 50–59. doi: 10.1016/j.aap.2014.04.021

Normalisation CED (2011). *Head and Neck Impact, Burn And Noise Injury Criteria—A Guide For Cen Helmet Standards Committees. CEN/TR 16148*. Brussels: Comite Europeen de Normalisation.

Nusholtz, G. S., Lux, P., Kaiker, P., and Janicki, M. A. (1984). Head impact response-skull deformation and angular accelerations. *SAE Technical Paper*. doi: 10.4271/841657

Nusholtz, G. S., Wylie, B., and Glascoe, L. G. (1995). Cavitation/boundary effects in a simple head impact model. *Aviat. Space Environ. Med.* 66, 661–667.

Ommaya, A. K. (1985). "Biomechanics of head injury: experimental aspects," in *The Biomechanics of Trauma* (Norwalk, CT: Appleton & Lange), 245–258.

Ono, K., Kikuchi, A., Nakamura, M., Kabayashi, H., and Nakamura, N. (1980). *Human Head Tolerance To Sagittal Impact: Reliable Estimation Deduced From Experimental Head Injury Using Primates And Human Cadaver Skulls, SAE Technical Paper, No: 801303*. Warrendale, PA: SAE.

Pascoletti, G., Catelani, D., Conti, P., Cianetti, F., and Zanetti, E. M. (2019a). A multibody simulation of a human fall: model creation and validation. *Procedia Struct. Integr.* 24, 337–348. doi: 10.1016/j.prostr.2020.02.031

Pascoletti, G., Catelani, D., Conti, P., Cianetti, F., and Zanetti, E. M. (2019b). Multibody models for the analysis of a fall from height: accident, suicide, or murder? *Front. Bioeng. Biotechnol. 7*:419. doi: 10.3389/fbioe.2019.00419

Patton, D., McIntosh, A., Kleiven, S., and Frechede, B. (2012). Injury data from unhelmeted football head impacts evaluated against critical strain tolerance curves. *J. Sports Eng. Technol.* 226, 177–186. doi: 10.1177/1754337112438305

Peng, Y., Chen, Y., Yang, J. K., Otte, D., and Willinger, R. (2012). A study of pedestrian and bicyclist exposure to head injury in passenger car collisions based on accident data and simulations. *Saf. Sci.* 50, 1749–1759. doi: 10.1016/j.ssci.2012.03.005

Pincemaille, Y., Trosseille, X., Mack, P., Tarrière, C., Breton, F., and Renault, B. (1989). *Some New Data Related To Human Tolerance Obtained From Volunteer Boxers. SAE Technical Paper, No: 892435*. Warrendale, PA: SAE.

Richards, D., and Carroll, J. (2012). Relationship between types of head injury and age of pedestrian. *Acci. Anal. Prev.* 47, 16–23. doi: 10.1016/j.aap.2012.01.009

Rowson, S., Duma, S. M., Beckwith, J. G., Chu, J. J., Greenwald, R. M., Crisco, J. J., et al. (2012). Rotational head kinematics in football impacts: an injury risk function for concussion. *Ann. Biomed. Eng.* 40, 1–13. doi: 10.1007/s10439-011-0392-4

Sahoo, D., Deck, C., and Willinger, R. (2016). Brain injury tolerance limit based on computation of axonal strain. *Acci. Anal. Prev.* 92, 53–70. doi: 10.1016/j.aap.2016.03.013

Shi, L., Han, Y., Huang, H., He, W., Wang, F., and Wang, B. Y. (2019). Effects of vehicle front-end safety countermeasures on pedestrian head injury risk during ground impact. *Proc. Instit. Mech. Eng. D J. Automob. Eng.* 233, 0954407019828845. doi: 10.1177/0954407019828845

Shi, L., Han, Y., Huang, H., Li, Q., Wang, B., and Mizuno, K. (2018). Analysis of pedestrian-to-ground impact injury risk in vehicle-to-pedestrian collisions based on rotation angles. *J. Saf. Res.* 64, 37–47. doi: 10.1016/j.jsr.2017.12.004

Shi, L., Han, Y., Huang, H. W., Davidsson, J., and Thomson, R. (2020). Evaluation of injury thresholds for predicting severe head injuries in vulnerable road users resulting from ground impact via detailed accident reconstructions. *Biomech. Model. Mechanobiol.* 19, 1845–1863. doi: 10.1007/s10237-020-01312-9

TABC (2017). *Statistics of Road Traffic Accidents in PR of China*. Chongqing: Traffic Administration Bureau of China.

Takhounts, E., Craig, M., Moorhouse, K., Mcfadden, J., and Hasija, V. (2013). Development of brain injury criteria (BrIC). *Stapp Car Crash J.* 57, 243–266.

Takhounts, E., Eppinger, R., Campbell, J., Tannous, R., Power, E., and Shoo, L. (2003). On the development of the simon finite element head model. *Stapp Car Crash J.* 47, 107–133.

Takhounts, E., Hasija, V., Ridella, S., Rowson, S., and Duma, S. (2011). "Kinematic rotational brain injury criterion (BRIC)," in *Proceedings of the 22nd Enhanced Safety Of Vehicles (ESV) Conference* (Washington, DC: ESV).

Tamura, A., Koide, T., and Yang, K. H. (2014). Effects of ground impact on traumatic brain injury in a fender vault pedestrian crash. *Int J Veh Saf* 8, 85–100. doi: 10.1504/ijvs.2015.066278

Thibault, L., Gennarelli, T., Margulies, S., Marcus, J., and Eppinger, R. (1990). "The strain dependent pathophysiological consequences of inertial loading on central nervous system tissue," in *Proceedings of the International Conference on the Biomechanics of Impacts (IRCOBI)* (Bron), IRCOBI. doi: 10.4103/2468-5690.191932

Unterharnscheidt, F. (1971). *Translational Versus Rotational Acceleration: Animal Experiments With Measured Input. SAE Technical Paper, No: 710880*. Warrendale, PA: SAE.

Versace, J. (1971). *A Review Of The Severity Index. SAE Technical Paper, No: 710881*. Warrendale, PA: SAE.

Ward, C., Chan, M., and Nahum, A. (1980). *Intracranial Pressure-A Brain Injury Criterion. SAE Technical Paper, No: 801304*. Warrendale, PA: SAE.

Willinger, R., and Baumgartner, D. (2003). Human head tolerance limits to specific injury mechanisms. *Int. J. Crashworthiness* 8, 605–617. doi: 10.1533/ijcr.2003.0264

Wood, D., and Simms, C. (2000). Coefficient of friction in pedestrian throw. *Impact J.* 9, 12–14.

World Health Organization (2018). *Global Status Report On Road Safety 2018*. Geneva: World Health Organization.

Wu, H., Han, Y., Shi, L., and Xu, W. (2020). Research on high-precision accident reconstruction method based on video information. *Automot. Eng.* 42, 74–79+88.

Yang, J. K., Lövsund, P., Cavallero, C., and Bonnoit, J. (2000). A human-body 3d mathematical model for simulation of car-pedestrian impacts. *J. Crash Prev. Inj. Control* 2, 131–149. doi: 10.1080/10286580008902559

Yao, J. F., Yang, J. K., and Otte, D. (2008). Investigation of head injuries by reconstructions of real-world vehicle-versus-adult-pedestrian accidents. *Saf. Sci.* 46, 1103–1114. doi: 10.1016/j.ssci.2007.06.021

Young, J. K. (1997). "Development and validation of a human-body mathematical model for simulation of car-pedestrian collisions," in *Proceedings of the International Conference on the Biomechanics of Impacts (IRCOBI)* (Isle of Mann: IRCOBI).

Zhang, L., Yang, K., and King, A. (2004). A proposed injury threshold for mild traumatic brain injury. *J. Biomech. Eng.* 126, 226–236. doi: 10.1115/1.1691446

Conflict of Interest: The authors declare that the research was conducted in the absence of any commercial or financial relationships that could be construed as a potential conflict of interest.

frontiers in Bioengineering and Biotechnology

ORIGINAL RESEARCH
published: 29 June 2021
doi: 10.3389/fbioe.2021.677982

Evaluation of Head Injury Criteria for Injury Prediction Effectiveness: Computational Reconstruction of Real-World Vulnerable Road User Impact Accidents

Fang Wang[1], Zhen Wang[2], Lin Hu[1], Hongzhen Xu[2], Chao Yu[2] and Fan Li[3]*

[1] School of Automotive and Mechanical Engineering, Changsha University of Science and Technology, Changsha, China, [2] School of Mechanical and Automotive Engineering, Xiamen University of Technology, Xiamen, China, [3] State Key Laboratory of Advanced Design and Manufacturing for Vehicle Body, Hunan University, Changsha, China

This study evaluates the effectiveness of various widely used head injury criteria (HICs) in predicting vulnerable road user (VRU) head injuries due to road traffic accidents. Thirty-one real-world car-to-VRU impact accident cases with detailed head injury records were collected and replicated through the computational biomechanics method; head injuries observed in the analyzed accidents were reconstructed by using a finite element (FE)-multibody (MB) coupled pedestrian model [including the Total Human Model for Safety (THUMS) head–neck FE model and the remaining body segments of TNO MB pedestrian model], which was developed and validated in our previous study. Various typical HICs were used to predict head injuries in all accident cases. Pearson's correlation coefficient analysis method was adopted to investigate the correlation between head kinematics-based injury criteria and the actual head injury of VRU; the effectiveness of brain deformation-based injury criteria in predicting typical brain injuries [such as diffuse axonal injury diffuse axonal injury (DAI) and contusion] was assessed by using head injury risk curves reported in the literature. Results showed that for head kinematics-based injury criteria, the most widely used HICs and head impact power (HIP) can accurately and effectively predict head injury, whereas for brain deformation-based injury criteria, the maximum principal strain (MPS) behaves better than cumulative strain damage measure ($CSDM_{0.15}$ and $CSDM_{0.25}$) in predicting the possibility of DAI. In comparison with the dilatation damage measure (DDM), MPS seems to better predict the risk of brain contusion.

Keywords: head injury criterion, injury prediction, vulnerable road user, impact accident reconstruction, computational biomechanics model

OPEN ACCESS

Edited by:
Mats Yngve Svensson, Chalmers University of Technology, Sweden

Reviewed by:
Kenneth L. Monson, The University of Utah, United States
Uriel Zapata, EAFIT University, Colombia

****Correspondence:***
Lin Hu
hulin888@sohu.com

Specialty section:
This article was submitted to Biomechanics, a section of the journal Frontiers in Bioengineering and Biotechnology

Received: *08 March 2021*
Accepted: *21 May 2021*
Published: *29 June 2021*

Citation:
Wang F, Wang Z, Hu L, Xu H, Yu C and Li F (2021) Evaluation of Head Injury Criteria for Injury Prediction Effectiveness: Computational Reconstruction of Real-World Vulnerable Road User Impact Accidents. Front. Bioeng. Biotechnol. 9:677982. doi: 10.3389/fbioe.2021.677982

INTRODUCTION

Traumatic brain injury (TBI) has become a global health problem due to its corresponding high fatality and disability rates (Corrigan et al., 2010). Statistics show that about 10 million people suffer from TBI each year worldwide (Fahlstedt et al., 2016). Deaths due to TBI were reported to account for 40% of all deaths annually, and TBI is the main reason for mortality under the age

of 45 in the United States. The incidence of TBI in the population of young people (15–30 years) was 154–415/100,000 in the United States, 535/100,000 in France, and 240/100,000 in Australia (Popescu et al., 2015). Currently, there is no ongoing large-scale epidemiological investigation of TBIs in China; however, according to statistics based on the national TBI database, the mortality rate of patients hospitalized for TBI is known as 27.23% (Yang et al., 2017). TBIs not only bring immeasurable pain to patients but also cause huge losses to the whole society. The main causes of TBI are traffic accidents, falls, and attacks, with traffic accidents being the second largest cause of TBI (Gabler et al., 2016; Hu et al., 2020, 2021). Therefore, studies on TBIs in traffic accidents have great practical significance.

In order to reduce the risk of brain injury from traffic accidents and other impact loads, a great deal of knowledge on the biomechanics of brain injury has been accumulated through research work, in which different injury evaluation criteria for different types of head injuries were also proposed. These criteria were initially derived from the well-known Wayne State Tolerance Curve (WSTC; Lissner et al., 1960) and is based on human cadaver head impact tests, which show the relationship between the average acceleration of head movement and its duration (Antona-Makoshi, 2016). Based on the WSTC, the severity index (SI) was later proposed by Gadd (1966), and Versace further modified the SI as a head injury criterion (HIC; Versace, 1971a). In 1974, the US government included HIC in Federal Motor Vehicle Safety Standard 208, which is the only HIC so far that is widely used in global automotive safety regulations. However, as the HIC only considers linear acceleration and action time and does not regard the rotational movement of the head, its deficiencies are gradually pointed out (Gabler et al., 2016). Over a decade later, Newman et al. proposed the Generalized Acceleration Model for Brain Injury Threshold (GAMBIT; Newman, 1986). Moreover, the head impact power (HIP) was proposed on the basis of GAMBIT a few years later (Newman et al., 2000). Both of these criteria consider both the linear and rotational accelerations of the head. With the expansion of in-depth research on the mechanism of head injury, researchers have put forward many head injury evaluation criteria, among which two representative ones are the rotational injury criterion (RIC) proposed by Kimpara and Iwamoto (2012) and the brain rotational injury criterion (BrIC) presented by Takhounts et al. (2013).

At present, the evaluation criteria of head injury are mainly divided into two categories: one is based on head kinematics response, and the other relies on brain tissue deformation response; all of the above-mentioned HICs utilize the head kinematics response. Head injuries have essentially two types, skull fracture and brain injury, with the latter divided into local brain injury and diffuse brain injury. Local brain injury includes contusion, acute subdural hematoma (SDH), epidural hematoma (EDH), and subarachnoid hemorrhage. The main manifestations of diffuse brain injury are concussion and diffuse axonal injury (DAI). The principal causes of the above injuries include concentrated pressure, intracranial viscous load, and craniocerebral inertial load (Yang, 2005), which can also be considered as collision force factors and inertia factors (including linear acceleration and rotational acceleration). In view of these common brain injuries, researchers have established corresponding injury criteria to effectively evaluate various injury types, such as cumulative strain damage measure (CSDM; Takhounts et al., 2003, 2008, 2013; Gabler et al., 2016) and maximum principle strain (MPS; Takhounts et al., 2008; Gabler et al., 2016) for the evaluation of DAI, or dilatation damage measure (DDM; Takhounts et al., 2003) and MPS (Bain and Meaney, 2000) to evaluate contusion. The relative motion damage measure (RMDM) is used to assess SDH (Takhounts et al., 2003; Gabler et al., 2016).

Biomechanical experiments have played a significant role in the development of these HICs (Nahum et al., 1977; Al-Bsharat et al., 1999). However, the subjects of biomechanical experiments are mostly animals and postmortem human subjects (PMHSs), causing deviations of the experimental measurement accuracy. Moreover, the loading conditions of human and animal cadavers and the consequent injuries are significantly different from those in traffic accidents (Kleiven, 2007; Gabler et al., 2016). Traffic accident reconstruction can provide researchers with more realistic injury data, thus making up for the lack of real information in this area. Therefore, many researchers believe that traffic accident reconstruction is one of the most effective methods to study head and brain injuries (Kleiven, 2007; Li and Yang, 2010). With the rapid development of computer technology and the computational biomechanics model of the human body, traffic accident reconstruction has become a common tool to study the complex biomechanical response of the head due to impact (Miller et al., 1998; Hu et al., 2007; Gabler et al., 2016; Wittek et al., 2016; Wang et al., 2018; Li et al., 2019). In previous studies on vulnerable road user (VRU) head injuries in traffic accidents, multi-rigid body [or multibody (MB)] models were mostly used for accident reconstruction and injury analysis (Lyons and Simms, 2012; Li et al., 2017; Shi et al., 2018); however, the MB models were only able to obtain head kinematics response and head kinematics-based injury parameters but not brain tissue injury parameters. Although a few studies (Katsuhara et al., 2014) have used finite element (FE) models to simulate collisions between vehicles and VRUs, such methods have high time cost and low adjustment flexibility, which in turn affects the efficiency of accident reconstruction. In order to shorten the calculation time, other researchers (Marjoux et al., 2008; Li and Yang, 2010) used an FE windshield and human head model to simulate the impact process between human head and windshield, and the boundary condition of collision is based on the result of a kinematics reconstruction with MB models. Obviously, although this method can obtain the brain tissue injury parameters and improve the calculation efficiency, it ignores the influence of other body segments on head injury (Ruan et al., 2007; Gabler et al., 2016; Jones et al., 2016; Wang et al., 2018).

In view of the above deficiencies, we proposed a coupled FE–MB human body model [coupled pedestrian computational biomechanics model (CPCBM)] in our previous study (Yu et al., 2020), where it was confirmed that the risk of brain injury in

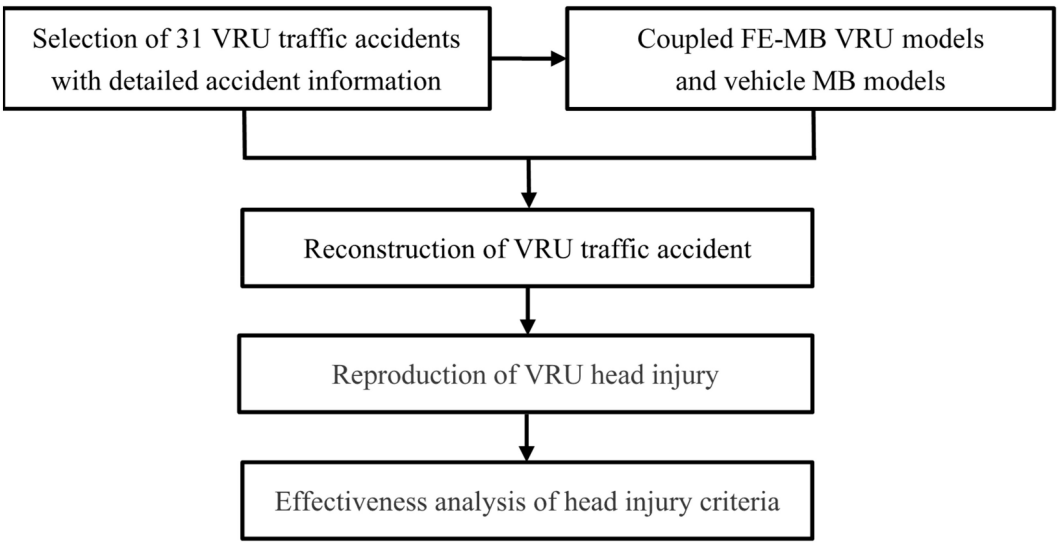

FIGURE 1 | Schematic of the research process.

an accident is lower than the real injury when only the head model (i.e., head-only model) is used to reconstruct the accident (Wang et al., 2020). Therefore, the coupled FE–MB human body model is used in the present study to reconstruct the accident and reproduce the head injury. In addition, the applicability and effectiveness of the HIC is subsequently analyzed and evaluated to assess the head injury in traffic accidents with the aim to reduce the risk of head injury of VRUs in traffic accidents.

MATERIALS AND METHODS

Research Protocol

The schematic of the procedures performed in the present study is shown in **Figure 1**. First, 31 real-world VRU traffic accidents with detailed accident information were selected from the traffic accident database (section "Accident Data"), and the computational modeling of the accident participants is completed (section "Model Description"). Second, VRU traffic accident reconstruction and VRU injury replication (section "Accident Reconstruction") were carried out. Finally, the effectiveness of HICs in predicting head injury in VRU traffic accidents was analyzed (sections " Analysis of Head Kinematics-Based Injury Criteria" and "Analysis of Injury Criteria Based on Brain Tissue Deformation").

All FE computations in this study were conducted using the LS-DYNA R10.0 non-linear explicit dynamics code by Livermore Software Technology Corporation LSTC (Livermore, CA, United States)[1]. Explicit dynamics analysis is an extremely popular method for FE models of injury biomechanics (Yang et al., 2011). The MB models were implemented using the MADYMO V7.7 MB analysis package by TASS (Helmond, Netherlands)[2], which is widely used in injury biomechanics. The interfacing between the FE and MB models was performed using the coupling assistant module/function of the MADYMO MB analysis package.

Accident Data

The VRU traffic collision accidents analyzed in this study were selected from the In-Depth Investigation of Vehicle Accident in Changsha (IVAC) database (Kong and Yang, 2010). This database was established by Hunan University in 2006, which has conducted comprehensive, in-depth, and systematic accident investigation activities in Changsha, China, and carried out detailed research on traffic accidents and subsequent human injuries. It is a highly valued database widely used by researchers to study the biomechanics of human injury, the epidemiology of traffic injury, and road traffic safety (Kong and Yang, 2010; Li and Yang, 2010; Nie and Yang, 2014, 2015).

In the present study, 31 typical vehicle-to-VRU impact accidents were selected from the IVAC database, among which accident Cases 1–17 were pedestrian impact accidents and accident Cases 18–31 were two-wheeler impact accidents. The selection process was based on the following criteria:

1. VRU impacts with the vehicle;
2. VRU head impacts with the front windshield of the car; and
3. head injury occurs in the accident.

The VRU and vehicle information of the selected 31 accidents is shown in **Table 1**.

According to the accident information recorded in the IVAC database, head injury rating data were obtained for the 31 selected accident cases, as shown in **Table 2**.

[1]http://www.lstc.com

[2]https://www.tassinternational.com/madymo

TABLE 1 | Basic information of 31 road traffic accidents selected for this study.

Case ID	VRU information					Vehicle information			Impact velocity (km/h)	
	Type	Gender	Stature (cm)	Weight (kg)	Age	Brand and model	Weight (kg)	Size (mm)	Vehicle	VRU
1	Pedestrian	Male	171	80	17	Volkswagen Jetta	1,490	4,428 × 1,660 × 1,420	30.0	2.1
2	Pedestrian	Male	172	60	20	Honda Accord	1,442	4,814 × 1,821 × 1,463	17.1	1.1
3	Pedestrian	Male	174	70	50	Volkswagen Jetta	1,490	4,428 × 1,660 × 1,420	37	0
4	Pedestrian	Male	173	68	63	Volkswagen Golf	1,275	4,400 × 1,735 × 1,470	43.2	5.0
5	Pedestrian	Male	176	76	35	Mercedes E-Class	1,455	4,800 × 1,800 × 1,400	46.8	7.0
6	Pedestrian	Male	180	77	57	Opel Astra	1,150	3,817 × 1,646 × 1,440	37.4	1.0
7	Pedestrian	Male	153	61	89	Volkswagen Passat	1,850	4,669 × 1,740 × 1,466	58.7	3.2
8	Pedestrian	Male	170	55	42	Volkswagen Jetta	1,490	4,428 × 1,660 × 1,420	43.6	6.5
9	Pedestrian	Male	176	75	50	Volkswagen Tiguan	1,545	4,506 × 1,809 × 1,685	48	5
10	Pedestrian	Male	174	75	52	Volkswagen Passat	1,590	4,789 × 1,765 × 1,470	40	5
11	Pedestrian	Male	166	65	70	Volkswagen Lavida	1,285	4,608 × 1,743 × 1,465	36	0
12	Pedestrian	Male	159	50	72	Volkswagen Polo	1,270	4,187 × 1,650 × 1,465	35	0
13	Pedestrian	Male	168	75	68	BYD F3	1,170	4,325 × 1,705 × 1,490	30	3.6
14	Pedestrian	Female	154	48	78	Zotye T600	2,000	4,648 × 1,893 × 1,686	36	0
15	Pedestrian	Male	175	70	56	Volkswagen Passat	1,850	4,789 × 1,765 × 1,470	70	5
16	Pedestrian	Male	158	55	79	Chevrolet Aveo	1,210	4,399 × 1,735 × 1,517	55	3
17	Pedestrian	Male	170	60	79	Hyundai Elantra	1,348	4,543 × 1,777 × 1,490	91	12
18	Cyclist	Female	157	60	55	Mazda Axela	1,286	4,461 × 1,795 × 1,474	30	10.5
19	Cyclist	Male	168	67	63	Geely Meiri	1,270	4,150 × 1,620 × 1,450	30	15.8
20	Cyclist	Male	170	60	54	Dongfeng Sokon	1,576	3,795 × 1,560 × 1,925	16.5	9.7
21	Cyclist	Male	170	80	58	Volkswagen Santana	1,540	4,595 × 1,750 × 1,430	34.7	7.2
22	Cyclist	Male	175	70	57	Iveco	2,325	4,845 × 2,000 × 2,500	40	4.3
23	Cyclist	Male	170	65	67	BAIC Hyosow S3	1,335	4,380 × 1,730 × 1,760	40.3	18.7
24	Cyclist	Male	158	49	65	Volkswagen Santana	1,540	4,595 × 1,750 × 1,430	31	5.5
25	Cyclist	Female	158	48	42	Volkswagen Santana	1,540	4,595 × 1,750 × 1,430	22	7.2
26	Cyclist	Male	165	60	65	Audi A4L	1,565	4,818 × 1,843 × 1,432	35	4.3
27	Cyclist	Female	161	45	23	Volkswagen Santana	1,540	4,595 × 1,750 × 1,430	34.7	0
28	Cyclist	Male	165	55	62	Volkswagen Jetta	1,500	4,428 × 1,660 × 1,420	40	7.2
29	Cyclist	Female	152	55	50	Wu Ling Sunshine	1,030	3,730 × 1,510 × 1,860	70	10.6
30	Electric two-wheeler	Female	155	40	13	Mitsubishi Outlander	1,500	4,695 × 1,810 × 1,680	35	3.6
31	Electric two-wheeler	Male	173	75	43	Hyundai Elantra	1,236	4,542 × 1,775 × 1,490	60	10.8

VRU, vulnerable road user.

TABLE 2 | VRU head injury rating information for the road traffic accidents subject to this study.

Case ID	Head injury		
	DAI AIS	Contusion AIS	MAIS
1	2	–	2
2	1	–	1
3	3	4	4
4	0	–	0
5	2	–	2
6	3	2	3
7	4	–	4
8	–	3	4
9	–	2	2
10	–	–	4
11	–	3	3
12	–	5	5
13	–	–	5
14	–	–	1
15	4	–	4
16	–	–	1
17	–	–	5
18	–	–	6
19	–	–	0
20	–	–	0
21	–	–	1
22	–	2	2
23	–	–	6
24	–	–	1
25	–	–	2
26	–	–	6
27	–	–	1
28	–	–	1
29	–	–	6
30	–	–	5
31	–	–	5

VRU, vulnerable road user; DAI, diffuse axonal injury.
AIS, Abbreviated Injury Scale, which is the most widely used injury scale to quantify the injury severity of the human body organs/segments (AAAM, 2008).
MAIS, Maximum Abbreviated Injury Scale; maximum AIS scores of all types of head injury.

Model Description

Coupled Finite Element–Multibody Human Body Model

The numerical model of the human body used for accident reconstruction in this study is composed of an MB model and an FE model, which consists of the MB model of the 50th percentile adult male pedestrian model developed by TNO (The Netherlands Organization for Applied Scientific Research[3]) (TASS, 2013a,b,c), and the FE head–neck complex of the Total Human Model for Safety (THUMS) (Version 4.01) of the 50th percentile adult male by Toyota Central R&D Laboratories[4] (Shigeta et al., 2009; Watanabe et al., 2011).

Due to the complex anatomical structure of the brain, biomechanical responses to head injury in VRUs involved in road traffic accidents cannot be simulated by the MB model, whereas the FE model with detailed structure is more useful in this regard. The current study uses the head and neck model of the widely used THUMS. The THUMS FE head model includes the key anatomical structures of the human brain, such as the scalp, skull, meninges, cerebrospinal fluid, brain, cerebellum, brain stem, falx, and tentorium, as shown in **Figure 2A**.

The TNO 50th percentile adult male pedestrian model is composed of 52 rigid bodies (**Figure 2B**), which are connected by kinematics hinges to simulate the stiffness characteristics of human tissues and joints. In order to simulate the interaction between various parts of the human body, as well as the interaction between the human body and the external environment, 64 ellipsoid surfaces and two planes attached to the rigid bodies are used to represent the outer body surface, and the contact characteristics are set for the rigid body surface of different parts.

For the coupling of the two models, the head and neck of the MB model are first removed, and the head–neck complex of the THUMS model and the remaining body segments of TNO pedestrian model are connected by using the coupling assistant module in MADYMO. The end node of muscle and cervical vertebra unit, originally connected with the trunk of THUMS model, are connected to the corresponding rigid bodies (left clavicle, upper torso, and right clavicle), as shown in **Figure 2C**. The coupled FE–MB human body model is shown in **Figure 2D**. For more detailed information about the coupled model, the reader is referred to our previous publications (Wang et al., 2020; Yu et al., 2020).

Bicycle Model

The bicycle model involved in the selected cases is established based on the information recorded in the accident investigation and the corresponding actual geometric information. Take Case 21 as an example: the developed bicycle model consists of five rigid bodies, including front wheel, rear wheel, frame, front fork, and pedal, connected to each other by hinges (**Figure 3**). The mechanical characteristics of each part are used following the literature (Nie et al., 2015).

Electric Two-Wheeled Vehicle Model

The modeling of the electric two-wheeler (ETW) is similar to the bicycle model. Take Case 31 as an example, where the ETW model consists of four rigid bodies, which are connected by hinges (**Figure 4**), including front wheels, rear wheels, frame, and front forks. The mechanical contact characteristics of each part have been studied and verified by predecessors (Deguchi, 2003).

Vehicle Model

The vehicle model used in accident reconstruction consists of two parts: the MB vehicle model and the FE front windshield model. The MB vehicle model is established based on the structure and size of each part of the vehicle in a real accident, with the car involved in Case 11 for the example seen in **Figures 5A,B**. The FE front windshield model is composed of glass and the surrounding metal frame, and the glass model is composed of two shell elements: glass and the other polyvinyl butyral (PVB;

[3]https://www.tno.nl/en/

[4]https://www.toyota.co.jp/thums/

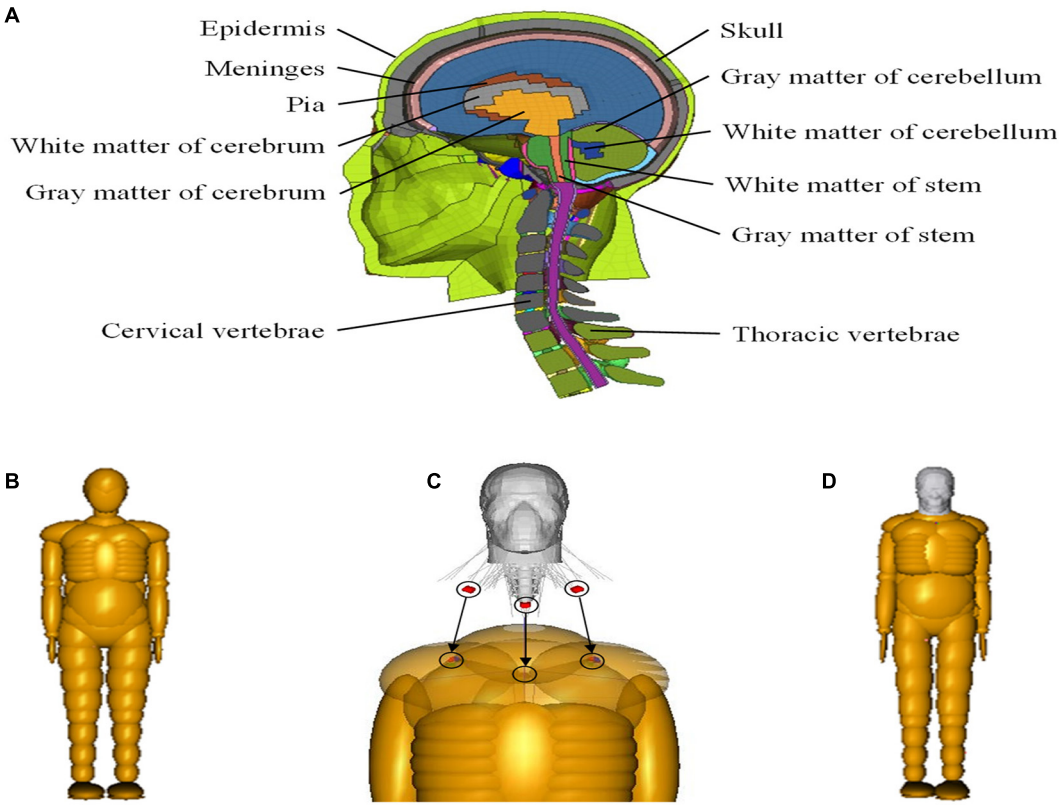

FIGURE 2 | (A) THUMS head–neck FE model; **(B)** TNO 50th percentile adult male model; **(C)** coupling process between FE and MB models; and **(D)** coupled FE–MB human body model. FE, finite element; MB, multibody.

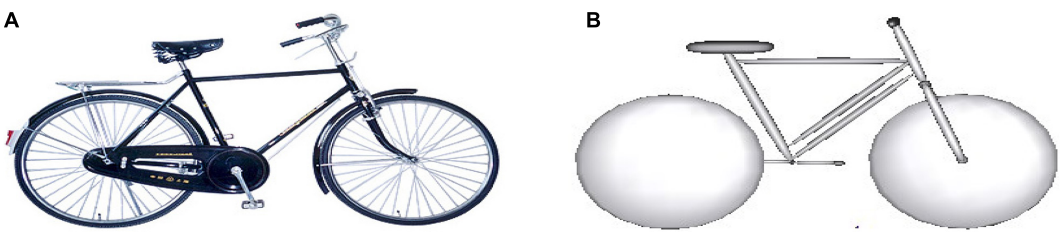

FIGURE 3 | Modeling of the bicycle involved in Case 21: **(A)** the bicycle in the real-world accident; and **(B)** MB model of the bicycle. MB, multibody.

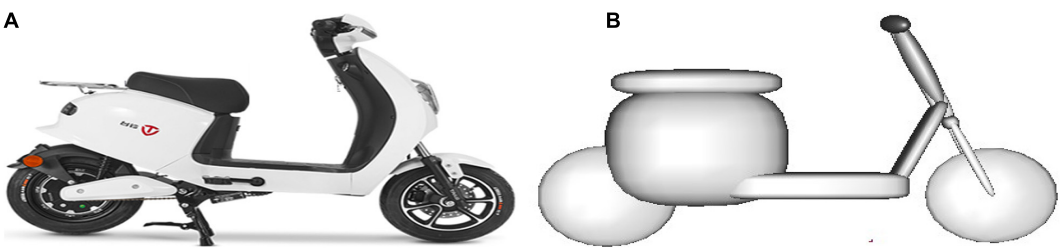

FIGURE 4 | Modeling of the electric two-wheeler involved in Case 31: **(A)** the ETW in the real-world accident and **(B)** MB model of the ETW. ETW, electric two-wheeler; MB, multibody.

Figure 5C); the corresponding material parameters and modeling methods have been verified in the literature (Yao et al., 2008; Li and Yang, 2010).

Accident Reconstruction

The MB dynamics analysis software MADYMO is used to reconstruct the VRU impact accident. The MB human body model needed for accident reconstruction is obtained by scaling the TNO 50th percentile human body model introduced above according to human body information from the real accident using the Generator of Body Data (GEBOD) module in MADYMO software. The flowchart of VRU traffic accident reconstruction is shown in **Figure 6**.

With the completion of the VRU traffic accident reconstruction, the MB human body model is replaced with the coupled FE–MB human body model described in section "Coupled Finite Element–Multibody Human Body Model," and its posture is adjusted accordingly; meanwhile, the MB front windshield model is replaced with the FE model. According to the boundary conditions of car-to-VRU impact obtained from the MB kinematics reconstruction, the accident is re-simulated to obtain the head injury parameters. The MB model of the vehicle and the pedestrian in accident Case 11 is shown in **Figure 7A**, and the coupled FE–MB vehicle and pedestrian model is shown in **Figure 7B** as an example.

Analysis of Effectiveness of Head Injury Evaluation Criteria

The head injury evaluation criteria and corresponding calculation methods employed in the present study, as shown in **Table 3**, were divided into two types: criteria based on head kinematics response (HIC, GAMBIT, BrIC, RIC, and HIP) and criteria based on brain tissue deformation (MPS, CSDM, and DDM). Among these criteria, HIC is most widely used in main stream vehicle safety standards/programs to evaluate the severity of head injury (Kleiven, 2007); however, this criterion solely relies on the linear kinematics of the head center of gravity (COG), without considering the influence of head rotational movement. The RIC is similar to the HIC, except that it uses rotational acceleration instead of linear acceleration. The GAMBIT and HIP criteria consider both the effects of linear and rotational acceleration of head COG. The BrIC considers the influence of maximum rotational velocity and maximum rotational acceleration. The CSDM measures the volume percentage of the area with brain strain exceeding a certain threshold in the whole brain volume, while DDM measures the volume percentage of the area with negative pressure exceeding a certain threshold in the whole brain.

Based on the selected 31 VRU traffic accident cases and subsequent reproduction of head injury as described above, the injury parameter values were calculated according to the formula of each criterion and compared with the Abbreviated Injury Scale/Maximum Abbreviated Injury Scale (AIS/MAIS) score for each accident head in **Table 2**.

Pearson's correlation coefficient analysis method was used to analyze the effectiveness of each criterion in predicting head injury. Pearson's correlation coefficient is a measure of the degree of linear correlation between variables, generally represented by the letter *r*. It is calculated by the product-difference method, which is based on the dispersion of two variables and their respective average values and reflects the correlation degree between two variables by multiplying the two dispersion values. The overall correlation coefficient of random variables X and Y is $\rho(X, Y) = (\mathrm{Cov}(X, Y)) \big/ (\sigma_X . \sigma_Y)$, where $Cov\ (X,\ Y)$ is the covariance of X and Y, σ_X indicates the standard deviation of X, whereas σ_Y is the standard deviation of Y. However, the overall correlation coefficient $\rho\ (X,\ Y)$ generally cannot be obtained, but only an estimate of $\rho\ (X,\ Y)$ can be given according to the observed values of samples, which is called the sample correlation coefficient. Pearson's correlation coefficient can be acquired by estimating the covariance and standard deviation of samples, which is often represented by *r*, and its expression is as follows:

$$r = \frac{\sum_{i=1}^{n} \left(X_i - \bar{X}\right)\left(Y_i - \bar{Y}\right)}{\sqrt{\sum_{i=1}^{n} \left(X_i - \bar{X}\right)^2} \sqrt{\sum_{i=1}^{n} \left(Y_i - \bar{Y}\right)^2}} \tag{1}$$

In this formula, $\bar{X}$ and $\bar{Y}$ represent the average value of X and Y, respectively. The value of r is between -1 and 1. The greater the absolute value of r, the stronger the correlation between variable x and variable y. If $r > 0$, the correlation between the two variables is positive, whereas if $r < 0$, this correlation is negative.

Moreover, the current research particularly focuses on the investigation of brain injury prediction for the analyzed accidents by using HICs based on brain tissue deformation. As mentioned in section "Accident data," two types of brain injury occurred in the selected 31 VRU accident cases: DAI and brain contusion (see **Table 2**). For DAI, CSDM (Takhounts et al., 2003, 2008, 2013; Gabler et al., 2016), and MPS (Takhounts et al., 2008; Gabler et al., 2016) injury criteria were analyzed; for brain contusion, DDM (Takhounts et al., 2003), and MPS (Bain and Meaney, 2000) injury criteria were investigated. Finally, the predicted injury criteria, in combination with the existing brain injury risk curves reported in the literature (Takhounts et al., 2003, 2008), were compared with the AIS scores of each accident in **Table 2**, and the effectiveness of each HIC in predicting human DAI and brain contusion in the accident was subsequently analyzed.

RESULTS

Results of Vulnerable Road User Impact Accident Reconstruction

The results of the predicted kinematics response parameters of the accidents, including collision point between VRUs and vehicles, and the final rest positions, are consistent with the actual accident information. Using these kinematics reconstructions, we can obtain the initial boundary conditions of the accident cases, such as the impact velocities of both VRUs and vehicles, and the VRU trajectories.

Taking Case 1 as an example, the kinematics responses of the pedestrian during the impact by using both MB and the coupled

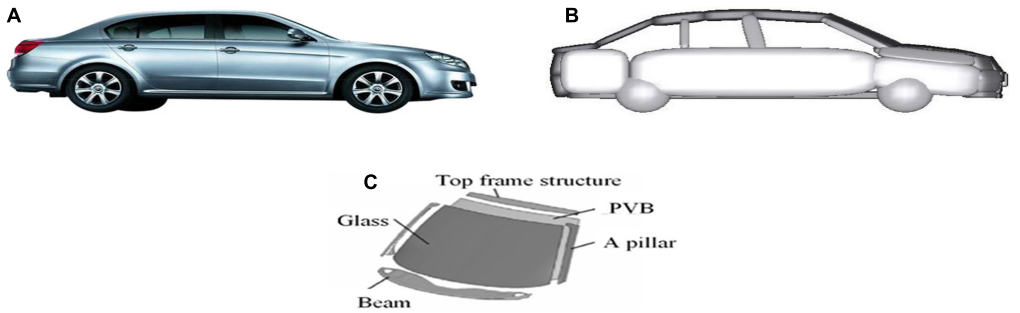

FIGURE 5 | (A) The vehicle involved in the real-world accident; **(B)** MB model of the vehicle; and **(C)** FE front windshield model. MB, multibody; FE, finite element.

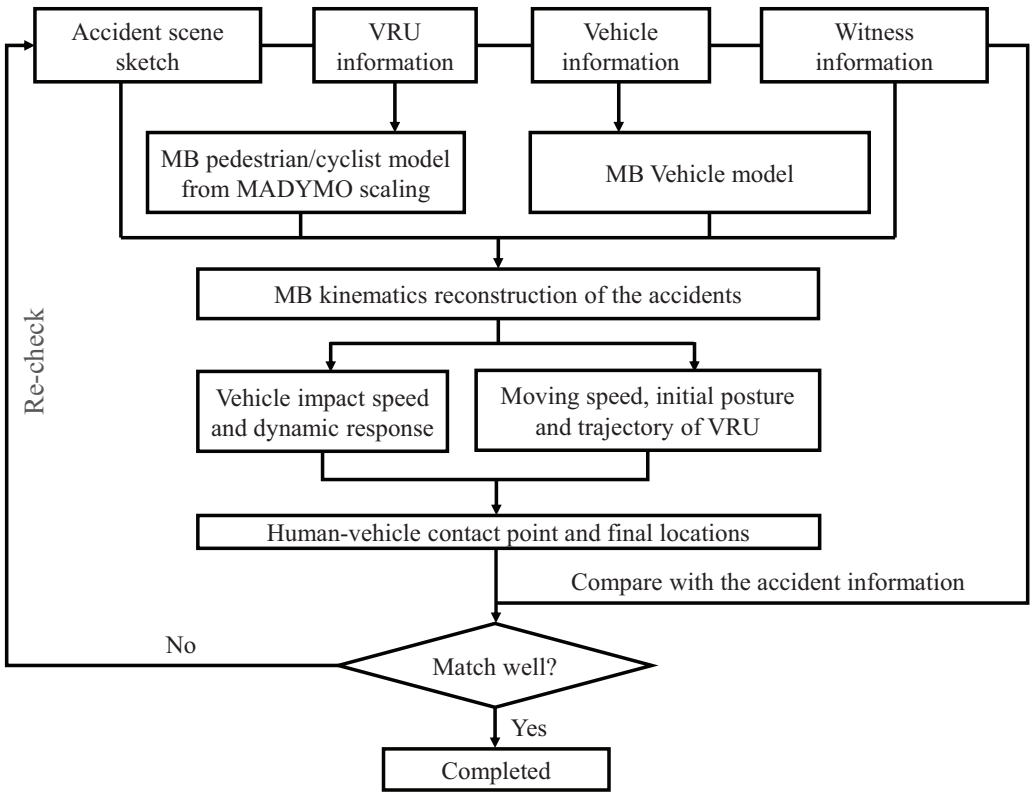

FIGURE 6 | Flowchart of VRU traffic accident kinematics reconstruction. VRU, vulnerable road user.

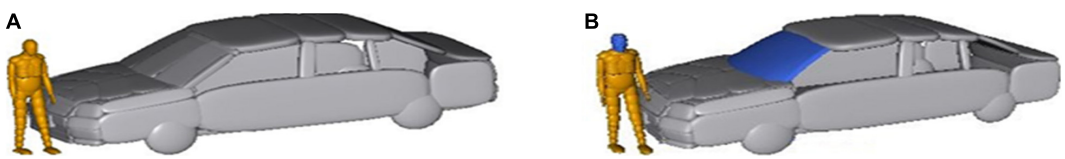

FIGURE 7 | (A) MB model of vehicle and VRU and **(B)** coupled vehicle and VRU model. MB, multibody; VRU, vulnerable road user.

FE–MB models are shown in **Figure 8**. It can also be seen that the predicted damaged locations of the vehicle by FE method matches well with those in the real accident. Moreover, the trajectory of the head COG of the pedestrian in the YOZ plane (composed of vehicle moving Y-direction and vertical Z-direction) is also compared between the sole MB model and the coupled FE–MB model, as shown in **Figure 9** and see **Supplementary Appendix 1** for other cases.

TABLE 3 | Evaluation criteria of head injury.

Evaluation criteria	Calculation method	Description
Head injury criterion, HIC (Versace, 1971b)	$HIC_{15} = \left\{ \left[(t_2 - t_1) \left(\frac{1}{(t_2 - t_1)} \int_{t_1}^{t_2} a(t)dt \right) \right]^{2.5} \right\}_{max}$	a(t): Resultant linear acceleration of head centroid, g = 9.8 m/s^2
Rotational injury criterion, RIC (Kimpara and Iwamoto, 2012)	$RIC = \left\{ \left[(t_2 - t_1) \left(\frac{1}{(t_2 - t_1)} \int_{t_1}^{t_2} \alpha(t)dt \right) \right]^{2.5} \right\}_{max}$	$_{\alpha(t)}$: Rotational acceleration of head centroid, rad/s^2, t_2-t_1 = 36 ms
Generalized Acceleration Model for Brain Injury Threshold, GAMBIT (Newman, 1986)	$GAMBIT = \left[\left(\frac{a_{max}}{a_{cr}} \right)^n + \left(\frac{\alpha_{max}}{\alpha_{cr}} \right)^m \right]^{\frac{1}{s}}$	a_{max} : Maximum linear acceleration, g; a_{cr} : Given the critical linear acceleration, its value is 350 × g; α_{max} : Maximum rotational acceleration, rad/s^2; α_{cr}: Given critical rotational acceleration, its value is 12,000 rad/s^2
Head impact power, HIP (Marjoux et al., 2008)	$HIP = ma_x \int a_x dt + ma_y \int a_y dt + ma_z \int a_z dt + I_{xx}\alpha_x \int \alpha_x dt + I_{yy}\alpha_y \int \alpha_y dt + I_{zz}\alpha_z \int \alpha_z dt$	a_x, a_y, a_z: translational acceleration, m/s^2; α_x, α_y, α_z: Rotational acceleration, rad/s^2. In this study, the head centroid mass m = 4.5 kg; head centroid moment of inertia: I_{xx} = 0.016 kg/m^2, I_{yy} = 0.024 kg/m^2, I_{zz} = 0.022 kg/m^2
Brain injury criterion, BrIC (Takhounts et al., 2013)	$BrIC = \frac{\omega_{max}}{\omega_{cr}} + \frac{\alpha_{max}}{\alpha_{cr}}$	ω_{max}: Maximum rotational velocity, rad/s; ω_{cr}: Given critical rotational velocity is 140 rad/s; α_{max}: Maximum rotational acceleration rad/s^2; α_{cr} : Given critical rotational acceleration, its value is 12,000 rad/s^2
Maximum principal strain, MPS (Gabler et al., 2016)	Used to predict diffuse axonal injury (DAI) and brain contusion	Measures the amount of strain in the tensile direction
Simulated Injury Monitor, SIMon (Takhounts et al., 2003)	Cumulative strain damage measure, CSDM; used to predict diffuse axon injury (DAI), with generally 15% or 25% as the threshold	Measures the volume percentage of the area with brain strain exceeding a certain threshold in the whole brain volume
Simulated Injury Monitor, SIMon (Takhounts et al., 2003)	Dilatation damage measure, DDM. To predict brain contusion and laceration, -100 kPa is generally set as the threshold of negative pressure	Measures the volume percentage of the area with negative pressure exceeding a certain threshold in the whole brain

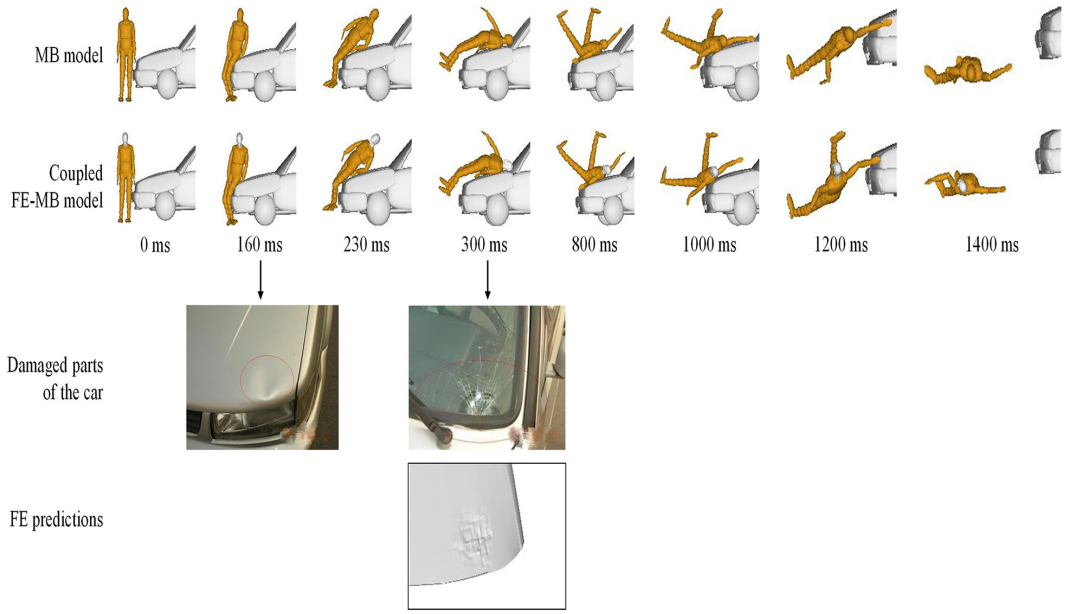

FIGURE 8 | Predicted pedestrian kinematics and the comparison of vehicle deformation between accident reconstruction and real accident, with Case 1 as the example.

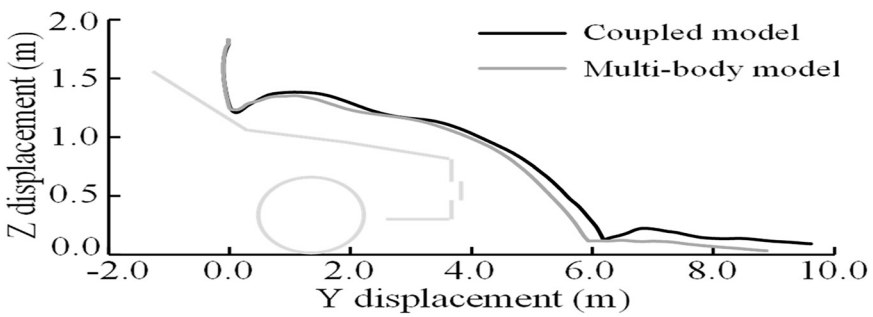

FIGURE 9 | Comparison of the trajectory of VRU head COG in the YOZ plane in Case 1 between using MB and coupled FE–MB models. VRU, vulnerable road user; COG, center of gravity; MB, multibody; FE, finite element.

Analysis of Head Kinematics-Based Injury Criteria

On the basis of the description of the head kinematics-based injury criteria in section "Analysis of Effectiveness of Head Injury Evaluation Criteria" (HIC, GAMBIT, BrIC, RIC, and HIP), the injury criteria are calculated for each accident case (**Table 4**) and compared with the recorded MAIS scores in **Table 2**. Pearson's correlation coefficient is used to analyze and evaluate the prediction and evaluation performance of each injury criterion for head injury.

Assuming that X in formula (1) is the calculated value of HICs in each case, and Y in formula (1) is the MAIS of head injury, formula (1) is used to calculate the correlation coefficient of predicted criterion and head injury MAIS, as shown in **Table 5**. The results of correlation coefficient analysis seem to indicate that HIC, the most widely used injury criterion, has the best correlation with head injury MAIS, followed by HIP, RIC, BrIC, and GAMBIT, with the latter showing the worst correlation.

The predicted HIC, GAMBIT, BrIC, RIC, HIP, and their corresponding MAIS in 31 VRU traffic accidents selected for this study are also graphically displayed in **Figure 10**.

Analysis of Injury Criteria Based on Brain Tissue Deformation

Based on the actual DAI and brain contusion injury records observed in accidents, the HICs based on brain tissue deformation are also computed, which include CSDM (Takhounts et al., 2003, 2008, 2013; Gabler et al., 2016) (for DAI), MPS (Takhounts et al., 2008; Gabler et al., 2016) (for DAI and brain contusion), and DDM (Takhounts et al., 2003) (for brain contusion), as shown in **Tables 6**, **7**.

TABLE 4 | Calculated parametric values of head injury criteria.

Case ID	HIC	GAMBIT	BrIC	RIC	HIP (kW)
1	780.02	4.33	4.45	189,537,000	4.88
2	184.69	1.73	1.95	54,634,500	6.29
3	1,586.97	3.30	3.60	136,134,000	4.56
4	1,031.01	5.15	5.37	249,415,000	20.19
5	2,939.93	2.09	2.25	48,786,900	15.80
6	1,391.30	6.33	6.55	379,812,000	4.22
7	3,833.51	10.11	10.09	350,811,000	10.00
8	2,051.95	11.14	11.36	385,087,000	19.64
9	699.90	1.89	2.00	73,385,300	11.97
10	1,288.22	4.54	4.73	208,250,000	14.04
11	3,569.25	9.12	9.35	653,978,000	15.41
12	3,395.78	8.60	8.72	619,131,000	22.46
13	2,369.58	9.94	9.94	845,224,000	6.55
14	2,503.95	2.89	2.94	244,043,000	4.39
15	1,499.24	1.78	2.35	160,381,000	14.43
16	772.20	2.45	2.73	38,496,500	2.73
17	1,533.34	2.23	2.23	142,236,000	7.53
18	8,107.39	5.26	5.53	625,871,900	19.88
19	197.54	0.72	0.91	9,397,440	5.07
20	254.16	1.80	1.84	13,210,200	6.62
21	311.20	0.99	1.09	6,189,740	8.17
22	1,205.82	3.53	3.94	271,328,000	4.16
23	9,256.10	6.29	6.36	710,420,000	16.89
24	1,757.95	6.57	6.60	453,202,000	21.64
25	678.03	0.77	0.63	3,555,080	1.51
26	7,249.62	5.93	5.91	437,064,000	28.70
27	883.26	2.11	2.26	175,018,000	7.88
28	3,365.14	9.04	9.07	786,648,000	4.79
29	1,423.95	2.46	2.92	152,093,000	11.26
30	2,013.30	4.29	4.42	146,262,000	13.69
31	1,411.30	1.74	1.95	59,559,500	5.68

HIC, head injury criterion; GAMBIT, Generalized Acceleration Model for Brain Injury Threshold; BrIC, brain rotational injury criterion; RIC, rotational injury criterion; HIP, head impact power.

TABLE 5 | Correlation coefficients between calculated injury criteria and MAIS.

Evaluation criterion	HIC	GAMBIT	BrIC	RIC	HIP
Correlation coefficient	0.606	0.332	0.340	0.398	0.403

MAIS, Maximum Abbreviated Injury Scale; HIC, head injury criterion; GAMBIT, Generalized Acceleration Model for Brain Injury Threshold; BrIC, brain rotational injury criterion; RIC, rotational injury criterion; HIP, head impact power.

In order to establish a relationship between the predicted injury criterion and the severity of actual brain injury, the brain injury risk curves in the existing literature are selected to analyze the effectiveness of the criteria in predicting brain injuries. Herein, the injury risk curve established by Takhounts et al. (2003, 2008) is selected for DAI. Combined with the predicted criterion in **Table 6**, the effectiveness of CSDM and MPS injury criteria in predicting DAI is analyzed separately, as shown in **Figure 11**. For brain contusion, the injury risk curve selected herein is that established by Takhounts et al. (2003, 2008). The calculated criterion values in **Table 7** are used to analyze/evaluate the effectiveness of DDM and MPS in predicting brain contusion, as shown in **Figure 12**.

As seen in **Figure 11A**, the predicted brain injury risks based on $CSDM_{0.15}$ for the eight accidents with DAI injury has no clear distribution pattern in relation to the DAI AIS scores; **Figure 11B** demonstrates that only the injury risks calculated from $CSDM_{0.25}$ for the cases with AIS1 and AIS4 show certain regularity, those of the two cases with AIS3 scores are significantly different, and the injury risk corresponding to AIS0 is fairly high and close to that of AIS4 cases. In **Figure 11C**, the cases of AIS1, AIS2, and AIS4 show relatively appropriate uniformity along with the brain injury risk calculated from MPS. As for brain contusion, **Figure 12A** shows that the risk of brain contusion reflected by DDM injury criterion is far lower than the actual injury, implying that brain contusion cannot be predicted through DDM. For the brain contusion risk (**Figure 12B**), certain regularity can be observed in relation to the AIS scores for a case with AIS2 (the lower one) and cases with AIS3 and AIS5, while the risk corresponding to AIS4 case is relatively small.

From the analysis results above, it is suggested that the MPS injury criterion can better predict the possibility of DAI injury compared with $CSDM_{0.15}$ and $CSDM_{0.25}$, and it behaves better than DDM in predicting the risk of brain contusion.

DISCUSSION

Coupled Finite Element–Multibody Human Body Model

In the present study, a coupled FE–MB human body model, developed and validated in our previous study, was used in the reconstruction of VRU impact accidents. The head trajectories predicted by using the MB model or the coupled FE–MB human body model (as shown in **Figure 9** and **Supplementary Appendix 1**) appear to show a good match, especially before the VRU head contacts the windshield. This coupled model was initially proposed in our previous study to overcome the well-known limit of head-only FE model (representing only the pedestrian head and brain) in predicting pedestrian brain injury due to car impact and validated against a real-world car-to-pedestrian impact accident (Wang et al., 2020). That model was later further validated in our study (Yu et al., 2020) in which three cadaver experiments reported in the literature were reproduced with both the coupled body model and an MB body model, and the effectiveness of the coupled model was verified by comparing the pedestrian head kinematics and injury response produced by both models with the experimental results. In the current study, the coupled model was used to reconstruct all of the selected real-world VRU impact accidents and subsequently showed quite similar performance with the MB model in predicting the VRU kinematics, which also confirms its effectiveness.

The FE model has better biofidelity than the MB human body model in reflecting the biomechanical response of the human head in impact accidents (Chai et al., 2011). Nonetheless, the shortcomings of the FE human body model in the accident reconstruction are also clear: the calculation time is too long, the human body posture adjustment is overly complicated, and the time cost is relatively high. The coupled FE–MB human body model is introduced to address these issues, which can predict

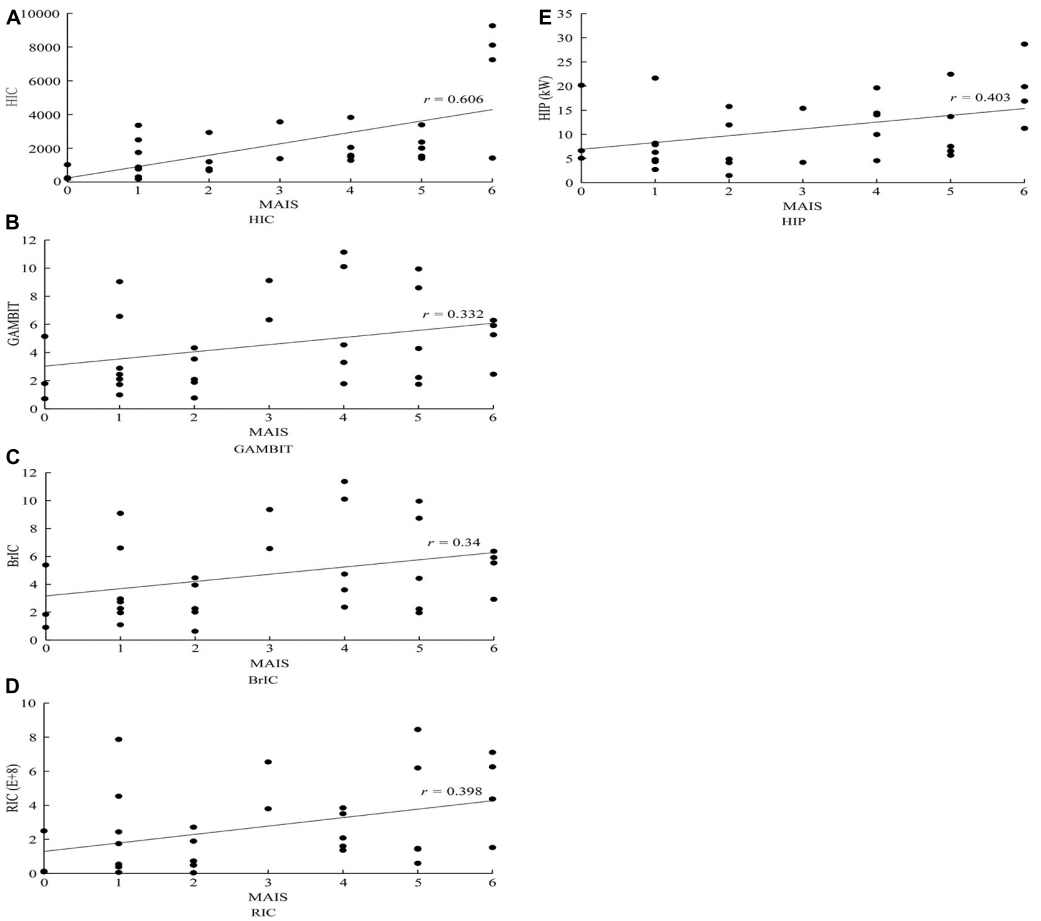

FIGURE 10 | Distribution of predicted head kinematics-based injury criteria and MAIS scores observed in the analyzed VRU impact accident cases. **(A)** HIC; **(B)** GAMBIT; **(C)** BrIC; **(D)** RIC; and **(E)** HIP. MAIS, Maximum Abbreviated Injury Scale; VRU, vulnerable road user; HIC, head injury criterion; GAMBIT, Generalized Acceleration Model for Brain Injury Threshold; MAIS, Maximum Abbreviated Injury Scale; RIC, rotational injury criterion; HIP, head impact power.

TABLE 6 | The AIS of DAI in accident cases included in this study and corresponding parametric values of head injury criteria.

Case ID	DAI AIS	$CSDM_{0.15}$	$CSDM_{0.25}$	MPS
1	2	0.98991727	0.850504137	0.881
2	1	0.82348759	0.389154602	0.603
3	3	0.840098242	0.362849018	0.556
4	0	0.998771975	0.942735264	1.29
5	2	0.997608583	0.916041882	1.019
6	3	0.998061013	0.990951396	2.457
7	4	0.999224405	0.944738883	2.32
15	4	0.993148914	0.985780765	1.402

AIS, Abbreviated Injury Scale; DAI, diffuse axonal injury; MPS, maximum principal strain.

TABLE 7 | AIS score of brain contusion in the accident cases included in this study and the corresponding damage evaluation criteria parameter values.

Case ID	Brain contusion AIS	MPS	DDM
3	4	0.556	0
6	2	2.457	0.020488625
8	3	1.181	0.043110134
9	2	0.818	0.000129266
11	3	0.934	0.000129266
12	5	1.833	0.032445708
22	2	1.092	0.018420372

AIS, Abbreviated Injury Scale; MPS, maximum principal strain; DDM, dilatation damage measure.

both the human body overall kinematics and brain soft tissue deformation responses and effectively improve the efficiency of collision simulation (by up to 82%) (Wang et al., 2020), thus avoiding frequent adjustments of the initial posture of the FE human body model during the reconstruction.

Head Injury Criteria

In this study, 31 car-to-VRU impact accident cases with detailed head injury records were recruited to analyze/evaluate various HICs based on kinematics and brain tissue deformation. The evaluation of head kinematics-based injury criteria in predicting overall head injury was conducted by using Pearson's correlation

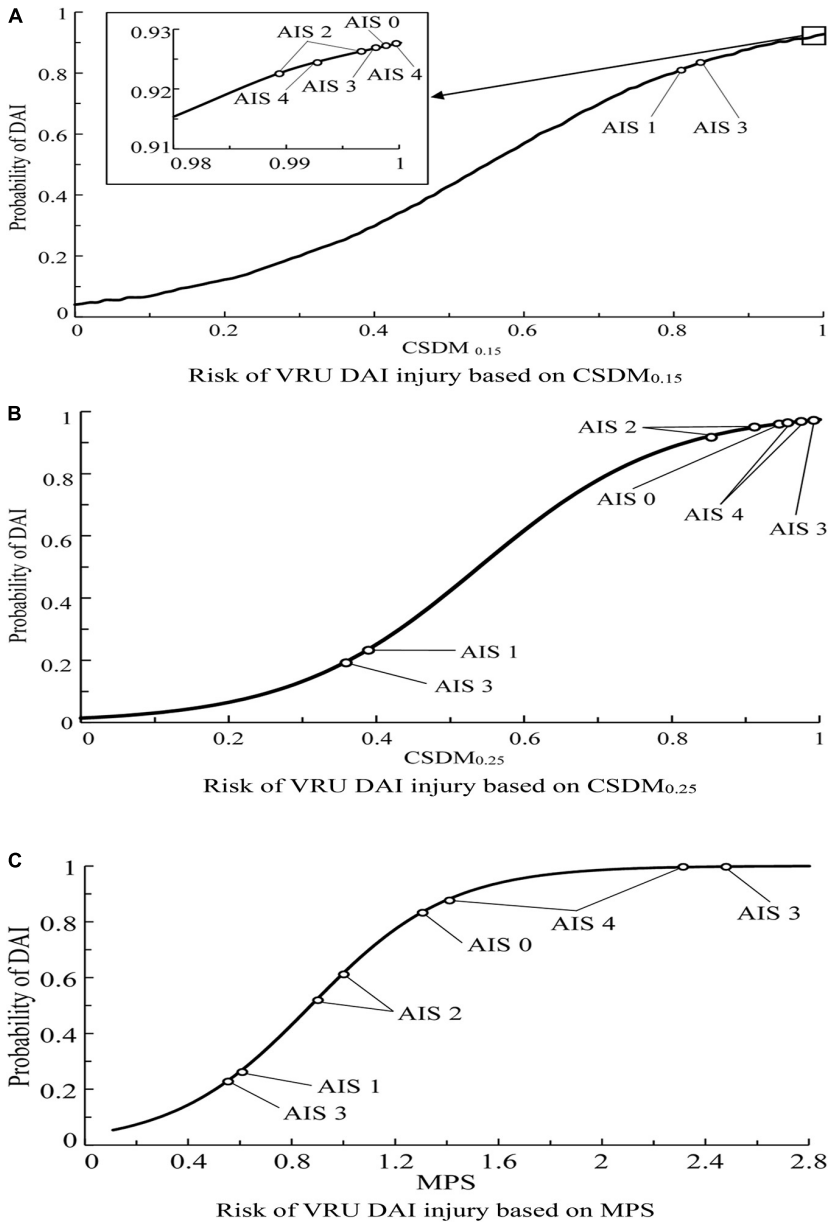

FIGURE 11 | Predicted probability of the DAI occurrence for the VRU impact accident cases analyzed in this study using brain injury risk curves reported in the literature (Takhounts et al., 2003, 2008). **(A)** Risk of VRU DAI injury based on $CSDM_{0.15}$, **(B)** Risk of VRU DAI injury based on $CSDM_{0.25}$, and **(C)** Risk of VRU DAI injury based on MPS. DAI, diffuse axonal injury; VRU, vulnerable road user; MPS, maximum principal strain.

coefficient method (**Tables 4**, **5**), and the brain deformation-based criteria were investigated using the brain injury risk curves in the existing literature combined with actual AIS scores (**Figure 11**).

The current study on the effectiveness of HICs in evaluating VRU head injury in traffic accidents is limited, and from the authors' point of view, it is due to the fact that the number of analyzed samples is not big enough and that the lack of video information of part of the accident cases would potentially affect the kinematics reconstruction of the accident. Differences can be observed between the current study and those reported in the literature (Takhounts et al., 2008; Hernandez et al., 2015; Jones et al., 2016; Feng, 2017; Shi et al., 2020). Shi et al. (2020) conducted similar research based on real-world VRU (including pedestrians and cyclists) impact accident reconstruction using both MB and FE human body models, in which the human body impact boundary conditions at the time of ground landing were extracted from the MB kinematics reconstruction and input into a full-scale FE human body model for head injury reproduction. Their results indicated that HIC, MPS, and $CSDM_{0.15}$ had the best ability to predict head injury, followed by $CSDM_{0.25}$, HIP, BrIC, and DDM, with the latter having the worst ability.

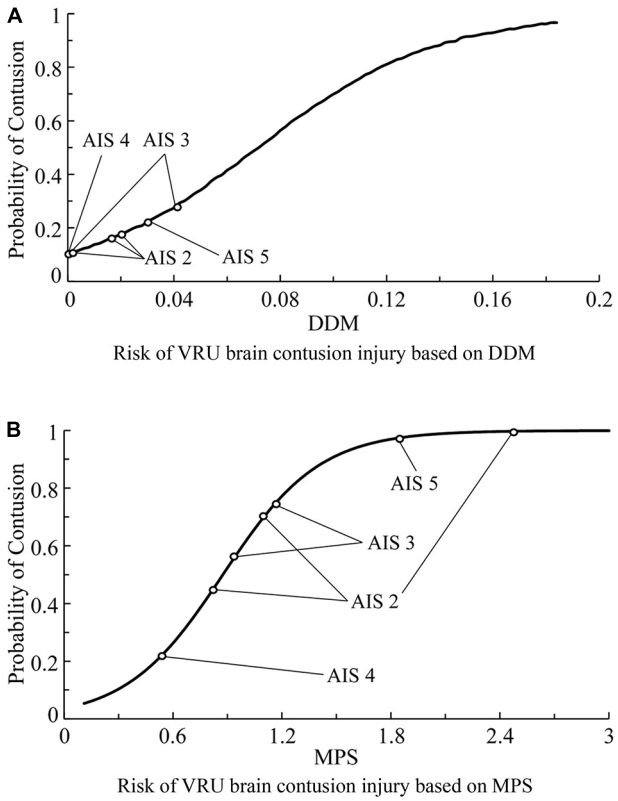

FIGURE 12 | Predicted probability of the brain contusion occurrence for the VRU impact accident cases analyzed in this study using brain injury risk curves reported in the literature (Takhounts et al., 2003, 2008). **(A)** Risk of VRU brain contusion injury based on DDM and **(B)** Risk of VRU brain contusion injury based on MPS. VRU, vulnerable road user; DDM, dilatation damage measure.

Jones et al. (2016) used the GHBMC 50th percentile adult male head–neck model to conduct a huge number of car-to-pedestrian impact simulations and obtain the head injury responses. Results on the analysis of the relationship between HIC and BrIC and brain injury severity suggested that the correlation between BrIC and brain contusion/DAI is higher than that of HIC. Takhounts et al. (2008) performed a similar research focusing on American football accidents and concluded that $CSDM_{0.25}$ and MPS had good correlations with DAI, whereas DDM was not related to contusion or focal lesion. Hernandez et al. (2015) demonstrated that MPS had the best ability to predict mild TBI (MTBI), followed by HIP and GAMBIT. Feng (2017) used head-only FE model to predict pedestrian head/brain injury responses during the head-windscreen impact of a real-world accident and found that MPS had the best ability to predict DAI.

In the present work, HIC and HIP injury criteria were shown to have the best correlation with MAIS, which is consistent with the study by Shi et al. (2020). In comparison with $CSDM_{0.15}$ and $CSDM_{0.25}$, the MPS damage criterion appeared to better predict the occurrence of DAI injury, which is in good agreement with the conclusions of Takhounts et al. (2008) and Feng (2017). With regard to predicting brain contusion, MPS can provide better ability than DDM, and this finding is consistent with the research by Takhounts et al. (2008). Meanwhile, differences exist between the current research and those reported in the literature, especially for the evaluation of brain deformation-based injury criteria. This can be explained by the application of the coupled FE–MB human body model that accounted for the influences of the rest of the human body on the head kinematics/injury responses compared with FE head-only models (Wang et al., 2020), which we believe could bring more confidence about the novelty of this study in the accuracy of HICs.

Limitations

The main limitation of this study is that the number of reconstructed traffic accident cases is limited, and the methods of accident reconstruction are backward, which may lead to potential variations in the behavior of certain injury criteria. Moreover, since many factors influence the kinematics reconstruction of the accident, such as VRU initial posture, thereby it cannot be guaranteed that the simulation accurately reproduces the actual accidents, leading to a potential impact on the accuracy of head injury analysis. Lastly, the head–neck FE model used in this study is extracted from the THUMS model, which represents the 50th percentile adult male. In fact, the biomechanical properties of the head tissues of adults and the elderly are different, which leads to different injury tolerance and kinematics response by different ages.

CONCLUSION

In this work, the coupled FE–MB human body model was used to simulate VRU injury in real traffic accidents, kinematics reconstruction, and head/brain injury reproduction of a series of real-world car-to-VRU impact accidents to investigate the effectiveness of various HICs in predicting the head injury risk due to VRU–car collision. According to the results, the following conclusions can be drawn:

1. The coupled FE–MB human body model can efficiently and accurately simulate the kinematics response and head/brain injuries of VRUs in impact accidents and can be effectively used for the analysis of head/brain injury due to VRU–car collision.
2. Among the injury criteria based on head kinematics response, the most widely used HIC and HIP are the most accurate and effective criteria in predicting head injury. Considering brain tissue deformation-based injury criteria, the MPS injury criterion can more effectively predict the possibility of DAI than the $CSDM_{0.15}$ and $CSDM_{0.25}$. For brain contusion, the MPS injury criterion shows enhanced ability to predict the injury risk compared with the DDM criterion.

DATA AVAILABILITY STATEMENT

The original contributions presented in the study are included in the article/**Supplementary Material**, further inquiries can be directed to the corresponding author.

AUTHOR CONTRIBUTIONS

FW: conceptualization, project administration, methodology, funding acquisition, and writing—review and editing. ZW: software and writing—original draft. LH: supervision and funding acquisition. HX: formal analysis and visualization. CY: validation and methodology. FL: investigation and resources. All authors contributed to the article and approved the submitted version.

FUNDING

The authors acknowledge the financial support of Hunan Province Natural Science Outstanding Youth Fund (Grant No. 2019JJ20017), the National Natural Science Foundation of China (Grant Nos. 51875049 and 51605407), and Hunan Key Research and Development Program, China (Grant No. 2020SK2099).

SUPPLEMENTARY MATERIAL

The Supplementary Material for this article can be found online at: https://www.frontiersin.org/articles/10.3389/fbioe.2021.677982/full#supplementary-material

Supplementary Appendix 1 | Comparison of the trajectory of VRU head COG in the YOZ plane in Cases 2–31 when using MB or coupled FE–MB models. VRU, vulnerable road user; COG, center of gravity; MB, multibody; FE, finite element.

REFERENCES

AAAM (2008). *Abbreviated Injury Scale 2005,Update 2008*. Barrington: Association for Advancement of Automatic Medicine.

Al-Bsharat, A. S., Hardy, W. N., Yang, K. H., Khalil, T. B., Tashman, S., and King, A. I. (1999). *Brain/Skull Relative Displacement Magnitude Due to Blunt Head Impact: New Experimental Data and Model (No. 99SC22)*. Warrendale: SAE.

Antona-Makoshi, J. (2016). *Traumatic Brain Injuries: Animal Experiments and Numerical Simulations to Support the Development of a Brain Injury Criterion*. Sweden: Chalmers University of Technology Gothenburg.

Bain, A. C., and Meaney, D. F. (2000). Tissue-level thresholds for axonal damage in an experimental model of central nervous system white matter injury. *J. Biomech. Eng.* 122, 615–622. doi: 10.1115/1.1324667

Chai, X., Jin, X., Zhang, X., and Hou, X. (2011). The application for skull injury in vehicle–pedestrian accident. *Int. J. Crashworthiness* 16, 11–24.

Corrigan, J. D., Selassie, A. W., and Orman, J. A. L. (2010). The epidemiology of traumatic brain injury. *J. Head Trauma Rehabil.* 25, 72–80.

Deguchi, M. (2003). "Modeling of a motorcycle for collision simulation," in *Proceedingsof the International Technical Conference on the Enhanced Safety of Vehicles*, Gothenburg.

Fahlstedt, M., Halldin, P., Alvarez, V., and Kleiven, S. (2016). "Influence of the body and neck on head kinematics and brain injury risk in bicycle accident situations. *Paper Presented at the IRCOBI 2016*, (Zurich: IRCOBI).

Feng, C. (2017). *Prediction of Pedestrian Death Risk and Brain Injury Type in Vehicle Collision*. Chongqing: Third Military Medical University.

Gabler, L. F., Crandall, J. R., and Panzer, M. B. (2016). Investigating brain injury tolerance in the sagittal plane using a finite element model of the human head. *Int. J. Automotive Eng.* 7, 37–43. doi: 10.1089/neu.2016.4758

Gadd, C. W. (1966). *Use of a Weighted-Impulse Criterion for Estimating Injury Hazard (No. 660793)*. Warrendale: SAE.

Hernandez, F., Wu, L. C., Yip, M. C., Laksari, K., Hoffman, A. R., Lopez, J. R., et al. (2015). Six degree-of-freedom measurements of human mild traumatic brain injury. *Ann. Biomed. Eng.* 43, 1918–1934.

Hu, J., Jin, X., Lee, J. B., Zhang, L., Chaudhary, V., Guthikonda, M., et al. (2007). Intraoperative brain shift prediction using a 3D inhomogeneous patient-specific finite element model. *J. Neurosurg.* 106, 164–169. doi: 10.3171/jns.2007.106.1.164

Hu, L., Bao, X., Lin, M., Yu, C., and Wang, F. (2021). Research on risky driving behavior evaluation model based on CIDAS real data. *Proc. Instit. Mech. Eng. Part D J. Automobile Eng.* 235:095440702098597. doi: 10.1177/0954407020985972

Hu, L., Hu, X., Wang, J., Kuang, A., Hao, W., and Lin, M. (2020). Casualty risk of e-bike rider struck by passenger vehicle using China in-depth accident data. *Traf. Injury Prevent.* 21, 283–287. doi: 10.1080/15389588.2020.1747614

Jones, D. A., Urban, J. E., Weaver, A. A., and Stitzel, J. D. (2016). "Investigation of head injury mechanisms through multivariate finite element simulation," in *Proceedings of the 12th Ohio State University Injury Biomechanics Symposium*, Columbus, OH.

Katsuhara, T., Miyazaki, H., Kitagawa, Y., and Yasuki, T. (2014). "Impact kinematics of cyclist and head injury mechanism in car-to-bicycle collision," in *Proceedings of the IRCOBI conference 2014*, Zurich.

Kimpara, H., and Iwamoto, M. (2012). Mild traumatic brain injury predictors based on angular accelerations during impacts. *Ann. Biomed. Eng.* 40, 114–126.

Kleiven, S. (2007). *Predictors for Traumatic Brain Injuries Evaluated Through Accident Reconstructions (No. 2007-22-0003)*. Warrendale: SAE.

Kong, C., and Yang, J. (2010). Logistic regression analysis of pedestrian casualty risk in passenger vehicle collisions in China. *Accident Anal. Prevent.* 42, 987–993.

Li, F., Liu, N. S., Li, H. G., Zhang, B., Tian, S. W., Tan, M. G., et al. (2019). A review of neck injury and protection in vehicle accidents. *Transp. Saf. Environ.* 1, 89–105.

Li, F., and Yang, J. (2010). A study of head–brain injuries in car-to-pedestrian crashes with reconstructions using in-depth accident data in China. *Int. J. Crashworthiness* 15, 117–124.

Li, G., Yang, J., and Simms, C. (2017). Safer passenger car front shapes for pedestrians: a computational approach to reduce overall pedestrian injury risk in realistic impact scenarios. *Accident Anal. Prevent.* 100, 97–110. doi: 10.1016/j.aap.2017.01.006

Lissner, H., Lebow, M., and Evans, F. (1960). Experimental studies on the relation between acceleration and intracranial pressure changes in man. *Surg. Gynecol. Obstetr.* 111:329.

Lyons, M., and Simms, C. K. (2012). "Predicting the influence of windscreen design on pedestrian head injuries," in *Paper presented at the IRCOBI Conference*, (Zurich: IRCOBI).

Marjoux, D., Baumgartner, D., Deck, C., and Willinger, R. (2008). Head injury prediction capability of the HIC, HIP, SIMon and ULP criteria. *Accident Anal. Prevent.* 40, 1135–1148. doi: 10.1016/j.aap.2007.12.006

Miller, R. T., Margulies, S. S., Leoni, M., Nonaka, M., Chen, X., Smith, D. H., et al. (1998). Finite element modeling approaches for predicting injury in an experimental model of severe diffuse axonal injury. *SAE Trans.* 4, 2798–2810.

Nahum, A. M., Smith, R., and Ward, C. C. (1977). *Intracranial Pressure Dynamics During Head Impact (No. 770922)*. Warrendale: SAE.

Newman, J., Barr, C., Beusenberg, M. C., Fournier, E., Shewchenko, N., Welbourne, E., et al. (2000). "A new biomechanical assessment of mild traumatic brain injury. Part 2: results and conclusions," in *Proceedings of the International Research Council on the Biomechanics of Injury conference*, Zurich. doi: 10.1227/01.neu.0000196265.35238.7c

Newman, J. A. (1986). "A generalized acceleration model for brain injury threshold (GAMBIT)," in *Proceedings of the 1986 International Research Council on the Biomechanics of Injury Conference*, Zurich. doi: 10.1007/s10439-019-02382-2

Nie, J., and Yang, J. (2014). A study of bicyclist kinematics and injuries based on reconstruction of passenger car–bicycle accident in China. *Accident Anal. Prevent.* 71, 50–59. doi: 10.1016/j.aap.2014.04.021

Nie, J., and Yang, J. (2015). A study on the dynamic response and injury of cyclist based on car-bicycle accident reconstruction. *Automotive Eng.* 37, 160–166.

Nie, J., Li, G., and Yang, J. (2015). A study of fatality risk and head dynamic response of cyclist and pedestrian based on passenger car accident data analysis

and simulations. *Traffic Inj. Prevent.* 16, 76–83. doi: 10.1080/15389588.2014.881477

Popescu, C., Anghelescu, A., Daia, C., and Onose, G. (2015). Actual data on epidemiological evolution and prevention endeavours regarding traumatic brain injury. *J. Med. Life* 8:272.

Ruan, S., Li, H., Wang, X., and Liu, W. (2007). A new exploration of the applicability and usability of criteria for judging head injury. *J. Biomed. Eng.* 24, 1373–1377.

Shi, L., Han, Y., Huang, H., Davidsson, J., and Thomson, R. (2020). Evaluation of injury thresholds for predicting severe head injuries in vulnerable road users resulting from ground impact via detailed accident reconstructions. *Biomech. Model. Mechanobiol.* 19, 1845–1863. doi: 10.1007/s10237-020-01312-9

Shi, L., Han, Y., Huang, H., Li, Q., Wang, B., and Mizuno, K. (2018). Analysis of pedestrian-to-ground impact injury risk in vehicle-to-pedestrian collisions based on rotation angles. *J. Saf. Res.* 64, 37–47. doi: 10.1016/j.jsr.2017.12.004

Shigeta, K., Kitagawa, Y., and Yasuki, T. (2009). "Development of next generation human FE model capable of organ injury prediction," in *Proceedings of the 21st Annual Enhanced Safety of Vehicles*, Zurich.

Takhounts, E. G., Craig, M. J., Moorhouse, K., McFadden, J., and Hasija, V. (2013). Development of brain injury criteria (BrIC). *Stapp. Car Crash J.* 57, 243–266.

Takhounts, E. G., Eppinger, R. H., Campbell, J. Q., Tannous, R. E., Power, E. D., and Shook, L. S. (2003). On the development of the SIMon finite element head model. *Stapp. Car Crash J.* 47, 107–133.

Takhounts, E. G., Ridella, S. A., Hasija, V., Tannous, R. E., Campbell, J. Q., Malone, D., et al. (2008). *Investigation of Traumatic Brain Injuries using the Next Generation of Simulated Injury Monitor (SIMon) Finite Element Head Model (No. 2008-22-0001)*. Warrendale: SAE.

TASS (2013a). *Coupiling Manual. version 7.5*. Netherlands: TASS.

TASS (2013b). *MADYMO Human Body Models Manual Release 7.5*. Netherlands: TASS.

TASS (2013c). *MADYMO Manual Version 7.5*. Netherlands: TASS.

Versace, J. (1971a). *A Review of the Severity Index (0148–7191)*. Warrendale: SAE.

Versace, J. (1971b). "A review of the severity index," in *Proceedings of the 15th Stapp Car Crash Conference*, Coronado.

Wang, F., Han, Y., Wang, B., Peng, Q., Huang, X., Miller, K., et al. (2018). Prediction of brain deformations and risk of traumatic brain injury due to closed-head impact: quantitative analysis of the effects of boundary conditions and brain tissue constitutive model. *Biomech. Model. Mechanobiol.* 17, 1165–1185. doi: 10.1007/s10237-018-1021-z

Wang, F., Yu, C., Wang, B., Li, G., Miller, K., and Wittek, A. (2020). Prediction of pedestrian brain injury due to vehicle impact using computational biomechanics models: are head-only models sufficient? *Traffic Inj. Prevent.* 21, 102–107. doi: 10.1080/15389588.2019.1680837

Watanabe, R., Miyazaki, H., Kitagawa, Y., and Yasuki, T. (2011). "Research of collision speed dependency of pedestrian head and chest injuries using human FE model (THUMS version 4)," in *Proceedings of the 22nd Int. Technical Conf. on the Enhanced Safety of Vehicles (ESV)*, Zurich.

Wittek, A., Grosland, N. M., Joldes, G. R., Magnotta, V., and Miller, K. (2016). From finite element meshes to clouds of points: a review of methods for generation of computational biomechanics models for patient-specific applications. *Ann. Biomed. Eng.* 44, 3–15. doi: 10.1007/s10439-015-1469-2

Yang, J. (2005). Review of injury biomechanics in car-pedestrian collisions. *Int. J. Vehicle Saf.* 1, 100–117.

Yang, K. H., Mao, H., Wagner, C., Zhu, F., Chou, C. C., and King, A. I. (2011). "Modeling of the brain for injury simulation and prevention," in *Biomechanics of the Brain*, ed. K. Miller (New York, NY: Springer), 99–110.

Yang, Y., Chang, T., Luo, T., Li, L., and Qu, Y. (2017). Research progress of multimodal monitoring in the treatment of severe traumatic brain injury. medical review. *Med. Life* 23, 1346–1349.

Yao, J., Yang, J., and Otte, D. (2008). Investigation of head injuries by reconstructions of real-world vehicle-versus-adult-pedestrian accidents. *Saf. Sci.* 46, 1103–1114.

Yu, C., Wang, F., Wang, B., Li, G., and Li, F. (2020). A computational biomechanics human body model coupling finite element and multibody segments for assessment of head/brain injuries in car-to-pedestrian collisions. *Int. J. Environ. Res. Public Health* 17:492. doi: 10.3390/ijerph17020492

Conflict of Interest: The authors declare that the research was conducted in the absence of any commercial or financial relationships that could be construed as a potential conflict of interest.

frontiers in Bioengineering and Biotechnology

ORIGINAL RESEARCH
published: 30 June 2021
doi: 10.3389/fbioe.2021.682974

Comparison of Upper Neck Loading in Young Adult and Elderly Volunteers During Low Speed Frontal Impacts

Carmen M. Vives-Torres[1]*, *Manuel Valdano*[1], *Jesus R. Jimenez-Octavio*[1], *Julia Muehlbauer*[2], *Sylvia Schick*[2], *Steffen Peldschus*[2] *and Francisco J. Lopez-Valdes*[1]

[1] *Instituto de Investigacion Tecnologica, ICAI, Engineering School, Universidad Pontificia Comillas, Madrid, Spain,*
[2] *Biomechanics and Accident Analysis, Ludwig Maximilians University (LMU), Munich, Germany*

Cervical pain and injuries are a major health problem globally. Existing neck injury criteria are based on experimental studies that included sled tests performed with volunteers, post-mortem human surrogates and animals. However, none of these studies have addressed the differences between young adults and elderly volunteers to date. Thus, this work analyzed the estimated axial and shear forces, and the bending moment at the craniocervical junction of nine young volunteers (18–30 years old) and four elderly volunteers (>65 years old) in a low-speed frontal deceleration. Since the calculation of these loads required the use of the mass and moment of inertia of the volunteers' heads, this study proposed new methods to estimate the inertial properties of the head of the volunteers based on external measurements that reduced the error of previously published methods. The estimated mean peak axial force (Fz) was −164.38 ± 35.04 N in the young group and −170.62 ± 49.82 N in the elderly group. The average maximum shear force (Fx) was −224.42 ± 54.39 N and −232.41 ± 19.23 N in the young and elderly group, respectively. Last, the estimated peak bending moment (My) was 13.63 ± 1.09 Nm in the young group and 14.81 ± 1.36 Nm in the elderly group. The neck loads experienced by the elderly group were within the highest values in the present study. Nevertheless, for the group of volunteers included in this study, no substantial differences with age were observed.

Keywords: frontal impact, head inertial properties, inverse dynamics, volunteer testing, occipital condyle loads

OPEN ACCESS

Edited by:
Ridha Hambli,
Polytech Orléans, France

Reviewed by:
Amber Rath Stern,
Engineering Systems Inc. (ESi),
United States
John Bolte,
The Ohio State University,
United States

***Correspondence:**
Carmen M. Vives-Torres
201604102@alu.comillas.edu

Specialty section:
This article was submitted to Biomechanics, a section of the journal Frontiers in Bioengineering and Biotechnology

Received: *19 March 2021*
Accepted: *04 June 2021*
Published: *30 June 2021*

Citation:
Vives-Torres CM, Valdano M, Jimenez-Octavio JR, Muehlbauer J, Schick S, Peldschus S and Lopez-Valdes FJ (2021) Comparison of Upper Neck Loading in Young Adult and Elderly Volunteers During Low Speed Frontal Impacts. Front. Bioeng. Biotechnol. 9:682974. doi: 10.3389/fbioe.2021.682974

1. INTRODUCTION

Neck injuries and pain are serious public health problems in the general population. The Global Burden of Diseases, Injuries, and Risk Factors Study 2017 estimated the point rate prevalence in 3551.1 cases and the number of years lived with disability associated to neck pain in 352 years per 100,000 population, globally (Safiri et al., 2020). The prevalence of neck pain has been reported to increase with age up to 70–74 years and then to decrease (Safiri et al., 2020). Motor vehicle crashes (MVC) are one of the main causes for neck injuries worldwide (Yadollahi et al., 2016; Umana et al., 2018). Although rare when compared to other injuries occurring in MVC, severe neck injuries can be life threatening or are associated with a high risk of severe impairment. A review of NASS-CDS data between 1994 and 2011 showed that spinal cord injury (SCI) occurred in one out of 1860 front seat occupants in tow-away crashes in the United States, with fracture-dislocation injuries occurring 5.3 times more often than SCI (Parenteau and Viano, 2014).

In frontal impacts, these injuries have been traditionally associated to the dynamic loading of the neck that occurs when the torso is suddenly stopped by the seat belt while the head continues pulling from the neck. As these loads cannot be measured directly without altering the tissue, the use of inverse dynamics methods has been proposed as a valid, non-invasive, method to estimate the craniocervical forces and moments experienced by volunteers and PMHS during frontal impacts (Funk et al., 2007; Lopez-Valdes et al., 2010; Seacrist et al., 2011; Beeman et al., 2016). However, this method requires calculating the mass and moment of inertia of the head, which cannot be directly measured when using human volunteers. In early studies with PMHS, the analysis of the head mass and moment of inertia involved the separation of the head from the neck (Walker et al., 1973). In more recent studies, less invasive methods, including the use of non-destructive computer models, have been used to accurately determine the human head anthropometry (Albery and Whitestone, 2003; Plaga et al., 2005; Damon, 2009). Other studies attempted to relate head inertial characteristics to external measurements (Clauser et al., 1969; McConville et al., 1980; Loyd et al., 2010; Seacrist et al., 2011). Such procedures have not been consistently used yet, requiring a more thorough investigation that could lead to the consolidation of a robust method to estimate such parameters.

As aforementioned, the prevention of MVC cervical injuries relies on monitoring the axial and shear forces and the bending moment measured at the upper and lower cervical spine of Anthropomorphic Test Devices (ATD) or dummies in simulated collisions to calculate neck injury indicators, such as the Neck Injury Criterion (Nij) that combines the axial force with the flexion/extension moment to predict the likelihood of cervical trauma (Li et al., 2019). These indices are then compared to corresponding thresholds that are based on previous experiments performed with Post Mortem Human Surrogates (PMHS), animals and live human volunteers (Mertz and Patrick, 1971; Prasad and Daniel, 1984), where severe injuries such as hemorrhages at the atlanto-occipital junction, cord transections, ligament and capsular partial and complete tears injuries were observed. The non-injury data obtained from these experiments have been used to propose the intercept values used in the development of the Nij injury criterion (Eppinger et al., 2000; Mertz et al., 2003). Despite the aforementioned experiments, cervical data from whole body experiments with volunteers in an automotive setup are still limited (Mertz and Patrick, 1971; Arbogast et al., 2009; Seacrist et al., 2011) and, only in a few cases, allow to study differences across different age groups which has focused mainly on understanding the differences between pediatric and adult subjects. Arbogast et al. (2009) found a decrease in the magnitude of flexion rotation with increasing age in the comparison between children (6–14 years old) and young adults (18–30 years old). For the same subjects, Seacrist et al. (2011) utilized inverse dynamics to estimate upper cervical neck loads and reported increasing bending moment and decreasing peak axial force with increasing age.

This work reviewed all the studies mentioned above and used the already available experimental data to propose a new method to calculate the head inertial properties of volunteers based on external measurements. This new method reduced considerably the error generated using the previously published methods. In addition, the axial and shear forces and the flexion moment at the craniocervical junction were estimated using inverse dynamics during a low-speed frontal deceleration of a set of volunteers. Two different volunteer age groups were analyzed: nine young adults (18–30 years old) and four elderly volunteers (>65 years old).

Thus, the current study had two objectives: to estimate the head mass and principal moment of inertia improving the mean error obtained in previous studies, and to verify whether there were age-related differences in the craniocervical loads in low-speed frontal impacts using inverse dynamics.

2. MATERIALS AND METHODS

The experimental data used in this study were generated within the SENIORS project, funded by the European Union under the Horizon 2020 program (Grant agreement ID: 636136). The data used in this study correspond to low-speed frontal tests performed with volunteers from two different age groups.

A complete description of the test conditions, volunteers' characteristics, experimental data recorded during these tests and general kinematic and dynamic results can be downloaded from the website of the THUMS User Community (THUMSUserCommnunity, 2021).

2.1. Volunteer Characteristics and Procedures

Four elderly (>65 years old) and nine young (18–30 years old) male volunteers were recruited for the study. Subjects were chosen to be as close in height and weight as possible to the 50th male percentile (nominally: 175 cm, 78 kg). Volunteers reported not to have any health condition susceptible of being aggravated during the study. Prior to being exposed to the low-speed test, volunteers were measured and instrumented. **Table 1** provides detailed information on the anthropometry of each of the test subjects.

The information sheet, informed consent, and the whole study procedure was reviewed and approved by CEICA (Ethical Commission for Clinical Research of Aragon), which was the official review board to ensure that the study was performed according to the required Ethical principles.

2.2. Calculation of Head Inertial Properties

The head mass and principal moment of inertia about the *y*-axis had to be estimated using anthropometric parameters that could be measured externally on the volunteers. The experimental data in Damon (2009), which included measurements of the head mass, moment of inertia and head dimensions from 100 PMHS (79 male and 21 female), were used to derive the estimations of the head inertial properties to be used in this study.

2.2.1. Estimation of the Head Mass

Regression curves were generated for different potential predictors of the mass of the head (i.e. length, depth, width, circumference). The characteristic length, which is the sum of

TABLE 1 | Anthropometry and main characteristics of volunteers.

Subject ID	Age (years)	Stature (cm)	Weight (kg)	Neck girth (cm)	Head girth (cm)	Head breadth (cm)	Head depth (cm)
Vol 01	18	171.0	75.5	38.0	59.5	15.3	19.4
Vol 02	18	176.5	77.7	36.5	57.0	15.9	19.9
Vol 03	21	179.5	73.0	37.0	59.0	15.7	20.1
Vol 04	21	179.0	79.4	37.0	58.0	15.5	19.9
Vol 05	22	167.0	75.3	38.5	55.0	14.4	19.2
Vol 07	71	176.5	99.0	46.0	60.0	16.3	20.5
Vol 08	82	165.3	78.2	41.5	57.0	16.9	19.3
Vol 09	67	169.0	88.2	44.5	59.5	15.8	20.3
Vol 10	28	172.0	68.4	37.5	56.0	14.8	20.0
Vol 11	70	172.5	89.6	41.0	58.0	16.0	20.0
Vol 12	25	174.0	73.0	38.0	59.5	17.0	22.0
Vol 13	26	174.0	64.6	37.0	57.0	15.0	20.0
Vol 14	21	173.0	86.7	43.0	61.0	15.5	22.0

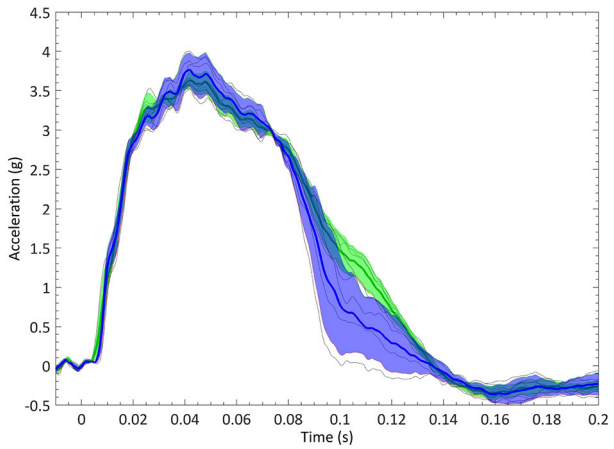

FIGURE 1 | Sled deceleration pulse corridors in the young (blue) and elderly (green) groups. Solid lines are the average deceleration within the group. Shaded area corresponds to the one standard deviation corridor.

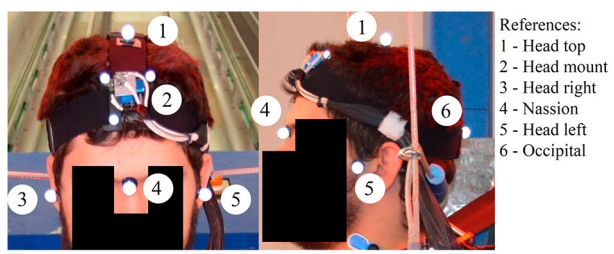

FIGURE 2 | Detail of the 6 degree-of-freedom head cube and of the position of the sensors on the head of one of the volunteers.

the head breadth, depth, and circumference, was also used. To test the accuracy of the estimations, the data in Damon (2009) were divided into a training set (80% of the data), and a test set (20% of the data).The normality of the residuals was studied, and the overall mean errors were calculated.

2.2.2. Estimation of the Head Principal Moment of Inertia

Two regression models were analyzed including either head dimensions and the head mass as independent variables, or just head mass, due to the high correlation between the moment of inertia and the head mass reported in previous studies (Plaga et al., 2005). To test the accuracy of the estimations, the data in Damon (2009) were again divided into a training set (80% of the data) and a test set (20% of the data). Due to the high error obtained, a third approach was used in which the moment of inertia of the head was approximated by those of three-dimensional objects (ellipsoid and sphere) as shown in Equations (1, 2).

$$I_{Ellipsoid}(kg\ m^2) = \frac{1}{5} \cdot [Head\ mass] \cdot [a^2 + b^2] \quad (1)$$

$$I_{Sphere}(kg\ m^2) = \frac{2}{5} \cdot [Head\ mass] \cdot r^2 \quad (2)$$

The least-squares approach was used with combinations of the head depth, breadth, and circumference, to calculate the parameters needed (a, b, and r in Equations 1, 2).

2.3. Experimental Test Setup, Crash Pulse and Description of Tests

The experimental test fixture was designed to represent the seating posture of a passenger car occupant in a simplified manner. This test fixture had been used before in experiments simulating frontal crashes with other surrogates (the THOR dummy, PMHS tests) (Lopez-Valdes et al., 2018; Muehlbauer et al., 2019). The fixture consisted of a rigid seat, a rigid footrest, and a flexible backrest made out of three segments of metal wire. The seat geometry included several inclined plates in the rear-forward and mid-lateral directions, and was designed so

TABLE 2 | Filters and cutoff frequencies used for each test.

Subject ID	Head angular velocity	Head linear acceleration
Vol 01	CFC 20	CFC 60
Vol 02	CFC 20	CFC 60
Vol 03	CFC 20	CFC 60
Vol 04	CFC 60	CFC 60
Vol 05	CFC 20	CFC 60
Vol 07	CFC 20	CFC 60
Vol 08	CFC 10	CFC 10
Vol 09	CFC 20	CFC 20
Vol 10	CFC 20	CFC 60
Vol 11	CFC 20	CFC 60
Vol 12	CFC 60	CFC 60
Vol 13	CFC 60	CFC 60
Vol 14	CFC 10	CFC 10

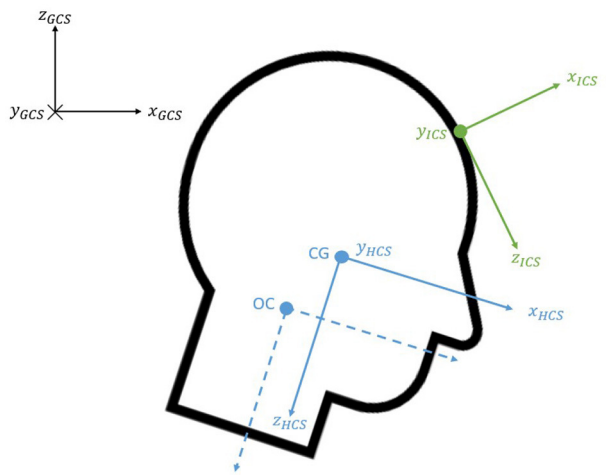

FIGURE 3 | Coordinate systems.

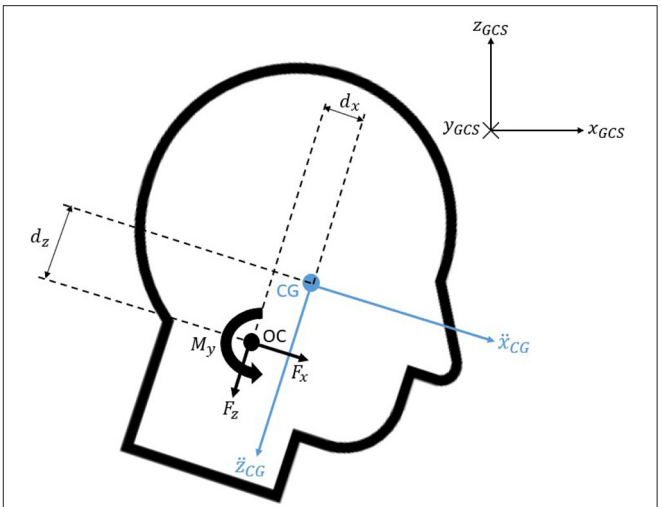

FIGURE 4 | Free body diagram of the head.

that the pelvic sagittal displacement of the occupant in a frontal crash was similar to the one observed in a production car seat (Pipkorn et al., 2016b). Occupants were restrained by a non-retractor three-point seat belt. The position of the anchoring points of the seat belt was chosen based on previous studies to allow the comparison of the results (López-Valdés et al., 2016; Pipkorn et al., 2016a). The position of the footrest and of the seat belt D-ring were adjusted depending on each volunteer's anthropometry, but ensuring that the loading scenarios were dynamically similar. The magnitude and the time history of the sled deceleration were chosen based on previous studies to ensure a safe experimental environment for the volunteers (Arbogast et al., 2009; Lopez-Valdes et al., 2010). These previous studies had exposed volunteers to a triangular pulse with a peak of 3.5 g and a duration of 100 ms, and had reported that no volunteer had experienced pain or discomfort. The selected test pulse for this study is shown in **Figure 1**.

Each volunteer was exposed to a minimum of three tests, with the exception of volunteer 8, who participated only in two tests. A preliminary analysis of the data showed a different kinematic behavior between the first trial and the subsequent ones for each volunteer, which were more similar. Only the third trial of each volunteer was chosen for the inverse dynamics analyses. This gave the volunteers enough time to understand the testing procedure. Volunteers received an acoustic signal immediately before the start of the test and they were asked to remain relaxed. The second trial had to be used for volunteers 8 and 9, instead of the third one. For volunteer 9, the second test was chosen as the head band on which the forehead markers and sensors were placed moved with respect to the head in the third trial.

2.4. Experiments Instrumentation and Data Processing

A head mount that included a tridimensional accelerometer cube (Endevco 7264C, Meggitt, Irvine, US) and a tridimensional angular rate sensor (ARS PRO-18K, DTS, Seal Beach, US) was attached to an adjustable headband that was fastened around the head of the volunteers providing a secure fit to avoid any relative motion between the head and the instrumentation (**Figure 2**). All sensor data were recorded at 10,000 Hz using an external data acquisition system (PCI-6254, National Instruments; Austin, TX). Sensor data were filtered using a low pass filter with a cutoff frequency selected based on the characteristics of each of the signals to ensure that essential information was not removed in the filtering process. **Table 2** shows the CFC class filters used in the analysis of each volunteer's data.

In addition to the above sensors, reflective markers were attached to selected anatomical landmarks on the volunteers, including: most lateral point of the Zygomatic bone (bilateral), Nasion and Opistocranion. Kinematic data were collected at 1,000 Hz using an optoelectric stereophotogrammetric system consisting of 10 cameras (Vicon, TS series, Oxford, UK). The

TABLE 3 | Mean errors and standard deviations obtained in the estimation of the head inertial properties.

	Present study			Seacrist et al., 2011
	Training set (80%)	Validation set (20%)	Overall (100%)	Overall (100%)
Head mass	11.00 ±9.39%	12.78 ±7.68%	11.36 ±9.07%	18.16 ±19.61%
I_{yy}	7.15 ±6.85%	8.30 ±5.62%	13.93 ±12.38%	27.89 ±31.19%

system captured the position of the aforementioned retro-reflective spherical markers within a calibrated 3D volume. A calibration procedure, performed prior to testing, estimated the optical characteristics of each camera and established its position and orientation in a global coordinate system (GCS) that was fixed to the laboratory. The *x*-axis of the GCS pointed forward parallel to the moving direction of the sled, the *z*-axis pointed upwards and the *y*-axis was chosen to complete a right-hand coordinate system, resulting in a coordinate system in which the y and z axes pointed opposite to the SAE J211 recommendations. A photogrammetric algorithm within the Vicon Nexus software package (Nexus 1.8.5, Vicon, Oxford, UK) reconstructed the 3D position of each target for each video sample increment from the multiple 2D camera images.

2.5. Definition of Coordinate Systems

Several coordinate systems were used in the study as illustrated in **Figure 3**. The position of the Vicon targets was expressed with respect to the fixed global coordinate system (GCS). The tridimensional accelerometer and the tridimensional angular rate sensor provided the corresponding data with respect to their local instrumentation coordinate system (ICS). The ICS was determined so that it would meet the criteria established in the SAE J211 standard. The origin was established at the point where the angular rate sensor was placed, which was estimated to be at the midpoint between two of the forehead markers.The polarity of the tridimensional angular rate sensor had been fixed so that the flexion motion was expressed according to the SAE J211 regulations.

The head anatomical coordinate system (HCS) was established at the center of gravity using the Frankfort plane and head anatomical landmarks (Beier et al., 1980; Albery and Whitestone, 2003; Plaga et al., 2005). The *y*-axis was the vector joining both tragions; the *x*-axis was perpendicular to this vector and passed through the midpoint of the infraorbitals pointing forward; the *z*-axis completed the standard orientated coordinate system and pointed downwards (SAE, 2007). Like previous studies (Lopez-Valdes et al., 2010; Seacrist et al., 2011), a coordinate system, parallel to the HCS and located at the Occipital-Condyle joint (OC), was used to express the upper neck loads.

2.6. Upper Neck Loading

Upper neck loads were estimated for the volunteers during low speed frontal sled tests using inverse dynamics. The analysis was performed only in the sagittal plane, as the out-of-plane motion was shown to be negligible by calculating the angle formed by the instrumentation *y*-axis with the global *y*-axis (the misalignment between these two vectors was found to be under 2%).

TABLE 4 | Calculated head inertial properties.

Subject ID	Head mass (kg)	I_{yy} (kg m^2)
Vol 01	4.21	0.0232
Vol 02	4.14	0.0242
Vol 03	4.23	0.0250
Vol 04	4.17	0.0241
Vol 05	3.96	0.0211
Vol 07	4.32	0.0267
Vol 08	4.16	0.0235
Vol 09	4.27	0.0257
Vol 10	4.05	0.0234
Vol 11	4.20	0.0247
Vol 12	4.40	0.0310
Vol 13	4.11	0.0238
Vol 14	4.40	0.0303

The initial angle of the ICS about the global *y*-axis was estimated using the dot product between the ICS *x*-axis unit vector and the GCS *x*-axis unit vector (Equation 3). The initial head angle was calculated as the angle formed by the marker placed at the top of the head and the head center of gravity (Equation 4). The head center of gravity was computed to be at the midpoint between the markers located at either side of the head.

$$\theta_{Instrum}(t=0) = \arccos(\underline{X}_{ICS} \cdot \underline{X}_{GCS}) \tag{3}$$

$$\theta_{Head}(t=0) = -\arctan\left(\frac{X_{Head_T} - X_{Head_{CG}}}{Z_{Head_T} - Z_{Head_{CG}}}\right) \tag{4}$$

Once the initial values of these angles were known, the angles formed by the ICS and the HCS at any other instant in time were obtained through integration of the angular velocity time-history. The HCS was then determined according to the SAE J211-based ATD coordinate system. To double-check the negligibility of the out-of-plane motion, the deviation between the HCS *y*-axis and the GCS *y*-axis was computed again at each time step and was found to be minimal. As the forces and moments applied at the craniocervical joint were to be expressed with respect to the HCS, the necessary rotation matrices to transform the variables to the HCS were calculated.

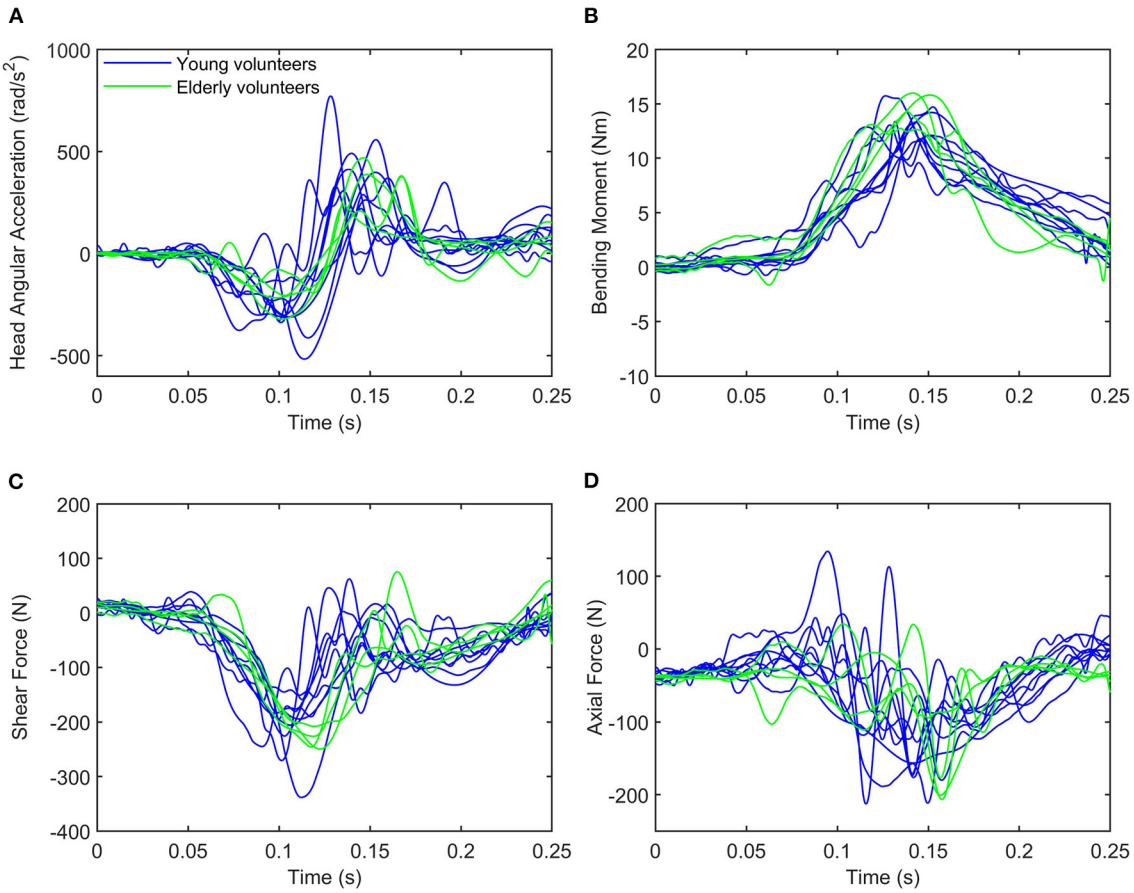

FIGURE 5 | Time history of **(A)** head angular acceleration, **(B)** bending moment, **(C)** shear force, and **(D)** axial force. The blue lines represent upper neck loading and head angular acceleration for young volunteers, while the green lines are used for elderly volunteers.

The angular velocity was differentiated to obtain the angular acceleration of the head, with an initial acceleration of zero. A CFC 60 filter was used to eliminate high frequency components that could have been introduced in the differentiation of the angular velocity, as suggested in previous publications (Lopez-Valdes et al., 2010; Seacrist et al., 2011).

The linear acceleration at the center of gravity of the head was computed using the existing kinematic relationship between the acceleration of two points belonging to the same rigid body as shown in Equation (5), where $\underline{a}_{CG}$ is the linear acceleration at the center of gravity of the head; $\underline{a}_{Instrum}$ is the linear acceleration measured using the tri-axial accelerometer at the origin of the ICS; and $\underline{\rho}$ is the vector from the origin of the ICS to the center of gravity of the head, which was calculated at $t = 0$ and then rotated according to the motion of the head.

$$\underline{a}_{CG} = \underline{a}_{Instrum} + \underline{\ddot{\theta}}_{Head} \times \underline{\rho} + \underline{\dot{\theta}}_{Head} \times (\underline{\dot{\theta}}_{Head} \times \underline{\rho}) \quad (5)$$

Then, the craniocervical forces and moment were calculated as shown in Equations (6, 7), where the head mass and the moment of inertia (I_{Head}) for each volunteer had been determined as aforementioned; ($\ddot{x}$) and ($\ddot{z}$) were the x and z components of the linear accelerations at the center of gravity of the head; and (d_x) and (d_z) represented the distances between the center of gravity of the head and the occipital condyle joint in the x and z direction with respect to the HCS. **Figure 4** illustrates the position and positive polarity of the estimated neck loads.

$$\sum \underline{F} = \begin{bmatrix} F_x \\ F_z \end{bmatrix} = [Head\ mass] \cdot \begin{bmatrix} \ddot{x} \\ \ddot{z} \end{bmatrix}_{CG} - [Head\ mass] \cdot g \cdot \begin{bmatrix} \sin\theta_{Head} \\ \cos\theta_{Head} \end{bmatrix} \quad (6)$$

$$M_y = I_{Head} \cdot \ddot{\theta}_{Head} - F_x \cdot d_z - F_z \cdot d_x \quad (7)$$

The distances between the center of gravity and the occipital condyle joint (d_x and d_z) were calculated for each subject according to their head depth and height, respectively, as suggested in previous research (Seacrist et al., 2011). This is shown in Equation (8).

$$\left\{ \begin{array}{l} d_x = 0.102 \cdot H_{Depth} \\ d_z = 0.260 \cdot H_{Height} \end{array} \right\} \quad (8)$$

TABLE 5 | Peak head angular acceleration.

Subject ID	$\ddot{\theta}_{min}$ (rad/s^2)	Time (s)	$\ddot{\theta}_{max}$ (rad/s^2)	Time (s)
Young volunteers				
Vol 01	–377.58	0.08	772.83	0.13
Vol 02	–412.96	0.12	558.83	0.15
Vol 03	–313.92	0.10	491.60	0.14
Vol 04	–142.70	0.09	288.12	0.15
Vol 05	–516.88	0.11	368.80	0.16
Vol 10	–303.45	0.10	412.24	0.14
Vol 12	–338.83	0.10	360.37	0.12
Vol 13	–331.98	0.10	307.35	0.14
Vol 14	–311.98	0.11	397.17	0.15
Elderly volunteers				
Vol 07	–194.72	0.12	235.19	0.14
Vol 08	–217.80	0.10	387.13	0.15
Vol 09	–206.42	0.10	375.19	0.17
Vol 11	–322.88	0.10	467.98	0.15

3. RESULTS

None of the volunteers experienced any cervical pain or discomfort, nor any other symptoms (headache, back pain, etc.), that could be associated to the tests.

3.1. Head Inertial Properties

As aforementioned, the experimental data in Damon (2009) were used to calculate the mean errors in the estimation of the inertial properties of the head of 100 PMHS using previous methods reported in the literature and the new relations proposed in the current study.

3.1.1. Head Mass

Two regression models were built to estimate the mass head of the 20% PMHS data in Damon (2009) used as validation data. The regression model that yielded the lowest error was the one shown in Equation (9), that used the characteristic length (CL) as the single predictor of head mass. **Table 3** shows the mean errors obtained in the estimation of the head mass using the method developed here and comparing it to the estimations obtained with the methods suggested in previous research. The same set of data taken from Damon (2009) was used for the comparison of the error between the different methods.

$$Head\ mass(kg) = 4.4655 \cdot [CL(m)] \tag{9}$$

The overall mean error using the procedure developed here was 11.36 ± 9.07%, which was below the error obtained in previous studies. Thus, this method was applied to estimate the mass of the head of the volunteers included in this study. The calculated values are shown in **Table 4**. The average and standard deviation head mass for the volunteer group was 4.20 ± 0.13 kg.

3.1.2. Head Moment of Inertia

As with the estimation of the head mass, the data in Damon (2009) was used to compare the accuracy of the estimation of the head moment of inertia using relationships available in the literature. As the error in these methods was high, alternative methods based on linear regression and in the approximation of the shape of the head by two 3D volumes of known moment of inertia were developed. These methods used 80% of the data in Damon (2009) as a training set. The relationship that found the minimum error between the newly ones proposed was the one based on considering the head as a 3D ellipsoid, as shown in Equation (10).

$$I_{yy}(kg\ m^2) = \frac{1}{5} \cdot [Head\ mass(kg)] \cdot [(0.7922 \cdot [H_{Depth}(m)])^2 + (0.4124 \cdot [H_{Breadth}(m)])^2] \tag{10}$$

This relationship proposed in Equation (10) resulted in a mean 13.93 ± 12.38% error that was substantially smaller than the one obtained using previously published methods. Even if the standard deviation (SD) obtained with the newly proposed methodology was almost as high as the mean error, this SD was also smaller than the one obtained with the existing published methods (see **Table 3**) . Thus, the moment of inertia of the head of the volunteers of the study were calculated using this procedure and are shown in **Table 4**. The average and standard deviation of the head principal moment of inertia for the volunteer group was 0.0251±0.0028 kg m^2.

3.2. Upper Neck Loading

The time history plots obtained for the estimation of the shear and axial forces, bending moment, and head angular acceleration for each volunteer are shown in **Figure 5**. Green solid traces show the results obtained for the volunteers in the elderly group, while blue solid ones correspond to the volunteers in the younger age group.

3.2.1. Head Angular Acceleration

The calculated head angular acceleration is shown in subplot A in **Figure 5**. The time history plot shows that the head is accelerated in the negative HCS *y*-axis up to approximately 100 ms (flexion) and then it accelerates in the opposite direction (extension) up to 200 ms. This trend is common to all volunteers regardless of the group age. Vol 02 and 05, both within the younger group, exhibited peak flexion values that were considerably greater than those of the other volunteers regardless of the age group (−412.96 and −516.88 rad/s^2). Vol 02 also sustained one of the two highest values in the angular acceleration in extension, although the peak value was observed in the results of Vol 01 (772.83 rad/s^2). Vol 04 exhibited the minimum value in the flexion motion for both age groups (−142.70 rad/s^2). With the exception of this subject, three out of the four elderly volunteers showed smaller peak values in flexion than any volunteer in the younger group. Vol 11 in the elderly group sustained a similar angular acceleration value than the ones observed in the younger group. The peak values of the head angular acceleration are shown in **Table 5**.

3.2.2. Shear and Axial Force, and Moment at the Craniocervical Junction

Time history plots of the forces and moment estimated at the craniocervical junction are shown in **Figures 5B–D**.

TABLE 6 | Peak upper neck loads.

Subject ID	F_x (N)	Time (s)	F_z (N)	Time (s)	M_y (Nm)	Time (s)
Young volunteers						
Vol 01	–244.97	0.09	–212.82	0.12	13.08	0.13
Vol 02	–190.28	0.12	–127.67	0.14	14.73	0.15
Vol 03	–205.83	0.11	–122.00	0.16	13.34	0.14
Vol 04	–154.82	0.12	–123.68	0.14	12.12	0.15
Vol 05	–338.32	0.11	–211.66	0.15	12.88	0.12
Vol 10	–225.80	0.10	–180.16	0.16	13.41	0.13
Vol 12	–270.61	0.10	–171.29	0.14	15.75	0.13
Vol 13	–194.72	0.10	–173.55	0.14	13.16	0.14
Vol 14	–194.45	0.11	–156.56	0.14	14.22	0.15
Elderly volunteers						
Vol 07	–245.85	0.12	–98.44	0.12	13.12	0.12
Vol 08	–249.54	0.12	–200.57	0.16	15.82	0.15
Vol 09	–207.97	0.12	–206.70	0.16	15.99	0.14
Vol 11	–226.29	0.12	–176.78	0.16	14.31	0.14

All volunteers exhibited a similar behavior regarding the time history of the shear neck force, showing a negative peak (indicating that the neck pulls from the head as the head moves forward) at around 100 ms. There was less variability in the timing within the elderly volunteer group (in which the peak shear force was always obtained at $t = 120$ ms) than within the younger volunteer group (in which the time of the peak force ranged between 90 and 120 ms). As for the magnitude, Vol 05 exhibited the largest shear force (−338.32 N) and Vol 04 the lowest shear force peak value (−154 N) observed for any of the volunteers. These observations coincide with the ones discussed above related to the angular acceleration and it is probably an indication of the link between the value of the shear force and the rotational acceleration of the head. The range of peak shear forces was greater for the young adults than for the elders, being (−338.32 N, −190.28 N) and (−207.97 N, −249.54 N), respectively. The peak values of the shear force estimated for all the volunteers are included in **Table 6**.

More variability could be observed in the results for the estimation of the neck axial force as shown in **Figure 5**. In particular, Vol 01 exhibited a different behavior than any of the other volunteers regardless of the age group: with a positive compression force observed at around $t = 90$ ms and the largest peak tension force (−212.82 N) obtained at $t = 120$ ms. No other volunteers exhibited this phase change. In general, volunteers sustained a peak tension force delayed some 30 ms from the peak shear force. This behavior indicates that the peak tension force occurs when the head has reached its maximum forward excursion and undergoes a flexion motion that will attempt to elongate the neck. Peak axial forces ranged between (−212.82 N, −122.00 N) in the young volunteer group and between (−206.70 N, −98.44 N) in the elderly volunteer group. These values are shown in **Table 6**.

The timing for the maximum moment My was more similar to the one of the peak tension force than to the one in which the peak shear force was observed. It is again linked to the fact that the flexion motion of the head starts only when the forward motion has finished. This timing of the peak flexion moment is very similar to the peak of the positive head angular acceleration discussed above. The time history plot of the My moment shown in **Figure 5** shows that there were no substantial differences neither in the magnitude nor in the phasing between the two age groups. Peak values of the My moment are included in **Table 6** and ranged between (12.12 Nm, 15.99 Nm).

4. DISCUSSION

This is the first study that reports axial and shear forces, and flexion moment at the atlanto-occipital junction of young and elderly volunteers using inverse dynamics. The current study complements the data presented by Seacrist et al. (2011) that included a comparison of the same upper cervical loads but between pediatric and young adult volunteers.

The craniocervical junction consists of two joints: the atlanto-occipital and the atlanto-axial. While the joint mechanics of the first one are determined by the geometry of the bony part, the motion in the second one is primarily determined by the ligamentous structures (Offiah and Day, 2017). These two joints are responsible for the large mobility exhibited by the human cervical spine. While the changes in the geometry (curvature of the different sections of the spine), size and structure of the vertebrae and intervertebral discs during development and up to maturity are extensively reported in the literature (Moore et al., 2010), the effects of aging on the spine are limited to the overall decrease in bone density that modifies the geometry of the vertebral bodies and facilities the development of osteophytes around the attachment of the intervertebral discs to the bone. In parallel, osteophyte growth around the joint capsules is also possible and is normally associated to the wearing out of the cartilage with age. Osteophytes may occur at any level of the spine, including the atlanto-axial joint (Alikhani et al., 2020). The combination of the stiffening

effect of the osteophytes and the degradation of the ligaments in the cervical spine with age has been suggested as a risk factor to the increased likelihood of upper cervical injuries (atlanto-axial junction, odontoid injuries) observed in elderly patients, as the lower cervical spine would become stiffer and transmit increased loads to the upper cervical spine region (Lomoschitz et al., 2002).

Subject-specific estimation of the inertial properties of the head of the volunteers is essential to obtain a good prediction of the loads calculated using inverse dynamics (Yoganandan et al., 2009; Seacrist et al., 2011; Beeman et al., 2016). Volunteer studies require non-invasive estimations of the head inertial properties, based on relationships of some external measurements taken on the volunteers (Loyd et al., 2010; Seacrist et al., 2011). This study combined data from several cadaveric studies that had measured the inertial properties of the head to propose new relationships to estimate the head mass and the moment of inertia of the head of the volunteers. Compared to previous estimations of these properties, the method developed here reduced the error of previous publications (achieving an estimated mean error of 11.4 ± 9.1% for the head mass and 13.9 ± 12.4% for the head moment of inertia). Nevertheless, previous studies (Seacrist et al., 2011) had used data from PMHS up to 16 years of age, which could explain the larger error obtained for adults. Compared to previous research, the results obtained for the head mass (4.20 ± 0.13 kg) and moment of inertia (0.0251 ± 0.0028 kg m^2) were within the expected range reported in earlier studies (Beier et al., 1980; Plaga et al., 2005; Damon, 2009). The present study also showed that, for the volunteers included in this study, head inertial parameters were independent of age, but were dependent, as expected, on head dimensions.

The inverse dynamics method used in this study to estimate the upper neck loads assumes a pin joint between the head and the first cervical vertebra, which is an oversimplification of the real anatomy of the head-neck junction. The forces and moments estimated here are not supported by a single point anatomical structure, but are in fact distributed among the condyles of C1 and the cervical ligaments and muscles. It is also not possible to apportion the load that each of the anatomical structures would receive in case of a sudden deceleration. However, the pin joint model is closer to the construction of the ATD neck and can be used to inform more biofidelic designs of the dummy neck.

With the experimental data available for this study, it was difficult to find differences in the time history plots of the upper cervical forces estimated for the young and elderly age groups. The potential differences that could be attributed to age, are included in the variability observed in each of the groups, which is especially significant in the younger group. It can be observed that the values estimated for the shear (F_x) and axial forces (F_z) experimented by the elderly volunteers are within the highest values observed in the young group, although one young volunteer (Vol 05) exhibited larger force values than the ones observed in the elderly group. The situation is slightly different looking at the estimation of the flexion moment which is maximum for two of the elderly volunteers, supporting the anatomical/clinical observations mentioned above (Lomoschitz et al., 2002). It is important to mention that none of the volunteers complained of any cervical pain or even discomfort during the tests. Vol 08 was exposed only to two trials as he was experiencing discomfort from the rigid seat plate used in the tests.

In Mertz and Patrick (1971), one volunteer was exposed to 46 sled runs at various degrees of severity to induce neck flexion. This volunteer experienced pain in the neck and back after one sled run, and did not desire to go further. The peak acceleration for this run was 9.6 g, the maximum head accelerations observed were 573 rad/s^2 in flexion and −760 rad/s^2 in extension, the estimated peak moment was 90.7 Nm, and the peak axial and shear forces were 647.6 N and 789.6 N, the latter occurring 20 ms after the peak axial force. These values exceeded the ones observed in the volunteer tests presented here. The researchers proposed the value $My = 90.7$ Nm as the injury threshold for living humans. In PMHS tests performed under similar conditions but with increasing acceleration levels, Mertz and Patrick (1971) did not find any indication of disc, ligament or bony cervical injuries for values up to $My = 189.8$ Nm, although the authors advised caution to accept this level as muscular injury could have happened in a living human. Focusing on the volunteer sled runs that occurred at deceleration levels comparable to those of our study (2.9–4.2 g), the peak moment observed in Mertz and Patrick (1971) varied between 11.7 and 20.75 Nm and the shear force ranged between 160.1 and 280.2 N. These values are much closer to the ones observed in this study. It should be noted that the volunteer in the Mertz and Patrick (1971) was restrained using a crisscross seatbelt over his chest, resulting in an earlier rotation of the head that could explain the different timing for the peak values observed in the two studies. The authors proposed that the best indicator for the degree of severity of neck flexion is the equivalent moment at the occipital condyles.

However, the suggested injury threshold for the flexion moment My in Mertz and Patrick (1971) is higher than the threshold suggested in a later study (Prasad and Daniel, 1984), which found severe neck injuries in piglets starting at neck moment values of 29.4 Nm. However, the data in the latter study are difficult to translate to the case of humans due to the use of juvenile surrogates and to reporting neck values measured with a pediatric ATD instead of using inverse dynamics. As there was one case in which the piglet did not suffer any neck injury after being exposed to a moment of 50.9 Nm, Prasad and Daniel (1984) hypothesized that the mechanism of neck injury required the combined action of a flexion moment and an axial load. This hypothesis could be related to the finding of this study in which the peak axial force and the peak bending moment occurred at very similar timing.

If the focus is on low-speed frontal impacts, several contemporary studies have calculated the upper cervical forces and moments of volunteers using inverse dynamics (Arbogast et al., 2009; Lopez-Valdes et al., 2010; Seacrist et al., 2011; Beeman et al., 2016). Although the deceleration level used in these studies

is similar, there were important differences in the experimental setup and in the initial position of the participants that affected the excursion of the head and the calculated neck loads (Beeman et al., 2016). The younger volunteer group in this study matches closely the 18–30 years old group studied in Seacrist et al. (2011).The latter reported mean peak values of $-162 \pm 24N$ and $13 \pm 2.7Nm$ for the axial force and bending moment, which are very close to the ones included here.

The values of the forces and moments obtained can be compared also to those reported by Funk et al. (2011) during everyday vigorous activities. The 20 volunteers included in this study spanned a range of age between 26 and 58 years and the results also showed a large variability between the peak values of the shear and axial force, and of the flexion moment measured during the tests. In general the shear forces measured in Funk et al. (2011) were smaller than the ones calculated in this study, while the axial forces peak values were larger. The estimated My flexion moment was comparable especially for some of the daily activities that occurred at a higher rate such as shaking the head ($15 \pm 5.7Nm$), or being dropped while seating supine in a chair ($15 \pm 5.7Nm$). Funk et al. (2011) did not find any effect of age and body size of the volunteers on the biomechanical measurements or symptoms being reported in any of the test scenarios.

There are some limitations of the study that need to be discussed. First, each volunteer was exposed to several trials (between two and five), but the results included here correspond to only one trial per volunteer. Volunteers were asked to remain relaxed during the simulated impact, but it must be assumed some level of reflex muscle contraction, which could have influenced the calculated loads (Beeman et al., 2016). To minimize the influence of this non-voluntary muscle response, and after performing a preliminary analysis that found differences in the kinematics between the first trial and the remaining ones for each volunteer, the third trial was the one used in the study (with the exception of two volunteers as discussed in the Methods section). Second, there were only four volunteers in the elderly group. Even if the recruitment period was open for several weeks, it was difficult to secure more volunteers willing to participate in the study. Despite of it, other studies have used groups with 5–6 subjects in similar analyses (Arbogast et al., 2009; Beeman et al., 2016) . Third, as the sample size was limited, it was decided to avoid averaging the responses of the volunteers so that individual differences among subjects could be appreciated. This decision implies that detecting the potential differences between the two age groups could have become more difficult, but respects the nature of the individual data.

As indicated in **Table 2**, the analyses of the kinematics of the volunteers required the differentiation of instrument data. These procedures usually involved the amplification of the noise in the signals that had to be filtered before calculating the estimated values of the neck loads, similarly to what had been reported in previous studies (Funk et al., 2007; Lopez-Valdes et al., 2010; Seacrist et al., 2011). In our case, as the head instrumentation was fixed to the head using a head band that did not provide a perfectly rigid attachment to the head, some of the experimental data required to be filtered before being able to process them. Since the rigidity of the head band attachment changed between the volunteers, different cutoff frequencies were used. To minimize the impact of the filtering on the original data, the cutoff frequency for the filters was selected after visual inspection of the original (unfiltered) and processed signals, together with the analysis of the frequency content of the original signal using the Fast Fourier Transform of the experimental data.

5. CONCLUSION

Using previously obtained data from PMHS, this study proposed new relationships to calculate the inertial properties of the human head that improved substantially the methods that had been used in previous literature. These relationships were used then in the estimation of the axial and shear force, and the sagittal moment experienced by volunteers at the craniocervical junction during low-speed frontal decelerations (9 km/h). Two groups of volunteers were analyzed: a young adult group (18–30 years old) and an elderly group (>65 years old). Although slightly greater values of the peak My moment were found in the elderly group, they were within the variability observed in the young group. Thus, with the limited sample analyzed in this study, no substantial differences were found in the comparison of craniocervical loads between the two age groups. The results reported here can be used to benchmark active human body models in low-speed frontal impacts. The findings of this study support that the active response of the cervical spine of human body models does not need to account for age effects in the adulthood.

DATA AVAILABILITY STATEMENT

The data analyzed in this study is subject to the following licenses/restrictions: Data of volunteers available on request. Requests to access these datasets should be directed to steffen.peldschus@med.uni-muenchen.de.

ETHICS STATEMENT

The studies involving human participants were reviewed and approved by CEICA (Ethical Comission for Clinical Research of Aragon). The patients/participants provided their written informed consent to participate in this study.

AUTHOR CONTRIBUTIONS

CV-T: data analyses, methodology, and manuscript writing. MV: data analyses, methodology, and manuscript review. JJ-O: conceptualization, supervision, and manuscript review. JM: conceptualization, experimental work, and manuscript review. SS: conceptualization, methodology, and manuscript review. SP: conceptualization, resources, methodology, and manuscript review. FL-V: conceptualization, experimental work, methodology, supervision, and manuscript review. All authors contributed to the article and approved the submitted version.

FUNDING

The tests included in this study were performed within the SENIORS project (Grant Agreement 636136), funded by the European Union Horizon 2020 Program. The experiments were carried out at the Impact Laboratory (I3A) of the University of Zaragoza, subcontracted by LMU.

ACKNOWLEDGMENTS

We would like to primarily thank the volunteers that participated in the program: without their generous collaboration, this study could not have been possible. We also thank the support of the SENIORS consortium and of the Impact Laboratory of the University of Zaragoza to perform these tests.

REFERENCES

Albery, C., and Whitestone, J. (2003). "Comparison of cadaveric human head mass properties: mechanical measurement vs. calculation from medical imaging," in *Proceedings of the 31st International Workshop Injury Biomechanics Research*, Vol. 157, 157–172.

Alikhani, P., Suradi, Y., Amin, S., and Amin, U. (2020). Complex c1-2 osteophyte presenting with severe dysphagia and ptosis. *Neurology* 94, 324–325. doi: 10.1212/WNL.0000000000008969

Arbogast, K., Balasubramanian, S., Seacrist, T., Maltese, M., García-España, J., Hopely, T., et al. (2009). Comparison of kinematic responses of the head and spine for children and adults in low-speed frontal sled tests. *Stap Car. Crash J.* 53, 329–732. doi: 10.4271/2009-22-0012

Beeman, S. M., Kemper, A. R., and Duma, S. M. (2016). Neck forces and moments of human volunteers and post mortem human surrogates in low-speed frontal sled tests. *Traffic Inj. Prev.* 17(Suppl. 1):141–149. doi: 10.1080/15389588.2016.1205190

Beier, G., Schuller, E., Schuck, M., Ewing, C. L., Becker, E. D., and Thomas, D. J. (1980). "Center of gravity and moments of inertia of human heads," in *Proceedings of the International Research Council on Biomechanics of Injury (IRCOBI)*, (Birmingham).

Clauser, C. E., McConville, J. T., and Young, J. W. (1969). *Weight, Volume, and Center of Mass of Segments of the Human Body*. Technical Report AMRL-TR-69-70, Air Force System Comand, Wright-patteron AFB.

Damon, A. (2009). *Characterizing the Geometric and Inertial Properties of the Adult Human Head*. Master's Thesis.

Eppinger, R., Kuppa, S., Saul, R., and Sun, E. (2000). *Supplement: Development of Improved Injury Criteria for the Assessment of Advanced Automotive Restraint Systems II*. Technical report, United States. National Highway Traffic Safety Administration.

Funk, J., Cormier, J., Bain, C., Guzman, H., and Bonugli, E. (2007). "An evaluation of various neck injury criteria in vigorous activities," in *Proceedings of the International Research Council on Biomechanics of Injury (IRCOBI)* (Maastricht), 19–21.

Funk, J., Cormier, J., Bain, C., Guzman, H., Bonugli, E., and Manoogian, S. (2011). Head and neck loading in everyday and vigorous activities. *Ann. Biomed. Eng.* 39, 766–776. doi: 10.1007/s10439-010-0183-3

Li, F., Liu, N.-S., Li, H.-G., Zhang, B., Tian, S.-W., Tan, M.-G., et al. (2019). A review of neck injury and protection in vehicle accidents. *Transport. Safety Environ.* 1, 89–105. doi: 10.1093/tse/tdz012

Lomoschitz, F., Blackmore, C., Mirza, S., and Mann, F. (2002). Cervical spine injuries in patients 65 years old and older: epidemiologic analysis regarding the effects of age and injury mechanism on distribution, type, and stability of injuries. *Am. J. Roentgenol.* 178, 573–577. doi: 10.2214/ajr.178.3.1780573

López-Valdés, F. J., Juste-Lorente, O., Maza-Frechin, M., Pipkorn, B., Sunnevang, C., Lorente, A., et al. (2016). Analysis of occupant kinematics and dynamics in nearside oblique impacts. *Traffic Inj. Prev.* 17(Suppl. 1):86–92. doi: 10.1080/15389588.2016.1189077

Lopez-Valdes, F. J., Lau, A., Lamp, J., Riley, P., Lessley, D. J., Damon, A., et al. (2010). Analysis of spinal motion and loads during frontal impacts. Comparison between pmhs and atd. *Ann. Adv. Autom. Med.* 54, 61–78.

Lopez-Valdes, F. J., Mroz, K., Eggers, A., Pipkorn, B., Muehlbauer, J., Schick, S., et al. (2018). Chest injuries of elderly postmortem human surrogates (pmhss) under seat belt and airbag loading in frontal sled impacts: comparison to matching thor tests. *Traffic Inj. Prev.* 19(Suppl. 2):S55–S63. doi: 10.1080/15389588.2018.1542139

Loyd, A., Nightingale, R., Bass, C., Mertz, H., Frush, D., Daniel, C., et al. (2010). Pediatric head contours and inertial properties for atd design. *Stapp Car Crash J.* 54, 167–196. doi: 10.4271/2010-22-0009

McConville, J. T., Clauser, C. E., Churchill, T. D., Cuzzi, J., and Kaleps, I. (1980). *Anthropometric Relationships of Body and Body Segment Moments of Inertia*. Technical Report AFAMRL-TR-80-119, Air Force System Comand, Wright-patteron AFB.

Mertz, H. J., Irwin, A. L., and Prasad, P. (2003). *Biomechanical and Scaling Bases for Frontal and Side Impact Injury Assessment Reference Values*. Technical report, SAE Technical Paper.

Mertz, H. J., and Patrick, L. M. (1971). "Strength and response of the human neck," in *Proceedings of the 15th Stapp Car Cash Conference* (Coronado, CA), SAE paper No. 710855:207–255.

Moore, K., Dalley, A., and Agur, A. (2010). *Clinically Oriented Anatomy*. Clinically Oriented Anatomy. Philadelphia, PA: Wolters Kluwer Health/Lippincott Williams & Wilkins.

Muehlbauer, J., Schick, S., Draper, D., Lopez-Valdes, F. J., Symeonidis, I., and Peldschus, S. (2019). Feasibility study of a safe sled environment for reclined frontal deceleration tests with human volunteers. *Traffic Inj. Prev.* 20(Suppl. 2):S171–S174. doi: 10.1080/15389588.2019.1659592

Offiah, C. E., and Day, E. (2017). The craniocervical junction: embryology, anatomy, biomechanics and imaging in blunt trauma. *Insights Into Imaging* 8, 29–47. doi: 10.1007/s13244-016-0530-5

Parenteau, C. S., and Viano, D. C. (2014). Spinal fracture-dislocations and spinal cord injuries in motor vehicle crashes. *Traffic Inj. Prev.* 15, 694–700. doi: 10.1080/15389588.2013.867434

Pipkorn, B., López-Valdés, F. J., Juste-Lorente, O., Insausti, R., Lundgren, C., and Sunnevång, C. (2016a). Assessment of an innovative seat belt with independent control of the shoulder and lap portions using thor tests, the thums model, and pmhs tests. *Traffic Inj. Prev.* 17(Suppl. 1):124–130. doi: 10.1080/15389588.2016.1201204

Pipkorn, B., Sunnevang, C., Juste-Lorente, O., Maza, M., and Lopez-Valdes, F. (2016b). "Exploratory study of the kinematics of the thor dummy in nearside oblique impacts," in *Proceedings of the International Research Council on Biomechanics of Injury (IRCOBI)* (Malaga).

Plaga, J. A., Albery, C., Boehmer, M., and Goodyear, C. (2005). *Design and Development of Anthropometrically Correct Head Forms for Joint Strike Fighter Ejection Seat Testing*. Wright-Pattersons AFB, OH.

Prasad, P., and Daniel, R. P. (1984). *A Biomechanical Analysis of Head, Neck, and Torso Injuries to Child Surrogates Due To Sudden Torso Acceleration*. SAE Transactions 784–799.

SAE (2007). *Instrumentation for Impact Test: Part 1-Electronic Instrumentation*. Technical Report, SAE J211/1.

Safiri, S., Kolahi, A.-A., Hoy, D., Buchbinder, R., Mansournia, M. A., Bettampadi, D., et al. (2020). Global, regional, and national burden of neck pain in the general population, 1990-2017: systematic analysis of the global burden of disease study 2017. *BMJ* 368:m791. doi: 10.1136/bmj.m791

Seacrist, T., Arbogast, K. B., Maltese, M. R., García-Espaňa, J. F., Lopez-Valdes, F. J., Kent, R. W., et al. (2011). Kinetics of the cervical spine in pediatric and adult volunteers during low speed frontal impacts. *J. Biomech.* 45, 99–106. doi: 10.1016/j.jbiomech.2011.09.016

THUMSUserCommnunity (2021). *Seniors Deliverable 2.3*. Available online at: https://tuc-project.org/frontal-sled-seniors/ (accessed May 14, 2021).

Umana, E., Khan, K., Baig, M., and Binchy, J. (2018). Epidemiology and characteristics of cervical spine injury in patients presenting to a regional emergency department. *Cureus* 10::e2179. doi: 10.7759/cureus.2179

Walker, L., Harris, E., and Pontius, U. (1973). "Mass, volume, center of mass, and mass moment of inertia of head and head and neck of human body," in *Proceedings of the Stapp Car Crash Conference* (Oklahoma City, OK), 525–538.

Yadollahi, M., Paydar, S., Ghaem, H., Ghorbani, M., Mousavi, S. M., Taheri Akerdi, A., et al. (2016). Epidemiology of cervical spine fractures. *Trauma Mon.* 21:e33608. doi: 10.5812/traumamon.33608

Yoganandan, N., Maiman, D. J., Guan, Y., and Pintar, F. (2009). Importance of physical properties of the human head on head-neck injury metrics. *Traffic Inj. Prev.* 10, 488–496. doi: 10.1080/15389580903132801

Disclaimer: The views expressed here are the sole opinion of the authors and not of the funding agency or the subcontractors.

Conflict of Interest: The authors declare that the research was conducted in the absence of any commercial or financial relationships that could be construed as a potential conflict of interest.

frontiers in Bioengineering and Biotechnology

ORIGINAL RESEARCH
published: 05 July 2021
doi: 10.3389/fbioe.2021.670498

Identifying and Characterizing Types of Balance Recovery Strategies Among Females and Males to Prevent Injuries in Free-Standing Public Transport Passengers

Jia-Cheng Xu[1], Ary P. Silvano[1], Arne Keller[2], Simon Krašna[3], Robert Thomson[4], Corina Klug[5] and Astrid Linder[1,4]*

[1] Swedish National Road and Transport Research Institute, Linköping, Sweden, [2] AGU Zürich, Zurich, Switzerland, [3] Faculty of Mechanical Engineering, University of Ljubljana, Ljubljana, Slovenia, [4] Mechanics and Maritime Science, Chalmers University of Technology, Gothenburg, Sweden, [5] Vehicle Safety Institute, Graz University of Technology, Graz, Austria

OPEN ACCESS

Edited by:
Jason Forman, University of Virginia, United States

Reviewed by:
Yun-Ju Lee, National Tsing Hua University, Taiwan
Natalya Kizilova, Warsaw University of Technology, Poland

***Correspondence:**
Jia-Cheng Xu
jia.cheng.xu@vti.se

Specialty section:
This article was submitted to Biomechanics, a section of the journal Frontiers in Bioengineering and Biotechnology

Received: *21 February 2021*
Accepted: *11 June 2021*
Published: *05 July 2021*

Citation:
Xu J-C, Silvano AP, Keller A, Krašna S, Thomson R, Klug C and Linder A (2021) Identifying and Characterizing Types of Balance Recovery Strategies Among Females and Males to Prevent Injuries in Free-Standing Public Transport Passengers. Front. Bioeng. Biotechnol. 9:670498. doi: 10.3389/fbioe.2021.670498

Free-standing passengers on public transport are subjected to perturbations during non-collision incidents caused by driver maneuvers, increasing the risk of injury. In the literature, the step strategy is described as a recovery strategy during severe perturbations. However, stepping strategies increase body displacement, ultimately subjecting passengers to higher risk of impacts and falls on public transport. This study investigates the influence of different recovery strategies on the outcome of balance recovery of free-standing public transport passengers, challenged in postural balance by the non-uniform vehicle dynamics. From high-speed video recordings, a qualitative investigation of the balance responses of volunteer participants in a laboratory experiment was provided. On a linearly moving platform, 24 healthy volunteers (11 females and 13 males) were subjected to perturbation profiles of different magnitude, shape and direction, mimicking the typical acceleration and deceleration behavior of a bus. A methodology categorizing the balancing reaction to an initial strategy and a recovery strategy, was used to qualitatively identify, characterize and, evaluate the different balance strategies. The effectiveness of different strategies was assessed with a grading criterion. Statistical analysis based on these ordinal data was provided. The results show that the current definition in the literature of the step strategy is too primitive to describe the different identified recovery strategies. In the volunteers with the most successful balancing outcome, a particularly effective balance recovery strategy not yet described in the literature was identified, labeled the *fighting stance*. High jerk perturbations seemed to induce faster and more successful balance recovery, mainly for those adopting the fighting stance, compared to the high acceleration and braking perturbation profiles. Compared to the pure step strategy, the characteristics of the *fighting stance* seem to increase the ability to withstand higher perturbations by increasing postural stability to limit body displacement.

Keywords: balance strategy, balance recovery, free-standing passengers, human balance, perturbation, public transport, step strategy

INTRODUCTION

Public transport is considered a safe mode of transportation. However, standing passengers on buses and trams are subjected to perturbations due to vehicle maneuvers that might cause injuries. The risk of injury due to falling in non-collision incidents on public transport has been estimated in a meta-analysis to be between 0.2 and 0.3 per million passenger km (Elvik, 2019). Factors contributing to the risk of falling include the perturbation profile (magnitude, duration, and orientation) and passenger capabilities (balance recovery, age, gender, and health condition). The literature highlights that harsh acceleration and sudden braking perturbations are important contributing factors, and that the group of female passengers aged 65+ are overrepresented in non-collision incidents on public transport (Kirk et al., 2003; Albertsson and Falkmer, 2005; Björnstig et al., 2005; Halpern et al., 2005). Furthermore, in a more recent study, Silvano and Ohlin (2019) found that female involvement is also high for other age groups with 87 and 86% involvement for the age group brackets of 16–24 and 25–65, respectively.

Postural balance is often described in terms of three fundamental balance strategies: (1) the ankle, (2) the hip, and (3) the step strategy (Nashner and McCollum, 1985; Winter, 2009). Another strategy found in the literature, yet not so extensively used, is the squat strategy, which incorporates both knee and hip flexion for stability (Hemami et al., 2006; Cheng, 2016). The ankle and hip strategies are fixed-support strategies, while the step strategy is a change-in-support (CIS) strategy induced during more severe perturbations as the center-of-mass (CoM) and base-of-support (BoS) are displaced due to the momentum of the perturbation. The BoS is defined as the area under and between the feet. To maintain the full-body system in balance, the CoM projecting on the floor must be within the BoS to maintain equilibrium. For less severe perturbations, the combination of ankle and hip adjustments is usually sufficient to maintain balance. Change-in-support strategies with single or multiple recovery steps are the most dominant strategies to avoid falls, by shifting the BoS to contain the displaced CoM (Maki and McIlroy, 1997; Maki et al., 2008). Multiple-step strategies have been shown to result in less effective balance recovery, compared to single-step recovery in translational perturbations (Robert et al., 2007; Carty et al., 2011; Barrett et al., 2012; Carty et al., 2012a,b; Mille et al., 2013; Crenshaw and Kaufman, 2014; Carty et al., 2015), and lateral perturbations (Mille et al., 2005, 2013; Hilliard et al., 2008; Bair et al., 2016; de Kam et al., 2017; Borrelli et al., 2021). Single-step responses are characterized by longer step lengths and shorter initiation times, usually utilized by younger subjects, and Cronin et al. (2013) suggested that a single-step strategy can be assumed as the most optimal response. This is biomechanically efficient, as a larger step increases balance recovery by relocating the stepping foot ahead of the CoM and generates larger contact forces between the foot and the ground (King et al., 2005). In contrast, older adults tend to execute a multiple-step strategy (Luchies et al., 1994; McIlroy and Maki, 1996; Hsiao and Robinovitch, 1999). However, increased step length and shorter step initiation time is observed for both younger and older subjects (Do et al., 1982; Luchies et al., 1994; Maki et al., 1996; Thelen et al., 1997; Hsiao and Robinovitch, 1999; Wojcik et al., 1999). This has been experimentally confirmed by measuring release angles to recover a stable upright stance with a single step, where recovery increased through larger and quicker steps, among both young and elderly women (Hsiao-Wecksler and Robinovitch, 2007). However, during more severe perturbations, multiple-step responses are natural and can be executed in various ways (Maki and McIlroy, 1996; Hsiao and Robinovitch, 1999). As multiple stepping increases body displacement and the risk of impacts with interior design or passengers on public transport, it can be hypothesized that recovery strategies increase dynamic postural stability with different effectiveness.

Tether-release methods to simulate trips and slips, for fall prediction, are very common in the literature (Thelen et al., 1997; Hsiao and Robinovitch, 1999, 2001; Cyr and Smeesters, 2007; Carty et al., 2011; Cheng, 2016; Okubo et al., 2019). This kind of experimental setup provides lean angle thresholds to study the difference between single- and multiple-step strategies to avoid falls, where single-step responses are used to identify perturbation threshold limits to successfully recover balance (Hsiao-Wecksler and Robinovitch, 2007; Barrett et al., 2012; Carbonneau and Smeesters, 2014; Carty et al., 2015). Graham et al. (2014) instructed younger and older volunteers to recover balance using a single step to model the muscle contribution for recovery, and the recovery strategy of older multiple steppers was considered less effective than for older single steppers. Hence, single-step strategies seem to be advantageous over multiple-step strategies, arguably important on public transport to avoid, e.g., head impacts due to increased body displacement (Robert et al., 2007). Pull perturbations (waist or shoulder) in multiple directions are also common to study stepping responses in a similar manner (Pai et al., 1998; Sturnieks et al., 2013; Fujimoto et al., 2015, 2017; Bair et al., 2016; Verniba and Gage, 2020).

Studies conducted with translational perturbations on a moving platform, which would be the most realistic laboratory setup to simulate a standing passenger on public transport, are less common due to the more complicated setups. These perturbation studies usually evaluate the stepping response limited to identification, i.e., only differentiating between individual responses, of single- and multiple stepping with minor specific illustration or description of the different executions (Rogers et al., 1996; Mille et al., 2005; Robert et al., 2007; Carty et al., 2012b; Lee et al., 2014; Honeycutt et al., 2016; de Kam et al., 2018; Borrelli et al., 2019). Furthermore, stepping responses comparing older to younger adults are also common since older adults constitute the most vulnerable age group to lose balance during platform perturbations (Brauer et al., 2002). Instead, the aforementioned studies, regardless of the perturbation type, characterize the stepping responses based on quantitative measures such as step initiation times, number of recovery steps, CoM or CoP kinematics, and margin of stability (Hof et al., 2005; Hof and Curtze, 2016). Ideally, qualitative identification and characterization of different stepping responses could complement such quantitative measures, since multiple step responses can have different effectiveness and execution. More importantly, since instructing volunteers to recover balance using a single step is considered as the most effective strategy,

characterizations of the single-step execution might also be vastly different among different age groups and genders. To the authors' best knowledge, there have been a few studies that have identified and characterized strategies in more detail than single- and multiple stepping (Eng et al., 1994; Cordero et al., 2003; de Boer et al., 2010; Mille et al., 2013; Krasovsky et al., 2014; Honeycutt et al., 2016; Karekla and Tyler, 2018a). For example, de Boer et al. (2010) characterized and confirmed previous findings (Eng et al., 1994; Cordero et al., 2003), regarding an elevating and a lowering strategy during induced stumble perturbations. Honeycutt et al. (2016) sought to identify main kinematic characteristics of stroke survivors' stepping responses, characterizing two additional compensatory step strategies (called "pivot" and "hopping") utilized to avoid falls beside the traditional pure step strategy.

Further characterization of the step strategy exists, but the perturbation levels used in the literature are rarely similar to those experienced on public transport. Robert et al. (2007) conducted linear sled perturbations to simulate emergency braking and a low collision scenario to study head excursion in three different starting positions (free-standing, backrest, and holding a vertical bar) and found a main and an alternative strategy. However, these strategies were differentiated mainly by head kinematics and not stepping characteristics. Schubert et al. (2017) subjected older passengers in standing upright postures to acceleration profiles similar to those encountered during regular start and stop maneuvers in traffic, measuring ground reaction and handgrip forces. Although grasping strategies, i.e., using hand support such as handrails to recover balance, is effective, it does not account for free-standing scenarios when handrails are out of reach. Karekla and Tyler (2018a; 2018b) analyzed stepping responses during normal gait without handrails of moving passengers inside an accelerating bus to determine perturbation thresholds with respect to standing postural balance. Here, some characterization of step responses between males and females were found based on number of steps. In that study, a recommended threshold of 2.0 m/s^2 to account for balance of all passengers using handrails, 1.0 m/s^2 to account for free-standing postures, and 1.5 m/s^2 for the majority of younger passengers during normal gait (Karekla, 2016; Karekla and Tyler, 2018a,b). These levels are commonly exceeded in regular operation of public transport (Karekla, 2016; Karekla and Tyler, 2018a,b). However, this was not in free-standing scenarios and only acceleration levels were considered with no jerk variations.

The literature assessing stepping responses during perturbations is very extensive, but a gap was identified between the literature on recovery strategies and different perturbation characteristics causing balance instability on public transport. Identifying balance strategies when subjected to perturbation profiles similar to those on public transport complements current literature on stepping strategies. Characterizing such stepping responses might provide insight on how effective balance recovery in free-standing scenarios can be executed, to benefit passengers. It might also provide insight on how to optimize vehicle dynamics for passenger safety and discomfort, especially with the development of automated vehicles for public transport. Therefore, the aim of this study was to provide a first investigation to identify and characterize recovery stepping strategies that healthy free-standing females and males display during perturbations of different characteristics, mimicking relatively strong bus accelerations and decelerations. The identified strategies were analyzed for their effectiveness in balance recovery by a qualitative measurement, to mainly provide insight on different CIS strategies and understand perturbation thresholds.

MATERIALS AND METHODS

The methodology used for the analysis of the balance strategies was based on visual analysis of video recordings of dynamic tests with volunteers, where the standing participants were exposed to translational acceleration/deceleration perturbations. It comprises three steps: (i) identification, aiming at distinguishing different strategies used among the volunteers; (ii) characterization, describing the execution and

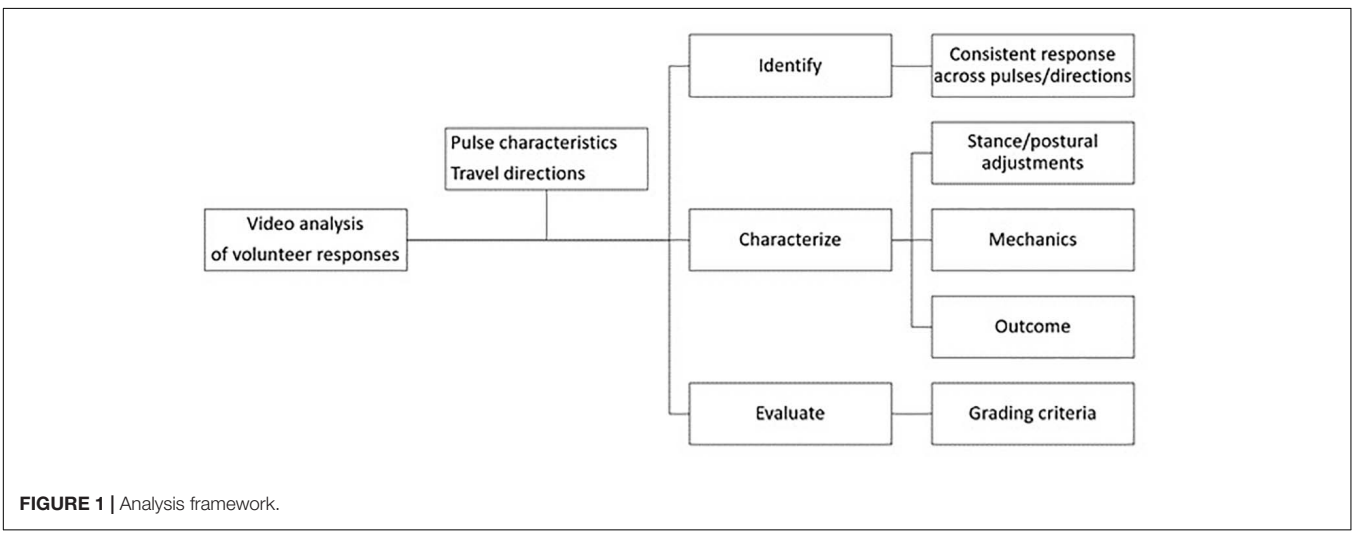

FIGURE 1 | Analysis framework.

TABLE 1 | Volunteer information.

No.	Gender	Age	Height (cm)	Weight (kg)	No.	Gender	Age	Height (cm)	Weight (kg)
1	M	37	185.0	83.3	13	F	23	178.5	68.7
2	M	42	191.5	110.5	14	F	25	167.0	79.8
3	M	63	177.0	102.7	15	F	33	160.0	80.3
4	F	30	168.0	57.5	16	F	38	170.5	54.6
5	F	38	161.0	54.7	17	M	24	174.0	75.5
6	F	34	165.0	58.6	18	M	32	173.0	78.6
7	M	40	179.0	84.2	19	M	30	171.0	82.9
8	F	22	155.0	53.6	20	M	34	182.0	83.4
9	F	28	168.0	64.0	21	M	44	180.0	103.8
10	F	46	167.5	67.5	22	M	35	180.0	75.7
11	M	21	180.0	79.5	23	M	30	181.5	86.0
12	M	30	176.0	74.1	24	F	31	160.0	72.6

TABLE 2 | Age, height, and weight summary statistics and gender.

Description	Mean ± SD	Minimum	Maximum
Age	33.8 ± 9.0	21	63
Female Age	31.6 ± 7.2	22	46
Male Age	35.5 ± 10.6	21	63
Height (cm)	172.9 ± 9.2	155	191.5
Female height (cm)	166.5 ± 6.4	155	178.5
Male height (cm)	179.2 ± 5.4	171	191.5
Weight (kg)	76.3 ± 15.3	53.6	110.5
Female weight (kg)	64.7 ± 9.9	53.6	80.3
Male weight (kg)	86.2 ± 11.8	74.1	110.5

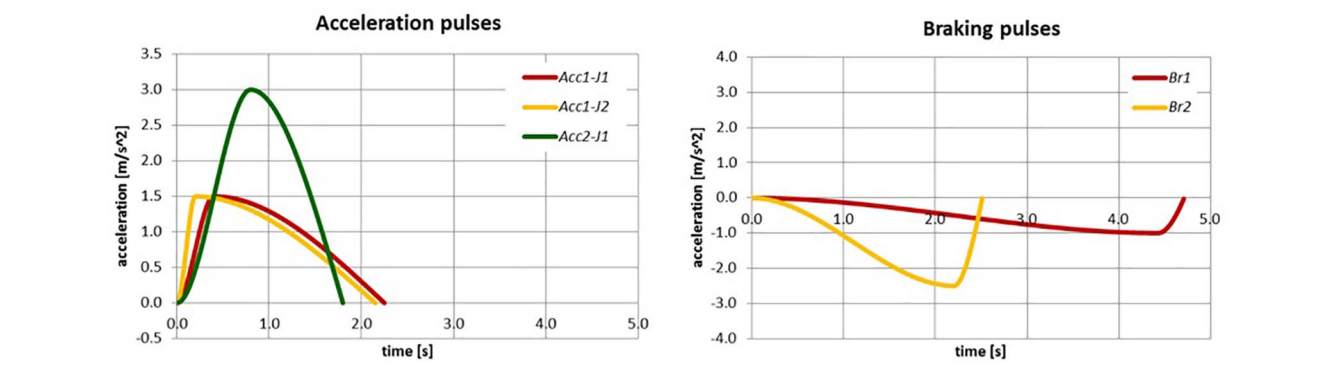

FIGURE 2 | Pulse profile characteristics of acceleration and braking pulses.

TABLE 3 | Main characteristics of the perturbation profiles used.

Consecutive trial	Profile name	Magnitude (m/s^2)	Rise time (s)	Duration (s)	Jerk (m/s^3)
1	Lowest braking (Br1)	1.0	4.43	4.72	0.3
2	Baseline (Acc1-J1)	1.5	0.4	2.25	5.6
3	Highest jerk (Acc1-J2)	1.5	0.2	2.15	11.3
4	Highest acceleration (Acc2-J1)	3.0	0.8	1.8	5.6
5	Highest braking (Br2)	2.5	2.2	2.9	1.7

characteristics of the identified strategies biomechanically, and (iii) evaluation, with the aim of systematically assessing the effectiveness of the identified and characterized strategies. The methodological framework is, therefore, based on a visual grading experiment approach which has been used in other fields such as clinical experiments and radiography (Ivanauskaite et al., 2008; Smedby and Fredrikson, 2010). The methodology is depicted in **Figure 1** below.

Volunteer Tests

The experiment was conducted on 24 healthy volunteers (11 females and 13 males) close to the 50th percentile stature, see **Tables 1**, **2**. While standing on a moving platform, the participants were exposed to five different acceleration profiles designed to mimic the behavior of buses in normal operation (see **Figure 2** and **Table 3**). The acceleration pulses is described in more detail in Linder et al. (2020). Each perturbation was tested both in forward and rearward direction, i.e., the participant either facing the direction of travel or the opposite direction. The volunteers were instructed to initially adopt a relaxed standing posture, feet hip-wide apart, on a designated spot on the platform, while trying to withstand the perturbation without grabbing any parts of the platform. For the safety of the participants, the platform was partly padded, and they were attached to a harness system to prevent them from falling off the platform. The tests were monitored laterally and transversally by two high speed cameras (VEO 640L, Vision Research, Wayne, NJ, USA), the footage of which the analysis in this article is based on.

Identification of Different Balance Strategies

To identify the different balance recovery strategies among the volunteers, the balance response of each volunteer during a specific perturbation trial was categorized into two phases:

Initial Phase

Indicated by the first balancing reactions occurring in the starting position when subjected to a perturbation. Hence, this is the first balance strategy executed by the volunteer. It is described by the fixed-support strategies, the ankle, hip, and squat strategies, since the BoS is stationary at this point and the CoM is displaced from its equilibrium at the start of the perturbation (causing an initial balance instability). If the perturbation is not severe, balance can be maintained by a fixed support strategy.

Recovery Phase

Defined as the phase where a recovery strategy, induced as the severity of the perturbation increases for the volunteer. Here, the initial strategy was not sufficient to maintain a stationary BoS. The balance instability displaces the CoM and BoS beyond static equilibrium limits and a CIS strategy (step strategy) was utilized to attempt to counteract the perturbation. The step strategy is utilized to keep the CoM within the translating BoS.

The hypothesis suggests that the step strategy is too primitive to characterize the differences in the balance responses among the volunteers. Therefore, different recovery strategies were defined, because they determine whether a volunteer is successful in withstanding the perturbation or not. Furthermore, the characterization of a specific recovery strategy was evaluated in relation to its balancing effectiveness, i.e., the resulting balance outcome during a specific perturbation, as a result of utilizing a successful recovery strategy. The characterization methodology describes how the step strategy adopted during balance instability enabled differentiation of the identified balance strategies.

Characterization of Balance Recovery Strategies

Exceeding the initial balance maintenance strategy activates a recovery strategy and initiates the CIS strategy in humans. Two reactions can occur without falling: (i) balance recovery occurs through returning to a fixed-support strategy (stationary BoS), or (ii) a continuous CIS strategy is applied (the BoS is translating beyond static equilibrium limits). A stable position (stationary BoS) represents body control (withstanding the perturbation) and increases stability (balance equilibrium), maintaining or recovering balance. When a step strategy is adopted to counteract the instability produced by perturbation, compensatory stepping is utilized to keep the CoM within the BoS, as the latter is displaced when the body is perturbed. A recovery strategy was established based on the identification of different balance strategies during each perturbation trial, using the factors denoted below in bold.

To regain a stationary BoS and, consequently, body control and the stability to counteract the momentum from the perturbation, a new posture is required. The identified new posture has been defined as a **stance**, i.e., a fixed-support strategy utilized to minimize continued compensatory stepping. Harness deployment resulting in a stance is not considered a successful recovery strategy. On the other hand, continuous **postural adjustments** denote movements to maintain or recover balance, i.e., taking compensatory steps to recover balance equilibrium when a stationary BoS cannot be achieved or maintained during a perturbed state.

The **mechanics** of the balance recovery can be described in terms of the BoS and the CoM during the perturbation. An effective strategy should allow the CoM to be within the BoS throughout the movement, to limit BoS translation from the starting position due to controlled CoM displacement. Minimal total translation from the starting position was considered ideal to display active counteraction to withstand the perturbation, resulting in balance recovery from a perturbed balancing state. A stable position, i.e., an efficient stance, facilitates balance equilibrium of the CoM and BoS, indicating that these components are not translating, and the volunteer has achieved balance equilibrium or returned to the starting position (through stepping) and has counteracted the perturbation. Postural adjustments denote continuous balance instability, where each adjustment is counteracting a perturbed balance equilibrium.

Strategy **outcome** identifies the effectiveness of the response in terms of balance recovery from perturbed states. If a combination of stance and/or postural adjustments allows the "mechanics" to act and turn a perturbed state into a state of balance equilibrium, then the strategy outcome is considered successful.

TABLE 4 | Grading table for balance recovery based on the characterization of strategy effectiveness.

Assessment	Effective (2 points)	Less effective (1 point)	Ineffective (0 point)
Stance	Finds and keeps a firm stance Stable position	Difficulties finding and keeping a stance Less stable position	Unable finding and keeping a stance Unstable position
Postural adjustment	Minimal body adjustments Body control	Body adjustments Less body control	Major body adjustments No body control
Mechanics	CoM within the BoS Minimal translation of CoM and BoS	CoM slightly outside BoS (action: compensatory stepping to try to maintain CoM within BoS) Some translation of CoM and BoS	CoM outside the BoS (rigorous stepping, difficulties in maintaining stable CoM within BoS, exhibiting many difficulties during a trial) Larger translation of CoM and BoS
Outcome	Firm and stable stance or returning to the starting position Few compensatory steps Clear body control and stability	Less firm and stable stance and/or multiple compensatory steps Displayed instability, some body control	Harness deployment No clear body control or stability

Given that a twofold classification "successful or not" in some cases would be too primitive to describe the strategy outcome, the following three categories were applied: effective, less effective, and ineffective.

Evaluation of Balance Recovery

To enable differentiation of different stepping strategies and evaluate the balance recovery qualitatively, a simple ranking system was developed to enable comparison of responses among the different perturbations. A statistical analysis based on the qualitative evaluation (ordinal data) is provided to understand the difference between genders and identified strategies.

To understand and interpret the identified strategies, a grading system was established to analyze the outcome of the different strategies utilized during a perturbation to recover/maintain balance. This is an ordinal scale of effectiveness, i.e., balance responses were scaled to obtain so-called ordinal data (Merbitz et al., 1989). Different criteria constitute the grading system used during the video analysis when the volunteers were subjected to perturbation. A grading scale of 2 (*effective*), 1 (*less effective*), or 0 (*ineffective*) points were used to determine the effectiveness of the adopted strategy when analyzing a pulse trial. The properties defined in Section "Characterization of Balance Recovery Strategies" were used for the evaluation.

If the volunteer managed to hold a stable position (stance) or return to the starting position (fully controlled step strategy), then the strategy has been considered effective. The postural adjustments were deemed "*effective*" if it was evident that the volunteer had recovered balance, and displayed control through compensatory movements, to counteract additional perturbed balance to recover balance equilibrium. In contrast, the strategy was deemed *"ineffective"* if the volunteer showed instability in the stance or postural adjustments, and exhibited an unstable balancing state, i.e., continuous compensatory stepping representing difficulties in counteracting the perturbation, or harness deployment). However, a strategy would be *"less effective"* if balance has been achieved yet showing some instability or constant utilization of compensatory steps or adjustments throughout the perturbation. Displayed instability through compensatory stepping has been considered to increase the risk of harness deployment and is therefore not ideal inside a public transport vehicle to avoid the risk of impacts. **Table 4** below, defines the grading which represents the effectiveness of each balance strategy based on the outcome during a perturbation.

Gender Comparisons

It is well known that there are anthropometric differences between females and males, generally more evident in terms of height, musculature and fat mass, to name a few (Schneider et al., 1983; Al-Haboubi, 1998; Glenmark et al., 2004; Schorr et al., 2018). Physical capabilities, either through gender and anthropometrical differences or athletic background and experience, might affect the execution of a balance strategy. Thus, from the identification and evaluation of balance strategies, gender differences have been examined to understand the effectiveness of utilized strategies and their execution.

Pulse Severity

The volunteer tests provided the opportunity to analyze how the different perturbation characteristics (see **Figure 2** and **Table 3**) disturb a standing passengers' equilibrium and how passengers counteract the disturbance. This was achieved by analyzing and comparing the balance recovery and reaction strategies among the volunteers for the different perturbation profiles. In order to reduce the risk of injury to standing passengers, the success and failure ratios of the volunteers due to the different pulse severities, have been estimated to identify the most challenging perturbations to understand the magnitude thresholds.

Statistical Analysis

In addition to the qualitative evaluation, statistical tests were carried out on the ranked score data (so-called ordinal data) to evaluate whether there are statistical differences among the identified strategies or between genders. The non-parametric (Kruskal and Wallis, 1952) was applied for ordinal data at 5% level of significance. The Null hypothesis is that the sample distributions come from the same population, Whereas the alternative hypothesis states that the distributions are from different populations.

RESULTS

The following subsections describe the tabulated results that constitute the findings of the identification of different balance strategies, characterization of these strategies, and how the recovery strategy of the volunteers affected balancing outcome.

Identification and Characterization of Balance Strategies

From the qualitative video analysis, different strategies were identified. Different execution of similar strategies was found among the volunteers, also between the genders. **Supplementary Appendix 1** shows the identified strategies for each volunteer during each perturbation trial, categorized into the characterization of an initial and a recovery strategy. The overall initial and recovery strategies were determined based on the most frequently used strategy by a volunteer. In **Table 5**, the volunteers were ranked based on their performance according to the grading criteria. The different perturbations affected the volunteers' responses, and the different pulse severities have been highlighted in the columns of **Supplementary Appendix 1**. The success and failure rate presents how well the volunteers performed as a group and also denotes the most challenging perturbation.

The initial strategy was identified as the first reaction where the perturbation disturbed the balance equilibrium from the starting position. **Table 5** shows that the main initial strategy for the volunteers was the ankle strategy. Knee flexion reactions were in some cases found as part of the initial strategies, indicating a knee strategy. The hip strategy was also identified as an initial strategy, although not as frequently as the ankle and knee strategies. For more severe perturbations, the step strategy was executed quicker after a brief ankle strategy, displaying the balance instability caused by the perturbation. The step strategy was identified as the most prevalent strategy to recover balance as the BoS was displaced. Two specific variants were identified, mainly continuous stepping, stretching the harness out (denoted as a pure step strategy) or a counteraction to the CIS reaction by utilizing a stance to recover a stationary BoS (denoted as the *fighting stance* later on). **Figures 3–5** illustrate typical examples of the identified strategies for one perturbation, including frames from the starting position, initial strategy, and the recovery strategy phase. Variations in execution of the identified strategies are depicted in **Supplementary Appendix 2,3**. Section "Characterization of Identified Recovery Strategies" aims to characterize different identified fixed-support responses during the recovery phase, used for balance recovery during the step strategy, caused by a more severe perturbation. Section "Overall Description of the Execution of a Strategy" aims to characterize these variations based on their execution to provide the basis of evaluation.

Characterization of Identified Recovery Strategies

Three different recovery strategies were identified during the recovery phase, different from a pure step response.

The **fighting stance** strategy (see **Figure 3**) is characterized by positioning the lower body in a stable position utilizing a stance constituting of a front and rear leg, with the ankle, knee, and hip of the front leg flexed coupled with a slightly flexed torso. The rear leg has less ankle and knee flexion but is mostly characterized by a hip extension due to the leg position. The degree of external rotation of the ankle of the rear leg was more pronounced in some volunteers. From the video analysis, compensatory steps were included in the execution, to reach the stance. The fighting stance is also characterized by fixating a larger step, utilizing the step strategy. A fixed-support strategy, through a stable stance, is therefore obtained during the step strategy. The lower body musculature is utilized to position the body in a fixed position, i.e., a stance, by increasing knee and hip flexion in the front leg to control the CoM displacement within the BoS, utilizing the hip-extended rear leg for support. Furthermore, the rear leg executes the majority of the compensatory steps to maintain the stance, to adjust the BoS and stabilize the CoM.

The **surfer stance strategy** (**Figure 5A**), only utilized by Volunteer 19, resembles a surfer standing on a surfboard, and in contrast to the fighting stance it includes a larger rotation of the torso and the lower body. Should the weight of the torso be shifted to either leg, the torso rotates and leans over the front or the rear leg, whereas in the fighting stance the weight is mostly distributed on the front leg. The legs support the weight of the torso, however, compared to the fighting stance, the surfer stance can support the weight on either leg due to the stance being more symmetrical.

The **small-step squat strategy** (**Figure 5B**), utilized only by Volunteer 24, is characterized by a synergetic knee and hip action complex (squatting posture) with a step strategy utilizing small compensatory steps. The lower body musculature is utilized to lower the CoM accompanied by a broader stance to increase the width of the BoS. The small-step strategy keeps the feet close to the ground to maintain as close contact as possible, while taking small compensatory steps deaccelerate the BoS as the CoM is perturbed during the perturbation. From the video analyses, Volunteer 24 seemed to have a larger lower body, and her stepping seemed to be executed cautiously. The combination of smaller multiple compensatory steps with a squatting posture allowed the volunteer to increase body control (with the help of cautious stepping) and stability (maintaining a squat posture, to lower the CoM). Therefore, the small-step strategy can be used to counteract the momentum from the perturbation and withstands the perturbation by using smaller cautiously taken steps, while the squat strategy increases the stability of the CoM and BoS by lowering the CoM.

Overall, the fighting stance strategy converts balance instability (multiple-step response) into a stable stance, withstanding the need for stepping to control an unstable body by stabilizing the CoM within the BoS. Body control is increased due to the positioning of the legs, allowing discrepancies of CoM movement within a larger surface area (BoS), but with more stability due to flexible postural adjustments through multiple stepping and weight distribution advantages using both legs. The hip flexors and knee extensors (mainly quadriceps)

TABLE 5 | Tabulated grading of balance recovery during each perturbation and ranking of the volunteer outcome based on strategy effectiveness (M, male; F, female).

Volunteers	Gender	Initial strategy	Recovery strategy	*Lowest braking*		Baseline		*Highest jerk*		*Highest acceleration*		*Highest braking*		Number of pulses	Average score
				F	R	F	R	F	R	F	R	F	R		
12	M	An-kn	Fighting	2	2	2	2	2	2	1	0	2	2	10	1,7
18	M	Ankle	Fighting	1	2	2	2	2	2	2	0	2	2	10	1,7
7	M	Ankle	Fighting	2	2	2	2	2	2	0	0	2	2	10	1,6
17	M	Ankle	Fighting	2	2	2	2	2	2	0	0	2	2	10	1,6
11	M	Ankle	Fighting	2	2	2	2	2	2	1	0	2	0	10	1,5
9	F	Ankle	Fighting	0	2	2	2	2	2	0	0	2	2	10	1,4
16	F	Ankle	Fighting	2	2	2	2	2	2	0	0	1	1	10	1,4
24	F	Ankle	Squat-step	2	2	0	2	1	2	0	2	-	-	8	1,4
20	M	Ankle	Fighting	2	2	2	2	2	2	0	0	1	0	10	1,3
23	M	Ankle	Fighting	2	1	2	2	2	2	0	0	1	1	10	1,3
4	F	Ankle	Step	2	2	2	1	2	2	0	0	1	0	10	1,2
15	F	Ankle	Fighting	2	1	1	1	2	2	0	0	-	-	8	1,1
6	F	Ankle	Step	2	1	1	1	2	2	0	0	1	1	10	1,1
3	M	Ankle	Step	2	2	1	0	1	2	0	0	-	-	8	1
8	F	Ankle	Step	0	0	2	2	2	1	0	0	2	0	10	0,9
13	F	Ankle	Step	1	1	1	1	2	1	0	0	1	1	10	0,9
19	M	Ankle	Surfer	0	0	1	1	2	2	0	0	2	0	10	0,8
1	M	An-kn	Step	0	2	2	0	1	0	0	0	1	0	10	0,6
14	F	Ankle	Step	2	2	0	0	0	0	0	0	-	-	8	0,5
21	M	Ankle	Step	2	0	1	0	1	0	0	0	0	0	10	0,4
5	F	Ankle	Step	2	0	0	0	0	0	0	0	0	0	10	0,2
2	M	Ankle	Step	1	0	0	0	0	0	0	0	-	-	10	0,1
22	M	Ankle	Step	1	0	0	0	0	0	0	0	0	0	10	0,1
10	F	Ankle	Step	0	0	0	0	0	-	0	-	-	-	6	0
	Test performed			24	24	24	24	24	23	24	23	18	18		
	Total points			34	30	30	27	34	32	4	2	23	14		
	% Success			79	71	75	67	79	74	13	4	83	50		
	% Fail			21	29	25	33	21	26	87	96	17	50		
	% Success females			73	73	64	73	73	80	0	10	86	43		
	% Success males			85	69	85	62	85	69	23	0	82	45		

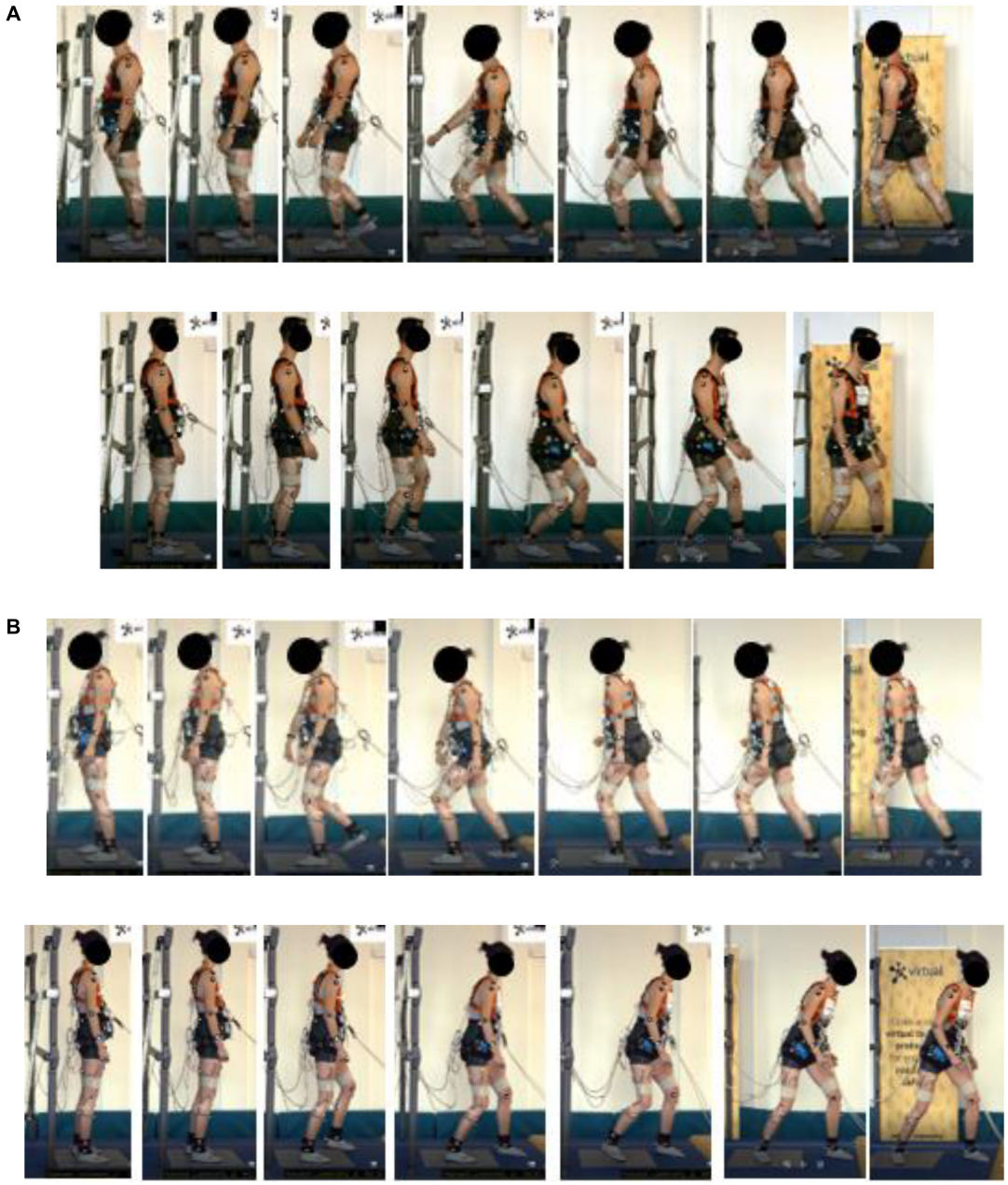

FIGURE 3 | Typical forward and rearward fighting stance, **(A)** male (Volunteer 12) and **(B)** female (Volunteer 16).

allow the torso to be supported by a front leg positioned with a stable knee and hip flexion and dorsi-flexed ankle, acting as a weight-bearing component. The rear leg, characterized by a noticeable hip extension and slight knee flexion and dorsi- or plantar-flexed ankle for stability, activates the lower part of the posterior chain (hamstrings, gluteus muscles, and calves). This acts as the supporting part, providing the base for postural adjustments to support the weight-bearing front leg and change in the torso angle, thus lowering the CoM which increases stability.

Overall Description of the Execution of a Strategy

Although not displayed during every perturbation, most volunteers showed a preferred recovery strategy when their balance recovery was effective. During the video analyses, multiple volunteers displayed efforts to execute their preferred recovery strategy, despite the preferred recovery strategy being more challenging to execute successfully during the more severe perturbations. This was evident for the volunteers utilizing the fighting stance, as denoted in **Supplementary Appendix 1** and **Table 5**. Volunteers with higher failure rates to maintain/recover

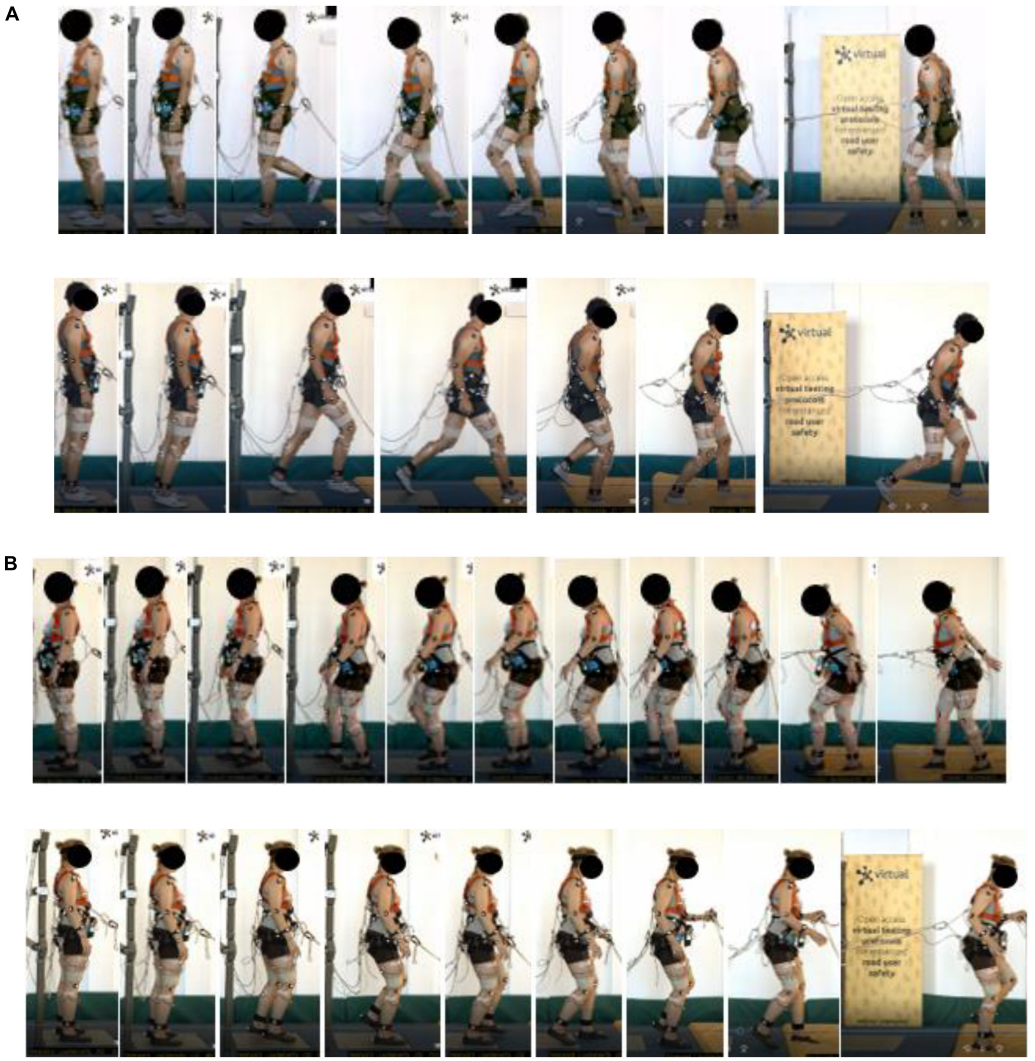

FIGURE 4 | Typical forward and rearward step strategy, **(A)** male (Volunteer 22) and **(B)** female (Volunteer 10).

balance usually used the pure step strategy, and showed no indication of trying to find a stance to stop the stepping, that would eventually induce harness deployment.

While the surfer stance strategy and the small-step squat strategy were only executed by Volunteer 19 and 24, respectively, the small-step squat strategy was executed differently in the forward and rearward perturbation. In the rearward direction, the squatting posture was more pronounced, as illustrated in **Figure 5B** with more flexion at the knees and the hips which resulted in more torso flexion and lower CoM. This was consistent for all rearward perturbations, with more flexion as the pulse severity increased. For the surfer stance strategy, closer to horizontal torso positioning was inspected for more severe perturbations although it was accompanied with difficulties in balance recovery. For example, during balance instability, the torso leaned forward such that Volunteer 19 lost his foothold and displayed cases where he braced using his hands to avoid falling. No clear differences in execution of this strategy were found in the video analysis.

The majority of the volunteers utilizing a step strategy as their recovery strategy presented continuous compensatory stepping throughout the perturbation, with the exception of those who managed to discontinue the stepping movements (stance) and recovered balance equilibrium as a result. No differences in execution among these users were found, specifically among genders, perturbation profiles or orientation. The initial strategy utilized was the ankle strategy, which caused larger ankle motion in the rearward perturbation and larger compensatory steps as a result.

Overall, the fighting stance was the most prevalent recovery strategy, together with the step strategy. Here, a wide variety of execution was found compared to the step strategy, as illustrated in **Supplementary Appendix 2**. Usually, some postural adjustments with regard to the stepping were made to find or

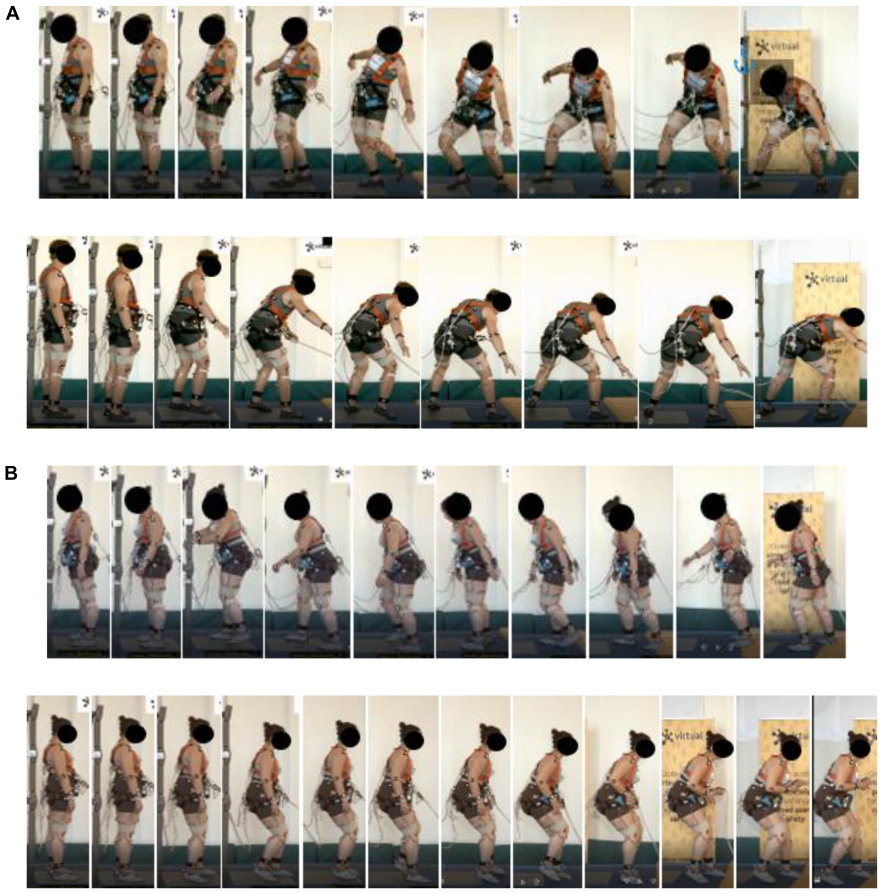

FIGURE 5 | Forward and rearward, **(A)** surfer (Volunteer 19) and **(B)** squat stance (Volunteer 24).

adjust the stance as the body became unstable. Furthermore, the step length was larger compared to the step strategy users. Overall, the characterization of this strategy was very similar among the volunteers, where the final position of all users can be described using the characterization in Section "Characterization of Identified Recovery Strategies," above. However, the transfer from stepping to the stance was different. Some volunteers displayed the execution of the stance more consistently than others as the stepping started, attempting to return to the stance in one single step, i.e., the stance was utilized to avoid further compensatory stepping as the BoS displaced from the starting position. This is illustrated in **Figure 3**. For other volunteers, multiple compensatory steps were utilized until the stance was found. No specific differences in the execution between genders were found.

Balance Recovery Outcome During the Different Perturbations

The average score in **Table 5** quantifies each volunteer's overall success in recovering balance. The top scoring participants utilized the fighting stance strategy as their preferred balance recovery strategy, illustrated in **Supplementary Appendix 1** and **Table 5**. The main recovery strategies were the fighting stance (10 out of 24) and the step strategy (12 out of 24). Based on the highest scores, seven out of 13 males utilized the fighting stance, of which five scored 2 points for most of the pulses, covering the top five ranking out of all volunteers. Only three out of 11 females utilized the fighting stance, with two of them ranking at the top of the grading table, below the five most successful male users of the strategy. For the squat-step (Volunteer 24) and surfer (Volunteer 19) recovery strategies, Volunteer 24 ranked tied among the top females (the other two had adopted the fighting stance strategy) while Volunteer 19 ranked in between the pure step strategy users, ranking low in **Table 5**.

The columns in **Table 5** can be used to illustrate the effect of pulse shape on the volunteer response. The rearward-facing perturbations were the most severe conditions. The volunteers had higher success rates for balance during the *highest jerk* perturbations. In general, all volunteers expressed consistency in their preferred balance recovery strategy throughout all perturbations in both forward and rearward facing orientation, as described in Section "Overall Description of the Execution of a Strategy". The top males were partly successful in the forward-facing perturbation of the *highest acceleration*, whereas the majority failed to fully recover balance. The

TABLE 6 | Statistical results based on recovery strategy and gender.

Pulse severity	Strategy (fighting = 10; stepping = 12)				Gender (males = 12; females = 10)			
	Forward		Rearward		Forward		Rearward	
	t-stat	*p-value*	*t*-stat	*p-value*	*t*-stat	*p-value*	*t*-stat	*p-value*
Lowest Braking	1.924	*0.165*	6.181	*0.012**	0.380	*0.537*	3.736	*0.053*
Baseline	9.177	*0.002**	14.305	*0.000**	1.364	*0.242*	0.249	*0.617*
Highest Jerk	9.535	*0.002**	10.717	*0.001**	0.037	*0.846*	0.027	*0.868*
Highest Acceleration	6.217	*0.012**	[a]	-	[b]	-	[a]	-
Highest Braking	6.217	*0.012**	6.199	*0.012**	0.277	*0.598*	0.34	*0.559*

**Statistically significant.* [a]*All participants lost balance.* [b]*Few observations.*

results indicate that the *highest acceleration* was the most troublesome perturbation, with a slight disadvantage during the corresponding rearward-facing orientation (13 vs. 4% success). The highest rearward-facing braking pulse was the next troublesome perturbation (50% success). The forward-facing highest magnitude braking pulse had the highest success rate. However, due to safety considerations for some volunteers, not all volunteers participated during the *highest braking* pulses as indicated by the lower number of tests performed (18 out of 24 volunteers). The forward *highest jerk* and *lowest braking* pulse had the highest success rate including all volunteers (79% success each), with the rearward *highest jerk* and *lowest braking* pulse having a similar success rate (74 vs. 71%). Overall, the females were more successful than the males in the rearward perturbations, and vice versa. For the *highest braking*, the success rate was reversed but with very minor difference in the success rate. The number of females participating for that pulse was decreased from 11 to seven, and for the males from 13 to 11.

The volunteers preferring the pure step strategy exhibited more compensatory steps with shorter single-support phases to withstand the more severe the perturbation, which resulted in either harness deployment (0 points) or major postural adjustments to recover balance to obtain 1 point. The success rate for balance recovery based on the grading criteria was higher for the *highest jerk* compared to the *highest acceleration*. The *highest jerk* perturbation induced the fighting stance faster and more successfully to counteract and recover balance and adopting a stable stance. Furthermore, details from the video analyses show that the *lowest braking* was usually not severe enough to cause major balancing instability for the majority of the volunteers. The volunteers' recovery strategies (mostly the fighting stance) were not challenged, and the execution was not problematic. In general, those who achieved 1 or 2 points for the *lowest braking* pulse, had little to no difficulties in balance recovery and at most exhibited only compensatory steps at the second half of the perturbation or utilized one step to find the stance. Also, the majority recovered balance fully, which was determined when a volunteer returned to the original starting position on the force plate. The surfer stance user failed in both perturbations during the *lowest braking* pulse. For the rest of the perturbations, the recovery strategies were used to counteract the perturbations, primarily for those utilizing the fighting stance. The fighting stance users required more compensatory steps to stabilize their stance since the CoM became more unstable. In addition, the *highest jerk* perturbations seemed to cause quicker transition into a successful fighting stance, as these volunteers displayed body control and stability after finding the stance and utilized very few postural adjustments, i.e., maintaining the stance. **Supplementary Appendix 1** shows that all fighting stance users utilized their preferred recovery strategy during the jerk perturbations to obtain the highest grading. On the contrary, during the *highest acceleration and braking*, the fighting stance users displayed more difficulties in maintaining the fighting stance, and hence more balance instability. However, the grading demonstrates that the braking pulse was associated with a higher success rate for these volunteers.

Statistical Results

The results of the statistical analysis in **Table 6** shows that the distributions of the *fighting stance* and the pure step strategy are not from the same population. This indicates that their characteristics differ statistically, and that the *fighting stance* has an impact on the outcome regarding balance recovery. Since the test does not indicate in which way they differ, further analysis is needed, e.g., investigating the step length or margin of stability.

On the other hand, the results show no differences in the outcome of the balance recovery due to gender. This can be an artifact of the data since the results based on gender do not differentiate between strategies. The analysis for gender differences within strategies (fighting/stepping) could not be performed due to small sample sizes ($n < 5$).

DISCUSSION

A proposed methodology for in-depth analysis of identified strategies was defined, (i) to first identify the initial reaction at the starting position using a fixed-support strategy, and (ii) then the recovery phase dominated by CIS strategies. The purpose was to understand how postural balance was affected during the recovery phase (as defined in Section "Identification of Different Balance Strategies"), through identification of individual CIS strategies which would result in different balancing outcomes

when subjected to different perturbations. The characterization serves to provide a description of the strategy execution to qualitatively understand the differentiation of the CIS strategies. This study is intended to be a first investigation of qualitatively evaluating if an effective CIS strategy to withstand higher severity perturbations exists. Hence, only healthy younger volunteers were included in this study to identify the upper perturbation thresholds (i.e., the limit where recovery could still be achieved) with respect to relevant acceleration and jerk magnitudes experienced on public transport.

The small-step squatting strategy, the surfer stance and the fighting stance were identified as recovery strategies different from pure stepping. The fighting stance was utilized by multiple volunteers with similar execution and high overall success rates, although not all managed the *highest acceleration*. The different strategies are briefly discussed in sections below.

Surfer Stance Strategy

The surfer stance has not previously been defined in the literature and the term was suggested due to the similarity with the stance of surfers. However, it is debatable how applicable such a strategy would be on board a bus or tram. It was unique in this study, with only Volunteer 19 (male) displaying this strategy. From the video analyses, the risk of falling head-first would increase, as Volunteer 19 did lose footing and used his hands for support, which might increase the risk of head injuries. Therefore, it can be hypothesized that such a strategy might not be suitable inside a public transport vehicle and have unnecessary biomechanical demands for its execution. Thus, it will not be discussed further.

Small-Step Squat Strategy

The next unique case is the small-step squat strategy, only utilized by Volunteer 24 (female, 160.0 cm, 72.6 kg). Generally, a step strategy is a countermeasure for balance instability, although from the more severe perturbation trials it has rarely been considered effective in balance recovery (as illustrated by **Table 5**), as most users deployed their harness. However, the small-step squat strategy increased body control and stability successfully, hence Volunteer 24 was ranked higher than the pure step strategy users, and tied with Volunteers 9 and 16 (both females utilizing the fighting stance strategy) in terms of successful outcomes. The cautious stepping might be effective to counteract the momentum caused by the perturbation, as it displayed slower stepping to withstand the perturbation, as opposed to the pure step strategy users that executed quicker steps (short single-support phase) and traveled a longer distance which deployed the harness. However, the less common anthropometry among the volunteers, with the above-mentioned combination of both strategies, could have been responsible for the successful outcome. The unique results in this study indicated that the small-step squat strategy was more effective than the pure step strategy to counteract the perturbed body movement, but the prevalence of this strategy was too low to draw any conclusions. Whether this strategy is useful for a general population needs further research, as it might be an outlier of mechanically efficient usage for this anthropometry rather than balance strategy effectiveness. As this strategy was also unique in this study, it will also not be discussed further.

Characteristic Differences Between *Fighting Stance* and Step Strategy

The highest prevalence of utilized strategies was found for the *fighting stance* (10 out of 24) and the pure step strategy (12 out of 24). Overall, the fighting stance resulted in the highest overall scores, displaying its effectiveness in balance recovery in both its female and male users. Although this study only included 11 females and 13 males, the males seemed to execute the fighting stance more frequently compared to the females (seven males and three females). Since the fighting stance can only be successful if the perturbation can be counteracted by stopping continuous compensatory stepping, more muscular strength and body control might be required to produce the stability needed to find a stance stable enough to avoid stepping and stabilizing the CoM within a stationary BoS. Since all volunteers were subjected to the same perturbations, this might suggest that females had more difficulties in executing the fighting stance due to anthropometric aspects. For example, it was harder to execute the fighting stance during the *highest acceleration* pulse, which represents the most severe condition for the volunteers. However, some of the top-ranked males consistently adopting the fighting stance were able to withstand the *highest acceleration* in the forward direction, displaying better execution than other users of the same strategy. Despite the less successful balance recovery among the female users in this study, these females showed how effective the fighting stance was for the other perturbations in that they were more successful than the males using the pure step strategy. Karekla and Tyler (2018a) found that younger volunteers, the strongest of the sample also containing older volunteers, utilized the least effective step strategies to withstand the perturbations of that study (1.5 m/s^2). The more effective steps were utilized by mainly male and older participants, while females were less challenged during walking which contradicted previous findings that argued that women sway more and have reduced balance (Lord et al., 1996; Hsue and Su, 2014). In the current study, there were more males than females executing the fighting stance and ultimately less females that could recover balance effectively. However, this study investigated stepping responses occurring from a stationary position as opposed to normal gait inside a moving bus and the highest effectiveness was found among males. Therefore, adopting the fighting stance might be an effective and proactive balance strategy to improve the success in recovering balance during perturbations, regardless of gender. Furthermore, the statistical analysis supports these findings, where the fighting stance does have an impact on the outcome regarding balance recovery, whereas gender does not have an impact. In other words, a female executing a given strategy (e.g., the fighting stance) would have the same outcome as a male using the same strategy. Thus, female passengers would benefit the most if they can switch from a pure stepping strategy to a stance strategy. However, the last argument is based on statistical analysis of ordinal data, and more studies are needed

FIGURE 6 | Fighting stance in martial arts (*left*) and Volunteers 12 and 16 displaying their fighting stance (*right*). Left picture from (attached link): Two Male Mannequins Black White Fighting Stock Illustration 1877892802 (shutterstock.com)–Accessed 3 Feb 2021.

(quantitative and qualitative) to understand the gender influence on the execution and utilization of the fighting stance.

The fighting stance utilizes the step strategy for execution, but the step characteristics between the strategies differ. From the video analysis, *fighting stance* users executed larger steps and intended to keep the stance using compensatory steps (usually changing the step length, i.e., moving either leg), and body displacement were lower compared to pure steppers. The pure steppers executed compensatory steps with increased body displacement, rather than maintaining a stance posture and executing steps for postural adjustments which all classified *fighting stance* volunteers utilized. The effectiveness of the *fighting stance* might be due to increased body control and stability as the severity of the perturbation increases, to induce effective balance with the lower body positioning (with a leg in front of the CoM, broadening the BoS) during unexpected perturbations to lower the risk of injury. During the lowest braking perturbations, all *fighting stance* volunteers were less challenged than pure steppers (**Table 5**), and the *fighting stance* was more similar to a single-step strategy. The *fighting stance* users maintained postural balance with a fixed-support strategy (usually ankle, **Table 5**) and increased recovery through a CIS strategy using a larger step (King et al., 2005; Wu et al., 2007) towards the end of the pulse. This larger step response was characteristic among the *fighting stance* volunteers. Pure steppers executed multiple-step strategies during the same perturbation, displaying a lower perturbation threshold than *fighting stance* volunteers, even though this was the least severe perturbation in this study.

With the identification of the *fighting stance*, the different characteristics can limit body displacement and increase dynamic postural stability compared to pure stepping. It provided insight on free-standing balance recovery thresholds to different magnitudes of acceleration, jerk, and braking (described in the later subsection). This stance can also be compared to an actual fighting stance, which is a stance adopted in martial arts, which might explain its effectiveness in maintaining balance as well as utilizing postural adjustments to withstand external disturbances. The lower body positioning is very similar, see **Figure 6**.

King et al. (2005) found that younger subjects take longer steps naturally, while older adults rather rely on shorter steps, which require less biomechanical strength. This study had a mean age of 33.8 ± 9.0 (**Table 2**) and therefore is not representative of the elderly. Whether the *fighting stance* is applicable and of benefit also to older adults, should be investigated further. Increasing lower body biomechanical strength (King et al., 2005; Carty et al., 2012a) might benefit older adults to execute larger steps more naturally and utilizing the single-step strategy over multiple stepping with less physical restraints. Hence, the opportunity to utilize effective recovery strategies might be possible. Previous studies (McIlroy and Maki, 1996; Hsiao and Robinovitch, 1999, 2001) have argued to not replace natural multiple stepping that occur during severe perturbations with a pure single-step response to recover balance, which ultimately can limit the perturbation thresholds, but to instead enhance (increased effectiveness) the multiple-step response (Hsiao-Wecksler and Robinovitch, 2007). Hence, it would be interesting to utilize the idea by Hsiao-Wecksler and Robinovitch (2007) to evaluate how multiple-step responses can be controlled, e.g., minimize body displacement, to improve postural control on public transport. From this, acting as one important factor among others [such as perturbation-based training (Mansfield et al., 2015)], an increased tolerance to higher perturbations could be feasible.

Recommended Perturbation Thresholds Based on the Recovery Outcomes

The execution of the balance strategies was rapid for the *higher jerk* perturbation with effective outcome. This was not seen for the *highest acceleration*. The *highest braking* event did not include all volunteers, but the execution and the absolute outcome was not as successful as during the jerk. As seen in this study

during the *higher acceleration* and *braking*, and in some of the *fighting stance* volunteers during the *highest jerk*, is that multiple compensatory steps were used to execute the *fighting stance*. Here, based on the effectiveness results in **Table 5**, successful recovery was less seen for the *highest acceleration* but more common for the *highest braking*, which indicates that the acceleration threshold was reached but not necessarily for the braking maneuver. This successful recovery was not seen for the pure steppers for the acceleration and braking perturbations. Multiple pure steppers were excluded from the braking pulses, the findings are mostly determined by the *fighting stance* responses. Thus, out of the higher severity pulses, the *highest jerk* perturbations might be more favorable for successful execution of balance recovery strategies compared to higher acceleration and braking.

Recent studies on bus perturbations (Karekla, 2016; Karekla and Tyler, 2018a,b; Karekla and Fang, 2021) recommended an acceleration level below 2.0 m/s^2 to account for postural balance during gait using handrails, and 1.0 m/s^2 without handrails. A jerk recommendation for comfort at 0.9 m/s^3 was mentioned, but is not comparable to the findings in this study considering the recovery outcome in this study for both the baseline pulse (5.6 m/s^3) and the *highest jerk* pulse (11.3 m/s^2) where the majority of the volunteers managed to recover balance successfully. However, the identification of the fighting stance with resulting volunteer responses showed that the *baseline* pulse (1.5 m/s^2) was not as problematic for this volunteer group together with the *highest jerk* and *lowest braking* pulses. Furthermore, the *baseline* pulse was too troublesome for the pure steppers, as most scored between 0 and 1 points, indicating that an acceleration of 1.0 m/s^2 might be more realistic and improving the stepping response using the fighting stance characteristics might increase the perturbation threshold to at least 1.5 m/s^2. It is also arguable that pure steppers should not exceed either jerk level, as their multiple step response was more unstable than volunteers with the *fighting stance*. This shows that higher perturbation thresholds can be allowed if the free-standing passengers are initially at a standstill, if *fighting stance* is utilized, but careful consideration is needed during gait such as boarding, alighting, or finding a seat inside a moving bus or tram. Avoiding pure stepping during free-standing scenarios by using the *fighting stance* might allow postural control and less body displacement, as the results in this study showed higher harness deployment rate for pure steppers (indicative of 0 points in **Table 5**). Providing hand support, such as handrails and/or horizontal/vertical bars, will increase the opportunity to maintain balance, as postural sway during perturbations decreases (Maki and McIlroy, 1997; Ustinova and Silkwood-Sherer, 2014; Karekla and Fang, 2021). Future studies should investigate hand support with an effective strategy, e.g., with characteristics such as the *fighting stance*, to increase the knowledge on utilizing effective CIS strategies and perturbation thresholds relevant for controlling vehicle dynamics for public transport. However, the *fighting stance* is a single-step strategy executed anteriorly to the CoM in a forward- or rearward-facing posture, which is a reasonable stepping characteristic during forward or rearward translations, but its relevancy in lateral configurations is unknown. The absence of lateral perturbations with respect to public transport needs to be addressed to complement the current study. The literature on lateral perturbations have provided more characterization by identifying different types of side-step and cross-step strategies (Borrelli et al., 2019; Batcir et al., 2020). However, recovery strategies when facing laterally to the direction of travel might induce other stepping responses when subjected to more severe perturbations as in the current study. Such literature with respect to public transport has not been found. Hence, studying acceleration and jerk perturbations in lateral-facing directions, to identify perturbation thresholds among free-standing passengers, is needed. More complex maneuvers, such as turning, should also be studied to identify and characterize stepping responses in free-standing scenarios.

CONCLUSION

The qualitative investigation of identification and characterization provided insight on different CIS strategies executed during severe perturbation levels similar to those on public transport. The *fighting stance* was identified as the most effective recovery strategy to limit body displacement and increase dynamic stability during severe perturbations, compared to pure stepping. It also displayed recovery (no harness deployment) during perturbations that were more challenging for pure steppers. Thus, *fighting stance* users have higher perturbation thresholds and could withstand all perturbations, with the exception of the *highest acceleration* in both directions being too severe. A limitation in this study was the exclusion of quantitative measures, which should be utilized in conjunction with in-depth qualitative analysis (identification and characterization of the step responses), to determine the effectiveness of a balance strategy. Identifying and characterizing recovery step strategies among older adults, using lower magnitudes of acceleration, jerk, and braking, should be investigated to identify relevant perturbation thresholds. For this group, instructing the *fighting stance* and compare to pure stepping should be explored, as it might increase postural balance by increasing the effectiveness of their multiple-step responses. Overall, the *fighting stance* supports previous findings on the higher effectiveness of a single-step strategy over multiple-step strategies, since the *fighting stance* characteristics are similar to a single-step strategy but utilizes multiple stepping for postural adjustments. This shows that additional characterization provides details on how to execute an effective multiple-stepping response.

DATA AVAILABILITY STATEMENT

The raw data supporting the conclusions of this article will be made available by the authors, without undue reservation.

ETHICS STATEMENT

The studies involving human participants were reviewed and approved by National Medical Ethics Committee, Ministry of Health, Republic of Slovenia, Štefanova 5, SI-1000 Ljubljana (http://www.kme-nmec.si/). Application number was: 0120-63/2019/4. The participants provided their written informed consent to participate in this study.

AUTHOR CONTRIBUTIONS

JX and AS designed the methodology and conducted the video analyses. JX analyzed the results and wrote the manuscript, with some assistance from AS. AS conducted the statistical analysis. AK, SK, RT, CK, and AL provided feedback during the video analyses. AK reviewed the methodology and improved the concepts. AS, AK, SK, RT, CK, and AL read and edited the manuscript. All the authors critically reviewed and approved the final manuscript.

FUNDING

This study has been conducted within the project VIRTUAL and has received funding from the European Union Horizon 2020 Research and Innovation Programme under Grant Agreement No. 768960.

ACKNOWLEDGMENTS

Thanks to Elisabet Agar for the appreciated and detailed language review.

SUPPLEMENTARY MATERIAL

The Supplementary Material for this article can be found online at: https://www.frontiersin.org/articles/10.3389/fbioe.2021.670498/full#supplementary-material

REFERENCES

Albertsson, P., and Falkmer, T. (2005). Is there a pattern in European bus and coach incidents? A literature analysis with special focus on injury causation and injury mechanisms. *Accid. Anal. Prev.* 37, 225–233. doi: 10.1016/j.aap.2004.03.006

Al-Haboubi, M. H. (1998). The female/male ratio of anthropometric dimensions. *J. Hum. Ergol.* 27, 9–16.

Bair, W. N., Prettyman, M. G., Beamer, B. A., and Rogers, M. W. (2016). Kinematic and behavioral analyses of protective stepping strategies and risk for falls among community living older adults. *Clin. Biomech.* 36, 74–82. doi: 10.1016/j.clinbiomech.2016.04.015

Barrett, R. S., Cronin, N. J., Lichtwark, G. A., Mills, P. M., and Carty, C. P. (2012). Adaptive recovery responses to repeated forward loss of balance in older adults. *J. Biomech.* 45, 183–187. doi: 10.1016/j.jbiomech.2011.10.005

Batcir, S., Shani, G., Shapiro, A., Alexander, N., and Melzer, I. (2020). The kinematics and strategies of recovery steps during lateral losses of balance in standing at different perturbation magnitudes in older adults with varying history of falls. *BMC Geriatr.* 20:249. doi: 10.1186/s12877-020-01650-4

Björnstig, U. L. F., Bylund, P. O., Albertsson, P., Falkmer, T., Björnstig, J., and Petzäll, J. (2005). Injury events among bus and coach occupants: non-crash injuries as important as crash injuries. *IATSS Res.* 29, 79–87.

Borrelli, J., Creath, R. A., Pizac, D., Hsiao, H., Sanders, O. P., and Rogers, M. W. (2019). Perturbation-evoked lateral steps in older adults: why take two steps when one will do? *Clin. Biomech.* 63, 41–47. doi: 10.1016/j.clinbiomech.2019.02.014

Borrelli, J., Creath, R., Gray, V. L., and Rogers, M. W. (2021). Untangling biomechanical differences in perturbation-induced stepping strategies for lateral balance stability in older individuals. *J. Biomech.* 114:110161. doi: 10.1016/j.jbiomech.2020.110161

Brauer, S. G., Woollacott, M., and Shumway-Cook, A. (2002). The influence of a concurrent cognitive task on the compensatory stepping response to a perturbation in balance-impaired and healthy elders. *Gait posture* 15, 83–93. doi: 10.1016/s0966-6362(01)00163-1

Carbonneau, E., and Smeesters, C. (2014). Effects of age and lean direction on the threshold of single-step balance recovery in younger, middle-aged and older adults. *Gait Posture* 39, 365–371. doi: 10.1016/j.gaitpost.2013.08.013

Carty, C. P., Barrett, R. S., Cronin, N. J., Lichtwark, G. A., and Mills, P. M. (2012a). Lower limb muscle weakness predicts use of a multiple-versus single-step strategy to recover from forward loss of balance in older adults. *J. Gerontol. A Biomed. Sci. Med. Sci.* 67, 1246–1252. doi: 10.1093/gerona/gls149

Carty, C. P., Cronin, N. J., Lichtwark, G. A., Mills, P. M., and Barrett, R. S. (2012b). Mechanisms of adaptation from a multiple to a single step recovery strategy following repeated exposure to forward loss of balance in older adults. *PLoS One* 7:e33591. doi: 10.1371/journal.pone.0033591

Carty, C. P., Cronin, N. J., Nicholson, D., Lichtwark, G. A., Mills, P. M., Kerr, G., et al. (2015). Reactive stepping behaviour in response to forward loss of balance predicts future falls in community-dwelling older adults. *Age Ageing* 44, 109–115. doi: 10.1093/ageing/afu054

Carty, C. P., Mills, P., and Barrett, R. (2011). Recovery from forward loss of balance in young and older adults using the stepping strategy. *Gait Posture* 33, 261–267. doi: 10.1016/j.gaitpost.2010.11.017

Cheng, K. B. (2016). Does knee motion contribute to feet-in-place balance recovery? *J. Biomech.* 49, 1873–1880. doi: 10.1016/j.jbiomech.2016.04.026

Cordero, A. F., Koopman, H. F., and Van der Helm, F. C. T. (2003). Multiple-step strategies to recover from stumbling perturbations. *Gait Posture* 18, 47–59. doi: 10.1016/s0966-6362(02)00160-1

Crenshaw, J. R., and Kaufman, K. R. (2014). The intra-rater reliability and agreement of compensatory stepping thresholds of healthy subjects. *Gait Posture* 39, 810–815. doi: 10.1016/j.gaitpost.2013.11.006

Cronin, N. J., Barrett, R. S., Lichtwark, G., Mills, P. M., and Carty, C. P. (2013). Decreased lower limb muscle recruitment contributes to the inability of older adults to recover with a single step following a forward loss of balance. *J. Electromyogr. Kinesiol.* 23, 1139–1144. doi: 10.1016/j.jelekin.2013.05.012

Cyr, M. A., and Smeesters, C. (2007). Instructions limiting the number of steps do not affect the kinetics of the threshold of balance recovery in younger adults. *J. Biomech.* 40, 2857–2864. doi: 10.1016/j.jbiomech.2007.03.012

de Boer, T., Wisse, M., and Van der Helm, F. C. T. (2010). Mechanical analysis of the preferred strategy selection in human stumble recovery. *J. Biomech. Eng.* 132:071012.

de Kam, D., Roelofs, J. M., Bruijnes, A. K., Geurts, A. C., and Weerdesteyn, V. (2017). The next step in understanding impaired reactive balance control in people with stroke: the role of defective early automatic postural responses. *Neurorehabil. Neural Repair* 31, 708–716. doi: 10.1177/1545968317718267

de Kam, D., Roelofs, J. M., Geurts, A. C., and Weerdesteyn, V. (2018). Body configuration at first stepping-foot contact predicts backward balance recovery capacity in people with chronic stroke. *PLoS One* 13:e0192961. doi: 10.1371/journal.pone.0192961

Do, M. C., Breniere, Y., and Brenguier, P. (1982). A biomechanical study of balance recovery during the fall forward. *J. Biomech.* 15, 933–939. doi: 10.1016/0021-9290(82)90011-2

Elvik, R. (2019). Risk of non-collision injuries to public transport passengers: synthesis of evidence from eleven studies. *J. Transport Health* 13, 128–136. doi: 10.1016/j.jth.2019.03.017

Eng, J. J., Winter, D. A., and Patla, A. E. (1994). Strategies for recovery from a trip in early and late swing during human walking. *Exp. Brain Res.* 102, 339–349.

Fujimoto, M., Bair, W. N., and Rogers, M. W. (2015). Center of pressure control for balance maintenance during lateral waist-pull perturbations in older adults. *J. Biomech.* 48, 963–968. doi: 10.1016/j.jbiomech.2015.02.012

Fujimoto, M., Bair, W. N., and Rogers, M. W. (2017). Single and multiple step balance recovery responses can be different at first step lift-off following lateral waist-pull perturbations in older adults. *J. Biomech.* 55, 41–47. doi: 10.1016/j.jbiomech.2017.02.014

Glenmark, B., Nilsson, M., Gao, H., Gustafsson, J. A., Dahlman-Wright, K., and Westerblad, H. (2004). Difference in skeletal muscle function in males vs. females: role of estrogen receptor-β. *Am. J. Physiol. Endocrinol. Metab.* 287, E1125–E1131.

Graham, D. F., Carty, C. P., Lloyd, D. G., Lichtwark, G. A., and Barrett, R. S. (2014). Muscle contributions to recovery from forward loss of balance by stepping. *J. Biomech.* 47, 667–674. doi: 10.1016/j.jbiomech.2013.11.047

Halpern, P., Siebzehner, M. I., Aladgem, D., Sorkine, P., and Bechar, R. (2005). Non-collision injuries in public buses: a national survey of a neglected problem. *Emerg. Med. J.* 22, 108–110. doi: 10.1136/emj.2003.013128

Hemami, H., Barin, K., and Pai, Y. C. (2006). Quantitative analysis of the ankle strategy under translational platform disturbance. *IEEE Trans. Neural Syst. Rehabil. Eng.* 14, 470–480. doi: 10.1109/tnsre.2006.886718

Hilliard, M. J., Martinez, K. M., Janssen, I., Edwards, B., Mille, M. L., Zhang, Y., et al. (2008). Lateral balance factors predict future falls in community-living older adults. *Arch. Phys. Med. Rehabil.* 89, 1708–1713. doi: 10.1016/j.apmr.2008.01.023

Hof, A. L., and Curtze, C. (2016). A stricter condition for standing balance after unexpected perturbations. *J. Biomech.* 49, 580–585. doi: 10.1016/j.jbiomech.2016.01.021

Hof, A. L., Gazendam, M. G. J., and Sinke, W. E. (2005). The condition for dynamic stability. *J. Biomech.* 38, 1–8. doi: 10.1016/j.jbiomech.2004.03.025

Honeycutt, C. F., Nevisipour, M., and Grabiner, M. D. (2016). Characteristics and adaptive strategies linked with falls in stroke survivors from analysis of laboratory-induced falls. *J. Biomech.* 49, 3313–3319. doi: 10.1016/j.jbiomech.2016.08.019

Hsiao, E. T., and Robinovitch, S. N. (1999). Biomechanical influences on balance recovery by stepping. *J. Biomech.* 32, 1099–1106. doi: 10.1016/s0021-9290(99)00104-9

Hsiao, E. T., and Robinovitch, S. N. (2001). Elderly subjects' ability to recover balance with a single backward step associates with body configuration at step contact. *J. Gerontol. A Biol. Sci. Med. Sci.* 56, M42–M47.

Hsiao-Wecksler, E. T., and Robinovitch, S. N. (2007). The effect of step length on young and elderly women's ability to recover balance. *Clin. Biomech.* 22, 574–580. doi: 10.1016/j.clinbiomech.2007.01.013

Hsue, B. J., and Su, F. C. (2014). Effects of age and gender on dynamic stability during stair descent. *Arch. Phys. Med. Rehabil.* 95, 1860–1869. doi: 10.1016/j.apmr.2014.05.001

Ivanauskaite, D., Lindh, C., and Rohlin, M. (2008). Observer performance based on marginal bone tissue visibility in Scanora panoramic radiography and posterior bitewing radiography. *Stomatologija* 10, 36–43.

Karekla, X. (2016). *Improving Accessibility of Public Transport Systems: The Influence of Double-Decker Bus Acceleration on Passenger Movement* Doctoral dissertation. London: University College London.

Karekla, X., and Fang, C. (2021). Upper body balancing mechanisms and their contribution to increasing bus passenger safety. *Safety Sci.* 133:105014. doi: 10.1016/j.ssci.2020.105014

Karekla, X., and Tyler, N. (2018a). Maintaining balance on a moving bus: the importance of three-peak steps whilst climbing stairs. *Transp. Res. Part A Policy Pract.* 116, 339–349. doi: 10.1016/j.tra.2018.06.020

Karekla, X., and Tyler, N. (2018b). Reducing non-collision injuries aboard buses: passenger balance whilst walking on the lower deck. *Safety Sci.* 105, 128–133. doi: 10.1016/j.ssci.2018.01.021

King, G. W., Luchies, C. W., Stylianou, A. P., Schiffman, J. M., and Thelen, D. G. (2005). Effects of step length on stepping responses used to arrest a forward fall. *Gait Posture* 22, 219–224. doi: 10.1016/j.gaitpost.2004.09.008

Kirk, A., Grant, R., and Bird, R. (2003). "Passenger casualties in non-collision incidents on buses and coaches in Great Britain," in *Proceedings of the 18th International Technical Conference on the Enhanced Safety of Vehicles*, (Nagoya), 19–22.

Krasovsky, T., Lamontagne, A., Feldman, A. G., and Levin, M. F. (2014). Effects of walking speed on gait stability and interlimb coordination in younger and older adults. *Gait Posture* 39, 378–385. doi: 10.1016/j.gaitpost.2013.08.011

Kruskal, W. H., and Wallis, W. A. (1952). Use of ranks in one-criterion variance analysis. *J. Am. Stat. Assoc.* 47, 583–621. doi: 10.1080/01621459.1952.10483441

Lee, P. Y., Gadareh, K., and Bronstein, A. M. (2014). Forward–backward postural protective stepping responses in young and elderly adults. *Hum. Mov. Sci.* 34, 137–146. doi: 10.1016/j.humov.2013.12.010

Linder, A., Davidse, R. J., Iraeus, J., John, J. D., Keller, A., Klug, C., et al. (2020). "VIRTUAL-a European approach to foster the uptake of virtual testing in vehicle safety assessment," in *Proceedings of the 8th Transport Research Arena TRA 2020,* April 27-30, 2020, (Conference canceled), (Helsinki).

Lord, S. R., Lloyd, D. G., and Keung Li, S. E. K. (1996). Sensori-motor function, gait patterns and falls in community-dwelling women. *Age Ageing* 25, 292–299. doi: 10.1093/ageing/25.4.292

Luchies, C. W., Alexander, N. B., Schultz, A. B., and Ashton-Miller, J. (1994). Stepping responses of young and old adults to postural disturbances: kinematics. *J. Am. Geriatr. Soc.* 42, 506–512. doi: 10.1111/j.1532-5415.1994.tb04972.x

Maki, B. E., and McIlroy, W. E. (1996). Postural control in the older adult. *Clin. Geriatr. Med.* 12, 635–658. doi: 10.1016/s0749-0690(18)30193-9

Maki, B. E., and McIlroy, W. E. (1997). The role of limb movements in maintaining upright stance: the "change-in-support" strategy. *Phys. Ther.* 77, 488–507. doi: 10.1093/ptj/77.5.488

Maki, B. E., Cheng, K. C. C., Mansfield, A., Scovil, C. Y., Perry, S. D., Peters, A. L., et al. (2008). Preventing falls in older adults: new interventions to promote more effective change-in-support balance reactions. *J. Electromyogr. Kinesiol.* 18, 243–254. doi: 10.1016/j.jelekin.2007.06.005

Maki, B. E., McIlroy, W. E., and Perry, S. D. (1996). Influence of lateral destabilization on compensatory stepping responses. *J. Biomech.* 29, 343–353. doi: 10.1016/0021-9290(95)00053-4

Mansfield, A., Wong, J. S., Bryce, J., Knorr, S., and Patterson, K. K. (2015). Does perturbation-based balance training prevent falls? Systematic review and meta-analysis of preliminary randomized controlled trials. *Phys. Ther.* 95, 700–709. doi: 10.2522/ptj.20140090

McIlroy, W. E., and Maki, B. E. (1996). Age-related changes in compensatory stepping in response to unpredictable perturbations. *J. Gerontol. A Biol. Sci. Med. Sci.* 51, M289–M296.

Merbitz, C., Morris, J., and Grip, J. C. (1989). Ordinal scales and foundations of misinference. *Arch. Phys. Med. Rehabil.* 70, 308–312.

Mille, M. L., Johnson, M. E., Martinez, K. M., and Rogers, M. W. (2005). Age-dependent differences in lateral balance recovery through protective stepping. *Clin. Biomech.* 20, 607–616. doi: 10.1016/j.clinbiomech.2005.03.004

Mille, M. L., Johnson-Hilliard, M., Martinez, K. M., Zhang, Y., Edwards, B. J., and Rogers, M. W. (2013). One step, two steps, three steps more…directional vulnerability to falls in community-dwelling older people. *J. Gerontol. A Biomed. Sci. Med. Sci.* 68, 1540–1548. doi: 10.1093/gerona/glt062

Nashner, L. M., and McCollum, G. (1985). The organization of human postural movements: a formal basis and experimental synthesis. *Behav. Brain Sci.* 8, 135–150. doi: 10.1017/s0140525x00020008

Okubo, Y., Brodie, M. A., Sturnieks, D. L., Hicks, C., and Lord, S. R. (2019). A pilot study of reactive balance training using trips and slips with increasing unpredictability in young and older adults: biomechanical mechanisms, falls and clinical feasibility. *Clin. Biomech.* 67, 171–179. doi: 10.1016/j.clinbiomech.2019.05.016

Pai, Y. C., Rogers, M. W., Patton, J., Cain, T. D., and Hanke, T. A. (1998). Static versus dynamic predictions of protective stepping following waist–pull perturbations in young and older adults. *J. Biomech.* 31, 1111–1118. doi: 10.1016/s0021-9290(98)00124-9

Robert, T., Beillas, P., Maupas, A., and Verriest, J. P. (2007). Conditions of possible head impacts for standing passengers in public transportation: an experimental study. *Int. J. Crashworthiness* 12, 319–327. doi: 10.1080/13588260701433552

Rogers, M. W., Hain, T. C., Hanke, T. A., and Janssen, I. (1996). Stimulus parameters and inertial load: effects on the incidence of

protective stepping responses in healthy human subjects. *Arch. Phys. Med. Rehabil.* 77, 363–368. doi: 10.1016/s0003-9993(96)90085-4

Schneider, L. W., Robbins, D. H., Pflüg, M. A., and Snyder, R. G. (1983). *Anthropometry of Motor Vehicle Occupants*. Final Report, UMTRI-83-53-1, University of Michigan Transportation Research Institute.

Schorr, M., Dichtel, L. E., Gerweck, A. V., Valera, R. D., Torriani, M., Miller, K. K., et al. (2018). Sex differences in body composition and association with cardiometabolic risk. *Biol. Sex Diff.* 9, 1–10. doi: 10.1007/978-1-60327-250-6_1

Schubert, P., Liebherr, M., Kersten, S., and Haas, C. T. (2017). Biomechanical demand analysis of older passengers in a standing position during bus transport. *J. Transp. Health* 4, 226–236. doi: 10.1016/j.jth.2016.12.002

Silvano, A. P., and Ohlin, M. (2019). Non-collision incidents on buses due to acceleration and braking manoeuvres leading to falling events among standing passengers. *J. Transp. Health* 14:100560. doi: 10.1016/j.jth.2019.04.006

Smedby, Ö, and Fredrikson, M. (2010). Visual grading regression: analysing data from visual grading experiments with regression models. *Br. J. Radiol.* 83, 767–775. doi: 10.1259/bjr/35254923

Sturnieks, D. L., Menant, J., Delbaere, K., Vanrenterghem, J., Rogers, M. W., Fitzpatrick, R. C., et al. (2013). Force-controlled balance perturbations associated with falls in older people: a prospective cohort study. *PLoS One* 8:e70981. doi: 10.1371/journal.pone.0070981

Thelen, D. G., Wojcik, L. A., Schultz, A. B., Ashton-Miller, J. A., and Alexander, N. B. (1997). Age differences in using a rapid step to regain balance during a forward fall. *J. Gerontol. A Biol. Sci. Med. Sci.* 52, M8–M13.

Ustinova, K. I., and Silkwood-Sherer, D. J. (2014). Postural perturbations induced by a moving virtual environment are reduced in persons with brain injury when gripping a mobile object. *J. Neurol. Phys. Ther.* 38, 125–133. doi: 10.1097/npt.0000000000000035

Verniba, D., and Gage, W. H. (2020). A comparison of balance-correcting responses induced with platform-translation and shoulder-pull perturbation methods. *J. Biomech.* 112:110017. doi: 10.1016/j.jbiomech.2020.110017

Winter, D. A. (2009). *Biomechanics and Motor Control of Human Movement*. Hoboken, NJ: John Wiley & Sons.

Wojcik, L. A., Thelen, D. G., Schultz, A. B., Ashton-Miller, J. A., and Alexander, N. B. (1999). Age and gender differences in single-step recovery from a forward fall. *J. Gerontol. A Biomed. Sci. Med. Sci.* 54, M44–M50.

Wu, M., Ji, L., Jin, D., and Pai, Y. C. (2007). Minimal step length necessary for recovery of forward balance loss with a single step. *J. Biomech.* 40, 1559–1566.

Conflict of Interest: The authors declare that the research was conducted in the absence of any commercial or financial relationships that could be construed as a potential conflict of interest.

frontiers in Bioengineering and Biotechnology

ORIGINAL RESEARCH
published: 16 July 2021
doi: 10.3389/fbioe.2021.687058

Design and Evaluation of the Initial 50th Percentile Female Prototype Rear Impact Dummy, BioRID P50F – Indications for the Need of an Additional Dummy Size

Anna Carlsson[1], Johan Davidsson[2], Astrid Linder[2,3] and Mats Y. Svensson[2]*

[1] Chalmers Industrial Technology (Chalmers Industriteknik), Gothenburg, Sweden, [2] Vehicle Safety Division, Chalmers University of Technology, Gothenburg, Sweden, [3] Swedish National Road and Transport Research Institute (VTI), Gothenburg, Sweden

OPEN ACCESS

Edited by:
Michael Kleinberger, United States Army Research Laboratory, United States

Reviewed by:
Liming Voo, Johns Hopkins University, United States
Michael Tegtmeyer, United States Army Research Laboratory, United States
Kevin Moorhouse, National Highway Traffic Safety Administration, United States

***Correspondence:**
Anna Carlsson
anna.carlsson@chalmers.se

Specialty section:
This article was submitted to Biomechanics, a section of the journal Frontiers in Bioengineering and Biotechnology

Received: *28 March 2021*
Accepted: *23 June 2021*
Published: *16 July 2021*

Citation:
Carlsson A, Davidsson J, Linder A and Svensson MY (2021) Design and Evaluation of the Initial 50th Percentile Female Prototype Rear Impact Dummy, BioRID P50F – Indications for the Need of an Additional Dummy Size. Front. Bioeng. Biotechnol. 9:687058. doi: 10.3389/fbioe.2021.687058

The objective of this study was to present the design of a prototype rear impact crash test dummy, representing a 50th percentile female, and compare its performance to volunteer response data. The intention was to develop a first crude prototype as a first step toward a future biofidelic 50th percentile female rear impact dummy. The current rear impact crash test dummy, BioRID II, represents a 50th percentile male, which may limit the assessment and development of whiplash protection systems with regard to female occupants. Introduction of this new dummy size will facilitate evaluation of seat and head restraint (HR) responses in both the average sized female and male in rear impacts. A 50th percentile female rear impact prototype dummy, the BioRID P50F, was developed from modified body segments originating from the BioRID II. The mass and rough dimensions of the BioRID P50F is representative of a 50th percentile female. The prototype dummy was evaluated against low severity rear impact sled tests comprising six female volunteers closely resembling a 50th percentile female with regard to stature and mass. The head/neck response of the BioRID P50F prototype resembled the female volunteer response corridors. The stiffness of the thoracic and lumbar spinal joints remained the same as the average sized male BioRID II, and therefore likely stiffer than joints of an average female. Consequently, the peak rearward angular displacement of the head and T1, and the rearward displacement of the T1, were lesser for the BioRID P50F in comparison to the female volunteers. The biofidelity of the BioRID P50F prototype thus has some limitations. Based on a seat response comparison between the BioRID P50F and the BioRID II, it can be concluded that the male BioRID II is an insufficient representation of the average female in the assessment of the dynamic seat response and effectiveness of whiplash protection systems.

Keywords: crash test dummy, females, rear impact, sled testing, soft tissue neck injury, vehicle safety, volunteer tests, whiplash

INTRODUCTION

Vehicle crashes causing Whiplash Associated Disorder (WAD) are still of worldwide concern. Despite new seat designs intended to lessen the risk of whiplash injury and Advanced Driver Assistance Systems (ADAS) that reduces the number of rear impacts, the long-term consequences of whiplash injuries remain (Kullgren et al., 2020). Cars equipped with advanced whiplash protection systems posed on average a ∼50% lower risk of long-term whiplash injuries in comparison to cars equipped with standard seats (Davidsson and Kullgren, 2013). According to a review by Carlsson, 2012, accident data have shown that females typically have twice the risk of sustaining whiplash injuries than males, even under similar crash conditions.

In rear impacts, the whiplash injury risk in cars equipped with conventional seats generally shows a growing trend for increasing statures for both females and males, where tall females are associated with the greatest risk (Temming and Zobel, 1998; Jakobsson et al., 2000). It is however important to note that the greatest whiplash injury frequencies are associated with females and males of average statures (Carlsson et al., 2014). Based on Swiss and Swedish insurance records, Carlsson et al. (2014) concluded that the stature and mass of the females most frequently injured, correspond reasonably well with the average stature and mass of females in the European countries.

Today, rear impact testing is performed with 50th percentile male dummies, mainly the BioRID II, which may limit the assessment and development of whiplash protection systems since the female part of the population is not represented. In terms of stature and mass, the 50th percentile male crash test dummy roughly corresponds to the 90th–95th percentile female (Welsh and Lenard, 2001), resulting in females not being adequately represented by the BioRID II. Previous studies show that the BioRID II matches 50th percentile male volunteer responses (Davidsson et al., 1999, 2000). However, more recent volunteer studies show that the response of 50th percentile females is clearly different to 50th percentile males (Linder et al., 2008; Carlsson et al., 2010, 2011; Carlsson, 2012). Similar differences were found in a comparison between the BioRID II and a prototype rear impact crash test dummy, representing a 50th percentile female, Schmitt et al. (2012). The BioRID II is thus not adequately representative of 50th percentile females. Since the male BioRID II has only been validated with regard to tests with male volunteers, current seats are assessed without consideration of female properties, despite a higher whiplash injury risk in females. This limitation may contribute to whiplash protection systems being more effective for males than for females. According to insurance claims records (Kullgren and Krafft, 2010), the risk reduction for permanent medical impairment was approximately 30% greater for males than for females. In recent years, injury statistics show that whiplash injuries still present a major problem, and that the whiplash injury risk females are exposed to is substantially higher (Kullgren et al., 2020).

The objective of this study was to present the design of the prototype rear impact crash test dummy, representing a 50th percentile female, used in Schmitt et al. (2012). Furthermore, the performance of this prototype dummy was compared to volunteer response data. The intention was to develop a first crude prototype as a first step toward a future biofidelic 50th percentile female rear impact dummy. Introduction of this new dummy size will facilitate evaluation of seat and head restraint (HR) responses in both the average sized female and male in rear impacts.

MATERIALS AND METHODS

A rear impact dummy prototype, called BioRID P50F, representing a 50th percentile female in size, was built by modifying/downsizing a 50th percentile male BioRID II dummy. The dynamic response of the BioRID P50F prototype was evaluated with regard to rear impact sled tests comprising female volunteers close to the 50th percentile female size (Carlsson et al., 2021).

Construction of the BioRID P50F

The BioRID P50F prototype was assembled using modified parts originating from a BioRID II. Target dimensions and masses of the BioRID P50F's body segments were mainly based on the EvaRID LS-Dyna Model, release version 1.0, by Humanetics (Carlsson et al., 2014). The EvaRID V1.0 model was based on the anthropometric measures of the 50th percentile female from the University of Michigan Transport Research Institute (UMTRI) study (stature 161.8 cm, mass 62.3 kg; Schneider et al., 1983; **Table 1**).

The BioRID's torso was modified and adjusted to match the overall dimensions and masses of the EvaRID LS-Dyna Model. Two lumbar vertebrae (L4 and L5) were removed from the spine and the height of the sacral vertebra (S1) was reduced by 20 mm (**Figure 1**). Consequently, the full range of lumbar angular motion was reduced. With these changes, the seated height of the BioRID P50F matched that of the EvaRID model. The construction of the BioRID P50F's spine, however, deviated from that of the EvaRID model, which has a complete, scaled-down BioRID II spine.

Two segments were removed from the torso jacket (**Figure 2**), one mid-sagittal segment to reduce the width of the dummy torso and one horizontal segment in the lower region to reduce the height of the torso. The size of the removed mid-sagittal segment was selected to achieve the same width as the EvaRID model. The shoulder joint and the 10th rib levels were used as landmarks to determine the width of the mid-sagittal segment. At the shoulder joint level, the width of the removed segment was 40 mm, and correspondingly, at the 10th rib level it was 51 mm wide (**Figure 2**). The size of the removed horizontal segment (88 mm) was selected for the torso jacket to fit the length of the spine. Two-component silicon (Wacker M4601 mixed with a thixotropic stabilizer 43) was used to reassemble the jacket. These modifications resulted in a lateral distance of 305 mm between the shoulder joints. The pins that connect the spine with the jacket were shortened to match the new jacket width.

The stiffness and damping properties of the neck and spine of the EvaRID model were scaled to 70% of the original values

TABLE 1 | The length and mass of each body segment of the BioRID II, BioRID P50F, EvaRID model, and the 50th percentile female.

Dummy segment	BioRID II dummy	BioRID P50F prototype	EvaRID model	50th percentile female
		Length (cm)		
Head[1]	21.59	19.8	20.30	20.30[8]
Neck[2]	12.04	12.0	10.28	10.28[8]
Torso	52.65[3]	43.8[3]	47.94[3]	41.1[9,10]
Pelvis	25.83	25.8	25.82	25.82[9]
Arm (upper)[4]	26.14	26.1	26.40	26.4[8]
Arm (lower)[5]	24.88	23.4	23.40	23.4[8]
Leg (upper)[6]	40.55	38.9	38.90	38.9[8]
Leg (lower)[7]	49.55	45.7	45.70	45.7[8]
		Mass (kg)		
Head	4.44	3.32	3.58	3.58
Torso[11]	27.16	22.43	19.58	19.58
Pelvis	11.67	12.03	15.84	15.84
Arm (upper) × 2	2.02	1.46	1.40	1.40
Arm (lower) × 2	2.26	1.25	1.16	1.15
Leg (upper) × 2	6.86	5.72	5.67	5.68
Leg (lower) × 2	5.80	3.83	3.43	3.43
Total	**77.15**	**62.30**	**62.30**	**62.30**

Additional details can be found in Carlsson et al. (2014).
[1] *Top of head to chin.*
[2] *C0/C1 joint to C7/T1 joint.*
[3] *C7/T1 joint to mid-point of hip joints.*
[4] *Shoulder joint to elbow joint.*
[5] *Elbow joint to wrist joint.*
[6] *Hip joint to knee joint.*
[7] *Knee joint to bottom of heel along tibia.*
[8] *Diffrient et al. (1974).*
[9] *Young et al. (1983).*
[10] *"Cervicale landmark" (superior tip of the spine of the 7th cervical vertebra) to "iliocristale landmark" (the highest point on the crest of each ilia in the midaxillary line).*
[11] *Including neck/spine.*

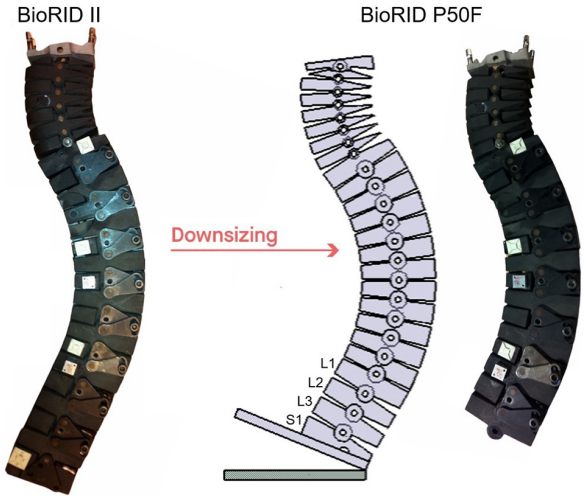

FIGURE 1 | The spine of the BioRID P50F prototype was made by removing two lumbar vertebrae (L4 and L5) from the BioRID II spine and the height of the sacral vertebra (S1) was reduced by 20 mm.

in the BioRID II model (Carlsson et al., 2014). This was the starting point for reducing the spine stiffness of the BioRID P50F, however, for practical reasons these reductions did not reach exactly 70%. The polyurethane bumpers, that provide the greatest resistance to flexion and extension of the spine, were decreased: from 15 mm × 10 mm × 10 mm (width × breadth × height) to 10 mm × 10 mm × 10 mm for the anterior and posterior bumpers between C1 and T1; from 25 mm × 15 mm × 2 mm to 20 mm × 15 mm × 2 mm for the posterior bumpers between T1 and T2; from 25 mm × 15 mm × 3 mm to 12.5 mm × 10 mm × 3 mm for the posterior bumpers between T2 and T9; and from 25 mm × 15 mm × 3 mm to 15 mm × 15 mm × 3 mm for the posterior bumpers between T9 and L1. Finally, the springs that control the stiffness of the neck muscle substitute wires (anterior: Stece Die spring No. 51780; L0 = 140.0 mm, C = 9.8 N/mm, posterior: Stece Die Spring No. 51620; L0 = 140.0 mm, C = 16.8 N/mm), were replaced by softer units (anterior: Stece Die spring No. 51820; L0 = 139.7 mm, C = 8.4 N/mm, posterior: Stece Die Spring No. 51780; L0 = 127.0 mm, C = 9.8 N/mm). The design of the spring cartridges and the length of the wires were modified to match the length of the new springs. The wire pretension was in total 14 mm, equivalent to that used with the BioRID II. No modifications were made to the pelvis.

The length of the BioRID II upper arm is 261 mm, measured between the shoulder and the elbow joints. The corresponding length of the EvaRID model is 264 mm (Carlsson et al., 2014, based on Diffrient et al., 1974), thus the length of the upper arms remained unchanged in the BioRID P50F. The lower arms, measured between the elbow and wrist joints, were shortened from 249 to 234 mm, based on Carlsson et al. (2014). Steel skeleton parts were machined, and interior portions of the flesh were removed to reduce mass. The parts reproducing the wrists and hands were removed (**Supplementary Appendix Figure A1.1**).

The original load cell imitations in the upper legs were replaced by 18 mm shorter aluminum cylinders, resulting in an upper leg length of 389 mm, measured between the hip and knee joints, in accordance with the EvaRID model dimensions (Carlsson et al., 2014). The length of the lower legs was reduced from 409 to 376 mm, measured from the knee joint to the ankle joint along the tibia, based on the EvaRID model dimensions (Carlsson et al., 2014). The polymer flesh parts that wrap around the metal parts of the upper and lower legs were cut to match the reduced lengths, and portions of the interior flesh were removed to reduce mass. The BioRID II ankles were replaced by a simplified and lighter design, consisting of an aluminum square profile (25 mm × 25 mm × 2.5 mm) to match the target mass (**Figure 3**).

The BioRID P50F head consisted of a BioRID II head unit with the anterior flesh removed (**Figure 4**) to match the target mass (**Table 1**). Body segment dimensions and masses for the BioRID P50F and the BioRID II are listed in **Table 1**.

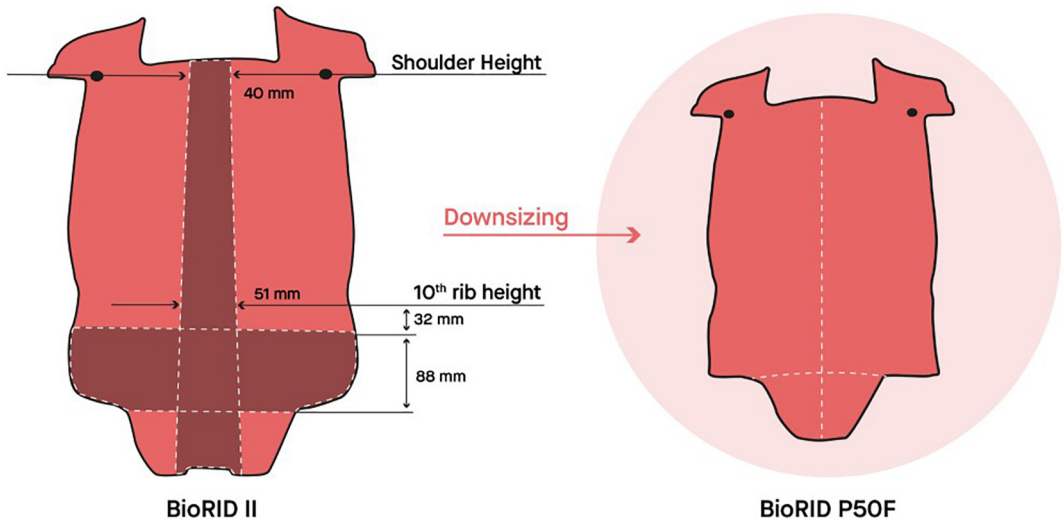

FIGURE 2 | The torso jacket of the BioRID P50F prototype was made by removing the dark segments from the torso jacket of the BioRID II. Illustration courtesy of A. Hedenström.

Test With the BioRID P50F Prototype in a Laboratory Seat

In order to evaluate the performance of the BioRID P50F, one test was performed with the prototype dummy in equivalent test conditions as previous tests comprising female volunteers (Carlsson et al., 2021). Eight female volunteers participated in the test series. Their age ranged between 22 and 29 years at an average of 26 years; their stature ranged between 161 and 166 cm at an average of 163 cm; and their mass ranged between 55 and 67 kg at an average of 60 kg. In comparison to the BioRID P50F, the female volunteers were on average 1% taller and 4% lighter. Results from a subset of six volunteer tests at ~15 cm initial head-to-HR distance, provided in Carlsson et al. (2021), were used as a reference. Carlsson et al. (2021) placed the remaining two tests in a separate category as those volunteers did not contact with the HR. The dummy was seated on a sled, a Hyper-G hydro pneumatic catapult type sled, that was accelerated forward. **Figure 5** shows the sled pulse for volunteer tests and the BioRID P50F test.

FIGURE 3 | The lower leg of the BioRID P50F prototype.

FIGURE 4 | The head of the BioRID P50F prototype.

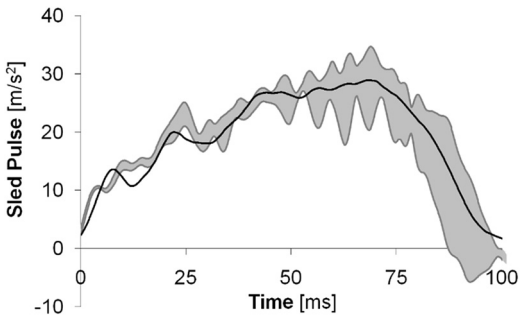

FIGURE 5 | The sled pulse for the tests comprising 50th percentile female volunteers (gray corridor) and the BioRID P50F prototype (solid black line).

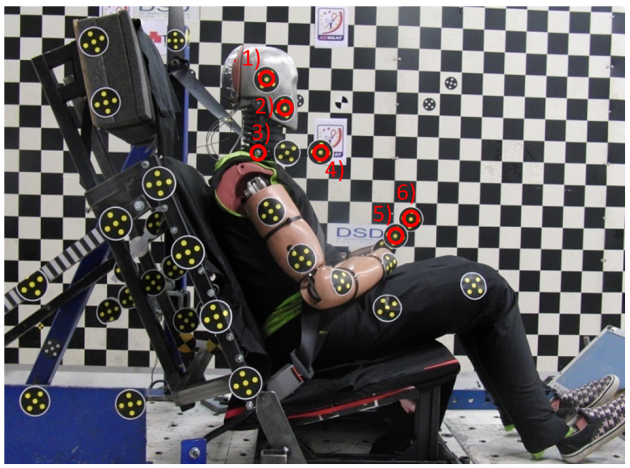

FIGURE 6 | The BioRID P50F prototype in the laboratory seat.

The BioRID P50F prototype was equipped with three single-axis accelerometers in the head (Endevco 7264C-2k) and a triaxial accelerometer (Meas-spec 1203-500) on the 1st thoracic vertebra (T1). A single-axis accelerometer (ICS/Disynet ICS 3022-200) was attached to the sled base. The coordinate systems were defined according to SAE J211 (orthogonal right-handed). The centers of the accelerometers' coordinate systems were fixed on the respective accelerometer positions. The head and T1 accelerometers were mounted with initial axes coinciding with the SAE J211 standards.

The same laboratory seat was used in this study as in the previous test series with female volunteers (Carlsson et al., 2021). The seatback consisted of four stiff panels covered with 20 mm foam. The panels were independently mounted to a rigid seatback frame by coil springs to allow easy implementation into a computational model. The seatback frame was adjusted to 24.1° from the vertical plane. The HR consisted of a plywood panel covered by firm padding (polyethylene 220-E) and was supported by a stiff steel frame mounted to the seatback. The initial head-to-HR distance was adjusted to 15 cm by adjusting the thickness of the padding (**Figure 6**). The rigid seat base was angled 16.9° from the horizontal plane. A plate was mounted on the sled to resemble a passenger floor pan surface of a car. The seatback, HR and seat base were covered with double layers of knitted lycra fabric. The pelvic part of the dummy was positioned in accordance with the European New Car Assessment Programme (Euro NCAP) test procedure [European New Car Assessment Programme (EuroNCAP), 2010]. The torso leaned against the seatback, and the T1 as well as the head were aligned with the horizontal plane. The lower arms were positioned on the upper legs (**Figure 6**).

Film targets were secured on the BioRID P50F and on the seat prior to the tests (**Figure 6**). Linear displacements of the head and T1 were derived from targets (1) and (3), respectively. Angular displacement of the head and T1 were derived from targets (1) and (2), as well as (3) and (4), respectively. The displacement data were set to zero at the time of impact (T = 0) and were expressed in a sled fixed coordinate system. For practical reasons, the volunteer tests had different target positions to derive the corresponding head and T1 displacements (Carlsson et al., 2021).

The tests were monitored by two high-speed digital video cameras (Kodak RO, 512 × 384 pixels); one providing an overview and one providing a detailed view from the side. The cameras were mounted on a stiff rack attached to the sled, approximately 1.5 m from the volunteers. The frame rate was 1,000 s^{-1} for both cameras. Film targets were digitized using Tema 3.5 software. None of the displacement data were filtered. The data acquisition unit Kayser-Trede MiniDau registered the sensor data at a sampling rate of 20 kHz and the data were filtered in accordance with SAE J211.

The dynamic response of the BioRID P50F prototype was compared to response corridors (the average ± one standard deviation) from the six tests with female volunteers used as reference (Carlsson et al., 2021). The head-to-HR contact time was documented. Additionally, the Neck Injury Criterion (NIC) values (Boström et al., 2000) were calculated.

RESULTS

The response of the BioRID P50F prototype dummy in comparison to the volunteer corridors is presented in **Figure 7** and **Table 2**.

The BioRID P50F's head remained stationary for a longer time which delayed the head x-acceleration onset compared to the volunteers. This led to an earlier rise in head x-displacement and a greater and somewhat earlier peak head x-acceleration for the BioRID P50F prototype compared to the volunteers. The T1 x-acceleration was similar for the volunteers and the BioRID P50F prototype during the first ∼85 ms. As the upper torso of the BioRID P50F prototype was pushed forward by the seatback, the T1 x-acceleration began to increase, peaking (142 ms) as the head reached the HR. The NIC value was on average 70% greater and occurred 13% earlier for the BioRID P50F prototype (8.5 m^2/s^2 at 106 ms), compared to the female volunteers (5.0 m^2/s^2 at 123 ms) (**Table 2**).

The head rearward angular displacement of the BioRID P50F prototype was close to the corridor of the female volunteers,

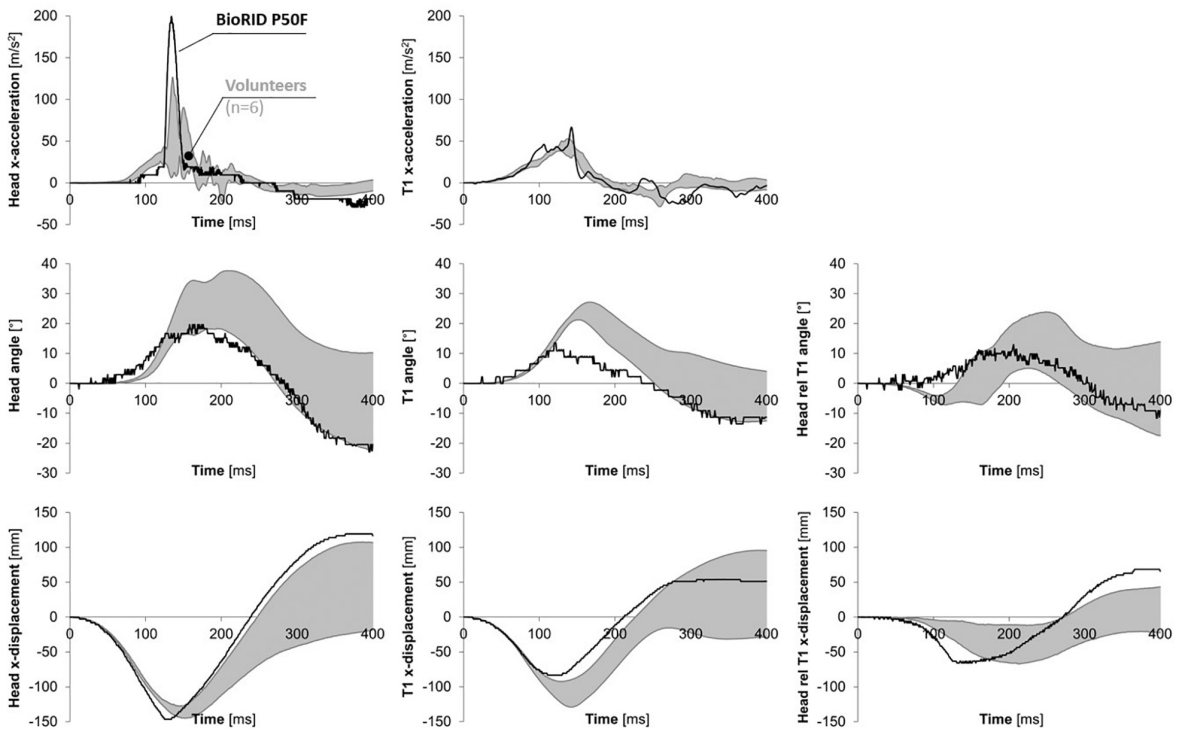

FIGURE 7 | X-acceleration of the head and T1 (NB: rotating coordinate systems); angular displacement of the head, T1 and the head relative to T1; and x-displacement relative to the sled for the head, T1 and the head relative to T1, for the 50th percentile female volunteers (gray corridor) and the BioRID P50F prototype (solid black line). The response corridors were calculated ± 1SD of the average response.

however, the onset began somewhat early. The peak T1 rearward angular displacement was lower and earlier for the BioRID P50F prototype compared to the female volunteers. The volunteers exhibited a small flexion of the head relative to the T1 angular displacement during the first ∼160 ms, since the rearward angular displacement of T1 began earlier than that of the head. This small flexion was not found in the BioRID P50F prototype due to the early onset of the head angular displacement. As the volunteers' heads began to rotate rearward, the flexion of the head relative to T1 changed into extension. The corresponding extension angle for the BioRID P50F prototype was within the corridor of the female volunteers.

The BioRID P50F rearward head x-displacement relative to the sled was similar to that of the volunteers. However, the peak occurred somewhat earlier for the BioRID P50F prototype due to the earlier head-to-HR contact, which in turn can be explained by the earlier head x-displacement. Compared to the volunteers, the rearward x-displacement of the T1 was slightly less for the BioRID P50F prototype.

DISCUSSION

The aim of this study was to present the design of the prototype rear impact crash test dummy, representing a 50th percentile female. The BioRID P50F prototype was assembled using BioRID II dummy parts, modified/downsized to match the anthropometric dimensions and mass distribution of the 50th percentile female (Carlsson et al., 2014; **Table 1**). BioRID P50F is thus based on the same design principle as the BioRID II. Previous studies have shown that the BioRID II is a highly repeatable and reproducible dummy design (Eriksson and Zellmer, 2007). Therefore, for the purpose of the present study, it was considered sufficient for performing a single test, exclusively. The head/neck response of the BioRID P50F prototype resembled the female volunteer response corridors (**Figure 7**).

The BioRID P50F included a BioRID II spine where two lumbar vertebrae (L4 and L5) were removed and the height of the S1 was reduced. Hence, the full range of lumbar angular motion was decreased. However, this had minor influence since the lumbar angular motion was restricted in the rear impact load case due to the support from the seatback. Furthermore, the thoracic and lumbar pin joint stiffnesses as well as the depth of the dummy torso of the BioRID II was kept in the BioRID P50F prototype. Therefore, it is most likely that the torso and thoraco-lumbar spine segments were stiffer than in an average female. Consequently, the rearward angular and x-displacements of the T1 were less for the BioRID P50F prototype in comparison to the female volunteers (**Figure 7** and **Table 2**). Furthermore, the NIC value was 70% greater in the BioRID P50F compared to the volunteers, which reflects the head and T1 x-accelerations (**Figure 6**) at the NIC peak at 106 ms (**Table 2**). In comparison to the volunteer x-accelerations at 106 ms, the amplitude of the head was 59% less, while the amplitude of the T1 was 57% greater, both

TABLE 2 | Summary of results obtained in the sled test with the BioRID P50F prototype compared with those of female volunteers.

Variable	Volunteers				BioRID P50F	
	Peak		Time		Peak	Time
	Average (SD)	Range	Average (SD)	Range		
X-acceleration	[m/s^2]	[m/s^2]	[ms]	[ms]	[m/s^2]	[ms]
Head	106 (40)	66→173	147 (8)	135→158	199	134
T1	47 (6)	38→54	135 (13)	113→153	67	142
NIC	[m^2/s^2]	[m^2/s^2]	[ms]	[ms]	[m^2/s^2]	[ms]
	5.0 (2.1)	3.0→7.8	123 (23)	79→141	8.5	106
Ang. displacement	(°)	(°)	[ms]	[ms]	(°)	[ms]
Head	28 (9)	16→38	202 (13)	185→216	20	167
T1	24 (3)	21→30	159 (8)	151→174	13	132
Head relative to T1[2]	−7 (2)	−9→−4	126 (27)	99→164	–	–
Head relative to T1[3]	15 (9)	5→26	235 (15)	212→258	12	200
X-displacement[1]	[mm]	[mm]	[ms]	[ms]	[mm]	[ms]
Head	−138 (9)	−147→−125	149 (7)	141→156	−147	130
T1	−103 (9)	−145→−94	136 (7)	129→145	−86	123
Head relative to T1	−52 (12)	−65→13	187 (36)	147→233	−63	132
Head restraint	[mm]	[mm]	[ms]	[ms]	[mm]	[ms]
Distance[4]	144 (6)	135→153	–	–	150	–
Contact	–	–	129 (8)	118→139	–	120

[1] *Relative to the sled.*
[2] *First peak.*
[3] *Second peak.*
[4] *At T = 0 ms (based on film analysis).*

contributing to a greater NIC value. The biofidelity of the BioRID P50F prototype thus have some limitations.

Despite these limitations, we realized that the BioRID P50F can be used to determine whether the male BioRID II also sufficiently represent the average female, in the assessment of the dynamic seat and HR response. This was investigated in a study by Schmitt et al. (2012), demonstrating the difference in seat interaction between the average male and female dummy sizes. A rear impact test series was performed in four different standard vehicle seats (A–D). Seats A, B and D were equipped with different types of whiplash protection systems, while Seat C was made in a basic seat design. According to Euro NCAP, Seats A, B and D were rated good, and Seat C performed marginally. Results comparing the BioRID P50F response with previously reported results for the BioRID II were presented by Carlsson (2012) (**Figure 8**) as well as by Schmitt et al. (2012) (**Supplementary Appendix Figure A1.2**).

Different trends were found for different seat models when comparing the female and male dummy responses (**Figure 8** and **Supplementary Appendix Figure A1.2**). The results indicate that there is no simple way to "reinterpret" or "scale" BioRID II data to address the female dynamic response. A fully validated 50th percentile female rear impact dummy would not only be an important tool for the design and evaluation of future protective systems, but also a tool useful in the process of further development and evaluation of injury criteria. An average female rear impact dummy could, together with the existing average male dummy, be used to complement the studies of Kullgren et al. (2003) and Linder et al. (2004) to find neck injury threshold values for female and male dummies separately. As a first estimate, Linder et al. (2013) suggested reducing the NIC threshold value from 15 to 12 m^2/s^2 for the average sized female. Furthermore, it was suggested to reduce the intercept values of the N_{km} from 47.5 Nm to 29 Nm for extension moment, from 88.1 to 53 Nm for flexion moment and from 845 N to 507 N for shear force, for the average sized female.

In the present study, the head-to-HR distance was adjusted to 15 cm, in accordance with the tests with female volunteers (Carlsson et al., 2021). It is important to note that this HR adjustment procedure deviates from the typical situation in a standard passenger vehicle seat. The study of Schmitt et al. (2012) compared the BioRID P50F to the BioRID II in four different standard seats. They reported a 28–96% greater head-to-HR distance for the BioRID P50F compared to the BioRID II (**Figure 8**). However, based on volunteer tests in seats without horizontal head-to-HR distance adjustment it has been reported that the head-to-HR distance is shorter for 50th percentile females than 50th percentile males (Welcher and Szabo, 2001; Linder et al., 2008; Carlsson et al., 2010; Carlsson et al., 2011; Carlsson et al., 2017). The greater head-to-HR distance for BioRID P50F may be a result of its thoracic spinal curvature, which is taken directly from the male BioRID II dummy. Sato et al. (2016) observed that the female thoracic spine curvature is far less kyphotic compared to the male. This suggests that the BioRID P50F T1 vertebra position is too far forward compared to an average female.

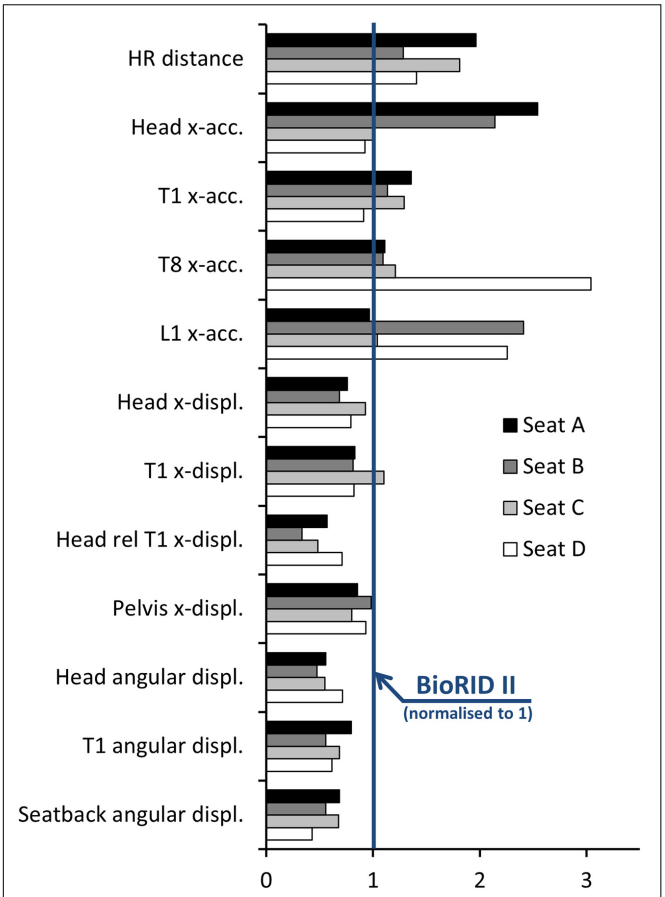

FIGURE 8 | Results from tests with the BioRID P50F prototype in four different standard seats (A–D) normalized with respect to the corresponding BioRID II Euro NCAP results (solid blue line); picture from Carlsson (2012).

To conclude, the overall response of the BioRID P50F prototype dummy resembled the female volunteer response corridors in low severity rear impacts. However, further refinements and additional validations would be needed in order to bring it to the same level of biofidelity as the BioRID II. This would include improved surface geometry and local mass distribution, as well as a modified spine, more representative of female properties with regards to the number of vertebrae, stiffness, curvature and range of motion. The targeted reduction to 70% of the spinal stiffness, in the present study, requires further tuning to match the outcome of the volunteer tests. Furthermore, sensor equipment corresponding to that of the BioRID II can be used in the present BioRID P50F. Additional validations could include alternative volunteer data sets, as well as Post Mortem Human Subject (PMHS) testing at higher impact severity. In future it would be of high value to have 50th percentile rear impact dummies of both the female and the male sizes. Ideally, these two dummy versions should be based on the same design principles and have the same level of biofidelity, which could be ensured by comparison to volunteer response data, using biofidelity ratings such as correlation and Analysis (CORA) or similar. The BioRID II represents the 50th percentile male which limits the assessment and development of whiplash protection systems with regard to female occupants. It is therefore important that future whiplash protection systems are developed and evaluated taking female properties into account. Thus, the need to develop a new fully validated rear impact 50th percentile female dummy, suitable for use in parallel with the current male dummy, is apparent.

DATA AVAILABILITY STATEMENT

The raw data supporting the conclusions of this article will be made available by the authors, without undue reservation.

AUTHOR CONTRIBUTIONS

AC: preparation, execution, documentation, and analysis of the test series. JD: preparation of the test series, advice based on earlier experience in experimental whiplash injury research including crash test dummy development, and internal review of the manuscript. AL: EU project coordinator, planning of the test series, advice based on earlier experience in experimental whiplash injury research, and internal review of the manuscript. MS: principal investigator, WP leader in the two involved EU projects, initiated the work in the present study, and contributed with advice based on earlier experience in experimental whiplash injury research including crash test dummy development. All authors contributed to the article and approved the submitted version.

FUNDING

This study was part of the ADSEAT (Adaptive Seat to Reduce Neck Injuries for Female and Male Occupants) project funded by the European Commission, Project No. 233904. The writing of the paper was funded by Folksams Forskningsstiftelse, Sweden, and has received funding from the European Union Horizon 2020 Research and Innovation Programme under Grant Agreement No. 768960, the VIRTUAL project.

ACKNOWLEDGMENTS

We thank Ernst Tomasch, Graz University of Technology (TU Graz), Austria, who organized the testing at Steffan Datentechnik (DSD) in Linz, Austria, and Elisabet Agar who performed the language review.

SUPPLEMENTARY MATERIAL

The Supplementary Material for this article can be found online at: https://www.frontiersin.org/articles/10.3389/fbioe.2021.687058/full#supplementary-material

REFERENCES

Boström, O., Fredriksson, R., Håland, Y., Jakobsson, L., Krafft, M., Lövsund, P., et al. (2000). Comparison of car seats in low speed rear-end impacts using the biorid dummy and the new Neck Injury Criterion (NIC). *Accid. Anal. Prev.* 32, 321–328. doi: 10.1016/s0001-4575(99)00105-0

Carlsson, A. (2012). *Addressing Female Whiplash Injury Protection – A Step Towards 50th Percentile Female Rear Impact Occupant Models*. Ph. D. Thesis. Gothenburg: Chalmers University of Technology.

Carlsson, A., Chang, F., Lemmen, P., Kullgren, A., Schmitt, K.-U., Linder, A., et al. (2014). Anthropometric specifications, development, and evaluation of EvaRID – A 50th percentile female rear impact finite element dummy model. *Traffic Inj. Prev.* 15, 855–865. doi: 10.1080/15389588.2014.885647

Carlsson, A., Horion, S., Davidsson, J., Schick, S., Linder, A., Hell, W., et al. (2021). Dynamic Responses of Female Volunteers in Rear Impact Sled Tests at Two Head Restraint Distances. *Front. Bioeng. Biotechnol.* 9:684003. doi: 10.3389/fbioe.2021.684003

Carlsson, A., Linder, A., Davidsson, J., Hell, W., Schick, S., and Svensson, M. (2011). Dynamic kinematic responses of female volunteers in rear impacts and comparison to previous male volunteer tests. *Traffic Inj. Prev.* 12, 347–357. doi: 10.1080/15389588.2011.585408

Carlsson, A., Pipkorn, L., Kullgren, A., and Svensson, M. (2017). Real-World adjustments of driver seat and head restraint in saab 9-3 vehicles. *Traffic Inj. Prev.* 18, 398–405. doi: 10.1080/15389588.2016.1217522

Carlsson, A., Siegmund, G. P., Linder, A., and Svensson, M. (2010). "Motion of the head and neck of female and male volunteers in rear impact car-to-car tests at 4 and 8 km/h," in *Proceedings of the IRCOBI Conference* (Switzerland: IRCOBI).

Davidsson, J., Flogård, A., Lövsund, P., and Svensson, M. Y. (1999). "BioRID P3 – Design and Performance Compared to Hybrid III and Volunteers in Rear Impacts at ΔV=7 km/h," in *Proceeding of the 43rd STAPP Car Crash Conference* (Pennsylvania.: Society of Automotive Engineers).

Davidsson, J., and Kullgren, A. (2013). "Evaluation of seat performance criteria for rear-end impact testing BioRID II and insurance data," in *Proceedings of the IRCOBI Conference*(Switzerland: IRCOBI).

Davidsson, J., Lövsund, P., Ono, K., Svensson, M. Y., and Inami, S. (2000). A Comparison of Volunteer, BioRID P3 and Hybrid III performance in Rear Impacts. *J. Crash Prev. Inj. Control.* 2, 203–220. doi: 10.1080/10286580108902565

Diffrient, N., Tilley, A. R., and Bardagjy, J. C. (1974). *Humanscale 1/2/3 – A Portfolio of Information*. Cambridge: The MIT Press.

Eriksson, L., and Zellmer, H. (2007). "Assessing the BioRID II repeatability and reproducibility by applying the Objective Rating Method (ORM) on rear-end Sled tests," in *Proceedings of the 20th International Technical Conference on the Enhanced Safety of Vehicles (ESV)*. Lyon: National Highway Traffic Safety Administration (NHTSA).

European New Car Assessment Programme (EuroNCAP). (2010). *The Dynamic Assessment of Car Seats for Neck Injury Protection Testing Protocol. Version 3.0*. Belgium: European New Car Assessment Programme.

Jakobsson, L., Lundell, B., Norin, H., and Isaksson-Hellman, I. (2000). WHIPS – Volvo's whiplash protection study. *Accid. Anal. Prev.* 32, 307–319. doi: 10.1016/s0001-4575(99)00107-4

Kullgren, A., Eriksson, L., Boström, O., and Krafft, M. (2003). "Validation of neck injury criteria using reconstructed real-life rear-end crashes with recorded crash pulses," in *Proceedings of the 18th ESV Conference* (USA: National Highway Traffic Safety Administration).

Kullgren, A., and Krafft, M. (2010). "Gender analysis on whiplash seat effectiveness: results from real-world crashes," in *Proceedings of the IRCOBI Conference* (Switzerland: IRCOBI).

Kullgren, A., Stigson, H., and Axelsson, A. (2020). "Developments in car crash safety since the 1980s," in *Proceedings of the IRCOBI Conference 2020 (the conference was not held in person, due to Concerns Related to the Corona Pandemic, but the Proceedings are the Official Record of the Conference)* (Switzerland: IRCOBI).

Linder, A., Avery, M., Kullgren, A., and Krafft, M. (2004). "Real-world rear impacts reconstructed in sled tests," in *Proceedings of the IRCOBI Conference* (Switzerland: IRCOBI).

Linder, A., Carlsson, A., Svensson, M. Y., and Siegmund, G. P. (2008). Dynamic responses of female and male volunteers in rear impacts. *Traffic Inj. Prev.* 9, 592–599. doi: 10.1080/15389580802384669

Linder, A., Schick, S., Hell, W., Svensson, M., Carlsson, A., Lemmen, P., et al. (2013). ADSEAT – Adaptive seat to reduce neck injuries for female and male occupants. *Accid. Anal. Prev.* 60, 334–343. doi: 10.1016/j.aap.2013.02.043

Sato, F., Odani, M., Miyazaki, Y., Nakajima, T., Makoshi, J. A., Yamazaki, K., et al. (2016). "Investigation of whole spine alignment patterns in automotive seated posture using upright open MRI systems," in *Proceedings of the IRCOBI Conference* (Switzerland: IRCOBI).

Schmitt, K.-U., Weber, T., Svensson, M., Davidsson, J., Carlsson, A., Björklund, M., et al. (2012). "Seat testing to investigate the female neck injury risk – preliminary results using a new female dummy prototype," in *Proceedings of the IRCOBI Conference* (Switzerland: IRCOBI).

Schneider, L. W., Robbins, D. H., Pflüg, M. A., and Snyder, R. G. (1983). *Development of Anthropometrically Based Design Specifications for an Advanced Adult Anthropomorphic Dummy Family, Final Report, UMTRI-83-53-1*. Michigan: University of Michigan Transportation Research Institute.

Temming, J., and Zobel, R. (1998). "Frequency and risk of cervical spine distortion injuries in passenger car accidents: significance of human factors data," in *Proceedings of the IRCOBI Conference* (Switzerland: IRCOBI).

Welcher, J. B., and Szabo, J. S. (2001). Relationships between seat properties and human subject kinematics in rear impact tests. *Accid. Anal. Prev.* 33, 289–304. doi: 10.1016/s0001-4575(00)00043-9

Welsh, R., and Lenard, J. (2001). "Male and female car drivers – Differences in collision and injury risks," in *Proceedings of the 45th AAAM Conference* (USA: AAAM).

Young, J. W., Chandler, R. F., Snow, C. C., Robinette, K. M., Zehner, G. F., and Lofberg, M. S. (1983). *Anthropometric and Mass Distribution Characteristics of Adult Female Body Segments*. USA: Civil Aeromedical Institute.

Conflict of Interest: The authors declare that the research was conducted in the absence of any commercial or financial relationships that could be construed as a potential conflict of interest.

frontiers in Bioengineering and Biotechnology

ORIGINAL RESEARCH
published: 23 July 2021
doi: 10.3389/fbioe.2021.680883

Human Response to Longitudinal Perturbations of Standing Passengers on Public Transport During Regular Operation

Simon Krašna[1], Arne Keller[2], Astrid Linder[3,4], Ary P. Silvano[3], Jia-Cheng Xu[3], Robert Thomson[4] and Corina Klug[5]*

[1]Faculty of Mechanical Engineering, University of Ljubljana, Ljubljana, Slovenia, [2]AGU Zürich, Zürich, Switzerland, [3]Swedish National Road and Transport Research Institute, Linköping, Sweden, [4]Mechanics and Maritime Science, Chalmers University, Gothenburg, Sweden, [5]Vehicle Safety Institute, Graz University of Technology, Graz, Austria

This study investigates the response of standing passengers on public transport who experience balance perturbations during non-collision incidents. The objective of the study was to analyse the effects of the perturbation characteristics on the initial responses of the passengers and their ability to maintain their balance. Sled tests were conducted on healthy volunteers aged 33.8 ± 9.2 years (13 males, 11 females) standing on a moving platform, facilitating measurements of the initial muscle activity and stepping response of the volunteers. The volunteers were exposed to five different perturbation profiles representing typical braking and accelerating manoeuvres of a public transport bus in the forward and backward direction. The sequence of muscle activations in lower-extremity muscles was consistent for the perturbation pulses applied. For the three acceleration pulses combining two magnitudes for acceleration (1.5 and 3.0 m/s^2) and jerk (5.6 and 11.3 m/s^3), the shortest muscle onset and stepping times for the passengers to recover their balance were observed with the higher jerk value, while the profile with the higher acceleration magnitude and longer duration induced more recovery steps and a higher rate of safety-harness deployment. The tendency for a shorter response time was observed for the female volunteers. For the two braking pulses (1.0 and 2.5 m/s^2), only the lower magnitude pulse allowed balance recovery without compensatory stepping. The results obtained provide a reference dataset for human body modelling, the development of virtual test protocols, and operational limits for improving the safety of public transportation vehicles and users.

Keywords: balance recovery, non-collision incidents, public transport, standing passengers, volunteer tests

OPEN ACCESS

Edited by:
Jason Forman,
University of Virginia, United States

Reviewed by:
Xenia Karekla,
University College London, United Kingdom
Valentina Graci,
Children's Hospital of Philadelphia, United States

****Correspondence:***
Simon Krašna
simon.krasna@fs.uni-lj.si

Specialty section:
This article was submitted to Biomechanics, a section of the journal Frontiers in Bioengineering and Biotechnology

Received: *15 March 2021*
Accepted: *08 July 2021*
Published: *23 July 2021*

Citation:
Krašna S, Keller A, Linder A, Silvano AP, Xu J-C, Thomson R and Klug C (2021) Human Response to Longitudinal Perturbations of Standing Passengers on Public Transport During Regular Operation. Front. Bioeng. Biotechnol. 9:680883. doi: 10.3389/fbioe.2021.680883

INTRODUCTION

The safety of passengers on public transport is a prerequisite for a sustainable transport system, as even minor incidents and frequent discomfort can discourage vulnerable people from using public transport. On public transport vehicles, such as buses and trams, standing passengers are exposed to the risk of injury due to falling during regular trips (so-called non-collision incidents). The risk of falling in a moving vehicle was estimated to be between 0.3 and 0.5 falls per million passenger kilometres (Elvik, 2019). A recent study (Silvano and Ohlin, 2019) found that the circumstances for

which passenger falls occur, and the groups typically affected, are different during acceleration and braking. During acceleration and turning from the bus stop, passengers fall after boarding, while attempting to become seated. This affects those aged 65+ and female users in particular, who are also overrepresented among public transport users in these type of non-collision incidents on buses (Kirk et al., 2003; Albertsson and Falkmer, 2005; Björnstig et al., 2005; Halpern et al., 2005; Kendrick et al., 2015; Barnes et al., 2016). In contrast, during braking, falling events typically occur while travelling and affect males, females and different age groups similarly (Silvano and Ohlin, 2019). Apart from age, different body proportions, compositions, and muscle strengths in males and females are important factors when studying and improving traffic safety (Vasavada et al., 2001; Carlsson et al., 2011; Jin et al., 2019). However, some researchers observed no gender-related differences in the response to standing-posture perturbations (De Graaf and Van Weperen, 1997).

Balance is maintained if the centre of mass of the human body is within the base of support—an area projected onto the floor under and between the feet (Maki and McIlroy, 1997). In order to achieve this, three major strategies have been identified: ankle, hip and stepping strategies (Winter, 1995). The ankle and hip strategies, also referred to as fixed-support strategies, are applied during less severe perturbations. Step responses are referred to as a change in support strategies if the centre of mass moves beyond the base of support. All these strategies represent two ends of a continuum of responses that involve a combination of both strategies (fixed-support and change-in-support) with different muscle-activation patterns. In the ankle strategy, the anterior muscles of the lower extremities are typically activated in a distal-to-proximal sequence in response to small forward perturbations, while posterior muscles counteract inertia of the body when a backward perturbation is applied. In more severe perturbations, the hip strategy is evoked, where hip flexors (abdominal muscles, quadriceps) are activated in backward perturbations and hip extensors (lower back, biceps femoris) in forwards perturbations to generate hip torques (Horak and Nashner, 1986; Runge et al., 1999; Blenkinshop et al., 2017). The hip strategy is characterized by longer muscle onset latencies (Torres-Oviedo and Ting, 2007). Generally, muscle onset latencies obtained from electromyography (EMG) were found to be closely correlated with the timing of joint motions (Hwang et al., 2009).

Change-in-support strategies, where a recovery step changes the base of support for stability, are used when fixed-support strategies are no longer effective, which can be the case for the perturbation levels encountered on public transport vehicles. Compensatory stepping is initiated and executed faster than volitional movements (Maki and McIlroy, 1997). The reaction times of the muscles are approximately 90–130 ms, and about one second is needed to retain balance in the case of larger movements (Horak and Nashner, 1986; Winter, 1995; Runge et al., 1999; Simoneau and Corbeil, 2005; Powell and Palacín, 2015). Owings et al. (2001) studied stepping strategies in volunteers standing on a treadmill accelerating to 0.89 m/s in 150 ms. The average reaction time between the onset of the treadmill motion and the recovery step toe-off was estimated to be 0.24 ± 0.03 s for a successful recovery and 0.28 ± 0.05 s for a failed recovery group of older volunteers. The subjects exposed to a high jerk do not have sufficient time to react, even to low acceleration levels. The ability to perform fast and effective compensatory stepping is important for successful balance recovery in response to a standing-posture perturbation—a shorter step initiation and completion time can be related to improved balance (Rogers et al., 2003). Young, healthy adults were reported to mostly use a single recovery step, while for the same balance perturbations, elderly people tend to use multiple stepping, which was also identified as a robust predictor of fall risk in the elderly, particularly in lateral perturbations (Mille et al., 2013). Increasing perturbation intensity requires modifying the fixed-support strategies to a single-stepping or multiple-stepping response (de Kam et al., 2017). Multiple steps can also result in larger displacements of the whole body, particularly the head, implying an increased injury risk from impacting elements of the bus interior (Robert et al., 2007a; Siman-Tov et al., 2019; Zhou et al., 2020).

The shape, magnitude and duration of a perturbation profile can have a significant effect on the standing passenger's response during non-collision incidents (Robert et al., 2007a; Robert et al., 2007b). A typical bus deceleration (braking) profile is characterized by a rather long magnitude rise time. A vehicle acceleration profile exhibits a sharp initial slope (high jerk), with a gradual decrease of the acceleration magnitude afterwards. For normal bus braking, the reported values of deceleration magnitude ranged from 1.2 to 3.0 m/s^2 (Kühn, 2013; Kirchner et al., 2014; Schubert et al., 2017). The acceleration magnitudes for bus departures were reported to be 0.8–2.5 m/s^2, and the jerk magnitude values reported were up to 15.7 m/s^3 (Brooks et al., 1980; Kühn, 2013; Kirchner et al., 2014; Schubert et al., 2017). The duration of normal acceleration and braking can range from 8.4 to 13.6 s, depending on the velocity change of the vehicle (Kirchner et al., 2014; Schubert et al., 2017). An increased risk of falling is related to the magnitudes of acceleration and jerk that require recovery stepping in response to perturbation, thus exceeding the level of comfort (Powell and Palacín, 2015). Karekla and Fang (2021) proposed a threshold of 1.0–1.5 m/s^2 for comfortable gait and balance without handrails on a bus during operation.

In addition to field studies (Hoberock, 1976; Brooks et al., 1980; Schubert et al., 2017; Karekla and Tyler, 2018; Karekla and Fang, 2021), laboratory research enabling more controlled conditions has addressed the balance recovery of standing people by exposing volunteers to external perturbations in different settings. The perturbation can be generated in different ways, such as waist-pulls, sudden release of a person held in a tilted position by a rope, and moving platforms (Owings et al., 2001; Hsiao-Wecksler and Robinovitch, 2007; Cyr and Smeesters, 2009; Mille et al., 2013; Bair et al., 2016; Čamernik et al., 2016; Borelli et al., 2019). For practical reasons, the moving platforms and treadmills typically exhibited smaller displacements and durations of platform motion than expected on public transport vehicles (De Graaf and Van Weperen, 1997; Szturm and Fallang, 1998; Carpenter et al., 2005; Tokuno et al., 2010; Kirchner et al., 2014; Sarraf et al., 2014; Zemková et al., 2016; Koushyar et al., 2019).

A series of volunteer tests with standing people on a moving platform was performed by Robert et al. (2007a and Robert et al., 2007b), employing 2.0–10.0 m/s^2 perturbations of 400-ms duration and different set-up configurations (free-standing, grasping). Comparing the horizontal excursion and the velocity of the head revealed that the volunteers applied different strategies for balance recovery. In a simulation study with a multibody human body model, the time to fall was estimated to be about 2.5 s (Palacio et al., 2009). This suggests that a volunteer test needs to employ perturbations longer than 2.0–2.5 s to fully investigate the potential outcome of a passenger losing balance, but the measurement system must have the resolution to detect nuances in the kinematic responses during 300–400-ms intervals.

Providing experimental data that characterise the response of standing passengers in realistic conditions is necessary to assess the injury risk of standing passengers in different traffic situations. Furthermore, such a dataset is needed for the development of a validated human body model (HBM) for a standing passenger, which can utilize the advantages of numerical simulations for the safety improvements of vehicle designs and operation, in addition to the traditionally recommended measures of prevention (Siman-Tov et al., 2019; Zhou et al., 2020).

The current knowledge of how vehicle motion influences the risk of non-collision incidents is still insufficient to provide guidance to the drivers of today's buses and trams and to the developers of future autonomous vehicles. In particular, a better understanding of the factors that cause a person to lose balance when faced with a given perturbation is needed. The overall objective of this study was to collect experimental data for the development of a standing passenger HBM as a tool for assessing a passenger's response to different balance perturbations. A novel test setup for standing-passenger volunteers is introduced and the first analysis of the recorded data from a test series with healthy volunteers is presented. The first objective was to identify how the characteristics of the perturbation pulse affect the initial passenger responses, in particular how passengers react to the direction, magnitude and duration of a balance perturbation resulting from a bus braking or accelerating. The second objective was to understand the consequences of the pulses on different passengers, specifically the possible differences between the initial response of male and female volunteers. The literature identified different demographics and injury scenarios that warrant further investigation.

METHODS

Test Set-Up

In this study, 24 instrumented volunteers were exposed to five different perturbation pulses in the forward and backward directions. The tests were conducted on the linear translational platform shown in **Figure 1**. Two servomotors were used to propel the platform according to predefined motion profiles. The volunteers were perturbed from a stationary position by the motion profile of interest. After the initial perturbation, the platform was brought back to rest. The displacement of the platform during the perturbation and the subsequent deceleration to rest were limited by the range of motion of the test device (5.5 m).

The acceleration profiles were reviewed to define the test pulses that could be used for the volunteer testing in a laboratory. In addition to the literature reviewed, proprietary measurements of urban-bus accelerations were performed during regular service and closed track tests (unpublished in-house experimental data) to estimate the main pulse characteristics. Emergency manoeuvres that substantially exceeded the passengers' balance thresholds were beyond the scope of the study.

The pulses for the volunteer tests were selected to represent severity levels typically arising during regular travel for non-collision incidents, but greater than the published comfort thresholds. The pulse durations were selected to study the initial response of the participating volunteers, as well as a time frame that captures their balance strategies. Furthermore, the pulse should be long enough to estimate whether the resulting motion of the participant would put a real bus passenger at risk of colliding with the vehicle interior. After the initial pilot tests with volunteers were carried out, the magnitude and duration of the final set of pulses were defined, aiming to have a mix of pulses where volunteers are able to maintain, but also lose their balance.

Each volunteer could experience up to five different perturbation profiles, described in **Table 1**, representing the typical braking and accelerating manoeuvres of a public transport bus. For the braking pulses *Br1* and *Br2,* two platform acceleration magnitudes were selected (1.0, 2.5 m/s^2). For the acceleration pulses *Acc1-J1*, *Acc1-J2* and *Acc2-J1*, two magnitudes of acceleration (1.5, 3.0 m/s^2) were combined with two magnitudes of jerk (5.6, 11.3 m/s^3) to define five different sled motion profiles. The programmed time profile of the perturbation pulses is depicted in **Figure 1** and compared to the sled accelerations measured in a set of pilot trials.

The study of the volunteers' response was limited to the pulse segments denoted as the initial rise time (time to peak) of the braking pulses (**Figure 1A**) and the duration of the acceleration pulses (**Figure 1B**), before the sled starts to decelerate in order to bring the platform to a stop. Although longitudinal manoeuvres of the bus could take longer on regular trips, e.g., when braking from or accelerating to cruising travel speed, the pulse segments considered still enabled an analysis of the initial volunteer response to characteristic perturbation pulses. As the bus braking and acceleration pulses were simulated in the same sled direction, a forward-facing volunteer experienced the accelerations similar to a transit passenger facing the direction of travel, whereas the braking pulses were experienced as if the passenger were facing backwards in the vehicle, opposite to the direction of travel. The opposite was true for the backward-facing passenger.

Volunteers

A total of 24 volunteers participated in the study (13 males and 11 females), representing on average a body weight and height close to a 50th percentile anthropometry (**Table 2**). The height of the

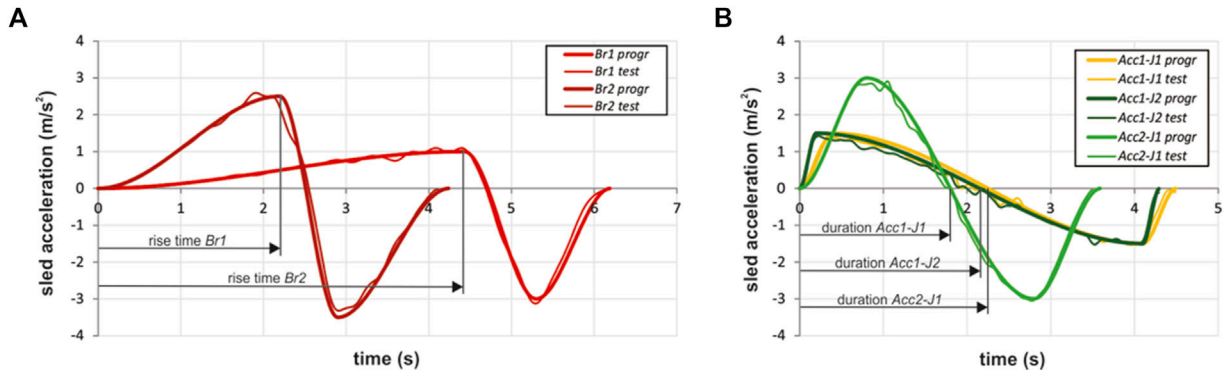

FIGURE 1 | Perturbation pulses applied to the moving platform with standing volunteers, representing braking **(A)** and acceleration **(B)** of a public transport bus; programmed pulses (thick lines), exemplary measured pulses (thin lines). Arrow lines indicate the parts of the pulses used in analysis of the volunteers' responses.

TABLE 1 | Perturbation profile characteristics.

Profile name	Sequence	Magnitude	Rise time	Duration	Jerk	Displacement	Max. Speed
		m/s^2	s	s	m/s^3	m	m/s
Br1	1	1.0	4.4	4.7	0.3	2.94	2.4
Br2	5	2.5	2.2	2.5	1.7	1.82	3.2
Acc1-J1	2	1.5	0.4	2.3	5.6	2.65	2.0
Acc1-J2	3	1.5	0.2	2.2	11.3	2.58	2.0
Acc2-J1	4	3.0	0.8	1.8	5.6	2.69	3.1

TABLE 2 | Basic anthropometric and demographic data for the volunteers (mean ± SD).

	Age	Mass	Height	Centre of mass height
	years	kg	cm	cm
11 females	31.6 ± 7.2	64.7 ± 9.9	165.5 ± 6.4	91.2 ± 3.9
13 males	35.5 ± 10.6	86.2 ± 11.8	179.2 ± 5.4	99.2 ± 3.6

centre of gravity from the ground was estimated using the centre of volume from the 3D scans of the volunteers performed prior to the tests with an infrared scanning device. The volunteers that were recruited (general health was required) were asked if they had any health issues that could affect the balance. Additionally, a participating physician made a quick assessment of each volunteer to confirm the absence of health issues. Considering the age group (younger adults, average), no further tests were performed to assess the volunteers' capabilities or to profile them. Prior to the tests, the volunteers were familiarized with the scope of tests and signed an informed consent. The design of the study and the consent form were approved by Slovenian National Medical Ethics Committee (application number 0120-63/2019/4).

The study was focused on free-standing occupants subjected to perturbations in anterior-posterior directions. The volunteers stood on the moving platform with their feet hip-width apart to provide uniform initial conditions for the volunteers. This posture could also represent the standard posture for a standing HBM. Each volunteer experienced two series of perturbations in the following order: 1. *Br1*, 2. *Acc1-J1*, 3. *Acc1-J2*, 4. *Acc2-J1*, 5. *Br2*. During the first series, the test subjects were facing the direction of travel, while for the second series, they were facing backwards. During a series of pre-tests, *Br2* was identified as the most challenging perturbation, with a high magnitude needed to stop the platform due to design limitations (**Figure 1A**). Therefore, if the participants visibly had trouble withstanding the first four perturbations, *Br2* was omitted for safety reasons. The time between two sequential tests was approximately 3 min. In order to prevent a possible adaptation to the perturbations, the volunteers were not informed about the pulse characteristics and the sequence of application prior to the tests. About 30 s before a test was initiated, the volunteers were instructed to maintain a relaxed free-standing posture on the moving platform as they would as passengers on a bus. To reduce the effect of possible anticipation, no indication was given to when the test was to start. The main switch for controlling the sled was out of sight and no noise from the motors and linear drive was generated when the sled was at rest. If technical difficulties occurred during one or several of the tests, they were repeated at the end of the test series and only the data from the repeated tests were included in the further analyses.

The volunteers wore uniform tight outfits and flexible thin rubber-soled shoes. For safety reasons, a cushion was placed in

the location on the platform where a fall could have happened. Additionally, to prevent the volunteers from falling off the platform or hitting the sled frame, they wore a full-body harness and were attached to the moving platform with two ropes. The length of the ropes was adjusted to each individual volunteer so as not to obstruct their motion during an attempt to recover their balance, allowing approximately 1.3 m of horizontal excursion before the harness was deployed.

Instrumentation

Two high-speed cameras (VEO 640L, Vision Research, Wayne, NJ, United States) captured the volunteer's motion in the sagittal and frontal planes. The muscle activity was measured using an 8-channel TeleMyo 2400T G2 system (Noraxon, Scottsdale, AZ, United States) for electromyography (EMG) at a 3-kHz sampling frequency. Bipolar Ag/AgCl surface electrodes (Skintact F-301, Innsbruck, Austria) were attached to the lower extremity muscles after the skin surface was shaved and cleaned with a propanol-based solution. The EMG electrodes were placed and fixed bilaterally according to SENIAM recommendations on the rectus femoris (RF), tibialis anterior (TA), biceps femoris (BF) and gastrocnemius medialis (GM).

Body-segment motions were captured with a system of eight cameras Oqus 3+ (Qualisys, Gothenburg, Sweden) tracking 56 passive reflective markers attached to the volunteer's body at a sampling rate of 200 fps. For measuring the ground-reaction forces, a force plate (HE600600-2k, AMTI, Watertown, MA, United States) was rigidly attached to the moving platform and connected to a LabVIEW data-acquisition card sampling at a 1-kHz frequency using an analogue low-pass filter with a 100-Hz cut-off frequency. The main switch was connected to the trigger providing the synchronisation signal. Additionally, six wearable inertial measurement units (MetaMotionR, MbientLab, San Francisco, CA, United States) were attached to the volunteer's body segments (lower legs, lower arms, head and pelvis) to track their motion by streaming the accelerometer and gyroscope data at 100 Hz.

Data Analysis

To study the effect of the pulse characteristics on the initial response of the passenger, tables were generated with variables describing the pulse characteristics like direction and magnitude, as well as the volunteer-response parameters like foot-contact times and EMG reference times. These tables allow for statistical analyses that identify the main and combined effects of the perturbation variables on the volunteers' responses. The acceleration and braking pulses were analysed independently.

The recorded EMG signals were band-pass filtered with a 4th-order zero-lag Butterworth filter (20–500 Hz), full-wave rectified, and low-pass filtered with a 6th-order zero-lag Butterworth filter with a 6-Hz cut-off frequency. For detecting muscle onset, the band-passed signals were filtered with a low-pass 4th-order zero-lag Butterworth filter with a 50-Hz cut-off frequency. The onset was defined as the first sample of a 50-ms moving-average window exceeding the threshold of 2.5 standard deviations of the EMG signal over the resting period before the initiation of the perturbation (Hodges and Bui, 1996) and was checked visually for each signal measured. The EMG signal processing was performed in Matlab (Natick, United States).

The sequence of events during the balance recovery was identified from the high-speed video recordings, where up to four sequential steps were tracked. The timing of the first frame when the contact between the foot and the ground (the moving platform) was lost was identified as the *contact-off* time, while the time of re-establishing the contact was identified as the *contact-on* time. The difference between *contact-off* and *contact-on* for the same (swing) foot represented the *swing time*. If the volunteer's motion was restricted by the harness before the end of the pulse, the event was identified as *harness deployment*. The sequential step-count and harness-deployment events were included in further analyses, if they occurred within the observed segment of the perturbation pulse.

To examine the volunteer's response time as a dependent variable of the pulse type and direction as factors, two-way repeated measures ANOVA analyses were used. ANOVAs of 3×2 design were performed for the acceleration pulses (*Acc1-J1*, *Acc1-J2*, *Acc2-J1*) and directions (forwards, backwards), while a 2×2 design was used for the braking pulses (*Br1*, *Br2*) and the two directions. Dependent variables for the ANOVAs were the contact-off time, the swing-time and the muscle onset latency for each of the muscles measured. Prior to the ANOVAs, Grubb's test and Shapiro-Wilk's test were used to detect outliers and to test the normality. The sphericity of the datasets was checked with Mauchly's test and a Greenhouse-Geisser correction was applied in the case of violation. The Bonferroni method for pairwise comparisons was applied. The significance level was set to 0.05. Additionally, the pulse type and gender (male, female) were considered as factors in the two-way repeated measures ANOVAs of 3×2 design for the acceleration pulses and 2×2 design for the braking pulses, which were used to test for the differences between the male and the female volunteers in the forward and backward directions. Spearman's correlation coefficient was used to estimate whether the muscle onset latency, contact-off time and swing time were correlated with the volunteer's body mass and the height of the centre of mass. Statistical analyses were conducted in OriginPRO 2019b (Northampton, MA, United States). The numbers of compensatory steps and harness deployments for each pulse configuration were analysed. In this approach no statistical analysis was conducted, but separate tables were created for the male and female subjects in order to identify the overall response of the volunteers to the pulse type.

RESULTS

Eleven volunteers finished a complete set of tests with five different pulses in the forward (**Figure 2A**) and backward (**Figures 2B,C**) directions, while seven volunteers repeated at least one of the tests. For six volunteers, the higher severity pulses were omitted due to safety considerations. In total, 223 tests were included in the analysis, out of 238 tests conducted with 24 volunteers. More than half (57%) of the volunteers needed at least one compensatory step to maintain their balance for the 1.0 m/s^2

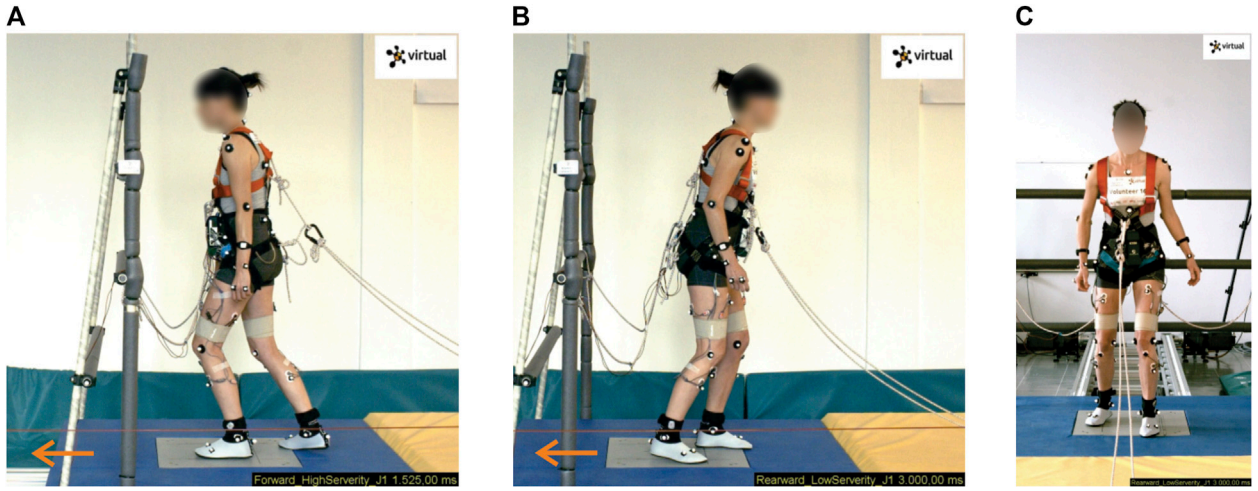

FIGURE 2 | Forward and backward orientation of the volunteers studied in the sled tests. The moving platform induced backward stepping when the volunteers were facing forwards **(A)**, and forward stepping when facing backwards **(B, C)**. The volunteer depicted (Volunteer 16) shows a typical kinematic response during the stepping strategy.

TABLE 3 | Percentage of sequential steps (1st–4th) during balance recovery and the percentage of harness deployments for the forward- and backward-facing volunteers (Males/Females).

Profile name	Forwards					Backwards				
	1st	2nd	3rd	4th	Harness	1st	2nd	3rd	4th	Harness
	%	%	%	%	%	%	%	%	%	%
Br1	57	52	30	9	4	96	70	57	30	9
M + F	58	58	25	17	8	100	50	58	17	17
M	55	45	36	0	0	91	91	55	45	0
F										
Br2	100	82	71	24	0	100	100	83	39	11
M + F	100	73	64	18	0	100	100	91	36	9
M	100	100	83	33	0	100	100	71	43	14
F										
Acc1-J1	100	100	67	54	21	100	92	79	33	21
M + F	100	100	69	46	15	100	85	69	23	23
M	100	100	64	64	27	100	100	91	45	18
F										
Acc1-J2	100	83	70	48	17	100	78	43	17	22
M + F	100	77	62	23	15	100	75	25	8	25
M	100	90	80	80	20	100	82	64	27	18
F										
Acc2-J1	100	100	92	46	75	100	100	88	50	88
M + F	100	100	85	31	69	100	100	92	46	92
M	100	100	100	64	82	100	100	82	55	82
F										

braking pulse (*Br1*) when facing in the direction of the sled travel and almost all stepped when backward-facing (**Table 3**). The safety harness was deployed extensively for the *Acc2-J1* profile, again with higher rates in the backward-facing direction. **Table 3** shows the general responses to all profiles in both directions.

Four outliers were detected with Grubb's test and removed from the datasets for the contact-off time; Shapiro-Wilk's test rejected a normal distribution for *Acc1-J1* forwards. Mauchly's test showed no violations of sphericity for the datasets. For the swing time, two outliers were found and removed; normal distribution was rejected for *Br1* forwards and *Acc1-J2* backwards. The analysis yielded significant main effects of pulse ($F(2,38) = 94.3$, $p < 0.001$) and direction ($F(1,19) = 56.3$, $p < 0.001$) on the contact-off time, while the interaction effect of the pulse and direction was not significant ($F(2,38) = 0.16$, $p = 0.851$). The contact-off time in *Acc1-J1* and *Acc2-J1* was

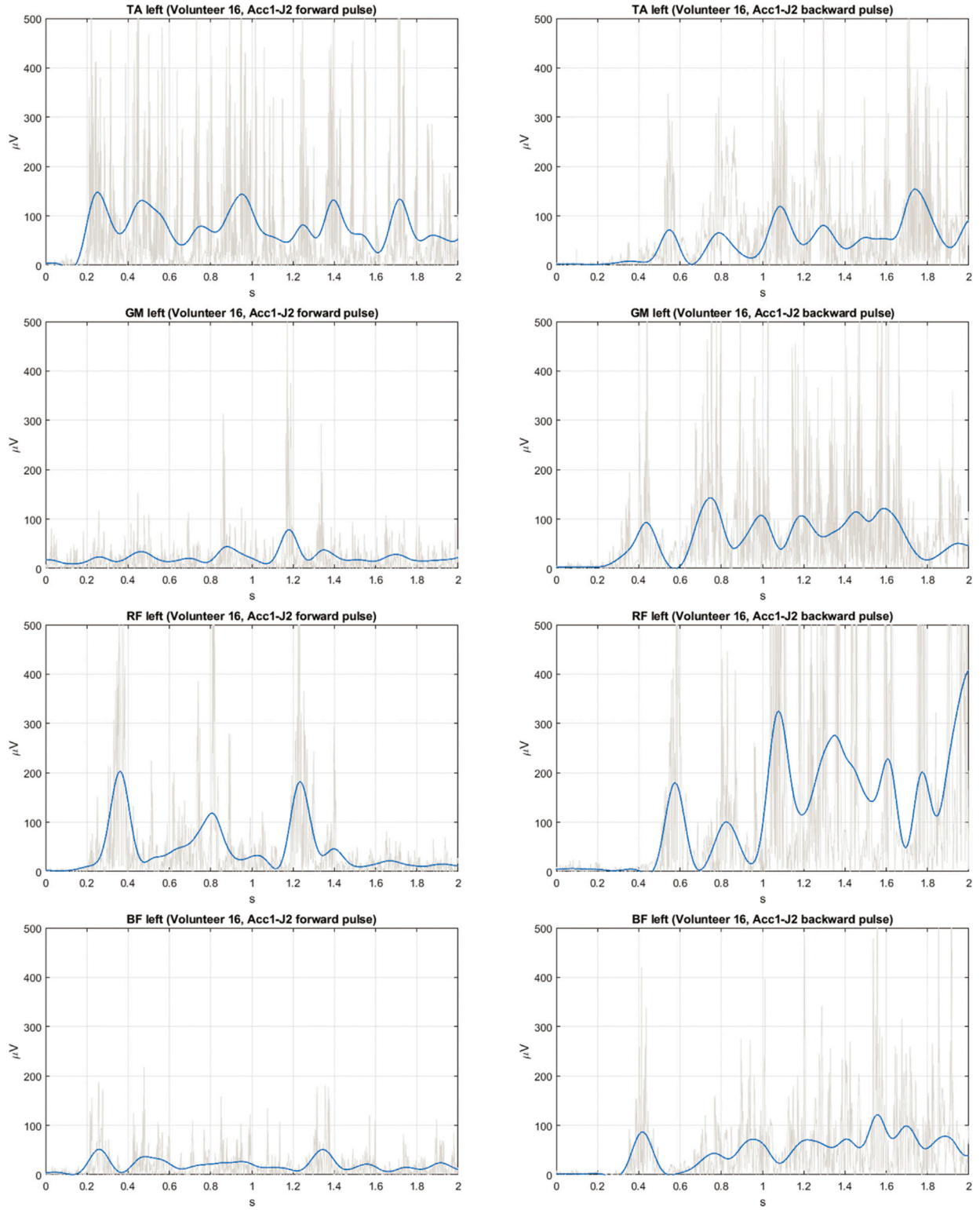

FIGURE 3 | Exemplary EMG signals measured on leg muscles (raw—grey, filtered—blue) for the *Acc1-J2* pulse in forward direction **(left column)** and backward direction **(right column)**; TA, tibialis anterior; GM, gastrocnemius medialis; RF, rectus femoris; BF, biceps femoris.

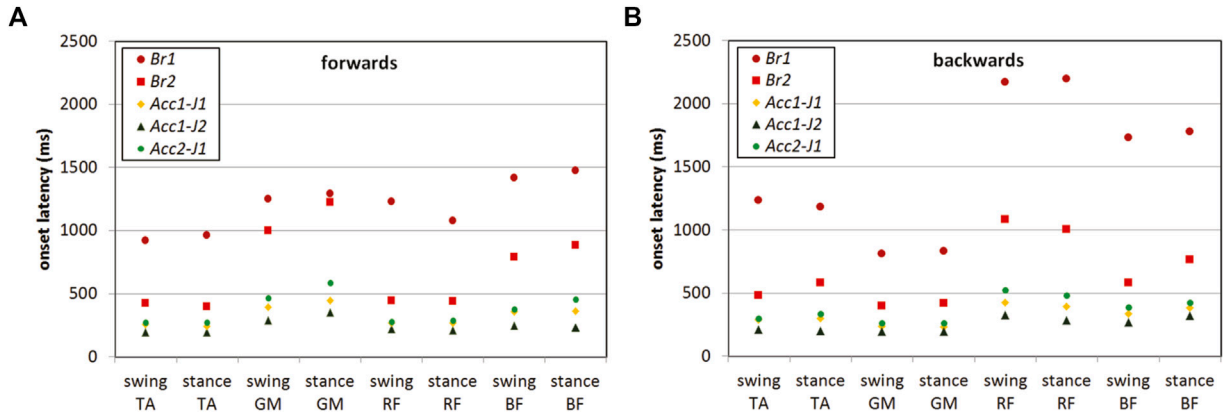

FIGURE 4 | Average EMG onset latencies for the muscles of the swing leg and the stance leg for each pulse type in forward **(A)** and backward **(B)** direction; TA, tibialis anterior; GM, gastrocnemius medialis; RF, rectus femoris; BF, biceps femoris. In both directions, shorter onset latencies were observed in the acceleration pulses, compared to the braking pulses. The shortest active muscle response was evoked by *Acc1-J2* pulse.

longer than in *Acc1-J2* in both directions ($p < 0.001$). However, no significant difference was found between the contact-off time in *Acc1-J1* and *Acc2-J1*. For the braking pulses, the analysis showed a significant effect of the pulse (F (1,6) = 808.3, $p < 0.001$), with the contact-off time in *Br2* being shorter in both directions. For the acceleration pulses, a significant main effect on swing time was found for the direction (F (1,20) = 10.21, $p = 0.005$), but not for the pulse (F (2,40) = 0.77, $p = 0.469$). The swing time was shorter in the forward direction *Acc1-J1* ($p = 0.011$). For the braking pulses, no significant effects of the pulse or the direction were found. No significant effect of gender on the contact-off and swing time was found.

In 17% of the EMG signals recorded, the onset detected was corrected manually, while in 5% it was not possible to estimate the muscle onset. For each of the eight muscles analysed, 10 datasets on the onset latencies were collected for the five perturbation pulses and two directions. Grubb's test detected 25 outliers that were removed from the EMG datasets. A Shapiro-Wilk test showed that the assumption of a normal distribution was not met in 29 out of 80 datasets. Based on a further examination of those cases by means of quantile-quantile plots, it was decided to continue with the analysis on the original data-sets without a transformation. An example of the EMG signals recorded on the lower leg muscles is depicted in **Figure 3**.

Similar to the analysis of the step initiation, the average response times for the volunteers were calculated and are presented in **Figure 4** and **Tables 5**, **6**. The responses for all the volunteers as well as for the male and female subgroups are provided.

For the braking pulses *Br1* and *Br2*, a significant main effect of the pulse was observed for all the muscles analysed. As expected, the onset latencies were shorter with a higher acceleration magnitude of *Br2*, compared to *Br1* (**Tables 5**, **6**). In addition, the main effect of direction was observed, except for the swing BF (F (1,8) = 0.15, $p = 0.710$, $\eta_p^2 = 0.02$) and the stance BF (F (1,10) = 0.69, $p = 0.424$, $\eta_p^2 = 0.06$). Shorter onset latencies in forward-direction pulses were found for the swing TA ($p = 0.003$) and the stance TA ($p = 0.003$), the swing RF ($p < 0.001$) and the stance RF ($p < 0.001$), while the latencies were shorter in the backward-direction pulses for the swing MG ($p = 0.011$) and the stance GM ($p = 0.001$). An interaction effect (pulse × direction) was found for the swing TA (F (1,15) = 7.59, $p = 0.014$, $\eta_p^2 = 0.34$) and the swing RF (F (1,15) = 5.38, $p = 0.035$, $\eta_p^2 = 0.26$). Pairwise comparisons showed that the onset latency of the swing TA was shorter in the forwards *Br1* ($p = 0.005$), but not in *Br2*.

For the acceleration pulses *Acc1-J1*, *Acc1-J2*, and *Acc2-J1*, the main effects of the pulse and direction were found for all the muscles analysed, with the exception of a non-significant direction effect for the swing BF (F (1,16) = 0.20, $p = 0.661$, $\eta_p^2 = 0.01$) and the stance BF (F (1,13) = 0.47, $p = 0.506$, $\eta_p^2 = 0.03$). The main effect of direction followed the same pattern as in *Br1* and *Br2*, where the onset latencies were shorter in the forward-

TABLE 4 | Average times for initiation (contact-off time) and duration (swing time) of the first step, where observed (Males/Females, mean ± SD).

Profile name	1st step contact-off time		1st step swing time	
	Forwards ms	Backwards ms	Forwards ms	Backwards ms
Br1	3,358 ± 434	3,205 ± 441	153 ± 69	166 ± 67
M + F	3,351 ± 447	3,183 ± 434	177 ± 68	173 ± 68
M	3,366 ± 460	3,236 ± 475	125 ± 65	158 ± 68
F				
Br2 (M + F)	1,259 ± 228	1,239 ± 234	168 ± 58	177 ± 57
M	1,244 ± 186	1,220 ± 263	177 ± 63	181 ± 62
F	1,288 ± 310	1,269 ± 197	152 ± 46	171 ± 54
Acc1-J1	541 ± 96	634 ± 89	136 ± 44	171 ± 55
M + F	556 ± 94	641 ± 79	150 ± 41	181 ± 65
M	523 ± 100	626 ± 104	120 ± 43	160 ± 40
F				
Acc1-J2	408 ± 29	505 ± 71	147 ± 57	172 ± 44
M + F	418 ± 30	528 ± 65	150 ± 65	183 ± 49
M	393 ± 21	476 ± 69	143 ± 47	160 ± 36
F				
Acc2-J1	577 ± 96	672 ± 92	155 ± 54	165 ± 40
M + F	601 ± 90	682 ± 61	173 ± 44	169 ± 48
M	549 ± 98	660 ± 124	133 ± 60	161 ± 29
F				

TABLE 5 | Descriptive statistics on EMG onset latencies in forward-direction trials (Males/Females, mean ± SD).

Profile name	Swing leg				Stance leg			
	TA	GM	RF	BF	TA	GM	RF	BF
	ms	ms	ms	ms	ms	ms	ms	ms
Br1	919 ± 261	1,251 ± 496	1,228 ± 584	1,419 ± 514	963 ± 256	1,291 ± 457	1,079 ± 502	1,475 ± 648
M + F	991 ± 224	1,274 ± 471	1,254 ± 691	1,546 ± 629	967 ± 245	1,161 ± 561	1,090 ± 624	1,451 ± 807
M	834 ± 287	1,226 ± 550	1,194 ± 442	1,245 ± 229	959 ± 280	1,394 ± 351	1,064 ± 355	1,594 ± 427
F								
Br2	421 ± 143	999 ± 320	445 ± 117	790 ± 352	396 ± 97	1,222 ± 326	440 ± 94	886 ± 378
M + F	434 ± 175	1,132 ± 226	444 ± 153	865 ± 383	395 ± 116	1,331 ± 293	436 ± 117	979 ± 365
M	401 ± 75	809 ± 353	446 ± 42	672 ± 283	398 ± 66	1,049 ± 329	447 ± 46	754 ± 383
F								
Acc1-J1	254 ± 27	392 ± 153	266 ± 37	357 ± 101	238 ± 42	445 ± 207	267 ± 25	359 ± 122
M + F	265 ± 24	457 ± 171	274 ± 41	392 ± 116	259 ± 25	557 ± 192	269 ± 21	395 ± 127
M	241 ± 25	321 ± 94	257 ± 32	318 ± 68	213 ± 45	323 ± 148	264 ± 29	324 ± 111
F								
Acc1-J2	195 ± 24	286 ± 88	221 ± 41	248 ± 78	193 ± 28	349 ± 127	208 ± 15	231 ± 66
M + F	204 ± 29	312 ± 105	238 ± 50	263 ± 104	208 ± 16	386 ± 123	214 ± 12	238 ± 89
M	184 ± 12	257 ± 58	203 ± 16	233 ± 33	176 ± 29	290 ± 118	201 ± 15	222 ± 18
F								
Acc2-J1	270 ± 27	465 ± 123	278 ± 37	376 ± 90	271 ± 27	584 ± 227	286 ± 23	455 ± 206
M + F	275 ± 31	493 ± 120	279 ± 47	408 ± 104	280 ± 27	657 ± 187	290 ± 25	519 ± 212
M	265 ± 22	432 ± 124	276 ± 24	341 ± 56	261 ± 25	512 ± 249	282 ± 22	390 ± 186
F								

TA, tibialis anterior; GM, gastrocnemius medialis; RF, rectus femoris; BF, biceps femoris.

direction pulses for TA and RF, and in backward-direction pulses for GM. Pairwise comparisons showed that the onset latencies were significantly shorter in *Acc1-J2* than in *Acc1-J1* and *Acc2-J2* for all the muscles except for the stance GM, which was not significantly different from the latency in *Acc1-J1* ($p = 0.386$).

A significant interaction effect pulse × direction was found for the stance TA (F (1.49,26.82) = 6.89, $p = 0.007$, $\eta_p^2 = 0.28$), the stance GM (F (2,24) = 3.54, $p = 0.045$, $\eta_p^2 = 0.23$), the swing RF (F (2,36) = 14.63, $p < 0.001$, $\eta_p^2 = 0.45$), and the stance RF (F (2,32) = 10.62, $p < 0.001$, $\eta_p^2 = 0.40$). For the stance TA, post-hoc tests showed no significant effect of direction in *Acc1-J2* and no difference between *Acc1-J1* and *Acc2-J1* in forward perturbations. Direction also had no significant effect in *Acc1-J2* for the stance GM ($p = 0.072$). Furthermore, the onset latencies

TABLE 6 | Descriptive statistics on EMG onset latencies in backward-direction trials (Males/Females, mean ± SD).

Profile name	Swing leg				Stance leg			
	TA	GM	RF	BF	TA	GM	RF	BF
	ms	ms	ms	ms	ms	ms	ms	ms
Br1	1,236 ± 346	809 ± 315	2,172 ± 943	1733 ± 785	1,184 ± 273	829 ± 228	2,195 ± 846	1777 ± 988
M + F	1,214 ± 313	728 ± 296	2,334 ± 920	1809 ± 814	1,221 ± 298	787 ± 273	2,275 ± 797	1905 ± 999
M	1,265 ± 401	889 ± 329	1937 ± 980	1,675 ± 787	1,132 ± 239	860 ± 193	2091 ± 939	1,649 ± 1,008
F								
Br2	480 ± 133	395 ± 83	1,081 ± 264	578 ± 132	581 ± 127	416 ± 104	1,006 ± 325	765 ± 331
M + F	488 ± 124	424 ± 80	1,071 ± 283	630 ± 148	624 ± 125	402 ± 109	949 ± 320	773 ± 319
M	466 ± 161	349 ± 70	1,098 ± 252	502 ± 41	509 ± 101	435 ± 101	1,095 ± 336	755 ± 373
F								
Acc1-J1	288 ± 64	236 ± 49	425 ± 135	333 ± 58	297 ± 45	232 ± 45	393 ± 109	383 ± 127
M + F	296 ± 47	235 ± 65	437 ± 96	327 ± 60	310 ± 54	229 ± 50	374 ± 95	395 ± 121
M	279 ± 82	237 ± 22	410 ± 175	340 ± 59	284 ± 27	235 ± 41	418 ± 125	370 ± 137
F								
Acc1-J2	211 ± 34	195 ± 14	326 ± 109	267 ± 49	201 ± 43	194 ± 20	280 ± 71	321 ± 159
M + F	219 ± 17	202 ± 9	359 ± 110	295 ± 42	191 ± 52	195 ± 27	296 ± 71	336 ± 179
M	201 ± 48	187 ± 14	278 ± 93	237 ± 37	216 ± 24	193 ± 10	257 ± 67	303 ± 135
F								
Acc2-J1	296 ± 58	260 ± 25	521 ± 136	386 ± 97	336 ± 72	259 ± 36	481 ± 137	422 ± 127
M + F	297 ± 67	269 ± 26	521 ± 124	408 ± 95	365 ± 81	273 ± 40	512 ± 139	446 ± 94
M	295 ± 49	249 ± 20	520 ± 157	359 ± 98	302 ± 44	242 ± 23	436 ± 130	397 ± 154
F								

TA, tibialis anterior; GM, gastrocnemius medialis; RF, rectus femoris; BF, biceps femoris.

TABLE 7 | Correlations between body mass and EMG onset latencies, contact-off time and swing time in forward-direction trials.

Profile name	Swing leg				Stance leg					
	TA	GM	RF	BF	TA	GM	RF	BF	Contact-off time	Swing time
Br1	0.10	–0.23	–0.16	0.19	–0.04	–0.22	–0.16	–0.16	–0.15	0.51
Br2	**0.61**	0.35	**0.43**	**0.42**	**0.64**	0.38	0.29	0.40	–0.10	–0.03
Acc1-J1	**0.57**	0.14	**0.48**	0.21	**0.69**	0.29	**0.63**	**0.53**	0.08	–0.37
Acc1-J2	0.09	0.04	0.09	0.43	0.28	0.28	–0.08	0.41	0.15	0.18
Acc2-J1	–0.11	0.35	–0.22	**0.47**	–0.18	0.50	–0.10	0.40	–0.01	0.15

TA, tibialis anterior; GM, gastrocnemius medialis; RF, rectus femoris; BF, biceps femoris.
Values in bold indicate statistical significance.

TABLE 8 | Correlations between body mass and EMG onset latencies, contact-off time and swing time in backward-direction trials.

Profile name	Swing leg				Stance leg					
	TA	GM	RF	BF	TA	GM	RF	BF	Contact-off time	Swing time
Br1	–0.40	–0.23	0.08	0.07	0.03	0.08	0.04	–0.03	–0.15	–0.13
Br2	0.13	0.35	0.16	0.19	0.16	–0.06	–0.12	0.19	0.10	0.17
Acc1-J1	0.29	0.14	0.39	**0.66**	0.00	0.35	0.10	–0.07	0.11	0.12
Acc1-J2	–0.08	0.04	0.19	0.16	0.12	0.38	0.37	–0.03	0.16	0.03
Acc2-J1	–0.10	0.35	–0.17	0.23	0.21	–0.31	–0.21	–0.09	–0.17	0.34

TA, tibialis anterior; GM, gastrocnemius medialis; RF, rectus femoris; BF, biceps femoris.
Values in bold indicate statistical significance.

for the stance GM exhibited no differences between the backward-direction pulses, while the difference in the forward-direction pulses was found only between *Acc1-J2* and *Acc2-J1*, with the latter exhibiting a longer onset latency ($p = 0.001$). The onset latencies for the swing RF were not significantly different among the forward-direction pulses, which was also observed for the stance RF, where no direction effect was found in *Acc1-J2* ($p = 0.279$).

In addition to the main effect of the pulse, a significant main effect of the gender of the volunteers was found, with a tendency for a shorter onset latency with the female volunteers in the acceleration forward-direction trials for the stance TA, (F (1,9) =

TABLE 9 | Correlations between centre of gravity height and EMG onset latencies, contact-off time and swing time in forward-direction trials.

Profile name	Swing leg				Stance leg					
	TA	GM	RF	BF	TA	GM	RF	BF	Contact-off time	Swing time
Br1	0.29	0.40	0.23	0.18	–0.17	0.26	0.30	–0.05	0.06	0.09
Br2	**0.51**	**0.52**	0.20	**0.47**	**0.67**	**0.49**	0.20	0.41	0.19	0.39
Acc1-J1	**0.57**	0.15	**0.54**	0.28	**0.77**	0.19	**0.60**	0.36	**0.44**	–0.01
Acc1-J2	0.22	0.08	0.05	0.39	0.35	0.12	0.33	**0.66**	**0.51**	0.29
Acc2-J1	0.34	0.23	0.18	0.46	0.12	0.34	0.15	0.31	0.13	0.30

TA, tibialis anterior; GM, gastrocnemius medialis; RF, rectus femoris; BF, biceps femoris.
Values in bold indicate statistical significance.

TABLE 10 | Correlations between centre of gravity height and EMG onset latencies, contact-off time and swing time in backward-direction trials.

Profile name	Swing leg				Stance leg					
	TA	GM	RF	BF	TA	GM	RF	BF	Contact-off time	Swing time
Br1	–0.12	–0.39	0.44	0.06	0.19	–0.21	**0.45**	–0.12	0.06	0.19
Br2	0.09	0.08	0.41	0.01	0.41	–0.02	0.07	**0.57**	**0.61**	**0.59**
Acc1-J1	0.32	0.43	**0.66**	**0.51**	–0.21	0.22	0.32	0.14	**0.62**	0.31
Acc1-J2	0.05	0.19	**0.65**	0.28	0.32	0.16	**0.64**	0.40	0.36	**0.51**
Acc2-J1	0.05	0.20	–0.08	0.03	0.29	–0.51	0.19	–0.31	0.02	0.27

TA, tibialis anterior; GM, gastrocnemius medialis; RF, rectus femoris; BF, biceps femoris.
Values in bold indicate statistical significance.

9.32, $p = 0.014$, $\eta_p^2 = 0.51$), stance GM (F (1,4) = 40.53, $p = 0.003$, $\eta_p^2 = 0.91$), and the stance BF (F (1,5) = 7.51, $p = 0.041$, $\eta_p^2 = 0.60$). Although no significant differences for the contact-off time between the males and the females were observed, the p-value was close to the 0.05 significance level (F (1,8) = 5.27, $p = 0.051$, $\eta_p^2 = 0.40$). For the acceleration backward-direction trials, no significances for the gender-dependent analyses were found.

Significant positive correlations (Spearman's coefficient r = 0.42–0.69) were found between the body mass and the onset latencies of the TA, RF and BF muscles (**Tables 7**, **8**) in both the forwards and (even though less prevalent) backward-direction trials. Step timings were not found to have any significant correlation with body mass. The height of the centre of gravity was found to be positively correlated with the muscle onset latencies in both the forward- and backward-direction trials (r = 0.47–0.77) for some muscles, as well as for the contact-off and swing times (**Tables 9**, **10**).

DISCUSSION

We compared the characteristics of the initial muscle and kinematic responses of healthy volunteers subjected to typical balance perturbations that can be experienced by standing passengers on public transport. Based on a literature review and in-house measured data, a set of perturbation pulses was defined to simulate typical bus accelerations and decelerations in a laboratory environment. The severity of the perturbation pulses was targeted to exceed the comfort zone for standing passengers, yet enable an analysis of the passengers' initial response in typical accelerations and decelerations of public transport, potentially resulting in non-collision incidents. A strong individual variability was observed during the tests: while some of the participants showed a good ability to counteract the perturbation pulses used, others could not be exposed to the more severe perturbations for safety reasons, which also resulted in missing observations that could not be included in the analysis. No signs of the volunteers' adaptation to the perturbation pulses were observed.

In both directions of travel, the time until the participants initiated the first recovery step was longer for the braking pulses *Br1* and *Br2* than for the acceleration pulses (**Table 4**). The participants could maintain their balance without recovery stepping in only about half of the trials with the low-severity braking pulse *Br1*, characterized by a very gradual increase of the acceleration magnitude (**Table 3**), while at least one recovery step was needed in the acceleration pulses. This is in accordance with observations in another study (Schubert et al., 2017), where volunteers had to make recovery stepping when standing freely in a bus and subjected to accelerating and decelerating manoeuvres comparable to the *Acc1-J1* and *Acc1-J2* pulses, while the magnitude of the deceleration phase was between *Br1* and *Br2* pulses. These authors found characteristic patterns of muscle activity similar to the observations in our study and observed a correlation between the jerk and fast compensatory steps, even though the participating volunteers were elderly (age 68.1 ± 5.2). In addition, the current study presents a more detailed analysis of the timing of the muscle activity and the stepping.

The pattern of muscle activation was similar for all the pulses, despite being considerably longer for the braking than for the acceleration pulses (**Figure 4**). In the forward-direction trials, the anterior leg muscles TA and RF preceded the activation of GM and BF, while in the backward-direction trials the sequence was opposite. In both perturbation directions, the leg muscles tended to activate in distal to proximal sequences, which characterizes the ankle strategy, before making a compensatory step.

For acceleration trials, the tests showed shorter onset latencies in *Acc1-J2* with the highest jerk magnitude (11.3 m/s^3) compared to *Acc1-J1* and *Acc2-J1* (5.6 m/s^3), implying that the jerk magnitude is the more important factor in the excitation of the active response of the muscles, rather than the acceleration magnitude. This finding is in agreement with observations that the jerk magnitude and the frequency of occurrence significantly influence the comfort and safety, requiring a corrective response from the passengers (Levis, 1978; Brooks et al., 1980). A further comparison of the pulses *Acc1-J1* and *Acc2-J1* having the same jerk magnitude 5.6 m/s^3 and different acceleration magnitude yielded significantly shorter onset latencies for the stance TA, swing RF, and stance RF in *Acc1-J1* (1.5 m/s^2) than in *Acc2-J1* (3.0 m/s^2). A possible reason is that the jerk magnitude in *Acc1-J1* appeared at 0.1 s, but later in *Acc2-J1*, at 0.2 s (**Table 1**; **Figure 1**), evoking a more rapid reflex response in *Acc1-J1*, despite the lower acceleration magnitude. Following the muscle activation, the contact-off time of the first step was significantly shorter with a higher jerk magnitude, but similar with different acceleration magnitudes of the pulses. Hence, a higher acceleration magnitude of a perturbation profile might not necessarily evoke faster recovery stepping within the range of magnitudes tested.

Backward stepping in response to a forward motion of the platform was consistently faster than forward stepping, which can most likely be attributed to the asymmetry of the human body in the sagittal plane, resulting in different motion patterns for forward and backward displacements (Runge et al., 1999). In a study of young adult volunteers (Maki et al., 1996; Maki and McIlroy, 1997), a contact-off time of 409 ± 77 ms after the pulse was initiated and a foot-swing duration of 141 ± 69 ms were reported for backward perturbations, compared to a shorter contact-off time of 368 ± 85 ms and a foot-swing duration of 149 ± 63 ms in forwards perturbations with a 300-ms square acceleration pulse and 0.18-m linear displacements. Although the perturbation profiles used there (Maki et al., 1996; Maki and McIlroy, 1997) differed in duration and displacements from the present study, the contact-off times and swing duration for the first recovery step were comparable for the case of the acceleration pulses applied (**Table 4**), which could be attributed to the initial jerk of the square pulse, but were longer than the step preparation time of 150–160 ms assumed for the inverted pendulum model (Vallée et al., 2015; Aftab et al., 2016).

For the braking pulses applied, the muscle onset latencies and contact-off time of the first step were longer than for the acceleration pulses, but did not change with the direction of travel. This was present in particular for *Br1*, where the volunteers

applied non-stepping as well as stepping strategies to recover their balance, implying larger between-subject variations of the active response, possibly combining reflexive and voluntary reactions. However, the percentage of participants who took at least one recovery step was higher in the backward-direction trials (**Table 3**), which is in agreement with estimations of the single-step threshold being about 1.0 m/s^2 for the forward direction and lower for the backward direction, 0.7 m/s^2 (de Kam et al., 2017).

The rate of harness deployment, indicating excessive whole-body displacement, was greater when travelling backwards than forwards and particularly high in the *Acc2-J1* pulse, 88% (**Table 3**). An acceleration magnitude of 3.0 m/s^2 caused almost 90% of the backward-facing participants to fall into the harness, compared to 21% in *Acc1-J1* (which had the same jerk level, but only half the acceleration magnitude). These findings cannot be directly compared to previous studies due to the different setup and design of the safety system, but the sharp rise of the harness deployment between 1.5 and 3.0 m/s^2 acceleration magnitude confirms the threshold levels of 1.0–1.8 m/s^2, as recommended for public transport (De Graaf and Van Weperen, 1997; Szturm and Fallang, 1998; Karekla and Tyler, 2018; Karekla and Fang, 2021). The percentage of harness deployment was low in the trials with the *Br2* pulse, even though it was identified as the most challenging to participants during pre-tests and was not used for the volunteers during the tests who raised potential safety concerns. The likely reason was that the sled-stopping segment of *Br2* yielded a magnitude of 3.5 m/s^2 due to the setup design limitations (**Figure 1**), which caused the safety concerns, while the volunteers' response was observed during the rise segment of the pulse only. In 24% of the forward-direction trials and 44% of the backward-direction trials, the harness was deployed after the rise time of *Br2* pulse ended (2.2 s, **Table 1**), before the stopping of the sled had to be initiated due to the operational limits of the setup. Compared to a free-standing posture, the use of handrails and vertical bars substantially increases the possibility of the standing passengers keeping their balance (Robert et al., 2007a; Sarraf et al., 2014; Schubert et al., 2017). However, if public transport must accommodate free-standing passengers, the vehicle acceleration and braking actions should be such that they minimize the risk of these passengers losing their balance.

The initial response to the perturbations followed the same pattern for the male and female volunteers, although the results collected imply a faster response from the female volunteers (**Tables 4–6**). Furthermore, the muscle onset latency, contact-off time, and swing time were found to be correlated with the body-mass distribution (**Tables 7–10**). Hence, the lower body mass and the lower height of the centre of mass of the female volunteers (**Table 2**) could contribute to their faster response, particularly with the acceleration profiles applied that tend to evoke a mechanical response in the inverted-pendulum manner, possibly triggering sensory feedback and muscle activation faster to recover balance (Winter, 1995; Costello et al., 2012; Aftab et al., 2016; Le Mouel and Brette, 2019). Similar observations were reported in other studies comparing male and female volunteers (Maki et al., 1996; Karekla and Fang, 2021).

However, in order to provide more definite conclusions that could be applied to gender-specific HBM modelling, increasing the number of test subjects would provide more input data for the analysis methods used. The influence of age on balance recovery has not been examined in this study. It is reported in the literature that younger adults are capable of shorter step-initiation and completion times, while the elderly can respond as fast as younger populations in reflexive stepping (which is generally faster than voluntary stepping) (Rogers et al., 2003; Tokuno et al., 2010). Therefore, the outcomes of the present study with volunteers aged 33.8 ± 9.2 might also be representative for elderly passengers exposed to forward and backward perturbations.

Only the initial response of free-standing occupants to balance perturbations in the anterior-posterior direction was considered in the present study, which offers the smallest base of support to react against the applied loads and might lead to large body displacements, increasing the risk of impacts. Moreover, it is a suitable choice for the initial HBM standing position, which can be modified to other postures that might be used by the occupants of a bus. Passengers oriented laterally with respect to the perturbation might exhibit better resistance to perturbations due to a larger base of support. However, elderly people (above the age of 65–70) have been found to have a higher risk of falling and injury, tending to perform cross-over steps more often compared to lateral sidesteps that are used by younger adults (Maki et al., 2000; Mille et al., 2013; Borelli et al., 2019). Such complex balance strategies were out of the scope of this study, but future research should investigate occupant postures with different foot positions and study the use of handrails and vertical bars, as well as measuring other muscles that might contribute to balance recovery (Oude Nijhuis et al., 2010). The study was conducted in a laboratory setting, offering a high level of control over the test parameters. Yet, despite the preventive measures taken, the possibility of the volunteers getting habituated to the perturbation pulses cannot be entirely excluded. Furthermore, due to the safety aspect and technical limitations it was not possible to precisely replicate the environment of the bus and the perturbations that could be experienced by the bus passengers.

The results of this study suggest, as a starting point, that the peak accelerations of a bus should be below 1.5 m/s^2 during the journey, while the jerk magnitudes used in the study were higher (over 5 m/s^3) than recommended for comfortable travel, but still allowed the volunteers to recover their balance effectively with the room for compensatory stepping provided. For the braking event, the deceleration should be below 1.0 m/s^2. These values are based on volunteer tests with young volunteers. It is assumed that these values would need to be adjusted downwards when established for the range of the population using public transport. This work is still to be done. Once established, it would serve to define virtual testing procedures for public transport vehicles, providing an efficient approach to assessing the design and operational characteristics of the vehicles, as well as guidance both for bus drivers and for prescribing the take-off and braking of autonomous vehicles.

CONCLUSION

This study investigated the response of standing passengers on public transport to balance perturbations, establishing a reference set of experimental data for estimating safe operating envelopes. The focus was on muscle-activation patterns and the kinematic response to forwards and backwards platform translations. By testing several perturbation profiles based on real-world recorded data in a controlled laboratory setup, it was possible to estimate the neuromuscular response in transition from fixed-support strategies to single or multiple stepping strategies for balance recovery. The data collected provides a basis for further developing tools to improve passenger safety and public transit functions, including bus manoeuvring.

It was shown that the shape, magnitude and duration of the perturbation profile significantly affect the initial response of erect passengers. A higher jerk evoked faster muscle activity and recovery steps, which could be expected in both younger and older healthy adults. Bus acceleration can induce a higher risk of the passenger falling than braking due to the higher jerk content, as observed in the pulses used in this study. Greater passenger motion can also arise from longer perturbation durations as experienced in moderate accelerating and braking events. Different combinations of perturbation characteristics elicit a variety of balance-recovery responses. A combination of jerk and acceleration magnitude should be considered when analysing the balance response in virtual testing with generic perturbations. In addition, the study results imply that gender-specific modelling might improve the biofidelity of human body models for simulating the balance recovery of standing passengers in non-collision incidents of public transport vehicles, as gender-specific differences for the muscle onset times were observed. Future research should provide a larger sample of the volunteers subjected to a greater variety of load cases.

DATA AVAILABILITY STATEMENT

The raw data supporting the conclusions of this article will be made available by the authors, without undue reservation.

ETHICS STATEMENT

The studies involving human participants were reviewed and approved by National Medical Ethics Committee, Ministry of Health, Republic of Slovenia, Štefanova 5, SI-1000 Ljubljana (http://www.kme-nmec.si/). The patients/participants provided their written informed consent to participate in this study.

AUTHOR CONTRIBUTIONS

SK, CK, AL, AK and AS designed and conducted the experimental work. SK wrote the initial draft of the manuscript. AL, CK, AK, RT and J-CX revised the manuscript and added to all the sections and references.

FUNDING

This study has received funding from the European Union Horizon 2020 Research and Innovation Programme under Grant Agreement No. 768960 (project VIRTUAL).

REFERENCES

Aftab, Z., Robert, T., and Wieber, P.-B. (2016). Balance Recovery Prediction with Multiple Strategies for Standing Humans. *PLoS ONE.* 11 (3), e0151166. doi:10.1371/journal.pone.0151166

Albertsson, P., and Falkmer, T. (2005). Is There a Pattern in European Bus and Coach Incidents? A Literature Analysis with Special Focus on Injury Causation and Injury Mechanisms. *Accid. Anal. Prev.* 37 (2), 225–233. doi:10.1016/j.aap.2004.03.006

Bair, W.-N., Prettyman, M. G., Beamer, B. A., and Rogers, M. W. (2016). Kinematic and Behavioral Analyses of Protective Stepping Strategies and Risk for Falls Among Community Living Older Adults. *Clin. Biomech.* 36, 74–82. doi:10.1016/j.clinbiomech.2016.04.015

Barnes, J., Morris, A., Welsh, R., Summerskill, S., Marshall, R., Kendrick, D., et al. (2016). Injuries to Older Users of Buses in the UK. *Public Transp.* 8 (1), 25–38. doi:10.1007/s12469-015-0113-8

Björnstig, U., Bylund, P.-O., Albertsson, P., Falkmer, T., Björnstig, J., and Petzäll, J. (2005). Injury Events Among Bus and Coach Occupants. *IATSS Res.* 29 (1), 79–87. doi:10.1016/S0386-1112(14)60121-7

Blenkinsop, G. M., Pain, M. T. G., and Hiley, M. J. (2017). Balance Control Strategies during Perturbed and Unperturbed Balance in Standing and Handstand. *R. Soc. Open Sci.* 4 (7), 161018. doi:10.1098/rsos.161018

Borrelli, J., Creath, R. A., Pizac, D., Hsiao, H., Sanders, O. P., and Rogers, M. W. (2019). Perturbation-evoked Lateral Steps in Older Adults: Why Take Two Steps when One Will Do? *Clin. Biomech. (Bristol, Avon).* 63, 41–47. doi:10.1016/j.clinbiomech.2019.02.014

Brooks, B. M., Edwards, H. M., Fraser, C. R., Levis, J. A., and Johnson, M. A. (1980). *Passenger Problems on Moving Buses*. Supplementary Report 520. Crowthorn, Berkshire: Crowthorn: Transport and road research laboratory.

Čamernik, J., Potocanac, Z., Peternel, L., and Babič, J. (2016). Holding a Handle for Balance during Continuous Postural Perturbations-Immediate and Transitionary Effects on Whole Body Posture. *Front. Hum. Neurosci.* 10, 486. doi:10.3389/fnhum.2016.00486

Carlsson, A., Linder, A., Davidsson, J., Hell, W., Schick, S., and Svensson, M. (2011). Dynamic Kinematic Responses of Female Volunteers in Rear Impacts and Comparison to Previous Male Volunteer Tests. *Traffic Inj. Prev.* 12 (4), 347–357. doi:10.1080/15389588.2011.585408

Carpenter, M. G., Thorstensson, A., and Cresswell, A. G. (2005). Deceleration Affects Anticipatory and Reactive Components of Triggered Postural Responses. *Exp. Brain Res.* 167, 433–445. doi:10.1007/s00221-005-0049-3Costello

Costello, K. E., Matrangola, S. L., and Madigan, M. L. (2012). Independent Effects of Adding Weight and Inertia on Balance during Quiet Standing. *Biomed. Eng. Online.* 11, 20. doi:10.1186/1475-925X-11-20

Cyr, M.-A., and Smeesters, C. (2009). Kinematics of the Threshold of Balance Recovery Are Not Affected by Instructions Limiting the Number of Steps in Younger Adults. *Gait & Posture.* 29 (4), 628–633. doi:10.1016/j.gaitpost.2009.01.011

de Kam, D., Roelofs, J. M. B., Bruijnes, A. K. B. D., Geurts, A. C. H., and Weerdesteyn, V. (2017). The Next Step in Understanding Impaired Reactive Balance Control in People with Stroke: the Role of Defective Early Automatic Postural Responses. *Neurorehabil. Neural Repair.* 31 (8), 708–716. doi:10.1177/1545968317718267

Elvik, R. (2019). Risk of Non-collision Injuries to Public Transport Passengers: Synthesis of Evidence from Eleven Studies. *J. Transport Health.* 13, 128–136. doi:10.1016/j.jth.2019.03.017

Graaf, B. D., and Van Weperen, W. (1997). The Retention of Blance: An Exploratory Study into the Limits of Acceleration the Human Body Can Withstand without Losing Equilibrium. *Hum. Factors.* 39 (1), 111–118. doi:10.1518/001872097778940614

Halpern, P., Siebzehner, M. I., Aladgem, D., Sorkine, P., and Bechar, R. (2005). Non-collision Injuries in Public Buses: a National Survey of a Neglected Problem. *Emerg. Med. J.* 22 (2), 108–110. doi:10.1136/emj.2003.013128

Hoberock, L. L. (1976). *A Survey of Longitudinal Acceleration comfort Studies in Ground Transportation Vehicles*. Austin TX: The University of Texas. Research Report 40.

Hodges, P., and Bui, B. H. (1996). A Comparison of Computer-Based Methods for the Determination of Onset of Muscle Contraction Using Electromyography. *Electroencephalogr. Clin. Neurophysiol.* 101, 511–519. doi:10.1016/s0013-4694(96)95190-5

Horak, F. B., and Nashner, L. M. (1986). Central Programming of Postural Movements: Adaptation to Altered Support-Surface Configurations. *J. Neurophysiol.* 55 (6), 1369–1381. doi:10.1152/jn.1986.55.6.1369

Hsiao-Wecksler, E. T., and Robinovitch, S. N. (2007). The Effect of Step Length on Young and Elderly Women's Ability to Recover Balance. *Clin. Biomech.* 22, 574–580. doi:10.1016/j.clinbiomech.2007.01.013

Hwang, S., Tae, K., Sohn, R., Kim, J., Son, J., and Kim, Y. (2009). The Balance Recovery Mechanisms against Unexpected Forward Perturbation. *Ann. Biomed. Eng.* 37 (8), 1629–1637. doi:10.1007/s10439-009-9717-y

Jin, X., Begeman, P., Board, D., Pline, K., Shen, M., Sundararajan, S., and Yang, K. H. (2019). "Comparison of Small Female and Mid-sized Male PMHS Response with an Inflatable Seatbelt System during Drontal Impacts," in 2019 International Research Council on Biomechanics of Injury (IRCOBI) Conference, Florence (Italy), 11–13 September 2019. IRC-19-21. doi:10.2118/194709-ms

Karekla, X., and Fang, C. (2021). Upper Body Balancing Mechanisms and Their Contribution to Increasing Bus Passenger Safety. *Saf. Sci.* 133, 105014. doi:10.1016/j.ssci.2020.105014

Karekla, X., and Tyler, N. (2018). Reducing Non-collision Injuries Aboard Buses: Passenger Balance whilst Walking on the Lower Deck. *Saf. Sci.* 105, 128–133. doi:10.1016/j.ssci.2018.01.021

Kendrick, D., Drummond, A., Logan, P., Barnes, J., and Worthington, E. (2015). Systematic Review of the Epidemiology of Non-collision Injuries Occurring to Older People during Use of Public Buses in High Income Countries. *J. Transport Health.* 2 (3), 394–405. doi:10.1016/j.jth.2015.06.002

Kirchner, M., Schubert, P., and Haas, C. T. (2014). Characterisation of Real-World Bus Acceleration and Deceleration Signals. *Jsip* 05, 8–13. doi:10.4236/jsip.2014.51002

Kirk, A., Grant, R., and Bird, R. (2003). "Passenger Casualties in Non-collision Incidents on Buses and Coaches in Great Britain," in 18th International Technical Conference on the Enhanced Safety of Vehicles (ESV), Nagoya, Japan, 19–22 May 2003. Paper No. 296.

Koushyar, H., Bieryla, K. A., Nussbaum, M. A., and Madigan, M. L. (2019). Age-related Strength Loss Affects Non-stepping Balance Recovery. *PLoS ONE.* 14 (1), e0210049. doi:10.1371/journal.pone.0210049

Kühn, W. (2013). *Fundamentals of Road Design*. Southampton: WIT Press. doi:10.5772/55837

Le Mouel, C., and Brette, R. (2019). Anticipatory Coadaptation of Ankle Stiffness and Sensorimotor Gain for Standing Balance. *Plos Comput. Biol.* 15 (11), e1007463. doi:10.1371/journal.pcbi.1007463

Levis, J. A. (1978). The Seated Bus Passenger - a Review. *Appl. Ergon.* 9 (3), 143–150. doi:10.1016/0003-6870(78)90004-2

Maki, B. E., Edmondstone, M. A., and McIlroy, W. E. (2000). Age-related Differences in Laterally Directed Compensatory Stepping Behavior. *J. Gerontol. Ser. A: Biol. Sci. Med. Sci.* 55 (5), M270–M277. doi:10.1093/gerona/55.5.M270

Maki, B. E., McIlroy, W. E., and Perry, S. D. (1996). Influence of Lateral Destabilization on Compensatory Stepping Responses. *J. Biomech.* 29 (3), 343–353. doi:10.1016/0021-9290(95)00053-4

Maki, B. E., and McIlroy, W. E. (1997). The Role of Limb Movements in Maintaining Upright Stance: the "Change-In-Support" Strategy. *Phys. Ther.* 77 (5), 488–507. doi:10.1093/ptj/77.5.488

Mille, M.-L., Johnson-Hilliard, M., Martinez, K. M., Zhang, Y., Edwards, B. J., and Rogers, M. W. (2013). One Step, Two Steps, Three Steps More . . . Directional Vulnerability to Falls in Community-Dwelling Older People Directional Vulnerability to Falls in Community-Dwelling Older People. *J. Gerontol. A. Biol. Sci. Med. Sci.* 68 (12), 1540–1548. doi:10.1093/gerona/glt062

Oude Nijhuis, L. B., Allum, J. H. J., Valls-Solé, J., Overeem, S., and Bloem, B. R. (2010). First Trial Postural Reactions to Unexpected Balance Disturbances: A Comparison with the Acoustic Startle Reaction. *J. Neurophysiol.* 104 (5), 2704–2712. doi:10.1152/jn.01080.2009

Owings, T. M., Pavol, M. J., and Grabiner, M. D. (2001). Mechanisms of Failed Recovery Following Postural Perturbations on a Motorized Treadmill Mimic Those Associated with an Actual Forward Trip. *Clin. Biomech.* 16 (9), 813–819. doi:10.1016/S0268-0033(01)00077-8

Palacio, A., Tamburro, G., O'Neill, D., and Simms, C. K. (2009). Non-collision Injuries in Urban Buses-Strategies for Prevention. *Accid. Anal. Prev.* 41, 1–9. doi:10.1016/j.aap.2008.08.016

Powell, J. P., and Palacín, R. (2015). Passenger Stability within Moving Railway Vehicles: Limits on Maximum Longitudinal Acceleration. *Urban Rail Transit.* 1 (2), 95–103. doi:10.1007/s40864-015-0012-y

Robert, T., Beillas, P., Maupas, A., and Verriest, J.-P. (2007a). Conditions of Possible Head Impacts for Standing Passengers in Public Transportation: an Experimental Study. *Int. J. Crashworthiness.* 12 (3), 319–327. doi:10.1080/13588260701433552

Robert, T., Beillas, P., Maupas, A., and Verriest, J.-P. (2007b). "Possible Head Impacts for Standing Passengers in Public Transportation – Influence of an Obstacle on the Passenger Kinematics," in 2007 International Research Council on Biomechanics of Injury (IRCOBI) Conference, Maastricht, Netherlands, 19-21 September 2007, 393–396.

Rogers, M. W., Johnson, M. E., Martinez, K. M., Mille, M.-L., and Hedman, L. D. (2003). Step Training Improves the Speed of Voluntary Step Initiation in Aging. *Journals Gerontol. Ser. A: Biol. Sci. Med. Sci.* 58 (1), M46–M51. doi:10.1093/gerona/58.1.M46

Runge, C. F., Shupert, C. L., Horak, F. B., and Zajac, F. E. (1999). Ankle and Hip Postural Strategies Defined by Joint Torques. *Gait & Posture.* 10 (2), 161–170. doi:10.1016/S0966-6362(99)00032-6

Sarraf, T. A., Marigold, D. S., and Robinovitch, S. N. (2014). Maintaining Standing Balance by Handrail Grasping. *Gait & Posture.* 39 (1), 258–264. doi:10.1016/j.gaitpost.2013.07.117

Schubert, P., Liebherr, M., Kersten, S., and Haas, C. T. (2017). Biomechanical Demand Analysis of Older Passengers in a Standing Position during Bus Transport. *J. Transport Health.* 4, 226–236. doi:10.1016/j.jth.2016.12.002

Silvano, A. P., and Ohlin, M. (2019). Non-collision Incidents on Buses Due to Acceleration and Braking Manoeuvres Leading to Falling Events Among Standing Passengers. *J. Transport Health.* 14, 100560. doi:10.1016/j.jth.2019.04.006

Siman-Tov, M., Radomislensky, I., Marom, I., Kapra, O., Peleg, K., Bahouth, H., et al. (2019). A Nation-wide Study on the Prevalence of Non-collision Injuries Occurring during Use of Public Buses. *J. Transport Health.* 13, 164–169. doi:10.1016/j.jth.2019.03.019

Simoneau, M., and Corbeil, P. (2005). The Effect of Time to Peak Ankle Torque on Balance Stability Boundary: Experimental Validation of a Biomechanical Model. *Exp. Brain Res.* 165 (2), 217–228. doi:10.1007/s00221-005-2290-1

Szturm, T., and Fallang, B. (1998). Effects of Varying Acceleration of Platform Translation and Toes-Up Rotations on the Pattern and Magnitude of Balance Reactions in Humans. *J. Vestib. Res.* 8 (5), 381–397. doi:10.3233/VES-1998-8504

Tokuno, C. D., Cresswell, A. G., Thorstensson, A., and Carpenter, M. G. (2010). Age-related Changes in Postural Responses Revealed by Support-Surface Translations with a Long Acceleration-Deceleration Interval. *Clin. Neurophysiol.* 121 (1), 109–117. doi:10.1016/j.clinph.2009.09.025

Torres-Oviedo, G., and Ting, L. H. (2007). Muscle Synergies Characterizing Human Postural Responses. *J. Neurophysiol.* 98 (4), 2144–2156. doi:10.1152/jn.01360.2006

Vallée, P., Tisserand, R., and Robert, T. (2015). Possible Recovery or Unavoidable Fall? A Model to Predict the One Step Balance Recovery Threshold and its

Stepping Characteristics. *J. Biomech.* 48 (14), 3905–3911. doi:10.1016/j.jbiomech.2015.09.024

Vasavada, A. N., Li, S., and Delp, S. L. (2001). Three-dimensional Isometric Strength of Neck Muscles in Humans. *Spine* 26 (17), 1904–1909. doi:10.1097/00007632-200109010-00018

Winter, D. (1995). Human Balance and Posture Control during Standing and Walking. *Gait & Posture.* 3 (4), 193–214. doi:10.1016/0966-6362(96)82849-9

Zemková, E., Kováčiková, Z., Jeleň, M., Neumannová, K., and Janura, M. (2016). Postural and Trunk Responses to Unexpected Perturbations Depend on the Velocity and Direction of Platform Motion. *Physiol. Res.* 65, 769–776. doi:10.33549/physiolres.933177

Zhou, H., Yuan, C., Dong, N., Wong, S. C., and Xu, P. (2020). Severity of Passenger Injuries on Public Buses: A Comparative Analysis of Collision Injuries and Non-collision Injuries. *J. Saf. Res.* 74, 55–69. doi:10.1016/j.jsr.2020.04.003

Conflict of Interest: The authors declare that the research was conducted in the absence of any commercial or financial relationships that could be construed as a potential conflict of interest.

frontiers in Bioengineering and Biotechnology

ORIGINAL RESEARCH
published: 02 August 2021
doi: 10.3389/fbioe.2021.684043

The Effect of Seat Back Inclination on Spinal Alignment in Automotive Seating Postures

Fusako Sato[1,2]*, *Yusuke Miyazaki*[3], *Shigehiro Morikawa*[4], *Antonio Ferreiro Perez*[5], *Sylvia Schick*[6], *Karin Brolin*[7] *and Mats Svensson*[2]

[1] Safety Research Division, Japan Automobile Research Institute, Tsukuba, Japan, [2] Department of Mechanics and Maritime Sciences, Chalmers University of Technology, Gothenburg, Sweden, [3] Department of Systems and Control Engineering, Tokyo Institute of Technology, Tokyo, Japan, [4] Shiga University of Medical Science, Otsu, Japan, [5] Fundación de Investigación HM Hospitales, Madrid, Spain, [6] Department of Forensic Epidemiology, Institute of Legal Medicine, Ludwig Maximilian University of Munich, Munich, Germany, [7] Lightness by Design Aktiebolag (AB), Stockholm, Sweden

Experimental studies have demonstrated a relationship between spinal injury severity and vertebral kinematics, influenced by the initial spinal alignment of automotive occupants. Spinal alignment has been considered one of the possible causes of gender differences in the risk of sustaining spinal injuries. To predict vertebral kinematics and investigate spinal injury mechanisms, including gender-related mechanisms, under different seat back inclinations, it is needed to investigate the effect of the seat back inclination on initial spinal alignment in automotive seating postures for both men and women. The purpose of this study was to investigate the effect of the seat back inclination on spinal alignments, comparing spinal alignments of automotive seating postures in the 20° and 25° seat back angle and standing and supine postures. The spinal columns of 11 female and 12 male volunteers in automotive seating, standing, and supine postures were scanned in an upright open magnetic resonance imaging system. Patterns of their spinal alignments were analyzed using Multidimensional Scaling presented in a distribution map. Spinal segmental angles (cervical curvature, T1 slope, total thoracic kyphosis, upper thoracic kyphosis, lower thoracic kyphosis, lumbar lordosis, and sacral slope) were also measured using the imaging data. In the maximum individual variances in spinal alignment, a relationship between the cervical and thoracic spinal alignment was found in multidimensional scaling analyses. Subjects with a more lordotic cervical spine had a pronounced kyphotic thoracic spine, whereas subjects with a straighter to kyphotic cervical spine had a less kyphotic thoracic spine. When categorizing spinal alignments into two groups based on the spinal segmental angle of cervical curvature, spinal alignments with a lordotic cervical spine showed significantly greater absolute average values of T1 slope, total thoracic kyphosis, and lower thoracic kyphosis for both the 20° and 25° seat back angles. For automotive seating postures, the gender difference in spinal alignment was almost straight cervical and less-kyphotic thoracic spine for the female subjects and lordotic cervical and more pronounced kyphotic thoracic spine for the male subjects. The most prominent influence of seatback inclination appeared in Total thoracic kyphosis, with increased angles for 25° seat back, 8.0° greater in spinal alignments with a lordotic cervical spine, 3.2° greater in spinal alignments with a kyphotic

OPEN ACCESS

Edited by:
Yih-Kuen Jan,
University of Illinois at Urbana-Champaign, United States

Reviewed by:
Emanuela Bologna,
University of Palermo, Italy
Rizwan Arshad,
Royal Military College of Canada, Canada

***Correspondence:**
Fusako Sato
fsatou@jari.or.jp

Specialty section:
This article was submitted to Biomechanics, a section of the journal Frontiers in Bioengineering and Biotechnology

Received: *22 March 2021*
Accepted: *28 June 2021*
Published: *02 August 2021*

Citation:
Sato F, Miyazaki Y, Morikawa S, Ferreiro Perez A, Schick S, Brolin K and Svensson M (2021) The Effect of Seat Back Inclination on Spinal Alignment in Automotive Seating Postures. Front. Bioeng. Biotechnol. 9:684043. doi: 10.3389/fbioe.2021.684043

cervical spine. The difference in total thoracic kyphosis between the two seatback angles and between the seating posture with the 20° seat back angle and the standing posture was greater for spinal alignments with a lordotic cervical spine than for spinal alignments with a kyphotic cervical spine. The female subjects in this study had a tendency toward the kyphotic cervical spine. Some of the differences between average gender-specific spinal alignments may be explained by the findings observed in the differences between spinal alignments with a lordotic and kyphotic cervical spine.

Keywords: automotive seating posture, MRI, multi-dimensional scaling, seat back inclination, spinal alignment, spinal injury, spinal segmental angle

INTRODUCTION

In investigations of spinal injury biomechanics in road traffic accidents, it has been considered that cervical spinal alignment is one potential factor that may influence the severity of the cervical spinal injury. Experimental studies using human cadavers have demonstrated the influence of the initial cervical spinal alignment on the severity of cervical spinal injuries (Maiman et al., 1983, 2002; Yoganandan et al., 1986, 1999; Liu and Dai, 1989; Pintar et al., 1995). Because of load transmission between the head and the torso through the cervical spine, cervical spinal alignment can affect vertebral translational and rotational kinematics during impact. One computational study using a head-neck model found that kyphotic cervical spinal alignment was exposed to larger elongation of the facet joint capsular ligaments than lordotic cervical spinal alignment in rear impact loadings (Stemper et al., 2005). Therefore, the study concluded that a kyphotic cervical spine has a more potentially harmful effect on the risk of sustaining cervical spinal injuries. Indeed, a series of human volunteer rear impact sled tests showed that cervical vertebrae with kyphotic cervical spinal alignment rotated significantly more in extension than cervical vertebrae with lordotic cervical spinal alignment (Ono et al., 1997).

Another series of human volunteer rear impact sled tests have indicated the importance of interaction between the torso and seat back on cervical spinal kinematics (Ono et al., 1999). In computational studies using a whole-body human finite element (FE) model, the initial thoracolumbar spinal alignment influenced vertebral kinematics of the whole spine in rear impact reconstructions (Sato et al., 2010, 2017). Thoracolumbar vertebral kinematics govern the T1 kinematics, which can directly affect cervical spinal kinematics. Therefore, it seems that the initial whole spinal alignments are essential factors for clarifying spinal injury mechanisms.

Epidemiologic studies have shown that women are at a higher risk to sustain cervical spinal injuries, including whiplash-associated disorders (WADs), in traffic accidents compared with men (Kihlberg, 1969; O'Neill et al., 1972; Thomas et al., 1982; Otremski et al., 1989; Maag et al., 1990; Morris and Thomas, 1996; Dolinis, 1997; Temming and Zobel, 1998; Chapline et al., 2000; Richter et al., 2000; Krafft et al., 2003; Jakobsson et al., 2004; Storvik et al., 2009; Carstensen et al., 2012; Forman et al., 2019a). The gender differences in the risk of sustaining cervical spinal injuries are attributed partly to anatomical, biomechanical, and muscular differences between men and women (Stemper et al., 2011; Stemper and Corner, 2016). In the gender-dependent anatomical differences, cervical spinal alignment has been considered one of the possible causes of gender differences in the risk of sustaining cervical spinal injuries (Helliwel et al., 1994; Matsumoto et al., 1998; Stemper et al., 2011; Brolin et al., 2015; Stemper and Corner, 2016; Östh et al., 2017; Sato et al., 2017; John et al., 2018). In an asymptomatic population measured in an upright seated position, cervical lordosis was observed in the majority, and non-lordotic alignment was observed in 36% (Matsumoto et al., 1998) and 38% (Takeshima et al., 2002). Women are more likely to present non-lordosis (straight or kyphosis) than men, while men statistically present more pronounced lordosis (Helliwel et al., 1994; Hardacker et al., 1997; Matsumoto et al., 1998; Been et al., 2017).

Rear impact sled tests using head-neck complexes extracted from cadavers have demonstrated greater intervertebral angular displacements and shear displacements between facet joints for female specimens than for male specimens (Stemper et al., 2003, 2004). Using a FE model of the C5–C6 spinal segment, computational simulations based on the experiments conducted by Stemper et al. (2003) have shown that the straighter C5–C6 spinal segment exhibited greater posterior facet joint compression and anterior longitudinal ligament stretch (John et al., 2018). Consequently, the study concluded that these findings might explain the higher risk of sustaining cervical spinal injuries for women with a straighter cervical spine. However, these studies have been limited to the cervical spine region.

Human volunteer sled tests have also demonstrated greater intervertebral flexion in the upper cervical spine and greater intervertebral extension in the lower cervical spine (Ono et al., 2006; Sato et al., 2014, 2015). The whole spinal alignment, from C2 to the sacrum, was investigated in the same seating posture and the same seat configuration as the human volunteer sled tests conducted by Ono et al. (2006) and Sato et al. (2017). The study has reported straighter spinal alignment, almost straight cervical, and less-kyphotic thoracic spine for female subjects. By changing the spinal alignment of a whole-body human FE model, reconstruction simulations of the human volunteer sled tests have illustrated the female spinal alignment exhibited greater intervertebral flexion in the upper cervical spine and greater intervertebral extension in the lower cervical spine, explaining

the influence of the interaction between thoracolumbar spine and seat back on cervical vertebral kinematics. These studies were conducted using a laboratory seat with a 20° seat back angle.

Basically, the seat performance of occupant protection systems installed in cars is evaluated at a seat back angle of 25° (SAE Standard J826, 2015). Furthermore, highly automated vehicles have the potential to allow drivers in a reclined position (Forman et al., 2019b; Gepber et al., 2019). It is important to evaluate vertebral kinematics of a reclined spinal alignment for future crash safety with highly automated vehicles. Human cadaver sled tests have shown the effect of the seat back inclination on cervical vertebral rotations and facet joint shear displacements (Deng et al., 2000; Yang and King, 2003). To predict vertebral kinematics and investigate spinal injury mechanisms, including gender-related mechanisms, under different seat back inclinations, it is needed to investigate the effect of the seat back inclination on initial spinal alignment in automotive seating postures for both men and women.

In the past, whole spinal alignments have been studied through medical imaging data, either in a standing (Hardacker et al., 1997; Janssen et al., 2009; Ames et al., 2013; Park et al., 2013) or supine position (Parenteau et al., 2014). To be relevant for traffic safety research, it is important that spinal alignments are characterized in postures representative for male and female automotive occupants (hereafter referred to as automotive seating postures) (Chabert et al., 1998; Klinich et al., 2004, 2012; Reed and Jones, 2017; Sato et al., 2017, 2019; Izumiyama et al., 2018). Chabert et al. (1998) showed the whole spinal alignment of an automotive seating posture for one male human cadaver. Klinich et al. (2004, 2012) and Reed and Jones (2017) analyzed cervical spinal alignments in one automotive seating posture with a 19° seat back angle for 180 male and female volunteers. Recently, Sato et al. (2017, 2019) investigated representative spinal alignments from C2 to the sacrum and the relationship between the cervical, thoracic and lumbar spinal alignment for male and female volunteers in one automotive seating posture with a 20° seat back angle, as described above. However, as these studies only investigated a single automotive seating posture, it remains to be determined how different seat back inclinations affect initial whole spinal alignment for both male and female automotive occupants.

The purpose of this study was to investigate the effect of seat back inclination on the spinal alignment of automotive seating postures for both men and women. This study targeted a 20° seat back angle, which has been investigated in our previous studies (Sato et al., 2017, 2019), and a 25° seat back angle, which is used in car crash tests (SAE Standard J826, 2015). In addition, spinal alignments in automotive seating postures were compared with supine postures to provide information about spinal alignment in reclined automotive seating postures for highly automated vehicles. Spinal alignment of a standing posture was also compared with obtain fundamental knowledge of spinal alignment based on previous studies in the medical field.

MATERIALS AND METHODS

The effect of seat back inclination on spinal alignment was investigated by comparing automotive seating postures in 20° and 25° seat back angles and standing and supine postures.

The spinal columns of volunteers in the seating, standing, and supine postures were scanned in an upright open magnetic resonance imaging (MRI) system. The MRI dataset of the automotive seating posture in the 20° seat back angle for eight female and seven male subjects, as listed in Groups 1 and 2 in **Table 1**, were obtained from our previous study (Sato et al., 2017). The automotive seating posture with the 20° seat back angle was set to the same seating posture and the same seat configuration as in a series of volunteer rear impact sled tests (Ono et al., 2006). The volunteers in Groups 1 and 2 were also subjected to MRI scans in standing and supine postures. Additional MRI datasets were acquired for three female and five male subjects, Group 3 in **Table 2**, in the automotive seating postures with the 20° and 25° seat back angles and standing and supine postures. The seat back angle of 25° was applied based on the crash test dummy positioning (SAE Standard J826, 2015).

Spinal alignments were extracted from the MRI dataset. To visually describe the overall trend of spinal alignment, representative patterns of spinal alignment in each posture, including average gender-specific spinal alignments, were analyzed with multidimensional scaling (MDS), presenting a distribution map (Cox and Cox, 2000; Mochimaru and Kouchi, 2000; Borg and Groenen, 2005; Miyazaki et al., 2005), as described in Section Spinal Alignment Patterns and in detail in our previous study (Sato et al., 2017). The variation in spinal alignment due to individual differences in each posture was studied through MDS analyses, and the average gender-specific spinal alignments were compared between postures.

Spinal segmental angles were measured on the MRI dataset in order to analyse the spinal alignment similar to a commonly used method in previous publications (Rocabado, 1983; Harrison et al., 2000; Berthonnaud et al., 2005; Roussouly et al., 2005; Armijo-Olivo et al., 2006; Mac-Thiong et al., 2007; Park et al., 2015), as described in section Spinal Segmental Angles. To look at the overall trend in spinal alignment from the perspective of the spinal segmental angles, correlations between the spinal segmental angles were analyzed. Thereafter, spinal segmental angles were compared between postures.

All procedures have been approved by the Ethical Committee of Shiga University of Medical Science in Japan, Hospital Universitario HM Montepríncipe (Fundación de Investigación HM Hospitales) in Spain, Japan Automobile Research Institute, and Tokyo Institute of Technology in Japan.

Human Subjects

Subjects comprised a total of 11 female, and 12 male volunteers divided into three groups, as listed in **Table 1**. The age of the subjects ranged from 21 to 38 years averaging at 27 years. None of the subjects had any known history of spinal injury. The target height and weight [average ± SD (SD)] for selecting the Japanese subjects were based on the average Japanese female and male body sizes for 20–40 year-olds; 159 ± 5 cm and 51

TABLE 1 | Test groups and subjects.

Group ID	Seatback angle (deg)	Posture	Sex	No. of subjects	Height (cm)	Weight (kg)
1 (Japanese)	20	Supine	Female	5	159.9 (5.3)	47.8 (6.1)
			Male	3	171.4 (0.7)	64.5 (4.9)
2 (European)	20	Standing, Supine	Female	3	162.3 (4.4)	58.3 (2.3)
			Male	4	175.2 (0.5)	77.7 (4.5)
3 (European)	20, 25	Standing, Supine	Female	3	162.7 (2.1)	58.3 (3.2)
			Male	5	175.8 (1.6)	78.0 (3.5)

Average and SD in brackets.

TABLE 2 | Angular measurements of spinal segments.

Angular measurements	Description
Cervical curvature (CC)	Angle between C2 and C7 (Harrison et al., 2000)
T1 slope (TS)	Angle of T1 from the horizontal line (Rocabado, 1983; Armijo-Olivo et al., 2006; Park et al., 2015)
Total thoracic kyphosis (TTK)	Angle between T1 and T12 (Rocabado, 1983; Armijo-Olivo et al., 2006; Park et al., 2015)
Upper thoracic kyphosis (UTK)	Angle between T1 and T4 (Rocabado, 1983; Armijo-Olivo et al., 2006; Park et al., 2015)
Lower thoracic kyphosis (LTK)	Angle between T4 and T12 (Rocabado, 1983; Armijo-Olivo et al., 2006; Park et al., 2015)
Lumbar lordosis (LL)	Angle between L1 and sacrum (Rocabado, 1983; Armijo-Olivo et al., 2006; Park et al., 2015)
Sacral slope (SS)	Angle of sacrum from the horizontal line (Rocabado, 1983; Armijo-Olivo et al., 2006; Park et al., 2015)

$\pm$ 6 kg for women and 172 $\pm$ 6 cm and 67 $\pm$ 9 kg for men (Ministry of Education, 2013). For European subjects, the target height and weight were defined based on the 50th percentile female and male body sizes, as reported in the University of Michigan Transportation Research Institute study (Schneider et al., 1983); 161.8 cm and 62.3 kg for women and 175.3 cm and 77.3 kg for men.

MRI Acquisition

A non-metallic seat, designed to correspond to the seat of the volunteer sled tests (Ono et al., 2006) was installed in an upright open MRI system, Signa SP2 (GE Healthcare Inc., Madison, WI) at Shiga University of Medical Science and in a Fonar Upright Multi-Position MRI system (Fonar Inc., Melville, NY) at Hospital Universitario HM Montepríncipe. The seat consisted of two flat plates with a 20° or 25° seat back angle from the vertical plane and a 10° seat pan angle from the horizontal plane. As per the procedure in the sled tests (Ono et al., 2006), subjects were instructed to sit on the seat deeply, face forward in a relaxed manner, keeping physical contact from the pelvic level up to the shoulder blades against the seat back. The head was held such that the Frankfort plane angle was ∼10° upward from the horizontal plane. The femur lines, defined from the great trochanter to the knee joint center of rotation, were tilted at 25° upward from the horizontal plane. Similarly, subjects were instructed to stand straight and face forward in a relaxed manner for the standing posture, keeping the head with the Frankfort plane angle of ∼10° upward from the horizontal plane. For the supine posture, subjects were laid straight on their back on a flat horizontal table. The main acquisitions were carried out with a T1-weighted 3D gradient echo sequence in the sagittal plane. Due to the limitation of the field of view, the full spinal column was scanned in three or four serial images with enough overlap to cut off geometric warping of images at the edge of the field. The volunteer's position in the MRI system was adjusted to fit the field of view for each scan. All MRI scans were conducted at Shiga University of Medical Science for the Japanese subjects and Hospital Universitario HM Montepríncipe for the European subjects.

Spinal Alignment Patterns

Spinal alignments in this study were presented with the geometrical centers of the vertebral bodies in midsagittal images, as shown in **Figure 1**. For C2 and the sacrum, the midpoint of the inferior and superior surface of the vertebral body was used, respectively. The coordinates of these points, used to define spinal alignments, were extracted with the medical imaging software OsiriX (Pixmeo, Geneva, Switzerland). After that, spinal alignments were normalized by the C2-sacrum length and rotated around the sacrum, defined as the origin to move C2 to 1 on the normalized vertical axis.

Spinal alignment patterns were investigated with MDS (Cox and Cox, 2000; Mochimaru and Kouchi, 2000; Borg and Groenen, 2005; Miyazaki et al., 2005). MDS is a statistical method for high-dimensional data to create a distribution map, visualizing similarities between investigated objects by relative positions in reduced data dimensions, generally two or three dimensions less (Cox and Cox, 2000).

A distance matrix D in Equation 1, applied as the input data for an MDS analysis, comprised all possible inter-individual distances between two subjects. The inter-individual distance between subjects S and T, e_{st} in Equation (2) was represented as the sum of squared Euclidean pairwise distances between corresponding vertebral points s_i and t_i in the normalized

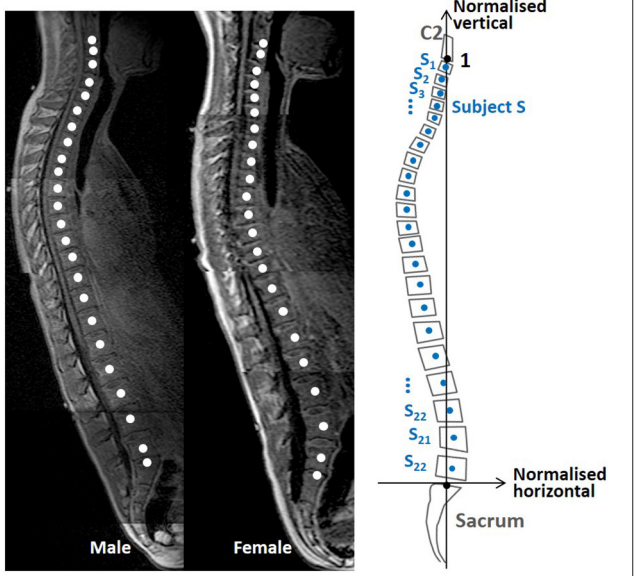

FIGURE 1 | Magnetic resonance imaging data spinal alignment and transfer to a normalized coordinate system.

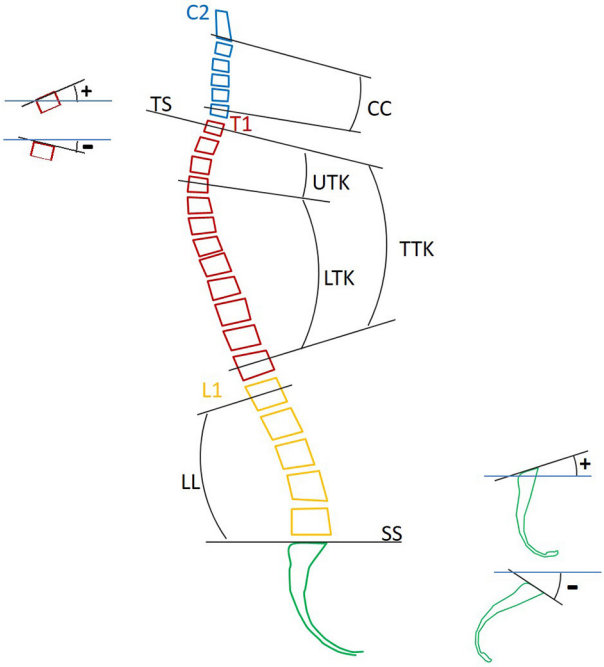

FIGURE 2 | Definitions of the angular measurements for the spinal segments.

coordinate system.

$$D = \begin{pmatrix} e_{11} & \cdots & e_{1n} \\ \vdots & \ddots & \vdots \\ e_{n1} & \cdots & e_{nn} \end{pmatrix} \quad (1)$$

$$e_{st} = \sum_{i=1}^{22} (s_i - t_i)^2 \quad (2)$$

where n means the *nth* subject, i means the *ith* vertebra from C3 to L5. s_i and t_i mean subject S or T's *ith* vertebral point containing normalized horizontal and vertical coordinates, a total of 22 points for each subject. By conducting MDS on the distance matrix D, a two-dimensional distribution map of the spinal alignments was obtained, identifying the two MDS dimensions with the largest inter-subject variance in spinal alignment.

In the distribution map, four spinal alignments were estimated as representative spinal alignments for each posture at the intersections of the 50% probability ellipse and the axes of the two MDS dimensions to describe underlying spinal alignment patterns indicated by each MDS dimension. Those spinal alignments were calculated by the weighted average of spinal alignments to minimize the difference between the MDS score of each estimated spinal alignment and the intersection. Similarly, average gender-specific spinal alignments were estimated at the average points for female and male subjects.

Spinal Segmental Angles

In accordance with previous investigations on spinal segmental angles (Rocabado, 1983; Harrison et al., 2000; Berthonnaud et al., 2005; Roussouly et al., 2005; Armijo-Olivo et al., 2006; Mac-Thiong et al., 2007; Park et al., 2015), the spinal segmental angles illustrated in **Figure 2** and **Table 2** were measured based on the vertebral angles in midsagittal images of the MRI data using the medical imaging software OsiriX (Pixmeo, Geneva, Switzerland). The spinal segmental angles measured in this study are cervical curvature (CC), T1 slope (TS), total thoracic kyphosis (TTK), upper thoracic kyphosis (UTK), lower thoracic kyphosis (LTK), lumbar lordosis (LL), and sacral slope (SS). In this study, each vertebral angle was defined as the angle of the median plane between the superior and inferior surface of the vertebral body on the midsagittal plane. The angle of the inferior and superior surfaces was used for C2 and the sacrum, respectively. The positive angle indicates a lordotic curvature or upward angle from the horizontal plane, while the negative angle indicates a kyphotic curvature or downward angle from the horizontal plane. For each segmental angle, the average and SD were obtained.

RESULTS

Spinal Alignment Patterns

Automotive Seating Postures in the 20° and 25° Seat Back Angles

The distribution maps of spinal alignments in the 20° and 25° seat back angles are illustrated in **Figures 3A**, **4A**. For the 20° seat back angle, the contribution ratio is 62.5% for the first MDS dimension, 31.0% for the second MDS dimension, 4.0% for the third MDS dimension, and 1.9% for the fourth MDS dimension. Limiting the distribution map of spinal alignments to the first two MDS dimensions captured 93.5% of the total inter-subject

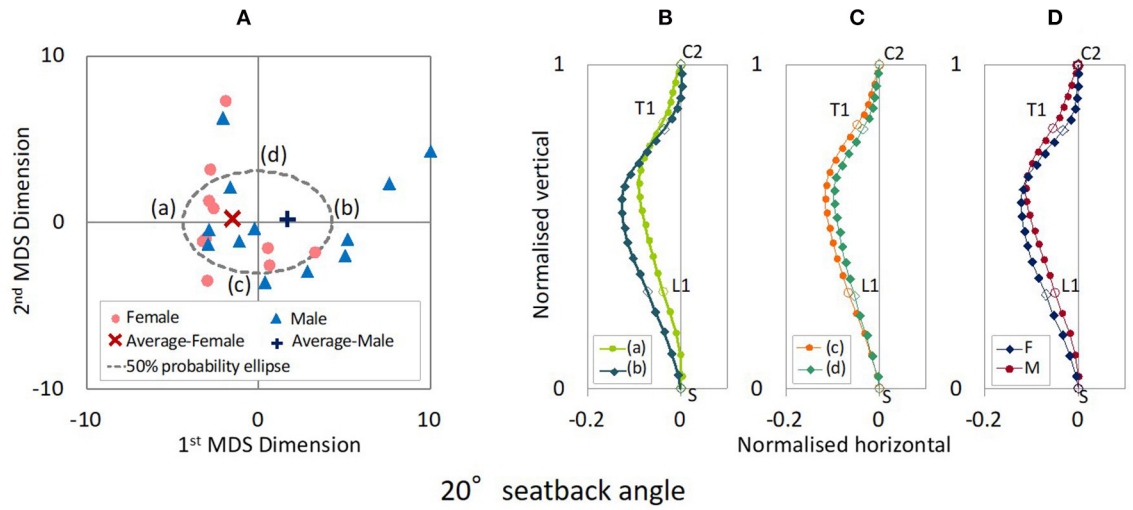

FIGURE 3 | (A) MDS distribution map of spinal alignments for the 20° seatback angle. **(B)** Spinal alignments estimated at the intersections of the 50% probability ellipse with the 1st MDS dimension (a,b) and **(C)** the 2nd MDS dimension (c,d), and **(D)** the female and the male average points (F and M).

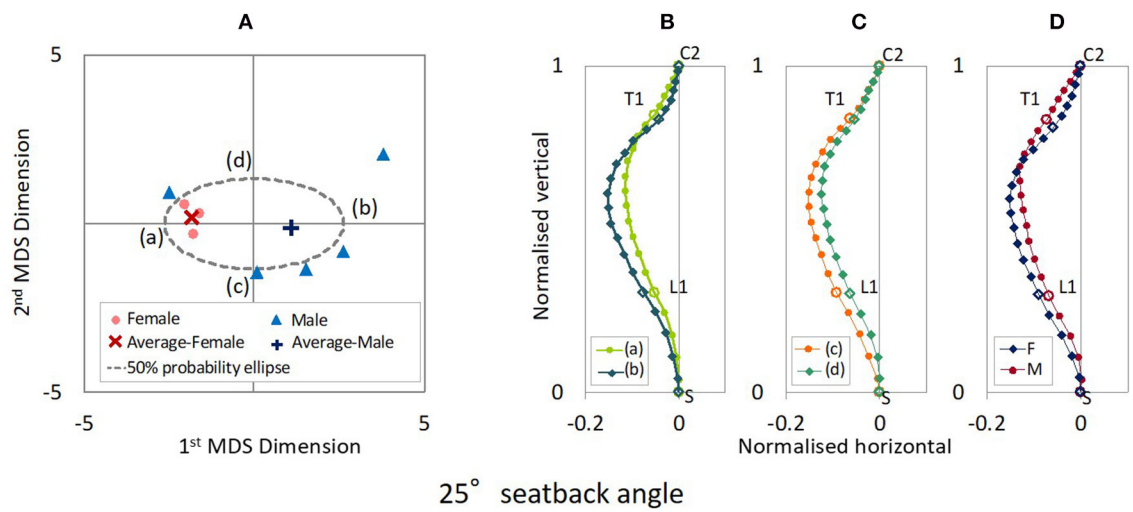

FIGURE 4 | (A) MDS distribution map of spinal alignments for the 25° seatback angle. **(B)** Spinal alignments estimated at the intersections of the 50% probability ellipse with the 1st MDS dimension (a,b) and **(C)** the 2nd MDS dimension (c,d), and **(D)** the female and the male average points (F and M).

variance. For the 25° seat back angle, the first to fourth MDS dimensions explained 72.0, 18.2, 8.5, and 1.1% of the total inter-subject variance, respectively. The two-dimensional distribution map consisting of the first two MDS dimensions captured 90.2% of the total inter-subject variance.

Figures 3B,C shows the spinal alignments estimated at the intersection of the 50% probability ellipse with the axes of the first and second MDS dimensions for the 20° seat back angle. The first MDS dimension explains the maximum variance of spinal alignment. Along the first MDS dimension, spinal alignment varies between an almost straight cervical and less kyphotic thoracic spine to a lordotic cervical and more pronounced kyphotic thoracic spine, comparing the spinal alignment (a) and (b) in **Figure 3B**. The second maximum variance of spinal alignment along the second MDS dimension illustrated that spinal alignment varies the thoracic spine between a rearward to a forward position with similar cervical spinal alignment, comparing the spinal alignment (c) and (d) in **Figure 3C**. The estimated average spinal alignment for each gender is shown in **Figure 3D**. On the distribution map, the average MDS point was located on the left side against the origin for female subjects and the right side for male subjects along the first MDS dimension, while the average MDS score of the second MDS dimension was close to zero for both genders. Hence, the estimated

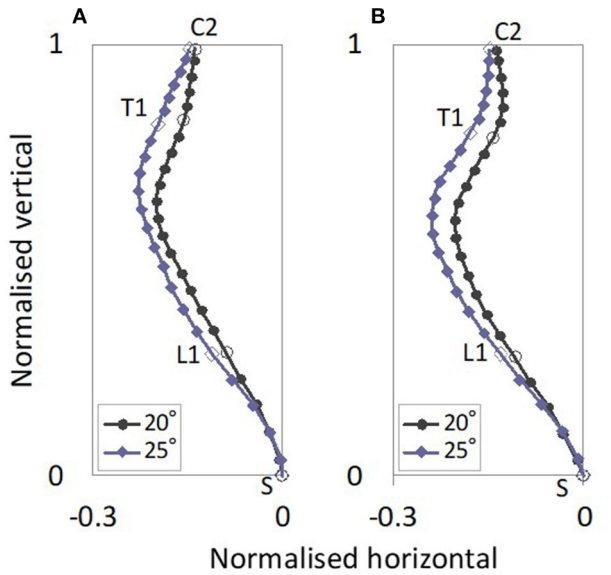

FIGURE 5 | Average gender-specific spinal alignments with 20° and 25° seat back angles. The average gender-specific spinal alignments were rotated back to the original position by average rotational angles for the female and male subjects in each posture, obtained in the normalization of the spinal alignment. **(A)** Female, **(B)** Male.

average gender-specific spinal alignments illustrated the variation indicated along the first MDS dimension, an almost straight cervical and less-kyphotic thoracic spine for the female subjects, and a lordotic cervical and more pronounced kyphotic thoracic spine for the male subjects. Similar trends in spinal alignment patterns were observed in the variation of spinal alignment for the 25° seat back angle as for the 20° seat back angle, as shown in **Figure 4**.

The estimated average gender-specific spinal alignments are shown in **Figure 5**. For both the female and male subjects, the spinal alignments in the 25° seat back angle were located rearward of the spinal alignments in the 20° seat back angle from L2 to C2, and came close at C2, exhibiting a similar spinal alignment pattern to that with the 20° seat back angle.

Standing and Supine Postures

The distribution map of spinal alignments in the standing posture is shown in **Figure 6A**. The first to fourth MDS dimensions explained 61.7, 22.2, 14.7, and 1.1% of total inter-subject variance, respectively. The two-dimensional distribution map consisting of the first two MDS dimensions captured 83.9% of the total inter-subject variance.

The estimated spinal alignments at the intersection of the 50% probability ellipse with the axes of the first and second MDS dimensions for the standing posture are illustrated in **Figures 6B,C**. To understand the maximum variance of spinal alignment illustrated by the first MDS dimension, the estimated spinal alignment (a) and (b) in **Figure 6B** were compared. Along the first MDS dimension, spinal alignment varies between the combination from a less kyphotic thoracic and lordotic lumbar spine with a slightly kyphotic cervical spine to a more pronounced kyphotic thoracic and lordotic lumbar spine with a lordotic cervical spine. The second maximum variance of spinal alignment along the second MDS dimension illustrated that thoracolumbar spinal alignments vary between straighter to more pronounced S-shape spine with similar cervical spinal alignment, comparing the spinal alignment (c) and (d) in **Figure 6C**. On the distribution map, the average MDS point was located on the left side against the origin for female subjects and the right side for male subjects, along the first MDS dimension. Hence, the estimated average gender-specific spinal alignments were in line with the trend observed along the first MDS dimension, as shown in **Figure 6D**.

The distribution map of spinal alignments in the supine posture is shown in **Figure 7A**. The first to fourth MDS dimensions explained 53.4, 25.5, 19.9, and 0.9% of total inter-subject variance, respectively. The two-dimensional distribution map consisting of the first two MDS dimensions captured 78.9% of the total inter-subject variance.

The estimated spinal alignments at the intersection of the 50% probability ellipse with the axes of the first and second MDS dimensions for the supine posture are illustrated in **Figures 7B,C**. Comparing the spinal alignment (a) and (b) in **Figure 7B**, the maximum variance of spinal alignment illustrated along the first MDS dimension that spinal alignment varies between a straighter cervicothoracic spine to a more pronounced kyphotic thoracic spine. Along the second MDS dimension, the second maximum variance of spinal alignment illustrated that spinal alignment varies between straighter to more pronounced S-shape thoracolumbar spine with, comparing the spinal alignment (c) and (d) in **Figure 7C**. The estimated average spinal alignment for each gender is shown in **Figure 7D**. The average MDS point on the distribution map shown in **Figure 7**a was located on the lower side against the origin for female subjects and the upper side for male subjects, along the second MDS dimension. Consequently, the estimated average gender-specific spinal alignments were consistent with the trend observed along the second MDS dimension, as shown in **Figure 7D**.

The estimated average gender-specific spinal alignments of the standing and supine postures, comparing spinal alignments of the automotive seating posture in the 20° and 25° seat back angle, are shown in **Figure 8**. For both the female and male subjects, the cervical and upper thoracic spine exhibited similar spinal alignment in the four postures, whereas the lumbar spine showed more pronounced lordosis for the standing and supine postures than for the seating postures.

Spinal Segmental Angles

Correlations Between Spinal Segmental Angles

Correlations between the spinal segmental angles were looked at, obtaining the Pearson product–moment correlation coefficients.

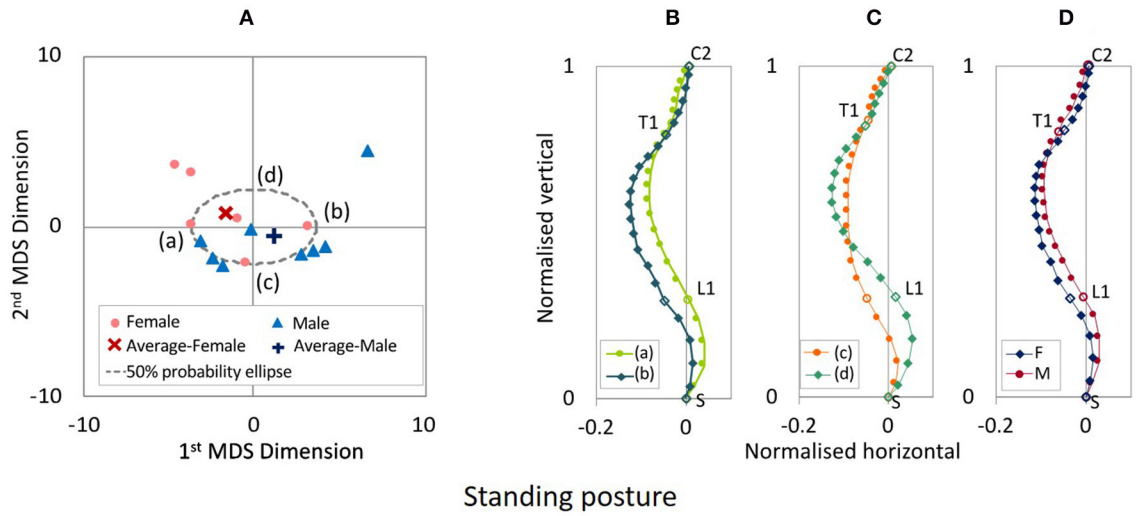

FIGURE 6 | (A) MDS distribution map of spinal alignments for the standing posture. **(B)** Spinal alignments estimated at the intersections of the 50% probability ellipse with the 1st MDS dimension (a,b) and **(C)** the 2nd MDS dimension (c,d), and **(D)** the female and the male average points (F and M).

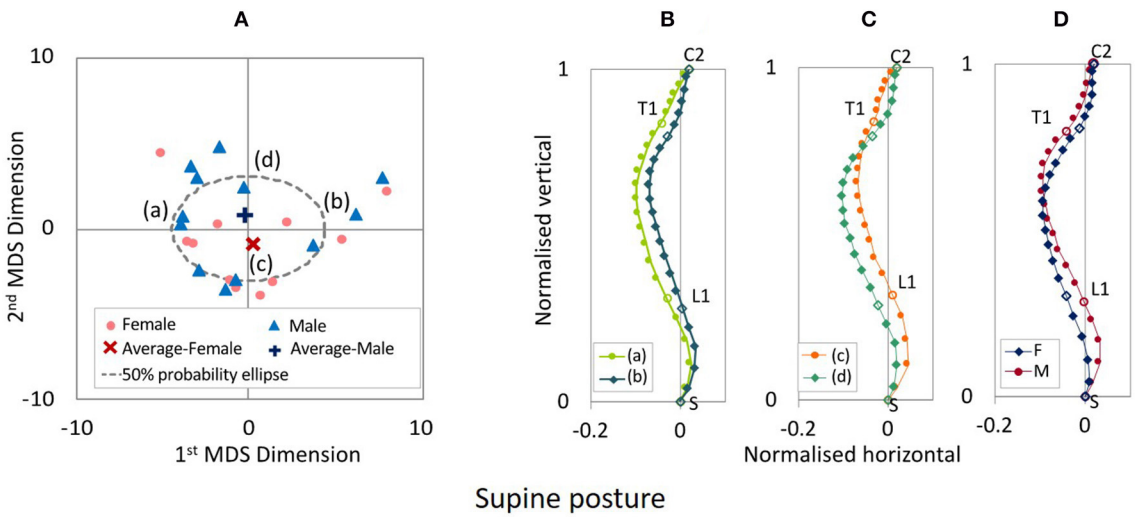

FIGURE 7 | (A) MDS distribution map of spinal alignments for the supine posture. **(B)** Spinal alignments estimated at the intersections of the 50% probability ellipse with the 1st MDS dimension (a,b) and **(C)** the 2nd MDS dimension (c,d), and **(D)** the female and the male average points (F and M).

The Pearson product–moment correlation coefficient between the spinal segmental angles is summarized in **Table 3** and **Figure 9**. For the automotive seating posture in the 20° and 25° seat back angles, correlations were observed between CC, TS, and TTK and between LL and SS. There was no correlation seen between cervicothoracic segmental angles and lumber segmental angles in this study. On the other hand, the standing posture had correlations between CC, TS and TTK, and between TTK and LL. For the supine posture, correlations were found between TS and TTK and between LL and SS.

Automotive Seating Postures in the 20° and 25° Seat Back Angles

The spinal segmental angles for the automotive seating postures are summarized in **Figure 10**. Subjects were categorized into two groups, according to the major trend of the spinal alignment patterns for the seating postures observed in the MDS analysis, based on gender and CC (cervical lordosis with positive values of CC or cervical kyphosis with negative values of CC). CC varied within the male and female groups for both seat back angles; negative CC (kyphotic) for nine females and six males and positive CC (lordotic) for two

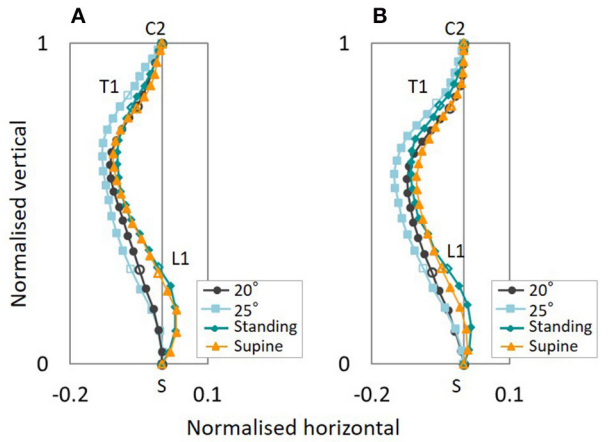

FIGURE 8 | Average gender-specific spinal alignments for the standing and supine postures, comparing the automotive seating posture with the 20° and 25° seat back angle. **(A)** Female, **(B)** Male.

TABLE 3 | Pearson product–moment correlation coefficient R between the spinal segmental angles.

	CC	TS	TTK	LL
(1) Automotive seating posture with the 20° seat back angle				
TS	−0.77	–	–	–
TTK	−0.65	0.84	–	–
LL	0.11	−0.17	−0.41	–
SS	0.02	0.03	0.10	−0.87
(2) Automotive seating posture with the 25° seat back angle				
TS	−0.90	–	–	–
TTK	−0.89	0.98	–	–
LL	0.14	−0.21	−0.29	–
SS	0.01	0.01	−0.01	−0.82
(3) Standing posture				
TS	−0.70	–	–	–
TTK	−0.60	0.92	–	–
LL	−0.25	−0.49	−0.72	–
SS	0.01	0.33	−0.22	−0.49
(4) Supine posture				
TS	−0.48	–	–	–
TTK	−0.23	0.82	–	–
LL	−0.47	−0.19	−0.50	–
SS	0.48	0.14	0.24	−0.88

females and six males in the 20°seat back angle, and negative CC (kyphotic) for two females and two males, and positive CC (lordotic) for one female and three males in the 25° seat back angle.

In the groups of subjects based on positive and negative CCs, as shown in **Figure 10B**, significant differences were observed for both the 20° and 25° seat back angles in CC, TS, TTK, and LTK. The absolute average values of TS, TTK, and LTK were greater for subjects with positive CCs (lordotic) than subjects with negative CCs (kyphotic). When comparing the 20° and 25° seat back angles, the absolute average value of TTK was significantly greater for the 25° seat back angle and showed the most prominent influence of seat back inclination on spinal alignment for subjects with positive CCs (lordotic). TS and UTK indicated similar angles in both the 20°and 25° seat back angles in each group. Hence, the effect of seat back inclination may be observed most predominantly in LTK.

Likewise, for both genders, as shown in **Figure 10A**, the absolute values of average TTK and LTK were relatively greater for the 25° seat back angle compared with the 20° seat back angle, even though no significant difference was observed between the two seat back angles. In comparing genders, a significant difference was observed in TS for the 20° seat back angle, and the absolute values of average TS, TTK, and LTK were greater for the male subjects than the female subjects in both the 20°and 25° seat back angles. The female subjects in this study tended to negative CC (kyphotic). Findings observed between spinal alignments with positive CCs (lordotic) and negative CCs (kyphotic) may affect differences in the average gender-specific spinal alignment.

Standing and Supine Postures

The spinal segmental angles for the standing and supine postures are summarized in **Figure 11**. Subjects were grouped based on gender and CC in a similar way to the automotive seating postures. CC varied within the male and female groups; negative CC (kyphotic) for five females and one male and positive CC (lordotic) for one female and seven males for the standing posture, and negative CC for eight females and six males, and positive CC for three females and six males for the supine posture.

In groups separating subjects into positive CC or negative CC, as shown in **Figure 11B**, significant differences were found in CC, TS, TTK, UTK, LTK for the standing posture, and CC, TS, LL, and SS for the supine posture. The absolute average values of TS, TTK, UTK, and LTK were greater for subjects with positive CCs (lordotic) than subjects with negative CCs (kyphotic) for both the postures. When comparing the spinal alignments in the two postures, the absolute values of average LTK were significantly greater for the standing posture than for the supine posture for subjects with both positive and negative CCs.

For both genders, as shown in **Figure 11A**, the absolute values of average LTK were significantly greater for the standing posture compared with the supine posture. In comparing genders, significant differences were observed in CC, TS, and LTK, and the absolute values of average TS and LTK were greater for the male subjects than the female subjects in both postures. Since the female subjects in this study tended toward negative CC (kyphotic), differences observed between spinal alignments with positive CCs and negative CCs (kyphotic) may affect the average gender-specific spinal alignment.

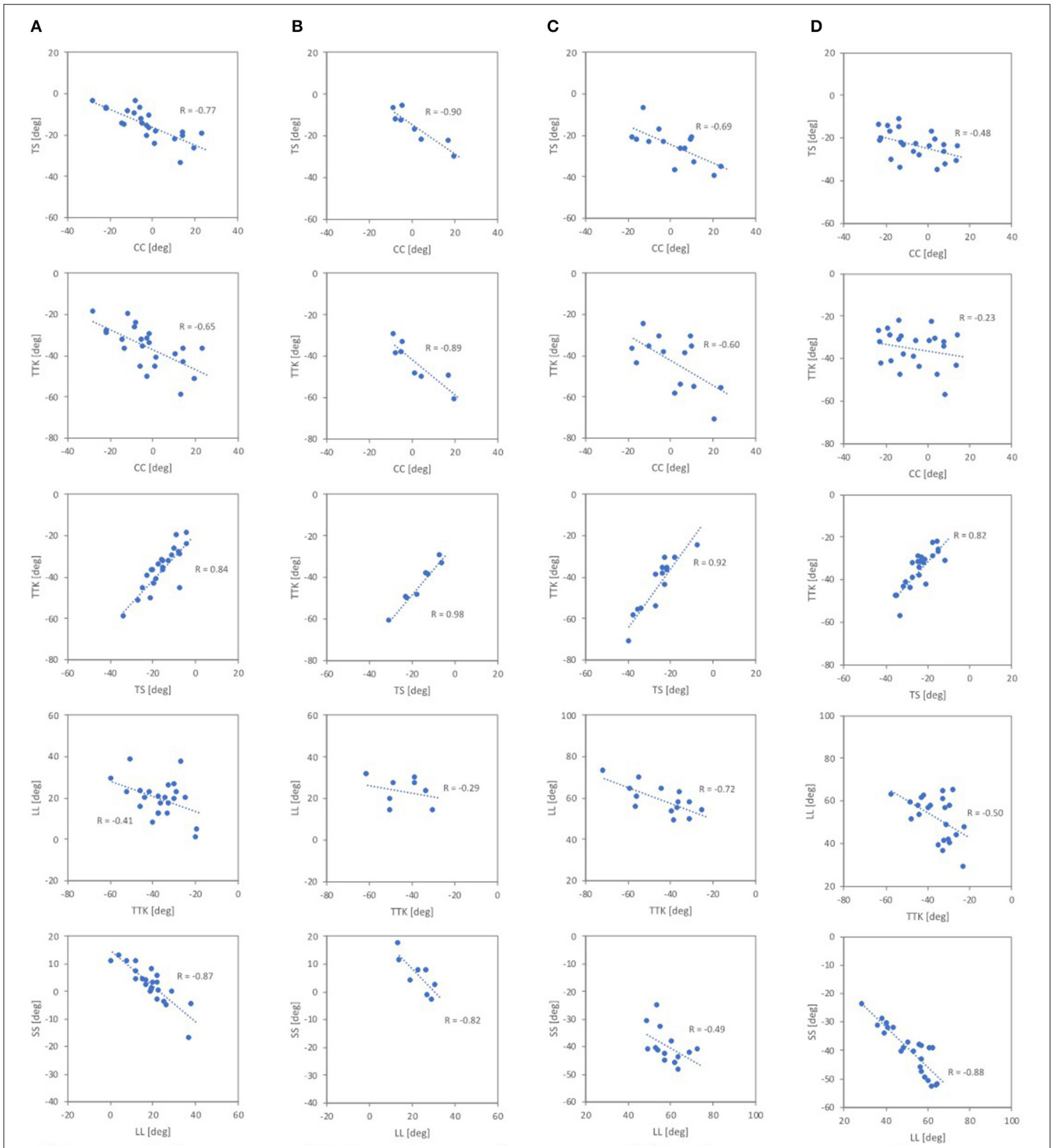

FIGURE 9 | Correlations between the spinal segmental angles. **(A)** 20° seat back angle, **(B)** 25° seat back angle, **(C)** standing, **(D)** supine.

Figure 12 illustrates differences in the seating posture with the seat back at 20° and the standing or supine posture. The prominent differences were found in LL and SS, followed by TS for both the postures. For the standing posture, the difference from the seating posture with the 20° seat back was significantly greater in LTK than for the supine posture, leading to more pronounced kyphosis in TTK, particularly for the male subjects and subjects with positive CCs (lordotic).

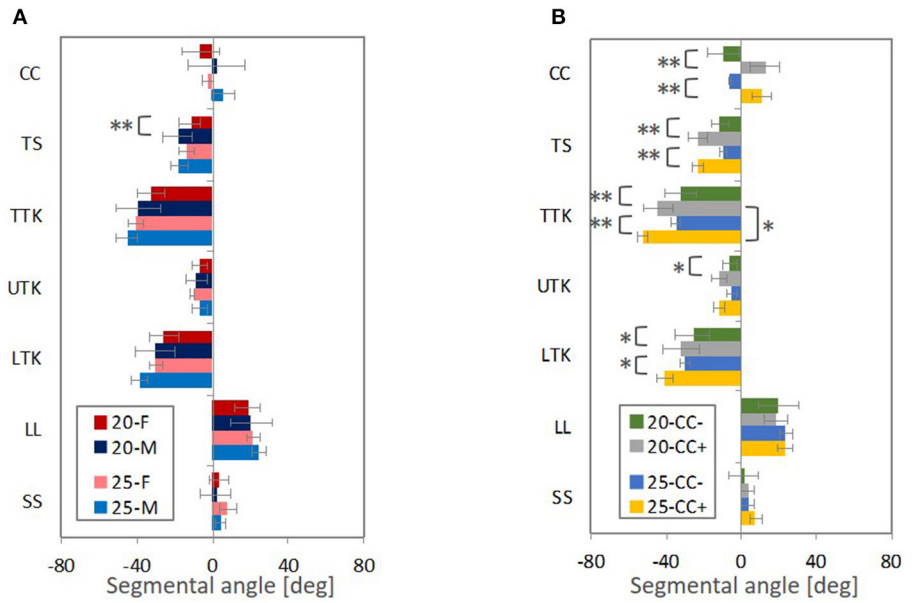

FIGURE 10 | The average segmental angles with standard deviation and *p*-value from *t*-test (** < 0.05, *<0.1), **(A)** comparing male and female subjects (M and F) and **(B)** the negative CC (CC−) and positive CC (CC+). Figures in legends indicate the seat back angles from the vertical line.

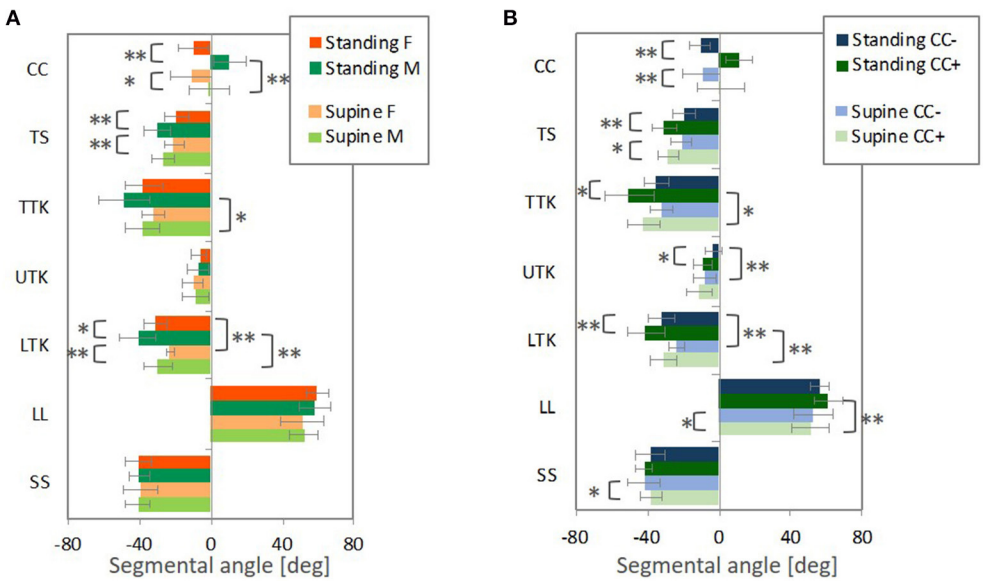

FIGURE 11 | The average segmental angles with standard deviation and *p*-value from *t*-test (** < 0.05, * < 0.1), **(A)** comparing male and female subjects (M and F) and **(B)** the negative CC (CC−) and positive CC (CC+).

DISCUSSIONS

Spinal Alignment in Automotive Seating Postures

The effect of seat back inclination on spinal alignment was investigated, comparing representative spinal alignment patterns in automotive seating postures with the seat back at 20° and 25° angles and standing and supine postures through MDS analyses on a data set of spinal alignment. The results of the MDS analysis indicated that the first MDS dimension, illustrating the maximum inter-subject variance, accounted for 62.5% of the total inter-subject variance of spinal alignments for the automotive seating posture with the 20° seat back angle, 72.0% for the 25° seat back angle, 61.7% for the standing posture and 53.4% for the supine posture, respectively. The first MDS dimension can explain a major part of the variety in spinal alignment for each posture. Since MDS detects meaningful underlying dimensions

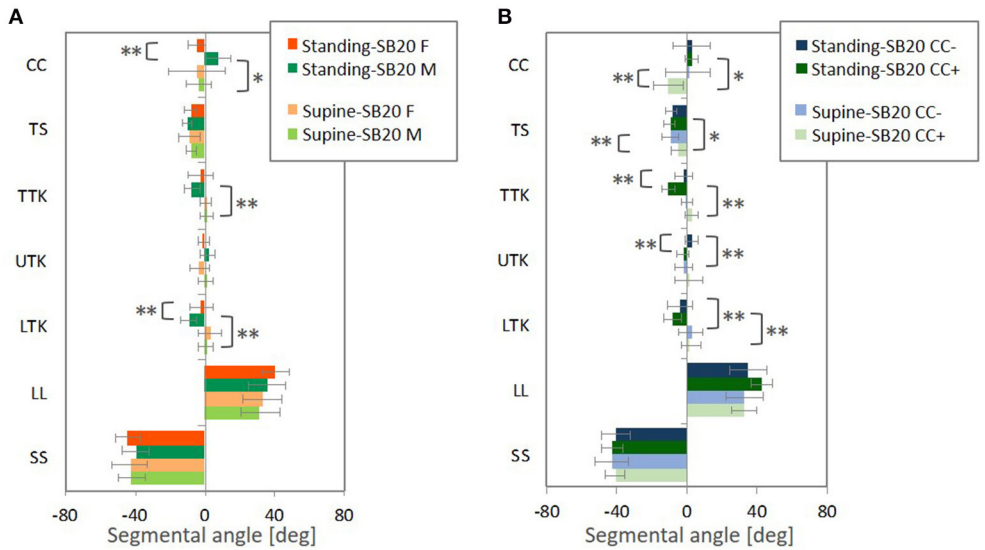

FIGURE 12 | The average with standard deviation and *p*-value from *t*-test (** < 0.05, * < 0.1) for differences of the segmental angles in the standing and supine postures relative to the seating posture with the 20° seatback angle, **(A)** comparing male and female subjects (M and F) and **(B)** the negative CC (CC−) and positive CC (CC+). Differences were calculated by subtracting the segmental angles in the seating posture from the segmental angles in the standing or supine posture, individually.

in a data set, spinal alignment patterns can be classified by applying an MDS analysis on a set of spinal alignment data (Mochimaru and Kouchi, 2000; Miyazaki et al., 2005). On a distribution map obtained by the MDS analysis, spinal alignments at the intersection of the 50% probability ellipse with the axes of the two MDS dimensions were estimated to interpret underlying spinal alignment patterns portrayed along each MDS dimension.

Comparing the estimated spinal alignments of the automotive seating postures along the axis of the first MDS dimension (**Figures 3B**, **4B**), the largest variance in spinal alignment due to individual differences showed a prominent relationship between the cervical and thoracic spinal alignment. The combination varies between a slight kyphotic or almost straight cervical spine with the less-kyphotic thoracic spine to lordotic cervical spine with a more pronounced kyphotic thoracic spine.

Reed and Jones (2017) reanalysed sagittal X-ray images of the head and the cervical spine, captured in a previous study by Snyder et al. (1975), of a total of 140 female and male volunteers seated on a hard seat resembling a vehicle seat. In their principal component analysis on cervical spines, the first principal component illustrated slightly kyphotic and pronounced lordotic cervical spinal alignments obtained at ± three SDs of the principal component score, respectively, with a straighter cervical spinal alignment obtained at the mean principal component score. The results are similar to the results in this study, thus supporting the observation of cervical spinal alignments on the distribution map in this study.

The correlation analysis on the spinal segmental angles of the automotive seating postures also indicated strong negative correlations between CC and TTK, as shown in **Table 3** (1) and (2) and **Figures 9A,B**. The MDS analyses and the correlation analyses supported a similar trend (cervical lordosis occurred with more pronounced thoracic kyphosis than cervical kyphosis). According to findings through the MDS analyses of the spinal alignment and the correlation analysis of the spinal segmental angles, spinal alignments were classified into two groups based on the CC angle in the investigation of spinal segmental angles. The absolute values of the average TS, TTK, and LTK angles were significantly greater for subjects with positive CC (lordotic) than subjects with negative CC (kyphotic) for both the 20° and 25° seat back angles, as shown in **Figure 10B**. In line with this, the influence of the seat back inclination on the spinal segmental angles was greater for subjects with positive CC (lordotic) than subjects with negative CC (kyphotic), indicating the most prominent influence in TTK. The comparison of the spinal alignments of the automotive seating postures estimated at the intersections of the 50% probability ellipse with the axis of the first MDS dimension on the distribution map (**Figures 3B**, **4B**) illustrated those findings observed in the spinal segmental angles.

For the cervicothoracic region, previous studies on spinal alignment have reported that cervical lordosis tends to have a more pronounced thoracic kyphosis (Hardacker et al., 1997; Erkan et al., 2010; Ames et al., 2013; Endo et al., 2016) with greater C7 (Endo et al., 2016) and T1 inclination (Ames et al., 2013; Lee et al., 2014; Park et al., 2015) in the standing posture. Conversely, cervical kyphosis tends to have a less-kyphotic thoracic spine with smaller C7 and T1 inclination. T1 inclination has been suggested as a predictor of whole spinal alignment in the standing posture due to relationships along

the cervical, thoracic and lumbar spines (Knott et al., 2010; Jun et al., 2014; Lee et al., 2015). In this study, the spinal alignment of the standing posture demonstrated consistency with these previous findings, as shown in **Figures 6B**, **11**, and **Table 3** (3). Spinal alignment trends in the automotive seating postures were similar to the previous findings in the standing posture. However, in **Figure 12**, differences of spinal alignment between the seating and standing postures were seen in TS and TTK including LTK, slightly in CC, due to maintaining spinal balance in the seating and standing postures, respectively.

For the lumbar region, the average LL angle indicated a similar value between subjects with positive CC (lordotic) and negative CC (kyphotic) in both the 20° and 25° seat back angle conditions, as shown in **Figure 10B**. The comparison of the spinal alignments estimated at the intersections of the 50% probability ellipse with the axis of the first MDS dimension on the distribution map (**Figures 3B**, **4B**) does not illustrate a pronounced difference in the lumbar spine, such as in the cervical and thoracic spine. In addition, CC, TS, and TTK do not correlate with LL, as described in **Table 3** (1) and (2).

Previous studies have reported that cervical lordosis tends to have a more pronounced thoracic kyphosis and less lumbar lordosis due to maintaining spinal balance in the standing posture (Gore et al., 1986; Roussouly and Pinheiro-Franco, 2011; Ames et al., 2013). On the other hand, another study has indicated that the cervical curvature does not have a prominent relationship with lumbar lordosis and sacral slope (Endo et al., 2016). Spinal alignment of the standing posture in this study demonstrated that CC had a negative correlation with TTK, and TTK also negatively correlated with LL. Consequently, cervical lordosis tends to have a more pronounced thoracic kyphosis and less lumbar lordosis, even though no correlation was found between CC and LL. As in the study by Endo et al. (2016), there was no correlation between LL and SS. Regarding the seating postures, the laboratory seat used in this study consisted of two stiff, flat plates. The subjects leaned in for good contact with the flat plane seat back along the entire back. Thus, the lumbar spine was straightened along with the seat back. Due to flexibility in the lumbar spine, this may not cause any significant difference in the lumbar spine between subjects with positive CC (lordotic) and negative CC (kyphotic) in both the 20° and 25° seat back angle conditions.

Gender Differences of Spinal Alignment

Average gender-specific spinal alignments were estimated at the average gender points on the distribution map of spinal alignment. For the automotive seating postures, the average spinal alignments include an almost straight cervical and less-kyphotic thoracic spine for the female subjects, and lordotic cervical and more pronounced kyphotic thoracic spine for the male subjects, as shown in **Figures 3D**, **4D**, **5**. The average gender-specific spinal alignments in the standing posture also illustrated these trends observed in the automotive seating posture. On the distribution map of spinal alignments (**Figures 3A**, **4A**, **6A**), the average gender-specific points were almost on the axis of the first MDS dimension, located at the left side against the origin for female subjects and the right side for male subjects, within the 50% probability ellipse. The origin indicates the average of all data. Therefore, average gender-specific spinal alignments were in line with the trend observed along the first MDS dimension, with a smaller difference than that between the estimated spinal alignments at the intersections of the 50% probability ellipse and the axis of the first MDS dimension.

In the investigation of spinal segmental angles, the average CC angle was greater for the male subjects than for the female subjects in the four postures, as shown in **Figures 10A**, **11A**. Also, the absolute values of the average TS, TTK, and LTK angles were greater for the male subjects than for the female subjects. The comparison of the estimated average gender spinal alignments (**Figures 3D**, **4D**, **6D**, **7D**) illustrated similar findings in the spinal segmental angles. However, for the automotive seating postures, only the TS in the 20° seat back angle condition indicated a significant difference between genders, whereas significant differences were observed in CC, TS, and LTK for the standing and supine postures.

As reported in previous studies on the variation in cervical spinal alignment in the standing or upright seating postures (Helliwel et al., 1994; Hardacker et al., 1997; Matsumoto et al., 1998), gender is an independent factor that correlates significantly with non-lordosis. Women are more likely to present non-lordosis (kyphotic or straight). Conversely, men present more pronounced lordosis. In this study, the average gender-specific spinal alignments in the cervical spine were almost straight for the female subjects and lordotic for the male subjects. The average CC angle was positive for the male subjects, whereas negative for the female subjects. Findings in this study correlate with previous studies.

At the cervicothoracic junction, relationships along the cervical spinal alignment, C7 or T1 inclination, and thoracic kyphosis have been investigated with focussing on gender differences (Lee et al., 2014; Park et al., 2015; Endo et al., 2016). A decrease in the C7 and T1 inclination is associated with kyphosis, or an increase in hypo-lordosis in cervical spinal alignment and less kyphosis in thoracic spinal alignment. Men tend to have greater C7 and T1 inclination (more forward-inclined C7 and T1), while women tend to have shorter C7 and T1 inclination (less forward-inclined C7 and T1). With decreasing T1 inclination, women are more likely to present a hypo-lordotic or kyphotic cervical spine and a less kyphotic thoracic spine than men. The average female spinal alignments in this study portrayed a less forward inclination around C7 and T1 displaying a straighter cervical and thoracic spine than the average male spinal alignment. The average CC angle and the absolute angles of the average TS, TTK, and LTK were smaller for female subjects than for male subjects. The gender differences observed in this study are in agreement with the above-mentioned previous studies.

Since CC of the female subjects tended to be negative, the trends observed in a comparison between subjects with negative (kyphotic) and positive (lordotic) CC (**Figures 10B**, **11B**) might affect differences between genders (**Figures 10A**, **11A**). Therefore, the average female exhibited less TS with less-kyphotic thoracic alignment and thus straighter cervicothoracic spinal alignment than the average male, despite no significant differences observed in CC, TTK, and LTK for the automotive seating postures. In addition, the influence of the seat back inclination on the spinal segmental angles was greater for subjects with positive CC (lordotic) than subjects with negative CC (kyphotic), indicating the most prominent influence in TTK, including LTK. This finding might have an impact on differences in the influence of the seat back inclination between genders. Indeed, the differences in LTK between the seating posture with the 20° seat back angle and the standing or supine posture were significantly greater for the male subjects. In the MDS analyses, the average gender-specific points were almost on the axis of the first MDS dimension on the distribution map of spinal alignment for the two seating and standing postures. Consequently, the average female point was positioned opposite the average male point across the origin, which may suggest gender as one of the factors affecting the largest inter-individual variance in spinal alignment.

The study of the lumbar region only revealed minor average gender-specific spinal alignment and LL differences. In a report by Endo et al. (2014), lumbar lordosis is significantly greater for women than men in the upright seating position, while the present study focused on an automotive seating posture instead of an upright seating posture. As mentioned in the preceding Section, subjects in this study were seated deeply on a stiff laboratory seat leaning the entire back against the flat plane seat back. This caused the lumbar spine to straighten and the seat back, showing no significant gender differences, such as in the upright seating posture.

LIMITATIONS

A limited number of subjects, in their 20s and 30s, were selected based on the average Japanese body sizes (Ministry of Education, 2013), the mid-sized female and male (Schneider et al., 1983). All subjects were close to the average body size in their gender. Due to the seat consisting of two flat plates, the spinal alignments observed in this study will likely not be affected by the seated height, although age and BMI might affect spinal alignment. A larger number of subjects will be needed to generalize spinal alignment patterns in other specific ages and body sizes.

The laboratory seat used in this study was designed to exclude the influence of seat properties (foam, frame stiffness and its distribution, etc.) and the external shape of the seat back and seat pan. This design was neutral to body size differences between individuals and genders compared with a regular car seat. However, these seat specifications may influence spinal alignment. Variations in designs of commercially available car seats would need to be considered for future studies in more realistic situations.

This study recruited only asymptomatic volunteers. Future studies could also compare the findings obtained in this study with whole spinal alignments of patients suffering from spinal pathologies. Providing the differences of whole spinal alignment between asymptomatic volunteers and patients to a human body FE model, computational simulations may show different vertebral kinematics and provide better knowledge of spinal injury mechanisms.

In addition, MRI scans take more test duration time than CT and X-rays scans. The test duration time may affect postural stability. Likewise, the duration of driving and the type of route driven may affect postural changes (Ghaffari et al., 2018), which is a topic of future study on spinal alignment of automotive seating postures.

CONCLUSIONS

The spinal alignment in the 25° seat back angle displayed more pronounced thoracic kyphosis than in the 20° seat back. The most prominent influence of seat back inclination on segmental angles appeared in TTK, including LTK when categorizing spinal alignments into two groups based on CC. The differences of TTK and LTK between the two seat back angles and between the seating posture with the 20° seat back and the standing posture were greater for spinal alignments with positive CCs than for spinal alignments with negative CCs. In this study, the female subjects tended negative CC. Some of the differences between average gender-specific spinal alignments may be explained by the findings observed in the differences between positive CC and negative CC spinal alignments.

DATA AVAILABILITY STATEMENT

The original contributions presented in the study are included in the article/supplementary material, further inquiries can be directed to the corresponding author/s.

ETHICS STATEMENT

The studies involving human participants were reviewed and approved by Ethical Committees of Shiga University of Medical Science in Japan, Hospital Universitario HM Montepríncipe (Fundación de Investigación HM Hospitales) in Spain, Japan Automobile Research Institute and Tokyo Institute of Technology in Japan. The patients/participants provided their written informed consent to participate in this study.

AUTHOR CONTRIBUTIONS

FS outlined this study. FS, SM, AF, MS, and SS conducted the MRI scans. FS and YM jointly analyzed and presented all data included in the paper. The paper was written by FS and reviewed

by all authors. All authors contributed to the article and approved the submitted version.

FUNDING

This study was supported by JSPS KAKENHI, Grant Number JP 16KK0137.

ACKNOWLEDGMENTS

The authors would like to thank J. Antona-Makoshi, H. Iguchi, J. Montero, T. Nakajima, and M. Yoshimura for their assistance with the MRI scanning and M. Odani for her assistance with analyzing spinal alignments.

REFERENCES

Ames, C. P., Blondel, B., Scheer, J. K., Schwab, F. J., Le Huec, J. C., Massicotte, E. M., et al. (2013). Cervical radiographical alignment: comprehensive assessment techniques and potential importance in cervical myelopathy. *Spine* 38, S149–S160. doi: 10.1097/BRS.0b013e3182a7f449

Armijo-Olivo, S., Jara, X., Castillo, N., Alfonso, L., Schilling, A., Valenzuela, E., et al. (2006). Comparison of the head and cervical posture between the self-balanced position and the Frankfurt method. *J. Oral Rehabil.* 33, 194–201. doi: 10.1111/j.1365-2842.2005.01554.x

Been, E., Shefi, S., and Soudack, M. (2017). Cervical lordosis: the effect of age and gender. *Spine J.* 17, 880–888. doi: 10.1016/j.spinee.2017.02.007

Berthonnaud, E., Dimmet, J., and Roussouly, P. (2005). Analysis of the sagittal balance of the spine and pelvis using shape and orientation parameters. *J. Spinal Disord. Tech.* 18, 40–47. doi: 10.1097/01.bsd.0000117542.88865.77

Borg, I., and Groenen, P. J. F. (2005). *Modern Multidimensional Scaling, 2nd Edn*. New York, NY: Springer.

Brolin, K., Östh, J., Svensson, M. Y., Sato, F., Ono, K., Linder,. A., et al. (2015). "Aiming for an average female virtual human body model for seat performance assessment in rear-end impacts," in *Enhanced Safety of Vehicles Conference* (Gothenburg).

Carstensen, T. B., Frostholm, L., Oernboel, E., Kongsted, A., Kasch, H., and Jensen, T. S. (2012). Are there gender differences in coping with neck pain following acute whiplash trauma? A 12-month follow-up study. *Eur. J. Pain* 16, 49–60. doi: 10.1016/j.ejpain.2011.06.002

Chabert, L., Ghannouchi, S., and Cavallero, C. (1998). "Geometrical characterisation of a seated occupant," in *Enhanced Safety of Vehicles Conference* (Windsor, ON).

Chapline, J. F., Ferguson, S. A., Lillis, R. P., Lund, A. K., and Williams, A. F. (2000). Neck pain and head restraint position relative to the driver's head in rear-end collisions. *Accident Anal. Prev.* 32, 287–297. doi: 10.1016/S0001-4575(99)00126-8

Cox, T. F., and Cox, M. A. A. (2000). *Multidimensional Scaling, 2nd Edn*. New York, NY: Chapman and Hall/CRC.

Deng, B., Begeman, P. C., Yang, K. H., Tashman, S., and King, A. I. (2000). Kinematics of human cadaver cervical spine during low speed rear-end impacts. *Stapp Car Crash J.* 44, 171–188. doi: 10.4271/2000-01-SC13

Dolinis, J. (1997). Risk factors for "Whiplash" in drivers: a cohort study of rear-end traffic crashes. *Injury* 28, 173–179. doi: 10.1016/S0020-1383(96)00186-6

Endo, K., Suzuki, H., Nishimura, H., Tanaka, H., Shishido, T., and Yamamoto, K. (2014). Characteristics of sagittal spino-pelvic alignment in Japanese young adults. *Asian Spine J.* 8, 599–604. doi: 10.4184/asj.2014.8.5.599

Endo, K., Suzuki, H., Sawaji, Y., Nishimura, H., Yorifuji, M., Murata, K., et al. (2016). Relationship among cervical, thoracic, and lumbopelvic sagittal alignment in healthy adults. *J. Orthopaed. Surg.* 24, 92–96. doi: 10.1177/230949901602400121

Erkan, S., Yercan, H. S., Okcu, G., and Özalp R. T. (2010). The influence of sagittal cervical profile, gender and age on the thoracic kyphosis. *Acta Orthop. Belg.* 76, 675–680. Available online at: http://www.actaorthopaedica.be/archive/volume-76/issue-5/original-studies/the-influence-of-sagittal-cervicalprofile-gender-and-age-on-the-thoracic-kyphosis/

Forman, J., Lin, H., Gepner, B., Wu, T., and Panzer, M. (2019b). Occupant safety in automated vehicles -effect of seatback recline on occupant restraint. *Int. J. Automot. Eng.* 10, 139–143. doi: 10.20485/jsaeijae.10.2_139

Forman, J., Poplin, G. S., Shaw, G., McMurry, T. L., Schmidt, K., Ash, J., et al. (2019a). Automobile injury trends in the contemporary fleet: belted occupants in frontal collisions. *Traffic Inj. Prev.* 20, 607–612. doi: 10.1080/15389588.2019.1630825

Gepber, B. D., Draper, D., Mroz, K., Richardson, R., Ostling, M., Pipkorn, B., et al. (2019). "Comparison of human body models in frontal crashes with reclined seatback," in *International Research Council on Biomechanics of Injury Conference (IRCOBI)* (Florence).

Ghaffari, G., Brolin, K., Bråse, D., Pipkorn, B., Svanberg, B., Jakobsson, L., et al. (2018). "Passenger kinematics in Lane change and Lane change with Braking Manoeuvres using two belt configurations: standard and reversible pre-pretensioner," in *International Research Council on Biomechanics of Injury Conference (IRCOBI)* (Athens).

Gore, D. R., Sepic, S. B., and Gardner, G. M. (1986). Roentgenographic findings of the cervical spine in asymptomatic people. *Spine* 11, 521–524. doi: 10.1097/00007632-198607000-00003

Hardacker, J. W., Shuford, R. F., Capicoto, P. N., and Pryor, P. W. (1997). Radiographic standing cervical segmental alignment in adult volunteers without neck symptoms. *Spine* 22, 1472–1480. doi: 10.1097/00007632-199707010-00009

Harrison, D. E., Harrison, D. D., Cailliet, R., Troyanovich, and, S. J., and Holland, B. (2000). Cobb method or harrison posterior tangent method. *Spine* 25, 2072–2078. doi: 10.1097/00007632-200008150-00011

Helliwel, P. S., Evans, P. F., and Wright, V. (1994). The Straight cervical spine: does it indicate muscle spasm? *J. Bone Joint Surg.* 76, 103–106. doi: 10.1302/0301-620X.76B1.8300650

Izumiyama, T., Nishida, N., Iwanaga, H., Chen, X., Ohgi, J., Mori, K., et al. (2018). "The analysis of an individual difference in human skeletal alignment in seated posture and occupant behavior using HBMs," in *International Research Council on Biomechanics of Injury Conference (IRCOBI)* (Athens).

Jakobsson, L., Norin, H., and Svensson, M. Y. (2004). Parameters influencing AIS1 neck injury outcome in frontal impacts. *Traffic Inj. Prev.* 5, 156–163. doi: 10.1080/15389580490435989

Janssen, M. M., Drevelle, X., Humbert, L., Skalli, W., and Castelein, R. M. (2009). Differences in male and female spino-pelvic alignment in asymptomatic young adults and its relation to spinal deformities – a three-dimensional analysis using upright low-dose digital biplanar X-rays. *Spine* 34, E826–E832. doi: 10.1097/BRS.0b013e3181a9fd85

John, J. D., Yoganandan, N., Arun, M. W. J., and Kumar, G. S. (2018). Influence of morphological variations on cervical spine segmental responses from inertial loading. *Traffic Inj. Prev.* 19, S29–S36. doi: 10.1080/15389588.2017.1403017

Jun, H. S., Chang, I. B., Song, J. H., Kim, T. H., Park, M. S., Kim, S. W., et al. (2014). Is it possible to evaluate the parameters of cervical sagittal alignment on cervical computed tomographic scans? *Spine* 39, E630–E636. doi: 10.1097/BRS.0000000000000281

Kihlberg, J. K. (1969). "Flexion-torsion neck injury in rear impacts," in *Association for the Advancement of Automobile Medicine* (Minneapolis, MN).

Klinich, K. D., Ebert, S. M., and Reed, M. P. (2012). Quantifying cervical spine curvature using Bézier splines. *J. Biomech. Eng.* 134, 114503–114508. doi: 10.1115/1.4007749

Klinich, K. D., Ebert, S. M., Van Ee, C. A., Flannagan, C. A. C., Prasad, M., Reed, M. P., et al. (2004). Cervical spine geometry in the automotive seated posture: variations with age, stature, and gender. *Stapp Car Crash J.* 48, 301–330. doi: 10.4271/2004-22-0014

Knott, P. T., Mardjetko, S. M., and Techy, F. (2010). The use of the T1 sagittal angle in predicting overall sagittal balance of the spine. *Spine J.* 10, 994–998. doi: 10.1016/j.spinee.2010.08.031

Krafft, M., Kullgren, A., Lie, A., and Tingvall, C. (2003). The risk of whiplash injury in the rear seat compared with the front seat in rear impacts. *Traffic Inj. Prev.* 4, 136–140. doi: 10.1080/15389580309862

Lee, J. H., Park, Y. K., and Kim, J. H. (2014). Chronic neck pain in young adults: perspectives on anatomic differences. *Spine J.* 14, 2628–2638. doi: 10.1016/j.spinee.2014.02.039

Lee, S. H., Son, E. S., Seo, E. M., Suk, K. S., and Ki, K. T. (2015). Factors determining cervical spine sagittal balance in asymptomatic adults: correlation with spinopelvic balance and thoracic inlet alignment. *Spine J.* 15, 705–712. doi: 10.1016/j.spinee.2013.06.059

Liu, Y. K., and Dai, Q. G. (1989). The second stiffest axis of a beam-column: implications for cervical spine trauma. *J. Biomech. Eng.* 111, 122–127. doi: 10.1115/1.3168352

Maag, U., Desjardins, D., Bourbeau, R., and Laberge-Nadeau, C. (1990). "Seat belts and neck injuries," in *International Research Council on Biomechanics of Injury Conference (IRCOBI)* (Bron).

Mac-Thiong, J. M., Labelle, H., Berthonnaud, E., Betz, R. R., and Roussouly, P. (2007). Sagittal spinopelvic balance in normal children and adolescents. *Eur. Spine J.* 16, 227–234. doi: 10.1007/s00586-005-0013-8

Maiman, D. J., Sances, A. Jr., Myklebust, J. B., Larson, S. J., Houterman, C., Chilbert, M., et al. (1983). Compression injury of the cervical spine. *Neurosurgery* 13, 254–260. doi: 10.1227/00006123-198309000-00007

Maiman, D. J., Yoganandan, N., and Pintar, F. A. (2002). Preinjury cervical alignment affecting spinal trauma. *J. Neurosurg.* 97, 57–62. doi: 10.3171/spi.2002.97.1.0057

Matsumoto, M., Fujimura, Y., Suzuki, N., Toyama, Y., and Shiga, H. (1998). Cervical curvature in acute whiplash injures: prospective comparative study with asymptomatic subjects. *Injury* 29, 775–778. doi: 10.1016/S0020-1383(98)00184-3

Ministry of Education, Culture, Sports, Science and Technology (2013). *Japan: Annual Report of Anthropometry Data by Age in 2012*. Available at: http://www.e-stat.go.jp/SG1/estat/List.do?bid=000001077241&cycode=0 (accessed February 1, 2015).

Miyazaki, Y., Ujihashi, S., Mochimaru, M., and Kouchi, M. (2005). "Influence of the head shape variation on brain damage under impact," in *SAE Digital Human Modeling for Design and Engineering Symposium* (Iowa City, IA).

Mochimaru, M., and Kouchi, M. (2000). "Statistics for 3D human body forms," in *SAE Digital Human Modeling for Design and Engineering Conference and Exposition* (Dearborn, MI).

Morris, A. P., and Thomas, P. D. (1996). "Neck injuries in the UK co-operative crash injury study," in *SAE Technical Paper*, No. Vol. 105, 1945–1957. doi: 10.4271/962433 Available online at: https://www.jstor.org/stable/44720911

O'Neill, B., Haddon, W., Kelley, A. B., and Sorenson, W. W. (1972). Automobile head restraints—frequency of neck injury claims in relation to the presence of head restraints. *Am. J. Public Health* 62, 399–406. doi: 10.2105/AJPH.62.3.399

Ono, K., Ejima, S., Suzuki, Y., Kaneoka, K., Fukushima, M., and Ujihshi, S. (2006). "Prediction of neck injury risk based on the analysis of localized cervical vertebral motion of human volunteers during low-speed rear impacts," in *International Research Council on Biomechanics of Injury Conference (IRCOBI)* (Madrid).

Ono, K., Inami, S., Kaneoka, K., Gotou, T., Kisanuki, T., Sakuma, S., et al. (1999). "Relationship between localized spine deformation and cervical vertebral motions for low speed rear impacts using human volunteersm," in *International Research Council on Biomechanics of Injury Conference (IRCOBI)* (Barcelona).

Ono, K., Kaneoka, K., Wittek, A., and Kajzer, J. (1997). "Cervical injury mechanism based on the analysis of human cervical vertebral motion and head-neck-torso kinematics during low speed rear impacts," in *SAE Technical Paper*, No. Vol. 106, 3859–3876. doi: 10.4271/973340 Available online at: https://www.jstor.org/stable/44720153

Östh, J., Mendoza-Vazquez, M., Sato, F., Svensson, M. Y., Linder A, and Brolin, K. (2017). A female head-neck model for rear impact simulations. *J. Biomech.* 51, 49–56. doi: 10.1016/j.jbiomech.2016.11.066

Otremski, I., Marsh, J. L., Wilde, B. R., McLardy Smith, P. D., and Newman, R. J. (1989). Soft tissue cervical injuries in motor vehicle accidents. *Injury* 20, 349–351. doi: 10.1016/0020-1383(89)90011-9

Parenteau, C. S., Zhang, P., Holcombe, S., and Wang, S. (2014). Characterization of vertebral angle and torso depth by gender and age groups with a focus on occupant safety. *Traffic Inj. Prev.* 15, 66–72. doi: 10.1080/15389588.2013.829217

Park, M. S., Moon, S. H., Lee, H. M., Kim, S. W., Kim, T. H., Lee, S. Y., et al. (2013). The effect of age on cervical sagittal alignment. *Spine* 38, E458–E463. doi: 10.1097/BRS.0b013e31828802c2

Park, S. M., Song, K. S., Park, S. H., Kang, H., and Riew, K. D. (2015). Does whole-spine lateral radiograph with clavicle positioning reflect the correct cervical sagittal alignments? *Eur. Spine J.* 24, 57–62. doi: 10.1007/s00586-014-3525-2

Pintar, F., Yoganandan, N., Voo, L., Cusick, J. F., Maiman, D. J., and Sances, A. Jr. (1995). "Dynamic characteristics of the human cervical spine," in *SAE Technical Paper*, No. Vol. 104, 3087–3094. doi: 10.4271/952722 Available online at: https://www.jstor.org/stable/44729362

Reed, M. P., and Jones, M. L. H. (2017). *A Parametric Model of Cervical Spine Geometry and Posture*. Final Report, UMTRI-2017–I-2011. Ann Arbor, MI: University of Michigan Transportation Research Institute.

Richter, M., Otte, D., Pohlemann, T., Krettek, C., and Blauth, M. (2000). Whiplash-type neck distortion in restrained car drivers: frequency, causes and long-term results. *Eur. Spine J.* 9, 109–117. doi: 10.1007/s005860050220

Rocabado, M. (1983). Biomechanical relationship of the cranial, cervical, and hyoid regions. *J. Craniomandib. Pract.* 1, 61–66. doi: 10.1080/07345410.1983.11677834

Roussouly, P., Gollogly, S., Berthonnaud, E., and Dimnet, J. (2005). Classification of the normal variation in the sagittal alignment of the human lumbar spine and pelvis in the standing position. *Spine* 30, 346–353. doi: 10.1097/01.brs.0000152379.54463.65

Roussouly, P., and Pinheiro-Franco, J. L. (2011). Sagittal parameters of the spine: biomechanical approach. *Eur. Spine J.* 20, S578–S585. doi: 10.1007/s00586-011-1924-1

SAE Standard J826 (2015). *SAE J826 Devices for Use in Defining and Measuring Vehicle Seating Accommodation, 2015 Edn*. Warrendale, PA: SAE International.

Sato, F., Antona, J., Ejima, S., and Ono, K. (2010). "Influence on cervical vertebral motion of the interaction between occupant and head restraint/seat, based on the reconstruction of rear-end collision using finite element human model," in *International Research Council on Biomechanics of Injury Conference (IRCOBI)* (Hanover).

Sato, F., Miyazaki, Y., Morikawa, S., Ferreiro-Perez, A., Schick, S., Yamazaki, K., et al. (2019). Relationship between cervical, thoracic, and lumbar spinal alignments in automotive seated posture. *J. Biomech. Eng.* 141:121006. doi: 10.1115/1.4045111

Sato, F., Nakajima, T., Ono, K., Svensson, M., Brolin, K., and Kaneoka, K. (2014). "Dynamic cervical vertebral motion of female and male volunteers and analysis of its interaction with head/neck/torso behavior during low-speed rear impact," in *International Research Council on Biomechanics of Injury Conference (IRCOBI)* (Berlin).

Sato, F., Nakajima, T., Ono, K., Svensson, M., and Kaneoka, K. (2015). "Characteristics of dynamic cervical vertebral kinematics for female and male volunteers in low-speed rear impact, based on quasi-static neck kinematics," in *International Research Council on Biomechanics of Injury Conference (IRCOBI)* (Lyon).

Sato, F., Odani, M., Miyazaki, Y., Yamazaki, K., Östh, J., and Svensson, M. Y. (2017). Effects of whole spine alignment patterns on neck responses in rear end impact. *Traffic Inj. Prev.* 18, 199–206. doi: 10.1080/15389588.2016.1227072

Schneider, L. W., Robbins, D. H., Pflüg, M. A., and Snyder, R. G. (1983). *Development of Anthropometrically Based Design Specifications for an Advanced Adult Anthropomorphic Dummy Family*. Final Report, UMTRI-83-53-1. Ann Arbor, MI: University of Michigan Transportation Research Institute.

Snyder, R. G., Chaffin, D. B., and Foust, D. R. (1975). *Bioengineering Study of Basic Physical Measurements Related to Susceptibility to Cervical Hyperextension-Hyperflexion Injury*. Final Report, UM-HSRI-BI-75–I-76. Ann Arbor, MI: University of Michigan Transportation Research Institute.

Stemper, B. D., and Corner, B. D. (2016). Whiplash-associated disorders: occupant kinematics and neck morphology. *J. Orthopaed. Sports Phys. Ther.* 46, 834–844. doi: 10.2519/jospt.2016.6846

Stemper, B. D., Pintar, F. A., and Rao, R. D. (2011). The influence of morphology on cervical injury characteristics. *Spine* 36, S180–S186. doi: 10.1097/BRS.0b013e3182387d98

Stemper, B. D., Yoganandan, N., and Pintar, F. A. (2003). Gender dependent cervical spine segmental kinematics during whiplash. *J. Biomech.* 36, 1281–1289. doi: 10.1016/S0021-9290(03)00159-3

Stemper, B. D., Yoganandan, N., and Pintar, F. A. (2004). Gender- and region-dependent local facet joint kinematics in rear impact. *Spine* 29, 1764–1771. doi: 10.1097/01.BRS.0000134563.10718.A7

Stemper, B. D., Yoganandan, N., and Pintar, F. A. (2005). Effects of abnormal posture on capsular ligament elongations in a computational model subjected to whiplash loading. *J. Biomech.* 38, 1313–1323. doi: 10.1016/j.jbiomech.2004.06.013

Storvik, S. G., Stemper, B. D., Yoganandan, N., and Pintar, FA. (2009). Population-based estimates of whiplash injury using NASS CDS data–biomed 2009. *Biomed. Sci. Instrum.* 45, 244–249. Available online at: https://europepmc.org/article/med/19369770; https://scholar.google.com/scholar_lookup?title=Population-based+estimates+of+whiplash+injury+using+NASS+CDS+data%2E&journal=Biomed%2E+Sci%2E+Instrum%2E&author=Storvik+S.+G.&author=Stemper+B.+D.&author=Yoganandan+N.&author=Pintar+F.+A.&publication_year=2009&volume=45&pages=244%E2%8%93249

Takeshima, T., Omokawa, S., Takaoka, T., Araki, M., Ueda, Y., and Takakura, Y. (2002). Sagittal alignment of cervical flexion and extension. *Spine* 27, E348–E355. doi: 10.1097/00007632-200208010-00014

Temming, J., and Zobel, R. (1998). "requency and risk of cervical spine distortion injuries in passenger car accidents: significance of human factors data," in *International Research Council on Biomechanics of Injury Conference (IRCOBI), 1998* (Gothenburg).

Thomas, C., Faverjon, G., Hartemann, F., Tarriere, C., Patel, A., and Got, C. (1982). "Protection against rear-end accidents," in *International Research Council on Biomechanics of Injury Conference (IRCOBI)* (Cologne).

Yang, K. H., and King, A. I. (2003). Neck kinematics in rear-end impacts. *Pain Res. Manag.* 8, 79–85. doi: 10.1155/2003/839740

Yoganandan, N., Pintar, F. A., Gennarelli, T. A., Eppinger, R. H., and Voo, L. M. (1999). "Geometrical effects on the mechanism of cervical spine injury due to head impact," in *International Research Council of Biomechanics of Injury Conference* (Sitges).

Yoganandan, N., Sances, A. Jr., Maiman, D. J., Myklebust, J. B., Pech, P., and Larson, S. J. (1986). Experimental spinal injuries with vertical impact. *Spine* 11, 855–860. doi: 10.1097/00007632-198611000-00001

Conflict of Interest: The authors declare that the research was conducted in the absence of any commercial or financial relationships that could be construed as a potential conflict of interest.

Publisher's Note: All claims expressed in this article are solely those of the authors and do not necessarily represent those of their affiliated organizations, or those of the publisher, the editors and the reviewers. Any product that may be evaluated in this article, or claim that may be made by its manufacturer, is not guaranteed or endorsed by the publisher.

frontiers in Bioengineering and Biotechnology

REVIEW
published: 17 August 2021
doi: 10.3389/fbioe.2021.684217

The Lack of Sex, Age, and Anthropometric Diversity in Neck Biomechanical Data

Gabrielle R. Booth[1,2], *Peter A. Cripton*[1,2]* *and Gunter P. Siegmund*[3,4]

[1]*Orthopaedic and Injury Biomechanics Laboratory, School of Biomedical Engineering and Departments of Orthopaedics and Mechanical Engineering, University of British Columbia, Vancouver, BC, Canada,* [2]*International Collaboration on Repair Discoveries, University of British Columbia, Vancouver, BC, Canada,* [3]*MEA Forensic Engineers & Scientists, Richmond, BC, Canada,* [4]*School of Kinesiology, University of British Columbia, Vancouver, BC, Canada*

Female, elderly, and obese individuals are at greater risk than male, young, and non-obese individuals for neck injury in otherwise equivalent automotive collisions. The development of effective safety technologies to protect all occupants requires high quality data from a range of biomechanical test subjects representative of the population at risk. Here we sought to quantify the demographic characteristics of the volunteers and post-mortem human subjects (PMHSs) used to create the available biomechanical data for the human neck during automotive impacts. A systematic literature and database search was conducted to identify kinematic data that could be used to characterize the neck response to inertial loading or direct head/body impacts. We compiled the sex, age, height, weight, and body mass index (BMI) for 999 volunteers and 110 PMHSs exposed to 5,431 impacts extracted from 63 published studies and three databases, and then compared the distributions of these parameters to reference data drawn from the neck-injured, fatally-injured, and general populations. We found that the neck biomechanical data were biased toward males, the volunteer data were younger, and the PMHS data were older than the reference populations. Other smaller biases were also noted, particularly within female distributions, in the height, weight, and BMI distributions relative to the neck-injured populations. It is vital to increase the diversity of volunteer and cadaveric test subjects in future studies in order to fill the gaps in the current neck biomechanical data. This increased diversity will provide critical data to address existing inequities in automotive and other safety technologies.

Keywords: injury biomechanics, injury prevention, population diversity, neck, ageing, obesity, sex differences, anthropometric differences

OPEN ACCESS

Edited by:
Sonia Duprey,
Université de Lyon, France

Reviewed by:
Anita Vasavada,
Washington State University, United States
John Henry Bolte,
The Ohio State University, United States

***Correspondence:**
Peter A. Cripton
peter.cripton@ubc.ca

Specialty section:
This article was submitted to Biomechanics, a section of the journal Frontiers in Bioengineering and Biotechnology

Received: *23 March 2021*
Accepted: *22 July 2021*
Published: *17 August 2021*

Citation:
Booth GR, Cripton PA and Siegmund GP (2021) The Lack of Sex, Age, and Anthropometric Diversity in Neck Biomechanical Data. Front. Bioeng. Biotechnol. 9:684217. doi: 10.3389/fbioe.2021.684217

INTRODUCTION

Injuries to the head and neck, which house and protect the brain and upper spinal cord, are some of the most catastrophic consequences of motor vehicle collisions. Over the past 7 decades, improvements in roads, vehicles, safety equipment, safety regulations, and enforcement have significantly reduced the injury, morbidity, and mortality burden associated with head and neck injuries. Despite these considerable achievements, many injury prevention approaches, including the computational models and anthropometric test devices (ATDs) used to design and evaluate safety equipment, have focused on 50th percentile adult male occupants (Linder and Svensson, 2019). As a

result, females and others who fall outside the anthropometric envelope of this "median male" are not as well represented in automotive safety equipment design. Assuming that ATDs and other surrogates are appropriate for developing vehicle safety technology, it follows that considerable numbers of injured and killed occupants were using safety equipment that may not have been optimally designed for them.

European and United States traffic safety regulatory standards are used worldwide, with minor alterations, to assess a vehicle's ability to prevent serious injuries for the occupants and other road users. These standards specify the use of 50th percentile adult male ATDs and representations of the 95th percentile male and 5th percentile female, which have been scaled from the 50th male by weight and height. While these three occupant representations attempt to approximate the median and extremes of height and weight of adult occupants, changes in size alone are not sufficient to represent the age, sex, and anthropometric variations seen in the population that safety technologies aim to protect (Linder and Svensson, 2019). Additionally, child restraint system performance evaluation is conducted using Hybrid III child dummies that were also derived from scalings of the Hybrid III 50th percentile adult male dummy and basic child anthropometry (Irwin and Mertz, 1997). Therefore, many ATDs used in traffic safety regulatory standards have been derived from a representation of a 'median-sized' adult male.

Anthropometry and size are not the only factors related to the use of ATDs that are median-male based. The injury assessment reference values (IARVs) for the neck, which were developed for relating the loads measured by ATDs to the potential for injury in humans, are based on a limited set of male human volunteer and cadaveric data (Mertz et al., 2003; Foster et al., 1977). These data have then been scaled using size (neck circumference) and tissue properties (calcaneal tendon strength) to provide IARVs for the 5th percentile female and 95th percentile male Hybrid III dummies. In the case of children, porcine models have been used to generate injury data, although the translation between animal and human data is outside the scope of the current study (Mertz et al., 2003).

There are considerable field data showing that female, elderly, and obese individuals are at greater risk than 50th percentile adult males of serious and fatal injuries across all body regions in similar severity collisions (Evans and Gerrish, 2001; Bédard et al., 2002; Hill and Boyle, 2006; Zhu et al., 2006; Bose, 2011; Rupp et al., 2013; Carter et al., 2014). Using data from the National Automotive Sampling System's Crashworthiness Data System (NASS-CDS), Bose et al. (2011) found that the odds of a belt-restrained female driver sustaining severe injuries were 47% higher than those for a belt-restrained male driver involved in a comparable crash. Hill and Boyle (2006) found that females and older occupants (75+ year olds) were at a significantly higher risk of a severe injury in crashes recorded in the United States General Estimate System (GES). Evans and Gerrish (2001) used the Fatality Analysis Reporting System (FARS) database to compare the risk of fatal injury in two-car crashes where the sex of one driver was male and the other was female and found the fatality risk to be 22% greater for female drivers. Bédard et al. (2002) also used the FARS database to examine fatality risk in single vehicle collisions with fixed objects and found the odds ratio of fatal injury increases with age (OR = 4.98 for 80+ year olds) and female sex (OR = 1.54). Rupp et al. (2013) found that obese subjects were at an increased risk of AIS 3+ spine injuries. While other vehicle- and crash-related factors that co-vary with sex, age, and occupant obesity may explain some of these findings, biomechanical factors related to these variables are plausible explanations for some proportion of the observed effects.

A similar pattern of increased injury risk for female, elderly, and obese individuals is also observed specifically for head and neck injuries. Carter et al. (2014) found that older individuals have a greater risk of severe spine injuries in frontal and rollover crashes. Furthermore, females are at about double the risk of males for whiplash injuries in low speed rear-end collisions (Krafft et al., 2003; Jakobsson et al., 2004; Linder and Svensson, 2019). Moreover, active head restraints have been shown to be more effective for men than women (Kullgren et al., 2013).

Sex and anthropometry also affect the kinematics of individuals in collisions. In volunteer studies, females exhibit higher magnitude head accelerations in both frontal and rear-end collisions (Siegmund et al., 1997; van den Kroonenberg et al., 1998). In rear impacts, females also exhibit greater forward rebound and larger intersegmental motion between adjacent vertebrae in the cervical spine (Ono et al., 2006). Reed et al. (2012) studied obese and non-obese subjects and showed that excess slack was introduced in the belt system in obese subjects. In post-mortem human subjects (PMHSs), obese subjects experienced greater excursion and tended to pitch forward less than the non-obese subjects in 48 km/h frontal collisions (Kent et al., 2010). Computational models have also predicted higher neck displacements for females than for males in low-speed rear-end collisions (Viano, 2003) and poor concordance has been observed between the Global Human Body Models Consortium (GHBMC) finite element model and obese PMHS tests (Gepner et al., 2018).

Sex differences in external neck morphology and anatomical differences in the cervical spine have also been established. The vertebral anatomy, curvature, head mass, neck strength, neck muscle morphometry, and neck muscle activation patterns have all been shown to differ between males and females (Brault et al., 1998; Kamibayashi and Richmond, 1998; Matsumoto et al., 1998; Siegmund et al., 2003a; Klinich et al., 2004; Stemper et al., 2008; Vasavada et al., 2008; Sato et al., 2017).

The above review suggests that injury prevention technologies (e.g., restraint systems, airbags, and head restraints) have been primarily designed using representations and scalings of mid-sized male occupants, and that sex, age, and anthropometry potentially affect neck injury risk, head and neck kinematics, and ultimately neck injury mechanics in automotive collisions. While the biomechanics of these relationships and the degree to which sex, age, and anthropometry explain these relationships remains unclear, an important first step in addressing this potential inequity in injury prevention is to understand the diversity—or lack of diversity—in the baseline biomechanical data that inform our understanding of occupant kinematics and tolerances, and motivate our designs of ATDs and safety

TABLE 1 | Study eligibility criteria.

Inclusion criteria	Exclusion criteria
• Test volunteer or cadaver subjects with or without helmets • Measure primary data on time history accelerations or displacements of both the human head and base of the neck or upper thorax (C6–T4 range) • Involve accelerating the head by means of inertial loading or direct head or body impact	• Solely use subjects who have undergone spinal surgery, have apparent or induced injuries, have been otherwise altered, or exhibit extreme spine pathologies • Involve modifying the kinematics of the head and neck through additional impacts (airbags, steering wheels, head restraints) or other factors • Poor methodology or insufficient detail to assess the quality of the methods used to obtain and modify data (requires the agreement of two reviewers)

technologies. Therefore, our objective here is to quantify the distributions of sex, age, height, weight, and BMI for volunteer and PMHS tests that make up the available neck biomechanical data and to compare the distributions of these parameters to reference data drawn from the neck-injured, fatally-injured, and general populations.

METHODS

Literature Search

A systematic search was performed for published studies that contained kinematic data for the head and torso in response to inertial loading and direct head and body impacts, and from which the neck response could be estimated. Five databases (PubMed, Web of Science Core Collection, Compendex Engineering Village, SportDiscus, and SAE Mobilus) were searched in June/July 2020 with no restrictions on year or language of publication. The search terms reflected the eligibility criteria, including keywords targeting human subjects and cadavers, head, neck and torso kinematics, and impact loading. Studies extracted from relevant review articles were also added to the results of these searches.

A sample Web of Science search is as follows:

#1 TS = (Volunteer* OR "*In Vivo*" OR Cadaver* OR "*Ex Vivo*" OR "Post mortem" OR PMHS).

#2 TS = (head).

#3 TS = (sled OR "crash test*" OR impact*)

#4 TS = (acceleration* OR displacement*)

#4 AND #3 AND #2 AND #1.

Studies from the search results were first compiled and deduplicated using Legacy RefWorks (ProQuest, Ann Arbor, MI). One author screened the titles and abstracts based on preset criteria (**Table 1**) and then performed a full-text review on the relevant subset to identify eligible studies containing the desired data using Covidence (Melbourne, Australia). A second author reviewed studies whose inclusion/exclusion was ambiguous. For eligible studies, we then determined if the kinematic data were available in the publication, appendix, supplementary material, by contacting the authors, or searching biomechanics databases (e.g., National Biodynamics Laboratory, Air Force Biodynamic, and NHTSA Biomechanics databases). We then extracted the sex, age, height, weight, and BMI for all volunteers and cadavers from each test within the included studies. These characteristics were compared to reference data for automotive neck injuries (NASS-CDS), automotive fatalities (FARS), and the general population (US Census Bureau, USCB).

Reference Data

From the NASS-CDS dataset that had AIS codes (1993–2015), we extracted all cases with cervical spine injuries (Region 6, Structures 02, 50 and 59 based on the 1998 Abbreviated Injury Scale) for light vehicles (Body types 1–49) and all types of crashes. For each unique individual (n = 25,889), we extracted the maximum Abbreviated Injury Scale (AIS) score for their cervical spine injury, as well as their sex, age, height, weight, and BMI when present. Individuals were removed from the dataset if their sex was unknown (n = 9) or if their age, height, and weight were all unreported (n = 4). Individuals with BMI >76 were removed, as there were continuous data up to a BMI of 76, after which the values doubled and were assumed to be errors (n = 17). The data were then grouped into three datasets based on injury severity: AIS1+, AIS2+, and AIS3+ injuries. Injuries of unknown severity (coded as AIS 7 in NASS) were included in the AIS1+ group but removed from AIS2+ and AIS3+ groups. Pregnant females were included in the age and height datasets but excluded from the weight and BMI datasets.

From the FARS data, we queried the Fatality and Injury Reporting System Tool (FIRST) to extract the sex and age of all drivers and occupants who died in motor vehicle crashes in the full date range of the available data (2005–2019). The FARS database did not contain height or weight data. The FARS data included deaths from all types of injuries, not just cervical spine injuries.

From the census data, we extracted the estimated 2017 United States population for females and males at each year of age between 0 and 100 years (US Census Bureau, 2021). All individuals over 100 years old were pooled into the 100-years category. To estimate the height and weight distributions of the general population, we first fit a lognormal distribution to the percentile distribution data (5, 10, 15, 25, 50, 75, 85, 90, and 95th percentiles) of the height and weight data for each sex and year of age (Fryar et al., 2021) and then calculated a weighted sum of these distributions based on the number of people in each age group. Separate height and weight distributions were used for each year from 2 to 19 years and for each decade thereafter (e.g., 20–29 years, 30–39 years, ... , 70–79 years, 80+ years). No information on the correlation between height and weight was available, therefore BMI for the general population was not computed.

Data Distributions

Histograms for age, height, weight and BMI were created for the number of volunteer tests, PMHS tests, AIS1+ injured individuals, AIS2+ injured individuals, AIS3+ injured individuals, fatalities, and people in the general population. We focused our analysis on the number of volunteer and PMHS tests rather than the number of volunteers or cadavers because each test yielded a unique set of data. As a result, a volunteer or cadaver could appear multiple times in the histograms. The histograms pooled both sexes and used bin widths of 1 year, 1 cm, 1 kg, and 1 kg/m^2 for age, height, weight, and BMI, respectively. For the AIS data, the bin widths for height were set to 2.54 cm (1 inch) and 2.258 kg (5 pounds) for weight. Separate density distributions for each sex were then generated using kernel density estimates (geom_density function in R). For a dataset with N observations, this function yields the sum of i = 1 to N normal distributions, where the mean of the ith distribution equals the value of the ith observation and the standard deviation for all N distributions equals the optimum bandwidth (Silverman, 1986). The optimum bandwidth for each dataset was calculated using **Eq. 1** (Silverman, 1986, pg 48), and then all bandwidths for a given parameter (age, height, weight, or BMI) were averaged to select a common bandwidth for all distributions of the same parameter. The average bandwidths for each parameter were as follows: age 2.90 years, height 1.40 cm, weight 2.95 kg, and BMI 1.01 kg/m^2. The bandwidth for height was doubled from 0.70 to 1.40 cm as the average optimum bandwidth created unrealistic peaks in the data with 1-cm bin widths.

$$\text{Optimum bandwidth} = 0.9\,\min(\text{SD}, \text{IQR}/1.34) \times \text{N}^{-0.2} \quad (1)$$

where SD = standard deviation of the dataset, and IQR = interquartile range of the dataset.

The histograms related to all distributions for a single parameter were plotted at the same scale, i.e., the areas of all related histograms are equal to one. The relative areas under the female and male distributions reflect their relative proportions of the population. The areas for the female and male distributions were doubled, i.e., their sum is double the area of the histogram, to improve their visibility relative to the histograms. The medians for the male and female data were computed using all of the data within a dataset. For the general population, the medians for the height and weight of adults (≥16 years) were also calculated. Dispersion within each of the datasets was quantified using the interquartile range (IQR).

RESULTS

Our search yielded 2,249 unique studies, of which 417 studies were relevant to our objectives, 91 of the 417 relevant studies measured the kinematic variables we sought, and 63 of these studies presented or otherwise allowed access to their data (**Figure 1**). The 63 studies contained 999 unique volunteers exposed to 5,229 tests and 110 unique PMHSs exposed to 202 tests (Ewing et al., 1969; Ewing and Thomas, 1972; Ewing et al., 1975; Ewing et al., 1977, Ewing et al., 1978; Kallieris et al., 1987; Buhrman and Perry, 1994; Margulies et al., 1998; Morris and Popper, 1999; Ono et al., 1999; Yoganandan and Pintar, 2000; Davidsson et al., 2001; Meijer et al., 2001; Fugger et al., 2002; Petitjean et al., 2002; Vezin et al., 2002; Deng and Wang, 2003; Perry et al., 2003; Siegmund et al., 2003a; Siegmund et al., 2003b; Vezin and Verriest, 2003; Doczy et al., 2004; Siegmund et al., 2004; Blouin et al., 2006; Rouhana et al., 2006; Wiechel and Bolte, 2006; Ejima et al., 2007; Pintar et al., 2007; Ejima et al., 2008; Siegmund et al., 2008; Arbogast et al., 2009; Funk et al., 2009; Lopez-Valdes et al., 2009; Siegmund and Blouin, 2009; White et al., 2009; Lopez-Valdes et al., 2010; Pintar et al., 2010; Funk et al., 2011; Sundararajan et al., 2011; Arbogast et al., 2012; Ejima et al., 2012; Stammen et al., 2012; Symeonidis et al., 2012; Forman et al., 2013; Mathews et al., 2013; Poulard et al., 2013; van Rooij et al., 2013; Crandall et al., 2014; Gutsche et al., 2014; Lessley et al., 2014; Lopez-Valdes et al., 2014; Seacrist et al., 2014; Shaw et al., 2014; Acosta et al., 2016; López-Valdés et al., 2016; Pietsch et al., 2016; Albert, Beeman and Kemper, 2018; Holt et al., 2018; Humm et al., 2018; Petit et al., 2019; Stark et al., 2019; Zaseck et al., 2019; Holt et al., 2020). About 66% of the volunteer tests and 84% of the PMHS tests were conducted with males (**Table 2**, also visible in **Figures 2–5**). Both values were higher than the proportion of males in the United States population (49%) and in the AIS1+, AIS12+, and AIS13+ neck injury groups (48, 60, and 63%, respectively), but landed on either side of the proportion of males seen in United States automotive fatalities (70%).

Of the four variables we examined, age showed the largest differences between datasets (**Figure 2**). The median ages for the PMHS tests were higher than all of the reference datasets, ranging from as little as 26 years older than the FARS data (males) up to 40 years older than the AIS1+ data (females). The youngest female and male PMHSs tested were 46 and 22 years old, respectively. The median ages for the volunteer tests, on the other hand, were lower than all of the reference datasets by a maximum of 14 years relative to the FARS data (females). In addition to differences in the medians, the age-related dispersions (IQRs) of both the volunteer tests and the PMHS tests were less than all of the reference datasets (**Table 2**). Dispersion was smallest for the female volunteer tests (7 years) and largest for the female fatalities and female population data (38 years). There were no volunteer or PMHS tests for female children or adolescents (≤17 years old) and the oldest female and male volunteer test subjects were 63 and 65 years old, respectively.

The median height of the female PMHS tests was only 2 cm shorter than the median female in the United States population, but 6–7 cm shorter than females with neck injuries (**Figure 3**). In contrast, the median height of the female volunteer tests was 3–4 cm taller than the females with neck injuries. For males, the median height for the volunteer tests was the same as the median for the adult United States population (**Figure 3**), but 3–4 cm shorter than the median heights for the PMHS tests and the neck injured populations. The dispersions in height for the female volunteer data and for both the male and female PMHS data were less than the dispersion for the neck-injured population and the general population.

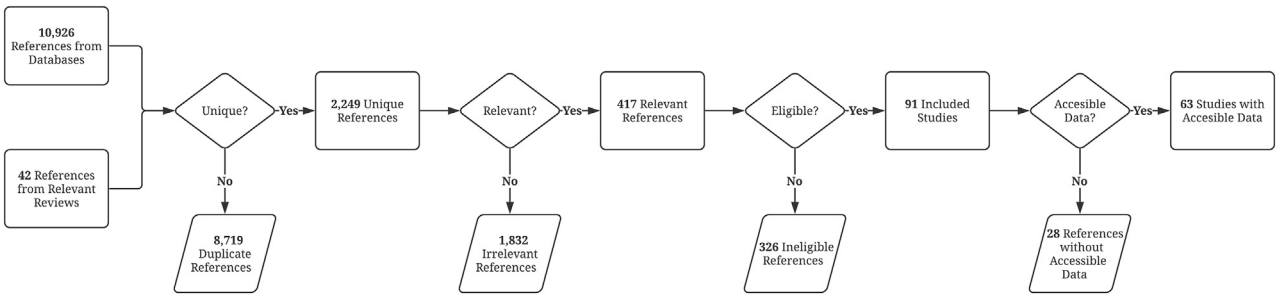

FIGURE 1 | Flowchart showing the number of studies at each stage of the selection process.

TABLE 2 | Sample size (n), median, and interquartile range (IQR) of the age, height, weight, and BMI data for the volunteer tests, PMHS tests, AIS1+, AIS2+, and AIS3+ from the NASS data, FARS data, and the United States population.

		Age (years)			Height (cm)			Weight (kg)			BMI (kg/m^2)		
		n	Median	IQR	n	Median	IQR	n	Median	IQR	n	Median	IQR
Volunteers	Total	5,296	26	11	5,296	172	10	5,296	69	14	5,296	23	3
	Male	3,544	26	11	3,544	174	10	3,544	75	13	3,544	24	3
	Female	1752	27	7	1752	168	6	1752	65	10	1752	23	2
PMHS	Total	195	65	17	196	176	11	196	75	17	196	24	5
	Male	166	65	15	166	177	6	166	77	18	166	25	4
	Female	29	72	20	30	157	7	30	54	25	30	22	9
AIS1+	Total	25,859	31	24	21,962	170	15	22,183	73	25	21,594	25	7
	Male	12,458	31	23	10,476	178	10	10,708	82	21	10,411	26	6
	Female	13,401	32	25	11,486	165	10	11,475	64	20	11,183	24	8
AIS2+	Total	4,410	35	29	3,810	173	15	3,866	76	24	3,769	25	7
	Male	2,658	34	26	2,270	178	10	2,318	82	19	2,257	26	6
	Female	1752	38	35	1,540	165	12	1,548	66	22	1,512	24	8
AIS3+	Total	1985	36	30	1,680	173	15	1,696	77	24	1,654	25	7
	Male	1,243	35	26	1,036	178	10	1,054	82	19	1,028	26	6
	Female	742	38	36	644	164	13	642	65	20	626	24	8
FARS	Total	455,886	39	33	—	—	—	—	—	—	—	—	—
	Male	320,917	38	31	—	—	—	—	—	—	—	—	—
	Female	134,969	41	38	—	—	—	—	—	—	—	—	—
United States Pop	Total	324,982,000	38	38	321,006,000	165	17	321,013,000	75	33	—	—	—
	Male	160,044,000	36	37	158,034,000	173	12	158,035,000	82	33	—	—	—
	Female	164,938,000	39	38	162,972,000	159	11	162,978,000	70	30	—	—	—

The weight data exhibited a similar pattern to the height data. The median weight of the female PMHS tests was 10–12 kg less than the females in the neck-injured groups and 16 kg less than females in the general population (**Figure 4**). For males, the median weights for the volunteer and PMHS tests were 5–7 kg less than both the neck-injured and general populations. Dispersion in the weight of the female volunteer tests was about half of the neck injured population and a third of the general population, whereas the dispersion in the PMHS data fell within the range between the neck-injured and general populations. For males, the dispersion in the volunteer tests was also about one third of the general population, but the PMHS and neck-injured populations were similar to one another.

Volunteers and PMHSs had slightly lower median BMIs than seen in the neck-injured populations (**Figure 5**). The median BMIs of the male volunteers and the female PMHSs differed the most, by 2 kg/m^2, from the neck-injury populations. Dispersion in the volunteer BMI's was one half of the neck-injured population for females and one quarter of the neck-injured population in males.

DISCUSSION

Our goal was to quantify the sex, age, and anthropometry of the volunteers and cadavers that comprise the available kinematic data for the human neck and to compare the distributions of these variables to those of the neck-injured, fatally-injured, and general populations. Overall, we found large differences in the sex and age distributions between the biomechanical data and the reference populations, and smaller, primarily female-specific, differences in the height, weight, and BMI distributions between the biomechanical data and reference populations. These findings point to an underlying lack of diversity in the biomechanical data

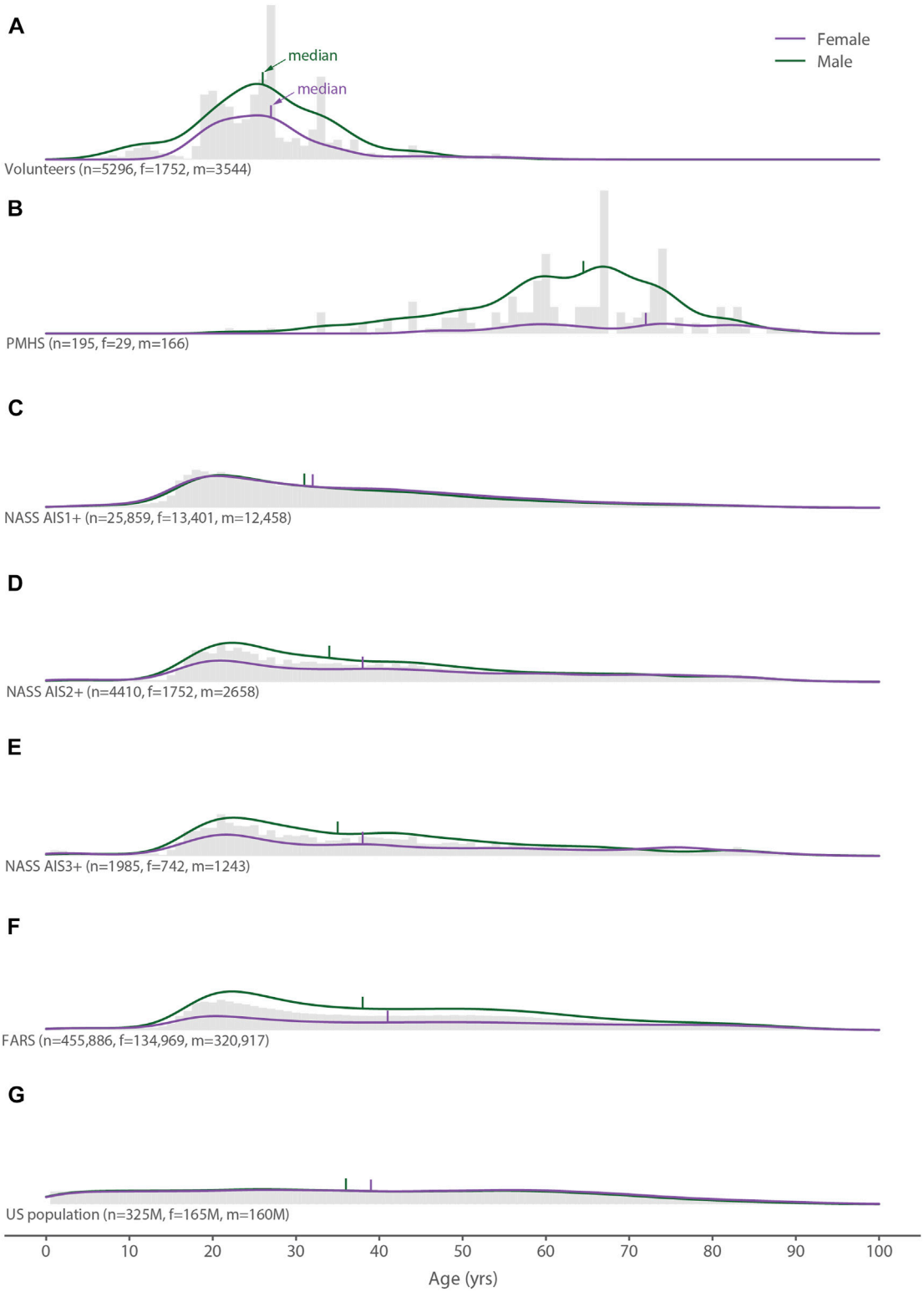

FIGURE 2 | Distribution of all age data (gray histograms), females (purple lines), and males (green lines) for **(A)** the volunteer tests, **(B)** the PMHS tests, **(C)** the NASS AIS1+ data, **(D)** the NASS AIS2+ data, **(E)** the NASS AIS3+ data, **(F)** the FARS data, and **(G)** the United States population.

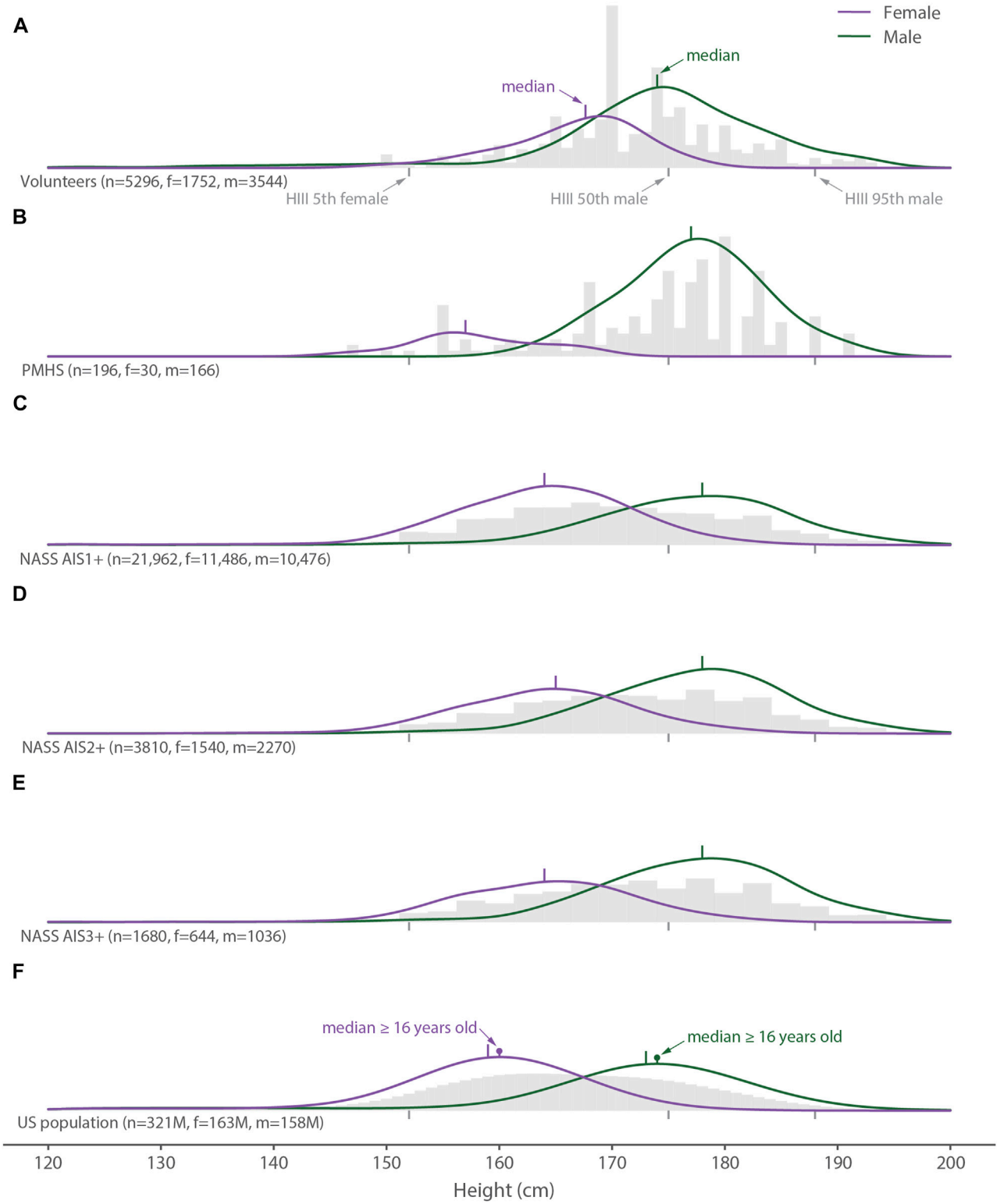

FIGURE 3 | Distribution of all height data (gray histograms), females (purple lines) and males (green lines) for **(A)** the volunteer tests, **(B)** the PMHS tests, **(C)** the NASS AIS1+ data, **(D)** the NASS AIS2+ data, **(E)** the NASS AIS3+ data, and **(F)** the United States population. The gray vertical bars below each histogram show the heights of the 5th percentile female, 50th percentile male, and 95th percentile male Hybrid III crash test dummies.

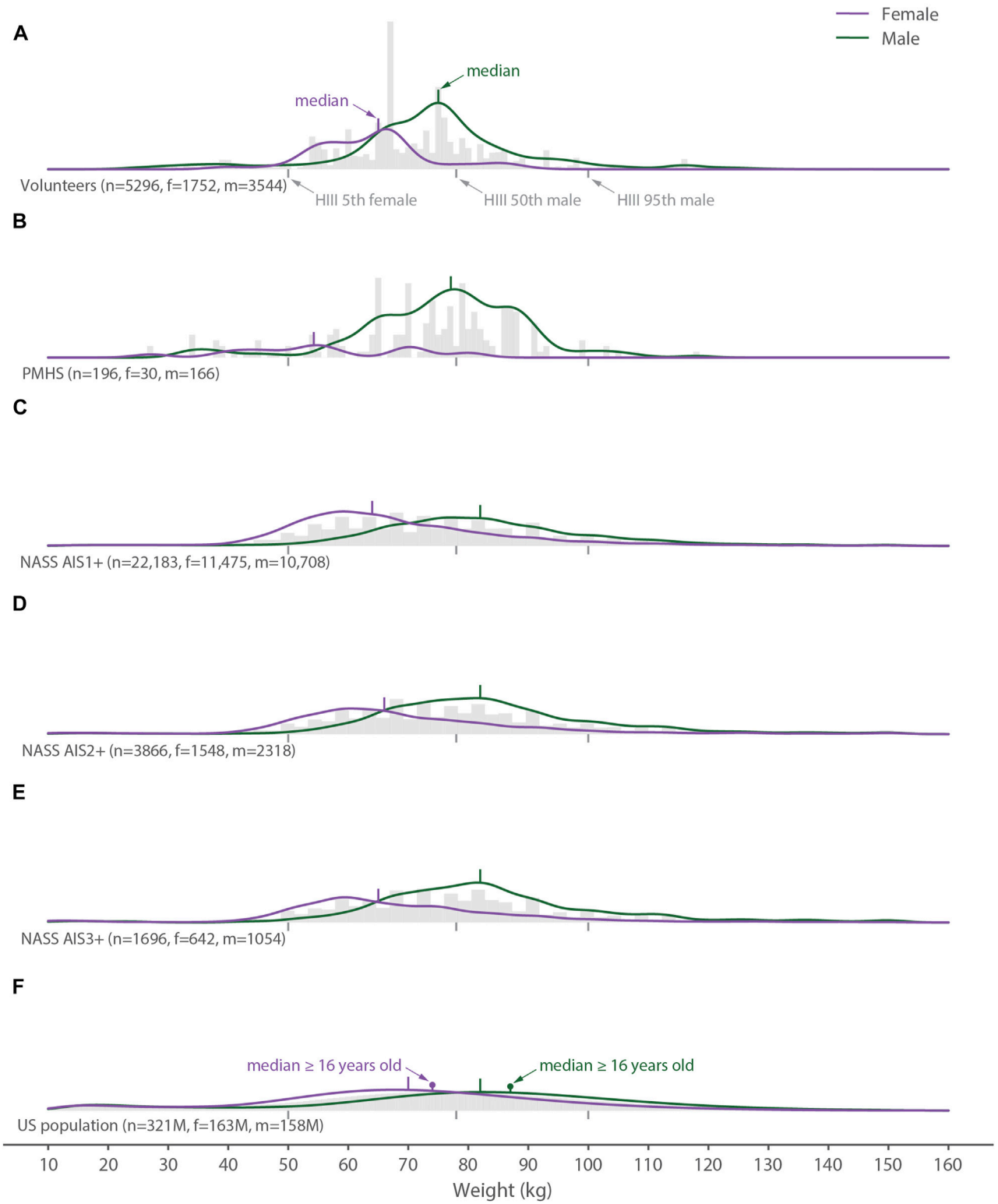

FIGURE 4 | Distribution of all weight data (gray histograms), females (purple lines) and males (green lines) for **(A)** the volunteer tests, **(B)** the PMHS tests, **(C)** the NASS AIS1+ data, **(D)** the NASS AIS2+ data, **(E)** the NASS AIS3+ data, and **(F)** the United States population. The gray vertical bars below each histogram show the weights of the 5th percentile female, 50th percentile male, and 95th percentile male Hybrid III crash test dummies.

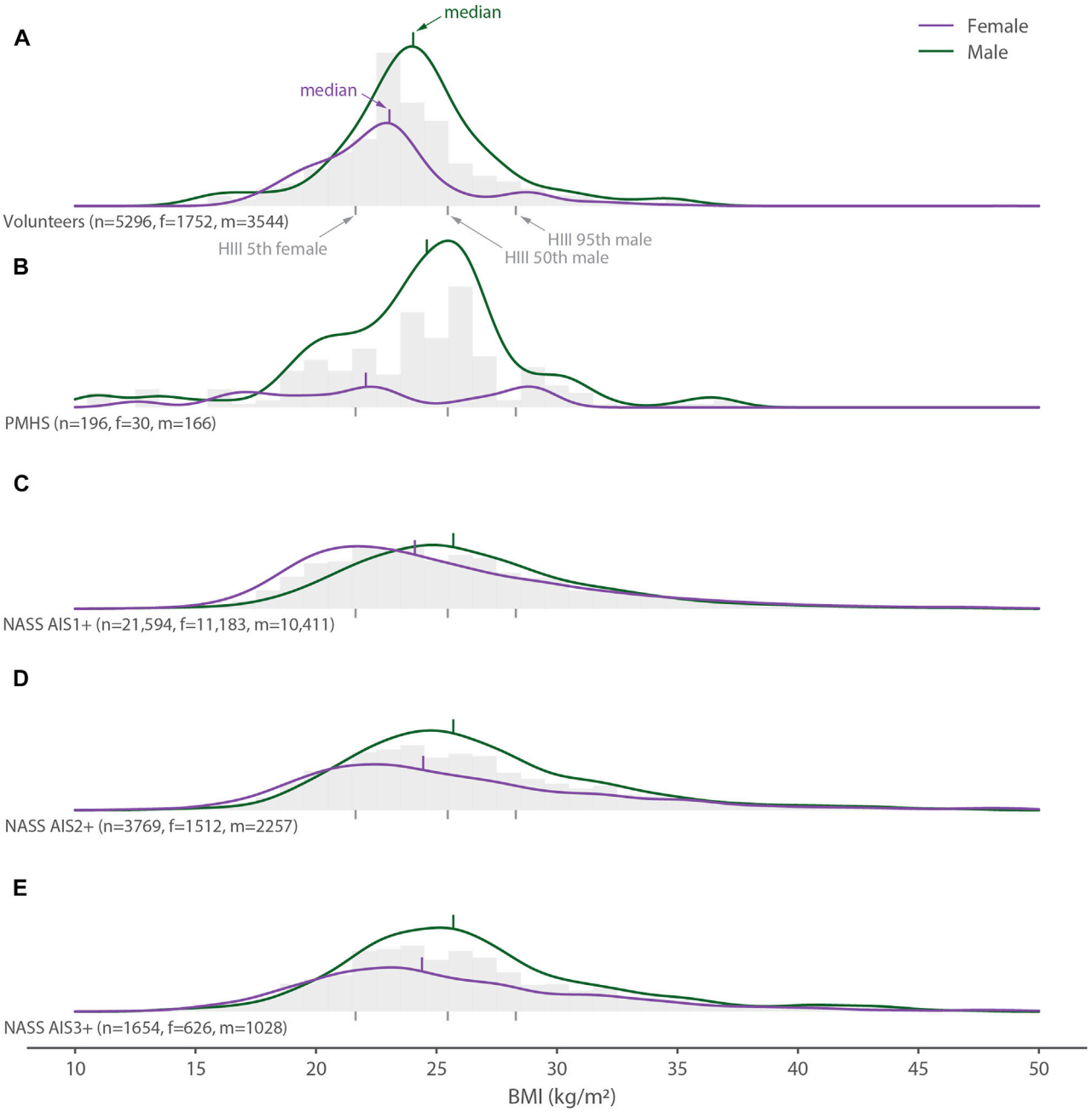

FIGURE 5 | Distribution of all body mass index (BMI) data (gray histograms), females (purple lines) and males (green lines) for **(A)** the volunteer tests, **(B)** the PMHS tests, **(C)** the NASS AIS1+ data, **(D)** the NASS AIS2+ data, and **(E)** the NASS AIS3+ data. The gray vertical bars below each histogram show the heights of the 5th percentile female, 50th percentile male and 95th percentile male Hybrid III crash test dummies.

being used to understand and ultimately prevent collision-related neck injuries.

The most obvious difference between the biomechanical and reference datasets is between males and females. There were twice as many male volunteer tests as female volunteer tests (67% male vs. 33% female) and over five times as many male PMHS tests as female PMHS tests (85 vs. 15%). In contrast, there were fewer males than females (48 vs. 52%) with neck injuries across the entire range of severities (i.e., AIS1+) and 1.67 times more males than females (63 vs. 37%) when only serious and more severe neck injuries (AIS3+) were considered. Although males were ~2.4 times more likely than females (70 vs. 30%) to die in a road crash based on FARS data, this database captures deaths from non-neck-related trauma and is therefore a poorer reference for the appropriate diversity needed in the neck biomechanical data. Based on these findings, more biomechanical data are needed for

females throughout the neck injury spectrum—from whiplash injury to neck fractures—although the optimum sex distribution of volunteers and PMHSs may vary for different neck injuries. For instance, volunteer tests may be more relevant for studying AIS1 injuries and therefore a bias toward more female than male subjects should be considered to better reflect the AIS1 injured population; whereas cadaver tests may be more relevant for studying severe neck injuries and therefore a bias toward more male than female cadavers—albeit less bias than currently exists—could be considered to reflect the AIS3+ injured population. More generally, our findings suggest that the applicability of biomechanical research could be improved if researchers queried the available field data for sex and anthropometry distributions relevant to the injury of interest and then enrolled volunteers and/or cadavers to match.

The age differences we observed between the biomechanical and reference datasets were primarily in the PMHS data. This finding is not surprising given that 75% of deaths in males and 85% of deaths in females occur at over 65 years of age (Shumanty, 2018), making old cadavers more readily available to researchers. Nevertheless, there are established age-related changes in tissue morphology and failure response that potentially confound comparisons between the volunteer and PMHS data (Yukawa et al., 2012; Yoganandan et al., 2018). These differences create problems when combining the geometric, kinematic, and neuromuscular data of young volunteers with the failure data of old cadavers, particularly when creating human body models, developing injury assessment reference values, or designing safety interventions. For example, the neck IARVs developed for correlating injury tolerances with the Hybrid III are scaled using tissue properties which are likely to be biased by the older age of cadaveric specimens (Mertz et al., 2003). Another key age-related difference is the complete absence of volunteer and cadaveric data for female children and adolescents. While injury rates to this sub-population are relatively low, the societal costs of injury to children are high and therefore biomechanical data from both sexes are needed to first understand if differences exist and then how to accommodate for them if present.

Though not a goal of the study, we observed that the neck-injured population was taller than the general population. The reasons for this difference cannot be discerned directly from our data, but possible explanations include a longer distance between the inertial mass of the head and the fulcrum created by the shoulder belt crossing the chest and shoulder during frontal crashes, a greater chance of head contact and neck loading during other types of impacts, and different interactions with airbags. Further work is needed to better understand this pattern and its possible importance when recruiting volunteers and selecting cadavers for studying neck injury. The height of female cadavers was even shorter than the general population and therefore matched the distribution of neck-injured females even more poorly. The heights of the three common Hybrid III dummies (5th female, 50th male, and 95th male; shown in **Figure 3**) appear to cover the range of injured individuals but result in many of the females landing in the gap between the 5th female and the 50th male dummy. Moreover, a median height for the neck-injured male population that is ~5 cm taller than the 50th-percentile male dummy, which is the most commonly used dummy for vehicle standards testing, may not be optimizing vehicle safety for taller male occupants.

In contrast to height, the weight distributions of neck-injured individuals and both the volunteer and PMHS data are lower than for the general population. The weight of female PMHSs is low compared to the other distributions, possibly signifying attempts by researchers to generate data related to the 5th-percentile female dummy. Although the BMI distribution of the general population was not determined because the covariance of height and weight was not available, the volunteer and PMHS test data was below the median levels for the neck-injured populations.

To interpret our findings, one should consider the different kinds of biomechanical data generated from volunteer and PMHS tests. Volunteers are exposed to lower, often sub-injurious conditions and the acquired data consist of kinematics from external sensors or motion tracking, intervertebral kinematics acquired via fluoroscopy, muscle activation data from surface or in-dwelling electromyography, kinetics computed via inverse dynamics, and potentially subjective or objective clinical data (including pre- and post-test imaging). Volunteer data can yield information related to realistic initial postures, neuromuscular responses, and potential pain measures. Cadavers, on the other hand, are often exposed to injurious loading conditions. These are the only human subjects that can be exposed to injurious or potentially injurious loads. The acquired data from PMHS tests consist of kinematic and kinetic data from external/embedded sensors or motion tracking, intervertebral data from high-speed x-ray, pre- and post-test imaging, and post-test dissection to identify injuries. Cadaver data can yield information regarding the tolerance to injuries detected via imaging, visible inspection and/or dissection, or post-impact mechanical testing. Given these differing conditions, outcomes, and ethical considerations, volunteer data may be more relevant to less severe neck injuries whereas PMHS data may be more relevant to more severe neck injuries.

Although our findings showed differences in the sex, age, and anthropometry of the biomechanical and reference populations, our analysis did not reveal whether the presence or scale of these differences was important. Previously documented morphological (Siegmund et al., 1997; Kamibayashi and Richmond, 1998; Matsumoto et al., 1998; Klinich et al., 2004; Stemper et al., 2008; Vasavada et al., 2008; Sato et al., 2017) and physiological differences (Ono et al., 2006; Vasavada et al., 2008) between male and female necks combined with the different risks for spine injuries in males and females in frontal and rollover crashes (Carter et al., 2014) suggests that some sex or sex-related variables could be responsible, but our understanding of the complex relationships amongst the many potential variables remains incomplete. For instance, sex, height, and weight are all interrelated, and even "normalized" metrics like BMI vary with sex and other variables (Heymsfield et al., 2014), and one variable could act as a surrogate for another in an exploratory correlational analysis. More mechanistic approaches, where individual variables or a small number of variables are systematically explored, are needed to determine which

variables are most important for a specific injury. Other factors, such as hormones, health, prior injury, disease state, and other variables further complicate our understanding of neck injury biomechanics.

We chose to tabulate volunteer and PMHS tests rather than the individual volunteers and cadavers. While we recognize that multiple tests from a single volunteer/cadaver do not generate independent data, many of the tests were not identical and therefore generated different, though not wholly independent data. From this perspective, our analysis provides an optimistic view of the amount of biomechanical data available for the human neck, and yet it still shows that there are large gaps in the overlap between the biomechanical data, the neck-injured population and the general population. A parallel set of figures reporting the data for individual volunteers and cadavers showed similar results (see the **Supplementary Materials**). In these alternate figures male subjects outnumber female subjects, the biases toward young volunteers and old cadavers remain, and the female anthropometry data remained shifted toward the 5th-percentile female.

The median and distribution of human anthropometry varies temporally and across the world's regions (Lee and Bro, 2008), and therefore using a reference population from a single year and country provides a perspective that may not be relevant to another year or country. We used recent measures of the United States population as a reference to directly compare with the United States injury datasets, however any population of interest to future researchers could be compared with the volunteer and PMHS figures. Additionally, safety systems in automobiles have changed considerably since 1993 and may confound our injury curves. To explore the effect of the differing time periods on the injury data, we split the NASS dataset into two groups: data preceding (1993–2004) and data overlapping (2005–2015) the available FARS data period. The greatest differences between the two groups were for age and weight. If we were to plot only the data from the later group, then compared to the overall data shown in the figures the mean age would increase 2.0 years for AIS1+, 1.1 years for AIS2+ and 0.7 years for AIS3+, whereas the average weight would increase 2.2 kg for AIS1+ and AIS2+ and 2.0 kg for AIS3+. Thus, at maximum, the age and weight histograms presented in the figures would shift about one bin width to the right, but would not change our overall findings. Another limitation of our work is that we did not separate either the biomechanical data or the neck-injured population by loading direction, crash type or injury type. Nevertheless, we recommend that researchers planning to conduct future volunteer and cadaver tests consider these specific factors when they specify or set up recruitment plans for the sex, age, and anthropometry distributions of their volunteers and cadavers.

CONCLUSION

We found large differences in the distributions of sex and age between the populations used to generate biomechanical data for the human neck and the neck-injured populations. Smaller differences were noted in the height, weight, and BMI distributions between these populations. Overall, our findings indicate that more female biomechanical data are needed, especially for females of average height and weight. Our findings also show that there is minimal biomechanical data for older volunteers, young cadavers, and volunteers of both sexes with high BMIs. More generally, we encourage researchers to consider the diversity of the population being injured when enrolling volunteers and cadavers for their biomechanical studies.

AUTHOR CONTRIBUTIONS

GB developed the study protocol with the assistance of PC and conducted the systematic literature search. PC reviewed papers where the methodology or relevance was ambiguous. GB collected and compiled the biomechanical subject data from papers, databases, or directly from the authors. GS queried the NASS-CDS database and calculated the United States Population distributions. GB queried the FARS data and synthesized each dataset into distributions. PC drafted the introduction, GB and GS drafted the methods and results, and GS drafted the discussion. All authors edited and approved the final article.

FUNDING

We gratefully acknowledge the Natural Sciences and Engineering Research Council of Canada for funding this project with a Discovery Grant (# RGPIN-2017-06013) and the Work Learn International Undergraduate Research Award at the University of British Columbia that supported author GB's work on this project.

ACKNOWLEDGMENTS

The authors would like to acknowledge Sarah Parker for her valuable assistance and expertise in developing the literature search protocol.

SUPPLEMENTARY MATERIAL

The Supplementary Material for this article can be found online at: https://www.frontiersin.org/articles/10.3389/fbioe.2021.684217/full#supplementary-material

REFERENCES

Acosta, S. M., Ash, J., Lessley, D., Shaw, C. G., Heltzel, S., Crandall, J., et al. (2016). Comparison of Whole Body Response in Oblique and Full Frontal Sled Tests, 2016 IRCOBI Conference Proceedings (Malaga, Spain: International Research Council on the Biomechanics of Injury), 15.

Albert, D. L., Beeman, S. M., and Kemper, A. R. (2018). Occupant Kinematics of the Hybrid III, THOR-M, and Postmortem Human Surrogates under Various Restraint Conditions in Full-Scale Frontal

Sled Tests. *Traffic Inj. Prev.* 19 (Suppl. 1), S50–S58. doi:10.1080/15389588.2017.1405390

Arbogast, K. B., Mathews, E. A., Seacrist, T., Maltese, M. R., Hammond, R., Balasubramanian, S., et al. (2012). The Effect of Pretensioning and Age on Torso Rollout in Restrained Human Volunteers in Far-Side Lateral and Oblique Loading. *Stapp Car Crash J.* 56, 443–467. doi:10.4271/2012-22-0012

Arbogast, K. B., Balasubramanian, S., Seacrist, T., Maltese, M. R., Garcia-Espana, J. F., Hopely, T., Constans, E., Lopez-Valdes, F. J., Kent, R. W., Tanji, H., and Higuchi, K. (2009). "Comparison of Kinematic Responses of the Head and Spine for Children and Adults in Low-Speed Frontal Sled Tests," in 53rd Stapp Car Crash Conference, November 2–4, 2009, Savannah, GA, 2009-22–0012. doi:10.4271/2009-22-0012

Bédard, M., Guyatt, G. H., Stones, M. J., and Hirdes, J. P. (2002). The Independent Contribution of Driver, Crash, and Vehicle Characteristics to Driver Fatalities. *Accid. Anal. Prev.* 34 (6), 717–727. doi:10.1016/S0001-4575(01)00072-0

Blouin, J.-S., Inglis, J. T., and Siegmund, G. P. (2006). Auditory Startle Alters the Response of Human Subjects Exposed to a Single Whiplash-like Perturbation. *Spine* 31 (2), 146–154. doi:10.1097/01.brs.0000195157.75056.df

Bose, D., Segui-Gomez, ScD, M., and Crandall, J. R. (2011). Vulnerability of Female Drivers Involved in Motor Vehicle Crashes: an Analysis of US Population at Risk. *Am. J. Public Health* 101 (12), 2368–2373. doi:10.2105/AJPH.2011.300275

Brault, J. R., Wheeler, J. B., Siegmund, G. P., and Brault, E. J. (1998). Clinical Response of Human Subjects to Rear-End Automobile Collisions. *Arch. Phys. Med. Rehabil.* 79, 72–80. doi:10.1016/s0003-9993(98)90212-x

Buhrman, J. R., and Perry, C. E. (1994). Human and Manikin Head/neck Response to +Gz Acceleration when Encumbered by Helmets of Various Weights. *Aviat Space Environ. Med.* 65 (65), 1086–1090.

Carter, P. M., Flannagan, C. A. C., Reed, M. P., Cunningham, R. M., and Rupp, J. D. (2014). Comparing the Effects of Age, BMI and Gender on Severe Injury (AIS 3+) in Motor-Vehicle Crashes. *Accid. Anal. Prev.* 72, 146–160. doi:10.1016/j.aap.2014.05.024

Crandall, J., Lessley, D., Shaw, G., and Ash, J. (2014). Displacement Response of the Spine in Restrained PMHS during Frontal Impacts. *Int. J. Automotive Eng.* 5 (2), 59–64. doi:10.20485/jsaeijae.5.2_59

Davidsson, J., Deutscher, C., Hell, W., Lövsund, P., and Svensson, M. Y. (2001). Human Volunteer Kinematics in Rear-End Sled Collisions. *J. Crash Prev. Inj. Control.* 2 (4), 319–333. doi:10.1080/10286580008902576

Deng, B., and Wang, J. T. (2003). "Assessment of H-Model Using Volunteer Tests," in Digital Human Modeling for Design and Engineering Conference and Exhibition, June 16, 2003, Montreal, QC, 2003-01–2220. doi:10.4271/2003-01-2220

Doczy, E., Mosher, S., and Buhrman, J. (2004). *The Effects of Variable Helmet Weight and Subject Bracing on Neck Loading during Frontal-GX Impact*. Dayton, OH: GENERAL DYNAMICS ADVANCED INFORMATION SYSTEMS DAYTON OH. Available at: https://apps.dtic.mil/sti/citations/ADA446621 (Accessed March 21, 2021).

Ejima, S., Ito, D., Satou, F., Mikami, K., Ono, K., Kaneoka, K., et al. (2012). Effects of Pre-impact Swerving/Steering on Physical Motion of the Volunteer in the Low-Speed Side-Impact Sled Test, 2012 IRCOBI Conference Proceedings (Dublin, Ireland: International Research Council on the Biomechanics of Injury), 15.

Ejima, S., Koshiro, O., Holcombe, S., Kaneoka, K., and Fukushima, M. (2007). *A Study on Occupant Kinematics Behaviour and Muscle Activities during Pre-impact Braking Based on Volunteer Tests*. Maastricht, Netherlands: International Research Council on the Biomechanics of Injury. Available at: https://regroup-production.s3.amazonaws.com/documents/ReviewReference/208080904/1_2.pdf?AWSAccessKeyId=AKIAJBZQODCMKJA4H7DA&Expires=1616359328&Signature=tjagKdHDPBiXu%2B%2Be%2Ffgug0ukqUE%3D (Accessed March 21, 2021).

Ejima, S., Zama, Y., Satou, F., Holcombe, S., Ono, K., Kaneoka, K., et al. (2008). Prediction of the Physical Motion of the Human Body Based on Muscle Activity during Pre-impact Braking, 2008 IRCOBI Conference Proceedings (Bern, Switzerland: International Research Council on the Biomechanics of Injury), 13.

Evans, L., and Gerrish, P. H. (2001). *Gender and Age Influence on Fatality Risk from the Same Physical Impact Determined Using Two-Car Crashes*. Warrendale, Pennsylvania, US: SAE International. doi:10.4271/2001-01-1174

Ewing, C. L., and Thomas, D., J. (1972). *Human Head and Neck Response to Impact Acceleration*. Pensacola, FL: NAVAL AEROSPACE MEDICAL RESEARCH LAB PENSACOLA FL, 386.

Ewing, C. L., Thomas, D. J., Lustick, L., Becker, E., Willems, G., and Muzzy, W. H. (1975). "The Effect of the Initial Position of the Head and Neck on the Dynamic Response of the Human Head and Neck to -Gx Impact Acceleration," in 19th Stapp Car Crash Conference (1975), November 17–19, 1975, San Diego, CA, 751157. doi:10.4271/751157

Ewing, C. L., Thomas, D. J., Lustick, L., Muzzy, W. H., Willems, G. C., and Majewski, P. (1978). *Effect of Initial Position on the Human Head and Neck Response to +Y Impact Acceleration*. Warrendale, PA: SAE Technical Paper #780888. doi:10.4271/780888

Ewing, C. L., Thomas, D. J., Lustik, L., Muzzy, W. H., Willems, G. C., and Majewski, P. (1977). *Dynamic Response of the Human Head and Neck to +Gy Impact Acceleration*. Warrendale, PA: SAE Technical Papers. doi:10.4271/770928

Ewing, C. L., Thomas, D. J., Patrick, L. M., Beeler, G. W., and Smith, M. J. (1969). "Living Human Dynamic Response to -Gx Impact Acceleration II-Accelerations Measured on the Head and Neck," in 13th Stapp Car Crash Conference (1969) (Warrendale, Pennsylvania, US: SAE International). doi:10.4271/690817

Fryar, C. D., Carroll, M. D., Gu, Q., Afful, J., and Ogden, C. L. (2021). Anthropometric Reference Data for Children and Adults : United States, 2015–2018. Available at: https://stacks.cdc.gov/view/cdc/100478.

Forman, J. L., Lopez-Valdes, F., Lessley, D. J., Riley, P., Sochor, M., Heltzel, S., et al. (2013). "Occupant Kinematics and Shoulder Belt Retention in Far-Side Lateral and Oblique Collisions: A Parametric Study," in 57th Stapp Car Crash Conference, November 11–13, 2013, Orlando, FL, 2013-22–0014. doi:10.4271/2013-22-0014

Foster, J., Kortge, J., and Wolanin, M. (1977). Hybrid III—A Biomechanically-Based Crash Test Dummy. *SAE Trans.* 86, 3268–3283. Available at: http://www.jstor.org/stable/44644622 (Accessed May 19, 2021).

Fugger, T. F., Randles, B. C., Wobrock, J. L., Welcher, J. B., Voss, D. P., and Eubanks, J. J. (2002). "Human Occupant Kinematics in Low Speed Side Impacts," in SAE 2002 World Congress & Exhibition, March 4–7, 2002, Detroit, United States, 2002-01–0020. doi:10.4271/2002-01-0020

Funk, J. R., Cormier, J. M., Bain, C. E., Guzman, H., Bonugli, E., and Manoogian, S. J. (2011). Head and Neck Loading in Everyday and Vigorous Activities. *Ann. Biomed. Eng.* 39 (2), 766–776. doi:10.1007/s10439-010-0183-3

Funk, J. R., Cormier, J. M., Bain, C. E., Guzman, H., and Bonugli, E. (2009). "Validation and Application of a Methodology to Calculate Head Accelerations and Neck Loading in Soccer Ball Impacts," in SAE World Congress & Exhibition, April 20–23, 2009, Detroit, MI, 2009-01–0251. doi:10.4271/2009-01-0251

Gepner, B. D., Joodaki, H., Sun, Z., Jayathirtha, M., Kim, T., Forman, J. L., et al. (2018). "Performance of the Obese GHBMC Models in the Sled and belt Pull Test Conditions," in IRCOBI Conference Proceedings, September 12–14, 2018, Athens, Greece.

Gutsche, A. J., Tomasch, E., Darok, M., Sinz, W., Ciglaric, I., Ravnik, D., et al. (2014). "Comparison of the Cervical Spine Bony Kinematics for Female PMHS with the Virtual EvaRID Dummy under Whiplash Loading," in *Effect of Countermeasures on Adult Kinematics during Pre-crash Evasive Swerving* (Berlin, Germany: International Research Council on the Biomechanics of Injury). Available at: https://regroup-production.s3.amazonaws.com/documents/ReviewReference/208079437/32.pdf?AWSAccessKeyId=AKIAJBZQODCMKJA4H7DA&Expires=1616361145&Signature=tVE0QuIrBNwFvnP42z2fszSf6WI%3D (Accessed March 21, 2021).

Heymsfield, S. B., Peterson, C. M., Thomas, D. M., Heo, M., Schuna, J. M., Hong, S., et al. (2014). Scaling of Adult Body Weight to Height across Sex and Race/ethnic Groups: Relevance to BMI. *Am. J. Clin. Nutr.* 100 (6), 1455–1461. doi:10.3945/ajcn.114.088831

Hill, J. D., and Boyle, L. N. (2006). Assessing the Relative Risk of Severe Injury in Automotive Crashes for Older Female Occupants. *Accid. Anal. Prev.* 38 (1), 148–154. doi:10.1016/j.aap.2005.08.006

Holt, C., Ethan, D., Valentina, G., Thomas, S., Jason, K., Richard, K., et al. (2018). Effect of Countermeasures on Adult Kinematics during Pre-crash Evasive Swerving, 2018 IRCOBI Conference Proceedings (Lonavala, India: International Research Council on the Biomechanics of Injury), 13.

Holt, C., Seacrist, T., Douglas, E., Graci, V., Kerrigan, J., Kent, R., et al. (2020). The Effect of Vehicle Countermeasures and Age on Human Volunteer Kinematics during Evasive Swerving Events. *Traffic Inj. Prev.* 21 (1), 48–54. doi:10.1080/15389588.2019.1679798

Humm, J. R., Yoganandan, N., Driesslein, K. G., and Pintar, F. A. (2018). Three-dimensional Kinematic Corridors of the Head, Spine, and Pelvis for Small Female Driver Seat Occupants in Near- and Far-Side Oblique Frontal Impacts. *Traffic Inj. Prev.* 19 (Suppl. 2), S64–S69. doi:10.1080/15389588.2018.1498973

Irwin, A., and Mertz, H. (1997). Biomechanical Bases for the CRABI and Hybrid III Child Dummies. *SAE Trans.* 106, 3551–3562. Available at: http://www.jstor.org/stable/44720132 (Accessed May 19, 2021).

Jakobsson, L., Norin, H., and Svensson, M. Y. (2004). Parameters Influencing AIS 1 Neck Injury Outcome in Frontal Impacts. *Traffic Inj. Prev.* 5 (2), 156–163. doi:10.1080/15389580490435989

Kallieris, D., Mattern, R., and Wismans, J. (1987). "Comparison of Human Volunteer and Cadaver Head-Neck Response in Frontal Flexion," in 31st Stapp Car Crash Conference, November 9–11, 1987, New Orleans, LA, 872194. doi:10.4271/872194

Kamibayashi, L. K., and Richmond, F. J. R. (1998). Morphometry of Human Neck Muscles. *Spine* 23 (12), 1314–1323. doi:10.1097/00007632-199806150-00005

Kent, R. W., Forman, J. L., and Bostrom, O. (2010). Is There Really a "Cushion Effect"?: A Biomechanical Investigation of Crash Injury Mechanisms in the Obese. *Obesity* 18 (4), 749–753. doi:10.1038/oby.2009.315

Klinich, K., Ebert, S., Van Ee, C., and Flannagan, C. (2004). *Cervical Spine Geometry in the Automotive Seated Posture: Variations with Age, Stature, and Gender*. Warrendale, PA: SAE Technical Paper No. 2004-22-0014. doi:10.4271/2004-22-0014

Krafft, M., Kullgren, A., Lie, A., and Tingvall, C. (2003). The Risk of Whiplash Injury in the Rear Seat Compared to the Front Seat in Rear Impacts. *Traffic Inj. Prev.* 4 (2), 136–140. doi:10.1080/15389580309862

Kullgren, A., Stigson, H., and Krafft, M. (2013). *Development of Whiplash Associated Disorders for Male and Female Car Occupants in Cars Launched since the 80s in Different Impact Directions*. Gothenburg, Sweden: International Research Council on the Biomechanics of Impact, 12.

Lee, S., and Bro, R. (2008). Regional Differences in World Human Body Dimensions: the Multi-Way Analysis Approach. *Theor. Issues Ergon. Sci.* 9, 325–345. doi:10.1080/14639220701511713

Lessley, D. J., Riley, P., Zhang, Q., Foltz, P., Overby, B., Heltzel, S., et al. (2014). Occupant Kinematics in Laboratory Rollover Tests: PMHS Response. *Stapp Car Crash J.* 58, 251–316. doi:10.4271/2014-22-0011

Linder, A., and Svensson, M. Y. (2019). Road Safety: the Average Male as a Norm in Vehicle Occupant Crash Safety Assessment. *Interdiscip. Sci. Rev.* 44 (2), 140–153. doi:10.1080/03080188.2019.1603870

Lopez-Valdes, F. J., Forman, J., Kent, R., Bostrom, O., and Segui-Gomez, M. (2009). A Comparison between a Child-Size PMHS and the Hybrid III 6 YO in a Sled Frontal Impact. *Ann. Adv. Automot Med.* 53, 237–246.

Lopez-Valdes, F. J., Lau, A., Lamp, J., Riley, P., Lessley, D. J., Damon, A., et al. (2010). Analysis of Spinal Motion and Loads during Frontal Impacts. Comparison between PMHS and ATD. *Ann. Adv. Automot Med.* 54, 61–78.

López-Valdés, F. J., Juste-Lorente, O., Maza-Frechin, M., Pipkorn, B., Sunnevang, C., Lorente, A., et al. (2016). Analysis of Occupant Kinematics and Dynamics in Nearside Oblique Impacts. *Traffic Inj. Prev.* 17 (Suppl. 1), 86–92. doi:10.1080/15389588.2016.1189077

Lopez-Valdes, F. J., Riley, P. O., Lessley, D. J., Arbogast, K. B., Seacrist, T., Balasubramanian, S., et al. (2014). The Six Degrees of Freedom Motion of the Human Head, Spine, and Pelvis in a Frontal Impact. *Traffic Inj. Prev.* 15 (3), 294–301. doi:10.1080/15389588.2013.817668

Margulies, S. S., Yuan, Q., and Guccione, S. J. (1998). Kinematic Response of the Neck to Voluntary and Involuntary Flexion. *Aviat Space Environ. Med.* 69 (9), 896.

Mathews, E. A., Balasubramanian, S., Seacrist, T., Maltese, M. R., Sterner, R., and Arbogast, K. B. (2013). Electromyography Responses of Pediatric and Young Adult Volunteers in Low-Speed Frontal Impacts. *J. Electromyogr. Kinesiol.* 23 (5), 1206–1214. doi:10.1016/j.jelekin.2013.06.010

Matsumoto, M., Fujimura, Y., Suzuki, N., Toyama, Y., and Shiga, H. (1998). Cervical Curvature in Acute Whiplash Injuries: Prospective Comparative Study with Asymptomatic Subjects. *Injury* 29 (10), 775–778. doi:10.1016/S0020-1383(98)00184-3

Meijer, R., van Hoof, J. F. A. M., Ono, K., Kaneoka, K., et al. (2001). "Analysis of Rear End Impact Response Using Mathematical Human Modelling and Volunteer Tests," in JSAE Spring Convention, May 23–25, 2001, Yokohama, Japan.

Mertz, H. J., Irwin, A. L., and Prasad, P. (2003). Biomechanical and Scaling Bases for Frontal and Side Impact Injury Assessment Reference Values. *Stapp Car Crash J.* 47, 155–188.

Morris, C. E., and Popper, S. E. (1999). Gender and Effect of Impact Acceleration on Neck Motion, *Aviat Space Environ. Med.* 70 (9), 851.

Ono, K., Ejima, S., Suzuki, Y., Kaneoka, K., Fukushima, M., Ujihashi, S., et al. (2006). *Prediction of Neck Injury Risk Based on the Analysis of Localized Cervical Vertebral Motion of Human Volunteers during Low-Speed Rear Impacts*. Madrid, Spain: Proc. IRCOBI Conf., 103–113.

Ono, K., Inami, S., Kaneoka, K., Gotou, T., Kisanuki, Y., Sakuma, S., et al. (1999). *Relationship between Localized Spine Deformation and Cervical Vertebral Motions for Low Speed Rear Impacts Using Human Volunteers*. Sitges, Spain: International Research Council on Biokinetics of Impact. Available at: https://regroup-production.s3.amazonaws.com/documents/ReviewReference/208077264/Ono%2C%201999.pdf?AWSAccessKeyId=AKIAJBZQODCMKJA4H7DA&Expires=1616363488&Signature=k%2FUo4INkBR6gUaYDnPAKkLcYLGQ%3D (Accessed: March 21, 2021).

Perry, C., John, R. B., Doczy, E., Mosher, S., et al. (2003). "The Effects of Variable Helmet Weight on Head Response and Neck Loading during Lateral +Gy Impact," in The Effects of Variable Helmet Weight on Head Response and Neck Loading During Lateral +Gy Impact. 41st Annual SAFE Symposium, September 22–24, 2003, Jacksonville, FL, 8.

Petit, P., Trosseille, X., Uriot, J., Poulard, D., Potier, P., Baudrit, P., et al. (2019). Far Side Impact Injury Threshold Recommendations Based on 6 Paired WorldSID/Post-Mortem Human Subjects Tests. *Stapp Car Crash J.* 63, 127–146. doi:10.4271/2019-22-0005

Petitjean, A., Lebarbe, M., Potier, P., Trosseille, X., and Lassau, J.-P. (2002). "Laboratory Reconstructions of Real World Frontal Crash Configurations Using the Hybrid III and THOR Dummies and PMHS," in 46th Stapp Car Crash Conference, November 11–13, 2002, Ponte Vedra Beach, FL, 2002-22–0002. doi:10.4271/2002-22-0002

Pietsch, H. A., Bosch, K. E., Weyland, D. R., Spratley, E. M., Henderson, K. A., Salzar, R. S., et al. (2016) 'Evaluation of WIAMan Technology Demonstrator Biofidelity Relative to Sub-injurious PMHS Response in Simulated Under-body Blast Events', in. 60TH Stapp Car Crash Conference, November 7–9, 2016, Washington, DC, United States, 2016-22–0009. doi:10.4271/2016-22-0009

Pintar, F. A., Yoganandan, N., and Maiman, D. J. (2010). Lower Cervical Spine Loading in Frontal Sled Tests Using Inverse Dynamics: Potential Applications for Lower Neck Injury Criteria. *Stapp Car Crash J.* 54, 133–166. doi:10.4271/2010-22-0008

Pintar, F. A., Yoganandan, N., Stemper, B. D., Bostrom, O., Rouhana, S. W., Digges, K. H., et al. (2007). Comparison of PMHS, WorldSID, and THOR-NT Responses in Simulated Far Side Impact. *Stapp Car Crash J.* 51, 313–360. doi:10.4271/2007-22-0014

Poulard, D., Bermond, F., and Bruyère, K. (2013). *In Vivo* Analysis of Thoracic Mechanical Response Variability under Belt Loading: Specific Behavior and Relationship to Age, Gender and Body Mass Index. *Stapp Car Crash J.* 57, 59–87. doi:10.4271/2013-22-0003

Reed, M. P., Ebert-Hamilton, S. M., and Rupp, J. D. (2012). Effects of Obesity on Seat Belt Fit. *Traffic Inj. Prev.* 13 (4), 364–372. doi:10.1080/15389588.2012.659363

Rouhana, S. W., Kankanala, S. V., Prasad, P., Rupp, J. D., Jeffreys, T. A., and Schneider, L. W. (2006). Biomechanics of 4-Point Seat Belt Systems in Farside Impacts. *Stapp Car Crash J.* 50, 267–298. doi:10.4271/2006-22-0012

Rupp, J. D., Flannagan, C. A. C., Leslie, A. J., Hoff, C. N., Reed, M. P., and Cunningham, R. M. (2013). Effects of BMI on the Risk and Frequency of AIS 3+ Injuries in Motor-Vehicle Crashes. *Obesity* 21 (1), E88–E97. doi:10.1002/oby.20079

Sato, F., Odani, M., Miyazaki, Y., Yamazaki, K., Östh, J., and Svensson, M. (2017). Effects of Whole Spine Alignment Patterns on Neck Responses in Rear End Impact. *Traffic Inj. Prev.* 18 (2), 199–206. doi:10.1080/15389588.2016.1227072

Seacrist, T., Locey, C. M., Mathews, E. A., Jones, D. L., Balasubramanian, S., Maltese, M. R., et al. (2014). Evaluation of Pediatric ATD Biofidelity as Compared to Child Volunteers in Low-Speed Far-Side Oblique and Lateral Impacts. *Traffic Inj. Prev.* 15 (Suppl. 1), S206–S214. doi:10.1080/15389588.2014.930832

Shaw, G., Lessley, D. J., Ash, J. L., Sochor, M. R., Crandall, J. R., Luzon-Narro, J., et al. (2014). Side Impact PMHS Thoracic Response with Large-Volume Air Bag. *Traffic Inj. Prev.* 15 (1), 40–47. doi:10.1080/15389588.2013.792109

Shumanty, R. (2018). Mortality: Overview, 2014 to 2016, Statistics Canada. Available at: https://www150.statcan.gc.ca/n1/pub/91-209-x/2018001/article/54957-eng.htm (Accessed March 22, 2021).

Siegmund, G. P., Sanderson, D. J., and Inglis, J. T. (2004). Gradation of Neck Muscle Responses and Head/Neck Kinematics to Acceleration and Speed Change in Rear-End Collisions. *Stapp Car Crash J.* 48, 419–430. doi:10.4271/2004-22-0018

Siegmund, G. P., Blouin, J.-S., Carpenter, M. G., Brault, J. R., and Inglis, J. T. (2008). Are Cervical Multifidus Muscles Active during Whiplash and Startle? an Initial Experimental Study. *BMC Musculoskelet. Disord.* 9 (1), 80. doi:10.1186/1471-2474-9-80

Siegmund, G. P., and Blouin, J.-S. (2009). Head and Neck Control Varies with Perturbation Acceleration but Not Jerk: Implications for Whiplash Injuries. *J. Physiol.* 587 (8), 1829–1842. doi:10.1113/jphysiol.2009.169151

Siegmund, G. P., David, J, K., and Lawrence, J. M.(1997). "Head/neck Kinematic Response of Human Subjects in Low-Speed Rear-End Collisions," in 41st STAPP Car Crash Conference, November 13–14, 1997, Lake Buena Vista, FL, 357–385.

Siegmund, G. P., Sanderson, D. J., Myers, B. S., and Inglis, J. T. (2003a). Awareness Affects the Response of Human Subjects Exposed to a Single Whiplash-like Perturbation. *Spine* 28 (7), 671–679. doi:10.1097/01.BRS.0000051911.45505.D3

Siegmund, G. P., Sanderson, D. J., Myers, B. S., and Inglis, J. T. (2003b). Rapid Neck Muscle Adaptation Alters the Head Kinematics of Aware and Unaware Subjects Undergoing Multiple Whiplash-like Perturbations. *J. Biomech.* 36 (4), 473–482. doi:10.1016/S0021-9290(02)00458-X

Silverman, B. W. (1986). *Density Estimation for Statistics and Data Analysis*. London, New York: Chapman & Hall. doi:10.1007/978-1-4899-3324-9

Stammen, J. A., Herriott, R., Kang, Y. S., Dupaix, R., and Bolte, J. (2012). Dynamic Properties of the Upper Thoracic Spine-Pectoral Girdle (UTS-PG) System and Corresponding Kinematics in PMHS Sled Tests. *Stapp Car Crash J.* 56, 65–104. doi:10.4271/2012-22-0003

Stark, D. B., Willis, A. K., Eshelman, Z., Kang, Y. S., Ramachandra, R., Bolte, J. H., et al. (2019). Human Response and Injury Resulting from Head Impacts with Unmanned Aircraft Systems. *Stapp Car Crash J.* 63, 29–64. doi:10.4271/2019-22-0002

Stemper, B. D., Yoganandan, N., Pintar, F. A., Maiman, D. J., Meyer, M. A., DeRosia, J., et al. (2008). Anatomical Gender Differences in Cervical Vertebrae of Size-Matched Volunteers. *Spine* 33 (2), E44–E49. doi:10.1097/BRS.0b013e318160462a

Sundararajan, S., Rouhana, S. W., Board, D., DeSmet, E., Prasad, P., Rupp, J. D., et al. (2011). Biomechanical Assessment of a Rear-Seat Inflatable Seatbelt in Frontal Impacts. *Stapp Car Crash J.* 55, 161–197. doi:10.4271/2011-22-0008

Symeonidis, I., Kavadarli, G., Erich, S., Graw, M., and Peldschus, S. (2012). Analysis of the Stability of PTW Riders in Autonomous Braking Scenarios. *Accid. Anal. Prev.* 49, 212–222. doi:10.1016/j.aap.2011.07.007

US Census Bureau (2021). Available at: https://www2.census.gov/programs-surveys/popest/tables/2010-2019/national/asrh/nc-est2019-syasexn.xlsx. (Accessed February 2, 2021).

van den Kroonenberg, A., Philippens, M., Cappon, H., Wismans, J., et al. (1998). "Human Head-Neck Response during Low-Speed Rear End Impacts," in 42nd Annual Stapp Car Crash Conference (Tempe, Arizona, USA: Society of Automotive Engineers, Inc., Warrendale, Pennsylvania, USA), 1–16.

van Rooij, L., Elrofai, H., Philippens, M. M., and Daanen, H. A. (2013). Volunteer Kinematics and Reaction in Lateral Emergency Maneuver Tests. *Stapp Car Crash J.* 57, 313–342.

Vasavada, A. N., Danaraj, J., and Siegmund, G. P. (2008). Head and Neck Anthropometry, Vertebral Geometry and Neck Strength in Height-Matched Men and Women. *J. Biomech.* 41 (1), 114–121. doi:10.1016/j.jbiomech.2007.07.007

Vezin, P., Bruyere-Garnier, K., Bermond, F., and Verriest, J. P. (2002). "Comparison of Hybrid III, Thor-α and PMHS Response in Frontal Sled Tests," in 46th Stapp Car Crash Conference, November 11–13, 2002, Ponte Vedra Beach, FL, 2002-22–0001. doi:10.4271/2002-22-0001

Vezin, P., and Verriest, J. P. (2003). Influence of the Impact and Restraint Conditions on Human Surrogate Head Response to a Frontal Deceleration, 2003 IRCOBI Conference Proceedings (Lisbon, Portugal: International Research Council on the Biomechanics of Injury), 18.

Viano, D. C. (2003). Seat Influences on Female Neck Responses in Rear Crashes: A Reason Why Women Have Higher Whiplash Rates. *Traffic Inj. Prev.* 4 (3), 228–239. doi:10.1080/15389580309880

White, N. A., Begeman, P. C., Hardy, W. N., Yang, K. H., Ono, K., Sato, F., Kamiji, K., Yasuki, T., and Bey, M. J. (2009). "Investigation of Upper Body and Cervical Spine Kinematics of Post Mortem Human Subjects (PMHS) during Low-Speed, Rear-End Impacts," in SAE World Congress & Exhibition, April 20–23, 2009, Detroit, MI, 2009-010387. doi:10.4271/2009-01-0387

Wiechel, J., and Bolte, J. (2006). "Response of Reclined Post Mortem Human Subjects to Frontal Impact," in SAE 2006 World Congress & Exhibition, April 3–6, 2006, Detroit, MI, United States, 2006-01–0674. doi:10.4271/2006-01-0674

Yoganandan, N., Chirvi, S., Voo, L., Pintar, F. A., and Banerjee, A. (2018). Role of Age and Injury Mechanism on Cervical Spine Injury Tolerance from Head Contact Loading. *Traffic Inj. Prev.* 19 (2), 165–172. doi:10.1080/15389588.2017.1355549

Yoganandan, N., and Pintar, F. (2000). "Biomechanics of Human Occupants in Simulated Rear Crashes: Documentation of Neck Injuries and Comparison of Injury Criteria," in 44th Stapp Car Crash Conference, April 6–8, 2000, Atlanta, GA, 2000-2001–SC14. doi:10.4271/2000-01-SC14

Yukawa, Y., Kato, F., Suda, K., Yamagata, M., and Ueta, T. (2012). Age-related Changes in Osseous Anatomy, Alignment, and Range of Motion of the Cervical Spine. Part I: Radiographic Data from over 1,200 Asymptomatic Subjects. *Eur. Spine J.* 21 (8), 1492–1498. doi:10.1007/s00586-012-2167-5

Zaseck, L. W., Anne, C. B., Carl, S. M., Nichole, R. O., Matthew, P. R., Constantine, K. D., et al. (2019). Kinematic and Biomechanical Response of Post-Mortem Human Subjects under Various Pre-impact Postures to High-Rate Vertical Loading Conditions. *Stapp Car Crash J.* 63, 235. doi:10.4271/2019-22-0010

Zhu, S., Layde, P. M., Guse, C. E., Laud, P. W., Pintar, F., Nirula, R., et al. (2006). Obesity and Risk for Death Due to Motor Vehicle Crashes. *Am. J. Public Health* 96 (4), 734–739. doi:10.2105/AJPH.2004.058156

Conflict of Interest: The authors declare that the research was conducted in the absence of any commercial or financial relationships that could be construed as a potential conflict of interest.

frontiers in Bioengineering and Biotechnology

ORIGINAL RESEARCH
published: 21 September 2021
doi: 10.3389/fbioe.2021.681134

Sex, Age and Stature Affects Neck Biomechanical Responses in Frontal and Rear Impacts Assessed Using Finite Element Head and Neck Models

*M. A Corrales and D. S Cronin**

Department of MME, University of Waterloo, Waterloo, ON, Canada

The increased incidence of injury demonstrated in epidemiological data for the elderly population, and females compared to males, has not been fully understood in the context of the biomechanical response to impact. A contributing factor to these differences in injury risk could be the variation in geometry between young and aged persons and between males and females. In this study, a new methodology, coupling a CAD and a repositioning software, was developed to reposture an existing Finite element neck while retaining a high level of mesh quality. A 5th percentile female aged neck model ($F05_{75YO}$) and a 50th percentile male aged neck model ($M50_{75YO}$) were developed from existing young ($F05_{26YO}$ and $M50_{26YO}$) neck models (Global Human Body Models Consortium v5.1). The aged neck models included an increased cervical lordosis and an increase in the facet joint angles, as reported in the literature. The young and the aged models were simulated in frontal (2, 8, and 15 g) and rear (3, 7, and 10 g) impacts. The responses were compared using head and relative facet joint kinematics, and nominal intervertebral disc shear strain. In general, the aged models predicted higher tissue deformations, although the head kinematics were similar for all models. In the frontal impact, only the $M50_{75YO}$ model predicted hard tissue failure, attributed to the combined effect of the more anteriorly located head with age, when compared to the $M50_{26YO}$, and greater neck length relative to the female models. In the rear impacts, the $F05_{75YO}$ model predicted higher relative facet joint shear compared to the $F05_{26YO}$, and higher relative facet joint rotation and nominal intervertebral disc strain compared to the $M50_{75YO}$. When comparing the male models, the relative facet joint kinematics predicted by the $M50_{26YO}$ and $M50_{75YO}$ were similar. The contrast in response between the male and female models in the rear impacts was attributed to the higher lordosis and facet angle in females compared to males. Epidemiological data reported that females were more likely to sustain Whiplash Associated Disorders in rear impacts compared to males, and that injury risk increases with age, in agreement with the findings in the present study. This study demonstrated that, although the increased lordosis and facet angle did not affect the head kinematics, changes at the tissue level were considerable (e.g., 26% higher relative facet shear in the female neck compared to the male, for rear impact) and relatable to the epidemiology. Future work will investigate tissue damage and failure through the incorporation of aged material properties and muscle activation.

OPEN ACCESS

Edited by:
Francisco J. Lopez-Valdes, Comillas Pontifical University, Spain

Reviewed by:
Jason Luck, Duke University, United States
Carolyn Roberts, University of Virginia, United States
Kevin Moorhouse, National Highway Traffic Safety Administration, United States

****Correspondence:***
D. S Cronin
duane.cronin@uwaterloo.ca

Specialty section:
This article was submitted to Biomechanics, a section of the journal Frontiers in Bioengineering and Biotechnology

Received: *15 March 2021*
Accepted: *06 September 2021*
Published: *21 September 2021*

Citation:
Corrales MA and Cronin DS (2021) Sex, Age and Stature Affects Neck Biomechanical Responses in Frontal and Rear Impacts Assessed Using Finite Element Head and Neck Models. Front. Bioeng. Biotechnol. 9:681134. doi: 10.3389/fbioe.2021.681134

Keywords: neck biomechanical response, age effects, sex effects, finite element model, frontal impact, stature effects, size effects, rear impact

INTRODUCTION

The elderly population has been identified to have an increased incidence of injury, compared to a young population, under similar loading in vehicular crashes (Lomoschitz et al., 2002; Kahane, 2013). The increased injury risk has been attributed, in part, to the change in posture associated with age (Park et al., 2016a). Specifically, within the neck, neck pain prevalence in the elderly (70–74 years old (YO)), is higher than in the younger population (Safiri et al., 2020) while vehicular crashes have been identified as one of the main causes of neck injuries (Umana et al., 2018). It has been found that the elderly exhibit increased lordosis of the cervical spine (D. Klinich et al., 2012) due to the combined effect of the increased kyphosis of the thoracic spine (Drzał-Grabiec et al., 2012) and orientation of the head to maintain the infraorbital-tragion line orientation. In addition to the increased lordosis in the neck with age, the cervical spine undergoes other morphological changes, such as an increase in facet angle (Parenteau et al., 2014). The isolated effect of the posture and morphological changes associated with increasing age on the tissue response has not been fully understood (Schoell et al., 2015) and has not been investigated in the neck region where some of the largest posture changes occur. In addition, it has been shown that small stature female occupants demonstrate a higher incidence of injury in car crash events (Bose et al., 2011) when compared to mid-size males. It has also been reported that females have a higher risk of Whiplash Associated Disorders (WAD) than males (Carlsson, 2012) in rear impacts. These outcomes are potentially related to the geometrical features (e.g., cervical lordosis, facet angle and size) of females, compared to males, and how they interact with the vehicle seat and safety systems (Kullgren et al., 2013).

Injury to the neck can occur as a catastrophic failure of tissues (e.g., ligament rupture and hard tissue failure) or sub-catastrophic tissue distraction that can lead to pain response (i.e. WAD), often associated with low severity impacts (Yang, 2018). Among the tissues associated with WAD in the neck, the sub-catastrophic collagenous fiber realignment of the capsular ligament (CL) and tears in the anterior annulus fibrosus of the intervertebral disc (IVD) has been associated with pain response (Yoganandan et al., 2001; Cavanaugh, 2006; Quinn and Winkelstein, 2007; Curatolo et al., 2011). In addition to direct tissue response (e.g. CL deformation), it has been proposed that relative facet joint kinematics (FJK) can be used to infer injury or pain response in the facet joint (Stemper et al., 2011b); for example, the relative displacement of the superior facet along the plane of the inferior facet surface represents shear displacement of the facet joint. Large shear displacements of the facet joint could be associated with an injurious capsular ligament strain. Similarly, nominal IVD shear strain has been used in experimental and computational studies to infer the likelihood of injury based on tissue kinematics (Panjabi et al., 2004; Fice and Cronin, 2012). Therefore, differences in catastrophic tissue failure, sub-catastrophic tissue strain and relative facet joint kinematics between young and aged subjects are of interest. Importantly, the quantification of the differences in the kinematic response and soft tissue response between males and females and the effect of the ageing process is limited.

With respect to the ageing geometrical changes, it has been shown that the cervical tissue morphology (Parenteau et al., 2014) and overall neck posture (Reed and Jones, 2017) change with age. Parenteau measured cervical facet angle, vertebral body depth and maximum spinal canal diameter of 251 CT scans of male subjects with an age range from 18 to 80 years old (YO). The sample was then divided into four age groups (18–29, 30–44, 45–59, and 60+), and it was found that the 60 + group had an increased facet angle ($p < 0.0001$), increased vertebral body depth at the C4, C5, and C6 levels ($p < 0.0001$), and a decreased spinal canal radius ($p < 0.1$) with respect to the 18–29 YO age group. In a separate study, Reed and Jones developed a cervical spine posture predictor (CSP) for a driving position based on gender, stature, seated stature, and age. A total of 177 seated position subjects from 18 to 74 YO were radiographed in neutral posture, maximum extension, and maximum flexion (Snyder et al., 1975) and digitized (Desantis Klinich et al., 2004) to serve as the database of the CSP. An increased lordosis in the cervical spine in the elderly population was identified, which was in agreement with previous studies (Boyle et al., 2002; Klinich et al., 2012). Both studies demonstrated an increased vertebral body depth and an increased facet angle with increasing age. Importantly, both studies suggest that the females had a higher increase in cervical lordosis and facet angle with age than the males. Another study (Park et al., 2016b) measured the posture in a driving-like environment (seated looking forward with hands on the steering wheel) of 46 male subjects with an age range of 21–95 YO. A general full-body posture predictor (FBP) in a driving position as a function of age, body mass index, stature, seated stature, seat height and seatback angle was developed. The predictor outputs coordinate points representing the center of the eye, tragion, C7/T1 joint, T12/L1 joint, mid-hip joint, knee joint and ankle joint. Regarding age, the study concluded that the aged occupants have a more anteriorly located head center of gravity than the young occupants, attributed to the increased thoracic kyphosis and cervical lordosis. Regarding the geometrical differences between males and females, the circumference of the female cervical spine relative to the length of the neck is smaller, as is the vertebral body sizes, and it has smaller muscle cross-sectional area for stature matched subjects (Vasavada et al., 2008; Stemper et al., 2011a).

Finite element (FE) models are commonly used to assess the effect of isolated factors in the mechanical response of a system, such as geometrical changes. Human body models (HBM) are widely used to increase the understanding of kinematics in impact events, such as vehicle crashes and injury risk. Two contemporary HBM include the Global Human Body Models Consortium (GHBMC) average stature male ($M50_{26YO}$) (GHBMC M50-O

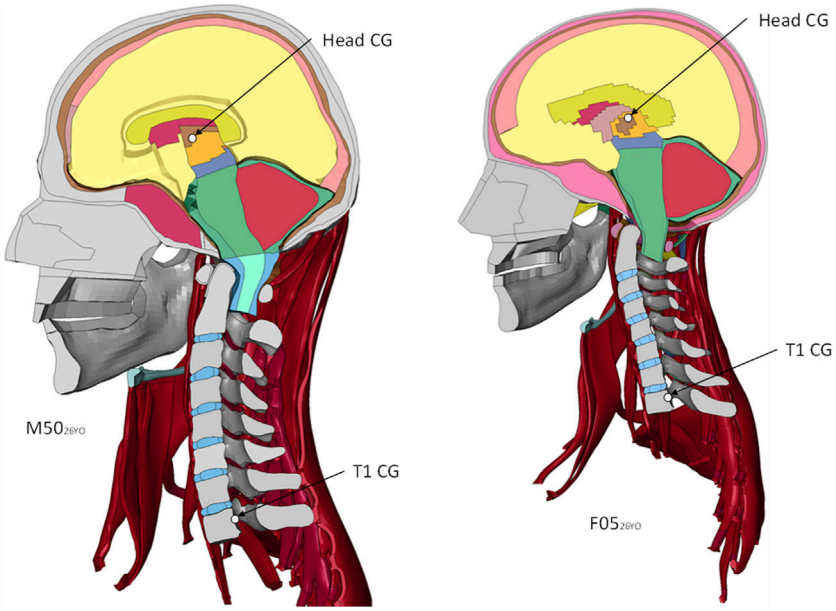

FIGURE 1 | Sagittal plane view of the detailed GHBMC Neck and Head models, showing the head center of gravity (CG) and the T1. Boundary conditions are applied at the T1.

v5.1) and small stature female ($F05_{26YO}$) (GHBMC F05-O v5.1) (**Figure 1**). The geometry of the existing (young) models was based on magnetic resonance imaging scans and computerized tomography scans of a 26 YO male volunteer representative of a 50th percentile male (Gayzik et al., 2011) and a 26 YO female volunteer representative of a 5th percentile female (Davis et al., 2014). (Gayzik et al., 2011; Davis et al., 2014) A recent study (Barker et al., 2017) validated the $M50_{26YO}$ neck model at the motion segment level against a wide range of experimental data in quasi-static and dynamic traumatic loading. At the full neck level, the model was validated (Barker and Cronin, 2021) in rear impacts using cadaveric full neck experimental data and in frontal and lateral impacts using human volunteer data. The active muscle activation scheme of the $M50_{26YO}$ and $F05_{26YO}$ was developed previously using volunteer data (Correia et al., 2020). The open-loop co-contraction muscle activation scheme (Correia et al., 2020) was designed to contract the neck muscles while maintaining the head in a neutral posture. The GHBMC neck model was objectively compared to the experimental data using the cross-correlation and corridor method (Correia et al., 2020; Barker and Cronin, 2021) with good cross-correlation ratings. The GHBMC $M50_{26YO}$ and $F05_{26YO}$ models include equivalent-plastic-strain-based element erosion criteria to model cortical and trabecular bone fracture. The cortical material model (Khor et al., 2018) was validated in a femur model under axial rotation and three-point bending. In the cervical spine, the cortical and trabecular bone models with bone fracture included were validated (Khor et al., 2017)in a C5-C6-C7 functional spinal unit under axial and eccentric compression with good agreement at the kinematic level (force-displacement response).

However, detailed HBMs have been developed in a limited number of positions (e.g., driving posture and pedestrian). Simplified models can be repositioned with simple transformation tools in pre-processor packages (e.g. LS-PrePost). For example, Frechede et al., 2006 investigated the effect of neck curvature in a simplified head and neck FE model by transforming the vertebra to achieve three postures (lordotic, straight and kyphotic) defined using Cobb angles. However, detailed models are challenging to reposition while retaining the mesh quality in the soft tissue (Janak et al., 2018). A recently released repositioning software (PIPER), developed to reposition and morph detailed HBM, without retaining the resultant stress state (Beillas et al., 2015), allows researchers to precisely reposition detailed FE models while retaining mesh quality (Janak et al., 2018).

There were two main objectives of this study. First, to investigate the effect of geometrical factors associated with the aging process on tissue-level response; therefore, the cervical spine lordosis and facet joint angle were modified while the material properties and the muscle activation scheme were held constant. The second objective was to compare the tissue-level response of the young and aged average stature male models to the young and aged small stature female models under frontal and rear impacts of various severities.

MATERIALS AND METHODS

In the present study, two existing young neck models (**Figure 1**) were extracted from contemporary detailed full HBMs M50-O v5.1 ($M50_{26YO}$) and F05-O v5.1 ($F05_{26YO}$). The $M50_{26YO}$ and $F05_{26YO}$ models were repostured to represent the posture of an average 75 YO subject, and the facet pillars were morphed to represent the facet angle change associated with age. Four models

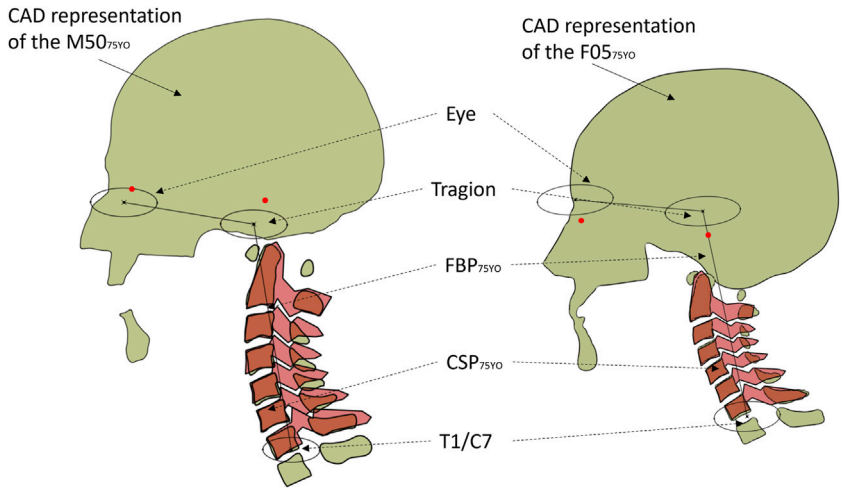

FIGURE 2 | The aged GHBMC CAD representation (light green) overlapped with the C-Spine predictor (red) for the aged M50$_{75YO}$ (left) and F05$_{75YO}$ (right). Red dots show the infraorbital and tragion of the head and neck models compared to the full-body predictor (black lines and ellipses).

were evaluated in the present study; the existing M50$_{26YO}$ and F05$_{26YO}$ and the newly developed aged models (M50$_{75YO}$ and F05$_{75YO}$) to assess the effect of age and sex differences on model response and the potential for injury. Head kinematics, FJK, and CL and IVD strain of the M50$_{75YO}$ and F05$_{75YO}$ were monitored and compared to those of the M50$_{26YO}$ and F05$_{26YO}$ models in frontal (2, 8, and 15 g) and rear (3, 7, and 10 g) impacts. The GHBMC HBMs are in the units of mm, ms and kg.

Posture Definition

A novel approach introduced in the current study is the use of CAD to improve the ease of comparing the model to literature data and to incorporate literature data to the definition of the reposturing targets in order to reduce reposturing time by 30–50%. A CAD (CATIA V5, Dassault systems) representation of the FE cervical spine model was developed (**Figure 2**). First, the posture of the M50$_{26YO}$ model was compared to the CSP (Reed and Jones, 2017) and FBP (Park et al., 2016b) data. The anthropometrics corresponding to the M50$_{26YO}$ model were used as input for the CSP and FBP models (1749 mm standing stature, 26 years old and 0.53 for the ratio standing/seated stature). It was found that the subject-specific M50$_{26YO}$ model had a longer neck (10.8%) than the single posture reported by the CSP neck length for the given stature, age and seated height ratio of the M50$_{26YO}$. A set of anthropometrics that match the posture and the neck length of the M50$_{26YO}$ model were found by increasing the stature to 1846 mm (5.5% increase in height with respect to the M50$_{26YO}$).

To define the aged posture, the age in the CSP was changed from 26 YO (1846 mm standing stature, 26 YO and 0.53 for the ratio standing/seated stature) to 75 YO (1846 mm standing stature, 75 YO and 0.53 for the ratio standing/seated stature). The change in stature with increasing age has been reported to be 2–4 cm over the life course (Fernihough and McGovern, 2015) and was excluded from this study. The vertebral bodies in the CAD assembly representing the M50$_{26YO}$ model were translated and rotated accordingly to the aged posture predicted by the CSP (Reed and Jones, 2017) to define the M50$_{75YO}$ posture. The superior endplate and the posterior edge of the vertebral body were prioritized over the inferior endplates when defining the aged posture. The aged posture was then compared to the FBP for posture validation (Park et al., 2016a). It was found that M50$_{75YO}$ had a longer neck than the average population measured in the FBP, but the general posture was considered in agreement given the variability of the lumbar and thoracic regions. For each vertebra, three landmarks were extracted from the CAD assembly for the aged neck posture: the geometric center of the superior endplate and the most distal point of the posterior transverse processes. Those landmarks served as input for the reposturing. The same procedure was applied to the F05$_{26YO}$ model to define the F05$_{75YO}$ model posture. The curvature and length of the F05$_{26YO}$ model agreed with both the CSP and the FBP. The specific locations of the landmarks used in the present study are included in the published F05 PIPER metadata (http://www.piper-project.eu).

Following the definition of the aged posture, the facet joint angles for the aged models were defined using the percentage of increase reported in the literature (Parenteau et al., 2014) at each segment level. Given that the intent of the present work was to develop the aged version of the existing subject-specific models, the relative percent increase in the facet angle from young to old was used to modify the facet angles from the young to old models. The females were reported to have an increase of 10.9% in the facet angle with age, whereas the males a 5.6% of increase when averaging all the segment levels (Parenteau et al., 2014).

Repositioning and Morphing

The young neck models were repostured to the aged target posture using contemporary repositioning software (PIPER) (Beillas et al., 2015). The reposturing process required model-specific metadata (skin definition, hard tissue definition and landmarks) within the HBM to successfully achieve the target

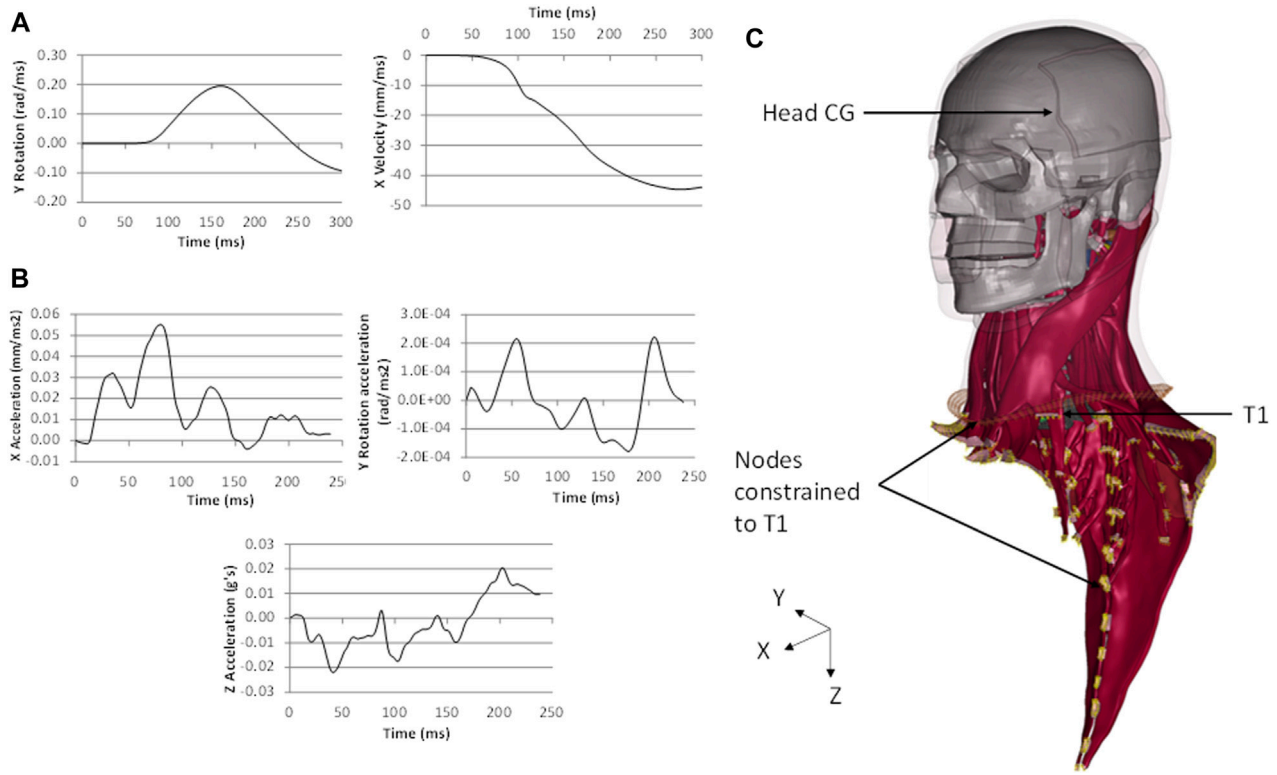

FIGURE 3 | Boundary conditions of (**A**) the 8 g frontal impact and (**B**) 7 g rear impact applied to (**C**) the first thoracic vertebrae (T1) of the head and neck models ($M50_{26YO}$ shown). Nodes constrained to T1 showed in yellow.

posture. The metadata required to reposture the neck region of the M50 and F05 models were developed in the present study. The F05 neck region metadata used in this study, along with full-body metadata, was made available to the community (http://www.piper-project.eu). Using the targets for an aged neck posture, the models were repositioned by moving the vertebrae to the desired location. After the target neck curvature was achieved, the facet pillars were morphed to achieve the target facet angle using PIPER. The behavior of the soft tissues was calculated by the PIPER software based on simplified material properties and the simulation engine "SOFA" (SOFA, National Institute for Research in Digital Science and Technology, France), another open-source package meant to simulate soft tissue behavior in clinical applications. The resultant stress-strain state after reposturing was not retained since the aged models were developed to be in a neutral posture for a specific age. All models in their respective neutral postures were assumed to be at a zero stress and strain state. After the target neck curvature was achieved, the facet pillars were morphed to increase the facet angle using PIPER. The PIPER engine calculates the position of the soft tissue during the repositioning simulation. Following the neck repositioning, the muscle, flesh, and skin meshes were smoothed using the transformation smoothing option (Janak et al., 2018) in PIPER. The mesh quality of the $M50_{75YO}$ and $F05_{75YO}$ models was assessed using the metrics and thresholds of the $M50_{26YO}$ and $F05_{26YO}$ models (including warpage <50°, aspect ratio <8, skew <70°, and Jacobian >0.4) and checked for penetrations. Static (50 ms with no boundary conditions) and dynamic (15 g frontal, 7 g lateral, and 7 g rear impacts for 235 ms) stability simulations ran to normal termination.

Model Evaluation

The four head and neck models were subjected to frontal (2, 8, and 15 g) and rear impact (3, 7, and 10 g) impacts using boundary conditions reported in the literature (Wismans et al., 1987; Deng et al., 2000) and developed for the GHBMC neck model (Barker and Cronin, 2021) (**Figures 3A,B**). The boundary conditions were applied to the first thoracic vertebra (T1). The nodes in the muscle insertions below T1, and the last layer of flesh and skin nodes were rigidly fixed to the T1. The rest of the model remained unconstrained (**Figure 3C**).

The models were assessed at three levels: head kinematics, relative FJK and nominal IVD shear strain. The head kinematics were extracted directly from the head CG of the model using a post-processor (LS-PrePost version 4.7.20). The head kinematic response of the young models was objectively compared to their aged counterparts using the cross-correlation method. The cross-correlation (CORA, pdb, Germany) is an objective method to compare the model response (e.g. aged model kinematic response) to a reference curve (e.g. young model kinematic response). The level of correlation is calculated as a value between 0 and 1, where 1 means perfect correlation and 0

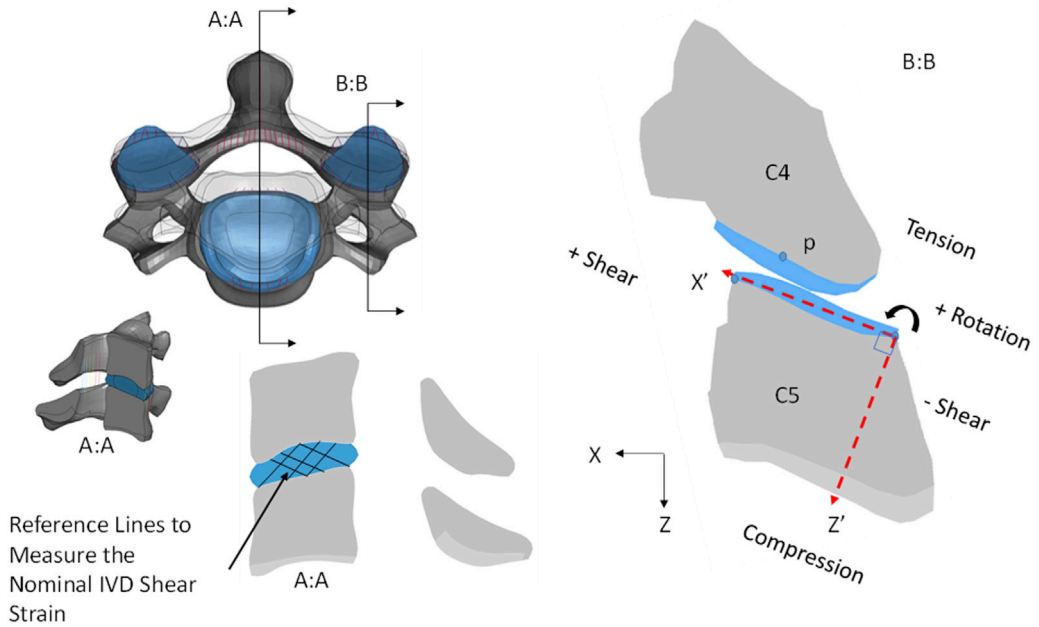

FIGURE 4 | (**A**) Nominal IVD shear strain measured using the change in angle between reference lines as in previous computational and experimental studies (Panjabi et al., 2004; Fice and Cronin, 2012) and (**B**) relative facet joint kinematics (FJK) calculated as the displacement of the point "p" in the inferior facet of the vertebra with respect to a local coordinate system in the superior facet of the lower adjacent vertebra ($M50_{26YO}$, C45 segment shown).

means no correlation. The FJK were calculated as the displacements of the point "p" in the inferior facet of the vertebra (C2 to C7) with respect to a local coordinate system (X′, Z′) in the superior adjacent vertebra (**Figure 4B**), similar to experimental (Stemper et al., 2011b) and computational studies (Corrales and Cronin, 2021). The FJK rotation was defined as the change in angle between the X′ axis and a line passing through the local coordinate system origin and the point "p". In the present study, FJK shear displacement was defined as the displacement of the point "p" along the X′ axis and the FJK compression defined as the displacement of the point "p" along the Z′ axis (**Figure 4B**). The nominal IVD shear strain was measured using the change in angle between reference lines formed by discrete points in the endplates of the adjacent vertebrae as reported in previous experimental (Panjabi et al., 2004) and computational (Fice et al., 2011) studies (**Figure 4A**). It should be noted that nominal IVD shear strain does not correspond to the strain in the tissue but rather the deformation of the IVD, based on the relative position of the vertebral bodies. In this study, it will be referred to as nominal IVD shear strain for consistency with the previous experimental and computational studies. The FJK and nominal IVD shear strain were calculated for each segment level (**Supplementary Appendix B and C**) and then averaged for clarity in the results section. In addition, the GHBMC neck model incorporates cortical and trabecular bone failure criteria (element erosion based on a critical effective plastic strain), ligament failure (displacement-based progressive element erosion), and IVD avulsion (tied interface criterion based on critical stress) (Barker et al., 2017; Barker and Cronin, 2021). Hard tissue failure (Khor et al., 2018), ligament failure and IVD avulsion (Barker et al., 2017) were monitored in the four models.

RESULTS

Aged Posture and Comparison to Geometric Data

The final position of the $M50_{75YO}$ and $F05_{75YO}$ models hard tissues was within 0.9 microns of the target positions, measured at the corners of the vertebral body. The location of the tragion and eye of the models were outside one standard deviation of the full-body predictions (Park et al., 2016b), attributed to the thoracic length and curvature of the subject-specific models. Importantly, the head orientation of the young and aged models matched the predicted head orientation of the full-body predictions in a driving position. The Bezier angles (**Figure 5**) of the $M50_{75YO}$ and $F05_{75YO}$ models where in agreement with the values reported in the literature (Klinich et al., 2012) for the aged population (**Table 1**).

The facet angle of the $M50_{75YO}$ and $F05_{75YO}$ models (**Figure 6**) were in agreement with the literature (Parenteau et al., 2014), within one standard deviation of the average with the exception of the C5 and C6 level in the male and C4 and C6 in the female, where the models had a higher facet angle compared to the literature (**Figure 6**).

Model Response Assessed With Head Kinematics and Tissue-Level Response

Four models were assessed under six impact conditions (24 analyses in total). The primary head kinematics will be shown together with the experimental data. The non-primary kinematics were monitored as well, but the magnitudes were small and

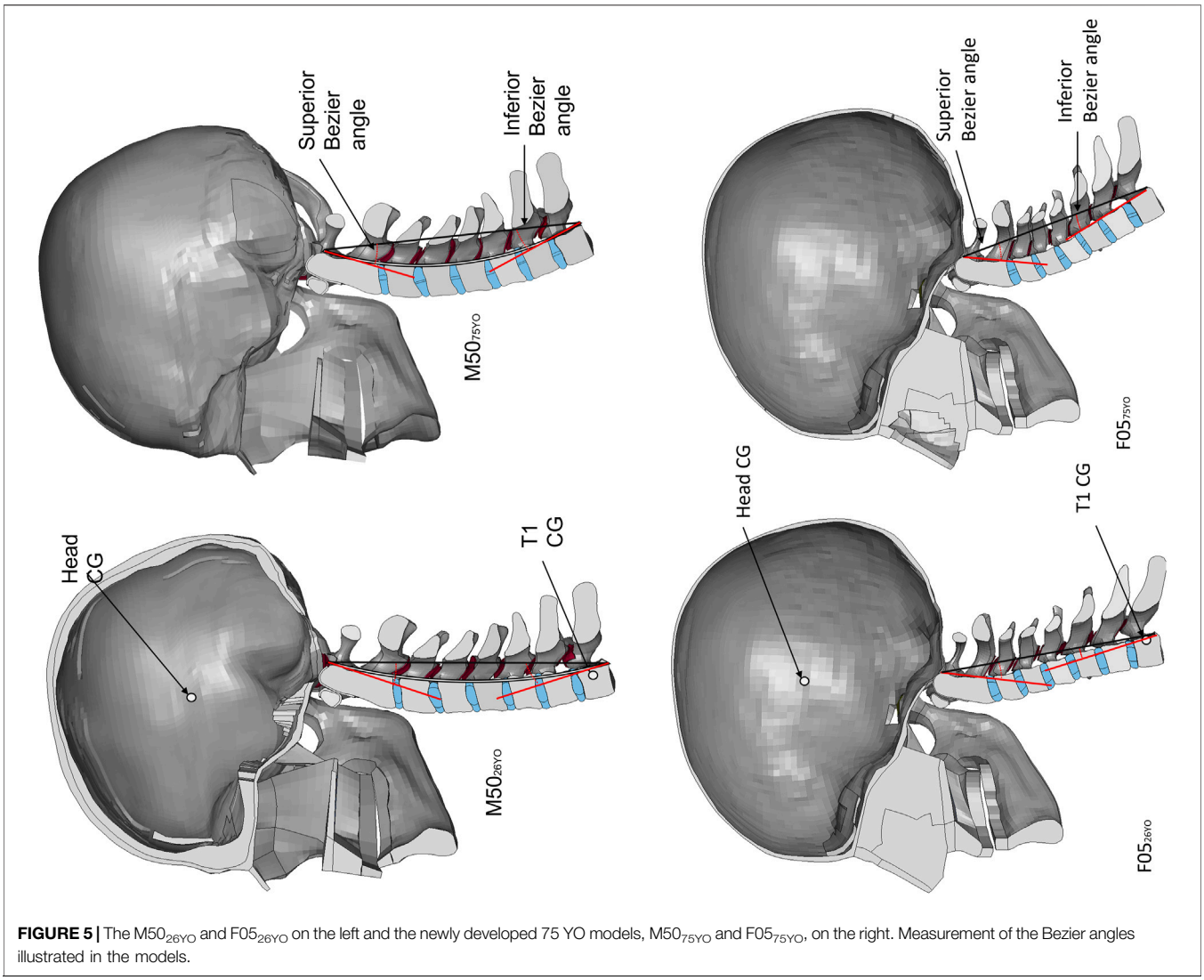

FIGURE 5 | The $M50_{26YO}$ and $F05_{26YO}$ on the left and the newly developed 75 YO models, $M50_{75YO}$ and $F05_{75YO}$, on the right. Measurement of the Bezier angles illustrated in the models.

TABLE 1 | Comparison of the Bezier angles of the existing models, $M50_{26YO}$ and $F05_{26YO}$, and the newly developed models, $M50_{75YO}$ and $F05_{75YO}$, to the literature data (Klinich et al., 2012).

	Bezier angle (deg)	26 YO model	Young (SD)	75 YO model	Older (SD)
M50	Superior	10.1	10.7 (7)	15.2	18.2 (10.3)
	Inferior	5.3	2.2 (7.3)	16.0	14.7 (12.3)
F05	Superior	15.0	17.1 (11.5)	21.4	24.9 (13.4)
	Inferior	2.2	5.2 (15.6)	14.3	18.1 (12.4)

therefore they were not reported in the current study. The FJK and nominal IVD strain was monitored at each segment level. The presented results demonstrate the trends and the effects of impact severity, sex and age for the 8 g frontal and 7 g rear impact cases. In general, the trends observed at the other impact severities (2 and 15 g frontal, 3 and 10 g rear) were similar to those observed at the intermediate impact severities (8 g frontal and 7 g rear). The complete set of results for all impact severities can be found in the supplemental material (**Supplementary Appendix A, B, C and D**). The head kinematics of the $M50_{26YO}$ and $M50_{75YO}$ under the frontal (2, 8 and 15 g) and rear (3, 7 and 10 g) impacts can be found in **Supplementary Appendix A**. The FJK and the nominal IVD shear strain at each segment level can be found in **Supplementary Appendix B**. Similarly, for the $F05_{26YO}$ and $F05_{75YO}$ models, the head kinematic response can be found in **Supplementary Appendix C** while FJK and the nominal IVD shear strain in **Supplementary Appendix D**.

Effect of Impact Severity

Increasing impact severity led to increases in the magnitude of the head kinematics, FJK, and nominal IVD shear strain, as expected. In that case, in agreement with the epidemiology data severity for the rear impact cases (**Figure 7**).

Age Effects

At the head kinematic level, the young and aged models demonstrated similar head kinematics shapes and peaks

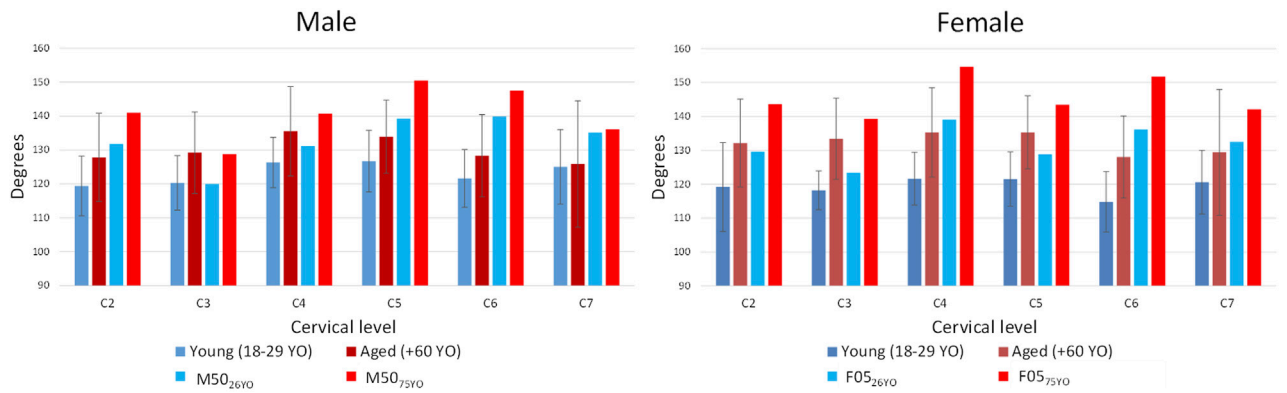

FIGURE 6 | Facet angle change with age reported in the literature and the facet angle of the developed models M50$_{75YO}$ and F05$_{75YO}$.

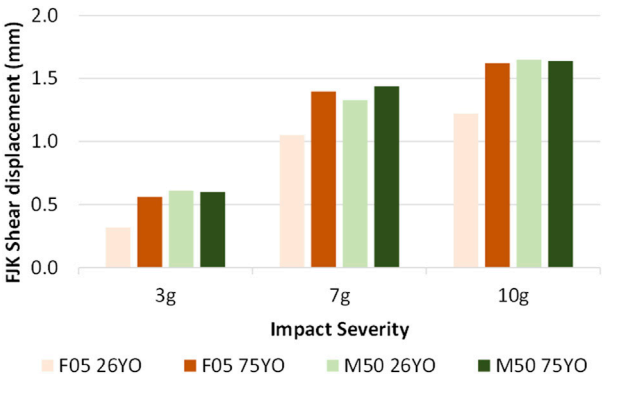

FIGURE 7 | FJK shear displacement, averaged at all segment levels for three rear impact severities, demonstrating increased response with increasing impact severity.

compared to the young models (cross-correlation ratings raging from 0.90 to 0.94 suggesting strong correlation). One notable difference was a spike in the head CG linear acceleration in the "X" and "Z" axis and in the rotational acceleration in the "Y" axis for the male model in the 8 g frontal (and 15 g frontal, **Supplementary Appendix A and C**) due to the hard tissue failure in the 6th vertebra of the M50$_{75YO}$ (**Figure 8A**). Hard tissue failure occurred only for the M50$_{75YO}$ model in the 8 and 15 g frontal simulations.

The FJK in the male models were similar to one another in the frontal and rear impacts (**Supplementary Appendix B**). In contrast, for the female models, the F05$_{75YO}$ predicted 26% higher relative facet shear in the rear impact while 36% lower relative facet rotation in the frontal (**Figures 8C,D**) when compared to the F05$_{26YO}$.

The nominal IVD shear strain between young and aged models was similar for all impact directions and severities, except for the female models in frontal impact (the F05$_{26YO}$ model predicted 17% more strain compared to the F05$_{75YO}$ model) (**Supplementary Appendix B and D**). However, for the M50$_{75YO}$ 8 g frontal impact, the maximum nominal IVD shear strain was affected by the predicted hard tissue failure. The nominal IVD strain time history demonstrated the maximum value at the moment prior to the hard tissue failure, followed by unloading of the IVD due to the vertebral body fracture (**Figure 8B**).

Sex and Size Effects

The differences between the head kinematic response between the male and female models were modest in general (with cross-correlation ratings ranging from 0.73 to 0.92). One notable difference was a spike in the head CG linear acceleration in the "X" and "Z" axis and in the rotational acceleration in the "Y" axis for the male model in the 8 g frontal (and 15 g frontal, **Supplementary Appendix A and C**) due to the hard tissue failure in the M50$_{75YO}$ (**Figure 8A**). Hard tissue failure occurred only for the M50$_{75YO}$ model in the 8 and 15 g frontal simulations. In general, the differences in tissue response observed between the M50$_{26YO}$ and F05$_{26YO}$ were similar in nature to those of the M50$_{75YO}$ compared to the F05$_{75YO}$. For example, male models predicted higher FJK shear displacement (12% more in the young models and 4% more in the aged models) regardless of age in the rear impact (**Figure 9A**). With respect to the FJK, in the rear impact, the female models predicted double the relative facet rotation on average than that of the male models (**Figure 9B**). Similarly, for the frontal impacts, the female models predicted 24% more relative facet joint rotation when compared to the male models (**Figure 9C**). The greater relative facet rotation predicted by the female models in frontal and rear impacts when compared to that of the male model was observed at most segment levels. However, in the C23 segment the facet joint rotation predicted by the male models was higher than that of the female in both in the frontal and in the rear impacts.

In the rear impact, the female model predicted 22% more nominal IVD shear strain on average than the male model (**Figure 9D**). In the frontal impact, the average nominal IVD shear strain of the male models was similar to that of the female models (**Supplementary Appendix B and D**) with the exception of the F05$_{75YO}$ that predicted 25% less nominal IVD shear strain than that of the M50$_{75YO}$

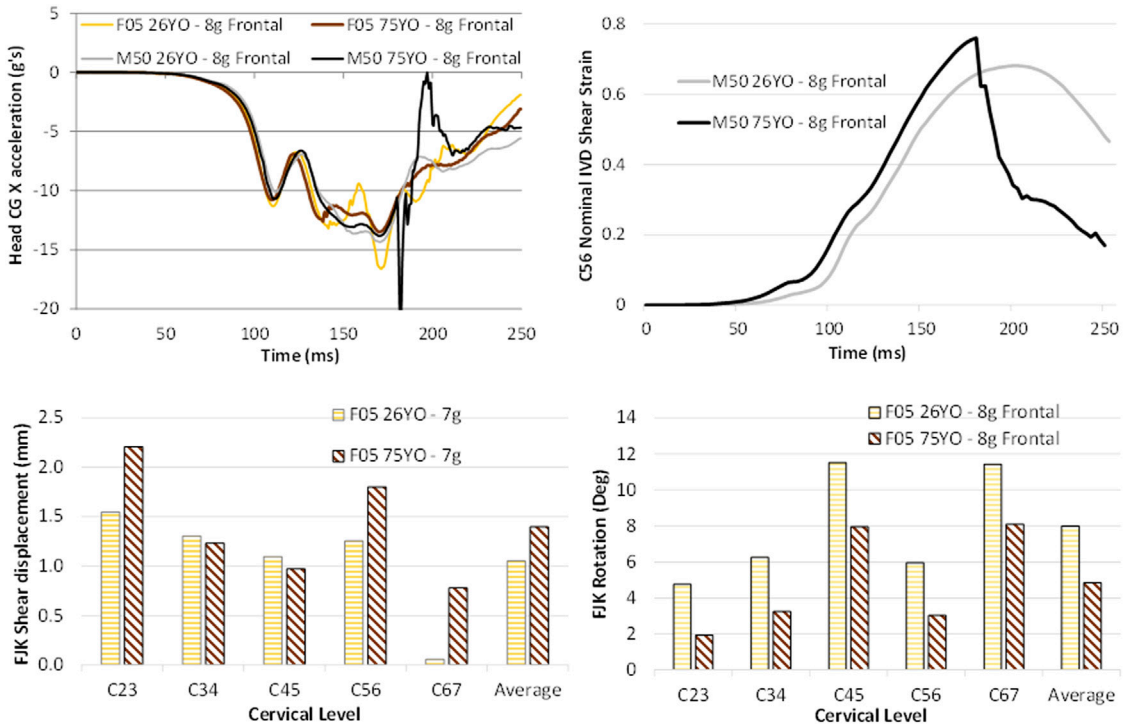

FIGURE 8 | Age effects on the (**A**) head kinematic response of the four assessed models, (**B**) the IVD space shear strain time history for the $M50_{75YO}$ and $M50_{26YO}$, demonstrating the effect of hard tissue failure, and (**C**) the relative facet joint kinematics in the rear and (**D**) frontal impact demonstrating the age-related differences in the female models.

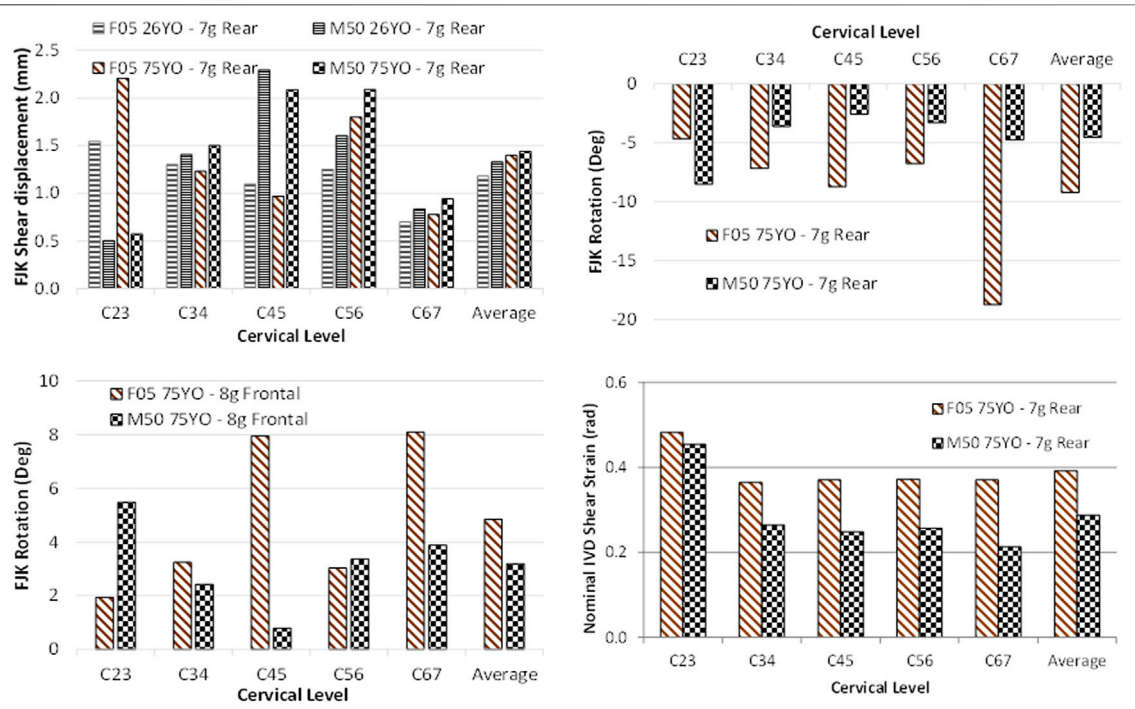

FIGURE 9 | Sex effects in the (**A**) relative facet shear displacement in the rear impact, the (**B**) relative facet rotation in the rear impact, the (**C**) relative facet rotation in the frontal impact, and the (**D**) nominal IVD shear strain in the rear impact demonstrating the differences associated with sex.

DISCUSSION

The neck models were geometrically aged by changing the curvature and the facet angle. A recent study (Reed and Jones, 2017) indicates that the change in facet joint angle is coupled with the change in spine curvature.

Reposturing Process

Early in the study, a preliminary assessment of simulation-based methods and a commercial morphing package was undertaken. Important limitations were found in terms of the output mesh quality, the difficulty of defining the boundary conditions for the target posture (for the simulation-based method) and the time-consuming process of defining the transformation rules for the soft tissues (for the morphing method). Although contemporary morphing tools may be able to achieve the same mesh quality as PIPER in the final posture, and can be further improved in efficiency, the open-source nature of the PIPER project allows for repeatability of the process by making the metadata and the software itself available to the community. The metadata used in this study for the F05 was made available through the PIPER web site. Within the PIPER project, metadata for the M50 was already freely available to the community.

Anthropometry

This study used male and female subject-specific young models repostured to represent average 75 YO subjects. The neck length of the subject-specific male model was higher than the average population reported in the literature. Although the subject selected for the development of the $M50_{26YO}$ model met the average mass and stature requirements, differences in anthropometries at the body region level could vary outside of the average for the target population. Interestingly, the $M50_{26YO}$ FE model neck curvature was straighter than the reported curvature of a 50th percentile 26 YO male, but when accounting for the neck length, the curvature of the $M50_{26YO}$ model was in agreement with the literature (Reed and Jones, 2017). This effect was identified using literature that reports individual vertebral positions. Such information may be obscured when using more general measurements, such as Bezier angles. Such measures depend more on the orientation, position, and shape of C7 and C2, with the mid-level vertebrae positions orientations having a lesser effect on the Bezier angles. Although the comparison of the cervical spine region in the models (male and female, both young and aged) to the FBP show a small discrepancy (within the mean plus two standard deviations), the FBP served to have confidence in the head orientation in a driving posture at the global level. The facet angles of the $M50_{26YO}$ and $M50_{75YO}$ models were within one standard deviation of the reported literature data for males for a given age group. The neck length and facet angles of the female models were within one standard deviation of the reported literature data for females at the given stature and age group.

Effect of Impact Severity

The effect of the increasing impact severities in frontal and rear impact was intuitive and in agreement with other post-mortem human subjects and anthropomorphic test device experiments (Nie et al., 2016) that predicted higher force peaks with higher impact severities. Higher impact severity led to higher head kinematic peaks, FJK, and nominal IVD shear strain. In the $M50_{75YO}$, the hard tissue failure with increased impact severity, however, led to lower peaks in the nominal IVD shear strain due to the subsequent unloading of the cervical spine as a consequence of the element erosion.

Age Effects

Higher compressive loads in the vertebral bodies of the $M50_{75YO}$ model, which led to hard tissue failure in the frontal impact, were attributed to the more anteriorly located head CG of the $M50_{75YO}$ when compared to the $M50_{26YO}$ that led to a higher moment-arm generating higher anterior compressive stresses in the vertebrae for frontal impact. Higher compressive loads were observed in the $M50_{75YO}$ model at all segment levels that led to hard tissue fracture at the 6th cervical vertebra within the vertebral body when compared to the $M50_{26YO}$ model. Similarly, higher nominal IVD shear strain was observed in the $M50_{75YO}$ when compared to the $M50_{26YO}$ model.

With respect to the female model, the increased age increased the relative facet shear in the rear impacts while the opposite in the frontal impacts. In the rear impact, the increased lordosis together with the increased facet angle (more horizontally oriented facet joints) of the $F05_{75YO}$ led to a more compliant neck under shear loading as the rotational range of motion was reduced by the change in the relative orientation of the facets. The straighter curvature of the $F05_{26YO}$ and the higher facet angle (more vertically oriented) led to higher relative facet rotation rather than relative facet shear.

The effect of age in the form of increased compressive forces observed in the $M50_{75YO}$ in the frontal impact and increased FJK in the rear impact observed in the $F05_{75YO}$ could imply a higher risk of injury with age for both males and females but related to different tissue-level injuries. Epidemiology shows higher chances of neck injury in the elderly population in general (Lomoschitz et al., 2002; Kahane, 2013) and higher for females in rear impacts (Carlsson, 2012), in agreement with the findings of the present study. Neck curvature and facet angle have demonstrated an effect on the tissue response often associated with injury and pain response (Yoganandan et al., 2001; Cavanaugh, 2006; Quinn and Winkelstein, 2007; Curatolo et al., 2011). Such factors could be important to consider in order to develop more effective safety equipment for the aged population.

Sex and Size Effects

When comparing the F05 to the M50 models, both young and aged, there were size factors (e.g. stature, neck length and head mass) and sex factors (e.g. facet angle, neck slenderness and neck lordosis). It has been shown that the 5th percentile female is not a simple scaled down geometry from a 50th percentile male (Singh and Cronin, 2017). In addition, it was found that sex differences in features like the facet joint angle were not well predicted using local scale factors, suggesting a complicated relationship between size and sex. A study including 50th percentile male and 50th percentile female would also include both size and sex effects;

similarly, including male and female size-matched individuals would include the two effects. Although computational models are a promising tool to isolate the sex effect from the size effect, the aim of the current study was to compare the response of an average male to a small stature female owing to the difference of incidence of injury between these two anthropometry groups. In the rear impact, the female ($F05_{26YO}$ and $F05_{75YO}$) models exhibited higher relative facet rotation and nominal IVD shear strain when compared to the male models ($M50_{26YO}$ and $M50_{75YO}$). The increased FJK and IVD deformation could be attributed to the female neck circumference relative to the length being smaller than in males, as is the vertebral body sizes, than males for size-matched subjects (Vasavada et al., 2008). In addition, the strength of the anterior and posterior muscles has been reported to be lower, 31.5 and 19.0%, respectively, than in males. The modest contribution of the female posterior musculature, when compared to the male in a rear impact, led to a higher sensitivity to geometrical and postural changes in the soft tissue response when compared to the frontal impact, where the posterior musculature is the major contributor. In addition, the increase in lordosis associated with age was higher in the females (2.9 deg increased lordosis when averaging the Bezier angles increase) than in the males (1.2 increased lordosis when averaging the Bezier angles increase) (Reed and Jones, 2017). In consequence, the lordosis of the $F05_{75YO}$ was higher than the lordosis of the $M50_{75YO}$ despite of the $F05_{26YO}$ lordosis being similar to the $M50_{26YO}$ lordosis (**Table 1**).

This is the first computational study that compares the neck response between an average stature male and a small stature female and between young and aged subjects. However, there were some limitations to the current study.

Limitations of the Study

Although specific injuries have not been linked to model response in the present study, higher tissue deformations could imply a higher likelihood of injury. In the context of this study, the higher facet joint kinematics could be associated with a higher likelihood of pain response in the facet joint, in that case, in agreement with the epidemiology data that suggest that females are more susceptible to injury in a rear impact. Future work includes the investigation of the injury assessment in the context of detailed HBMs using model tissue kinematics to infer injury risk. Importantly, the present study demonstrated that the assessment at the gross kinematic level might be insufficient to capture the effect of the geometric part of the ageing process. Tissue-level kinematic response assessments, such as FJK, were proved more informative than gross kinematic response, such as head kinematics, and might be required to understand the sex and age effects. To investigate the implication of injury related to the age and sex effects, more work is needed. A relationship between FJK and collagenous fibre realignment of the CL, for example, would be ideal to evaluate the injury risk associated with sex and age in HBMs.

The M50 model has been extensively validated at various levels (motion segment, ligamentous spine, and full neck with active musculature level) for a total of 82 validation cases. However, the F05 model has not been validated as extensively as the M50 has, owning, in part, to the lack of experimental data specific to small stature females. The F05 model was developed after the M50 model and based on a similar methodology used for the M50 model in terms of model and mesh design, material properties, and assessment using experimental data. One limitation of the assessments to date is that many experimental studies either report data for the average stature male, were scaled to represent an average stature male, or, in some cases, did not provide data regarding the subject anthropometric details. For example, the volunteer experimental data used to validate the active response of the M50 full neck model comes, in part, from the Naval Biodynamic Laboratory that performed human volunteer experiments using male military personnel. In a scaling study (Singh and Cronin, 2017), compared the response of the F05 to the M50 at the motion segment level and found that scaling based on the sagittal and transverse plane dimensions was appropriate for these models to compare kinematic response between models. It was noted that scaling did not apply specifically to the facet joint due to the fundamental differences in shape and angle between the male and female vertebrae. Importantly, the F05 validation using the same 82 cases as the M50, indicated a good correspondence to the experimental data, providing confidence in the model results.

The effective plastic strain based cortical and trabecular bone failure criteria should be further validated for the cervical spine under traumatic loading. Currently, the implementation has been validated in the cervical spine for non-catastrophic events, meaning that under the boundary conditions of volunteer human experiments, ligamentous spine experiments, and motion segment level experiments where bone failure was not observed, the model did not predict hard tissue failure. With respect to catastrophic events (Khor et al., 2018), validated the cortical material model in a femur fracture under axial rotation and three-point bending. In the cervical spine (Khor et al., 2017), evaluated the cortical and trabecular bone in the C5-C6-C7 functional spinal unit under axial and eccentric compression. However, the level of validation of the failure criteria, is not at the same level as the general validation of the GHBMC neck model under non-bone-fracture cases.

An important limitation of HBM is the uncertainty that exists with regards to the initial stress state of the modelled tissues in any posture. In a previous cervical motion segment investigation (Boakye-Yiadom and Cronin, 2018), using a C45 segment from the GHBMC M50 model, it was demonstrated that the initial stress state matters in terms of the tissue failure progression; suggesting that the stress state is important for the accurate prediction of the tissue response when considering repositioning. In this study, we aimed to develop neutral posture aged models from existing young neutral posture models. Including the induced strains in the soft tissues of the repostured aged models would have led to an unfair comparison, given that the young models did not account for the initial stress state of the soft tissues as well. Additional work is needed in order to define the stress states of the various tissues commonly modelled in HBM.

The geometric variability in biological tissues is often high. Importantly, the variability in anthropometry greatly increases with age (Parenteau et al., 2014), and it might be a dominant

factor in the increased incidence of injury in the aged population. In the present study, geometrical variability was not included. Variability of anthropometry in the ageing process can be challenging to implement in HBMs, partially due to the difficulty of reposturing models to a posture that might largely deviate from the original posture of the model. In addition, the relationship between local geometrical changes associated with age, such as facet angle, and the global changes, such as increased lordosis, is not clear. Subject-specific aged models could help researchers to understand such relationships and to encapsulate the geometrical changes associated with age in a more comprehensive manner; subject-specific modelling is part of future work. It is important to note that in the present study, a small stature female (5th percentile), due to the higher likelihood of injury of this anthropometry group, was compared to a medium-size male (50th percentile). Therefore, the size and sex effects were coupled in the present study. A comparison between the present $M50_{26YO}$ and a recently developed 50th female model (ViVA 50th percentile female model) could provide additional information regarding sex differences. However, the aim of this study was to compare the tissue-level response of an average stature male to that of a small stature female owing to the differences in incidence of injury between these two anthropometry groups. Importantly, in the present study, the material properties of the neck tissues and the muscle activation were not modified so that the known effect of geometric changes with age could be investigated. It is acknowledged that, with increasing age, biological material properties may change and increase in variability, joint stiffness may increase, and hard tissue strength decreases. In the context of the current study, increased joint stiffness may affect the FJK, and the lower strength hard tissue could lead to fractures, both monitored in the present study. Both the change in material properties and the potentially reduced muscle activation force could lead to more tissue distraction and higher injury risk. Including the effect of ageing in the material properties and in the muscle activation scheme is planned for future work. In addition, the boundary conditions applied to the T1 were the same for the four models. It is possible that the T1 response of the different anthropometry groups (young female compared to an aged female) changes under an impact scenario. Additional volunteer experimental data concerning female subjects is needed in order to develop boundary conditions for the neck that are representative of the female response under impact.

The interaction of the aged neck models with the safety systems in a car environment was not studied. Full body studies that compare young and aged models in a car environment or in a sled impact could be more informative about the effect of age on the effectiveness of the safety systems, which is the ultimate goal of the present research path and included in future work.

CONCLUSION

In this study, a methodology to modify the cervical spine geometry, using a hybrid approach with CAD and repositioning software (PIPER), successfully achieved the geometric hard tissue targets, while maintaining the overall mesh quality. This methodology could be applied to other models and body regions.

The head kinematic responses in terms of peaks and shape were similar for the four models and a given impact severity. However, the sex and size effects were evident in the tissue-level kinematic responses. Similarly, differences in tissue-level response between the young and aged models were observed and associated with the age-related geometric changes, suggesting that soft tissue metrics could be more informative than gross kinematic response. It is recommended to evaluate soft tissue metrics where possible in computational studies. In addition, detailed measurements of the soft tissue response along with a detailed description of the experimental set-ups in experimental studies would be beneficial for model development and validation at the tissue level. Similarly, when designing safety equipment, it could be more informative to evaluate the soft tissue response in the assessment of the effectiveness of the various safety systems to the protection of the subjects.

The epidemiology suggests that, in rear impacts, small stature female occupants demonstrate an increased risk of WADs when compared to males. This study is supported by those findings in the form of higher FJK predicted by the F05 (both young and aged) when compared to those of the M50 (both young and aged). Therefore, it is important to consider both sexes when evaluating safety systems. Although the importance of considering both females and males has been established before the present study, the present study has identified specific kinematics and could provide guidance for future investigations in injury risk.

The aged models demonstrated, in general, higher tissue deformation than their young counterparts. Higher tissue deformation could be associated with injury, but more work is needed to identify injury thresholds for the various tissues implicated in injury and pain response.

Age, sex and size effects were identified and found to be in general agreement with the existing literature suggesting a higher likelihood of injury for the aged population in general, and in rear impact for the female occupants.

DATA AVAILABILITY STATEMENT

The original contributions presented in the study are included in the article/**Supplementary Material**, further inquiries can be directed to the corresponding author.

AUTHOR CONTRIBUTIONS

All authors listed have made a substantial, direct, and intellectual contribution to the work and approved it for publication.

ACKNOWLEDGMENTS

The authors would like to acknowledge the Global Human Body Model Consortium for funding and use of the HBM, the

Compute Canada for computational resources, and the Natural Sciences and Engineering Research Council of Canada, FCA Canada, GM Canada, Honda R&D Americas and the Consejo Nacional de Ciencia y Tecnologia de Mexico for the financial support.

SUPPLEMENTARY MATERIAL

The Supplementary Material for this article can be found online at: https://www.frontiersin.org/articles/10.3389/fbioe.2021.681134/full#supplementary-material

REFERENCES

Barker, J. B., and Cronin, D. S. (2021). Multi-Level Validation of a Male Neck Finite Element Model with Active Musculature. *J. Biomechanical Eng.* 143 (1), 011004. doi:10.1115/1.4047866

Barker, J. B., Cronin, D. S., and Nightingale, R. W. (2017). Lower Cervical Spine Motion Segment Computational Model Validation: Kinematic and Kinetic Response for Quasi-Static and Dynamic Loading. *J. Biomechanical Eng.* 139 (6), 061009. doi:10.1115/1.4036464

Beillas, P., Petit, P., Kleiven, S., Kirscht, S., Chawla, A., Jolivet, E., et al. (2015). *Specifications of a Software Framework to Position and Personalise Human Body Models*. Lyon, France: IRCOBI, 594–595.

Boakye-Yiadom, S., and Cronin, D. S. (2018). On the Importance of Retaining Stresses and Strains in Repositioning Computational Biomechanical Models of the Cervical Spine. *Int. J. Numer. Meth Biomed. Engng.* 34, e2905. doi:10.1002/cnm.2905

Bose, D., Segui-Gomez, ScD, M., and Crandall, J. R. (2011). Vulnerability of Female Drivers Involved in Motor Vehicle Crashes: An Analysis of US Population at Risk. *Am. J. Public Health.* 101, 2368–2373. doi:10.2105/AJPH.2011.300275

Boyle, J. J. W., Milne, N., and Singer, K. P. (2002). Influence of Age on Cervicothoracic Spinal Curvature: An *Ex Vivo* Radiographic Survey. *Clin. Biomech.* 17 (5), 361–367. doi:10.1016/S0268-0033(02)00030-X

Carlsson, A. (2012). *Addressing Female Whiplash Injury Protection - A Step towards 50th Percentile Female Rear Impact Occupant Models*. Gothenburg, Sweden: Chalmers University of Technology.

Cavanaugh, J. M., Lu, Y., Chen, C., and Kallakuri, S. (2006). Pain Generation in Lumbar and Cervical Facet Joints. *J. Bone Jt. Surg. (American)* 88, 63–67. doi:10.2106/jbjs.e.01411

Corrales, M. A., and Cronin, D. S. (2021). Importance of the Cervical Capsular Joint Cartilage Geometry on Head and Facet Joint Kinematics Assessed in a Finite Element Neck Model. *J. Biomech.* 123, 110528. doi:10.1016/j.jbiomech.2021.110528

Correia, M. A., McLachlin, S. D., and Cronin, D. S. (2020). Optimization of Muscle Activation Schemes in a Finite Element Neck Model Simulating Volunteer Frontal Impact Scenarios. *J. Biomech.* 104, 109754. doi:10.1016/j.jbiomech.2020.109754

Curatolo, M., Bogduk, N., Ivancic, P. C., McLean, S. A., Siegmund, G. P., and Winkelstein, B. A. (2011). The Role of Tissue Damage in Whiplash-Associated Disorders. *Spine* 36, S309–S315. doi:10.1097/BRS.0b013e318238842a

Davis, M. L., Allen, B. C., Geer, C. P., Stitzel, J. D., and Gayzik, F. S. (2014). "A Multi-Modality Image Set for the Development of a 5th Percentile Female Finite Element Model," in *International Research Council on Biomechanics of Injury* (Berlin: IRCOBI). Available at: https://trid.trb.org/view/1324402.

Deng, B., Begeman, P. C., Yang, K. H., Tashman, S., and King, A. I. (2000). Kinematics of Human Cadaver Cervical Spine during Low Speed Rear-End Impacts. SAE Technical Papers. Stapp Car Crash. doi:10.4271/2000-01-SC13

Desantis Klinich, K., Ebert, S. M., Van Ee, C. A., Flannagan, C. A., Prasad, M., Reed, M. P., et al. (2004). Cervical Spine Geometry in the Automotive Seated Posture: Variations with Age, Stature, and Gender. *Stapp Car Crash J.* 48, 301–330. doi:10.4271/2004-22-0014

Drzał-Grabiec, J., Rykała, J., Podgórska, J., and Snela, S. (2012). Changes in Body Posture of Women and Men over 60 Years of Age. *Ortopedia, traumatologia, rehabilitacja.* 14 (5), 1–10. doi:10.5604/15093492.1012504

Fernihough, A., and McGovern, M. E. (2015). Physical Stature Decline and the Health Status of the Elderly Population in England. *Econ. Hum. Biol.* 16, 30–44. doi:10.1016/j.ehb.2013.12.010

Fice, J. B., and Cronin, D. S. (2012). Investigation of Whiplash Injuries in the Upper Cervical Spine Using a Detailed Neck Model. *J. Biomech.* 45 (6), 1098–1102. doi:10.1016/j.jbiomech.2012.01.016

Fice, J. B., Cronin, D. S., and Panzer, M. B. (2011). Cervical Spine Model to Predict Capsular Ligament Response in Rear Impact. *Ann. Biomed. Eng.* 39 (8), 2152–2162. doi:10.1007/s10439-011-0315-4

Frechede, B., Bertholon, N., Saillant, G., Lavaste, F., and Skalli, W. (2006). Finite Element Model of the Human Neck during Omni-Directional Impacts. Part II: Relation between Cervical Curvature and Risk of Injury. *Comp. Methods Biomech. Biomed. Eng.* 9 (6), 379–386. doi:10.1080/10255840600980940

Gayzik, F. S., Moreno, D. P., Geer, C. P., Wuertzer, S. D., Martin, R. S., and Stitzel, J. D. (2011). Development of a Full Body CAD Dataset for Computational Modeling: A Multi-Modality Approach. *Ann. Biomed. Eng.* 39 (10), 2568–2583. doi:10.1007/s10439-011-0359-5

Janak, T., Lafon, Y., Petit, P., and Beillas, P. (2018). *Transformation Smoothing to Use after Positioning of Finite Element Human Body Models*. Athens, Greece: IRCOBI, 224–236.

Kahane, J, C. (2013). Injury Vulnerability and Effectiveness of Occupant Protection Technologies for Older Occupants and Women. *National Highway Traffic Safety Administration*. Report No. DOT HS 811 766 (Accessed January 2021).

Khor, F., Cronin, D. S., Watson, B., Gierczycka, D., and Malcolm, S. (2018). Importance of Asymmetry and Anisotropy in Predicting Cortical Bone Response and Fracture Using Human Body Model Femur in Three-point Bending and Axial Rotation. *J. Mech. Behav. Biomed. Mater.* 87, 213–229. doi:10.1016/J.JMBBM.2018.07.033

Khor, F., Ds, C., and C, V. T. (2017). "Lower Cervical Spine Hard Tissue Injury Prediction in Axial Compression," in *International Research Council on Biomechanics of Injury* (Antwerp, Belgium: IRCOBI).

Klinich, K. D., Ebert, S. M., and Reed, M. P. (2012). Quantifying Cervical-Spine Curvature Using Bézier Splines. *J. Biomechanical Eng.* 134 (11), 114503. doi:10.1115/1.4007749

Kullgren, A., Stigson, H., and Krafft, M. (2013). "Development of Whiplash Associated Disorders for Male and Female Car Occupants in Cars Launched since the 80s in Different Impact Directions," in 2013 IRCOBI Conference Proceedings - International Research Council on the Biomechanics of Injury, Gothenburg (Sweden).

Lomoschitz, F. M., Blackmore, C. C., Mirza, S. K., and Mann, F. A. (2002). Cervical Spine Injuries in Patients 65 Years Old and Older. *Am. J. Roentgenology.* 178 (3), 573–577. doi:10.2214/ajr.178.3.1780573

Nie, B., Poulard, D., Subit, D., Donlon, J.-P., Forman, J. L., and Kent, R. W. (2016). Experimental Investigation of the Effect of Occupant Characteristics on Contemporary Seat belt Payout Behavior in Frontal Impacts. *Traffic Inj. Prev.* 17, 374–380. doi:10.1080/15389588.2015.1088944

Panjabi, M. M., Ito, S., Pearson, A. M., and Ivancic, P. C. (2004). Injury Mechanisms of the Cervical Intervertebral Disc during Simulated Whiplash. *Spine* 29, 1217–1225. doi:10.1097/00007632-200406010-00011

Parenteau, C. S., Wang, N. C., Zhang, P., Caird, M. S., and Wang, S. C. (2014). Quantification of Pediatric and Adult Cervical Vertebra-Anatomical Characteristics by Age and Gender for Automotive Application. *Traffic Inj. Prev.* 15 (6), 572–582. doi:10.1080/15389588.2013.843774

Park, J., Ebert, S. M., Reed, M. P., and Hallman, J. J. (2016a). A Statistical Model Including Age to Predict Passenger Postures in the Rear Seats of Automobiles. *Ergonomics* 59 (6), 796–805. doi:10.1080/00140139.2015.1088076

Park, J., Ebert, S. M., Reed, M. P., and Hallman, J. J. (2016b). Statistical Models for Predicting Automobile Driving Postures for Men and Women Including Effects of Age. *Hum. Factors.* 58 (2), 261–278. doi:10.1177/0018720815610249

Quinn, K. P., and Winkelstein, B. A. (2007). Cervical Facet Capsular Ligament Yield Defines the Threshold for Injury and Persistent Joint-Mediated Neck Pain. *J. Biomech.* 40, 2299–2306. doi:10.1016/j.jbiomech.2006.10.015

Reed, M. P., and Jones, M. L. H. (2017). *A Parametric Model of Cervical Spine Geometry and Posture A Parametric Model of Cervical Spine Geometry and Posture*. Michigan: University of Michigan Transportation Research Institute, Final report.

Safiri, S., Kolahi, A.-A., Hoy, D., Buchbinder, R., Mansournia, M. A., Bettampadi, D., et al. (2020). Global, Regional, and National burden of Neck Pain in the General Population, 1990-2017: Systematic Analysis of the Global Burden of Disease Study 2017. *Bmj* 368, m791. doi:10.1136/bmj.m791

Schoell, S. L., Weaver, A. A., Urban, J. E., Jones, D. A., Stitzel, J. D., Hwang, E., et al. (2015). Development and Validation of an Older Occupant Finite Element Model of a Mid-sized Male for Investigation of Age-Related Injury Risk. *Stapp Car Crash J.* 59 (April), 359–383. doi:10.4271/2015-22-0014

Singh, D., and Cronin, D. S. (2017). An Investigation of Dimensional Scaling Using Cervical Spine Motion Segment Finite Element Models. *Int. J. Numer. Meth Biomed. Engng.* 33 (11), e2872–13. doi:10.1002/cnm.2872

Snyder, R. G., Chaffin, D. B., and Foust, D. R. (1975). Bioengineering Study of Basic Physical Measurements Related to Susceptibility to Cervical Hyperextension-Hyperflexion Injury. UMTRI Final Report. Report No (Accessed December 2020).

Stemper, B. D., Pintar, F. A., and Rao, R. D. (2011a). The Influence of Morphology on Cervical Injury Characteristics. *Spine* 36, S180–S186. doi:10.1097/BRS.0b013e3182387d98

Stemper, B. D., Yoganandan, N., Pintar, F. A., and Maiman, D. J. (2011b). The Relationship between Lower Neck Shear Force and Facet Joint Kinematics during Automotive Rear Impacts. *Clin. Anat.* 24 (3), 319–326. doi:10.1002/ca.21172

Umana, E., Khan, K., Baig, M., and Binchy, J. (2018). Epidemiology and Characteristics of Cervical Spine Injury in Patients Presenting to a Regional Emergency Department. *Cureus* 10 (2), e2179. doi:10.7759/cureus.2179

Vasavada, A. N., Danaraj, J., and Siegmund, G. P. (2008). Head and Neck Anthropometry, Vertebral Geometry and Neck Strength in Height-Matched Men and Women. *J. Biomech.* 41, 114–121. doi:10.1016/j.jbiomech.2007.07.007

Wismans, J., Philippens, M., Van Oorschot, E., Kallieris, D., and Mattern, R. (1987). Comparison of Human Volunteer and Cadaver Head-Neck Response in Frontal Flexion. SAE Technical Papers. Society of Automotive Engineers. doi:10.4271/872194

Yang, K. H. (2018). *Basic Finite Element Method as Applied to Injury Biomechanics*. London, United Kingdom: Academic Press, Elsevier, 3–49. doi:10.1016/B978-0-12-809831-8.00001-5

Yoganandan, N., Cusick, J. F., Pintar, F. A., and Rao, R. D. (2001). Whiplash Injury Determination with Conventional Spine Imaging and Cryomicrotomy. *Spine* 26, 2443–2448. doi:10.1097/00007632-200111150-00010

Conflict of Interest: The authors declare that the research was conducted in the absence of any commercial or financial relationships that could be construed as a potential conflict of interest.

Publisher's Note: All claims expressed in this article are solely those of the authors and do not necessarily represent those of their affiliated organizations, or those of the publisher, the editors and the reviewers. Any product that may be evaluated in this article, or claim that may be made by its manufacturer, is not guaranteed or endorsed by the publisher.

Advantages of publishing in Frontiers

OPEN ACCESS
Articles are free to read for greatest visibility and readership

FAST PUBLICATION
Around 90 days from submission to decision

HIGH QUALITY PEER-REVIEW
Rigorous, collaborative, and constructive peer-review

TRANSPARENT PEER-REVIEW
Editors and reviewers acknowledged by name on published articles

Frontiers
Avenue du Tribunal-Fédéral 34
1005 Lausanne | Switzerland

Visit us: www.frontiersin.org
Contact us: frontiersin.org/about/contact

REPRODUCIBILITY OF RESEARCH
Support open data and methods to enhance research reproducibility

DIGITAL PUBLISHING
Articles designed for optimal readership across devices

FOLLOW US
@frontiersin

IMPACT METRICS
Advanced article metrics track visibility across digital media

EXTENSIVE PROMOTION
Marketing and promotion of impactful research

LOOP RESEARCH NETWORK
Our network increases your article's readership